A Publication of the
Marine Foundations Committee
of the Deep Foundations Institute

DEEP MARINE FOUNDATIONS

A Perspective on the Design and Construction of Deep Marine Foundations



Editors:
Robert B. Bittner
Roderic A. Ellman, Jr.

DFI SUSTAINING MEMBERS
1999-2008

AMERICAN CIVIL CONSTRUCTORS WEST COAST INC.
AMERICAN EQUIPMENT & FABRICATING CORP.
ANDERSON DRILLING
APE/J&M
ASC GEOSCIENCES INC.
BERKEL & COMPANY CONTRACTORS INC.
BRAYMAN CONSTRUCTION CORPORATION
CAJUN DEEP FOUNDATIONS LLC
CASE FOUNDATION COMPANY
CIPORT S.A.
DEAN CONSTRUCTION CO. LTD.
DEWITT CONSTRUCTION INC.
DGI-MENARD INC.
DOSDOURIAN ENTERPRISES INC.
FOUNDATION CONSTRUCTORS INC.
GEOKON INC.
HAYWARD BAKER INC.
HJ FOUNDATION INC.
KLEINFELDER
L.G. BARCUS & SONS INC.
LANGAN ENGINEERING AND ENVIRONMENTAL SERVICES
MACTEC ENGINEERING & CONSULTING INC.
McKINNEY DRILLING COMPANY
MORETRENCH
MUESER RUTLEDGE CONSULTING ENGINEERS
NICHOLSON CONSTRUCTION COMPANY
NORTH AMERICAN CONSTRUCTION GROUP
PILECO INC.
PND ENGINEERS INC.
RICHARD GOETTLE INC.
SAS STRESSTEEL INC.
SCHNABEL FOUNDATION COMPANY
STS-AECOM
THATCHER ENGINEERING CORPORATION
URBAN FOUNDATION/ENGINEERING LLC
WILLIAM F. LOFTUS ASSOCIATES FOUNDATION ENGINEERS
WURSTER ENGINEERING & CONSTRUCTION INC.

Deep Foundations Institute Sustaining Members are Corporate Members of DFI who have voluntarily granted funding to the Institute for expanded support of the industry. The Sustaining Membership Fund supports DFI Seminars and Educational programs for professionals as well as students through the Paul DeBruyn Memorial Student Scholarship Fund. DFI is proud to list the above Sustaining Member Organizations who support the Scholarship Fund and DFI ongoing conferences, seminars and programs. Both the Sustaining Membership Fund and the Paul DeBruyn Memorial Student Scholarship Fund are managed by the DFI Educational Trust.

DFI is grateful to The Sustaining Members and all its members as it continues as a resource for all persons and organizations involved in the design and construction of deep foundations.

Preface

Over the last six years since inception of the Marine Foundations Committee of DFI in 2002, the committee has been presenting annual seminars on a wide range of relevant technical issues relating to the design and construction of deep marine foundations. Over this same time period, the committee has been compiling the papers presented at these seminars and a few other relevant papers on deep marine foundations into a single volume for easy reference for designers, constructors, and suppliers to our industry. Hopefully this volume will assist designers and contractors in optimizing the efficiency of their deep marine foundations. The assembled volume contains 40 papers covering the following topics:

- Case histories of design and construction of deep marine foundations for major bridges
- Innovative concepts for temporary cofferdams
- Design and placement of tremie concrete
- Design and installation of large diameter driven piles for marine structures
- Design and installation of large diameter drilled shafts for marine structures
- Deep marine foundations for offshore wind turbines
- Miscellaneous topics dealing with deep marine foundations including: dredging, underwater geophysical investigation methods, driven-pile sound attenuation methods, ship-impact protection systems for bridges, corrosion of marine tiebacks, and underwater compaction using vibration.

The editors wish to thank the authors for their participation in the DFI Marine Foundations Committee Seminars and for their excellent contributions to this publication. The editors also wish to thank the peer review committee for their work. This committee included:

Alex Matlin – Parsons Brinckerhoff Quade & Douglas, Inc.
Dominic D'Argenzio – Mueser Rutledge Consulting Engineers
Joel Moskowitz – Mueser Rutledge Consulting Engineers
Ben C. Gerwick, Jr. – Ben C. Gerwick, Inc
Gerry Houlahan – Moffatt & Nichol
Jim Graham – James S. Graham, P.E.
Dennis Murphy – Kiewit Engineering Co.
Dennis Nottingham – PND Engineers, Inc.
John Fowler - Engineering & Construction Consultant
Jeff Sheldon - Moffatt & Nichol
Dennis Anderson - Kiewit Engineering Co.

The Marine Foundations Committee wishes to thank the Deep Foundations Institute and Theresa Rappaport, Executive Director of DFI, for her support and guidance during preparation of this publication.

Robert B. Bittner
Roderic A. Ellman, Jr.

January 31, 2009

DFI MARINE FOUNDATION COMMITTEE MEMBERS

Aly Mohammad	DMJM + Harris Inc.	aly.mohammad@aecom.com
Bernie Hertlein	STS-AECOM	bernie.hertlein@sts.aecom.com
Bill Marczewski, Jr.	BSM Consulting Engineers	bill@bsmengineering.com
Bob Bittner	Bittner-Shen Consulting Engineers Inc.	rbb@bittner-shen.com
David Borger	Skyline Steel LLC.	DBorger@skylinesteel.com
Dean Matthews	Timber Piling Council	dean@timberpilingcouncil.org
Don Tylenda	Skyline Steel LLC.	DTylenda@skylinesteel.com
Doug Scaggs	MENCK GmbH – An Acteon Company	douglas.scaggs@menck.com
Dr. Jinyuan Liu	Ryerson University	jinyuan.liu@ryerson.ca
Dr. Osama Safaqah	ExxonMobil	osama.safaqah@exxonmobil.com
Emad Farouz	CH2M Hill	efarouz@ch2m.com
Endi Zhai	Kleinfelder	EZhai@kleinfelder.com
Gerry Houlahan	Moffatt & Nichol	ghoulahan@moffattnichol.com
Gerry McShane	Skyline Steel LLC.	gmcshane@skylinesteel.com
Gianfranco DiCicco	GDConsulting LLC.	GDCons05@aol.com
Jeffrey Yachmetz	Langan Engineering and Environmental Services	jyachmetz@Langan.com
Jim Morrison	Kiewit Construction Group	jim.morrison@Kiewit.com
John Hammill	Roll Form Group	jhammill@rollformgroup.com
Koen Zuijdgeest	CBI	kz020304@yahoo.com
Larry Owens	Traylor Bros. Inc.	lowens@traylor.com
Mike Holloway	InSituTech Ltd.	Mike.Holloway@insitutech.com
Rick Ellman	Mueser Rutledge Consulting Engineers	rellman@mrce.com
Robb Swenson	General Construction Co.	Robb.Swenson@kiewit.com
Thomas Printz	Williams Form Engineering Corp.	tprintz@williamsform.com
Tshien Ma	TM Engineers Inc.	tm@tmengineers.com
William G. Duguay	Traylor Bros. Inc.	wduguay@traylor.com
Yingcai Han	Fluor Canada Ltd.	yingcai.han@fluor.com

The editors and the Deep Foundation Institute wish to thank the following organizations for allowing DFI to re-publish articles in this publication:

- **Structure Research Group, Public Works Research Institute of Japan** – *Skirt Suction Foundation* – Application to Strait Crossings, by Takashi Saito, Yoichi Yoshida, Masato Itoh and Naoki Masui

- **American Society of Civil Engineers** – *Substructure Construction Methods I-205 Columbia River Bridge*, by Robert B. Bittner

- **American Society of Civil Engineers** – *Underwater Concrete in Drilled Shafts: the Key Issues and Case Histories*, by Sam X. Yao and Robert B. Bittner

- **American Society of Mechanical Engineers** – *Foundations for Offshore Wind Energy Converters – A Review of Some Current Scandinavian Development Projects* by K. Viking and Lars Johansson

- **American Society of Mechanical Engineers** – *Offshore Wind Turbine Foundations in Denmark and Belgium* by Jorn H. Thomsen, Torben Forsberg and Robert Bittner

- **American Concrete Institute** – *Seal-Slab Prestressed Pile Interface Bond from Full-Scale Testing* by Gray Mullins, Ruben Sosa, Rajan Sen, and Moussa Issa

- **American Concrete Institute** – *Seal-Slab / Steel Pile Interface Bond from Full-Scale Testing* by Gray Mullins, Ruben Sosa, Rajan Sen and Moussa Issa

The editors and the Deep Foundation Institute also wish to thank Tacoma Narrows Constructors – A Joint Venture of Bechtel Corporation, Inc. and Kiewit Pacific Company for allowing use of the caisson photo from the construction of the new Tacoma Narrows Bridge for the cover of this publication.

Copyright © 2009 by Deep Foundations Institute
All Rights Reserved
ISBN: 978-0-9763229-1-7

DEEP MARINE FOUNDATIONS
A Perspective on the Design and Construction of Deep Marine Foundations
Table of Contents

Introduction…….. 1

Section 1 Design and Installation of Large Diameter Driven Piles for Deep Marine Foundations

1.1 Large Diameter Steel Tubular Piles for Optimum Seismic Performance …….. 3
Ben C. Gerwick, Jr. & Robert B. Bittner, Ben C. Gerwick Inc.

1.2 Design of the Marine Foundations for the Skyway Project of the San Francisco-Oakland Bay Bridge ……..…… 7
Gerry Houlahan, Moffatt & Nichol

1.3 Installation of Marine Pile Foundations at the Skyway Project for the San Francisco-Oakland Bay Bridge ……..….. 15
Robb L. Swenson, General Construction Company-a Kiewit Company

1.4 Underwater Pile Hammers ……...…….. 21
Douglas L. Scaggs, MENCK GmbH

1.5 Diameter Effects on p-y Curves ……..…….. 27
Ignatius P.O. Lam, Earth Mechanics, Inc.

1.6 Installation Checklist for Driving Mega Piles ……..……. 43
Douglas L. Scaggs, MENCK GmbH

1.7 Underwater Sound Attenuation in Construction Projects: Applying Science to Pile Driving Permits ……..….. 47
Alan Christopherson & Jennifer Lundberg, PND Incorporated

Section 2 Design and Installation of Large Diameter Drilled Shafts for Deep Marine Foundations

2.1 Construction of Large Diameter Drilled Shafts: The 2nd Mike O'Neill Lecture …… 53
Dan Brown, Dept. of Civil Engineering, Auburn University

2.2 Design of the Drilled Shaft Foundations for the Cooper River Bridge …… 65
Liang Shen, Osama Safaqah & Robert B. Bittner, Ben C. Gerwick, Inc.

2.3 Design and Construction of the Sutong Bridge Foundations …… 81
Robert B. Bittner & Osama Safaqah, Ben C. Gerwick, Inc., Xigang Zhang HPDI, China, Ole Juul Jensen & Ole Rud Hansen, COWI A/S, Denmark

2.4 Large Diameter Shafts – Youghiogheny Reservoir Bridge …… 101
Paul J. Lewis & David R. Scherer, Gannett Fleming, Inc.

2.5 Drilled Shaft Foundations for the Float-In Dam on the Monongahela River at Braddock, PA 113
Robert B. Bittner, Ben C. Gerwick, Inc. & William R. Miles, Bergmann Associates

Section 3 **Design and Installation of Caisson Foundations for Marine Structures**

3.1 Design and Construction of the Rion Antirion Bridge Foundations …… 123
Alain Pecker, Geodynamique & Structure, France

3.2 Construction of the Main Tower Pier Caissons for the Greenville Bridge in Mississippi ……. 137
F. Keith Jacobson, Massman Construction Co.

3.3 Skirt Suction Foundation – Application to Strait Crossings …….. 145
Takashi Saito, Public Works Research Group, Japan, Yoichi Yoshida, Masato Itoh & Naoki Masui, Obayashi Co Ltd., Japan

3.4 New Tacoma Narrows Bridge Caissons ……. 157
R. Bruce Patterson, Kiewit Pacific Co.

3.5 Mooring Bridge Caissons During Construction Using Jetted-In Driven Plate Anchors ……. 169
Osama Safaqah, Marc Gerin & Robert B. Bittner, Ben C. Gerwick, Inc.

3.6 Caisson Foundations for Mississippi River Bridges in the New Orleans Area …… 177
William B. Conway, Modjeski and Masters, Inc.

3.7 Open Well Caissons of A 1917 Railroad Bridge – How 19th Century Construction Can Influence 21st Century Construction …….. 185
Alan D. Fisher, Cianbro Corporation

3.8 Marine Foundations of Bridges in the Northeastern USA …….. 195
James S. Graham, Norwalk Marine Contractors & Joel Moskowitz, Mueser Rutledge Consulting Engineers

Section 4 **Innovative Concepts for Temporary Cofferdams**

4.1 Woodrow Wilson Bridge Cofferdams ……. 207
Roderic A. Ellman, Jr., Museser Rutledge Consulting Engineers, Jim X. Zhang & Bill Spence, Tidewater Skanska, Inc.

4.2 Float-In Cofferdams …….. 215
Robert B. Bittner, Ben C. Gerwick, Inc.

4.3 Finite Element Analyses and Cofferdam Excavations ……... 229
Dimitrios C. Konstantakos, Mueser Rutledge Consulting Engineers

4.4 Cooperative Effort Overcomes Problems with Pier and Cofferdam Construction Caused by Rock Slope ……. 239
Herbert F. "Buck" Darling III, Herbert F. Darling, Inc. & Richard J. Hartman, Hartman Engineering

4.5 Innovative Cofferdams used on the I-205 Columbia River Bridge ……. 249
Robert B. Bittner, Ben C. Gerwick, Inc.

Section 5 **Design and Placement of Tremie Concrete**

5.1 Underwater Concrete in Drilled Shafts: The Key Issues and Case Histories …… 257
Sam X. Yao & Robert B. Bittner, Ben C. Gerwick, Inc.

5.2 Seal Slab Prestressed Pile Interface Bond From Full-Scale Testing …….. 263
Gray Mullins, Ruben Sosa, Rajan Sen & Moussa Issa, University of South Florida

5.3 Seal Slab/Steel Pile Interface Bond From Full-Scale Testing ……..…... 277
Gray Mullins, Ruben Sosa, Rajan Sen & Moussan Issa, University of South Florida

5.4 Underwater Concrete – Mix Design and Construction Practices ……..289
Sam X. Yao, Ben C. Gerwick, Inc.

Section 6 **Deep Marine Foundations – Related Topics**

6.1 Marine Foundation Retrofit for the Richmond-San Rafael Bridge …… 297
Patrick E. Durnal & Henrik Dahl, Ben C. Gerwick, Inc.

6.2 Best Practices: Dredging and Dredged Material Disposal ……..…..…305
Raymond Sandiford, Port Authority of NY and NJ & Peter Dunlop, Gahagan & Bryant Associates, Inc.

6.3 Vessel Collision Design – Risk Analysis and Deep Foundation Issues for Bridges over Navigable Waterways ……..……..…… 311
Michael A. Knott, Moffatt & Nichol

6.4 The Underwater Cut-Off at the Water F. George Dam ……..….. 327
Gianfranco Di Cicco & Riccardo Pertocelli, Treviicos Corporation

6.5 Current State of Practice of Corrosion Protective Systems for Tierods and Tiebacks Used in Marine Applications ……... 335
Thomas A. Printz, John A. White and Tom Bird, Williams Form Engineering Corp.

6.6 Deep Compaction Using Vibratory Pile Hammers …….. 349
Dennis Nottingham, PND Incorporated

6.7 Statnamic Load Testing of High Capacity Marine Foundations ……..……. 355
Mike Muchard, Applied Foundation Testing, Inc.

6.8 Foundations for Offshore Wind Energy Converters – A Review of Some Current Scandinavian Development Projects ……. 373
K.Viking & Lars Johansson, Ramboll Sverige AB, Sweden

6.9 Geophysical Methods for Site Characterization for Marine Foundations ……. 381
Richard E. Sylwester, Golder Associates, Inc.

6.10 Offshore Wind Turbine Foundations – In Denmark and Belgium ……..… 391
Jørn H. Thomsen & Torben Forsberg, COWI A/S, Denmark & Robert B. Bittner, Ben C. Gerwick, Inc.

6.11 Berth Deepening A Three Decade Old Wharf Structure for the Next Generation of Container Ships ……..…….. 401
Bill Paparis & Michael Quadagno, Han-Padron Associates, LLP, Guy Buzzoni & James McQueen, APM Terminals N. America, Inc. and John Lizzo, Port Authority of NY & NJ

DEEP MARINE FOUNDATIONS – AN INTRODUCTION

Ben C. Gerwick, Jr., Ben C. Gerwick, Inc., San Francisco, CA, USA
Gerry Houlahan, P.E., Moffatt & Nichol, Walnut, Creek, CA, USA

This publication is intended to document recent innovations and technologies that have the best potential for effectively improving the quality of marine foundations while reducing the cost, time and risk of construction.

Marine foundations originated in Neolithic times with the Swiss Lake Dwellers who constructed pile-supported houses, safe from invading tribes. The Queen of Babylonia built the first recorded bridge in 1500 BC across the Tigris. The foundations were large flat stones laid on the river bottom. About the same time in India, builders extended their water well techniques to the construction of "well" foundations in the beds of their rivers. These were really the first open caissons; brick walls were built up in a circular ring while divers excavated sand from the bottom, sometimes at a depth of 100 feet. The Romans extended the clay-filled cribs of the Middle East to shallow cofferdams, which they sealed by underwater concrete made with pozzolanic cement from Mt. Vesuvius.

Look how far innovations have brought the Art of marine foundations in the intervening years, almost all of them in the last two centuries! While we still encounter the same environmental events, today's structures are far greater in depth and size, but most of our problems are similar.

Innovations in marine foundations have flourished at an accelerating pace. The marine field has been especially innovative, fuelled by the rapidly expanding harbor and coastal activities, being joined today by river navigation improvement projects. The first offshore platform was installed in 1947. The industry that grew from that beginning has provided us with numerous construction techniques, configurations and analysis techniques that are adaptable to the more traditional nearshore and riverine marine foundations that are the subject of this publication.

A list of modern innovations would fill this entire volume but we will present a few noteworthy cases that outline the range of capabilities that we see today. These are:

- screwed piles, invented in 1833 by a blind englishman Alexander Mitchell to support lighthouses in tidal waters,
- concrete slurry wall construction, which presents a much safer and more efficient means of constructing cofferdams and other retaining structures,
- prestressed concrete, which has extended the range of performance and cost-effectiveness of reinforced-concrete piles,
- post-tensioning, which permits rapid construction using precast segmental components,
- cast-in-drilled-hole (CIDH) and large diameter driven steel tubular piles, that are needed for today's very large structures,
- float-in construction of structures such as concrete footings and piers,
- air-bubble fish protection devices that nearly eliminate damage to marine life during pile driving,
- vibrators for ensuring good concrete compaction with high strength,
- hydraulic pile driving hammers, which provide very high controllable energy, can be used under water, eliminate the need for followers and minimize pollution,
- vibratory pile hammers that permit the flexible economic installation and removal of piles,
- suction-installed caissons, that can be used as anchors, or as foundations that can be ejected by pressure reversal, and
- tension-leg floating platforms and screeding barges, that are insensitive to tides and waves.

What made these innovations succeed?

Most made use of new technologies, including GPS, Side-Scan Sonar, ROVs, hydraulics and down-the-hole drills. Old problems could be tackled using new knowledge and techniques. Testing of piles for offshore platforms and the advent of modern powerful computers have enabled us to confidently predict even the dynamic behavior of soil-foundation systems in the time domain. Concrete admixtures such as high range water reducers, silica fume and anti-washout thixotropie admixtures made it possible for high strength workable concrete to be placed reliably underwater.

What factors drove their acceptance to where they are today State-of-the-Art?

Many of them filled needs that were beyond the practicable capability of past practice. A few, such as suction anchors filled new needs such as that of vertical uplift in deep water. T-headed reinforcing bars met the need to resist impact from ice and vessels. All were aimed at solving newly arisen problems and all were driven by the need for early application on specific projects.

What current areas are ripe for innovative developments?

There is an urgent need for a reliable method of joining slurry concrete walls in order to prevent leakage and to transfer moment. There is a need to develop a meaningful quantitative test for a workable concrete to be placed underwater and to flow around and through dense reinforcement. A promising start on this has been made by the Japanese with their J-tube flow test. The pile-supported raft, adapted and used brilliantly on the piers of the Rion-Antirion Bridge in Greece is a most revolutionary example of recent innovation. Can this concept be applied to other bridges and other sites? Construction of foundations in tidal and surf zones is still problematic. Can we develop a walking construction platform supported on suction caisson footings to increase our effectiveness in these conditions? Our ability to respond to breaches in levees is minimal. We must anticipate further problems and have the imagination and courage to develop and fund rapidly deployable containment systems that can minimize the loss of life and property damage in such events.

The history of the evolution of deep marine foundations indicates that dramatic and powerful innovations are still to come. We are fortunate to live in a society which is receptive to change. New challenges will arise and new opportunities will emerge. We challenge the marine industry to continue with the bold development that has brought us to our present capabilities. The state-of-the-art can be extended to produce new techniques, materials and methods that are limited only by our imagination and ability to fund their development.

The following chapters will discuss innovations in deep marine foundations in much greater detail. They provide valuable guidance and, hopefully, will stimulate new development, as well as act as a reference for those unfamiliar with modern marine design and construction techniques.

LARGE DIAMETER STEEL TUBULAR PILES FOR OPTIMUM SEISMIC PERFORMANCE

Ben C. Gerwick, Jr., Ben C. Gerwick, Inc., San Francisco, CA, USA
Robert B. Bittner, PE, Ben C. Gerwick, Inc., San Francisco, CA, USA

Large diameter steel tubular piles installed vertically or on a slight rake, offer many advantages as the foundations of major overwater bridge in regions of high seismicity. By proper selection of diameter and wall thickness, an optimum balance between stiffness and strength can be achieved. Under strong seismic motion, the piles will deflect and bend so as to reduce the acceleration forces transmitted to the superstructure, while still limiting drift. A major advantage of this concept is that the mass of the footing block is significantly reduced from that of the conventional pier. The design of the footing block requires great care in order to transfer the high shears and moments. Where the soils consist of significant depths of sediments, the kinematic interaction of soils, piles and structures must be considered. Moments will be a maximum just under the footing block. Filling the top portion of the pile with concrete will prevent local buckling and assure ductile behavior even under overload. Typically the piles will be long, with most or all of their support furnished by friction and will require the use of very large pile hammers to achieve the required capacities. Where the piles are founded on rock or in hardpan, sockets will be drilled and filled with reinforced concrete. For these piles, high moments can occur both at the head and just below the rock surface, so the concrete infill should extend the full length. This paper describes the use of tubular piles driven through the deep silty sands of the Jamuna River, Bangladesh, and also where socketed into the near-surface rock for the mail pylon pier of the new San Francisco-Oakland East Bay Bridge in California.

INTRODUCTION

1.1 Steel tubular cylinder piles with diameters of one to two meters have been previously employed for a number of major bridges, including the Rio Niteroi Bridge in Brazil, the Parana Bridges in Argentina, and on the new bridge across the Tagus River in Portugal. They have proved to be an efficient and economical solution for the foundations, because they enabled the footing block to be constructed near the waterline, thus obviating the need for a deep cofferdam or caisson.

In recent years it has been recognized that tubular piles of even greater diameter, 2.5 to 4.0 meters, have the ability to provide lateral stiffness to the pier along with ductility for overload events such as earthquakes, sea ice, and ship collision. (Figure 1) Combined with an efficiently designed footing block that develops both moment and shear, they can be optimized for drift (lateral deflection), and strength.

These piles are typically thick-walled so as to enable effective driving to deep penetrations, as well as to provide moment resistance and stiffness. The wall thickness can be varied along the length to suit the demands of both drivability and in-service stresses. Where piles are driven into deep sediments, the highest bending moment occurs in the 1 to 1 ½ diameters just below the footing block. Filling the upper part of the pile with concrete, locked to steel pile by means of shear rings, will give the pile increased stiffness and ductility. Stable hysteresis responses have been obtained in laboratory tests up to a ductility factor of 4.

As a result of the failure of many raked piles in wharves during earthquakes, the current trend has been to use only vertical piles in seismic zones. Vertical piles respond well to excitation from all directions. However, it has been recently realized that in soft sedimentary soils or deep water, a slight rake can be utilized and still not result in excessive moment, shear or axial forces during earthquake. The benefits are

greater lateral stiffness under serviceability environmental loadings, reduced drift during the seismic event and especially reduced residual displacement.

1.2 Design of these piles for lateral forces, such as those of earthquake, requires a full analysis of the soil-structure interaction. The free-field motions are modified by the kinematic interaction of the pile with the soil due to the pile's stiffness. In layered sediments, the load-deflection performance can be determined by the finite element method with soil springs input along the pile length.

Group effects due to "shadowing" must be considered. For extreme deflections, the moments and deformations resulting from eccentric loading may be important.

1.3 Installation of these large piles requires the use of very large crane barges and very heavy pile hammers. Templates are usually employed to position the piles accurately, especially when the piles are battered (raked). See Figure 2. Because there will be only a few such piles in a footing, each will be highly loaded e.g. to several thousand tons. Tolerances in pile head locations are very critical.

1.4 Design of the footing blocks requires consideration of the demands for moments, shear and axial force transfer and also the practicality of construction. Precast concrete shells are often employed, temporarily supported on the piles. Both circumferential and axial shear keys are employed. Because of the high forces in moment and shear, post-tensioning may also be required.

It should be noted that if the piles are slightly battered, the footing block can be reduced in size, thus reducing the mass which is subject to high accelerations under earthquake. It has been found that the largest contributor to the shear under earthquake is usually the mass of the footing block. Piles are usually designed for essentially elastic behavior under the design earthquake, with ductility employed for possible overload during a few cycles.

1.5 Large diameter steel tubular piles were utilized for the recently completed Jamuna River Multipurpose Bridge in Bagladesh, where very deep and unstable sediments, combined with variable river depths due to shifting channels as well as high Monsoon floods, demanded an unique solution. The piles varied from 2.5 to 3.15m in diameter. They were 80m in length, with wall thicknesses up to 65mm. They were driven in three sections, using a Menck hydraulic hammer developing 1800 KN-m of energy per blow. The piles were driven through medium dense to very dense sand, and founded in a gravel stratum at a depth of 80m below normal water level. Up to 12,000 blows per pile were required. Splicing of three sections was by full-penetration welding.

The 300 ton pile hammer and the pile sections were handled by a large offshore-type crane barge. Piles were installed at a rate up to 5 per week and the work was completed on schedule.

1.6 Tubular piles are also an excellent solution for overwater bridge piers founded in rock or hardpan. In this case, vertical piles will usually prove best. They are cleaned out and a socket drilled into the rock.

Past practice has then been there to install a reinforcing steel cage and to fill the pile with concrete. However, if there is inadequate overburden, the pile may develop high moments at or just below the rock line. In such cases, an oversize socket is drilled, and the tubular pile lowered or driven into it, assuring the full moment capacity is provided at this critical region. The annular space is then grouted and the pile filled with concrete.

This concept has been adopted for the seismic retrofit of the several major bridges across San Francisco Bay, in order to develop greater stiffness and thus reduce drift deflection to acceptable values. Steel tubular piles, socketed into rock, have been selected as the probable design for the major pylon pier suspension span of the new San Francisco-Oakland East Bay Bridge while driven tubular piles, 2.5m diameter and up to 100m in length will support the long approach viaduct.



Figure 1: 3m diameter x 80m long piles used to support this pier of the Jamuna River Multipurpose Bridge in Bangladesh.



Figure 2: Installation of piles on the Jamuna River Bridge

DESIGN OF THE MARINE FOUNDATIONS FOR THE SKYWAY PROJECT OF THE SAN FRANCISCO OAKLAND BAY BRIDGE

Gerry Houlahan, Moffatt & Nichol, Walnut Creek, CA, USA

The east span of the 3.5 km long SF-Oakland Bay Bridge is supported by different types of foundations along its span. Starting from the west, its first 460 m section comprising twin concrete box-girders is supported by sands and rock on Yerba Buena Island. A 620 m long steel suspension span then bridges a 25 m deep channel that is formed in sediments overlying rock. Twin concrete box girder structures, each 2.4 km long, complete the stretch over the remainder of San Francisco Bay to the engineered earth fill landing at its east end. For most of its length, the Skyway bridges water 3 to 10 m deep over soft surficial Young Bay Mud. The foundation types include spread footings with hold-downs, steel and concrete piles that are set in drilled rock sockets up to 3 m in diameter and 2.5 m diameter steel tubular piles driven to penetrations of up to 100 m. The design and construction-related considerations are presented. The different foundation types, influences of the site geology and earthquake demands on the substructures are discussed. The seismic motions of the bridge superstructures and substructures, as well as the depth-varying soil motions, influenced the foundation design. Together with performance-based design criteria, including post-earthquake footing displacement limits, these seismic demands influenced various aspects of the foundation design, including the use of battered and vertical piles.

INTRODUCTION

The geology along the new East Span of the San Francisco-Oakland Bay Bridge was the primary consideration in the selection of foundation types. Bridge structure types also were affected by this geology. The Safety Evaluation Earthquake (SEE), which was the extreme design earthquake with a return period of 1500 years, also affected the foundation design, as did variations in service loads. The bridge is described with an emphasis on the geotechnical and foundation aspects as they apply to each portion of the bridge. Design and construction aspects of the foundations include some cost-saving features made possible by the site geology.

THE BRIDGE AND ITS FOUNDATIONS

The bridge shown on Figure 1 consists of the Transition Structures, Suspension Bridge, Skyway Structures and Oakland Approach Structures. It starts on Yerba Buena Island (YBI) at the existing double deck tunnel. The structures on the island make the transition from a low, two-level reinforced concrete structure to two tall, side-by-side concrete structures. The roadway configuration for the new bridge is five lanes each way, at one level.

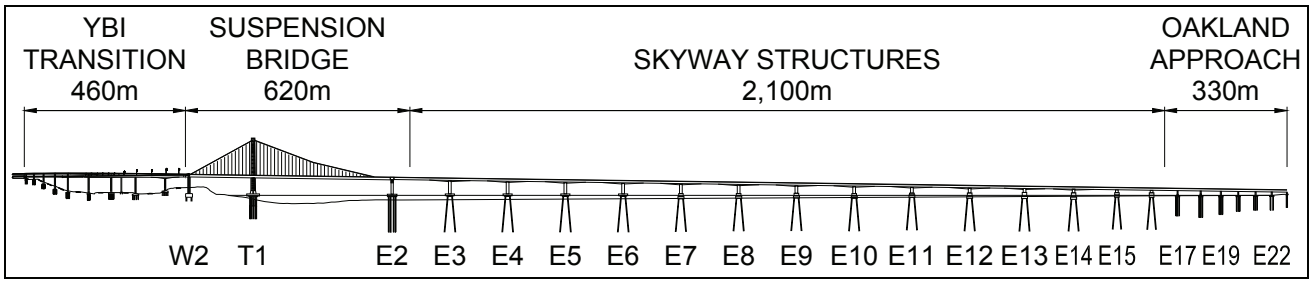


Figure 1: New Bay Bridge (East Span) - General Arrangement Looking North

The YBI Structures are complex cast-in-place prestressed concrete box girder structures with 22 m to 85 m spans. Many of its footings are on driven H-piles. Some are spread footings requiring tie-downs set in drilled rock sockets. One footing is founded on relatively short 2.4 m diameter Cast in Drilled Hole (CIDH) reinforced concrete piles because of its proximity to the rock surface.

The west piers of the Suspension Bridge (on YBI) are supported by 19 m square, 10 m deep gravity footings set in 25 m deep rock excavations. The north footing on the edge of YBI has four 2.5 m diameter 10 m long CIDH piles. The footing under the Suspension Bridge's steel tower, where the water is 16 m deep, is supported by 2.5 m diameter piles. The upper sections of the piles, where bending can occur, are composite concrete-filled steel tubes grouted into 3 m diameter holes drilled into the bedrock. These piles develop into, and are continuous with, 2.2 m diameter, 30 m long CIDH piles. The footings under the bridge's east piers, where the water is 12 m deep, are supported by vertical 2.5 m diameter steel pipe piles driven to penetrations of about 100 m. The upper sections of these piles are concrete-filled.

Most of the foundation costs for the bridge are associated with the Skyway portion because of its significant length. The Skyway spans are typically 160 m long with some shorter spans at its east end. The individual footings for this pair of separate precast concrete box girder structures are supported by 2.5 m diameter driven steel pipe piles similar to those at the Suspension Bridge's east pier foundation. However, these are driven at a slight batter, with penetrations up to about 100 m. The upper sections of these piles are also composite concrete-filled steel tubulars.

The Oakland Approach, which consists of a pair of separate cast-in-place concrete box girder structures with 42 to 64 m spans, is supported by 1.8 m diameter vertical steel pipe piles driven to penetrations as deep as 65 m. The abutment of these structures adjoins an engineered fill extension to the existing Oakland Mole.

FOUNDATION DESIGN ASPECTS

Local soil conditions dictated the foundation types. Where bedrock was close to the surface, spread footings sometimes with drilled piles or rock socket tie-downs were used. Where there was significant soil depth, driven piles were used. Because foundation cost was a high proportion of the total cost, emphasis was placed on developing designs and specification provisions that would reduce costs.

Site Characterization

An aggressive program was adopted by Caltrans to provide a good early geotechnical characterization of the site and the design earthquake motions. This enabled the designers to develop marine foundation designs that changed little from the conceptual phase to final design. However, on YBI, because of late access for the soils investigation, designs were progressed using assumed soils then updated as properties became available. The geology along the marine sections of bridge profile consists of soft Young Bay Mud overlying local sand layers, Old Bay Mud, Upper and Lower Alameda Formations (layers of stiff clay, silt, dense sand, gravel), overlying Franciscan Bedrock (Figure 2).

Design Considerations

Principal design criteria required the foundation to resist gravity and operational loads with appropriate factors of safety, to remain essentially elastic during the SEE, and to limit the post-earthquake horizontal displacements of the footings to 150 mm.

Cost-based optimization of the Skyway spans refined two aspects of normal practice for the design of the large diameter deep-driven piles.

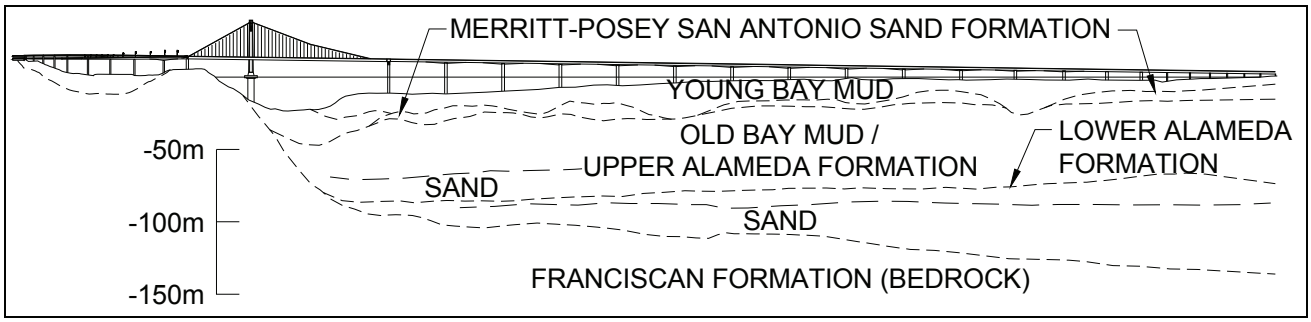


Figure 2: New Bay Bridge - Geologic Cross Section Design Considerations

Test-based Pile Capacity/Penetration. The measured resistance to driving large piles through clay-dominated formations is not a good indicator of the ultimate capacities of these piles after the dissipation of pore water pressure. This has long been recognized in the design of large piles, the use of which originated with large offshore oil and gas platforms. In such cases, the capacities of the piles have been based on tested soil properties. The measured resistance to driving is commonly in the range of 30% to 50% of the ultimate skin friction capacity. These piles drive unplugged and significant end bearing is available after setting concrete plugs in the piles. This also negates the use of resistance to driving as a measure of ultimate pile capacity. Therefore, we used target penetration as the primary basis of pile driving acceptance. This approach is appropriate where foundation behavior is predictable and extensive site investigations have been carried out. It also eliminates uncertainties that are reflected in higher bid prices. It was beneficial at this site that the elevation of the Lower Alameda formation, the end-bearing layer, is very predictable.

Displacement-Based SEE Design. Using traditional procedures, piles as designed for either skin friction or end bearing. We used skin friction capacity and force-based factors of safety to design the piles for load combinations of gravity, construction and deck shrinkage actions. However, the use of force-based criteria is not appropriate for these piles for the SEE because the ultimate capacity of the piles includes high end bearing in the Lower Alameda Formation in addition to the skin friction capacity. The six design SEE depth-varying ground motion records determined the post-earthquake settlement of the footings. In addition, sensitivity analyses of the effects of wide variations of end bearing confirmed the soundness of this approach, providing significant cost savings.

Earthquake Response

The following considerations affected the foundation seismic design:

Marine Footing Mass. The dynamic response of the over-water sections of the bridge to earthquakes shows that while the deck sway modes primarily drive the axial load in the piles, the footing sway modes cause most of the bending. Bending is significant in the SEE, creating a strong incentive to minimize the footing mass. Concrete-encased steel footing frames were used rather than more massive reinforced and post-tensioned concrete footings. In order to minimize the footing size, the Skyway foundations utilized slightly battered piles. These were spaced more closely at the footing but provide the spacing needed at depth to avoid detrimental group effects. In addition, it was found that battered piles were needed to meet the post-SEE footing displacement limits.

Kinematic Pile Response. The time-varying and depth-varying motions of the soil cause bending in the long large diameter piles. This kinematic response is incorporated in the total dynamic response of the soil-pile-structure system under SEE shaking. The design of the piles for this real phenomenon increases the reliability of the foundations over previously-used design methods, particularly at depth.

Vertical and Battered Piles. The east piers of the Suspension Bridge have vertical piles, while the Skyway has battered piles. This is because the east piers have relatively little dead load and are controlled by pile tension, whereas the Skyway has significant dead load, which reduces tension forces. Also, the soil at the east piers includes a thicker sand layer, which reduces the tension capacity of the piles. Vertical piles also reduce cyclic axial

loads in earthquakes, minimizing the total tension on the piles, with a small increase in pile bending.

Vertical piles are generally preferred for earthquake designs because they provide a more ductile response than highly battered piles. In addition, they are easier to install and have lower axial loads. In the design of the Skyway, slightly battered piles were found to be the most cost-effective way of meeting all of the design criteria, particularly the post-earthquake horizontal displacement limits.

Foundation Characteristics, by Structure

The following were considerations that affected the foundation characteristics for the individual bridge structures.

YBI Transition Foundations. Since the YBI portion of the bridge is founded on sand and bedrock, the Transition Structures are supported on a combination of spread footings that use driven H-piles, CIDH piles and tie-downs (see Figure 3).

Suspension Bridge. The steel tower, located about one third along the bridge deck, supports almost all of the structure's weight. Very little weight is applied to the back span piers (west end) or the forespan piers. These end piers, however, resist almost all of the horizontal earthquake and wind loads, as well as their associated vertical components.

The back span piers are supported by two concrete gravity footings that are cast in excavations in the YBI rock (see Figure 4a). These footings can resist potential uplift caused by increased cable tension that occurs during earthquake-induced sway of the deck and tower. This feature creates an inherently balanced bridge. The southern footing at this location is surrounded on all four sides by the vertical walls of the excavation, while the northern footing is partially exposed on its northern side. For this reason, four piles were cast in rock sockets to prevent potential rocking and sliding of the footing in the unsupported direction. The tower footing is pile-supported and set at water level. (See Figure 4b). Its size has been minimized to reduce its mass by a concrete-encased structural steel frame that provides full fixity for the piles. These piles are set into sockets drilled into rock. Because they are drilled foundations, practical construction dictates that they be vertical, which also suits the primary demand on the foundation, which is compressive.

The forespan piers are supported by two footings (see Figure 4c). Each footing is supported by eight vertical driven piles that are spaced to efficiently resist overturning and to minimize group-effect inefficiencies. They are connected at the waterline by a tie-beam. This links the transverse displacement of the two footings under SEE and minimizes structural demand on the top connections.

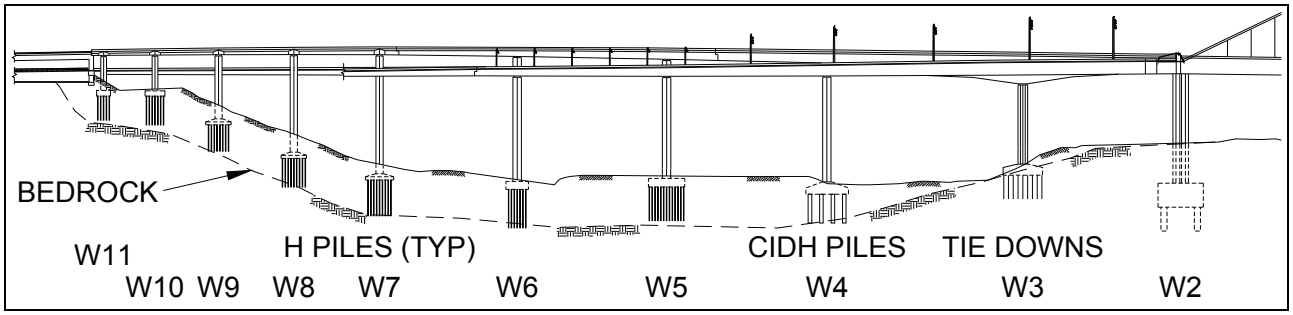


Figure 3: YBI Transition Structures

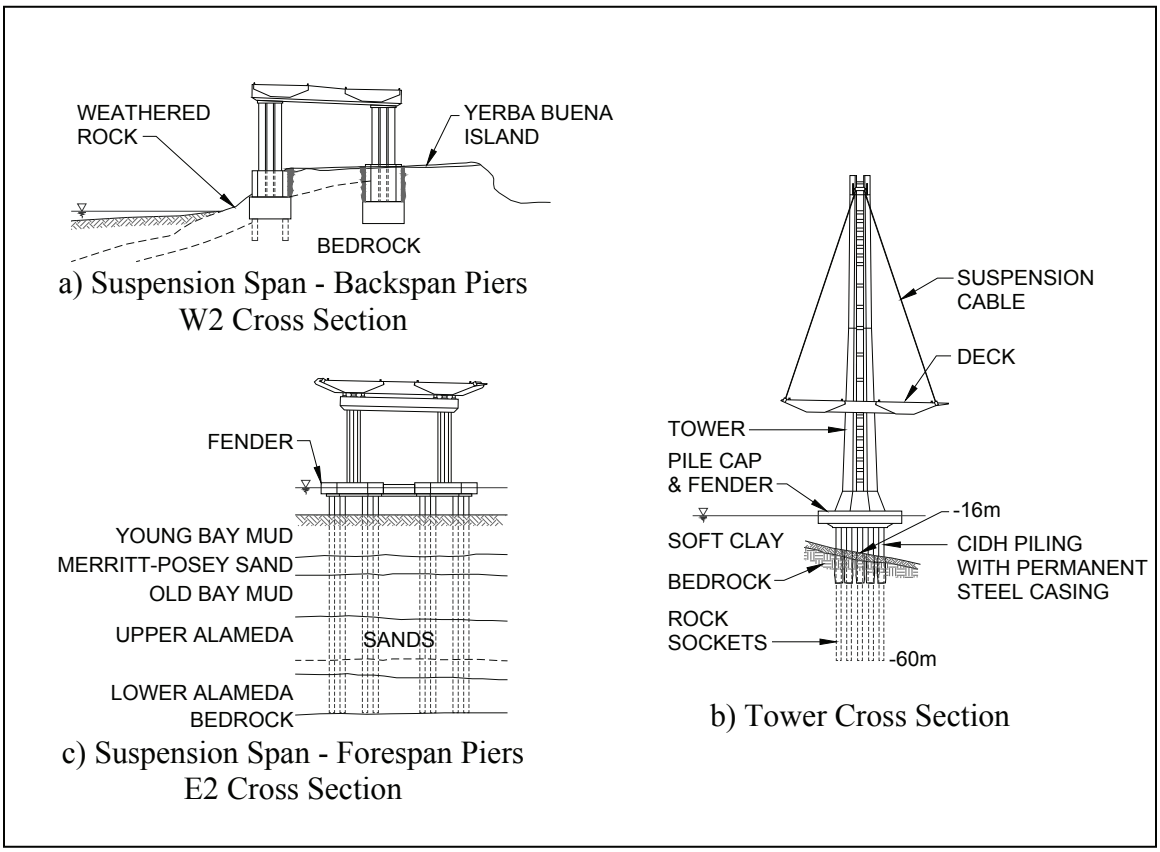


Figure 4: Suspension Bridge Sections

Skyway. The longitudinal framing of the Skyway consists of four multi-column fixed-top portal frames (see Figure 5). In the transverse direction, the substructures act as simple vertical cantilevers (see Figure 6). The Skyway foundations are influenced by several features of this structural system including high dead loads (concrete deck), balanced cantilever construction, shrinkage of pre-cast deck (under post-tension), jacking of half-frames and earthquake-induced motions. Loads from the construction, operating and earthquake design conditions all affect these foundations. The construction loads are applied within a few months of pile driving, before full skin friction capacity is developed, raising the importance of pile set-up.

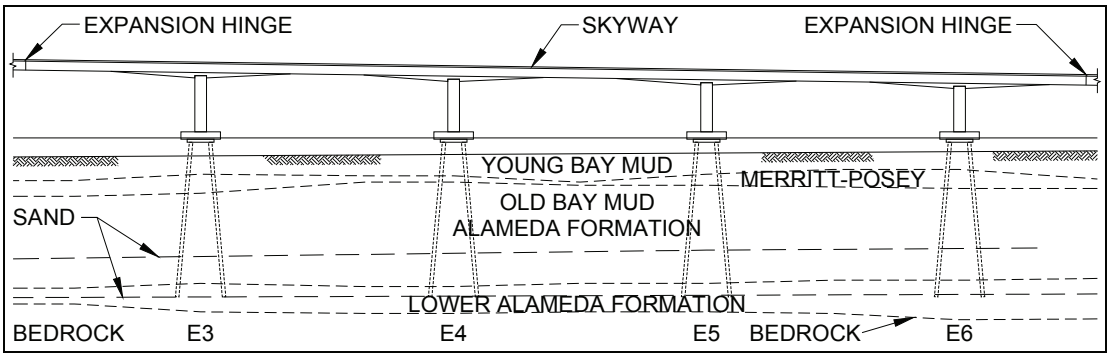


Figure 5: Typical Skyway Frame Arrangement

The gravity, construction and shrinkage demands on the footings led to the finding that the most economic typical foundation was six 2.5 m diameter steel tubular piles, driven into the Lower Alameda formation (penetrations up to 100 m). These piles provide the axial capacity, bending strength, ductility, redundancy and driveability that are needed. They also minimize the additional cost impacts of the SEE.

Oakland Approach. Piled footings were used to support these approach structures due to the presence of variable depths of Young Bay Mud on the Oakland side. Offshore footings were supported by 1.8 m diameter steel piles fitted with steel weldments that provide pile head fixity. Land portions use 610 mm diameter prestressed concrete piles. The remaining land portion of the bridge is on geofill.

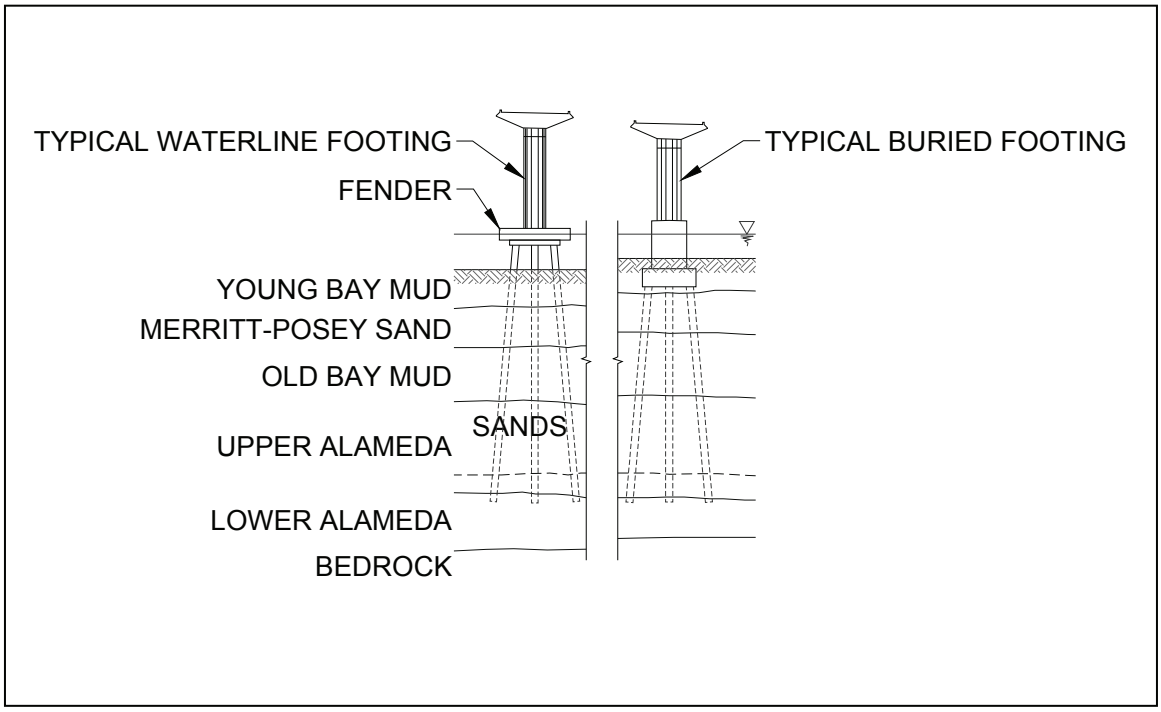


Figure 6: Typical Skyway Cross Sections

FOUNDATION CONSTRUCTION ASPECTS

The key construction considerations used during the design of the foundation systems for the new bridge included ease of construction, cost and service reliability. Design decisions were made to provide the contractors with significant flexibility.

Foundation Construction Procedures

The YBI Transition structures are on land and their foundation construction is complex, but conventional. The Suspension Bridge back-span piers are founded on rock, and deep rock excavation (controlled blasting) is significant in their construction. Mass concrete design required surface and internal tie reinforcement to control thermal cracking of the footing. Rock sockets were used at the northern, west-bound footing, and tall retaining walls were required around the piers to permit pier movement during earthquakes.

The construction of the marine foundations for the Tower, the forespan piers and the water-level Skyway piers uses temporary footing supports. Using this approach, piles are installed through the footings. After the Tower footing is in place, first stage pile sockets will be drilled into the surface materials and the permanent casings will be set with grout. The vertical rock sockets will then be drilled using the permanent casings as drilling risers. After the piles are connected to the foundation frame, the remaining concrete may be placed in preparation for the tower base plate.

For the Skyway, a separate temporary pile guide frame, supported on independent piles, is used to guide the piles during driving. The foundation piles do not touch the footing frame during driving. For the buried Skyway footings, a partially dewatered cofferdam system is utilized. Here, after excavation, a gravel bedding is placed, which supports the footing frame during pile driving.

Pile Size and Installation Equipment

The 2.5 m diameter piles used in the marine sections of the bridge are designed to be driven to the Lower Alameda Formation. Pile driving technology that is environmentally clean, portable and reliable (hydraulic hammers) has been available since about 1980. A free-riding 1700 kJ hammer (no sliding leads) has been specified for the deep-driven piles to ensure pile driveability. A uniform 2.5 m diameter was adopted for the most loaded piles to enable standardization of handling and installation equipment.

Installation Methods Sequence

The design of the foundations was necessarily based on assumed methods of construction. In general, the designs provided flexibility to the contractors for refinements when construction methods were known. Among the options that were considered were pile installation in one piece versus making field splices, and pile installation through the footing frames versus preinstalling the piles and lowering the footing onto the piles. The possibility of one-piece piles did not affect pile design, but did require limitations on the locations of field splice welding. To enable the preinstallation of one-piece battered Skyway piles, the footing frames were designed with oversized sleeves. After award, the Skyway contractor decided to install the piles through the footing frames, thus reducing the size and fabricated cost of the frames.

The additional pile loads caused by the out-of-balance moments inherent with the “balanced cantilever” Skyway deck erection technique are applied before full pile capacity has been realized. Caltrans’ Pile Installation Demonstration program, performed more than one year prior to bidding, calibrated the pile friction set-up rate, and minimized uncertainties in pile driving energy requirements. These two results helped to reduce construction bids.

ACKNOWLEDGMENTS:

The author would like to thank the following people for their contributions to the foundation design: Jal Birdy P.E., John Denis P.E., Dr. Sajid Abbas P.E., Dr. Marwan Nader P.E., Rick Nutt P.E., Kirsten Setterholm P.E., Godwin Mok P.E. and Siew Chee P.E.

INSTALLATION OF MARINE PILE FOUNDATIONS AT THE SKYWAY PROJECT FOR THE SAN FRANCISCO OAKLAND BAY BRIDGE

Robb L. Swenson, General Construction Company, a Kiewit Company, Poulsbo, WA, USA

Construction of foundations for the Skyway Segment of the San Francisco Oakland Bay Bridge required innovative techniques due to the mass of the structures being inserted and the unique subsurface of the Bay. Twenty of the pier structures required large sheet pile cofferdams. Eight other foundations were installed in open water without cofferdams at the deeper part of the Bay. This narrative will present the initial planning, as well as the stages of installation, for each type of foundation.

The first section will discuss foundation constructability modifications made during the initial planning phases of the project. Considerable effort was expended by Caltrans, the owner, T.Y. Lin the designer, and KFM (Kiewit/FCI/Manson) the contractor in modifying the design to assure that required tolerance would be maintained during the installation of the foundations.

The final section will describe the steps required for installation including: initial access dredging, installation of cofferdams, preparation required to install the footing boxes, footing box installation, foundation support pile installation, and pile to box connections.

FOUNDATION CONSTRUCTABILITY MODIFICATIONS

In the planning stages of the project, minimal redesign efforts were allowed to facilitate installation of the footing boxes and piling. These changes reduced the potential difficulties of obtaining the necessary horizontal and vertical tolerances of the structure.

The original design allowed for foundation piles to be driven before the installation of the footing boxes. The footing box was to be lowered over the driven piles in a watered condition. With the six, 2.5 m diameter driven piles battered in all directions the pile location tolerances to achieve this would be extremely difficult.

In the revised scheme the 900 ton footing box is preset in the required position and the piles are driven through the box. This guarantees the piles are in the required position relative to the box sleeve.

The original design for the pile to footing box connection required welding of the connector plate in confined space with limited access. Access was limited to the annulus between the outside of the driven pile and the sleeve in the footing box amounting to about 1.3 m of horizontal space.

In the revised installation, plan the sleeve in the footing box was redesigned to provide critical access by moving the welding of the plate to the inside of the pile and interior of the footing box outside the sleeve.

These modifications achieved a successful installation of all footing structures.

ACCESS DREDGING

Along the east shore of San Francisco Bay the accumulation of young bay mud deposits has created very shallow areas. These depths along the existing bridge reduced the allowable marine access for pier construction on the new structure. The owner recognized the need to obtain permits to allow the contractor to dredge materials in those areas.

The initial step in the construction of the bridge piers was to dredge an access causeway (299,000 cm) to provide the necessary water depths for marine equipment. Derrick barges,

utilizing clam shell digging buckets, excavated this material into dump barges. The material was then towed to an offshore location for disposal. (*Figure 1)*



Figure 1

Additional excavation called "glory hole dredging" was also utilized at several of the new pier locations. This dredging was designed to reduce the soil loads on the temporary cofferdams.

COFFERDAM CONSTRUCTION

Twenty of the twenty-eight piers required installation of sheet pile cofferdams. The soft bay mud deposits created difficult conditions to dewater cells without the assistance of typical concrete seals. Cell design depths and size dictated construction of massive supporting wale frames *(Figure 2).*

These frames were preassembled, moved into position and pinned to the sea floor with large diameter support piles. Once the frame was in place, sheet piles were driven to form a complete cofferdam. *(Figure 3)*

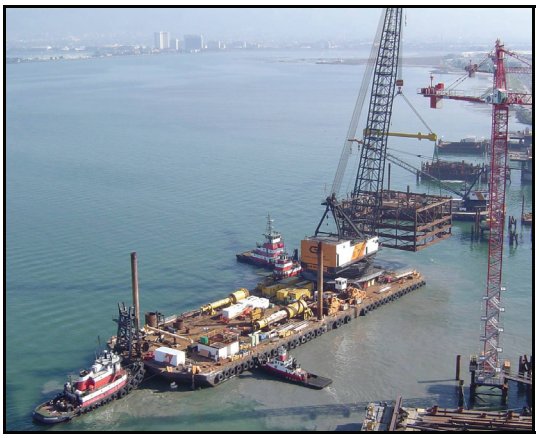


Figure 2

Once the sheets were in place, additional excavation was required to obtain the depths necessary for placement of a gravel bed for box installation. Derrick barges excavated the material which was deposited at offsite dredge disposal locations.

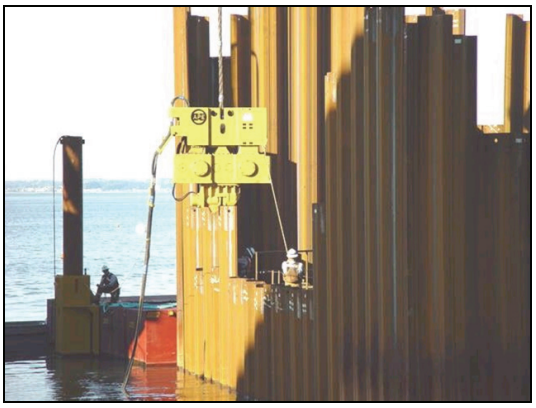


Figure 3

ALTERNATE PIER DESIGN

Eight of the piers, at the west end of the structure, did not require cofferdams. The structure design was modified due to the depth of water in this area. The footing boxes for these piers, which are identical to the other piers, were placed at or above the mean water levels of the bay. A steel frame with piling was installed to act as a cradle to support the footing box. The footing box was then placed in position for installation of large diameter piles.

PREPARATION FOR FOOTING BOX INSTALLATION

Critical design tolerances dictated that the footing box be set precisely in the bottom of the coffer cell relative to elevation and horizontal position.

A number of factors affected the design of the cofferdam, including: soil conditions, water depths, and timing of the cell dewatering. The footing box was an integral part of the cell design and was to act as the lower wale when the cell was dewatered. This demanded that the box be in place and in proper position before the cell was dewatered.

Once the cofferdam was installed a gravel bed was placed underwater to provide a level surface. A gravel screed was designed specifically to obtain the surface tolerance for the box *(Figure 4)*. This gravel surface was used to support the footing box structure.

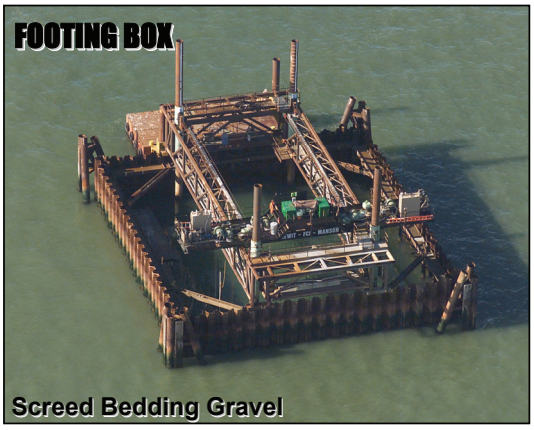


Figure 4

FOOTING BOX INSTALLATION

The footing box is a massive 900 ton steel structure designed to transfer the bridge pier load from the column through the box into the footing piles. Each footing box has six 3.0 m sleeves for driven piles and a center pocket to receive the structures column rebar and concrete for the bridge superstructure. The box is 19.5 m long, 16.0 m wide and 6.5 m tall. *(Figure 5)*

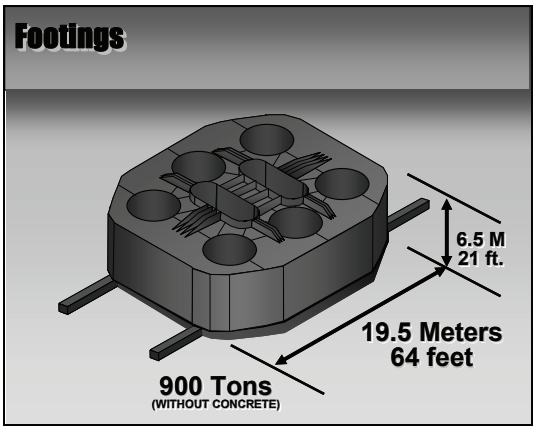


Figure 5

The footing boxes were fabricated at the Kiewit Offshore Facility in Ingleside, Texas and transferred via barge through the Panama Canal and up the coast to San Francisco. *(Figure 6)*

Figure 6

Once the boxes arrived an initial 1.5 m lift of concrete was placed in the box to act as ballast. The ballast created negative buoyancy in the box to assist in final placement in the cofferdam.

The box was then lifted off the transport barge utilizing a catamaran barge specially constructed for placement of the footing box. The catamaran barge moved the box over the cofferdam for final positioning *(Figure 7)*. The box was lowered into the flooded cell and onto the bedding material. The box position was then verified to assure its location met the required tolerances.





Figure 7

Locking fill was then placed between the wall of the cofferdam and the footing box to secure the structure and act as the lower wale for the cofferdam *(Figure 8).*

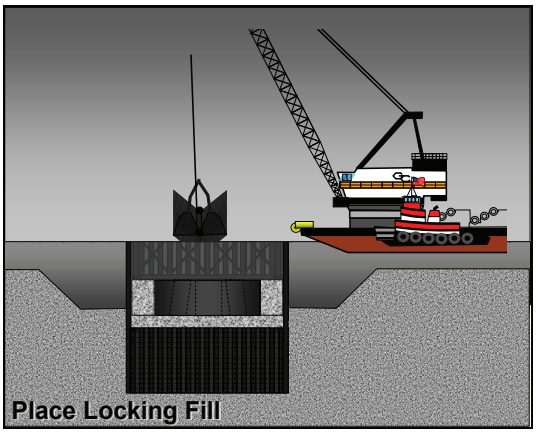


Figure 8

Once the locking fill was placed the cells were ready to be dewatered. Water was drawn down to just below the level of the top of the box. The footing box was then ready to receive the pile template for pile driving *(Figure 9)*.

SUPPORT PILE INSTALLATION

Large diameter piles supporting the fabricated steel boxes were driven several meters into various layers of bay mud. The pile driving operation required a large upper and lower template to provide support in driving the 2.5 m diameter piles.

The overall length of the piles averaged 108 m and piles were driven in two pieces. The template frame was designed to support the upper pile section during the splicing operation, as well as, maintaining the critical driving tolerances. *(Figure 9).*



Figure 9

The Menck 500 and 1700 Hydraulic pile hammers were used to drive the piles to their respective tip elevations. The smaller hammer was utilized for initial driving and the 1700 was used to restart the pile, after splicing, and drive to final tip elevation. All piles were driven within the required tolerances.



Figure 10

Once the pile reached grade it was cut off to meet the proper attitude of the box and the operation to remove the material from inside the pile began. Material was removed from the upper two hundred feet utilizing a digging tool called a “hammer grab”. This process was slow and difficult due to the sloping batter of all piles. A derrick barge was used to excavate and transfer the materials to a barge for disposal.

The inside of the pile was then cleaned and readied to receive a concrete seal plug. Once the bottom of the pile was sealed it was dewatered and prepared for installation of the pile head plate connectors.

DRIVEN PILE TO FOUNDATION BOX CONNECTORS

Attaching the piles to the footing boxes was achieved by inserting shear plates from the driven pile to the sleeve in the footing box.

The sleeves in the footing box were fabricated with 3.5 m slots, ready to receive the 75 mm thick shear connector plates. Before the plate could be inserted alignment of the slot was transferred to the pile and the required cuts were made.

The connector plate was then inserted through the inside of the pile and fed through the slots in the sleeve and pile for final welding *(Figure 11)*.



Figure 11

Welding of the shear plates, utilizing automated welding tools, completed plate installation.

Once all shear plates were installed in the foundation boxes the annulus at this location was grouted and the pile and box filled with the remaining concrete.

CONCLUSION

The modifications of the original design, made during the planning stages of the project, contributed to the constructability of a quality foundation. The ability of the designer, owner, and contractor to recognize the need for these modifications, in the early stages of the project, reduced or eliminated several potential construction problems.

This bridge design included a number of unique features that brought challenges not often seen in bridge construction. One of these features included large diameter piling with lengths not often used in such structures. As a result pile hammers typically used for offshore projects were required to drive these piles. The massive components, included in the foundation, required the largest marine cranes available. Needs also required a catamaran barge to be designed and constructed to handle the massive 900 ton footing boxes.

Despite the unique challenges inherent in this project, foresight in planning and the development of innovative construction techniques led to the successful installation of the bridge foundation for this project.

UNDERWATER PILE HAMMERS

Douglas L. Scaggs, MENCK GmbH, Houston, Texas, USA

Driving piles in under water applications has become more common place over the past twenty years. Where only a water depth reachable with a follower or dewatered cofferdam was the rule in the past, newer technologies developed for the offshore oil and gas industry have made depths of even several thousand feet possible offering new possibilities in foundation design and installation. With the new technology, engineers can now more efficiently design structures by placing foundations optimally thereby reducing weight and cost of the overall structure.

HISTORY

Underwater pile driving, while not an everyday occurrence, has become more commonplace in the last few years. Although there are a few exceptions, driving piles underwater generally required a follower or dewatered cofferdam and was limited to relatively shallow water. Since the late 1980s hammers capable of operating under water have simplified the job dramatically and made the task almost routine.

Before the introduction of enclosed hydraulic hammers, the air operated pile hammer manufacturers experimented with ways of operating their equipment under water. The enclosed air hammers would work under water as long as the exhaust port was vented to the surface. These were used on a few projects; most notably the Richmond - San Rafael Bridge near San Francisco, where modified MKT S-10 air/steam hammers were used to drive 4,000 H-Piles in 60 ft of water. Vulcan Iron Works designed their version of an underwater hammer called the Mariner series, but like the MKT hammers, loss of efficiency, limited market and cost of manufacture kept these from being overly successful. Steel shells, or cocoons, were experimented with enclosing standard open air/steam hammers, but again, they lacked efficiency and were too unreliable to be a market success. It wasn't until hydraulic hammers came into the market that underwater pile driving became more practical. Vulcan Iron Works' Don Warrington also designed an underwater hammer using sea water as the hydraulic fluid, but lack of adequate funding and an undefined market kept his idea from being developed.



Vulcan Mariner Hammer driving H-Piles

With the development of sealed hydraulic hammers, most notably from Menck GmbH of Germany and IHC Hydrohammer of The Netherlands, underwater pile driving became relatively simple. These hammers were developed for the offshore oil industry and were designed to operate in offshore underwater applications. Over the years, they have been proven to be very reliable. The smaller models can be operated either free hanging or leader guided and have provided contractors a very useful tool when underwater foundations are called for. Contractors found they could drive foundation piles in rivers without having to dewater a cofferdam first. In addition to the offshore market, the larger hammers have been successfully used to drive piles for bridges and port installations where the pile tops were below

the water's surface, again without the use of followers. Driven pile-anchored river buoys have become fairly common on the navigable rivers and waterways.

As the vibratory hammer manufacturers converted from electrically driven models to hydraulic, they too found opportunities taking them into underwater applications. Underwater dams reinforced with sheetpile are easily installed with vibratory hammers.



MKT V-35 Vibratory Hammer

HAMMER DESIGN

In order to efficiently drive piles under water, a hammer must be able to manage the water environment. For impact hammers, two things must be considered. First, the ram weight must be free to move in a dry environment. This is accomplished by sealing the hammer shell for shallow applications, and introducing compressed air or nitrogen into the hammer body to keep the water out for deeper conditions. Second, the impact zone, that is the area where the hammer strikes the pile, should be free of water. Otherwise hammer efficiency is compromised. This is done by pumping compressed air into the guide sleeve of the hammer which fits over the pile top, and pushing the level of the water down below the top of the pile. For shallow applications this can be done with standard air compressors able to pump enough air to blow bubbles through relief holes in the pile guide sleeve below the impact zone. For deeper applications, higher air pressures are required to overcome the increased hydrostatic pressures. Sensors in the pile sleeve tell the operator what air pressure is sufficient to keep the water level below the pile top.

For vibratory hammers, care must be taken to insure the transmission case is sealed to keep out water. This may be as simple as capping the breather vent, however the manufacturer should be contacted for the proper procedures. Adding compressed air to the transmission, or exciter case, may be required if the water depth is too deep for the standard seals and gaskets usually present in vibratory transmissions. The pressure must be increased as the hammer goes deeper, but slowly relieved as the hammer is brought back to the water's surface. Otherwise there is a likelihood of putting the seals under too much pressure and causing them to fail.

Whether a vibratory hammer or an impact hammer is used under water, the contractor must be sure that manufacturers' recommendations are strictly followed or damage costing several thousand dollars may result. However it should be pointed out that proper planning and preparation makes this relatively easy.

APPLICATION GUIDELINES

For monitoring what is going on under water, there are a couple of basic methods. Periodic checking by a diver or some type of remotely operated camera may be necessary. Another possibility is to attach an extension with reference markings to the hammer body long enough to reach the water's surface when the pile is at full penetration. Of course if the water is too deep, the use of a remote camera may be the only reliable method available. Modern hydraulic impact hammers have monitoring systems that can tell the operator how hard the hammer is hitting, blow frequency, and general information about the hammer operation. The more sophisticated systems can even provide water depth information, pile verticality, orientation, and pile penetration depth.

HAMMER SELECTION

There is a wide range of hammers available which have underwater capability. Most modern day vibratory hammers can go to shallow depths with very little preparation and some have been used in depths of a few hundred feet. The hydraulic impact hammers suitable for underwater driving are sealed units and are available with rated energies from just a few thousand foot pounds to over two million. (see

chart at end of paper) For depths of several hundred feet, conventional operation with a diesel powered power pack is adequate to operate the hammer. For deeper applications such as is the case in many offshore oil and gas production facility installations, Menck's patented electrically driven underwater power pack allows their hydraulic hammers to operate in several thousand feet of water with piles being driven recently in depths over 6000 ft.

Energy ratings are generally not affected in waters up to a few hundred feet in depth as long as the manufacturers' guidelines are followed. In fact, MENCK claims a reduction of less than 10% even when depths reach 3,300 ft (1,000 m).



MENCK MHU 500T with Underwater Power Pack

Virtually any pile that can be driven on land can be driven under water. Vibratory hammers can install most any low displacement piles including sheetpile, open end pipe piles, H-piles and even timber piles in some soils. Hydraulic impact hammers can install most any pile type under water with the exception of sheetpile with very little difficulty. Sheetpile can be driven with an underwater impact hammer, but it requires a mandrel and is generally not very practical. One exception to this rule is the Dawson hydraulic hammer produced by Dawson Construction Plant, Ltd. in the UK. With minimal modification, the double acting Dawson hammers can successfully drive steel sheetpile under water because of their drive head design. In fact, Dawson hammers have successfully operated in water up to 200 ft (60 m).



Dawson HPH 2400

Vibratory hammers can also be used for extracting piles under water. Just as is the case on dry land, if the pile top is such that the hammer can get a solid grip, a vibratory hammer probably offers the best chance of extracting it without jetting which is sometimes frowned upon for environmental reasons. These hammers are very useful when setting and removing pile templates for example.

CONCLUSION

With the exception of deepwater offshore pile driving, the latest hammer technologies have put underwater pile driving within the reach of most any contractor. However, before assumptions are made as to the suitability of a particular hammer to operate under water, the manufacturer or dealer should be contacted. A few simple steps can make all of the difference in how well the project goes, and can save many thousands of dollars in repairs caused by improper preparation. Contractors should not turn a job down just because it may have piles to be driven underwater, but they should always be careful to select a hammer properly prepared to do the work and be sure their methods are well thought out.

ACKNOWLEDGMENTS

Photographs courtesy of:

Dawson Construction Plant Ltd
Milton Keynes, England

MENCK GmbH
Kaltenkirchen, Germany

MKT Manufacturing, Inc.
St. Louis, MO, USA

Hammer Data from manufacturers' published brochures:

Dawson Construction Plant Ltd
Milton Keynes, England

IHC Hydrohammer BV
Kinderdijk, Holland

MENCK GmbH
Kaltenkirchen, Germany

Underwater hammers

Manufacturer	Model	Rated energy - ft.lbs.*	Weight - lbs. in air**
DAWSON	HPH1200	8,680	6,600
DAWSON	HPH1800	13,750	9,350
DAWSON	HPH2400	17,360	13,227
IHC	S-30	22,140	8,595
IHC	S-35	25,830	15,650
IHC	S-40	29,520	10,140
DAWSON	HPH4500	32,560	19,000
DAWSON	HPH6500	47,000	23,300
IHC	S-70	51,660	18,295
IHC	S-90	66,420	21,160
DAWSON	HPH10K	73,750	33,000
DAWSON	HPH12K	88,500	37,400
IHC	S-120	88,560	31,520
DAWSON	HPH15K	110,600	41,800
IHC	S-150	110,700	35,705
MENCK	MHU135T	110,700	46,505
IHC	S-200	147,600	54,000
MENCK	MHU200T	169,740	55,980
IHC	S-280	206,640	63,915
MENCK	MHU270T	225,090	67,885
MENCK	MHU400T	324,720	97,415
IHC	S-500	369,000	121,320
MENCK	MHU500T	405,900	119,455
IHC	S-600	442,800	141,055
MENCK	MHU600T	487,080	147,670
IHC	S-750	553,500	176,320
MENCK	MHU720T	590,400	175,440
IHC	S-900	664,200	275,500
MENCK	MHU900T	738,000	230,500
IHC	S-1200	885,600	304,150
MENCK	MHU1200S	885,600	262,700
MENCK	MHU1700S	1,276,750	418,760
IHC	S-1800	1,328,400	473,560
MENCK	MHU1900S	1,424,340	347,350
MENCK	MHU2100S	1,579,000	473,860
IHC	S-2300	1,697,400	573,040
MENCK	MHU2400S	1,793,300	528,960
MENCK	MHU2700S	1,992,600	562,000
MENCK	MHU3000S	2,250,900	617,120

* Energy ratings at sea level

** Hammer weights are shown without attachments. Consult manufacturer for applicable weights

DIAMETER EFFECTS ON p-y CURVES

Ignatius P.O. Lam, Earth Mechanics, Inc., Fountain Valley, CA. USA

This paper presents information on design analyses of large diameter piles using conventional p-y curves as recommended by the American Petroleum Institute (API RP2A, 1993). API RP2A adopted the soft clay criterion developed by Matlock (Matlock, 1970) based on 12.75-inch piles. API RP2A also adopted the API sand criteria originally introduced by Reese, Cox, and Koop (Reese et. al., 1974) based on 24-inch piles. Since Matlock and Reese published their original papers, there have been several publications recommending changes to their p-y criteria, especially regarding the need to adjust the Matlock p-y curves for pile diameter effects. The following sections attempt to clarify the issue of diameter effects on p-y curves.

REVIEW OF THE API p-y CURVE PROCEDURES

It would be appropriate to review the API RP2A p-y curve procedures and to clarify some of the definitions defining p-y curves. Figure 1 summarizes the API benchmark static p-y curve procedures for sands and clays. The sand p-y curve method was originally developed by Reese et al. (1974). Subsequently, API sponsored a study conducted by O'Neill and Murchison, (1983) which resulted in the currently described sand p-y criterion. The O'Neill and Murchison's sand p-y curve procedure is merely intended to simplify the original Reese's procedure and not meant to introduce fundamental changes to the Reese's p-y criteria. The proposed change largely relates to changing the hyperbolic curve shape from the parabolic curve shape originally used by Reese.

Otherwise, the O'Neill and Murchison's procedure is identical to the Reese's p-y procedure. The two anchoring parameters for the hyperbolic curve: (1) the initial tangent stiffness and (2) the ultimate capacity are identical to Reese's original recommendations. Therefore, this paper will continue to refer to the API sand p-y curve as the Reese's p-y curve procedure in this paper.

The definition defining soil reaction, p on the p-y curves varied in the literature and has been a source of confusion. For example, in API RP2A, there is an inconsistency in the definition for p between referencing the Reese's sand versus the Matlock's clay p-y procedure. In discussing Reese's sand p-y criteria, API RP2A defined p as the integrated soil reaction over the pile diameter, similar to our definition in this paper and p has the unit FL^{-1}. However, in referencing Matlock's soft clay p-y criteria, the API RP2A changed the definition for p to a pressure unit FL^{-2}. Such an inconsistency in defining p between sand and clay p-y procedures can be a source of confusion. This paper will define p similarly for both sands and clays. The unit will be FL^{-1} which is the soil pressure integrated over the entire pile diameter per unit length along the axial (vertical) dimension of the pile. As shown in Figure 1, the stiffness of the p-y curve, which is the ratio of p to deflection y, is defined as the modulus of subgrade reaction, E_s with unit of FL^{-2}. The modulus of subgrade reaction, E_s is the foundation model commonly adopted for pile design analysis modeling the soil support by discrete springs, commonly referred to as Winkler springs. The p-y curve is in fact a nonlinear Winkler spring model. The modulus of subgrade reaction E_s has been correlated to the soil model based on theory of elasticity, characterized by the Young's modulus of soil E_{soil}. Both the Winkler spring subgrade E_s and elasticity Young's modulus E_{soil} have the same unit in FL^{-2}. Further discussions on relations between the two soil moduli will be presented later.

COMMENTS ON THE REESE'S SAND p-y CURVE PROCEDURE

As shown in Figure 1 (a), the initial tangent modulus in the Reese's sand p-y curve is calculated from a coefficient of variation in subgrade modulus with depth, referred to as k which has a unit of FL^{-3}. This coefficient, after multiplying by depth z, gives rise to the

subgrade modulus E_s. In Reese's sand p-y curve formulation, the subgrade modulus E_s is

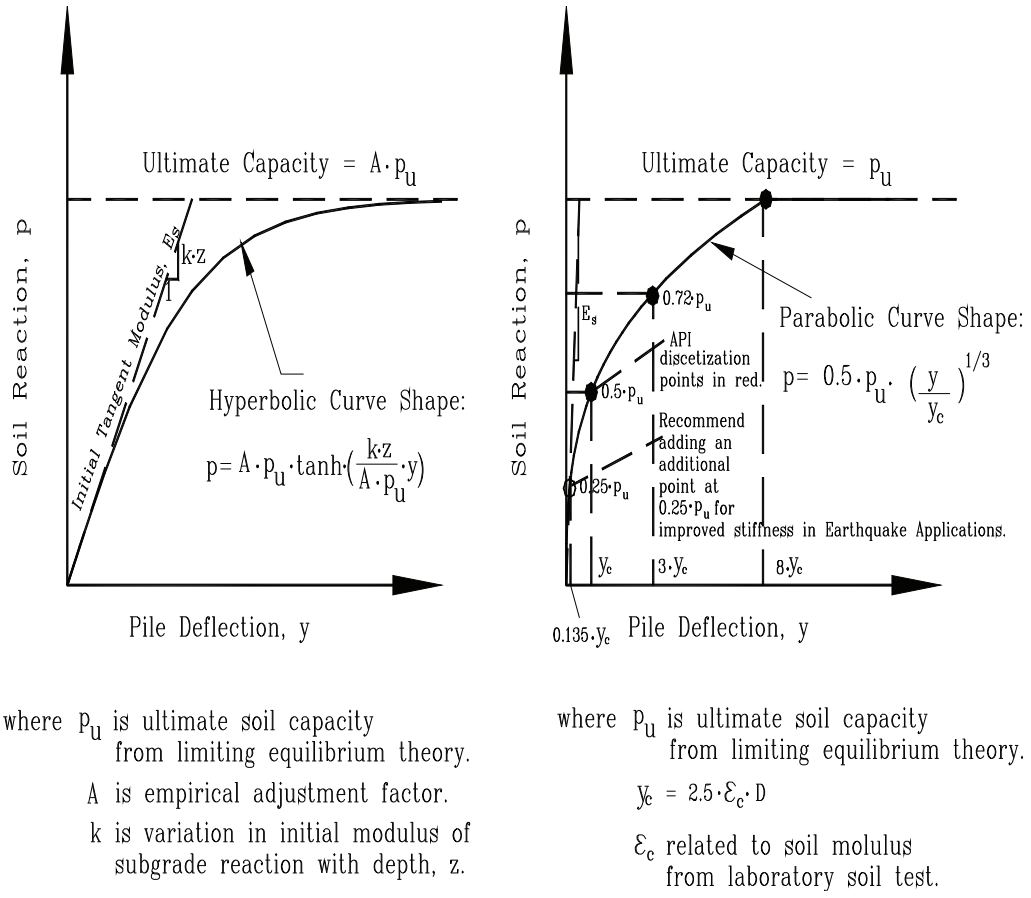


Figure 1: Review of API p-y Criteria for Piles

assumed to be independent of pile diameter, D. The ultimate capacity of the p-y curve (p_u) is primarily related to the shear strength, the unit weight and the depth of the p-y curve and will be roughly proportional to diameter. Strictly speaking, the statement that the p-y curve stiffness is independent of pile diameter is only true for the initial tangent modulus of the p-y curve. At any non-zero deflection values, the secant stiffness will be dependent on both the initial tangent modulus and the p_u value which is strongly dependent on diameter. Figure 2 illustrates variation of typical p-y curves with diameter based on Reese's static p-y procedure at a 5-ft depth for a 40-degree sand friction angle. It is evident from the figure that the statement that the subgrade modulus is independent of pile diameters applies to only the region at a very small deflection level (say at less than 0.02 inch) where the prescribed initial tangent modulus plays a stronger influence on the resultant p-y curve stiffness. However, even at a relatively small deflection value, say at deflection exceeding 0.1 inch, the resultant secant modulus from the Reese's p-y curve procedure would be diameter dependent due to the role p_u plays in the resultant p-y stiffness.

COMMENTS ON THE MATLOCK'S CLAY p-y CURVE PROCEDURE

As shown in Figure 1 (b), the clay p-y curve procedure (proposed by Matlock, 1970) makes use of a parabolic p-y curve shape. Parallel to the O'Neil and Murchison study for sand, API also sponsored a study for clay leading to an O'Neill and Gazioglu (1984) report. This report reviewed the Matlock soft clay criterion along with other available stiff clay p-y criteria and also attempted to reconcile the so-called pile diameter effects and eventually recommended an alternate clay p-y procedure referred to as Integrated Clay p-y procedure. However, to-date, API has not adopted the proposed changes by O'Neil and Gazioglu and the

Matlock clay p-y criteria remains the API recommended clay p-y procedure. The report also provided some discussions on pile diameter effects and we will provide some comments on the subject.

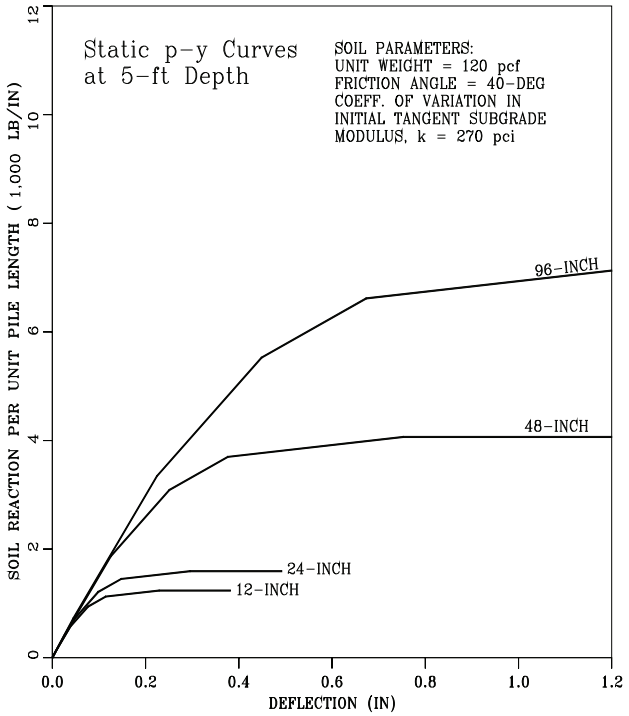


Figure 2: Static Sand p-y Curves for Various Diameters

Because Matlock has elected to make use of a parabolic curve shape, the theoretical initial tangent modulus at zero deflection will be infinite. However, in practice, pile analyses are conducted using computer programs which require inputting p-y curves by digitized numerical arrays and the initial tangent modulus is effectively defined by the first discretization point for the parabolic curve shape. The solid circles on the clay p-y curve shown in Figure 1(b) reflect the tabulation of the discrete parabolic clay p-y curve shape currently in API-RP2A. As seen from the figure, the first discrete point in the API code is the coordinate to half the ultimate capacity (i.e. p-y curve coordinate at y = y_c and p = 0.5 p_u). The fact that the theoretical initial tangent modulus be infinite for a clay p-y curve has often been criticized. However, for offshore soft clay sites, even at relatively small design loads, pile deflections at the significant soil-structure interaction zones (say the upper 10 pile diameters) will involve deflections above the so called initial tangent modulus range. The shortcoming in the theoretical infinite tangent modulus problem in the p-y criteria rarely leads to real problems in offshore wave loading design.

Interest in earthquake engineering applications often led to attempts to formulate the initial tangent p-y stiffness from low-strain shear modulus used for wave propagation site response analyses. However, from the author's experience, such efforts may be counter productive. This is partly because laterally loaded piles derive most of their soil resistance from the upper portion of the pile (say upper 10 pile diameters). At such depths, it will be difficult to obtain reliable soil modulus data, especially from direct shear wave velocity measurements. Also, from several soil-structure interaction experiments including full-scale and small model centrifuge pile load tests, or from embedded abutment-wall or bridge footing pile-cap tests sponsored by FHWA and various State Departments of Transportation, the initial tangent SSI stiffness observed from these experiments are usually much smaller than those implied from theoretical elasticity solutions with soil modulus based on low-strain shear wave velocity data. Discrepancies between experimental data and elasticity theories on initial tangent SSI modules based on low-strain soil modules in soil dynamics literature can be as much as a factor of 10. From the author's experience, the shortcoming of the infinite initial tangent modulus in the soft clay p-y criterion rarely poses serious practical problems. However, there is some danger in relying on elasticity theory using overly stiff soil modulus values adopted for wave propagation analysis.

From review of empirical pile, abutment wall and pile cap data, the SSI initial tangent modulus would be better based on soil modulus measurements from conventional static laboratory tests as opposed to the tendency using geophysical shear wave velocity measurements practiced in earthquake engineering. Based on pile-load test data, O'Neil and Gazioglu (1984) backfitted some typical soil modulus values for estimating the initial p-y stiffnesses and proposed an average E_{soil}/c ratio of about 40. Such as Young's modulus to undrained shear strength ratio corresponds to a much softer stiffness than typically assumed based on low-strain shear modulus used for site response analyses, with

typical relationship of E_{soil}/c ratio bigger than 1,000.

Furthermore, it should be mentioned that there is a tremendous range of scatter in literature information for estimating soil modulus values. Discrepancies arise from variations from the types of test: (1) insitu geophysical measurements, (2) soil dynamics soil sample tests and (3) static soil sample tests. Therefore, basing p-y curve construction methods on soil modulus directly can pose practical problems in design. This might be some of the factors that prompted Matlock to make use of the soil strain e_c occurring at one-half the maximum stress in a triaxial stress-strain curve to anchor the effective p-y stiffness. Generally, there is less uncertainty and less variations in literature correlations of e_c for a given clay soil (i.e. clay consistency). In Figure 1, some suggestion are offered for discretizing the parabolic p-y curve shape, using an additional discretization point in addition to the discretization scheme referenced in API RP2A. This additional point, denoted by the open circle, on the parabolic curve shape occurs at 0.25 p_u corresponding to deflection y = 0.135 y_c. From our experience, for typical soft clay profiles, the coordinate at this discretization point will result in an initial subgrade modulus E_s (E_s . E_{soil} soil Young's modulus) and will imply a more reasonable implied soil modulus value and be closer to the E_{soil}/c ratio suggested by the O'Neill and Gazioglu discussed earlier.

REVIEW OF TERZAGHI'S CLASSICAL SUBGRADE MODULUS THEORY

From previous discussions, it can be observed that the Reese's p-y criterion included concepts to define the initial tangent modulus of the p-y curve and intentionally defined this initial tangent modulus to be independent of pile diameter. The Matlock p-y criterion made no attempt to provide a theoretical basis for the initial tangent modulus and from the author's knowledge, Matlock relied purely on the first discrete point of the digital p-y curve shape for the implied initial tangent stiffness, but concluded that the parabolic curve shape formulation provided the best fit to empirical pile load test data.

However, from prior discussions and the illustration in Figure 2, it is obvious that that the implication of the elastic stiffness being independent of diameter would apply to only a small deflection range. Beyond this range, the nonlinear p-y curve formulation would result in diameter dependent p-y stiffnesses. In reading the original papers by Matlock and Reese, it is clear that both the Matlock and Reese p-y criteria followed the classical concept of modulus of subgrade reaction originally proposed by Terzaghi (Terzaghi and Peck, 1948) and Skempton (1955) in extrapolating smaller pile data to prototype design conditions, including adjustments for size effects.

The following provide some review of basic concepts in the modulus of subgrade reaction originated by Terzaghi and Peck (1948), and provide some explanation on why low-strain elastic foundation stiffness is independent of pile diameters and lastly procedures to extrapolate for size effects. Figure 3 discusses some of the reasoning on why the elastic subgrade modulus be independent of pile diameters. The figure considers the effective stiffness of two footings with size B and nB loaded to an equal vertical pressure q. One can assume without serious error that only stresses greater than a certain value, say 0.2q, produce any significant strains in the soil. The soil that is strained to this level lies within the stress bulbs shown in the figure. One may further simplify the problem by replacing the area inside the stress bulb with a rectangle whose dimensions are B and D. For the footing whose width is nB, the size of the stress bulb and rectangle is proportionally larger, as shown in the figure. If the soil modulus is constant with depth, the settlement r for the two footings can be approximated by the following equations:

$r_1 = Cq \bullet D / M$ $\qquad$ $r_2 = Cq \bullet n \bullet D / M$

The total integrated force loading the two footings are also proportional to the size of the footing as follows:

$F_1 = q \bullet B$ $\qquad$ $F_1 = q \bullet n \bullet B$

The resultant stiffness would be the ratio of the load to the settlement, and from the above two equations, the size parameter n will cancel out and the stiffness would become constant and identical to each other, independent of the size of the footing.

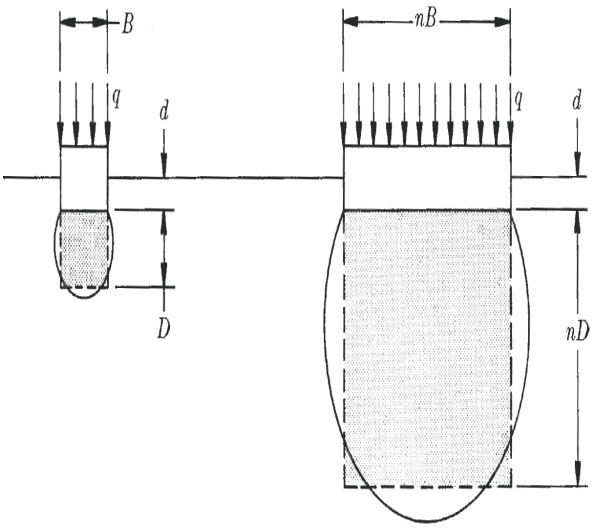


Figure 3: Schematics on Subgrade Stiffness based on Elastic Analysis

The above concept, based on elasticity theory, suggesting that the effective stiffness of a foundation supported by a soil medium be independent on size led Reese to the formulation that the initial tangent subgrade stiffness be independent of pile diameter.

Terzaghi and Peck also extended their subgrade modulus theory to the nonlinear range and provided recommendations on how to extrapolate settlement data from standard 1-ft by 1-ft plate load test to designing footings of much larger sizes. Several forms of equations were developed for extrapolation of smaller plate test data to larger sizes for several combinations of foundation configuration and soil stiffness profiles. Terzaghi's theory of Modulus of Subgrade Reaction has been proven over many years of application, and verified by numerous researchers both by analyses as well as by experiments. Skempton (1951) extended the Terzaghi's modulus of subgrade reaction theory to strip footings on clays. The y_c equation adopted by Matlock was based on work by Skempton.

The above discussions are intended to clarify some background in the Matlock and Reese's original p-y theories, especially, that they have a sound rational framework to account for size effects.

CORRELATING SUBGRADE STIFFNESS E_s WITH ELASTIC SOIL MODULUS

Confirmation in the above discussed theory that the soil elastic subgrade stiffness for piles be independent of diameter can also be observed by Vesic's classical solution (1961). Vesic's solution also formed the most widely cited procedure to estimate the Winkler spring stiffness, E_s, from elastic modulus parameters of soils (E_{soil} n_{soil}) as shown in the following equation.

$$E_s = \frac{0.65 E_{soil}}{1-\nu_{soil}^2} \sqrt[12]{\frac{E_{soil} D^4}{EI}} \qquad (1)$$

where D is the width of the beam, or pile diameter, and EI is the bending stiffness of the pile.

For typical materials and pile properties, the terms involved in the 12th root in the above equation will be close to unity. It is common practice to approximate the above equation by the following.

$$E_s \approx \frac{0.65 E_{soil}}{1-\nu_{soil}^2} \qquad (2)$$

and for a Poisson ratio closest to 0.5 for incompressible soils (a good approximation for undrained saturated offshore soils), the above equation can further be simplified by the more simple expression.

$$E_s \approx E_{soil} \qquad (3)$$

The above equation has been widely used by geotechnical engineers to estimate the Winkler spring subgrade modulus E_s from continuum soil modulus E_{soil} and Poisson ratio n_{soil}. It can be observed that the elastic subgrade modulus parameter E_s is independent of the diameter, D.

Confirmation in the above discussed theories that the initial subgrade stiffness be independent of pile diameter has also been verified by numerous cases of experimental data, including field plate load tests (Terzaghi and Peck, 1948) and more recently by Ashford from UCSD using full-scale pile load test data (Ashford and Juirnarongrit, 2003).

UNDERLYING THEORIES OF MATLOCK AND REESE'S p-y CRITERIA

The above discussions attempt to clarify some of the underlying background theory in the Matlock's and Reese's p-y curve procedure, especially the underlying theory to account for pile diameter effects. The following lists some of the key points discussed in prior sections:

1. First of all, it is a misnomer to state that the Reese and Matlock p-y curves are independent of pile diameter. Diameter effects are inherent in the Reese and Matlock p-y curve theories, especially for the ultimate capacity on the p-y curves. It may only be valid to state that the initial tangent p-y stiffness at very small deflection range in the Reese's sand p-y curve criterion is independent of pile diameter.

2. Secondly, the concept that the initial elastic subgrade modulus be independent of pile diameter is a well founded concept, supported by numerous publications. Formulation of the initial slope of p-y curves and then extrapolations of nonlinear load-deflection data from small model tests to larger foundation systems have been well developed, based on proven theories, collectively referred to as the modulus of subgrade reaction, originated by Terzaghi. There has been a long history of verifications and developments contributing to our basic understanding for adjustment for size effects using smaller foundation load-deflection test data. The Terzaghi's modulus of subgrade reaction has been advanced for designing various foundation types (e.g. square footings versus long strip footings which are also applicable for pile design). Size effect extrapolation procedures have been developed considering various forms of soil modulus profiles, including constant modulus with depth and soil modulus increasing with depth, etc.). Matlock and Reese are well versed in these background theories and their proposed p-y curves included well founded principals for size effect considerations.

LITERATURE PROMOTING DIAMETER DEPENDENT p-y STIFFNESS

Since Reese and Matlock proposed the API p-y curve criteria, there are occasional publications commenting that the API p-y curve criteria were based on smaller pile diameters, and that there are apparent pile diameter effects and stiffer/stronger p-y curves should be used for designing these large offshore piles, especially for the Matlock's clay p-y procedure.

These publications are reviewed in the following section and an attempt is made to reconcile evidences presented in these publications.

WORK OF STEVENS AND AUDIBERT

Stevens and Audibert (1979) presented a paper, entitled "Re-Examination of p-y Curve Formulations" which suggested that there is pile diameter effect and the Matlock soft clay p-y curve criteria should be modified in design. Stevens and Audibert compiled seven cases of full-scale pile load test data in clays, with pile diameters ranging from 11 inches to 59 inches. The paper presented hindsight analyses using the Matlock's soft clay p-y curves and compared their solutions to the compiled test data as shown in Figure 4.

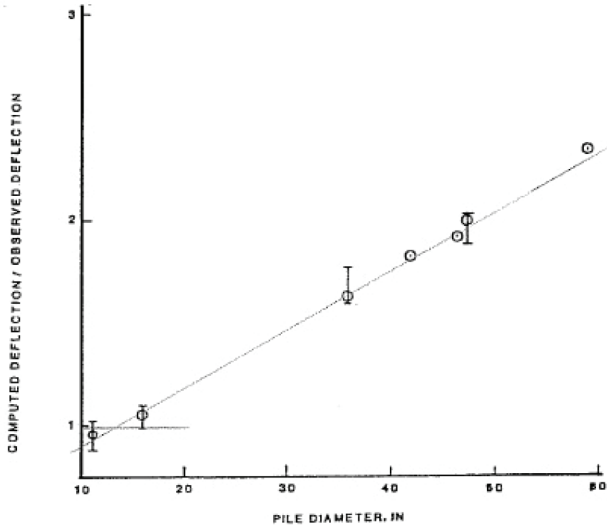


Figure 4: Comparison of Predictions based on Matlock p-y criterion with Test Data (after Stevens and Audibert, 1979)

From the above comparison, Stevens and Audibert concluded that there is an apparent pile diameter effect on p-y curves and they proposed some modifications to the Matlock p-y curve procedure as listed below:

1. y_c coefficient used to scale the deflection array in p-y curves be changed from the Matlock's equation of :

   $y_c = 2.5 \cdot e_{50} \cdot D$ to $y_c = 8.9 \cdot e_{50} \cdot D^{0.5}$.

2. Calculate the ultimate capacity N_p coefficient on the p-y curves from a depth-dependent function shown in Figure 5.

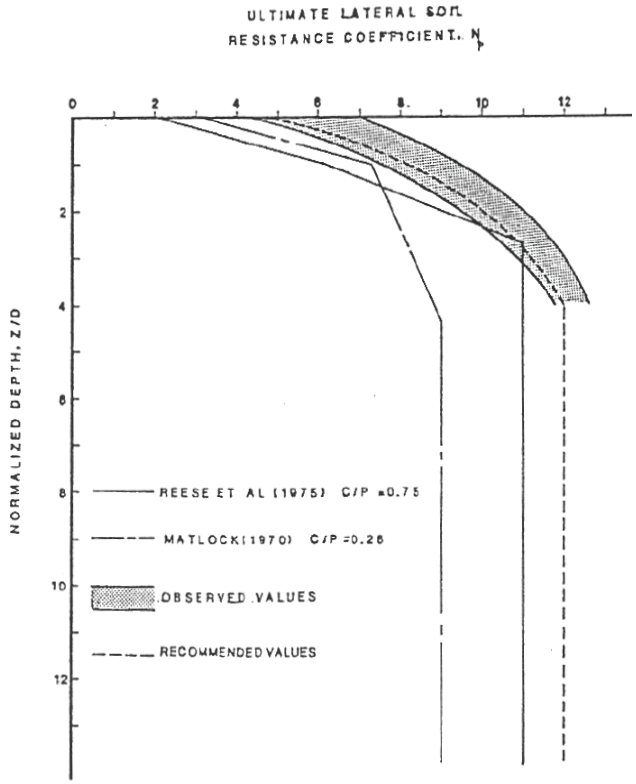


Figure 5: Ultimate Capacity Factor for Laterally Loaded Piles in Clay (after Stevens and Audibert, 1979)

COMMENTS ON THE STEVENS AND AUDIBERT'S PAPER

The major problem in the Stevens and Audibert's paper relates to their proposed equation for y_c. The Matlock's y_c formulation has been based on Skempton's work involving a comprehensive research program combining elasticity theory, ultimate strength methods, and laboratory soil property to estimate the short-time load-settlement characteristics of buried strip footings in clay soils. Skempton's work can be considered an extension of the Terzaghi's modulus of subgrade reaction theory for strip footings in clays, and the form of the equation is at least dimensionally correct in developing the y_c coefficient (i.e. the p-y curve procedure will generate consistent p-y curves independent of units used to develop the p-y curves). Steven's and Audibert's proposed y_c, however, has little theoretical support, and is based purely on several pile load tests. Whereas, the database is probably real, the paper did not provide any mechanistic reasons for the observed diameter effect. The fact that the proposed equation is not dimensionally correct leads to questions in the validity of the Stevens and Audibert y_c equation. Mechanistic reasoning for the apparent diameter effect is offered in later sections.

Figure 6 presents a comparison of y_c between Matlock's and Stevens and Audibert's p-y curve procedures. The figure reveals that y_c by the Matlock's method is typically about 2 to 3 times larger than the Steven's and Audibert's procedure. The Stevens and Audibert's proposal for y_c on p-y curves can be implemented by scaling the Matlock's p-y curve deflections by the appropriate y-multiplier. It can also be observed from Figure 5, that Stevens and Audibert proposed modification of the N_p from about 5 (as compared to 3 from Matlock) at a zero depth to about 12 (versus 9 from Matlock) at depth. The change would be about 70% at the most important ground surface zone to about 30% at depth. From the author's experience, modification of p-y curves by a p-multiplier of 1.7 will influence the overall pile solution to a far greater extent than a corresponding variation in the y-multiplier of say 0.4. Hence, it is apparent that Stevens and Audibert's proposed changes in the N_p formulation would be far more significant than their proposed changes in the y_c equation.

The Stevens and Audibert's proposed bearing capacity factor N_p is less problematic from theoretical reasoning. From the author's knowledge, the deviation between Audibert's proposed N_p with the Matlock's N_p is well within the range of uncertainty and can be easily accounted for by variation in the assumptions in the limiting equilibrium solutions developing the N_p relationship. Limiting equilibrium analysis forms the basis of most of the bearing capacity factors in classical soil mechanics, including the N_p in p-y curve theories. The analysis process involves making assumptions of the failure mechanism (failure surfaces) and then solving

for the implied soil capacity based on the assumed soil shear strength over the failure surface. The correct solution typically involves searching for the minimum capacity implied by various failure mechanisms. Any errors in the assumed failure surface (e.g. planar wedge failure surface versus log-spiral mechanism) tend to result in an overestimate of the bearing capacity factor N_p.

O'Neill and Gazioglu (1984) stated that it is easy to overestimate the bearing capacity factor N_p. However, our point of view is that the range of increase in the N_p factor proposed by Steven's and Audibert over the Matlock's proposal can be valid. The N_p value of 3 proposed by Matlock at zero depth suggests that the Matlock's N_p is based on limiting equilibrium solution for a smooth pile-soil interface. In reality, for the first loading cycle, after consolidation of soils around the pile, there is likely some adhesion effect of the clay on the pile wall, which can justify a higher soil resistance bearing capacity factor N_p. From limiting equilibrium solution for the simpler plane strain passive pressure problem of a rigid wall pushing toward a soil mass, a fully bonded (i.e. full soil adhesion factor) wall-soil surface will imply a 50% increase in the passive pressure capacity than a perfectly smooth wall-soil interface assumption. For a smooth wall case, the solution is reduced to the classical Rankine's equation solution.

However, it needs to be pointed out that the N_p profile suggested by Stevens and Audibert, was derived apparently for a specific shear strength profile of the clay. Stevens and Audibert did not clarify the shear strength profile they have assumed leading to the proposed N_p versus depth relationship, nor did they offer a comprehensive framework for developing N_p for varying shear strength profiles (e.g. linearly increasing shear strength with depth profile commonly found for offshore normally consolidated clay sites, or constant shear strength profile for stiff clay sites). It is also noteworthy that the Matlock soft clay p-y curve procedure included comprehensive basis for determining the governing bearing capacity factor, reflecting the failure mechanism transitioning from heaving soil wedge at shallow depth transitioning to lateral flow of soil around the pile at deeper depths. In a nutshell, the Matlock's soft clay p-y criterion is a more complete and a technically superior method for developing p-y curves for design.

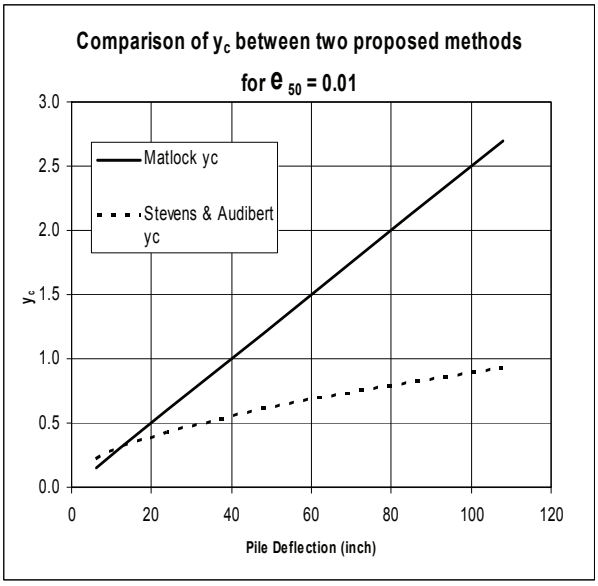


Figure 6: Comparison of Y_c between Matlock and Steven & Audibert

WORK OF O'NEILL AND GAZIOGLU

Following the Stevens and Audibert paper, O'Neill and Gazioglu also conducted a comprehensive review of the Matlock's soft clay p-y curve procedure as well as comparing the Matlock soft clay procedure to some other Reese's stiff clay p-y curve methods. In the O'Neill and Gazioglu study (1984), they also cited the so-called diameter effect and proposed their own modifications for the p-y curve method and referred their proposed method as the Integrated Clay Criteria. Their proposed changes are highlighted below:

1. O'Neill and Gazioglu proposed an even more complex equation than the one proposed by Stevens and Audibert for the y_c equation as follows.

$$y_c = A \bullet e_{50} \bullet D^{0.5} \bullet \left(\frac{EI}{E_{soil}}\right)^{0.125} \qquad (4)$$

2. However, they proposed a bearing capacity factor N_p that is remarkably similar to the original Matlock's formulation, with N_p increasing from 3 at a zero depth to an ultimate value of 9 below the critical depth where the failure mechanism changed to horizontal flow failure of soil around the pile. As mentioned earlier, they commented that there is danger in overpredictions in the N_p factor based solely on theoretical

solutions due to oversimplification in the gapping phenomenon in actual field conditions.

COMMENTS ON O'NEILL AND GAZIOGLU REPORT

Review of the O'Neill and Gazioglu API report suggested that much of the change in the so called Integrated Clay p-y curve procedure relates to changing to a rather complex y_c equation. O'Neill and Gazioglu stated that their y_c equation is dimensionally correct. Apparently the motivation in their y_c equation was intended to fix the dimensional problem stated by Steven's and Audibert in their y_c equation. It can be observed from Equation (4) that for a solid pile, the moment of inertia I will be proportional to diameter D to the fourth power (i.e. I % D^4). The 4^{th} power of D when operated by the 0.125 power explicit in the equation will give rise to a term of $D^{0.5}$, which in addition to the existing $D^{0.5}$ explicit in the O'Neill and Gazioglu's y_c equation, will lead to a y_c being directly proportional to diameter D, similar to what Matlock has proposed. It is interesting that in the O'Neill and Gazioglu's attempt to derive a dimensionally correct y_c, they might have unintentionally verified that the Matlock's formulation for y_c is dimensionally correct.

The O'Neill's and Gazioglu y_c formation can be traced back to a specific solution of pile embedded in an elastic half space. It is apparent that there are numerous hidden limiting assumptions implicit in the theoretical solution, including that the pile in the analysis is a solid pile. It is obvious that this is the only condition when the proposed y_c would become dimensionally correct. Also, there must be some limitations in the assumed variation in the soil modulus profile implicit in the solution (e.g. whether E_{soil} be constant or be increasing from linearly with depth). If the actual design problem deviates from the assumed conditions implicit in the elastic half space solution, the proposed y_c theory will break down. It is evident that the proposed y_c equation will become dimensionally incorrect for typical thin-wall hollow tubular offshore pipe piles. Also, the procedure requires estimating Young's modulus which can introduce unnecessary complexity in applications as compared to basing the y_c on e_{50} in the Matlock's and the Stevens and Audibert's y_c equations.

OTHER PUBLICATIONS ON DIAMETER EFFECTS

Other than the previously cited publications, observations that the overall pile-soil stiffness will increase as a function of pile diameter have also been cited in other literatures. Carter (1984) and Ling (1988), in reviewing pile load test data for various diameter piles (ranging from 3-inch to 3-ft diameters), found that the modulus of subgrade reaction, E_s increases for larger diameter piles. Hence, they proposed to modify the Vesic's subgrade modulus equation (Equations 2 and 3) based on the following equation:

$$E_{s2} = E_{s1} \frac{B_2}{B_1} \qquad (5)$$

where B_2 is the beam width for design and B_1 is the beam width from the reference test condition with measured subgrade stiffness E_{s1}. It should be noted that Carter's and Ling's recommendations are in a context of analysis using linear Winkler spring model as oppose to the nonlinear Winkler spring p-y curve method.

REASONS FOR DIAMETER EFFECTS IN PAST PILE LOAD TESTS

Despite the above discussions pointing out some shortcomings in suggested diameter effect theories, it is valid to ask the question why is there consistent observations of higher apparent p-y stiffnesses for larger diameter piles in prior pile load tests in the cited literatures.

Lam and Martin (1986) has pointed out that the observed pile diameter effects might be related to the fact that past load test data are predominantly free-head pile tests. For this free-head loading condition, there is a significant pile head rotation, which can mobilize additional modes of soil resistance in addition to the theoretical p-y curves of simple lateral translation of the pile. Some of the additional modes of resistance are schematically shown in Figure 7. The additional rotational component of soil stiffness increases with pile diameter and could be the cause for the apparent diameter effect of soil resistance beyond the simple lateral p-y curve resistance.

In fact, the electric and power industry (Davidson, 1982) has been practicing pile analysis making use of sources of soil

resistances beyond those from p-y curves, including moment-rotational springs acting along the pile and at the base of the shaft. In most cases, foundations for electric power transmission systems are designed for lateral loading conditions, as opposed to other structures such as offshore platforms and buildings, where vertical dead load would be the governing load condition. Hence, drilled shafts supporting electric power lines have usually much shorter embedded lengths and are designed for a much larger degree of foundation rotation and the discussed rotational component of resistance contributes substantially to the soil resistance to oppose the moment loading condition above the simple translational soil resistance modeled by p-y curves. This mode of mechanistic soil reaction could be the reason for the so-called diameter effect related soil resistance and accounting for this added soil resistance as appropriate would not be incompatible with the Matlock's and Reese's p-y curve theory, or the Terzaghi's classical theory of subgrade modulus reaction.

The above described additional sources of soil resistance for deep foundations mobilized by pile rotations should be revealed by comparing pile load tests with different pile head boundary conditions, including comparing free-head versus restrained pile head test data. Unfortunately, pile load test setups usually become much more complex for the restrained head pile case and are extremely rare in the literature. It would not be unreasonable to assume that most of the pile tests cited by prior papers commenting on pile diameter effects be dominated by free-head tests Matlock in his original soft clay p-y paper (Matlock, 1970) has some discussions on the issue of loading condition playing a role in the empirically derived p-y curves and has compared some test data between free-head versus restrained head pile load tests. Eventually, Matlock stated that much of the offshore design applications relate to designing jacket-leg platforms where the pile head will be restrained for rotation and formulated his p-y curve theory for the simpler lateral translational mode of deformation. Lam and Cheang (1995) presented a series of pile load test data for a sand site which included a test setup as shown Figure 8. A hydraulically controlled loading strut close to the mudline provides the primary pile loading mechanism for the load test. As shown in Figure 8, the test setup included an upper strut which can be

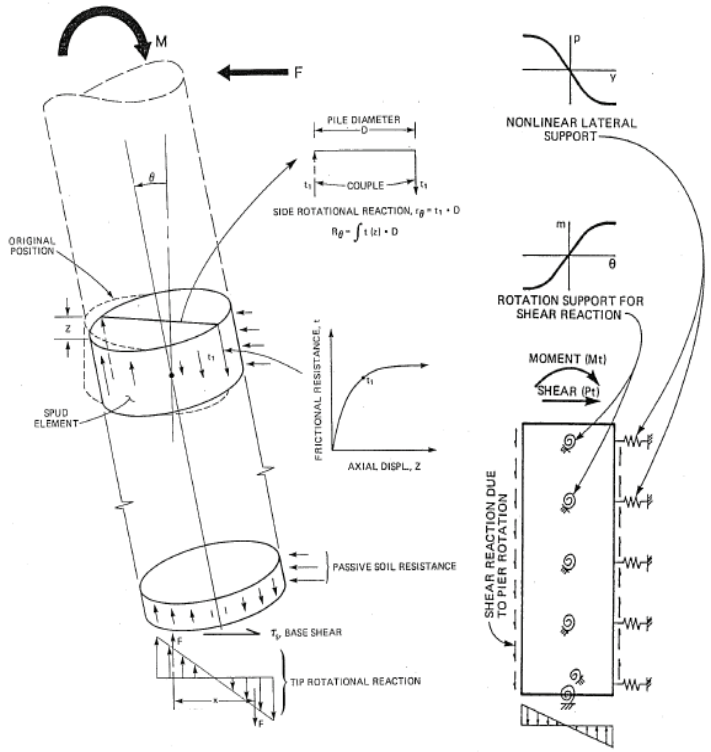


Figure 7: Various Sources of Soil Resistances for Deep Foundations (After Lam and Martin, 1986)

adjusted to provide varying degrees of pile head constraints at the mudline, including freeing the entire upper strut for a free-head test, and tightening the upper strut to the degree for an extreme rotational constraint (involving negative pile moment) at the pile head around the mudline elevation. From hindsight analyses using Reese's sands p-y criteria, Lam and Cheang (1995) observed that the apparent p-y stiffness increased for the free-head test over the fixed head test. A 42-degree friction angle provided the best fit to the free-head test, while the best fit friction angle reduces to about 38-degree for the fixed head test, representing about a 50% increase in the p-y curve soil resistance at shallow depth. The apparent increase in p-y capacity mobilized by pile rotation for even a 24-inch diameter pile used for the discussed pile load test resulted in the 50% increase in p-y capacity, which would be about the same order of increase in the N_p factor proposed by Stevens and Audibert.

The comparison between free-head versus fixed head test provides some evidence that it is plausible that the diameter effect may be actually due to pile rotation. It is obvious that

such an additional component of moment-rotation resistance would be highly dependent on the pile diameter D. Theoretically, the moment-rotational spring stiffness would be proportional to D^2, and the ultimate moment capacity will be proportional to D. The discussed mechanism is consistent with the observation of higher soil resistance for large diameter piles in past load tests dominated by free-head conditions. However, it is obvious that the additional capacity can only be realized if the pile rotation does occur, and needs to be in-phase with the imposed lateral load. Out of phase moment versus shear load on the pile can lead to a cancellation in the soil resistance. For jacket leg platforms, the jacket leg restrains the pile head to be close to zero rotation, and hence, even for large diameter piles, it is not justified to design for the added soil resistance.

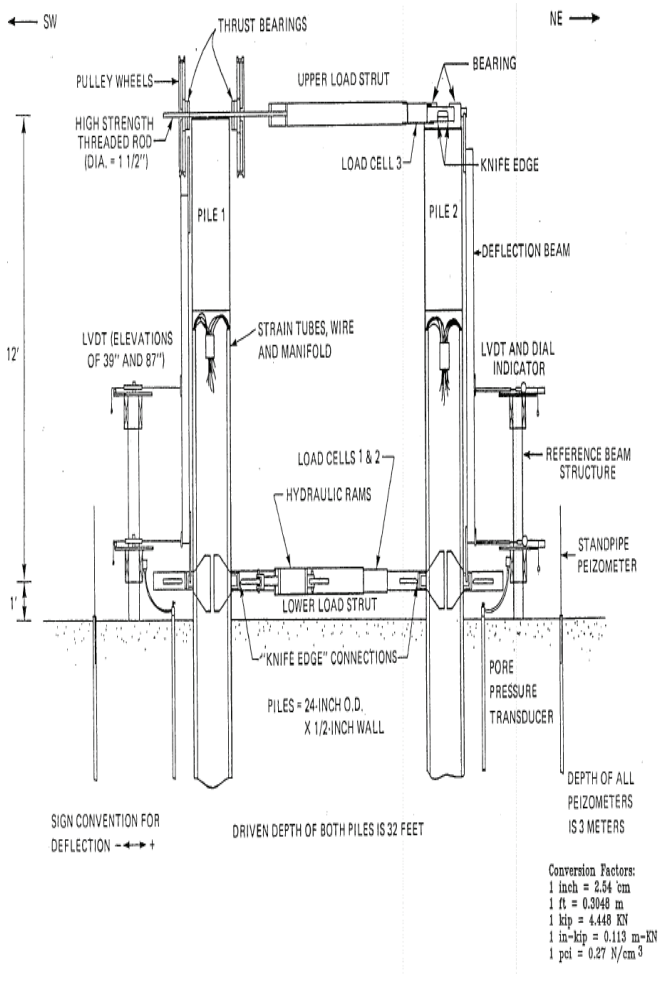
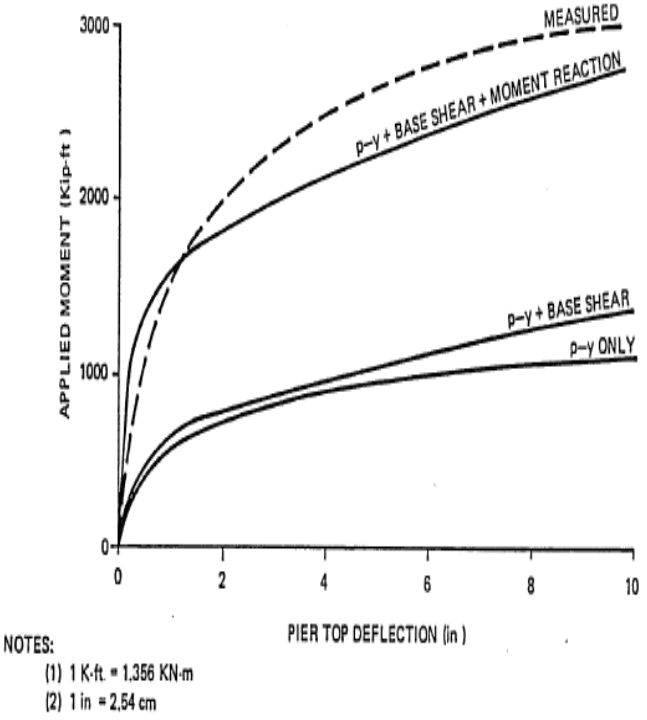


Figure 8: Pile Test Setup Reported by Lam and Cheang (1995)

CORRELATION FOR COMPONENT OF SOIL RESISTANCES ABOVE TRANSLATIONAL MODE p-y CURVES

Lam and Martin (FHWA, 1986) also conducted a series of backfitting analyses to evaluate the contribution of the above discussed rotational resistances of soils in addition to the traditional p-y curves making use of the database from the electric power full-scale large-diameter short drilled shaft tests from the comprehensive EPRI research program (Davidson, 1982). Lam conducted backfitting analyses for several EPRI drilled shaft tests, including a predominantly clay (cohesive) site and a predominantly sand, gravel and silt (cohesionless) site. The various soil resistances identified in Figure 7 were modeled. In addition to the conventional Matlock and Reese's p-y curves, distributed nonlinear moment-rotational springs were derived along the shaft of the pile. Nonlinear lateral and rotational springs were also modeled at the base of the shaft. The moment-rotational springs along the pile shafts were directly based on conventional skin-friction versus displacement t-z curves used for axial load-settlement analysis. The distributed axial skin-friction displacement characteristics acting on the vertical face of the shaft integrated over the shaft diameter were used to derive the nonlinear moment rotational springs. Similarly, the shaft tip moment rotational spring and shear traction-deflection spring at the shaft tip were based on relatively simple calculations, without inventing new p-y curve criteria. The drilled shaft at the clay site consists of a 5-ft diameter shaft with embedment length of 12.5-ft. The drilled shaft at the sand site consists of a 5.5-ft diameter shaft with embedment length of 16.2-ft. Figures 9 and 10 present the comparison between various load-deflection solutions with the experimental measurements. In a nutshell, the comparisons suggest that the additional component of moment-rotation soil resistance induced by pile rotation provided a rational account of the additional apparent increase in soil resistance for large diameter piles.



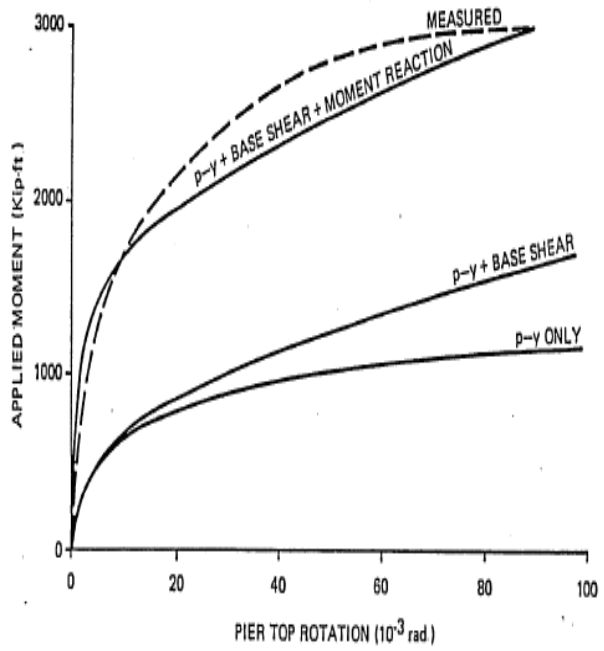
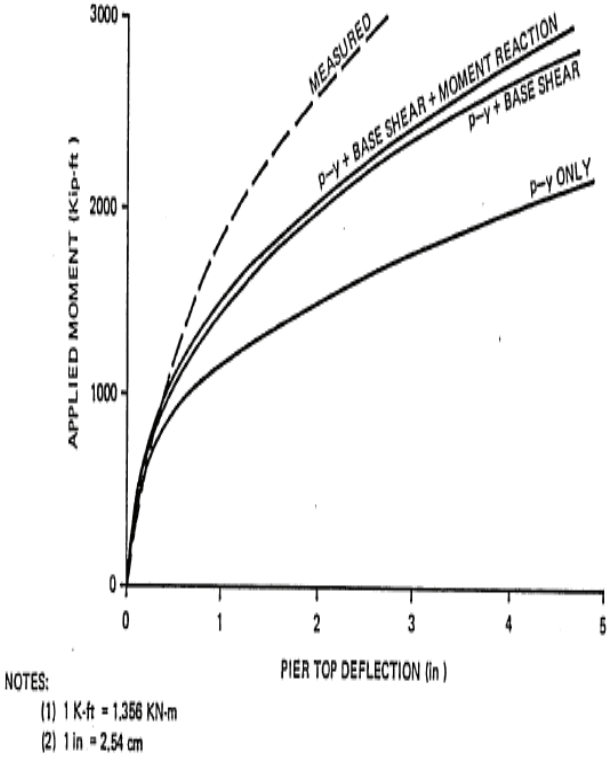


Figure 9: Solutions of EPRI Drilled Shaft compared to Test Data for Cohesive Soil Site (Lam and Martin, 1986)



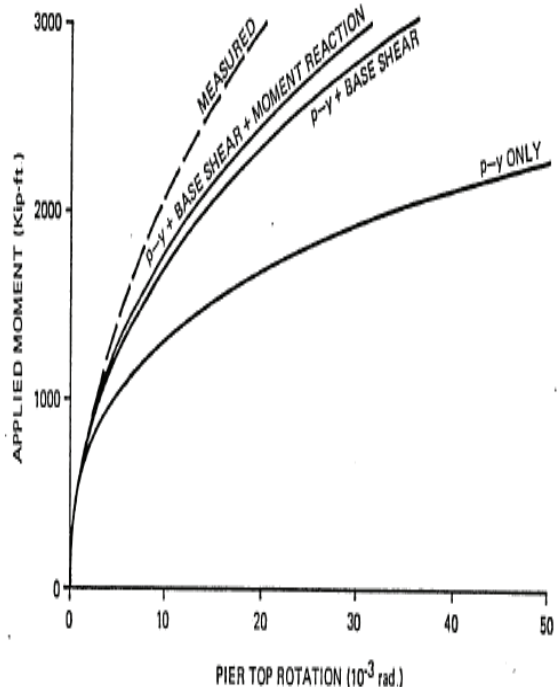


Figure 10: Solutions of EPRI Drilled Shaft compared to Test Data for Cohesionless Soil Site (Lam and Martin, 1986)

CONCLUSIONS

This paper presents a comprehensive review of available literatures postulating pile diameter effects and proposed various forms for modification of the Matlock's and Reese's p-y curves for larger diameter piles. This paper also reviewed the extensive theoretical background embodied in the Matlock's and Reese's p-y curve theories including detailing the inherent theory to account for size (diameter) effects based on well proven modulus of subgrade theories. The Matlock's and Reese's method for adjusting for diameter effect is not dissimilar with the classical Terzaghi's theory of modulus of subgrade reaction in projecting settlement measured from smaller plate load tests for designing larger foundations.

The apparent increase in soil resistance for large diameter piles cited in many of the diameter effect publications is probably due to additional component of soil reactions introduced by pile rotation in addition to the simple lateral translational mode of deformation implicit in the Matlock's and Reese's p-y curve theory. This issue was recognized by Matlock in his original paper on "Correlations for Design of Laterally Loaded Piles in Soft Clay". The p-y criterion postulated by Matlock was intentionally developed for designing offshore jacket-leg platforms where the pile head is restrained from rotation. For jacket-leg platforms, the Matlock's and Reese's p-y criteria still provide the best basis for design.

Despite the fact that diameter effects have been postulated by various publications since 1979, and more recently discussed in the API funded report reviewing the clay p-y curve criteria, the offshore design industry (API), apparently has elected to base the API code essentially on the original Matlock and Reese's p-y curve criteria. This is probably a sound decision on the API committee in this regard. All the cited methods for modifying the Matlock's p-y curve criteria for pile diameter effects have significant technical flaws and probably incomplete for replacing the Matlock's p-y curve criterion for treating potential variations in clay shear strength profiles, and consideration for designing for gapping and degradation effects for cyclically loaded piles. It is noteworthy that there have been numerous papers presented in past Offshore Technology (OTC) conferences and more recently in various geotechnical journals presenting both full-scale and model centrifuge test data. The majority of these publications suggest that the Matlock's and the Reese's p-y curve criteria provide reasonable platforms for design. Many of these publications included data from much larger diameter piles than piles tested by Matlock and Reese. For example, the two API reports (the O'Neill and Murchison report for sands, and the O'Neill and Gazioglu report for clays) included comparing the Matlock's and Reese's p-y curve criteria to pile data with diameters up to 59 inches. The comparison showed a large range of scatters inherent in the experimental database where the Matlock's and the Reese's p-y curves can sometimes be considered conservative, but also sometimes appeared unconservative.

However, in the earlier discussions, it has been pointed out that there are additional components of soil resistance induced by the more complex modes of deformation encountered in pile (deep) foundation systems from coupling effects of pile moment and pile shear loads. However, these additional components of soil resistance can potentially increase as well as to reduce the soil reaction from the simple translational mode of p-y curve resistance because the moment load can be acting in the same sense or in an opposite sense as the shear load. For conventional jacket-leg platform, where there are inherent rotational constrain at the pile head, the Matlock and Reese's criteria should be adequate without further modifications. However, in other structural configurations when the piles are cantilevered above the mudline to an elevation significantly above the mudline (a condition common for large diameter drilled shafts supporting bridge decks, often referred as a pile extension among bridge engineers) similar to shafts continuously cantilevered above mudline supporting electrical transmission lines, it would be valid to include additional components of soil resistance beyond the translational p-y curve model. The loading condition for such pile extension structural form typically involves a large positive pile moment deflecting the pile in the same sense as the lateral shear load. For these cases, we offer the following recommendations for design analysis.

RECOMMENDATIONS

The most technically sound approach in designing large diameter piles and for unusual structures, including for accounting the added

component of soil resistances beyond the simple translational mode of p-y curve resistance would be to formulate additional soil resistance curves for the foundation model such as those schematically shown in Figure 7. Then, the resultant analysis would automatically account for potential sources of soil resistance as appropriate. The additional moment-rotational springs along the pile, or base shear and base moment springs can contribute significant sources of resistance beyond the p-y model. The additional modes of moment-rotation resistance can be directly developed from side friction t-z curves, and pile tip bearing capacity curves using relatively simple geotechnical analyses without modifying the Matlock's and Reese's p-y curves. This is actually a standard design practice within the Electric Power Industry designing large diameter, but short drilled shafts used commonly for support of electric power transmission lines.

If the discussed procedure is considered impractical by the designer, one can fall back on modifying the Matlock's and Reese's p-y curves by p-multipliers and y-multipliers to increase the capacity and the stiffness of the p-y curves, as appropriate. Actually, a mature and a rational design practice should always make allowances to account for uncertainty in the real world situation with the discussed sensitivity studies including pile solutions exercising p and y multipliers to develop a feel for how uncertainties in p-y curves affect the eventual design. The designers are cautioned on the assumption that a softer p-y curve be considered conservative. This is valid only if the design is conducted using load controlled analyses (this is often the case for wave loading design). However, current seismic design practice often leads to displacement based analyses and softer p-y curves in the context of a pushover analysis to a given displacement demand can often lead to an unconservative solution of structural component stresses, or an unreasonable load distribution between the foundation versus the more vulnerable superstructure system. Ultimately the design should be sufficiently robust that the designed structural system should function adequately for a range of p-y curve characterization sufficiently wide to reflect inherent uncertainty in geotechnical engineering.

For the large diameter piles subjected to positive moment coupled with positive shear load discussed earlier, one might elect to develop y-multipliers less than unity for large diameter piles using the Carter and Ling equation Eq. (5). A reference pile diameter at say 24-inch might be reasonable as the reference diameter for anchoring the standard p-y curves considering that many of the pile load test database included pile diameters up to 24-inches in the literature as well as some of the Matlock's and Reese's pile load tests actually included 24-inch diameter piles. P-multipliers of say up to a factor ranging from 1.5 to 2.0 may be appropriate for the discussed pile loading problem to substitute for the rotational resistance not explicitly modeled in the analysis. Such a factor of up to 2 would be within the range of uncertainty in geotechnical engineering and soil properties.

From the author's experience, if the design process accounts for uncertainty in the p-y curves rationally, one often realizes that the resultant design is not very sensitive to large variations in the p-y curves. The key for rational treatments for uncertainty in p-y curves in design analyses is to be consistent in the p-y curve characterization throughout the design analysis process, especially consistency in demand versus capacity analysis processes.

It is the author's experience that the overall pile solution is much less sensitive to varying the y-multiplier, as opposed to varying the p-multipliers on the p-y curves. Also, uncertainty in p-y curves often merely imply a wider range in the deflection solutions as oppose to pile moment, especially in the context of the more common load-controlled design analyses.

REFERENCES

API RP2A (1993), American Petroleum Institute Recommended Practice for Planning, Designing and Constructing Fixed Offshore Platforms-Working Stress Design, API Recommended Practice 2A-WSD (RP 2A-WSD) Twentieth Edition, July 1, 1993.

Ashford, Scott and Juirnarongrit, Teerawut, 2003, "Evaluation of Pile Diameter Effect on Initial Modulus of Subgrade Reaction", Journal of Geotechnical and Geoenvironmental Engineering, ASCE. Vol. 129, No. 3, March, 2003.

Carter, D.P. (1984), “A Nonlinear Soil Model for Predicting Lateral Pile Response”, Report No. 359, Civil Engineering, University of Auckland.

Davidson, H.L., 1982, “Laterally Loaded Drilled Pier Research,” Vol. 1: Design Methodology, Vol. 2: Research Documentation, Final Report by GAI Consultants, Inc., to Electric Power Research Institute (EPRI), January, 1982.

Lam, Ignatius (Po), and Martin, Geoffrey, (1986) Seismic Design of Highway Bridge Foundations Vol. II Design Procedures and Guidelines, FHWA Report No. FHWA/RD-86/102.

Lam, Ignatius (Po) and Cheang, Lino, 1995, “Dynamic Soil-Pile Interaction Behavior in Submerged Sands”, ASCE Geotechnical Special Publications No. 55.

Ling, L.F., (1988), “Back Analysis of Lateral Load Tests on Piles”, M.E. Thesis, Civil Engineering Department, University of Auckland.

Matlock, Hudson, 1970, "Correlations for Design of Laterally Loaded Piles in Soft Clay," Proceedings, Second Annual Offshore Technology Conference, Paper No. 1204, Houston, Texas, April 22-24.

O’Neill, M.W., and Murchison, Jack M., (1983), An Evaluation of p-y Relationships in Sands, A Report to the American Petroleum Institute, (PRAC 82-41-1), University of Houston-University Park, Department of Civil Engineering, Research Report No. GT-DF02-83, May, 1983.

O’Neill, M.W., and Gazioglu, Sal M., (1984), An Evaluation of p-y Relationships in Clays, A Report to the American Petroleum Institute, (PRAC 82-41-2), University of Houston-University Park, Department of Civil Engineering, Research Report No. UHCE-84-3, April, 1984.

Reese, L.C., Cox, W.R., and Koop, F.D., 1974. “Analysis of Laterally Loaded Piles in Sand,” Proceedings, Sixth Annual Offshore Technology Conference, Vol. 2, Paper No. 2080, Houston, Texas.

Skempton, A.W., (1951), “The Bearing Capacity of Clays”, Building Research Congress, Division 1, Part 3, London, pp. 180-189.

Stevens, J.B. and Audibert, J.M.E., (1979), “Re-Examination of p-y Curve Formulations,” Proceedings, 11th Annual Offshore Technology Conference, Houston, Texas, Paper No. 3402, pp. 397-403.

Terzaghi, Karl and Peck, R.B. (1984), Soil Mechanics in Engineering Practice, Wiley, New York.

Vesic, A. (1961) “Beam on Elastic Foundations”, Proceedings, 5th ICSMFE, Paris, Vol. 2:1, pp. 24-28.

INSTALLATION CHECKLIST FOR DRIVING MEGA PILES

Douglas L. Scaggs, MENCK GmbH, Houston, TX, USA

Over the past several years, pile foundations have grown to meet the demands of larger and heavier structures. As the foundations have grown, so has the need for larger and more robust piles to carry the increased loads. Seismic considerations have also required larger and tougher piles to withstand the added component of supporting structures during earthquakes. While H-piles, precast concrete piles, timber piles and small pipe piles have been the product of choice, many applications are now calling for much larger piling requiring larger equipment and presenting the contractor with new challenges. This paper is not intended to be a "how to" guide as much as a discussion on the potential pitfalls a contractor should watch out for when considering a project where mega piles are required.

WHAT IS A MEGA PILE?

Although not defined by ASCE, mega piles are generally considered to be piles 8 feet in diameter or larger and some consider 15 feet as the starting point. Depending on the design load however, piles as small as 48 inches might even be considered mega piles when they are designed to carry very large loads requiring large installation equipment. Mega piles are gaining in popularity for a couple of reasons. First, in areas with a history of seismic activity, large steel cylinder piles are less likely to be damaged by an earthquake. Mega piles also make larger structures possible with fewer piles. Even with the higher cost of the piles and the equipment to install them, huge savings can be realized because of reduced time required to drive a few large piles versus high numbers of smaller piles.

There are several variations or designs that may come into play as well. Generally these piles are large steel cylinders of either constant or variable wall thicknesses. They may be vibrated into place, drilled out and filled with concrete and steel reinforcing. Or they may be driven with impact hammers and either left as is, or drilled out and filled with concrete and steel. In some instances such as the toll bridges around the Bay Area in California, these large piles are driven to rock and then a rock socket is drilled into the rock formation. When reinforcing steel and concrete are added, the rock and the pile are connected adding the stability needed to help prevent damage in the event of earthquakes. These are called Cast In Steel Shell (CISS) piles.

Needless to say, whether a pile is 8 feet in diameter, 15 feet or even larger, normal installation equipment and practices are not suitable. But whether the project calls for installing a simple H-pile for a building foundation, an 8 foot pile for a bridge, or an 18 foot pile for an offshore windmill turbine, the piles must still be forced into the earth's surface. Regardless of pile size, certain things are always constant.

SELECTING A HAMMER

A drivability analysis should be performed using collected soil data and pile design criteria. A program such as GRL-WEAP (GRL 2005) or similar programs are generally suitable to help select the appropriate driving solution for the pile. There are other programs similar to the GRL format, but they all ultimately calculate driving predictions based on the same general data. During this process, care must be taken by the engineer to assure that the pile can withstand the stresses of driving. Otherwise the pile design must be reviewed. This will help eliminate the embarrassing case of a pile which is suitable to carry the load once in place not being robust enough to withstand the stresses of driving without damage.

Once a hammer type and size have been established, the contractor must search the market for a hammer matching the engineer's specifications. The suitable hammer may not be available from a contractor's normal hammer source due to the size involved. Large hammers generally used in mega pile work were originally developed for the offshore oil and gas industry. Therefore, names such as MENCK GmbH of

Germany and IHC Hydrohammer of The Netherlands come to mind. Within the past few years, American Piledriving Equipment (APE) has produced a couple of large hydraulic hammers, the largest of which, the Model 750, is rated at 625,000 foot pounds. With the exception of the APE hammers, the other large hammers in the market were developed with offshore applications in mind. These hammers were built beginning in the 1970's with large steam powered models to answer the call from the contractors needing to install the huge steel structures required to drill and produce oil and gas offshore. As the structures got larger, so did the need for still larger hammers. The major offshore contractors and design engineers put pressure on the hammer builders to produce larger hammers. One contractor would align itself with one manufacturer ordering their largest hammer and then another contractor would do the same thing with another supplier specifying something even larger. The three main suppliers of these hammers, Vulcan Iron Works, Conmaco, Inc. and Menck were all too happy to oblige. The large hammer market resembled the horsepower race with the muscle cars of the 1960s. Everybody wanted to have a hammer bigger than their competitor. The race finally ended, at least for the steam hammers, when Vulcan produced two model 6300 steam hammers rated at 1,800,000 foot pounds for J. Ray McDermott in Louisiana. McDermott ordered these hammers to compete with Menck MRBS 12500 steam hammers rated at 1,582,200 foot pounds owned by the Dutch contractor, Heerema. These monsters weighed well over 400 tons. The Vulcan 6300's had rams weighing a massive 150 tons with a stroke height of 6 feet. They proved to be too big for the basic Vulcan design and although they did run, were never put into active service.

Following the end of the steam hammer race, hydraulic hammers were developed which raised the bar still further. The Netherlands based company IHC developed a hydraulic hammer that not only competed with the steam hammers in power, but could run under water. During the same time, Menck of Germany began switching their emphasis from steam to hydraulic and also developed an under water capable hammer. The largest of the IHC models currently is the S-2300 rated at 1.7 million foot pounds. Menck has built hydraulic hammers with rated energies up to 2.2 million foot pounds with their MHU 3000s. The hydraulic hammers have proven to be more efficient, lighter and easier to handle than their steam predecessors.



MENCK MHU1700 driving 102 in. pile

In the past several years a few diesel hammers have gotten into the large hammer market. Delmag of Germany has a D-200 rated near 500,000 foot pounds and APE of Kent, Washington has a model D-220 rated at 550,000 foot pounds.

Even vibratory hammers are getting in on the action. Depending on project requirements and the soil conditions, vibratory hammers may be suitable for certain applications where proven load bearing capacities are not an issue. APE has developed a quad arrangement utilizing four large vibratory hammers to install 40' diameter concrete cylinder piles in China. A series of connecting shafts and gear boxes synchronize the big vibros allowing them to work together. This design can be expanded to add additional units and drive even larger piles.



APE MODEL 400 QUAD VIBRO
driving 40' diameter concrete pile

Needless to say, regardless of what the design engineer might come up with, there is probably a hammer capable of driving it. However, it should be mentioned that availability of some of these very large hammers could be limited. The world market for hammers this large is quite limited, therefore very few may be available depending on the actual model selected.

When making the hammer selection decision, a word of warning should be noted concerning pile setup. If the pile is driven in segments, planning must be done to be sure that splices are made at a point before the driving resistance may make restarting the pile difficult. Pile setup is a concern since splicing very large piles can take several days. If the selected hammer is marginal, a restart after splicing or other interruption could create a major problem. It is advised that a hammer just barely large enough be avoided. Using a hammer with reserve power will make the job go easier and hammer related problems may be reduced when it doesn't have to run at full energy. While the larger hammer may be a little more expensive, it will likely pay for itself in the long run. Not only should it be more reliable, but in the case of hydraulic hammers, a larger hammer running at 70 or 80% energy will drive faster than a smaller one running at 100%.

When putting together the cost of renting these large hammers, the contractor should be reminded about transportation costs. These machines are generally made up of components requiring special handling and shipping. They may be shipped in several pieces and assembly once they reach the jobsite could require several days. Consideration should be given to including technicians from the manufacturer to assemble and possibly maintain and operate these hammers. Be careful that start and stop dates are clear on the rental contract as most offshore equipment is customarily rented portal to portal. That is, the rent begins when the equipment is shipped and ends when it returns. While these terms generally can be negotiated, the contractor should be aware and not overlook them.

CRANE SELECTION

After the hammer selection has been made, a suitable crane must be arranged. Boom length will be critical since pile length must be considered along with the long lengths of many large hammers. Keep in mind that many of these hammers were designed for barge mounted cranes where capacity was less of an issue. Most offshore hammers are free hanging either using guide sleeves which go over the top of the pile as much as 10 feet or more, or cage style leaders, and often weigh anywhere from 50 tons on up to over 200 tons. Because the pile must be able to support the hammer, it may have to be driven in sections and stabilized with a template. The use of a vibratory hammer to pre-set the piles is also a possibility which could eliminate the need for a pile template and drive the pile part way reducing the height needed to set the impact hammer on the pile.

NOISE CONTROL

It is no surprise that big hammers driving big piles make big noise. Depending on location, some type of noise control may be required. While a number of different approaches have been used, a perfect universal solution hasn't been found. IHC has developed a collapsible synthetic tube that surrounds the pile and lower part of the hammer that has proven effective, however it has never been used on very large piles. Menck has used a similar technique on somewhat larger piles. Others have used shields made of varying materials. In general, a solution specific to the local conditions may have to be designed.



MENCK 270T with pile noise mitigation

It could be that restrictions may be in the project specifications limiting the number of hours per day driving can be done. This too can impact cost since careful planning has to be done so that stoppages are not enforced at a time when pile set up mentioned above could create a problem.

If the piles are driven in the water, noise or shock control may be required to avoid harming marine life. Here again, several different approaches have been used. One solution is to install a cofferdam. It may require dewatering to be fully effective. Another solution is the use of a bubble curtain. One method of providing a bubble curtain is to use circular manifolds with air jets around the perimeter located near the mud line. This approach requires large air compressors and is only effective if there is little or no water movement. Gunderboom located in Anchorage, Alaska has solved this problem with a combination of air bubbles and a synthetic curtain that contains the bubbles. With the Gunderboom system, less air is required and water movement has far less influence on the effectiveness. There may be other creative ways to solve this problem, but it is a problem that must be addressed in many water based projects.



GUNDERBOOM SAS BUBBLE CURTAIN

CONCLUSION

Driving mega piles is technically little different from driving any other piles. However, contractors should be warned to not cut corners or approach a project using marginal equipment. If the selected crane is too small, it will slow the job down, increase the likelihood of accidents and possibly cause significant delays. If the hammer is too small, the project could be delayed for weeks or months while another hammer is located and shipped to the site. If noise mitigation is not effective, the project could be shut down while alternate methods are found. While many potential problems are the same as on any other pile driving job, the sheer size can make a problem very expensive to solve. However, proper planning and careful selection of equipment can make the mega pile project a success.

ACKNOWLEDGEMENTS:

Photographs courtesy of:

American Piledriving Equipment, Inc.
Kent, Washington, USA

Gunderboom, Inc.
Anchorage, Alaska, USA

MENCK GmbH
Kaltenkirchen, Germany

MKT Manufacturing, Inc.
St. Louis, Missouri, USA

UNDERWATER SOUND ATTENUATION IN CONSTRUCTION PROJECTS: APPLYING SCIENCE TO PILE DRIVING PERMITS

Alan Christopherson, PE, Senior Vice President, PND, Incorporated, Anchorage, AK, USA
Jennifer Lundberg, MES, Senior Environmental Scientist, PND, Incorporated, Anchorage, AK, USA

Nearshore construction projects often require installation of steel piles and specific methodologies of installing piles may adversely affect nearby species of concern. Water is an uncompressible medium which allows for easy transmission of energy through the water column. Energy transmission through water depends on the following factors for pile driving: 1) direct contact of the pile and the water; 2) the depth of the water column; 3) the size of the pile; 4) type of hammer; and 5) the energy of the hammer.

Seasonal restrictions are usually the best practicable alternative for reducing habitat impacts when pile driving activities may adversely affect the species of concern. When seasonal restrictions are not practical other options need to be evaluated, including mitigation and noise attenuation devices. The broad array of mitigation options will not be discussed as part of this presentation but instead will focus on noise attenuation technologies. Dewatered cofferdams can be effective noise attenuators as they eliminate direct contact of the pile with water while driving. Also, introduction of a compressible medium, like air, near the energy source can provide sound energy attenuation. An unconfined bubble curtain is relatively inexpensive but is not effective in tidal marine projects or rivers and may have unacceptable secondary effects. Secondary effects must be evaluated as these can increase exponentially for larger projects. Secondary effects to the environment include air quality degradation from air compressor use, transportation costs for fuel and equipment, and the potential for injecting oily compressed air into the water column. The confined bubble curtain works well in nearly all environments. It usually is more expensive initially, relative to an unconfined air curtain, but there is less potential for harmful secondary effects.

Generally, seasonal restrictions will be adequate to protect species of concern. However, there are conditions in which mitigation or one of the sound attenuation options should be utilized. Site specific factors, including the amount of energy being imparted into the environment, sensitivity of the species of concern, current, accessibility, length of time needed to complete the project, and the cost of the sound attenuation, should be factored into the permit evaluation.

INTRODUCTION

The need for continued development, or redevelopment, of the near shore area usually means that the shoreline must be modified to accommodate the uses. Dock structures and bridges are common shoreline developments. New techniques and materials can make the structure stronger to withstand natural forces, such as earthquakes and tsunamis, but also for supporting larger docks and bridges. One thing that these structures have in common is the use of some sort of pile. These include round piles made of steel and/or concrete and sheet piles usually made of steel but other materials such as fiberglass are becoming more common. This paper addresses steel round and sheet piles. These piles are usually driven with impact or vibratory hammer technology and sometimes a combination of both is used. Structural piles must be “proven-up” using the impact hammer so even on projects where the primary hammer is vibratory in nature; an impact hammer is always required to be on site.

PERMITTING ENVIRONMENT

For the regulatory agency, understanding the construction requirements is key to understanding what is reasonable as a stipulation in the permit and what will increase costs unnecessarily. The regulator must also understand many facets of the environment and the construction impacts to those resources that are under protection. The expansion of the Essential Fish Habitat requirements under the Magnuson-Stevens Fishery Conservation and Management Act is now looking at how pile driving affects protected species. This is partially a response to projects where there has been significant harassment and even death of protected species. Many of these projects utilize large steel pile (6 foot diameter and larger) and large impact hammer (250,000 ft/lb and larger). The traditional, and likely most effective, means of protecting species of concern is to stipulate seasonal restrictions in permits and to avoid, to the greatest extent possible, conducting projects when the species is likely to be in the area. Unfortunately, the list of species of concern is growing to the point where there can be at least one species of concern in the area at all times of the year. It is also appropriate for project owners and regulators to discuss other options when projects are in areas where the construction season is too short to be cost effective for construction of the project.

FACTORS IN SOUND ENERGY TRANSMISSION

The first step in determining what is reasonable for permit stipulations is understanding how energy is transmitted during the pile driving process to the water column and thus to the species of concern. Water is an incompressible medium, which allows for easy transmission of energy through the water column (Wilson (Lundberg), Christopherson et al., 2002). Energy transmission through water depends on the following factors for pile driving: 1) direct contact of the pile and the water; 2) the depth of the water column; 3) the size of the pile; 4) type of hammer; and 5) the energy of the hammer. Each project specific pile and hammer combination at each site will produce a different amount of energy that is transmissible into the water body. It should also be noted that some of this energy will be transferred directly into the sediment and not all the energy will be transmitted into the water. Variations in the substrate firmness or material type can also affect the amount of energy imparted into the water column. The worst case scenario, of all energy transferring into the water column, is most likely to occur at pile refusal and this is generally what regulators will be evaluating.

Assuming this worst case scenario, the intensity of sound at the pile can be estimated using the basic definition of intensity:

I=power/unit area

The power is the time rate of energy divided by the submerged area of the pile. A basic calculation using equation (1) for the source level (SL) of energy generated by the driving of a pile 12 meters (40 ft) in length and 2.5 meters (8 ft) in diameter is approximately 249 dB re 1μPa. This notation is a standardization of decibels (dB) that removes the need to discuss frequency. Damaging effects for most marine mammals and some fish begin at 170 dB re 1μPa(Federal Highways Administration, 2001). Since dB are logarithmic, this means that the calculated SL in the above example is not 1.5 times louder but more on the order of 800 times louder than what is considered damaging to most marine mammals and some fish.

Geometric spreading loss models provide a 20 dB (for spherical spreading in an unbound medium meaning “deep water”) to 40 dB (for cylindrical spreading in a bounded medium (meaning “shallow water”) loss at 100 meters distance from the source. These are theoretical losses and the actual loss at any project site is likely somewhere between these two values (Wilson (Lundberg), Christopherson et al., 2002). The loss of energy is actually an artifact of the spreading of the energy over a larger area and this is what produces the lower intensity.

UNDERWATER SOUND ATTENUATORS

There are several factors that determine the underwater sound level of a marine pile driving project. These include depth of water, velocity of the current, size of the hammer, size of the pile, characteristics of the soil/sediment, and, to a lesser extent, water quality characteristics like turbidity and salinity. The amount of sound that will be created by pile driving must be calculated for the site characteristics, usually after in situ testing has occurred.

Changing the medium that the energy travels through will act to dissipate the energy quickly (Wilson (Lundberg), Christopherson et al., 2002). Introduction of a compressible medium, like air, near the energy source can provide sound energy attenuation and a perfect layer of air, like a dewatered cofferdam, would achieve this. However, the installation of the cofferdam will require some sort of attenuation device itself since these structures are usually larger hollow steel piles driven into the sediment prior to driving the large structural steel. Dewatered cofferdams can be effective noise attenuators as they create a continuous air cushion around the pile while driving. Two methods have been used to introduce air bubbles into the water column near a pile: confined and unconfined air bubble curtains. See Figures 1 and 2 for an unconfined air bubble system diagram and confined air bubble system photograph, respectively.

The mathematical expression for why air bubbles work in noise attenuation is outside the scope of this paper and is well addressed in other reports and texts (Wilson (Lundberg), Christopherson et al., 2002). What is important for the regulator and designer of an air bubble curtain system to understand is that the air bubble curtain cannot have holes or gaps and there is frequency dependence for attenuation, which is directly and inversely related to bubble size (Wilson (Lundberg), Christopherson et al., 2002). Therefore, a bubble curtain must have many different sizes of bubbles and must surround a source completely in order to effectively attenuate the energy from the source for most of the frequencies being generated. So while there are ways to simplify the expression of energy for permitting purposes, the design of an attenuation device must consider the frequency being produced and which frequencies are most damaging to the species of concern. Several reports indicate that low frequency exposure is the most damaging to marine life (NOAA Fisheries, Wilson (Lundberg), Christopherson et al., 2002). The larger air bubbles, approximately the size of a basketball and larger, attenuate the lower frequency sound waves.

When the schedule requires a construction project to occur during a period of time when harassment or damaging effects to marine animals are likely, a confined air bubble curtain is likely the best available technology. An unconfined bubble curtain is relatively inexpensive but is not effective in high current situations such as tidal marine projects or rivers and may have unacceptable secondary effects. See Figure 1 for an elevation view of the typical layout of an unconfined air bubble curtain. Secondary effects must be evaluated as these can increase exponentially for larger projects. Potential secondary effects due to the unconfined air bubble curtain include air quality degradation due to the large number of air compressors required, transportation costs for fuel and equipment, and injection of potentially oily compressed air into the water column. The confined bubble curtain works well in nearly all environments. It usually is more expensive initially, relative to an unconfined air curtain, but the secondary effects are generally lower because less air is required to effectively run the system. See Figures 2 and 3 for a photograph of a confined air bubble curtain.

CASE STUDY

The San Francisco-Oakland Bay East Span Safety Project (East Span Project) provides an example of a large pile and hammer demonstration project that explored two air bubble curtain technologies for noise attenuation (NOAA Fisheries, Christopherson and Lundberg (Wilson), 2002; Wilson (Lundberg), Christopherson et al., 2002). California Department of Transportation (CalTrans) conducted a Pile Installation Demonstration Project (PIDP) using 6 ft (1.8 m) and 8 ft (2.5 m) diameter piles and a large hammer with a maximum energy of 1.2 million foot pounds. See Table 1 for the results of the CalTrans project.

Unconfined bubble curtains are attractive for several reasons. First, they appear to require little to no engineering and contractors are often responsible for designing and building them. Second, they appear to be inexpensive as the contractor usually dedicates a single air compressor to pump air into the system. Figure 1 demonstrates the primary problem with unconfined bubble curtains; they are subject to breaks in the curtain due to tidal action.

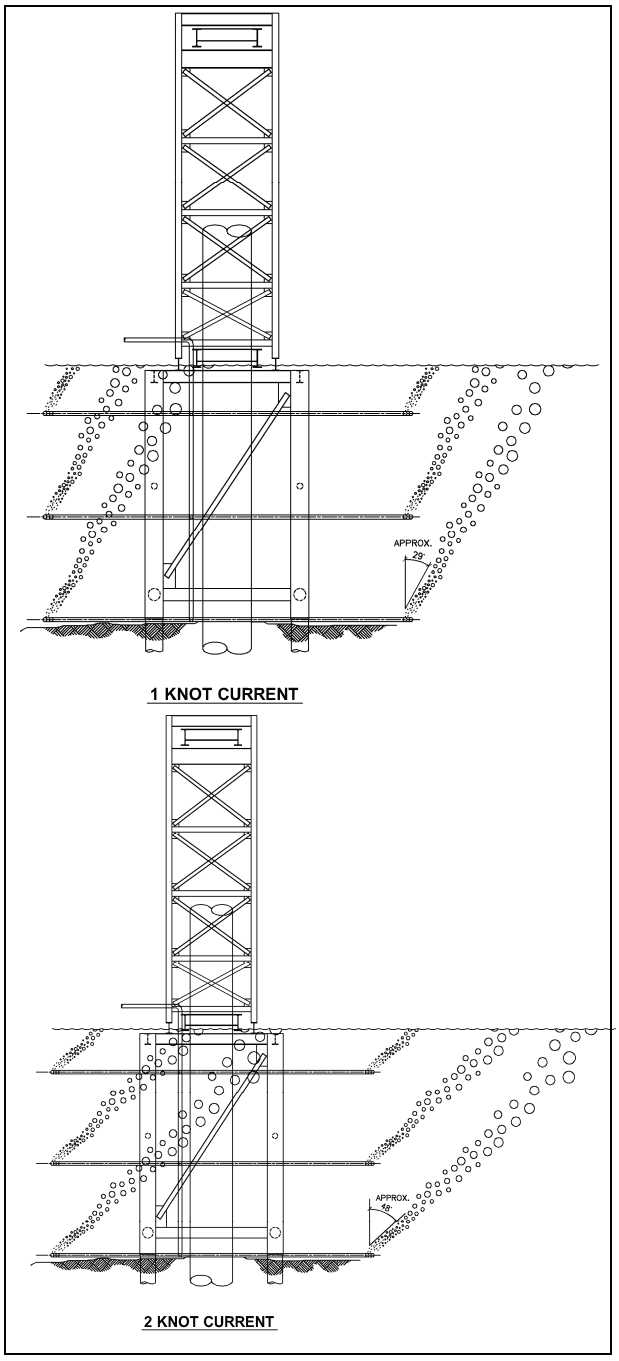


Figure 1: Diagram of Bubble Drift in 1 and 2 knot

The proponents of the unconfined bubble curtain for the East Span Project determined that more rings at different elevations of the water column and more air were required to make the unconfined air bubble curtain effective. PND determined that an additional barge containing at least eighteen, 1400 cfm air compressors were necessary to meet the stated objectives of the project proponents. However, it is unlikely that the increase in number of rings and amount of air would be effective in meeting the permit requirement of 10 dB reduction.

The secondary affects of the unconfined bubble curtain are also significant (NOAA Fisheries, Christopherson and Lundberg (Wilson), 2002; Wilson (Lundberg), Christopherson et al., 2002). The large number of air compressors required to approach effectiveness will introduce potentially oily compressed air into the water column, likely increase the percent dissolved oxygen, increase turbidity, and re-suspend solids into the water column. Oil-free air compressors are much more expensive and it is unlikely that large construction projects would be able to obtain the number and size of compressors necessary to run an unconfined air bubble system. The large number of air compressors will also increase fuel consumption requirements and increase air pollution. The risk for fuel spills will increase as the air compressors will require their own barge and significant amounts of fuel will need to be transferred from the shore. There is an increased risk of instability for work vessels in the vicinity of the unconfined air bubble curtain. Glosten Associates calculated a 23% reduction in stability/buoyancy for vessels in the case of the unconfined bubble curtain calculated above, which requires at least eighteen large air compressors. The often fragile nature of the air bubble rings for delivering the air into the water column and the large number of air compressors required increases the amount of maintenance required for the system. This could also lead to delays in the event of several air compressors being down for maintenance or repairs at one time. Finally, there is an increased risk for worker safety in the vicinity of a large number of air compressors.

Confined air bubble systems have clearly demonstrated their effectiveness. After-the-fact evaluations of several pile driving projects that used an unconfined air bubble system have been reported (Wilson (Lundberg), Christopherson et al., 2002). A project in Vancouver, British Columbia, used smaller hammers, about 1/5th the energy of the hammers used in the East Span Project, and smaller piles (24-inch) in calm waters (Longmuir and Lively, ; Wilson (Lundberg), Christopherson et al., 2002). The East Span project has effective water velocities of 3-5 knots whereas the Vancouver project has effective water

velocity of ¾ to 1 knot. See Table 1 for a comparison of the Vancouver and East Bay Projects. Note that the sound attenuation was measured for the confined air bubble system with the air turned on and off. The fabric that encloses the pile itself provided significant sound attenuation (See Figures 2 and 3). The sound attenuation numbers may be conservative as there was an incomplete seal at the bottom of the frame due to miscommunication on bottom topography. The system also required one 1400 cfm air compressor and the system is designed to be portable and reusable for multiple piles. The drawback of the system used in the East Bay Project is that it was expensive and requires engineering. However, continued research and development plus experience using the system in the field should bring down costs significantly.



Figure 2: A confined bubble curtain being transported to the project site. Two layers of non-woven geotextile fabric surround a frame. Air is bubbled from the bottom between the two layers.



Figure 3: Confined Air Bubble Curtain in place for pile driving.

RECOMMENDATIONS

In summary, the current strategy of timing restrictions is the most effective method of protecting species of concern during pile installation projects. However, if the project schedule or size of the project warrants further protection, sound attenuation is appropriate. One effective means of attenuating underwater noise is through the use of a confined air bubble curtain as it is not subject to breaks or gaps in the air bubble curtain due to currents.

Additionally, in situ research is also needed. The complex nature of noise propagation through the water column due to pile driving activities is poorly understood. Laboratory results have not translated well into the natural environment. The use of monitoring results has also been unsatisfactory.

REFERENCES

Christopherson, A., PE and J. Lundberg (Wilson) (2002). Technical Letter Report Regarding the San Francisco-Oakland Bay Bridge East Span Project Noise Energy Attenuation Mitigation. L. Kuhn, Esq. Anchorage, AK, PND Inc.

Federal Highways Administration (2001). Biological Opinion - San Francisco-Oakland Bay East Span Safety Project**:** 29.

Longmuir, C. and Lively, T. Bubble Curtain Systems for Use During Marine Pile Driving, Fraser River Pile & Dredge, Ltd.

NOAA Fisheries Summery of Potential Impacts to Fish from Pile Driving**:** 6.

Wilson (Lundberg), J., Christopherson, PE, A. et al. (2002). Report of Findings - Unconfirmed Air Bubble Curtain Technology. Anchorage, AK, PND, Incorporated.

Table 1: Comparison of the Canada Place Vancouver, BC pile driving project and the CalTrans East Bay Project.

Largest hammer used in Vancouver, BC was 225,000 ft/lb Delmag D80 Diesel Impact hammer on 24 inch steel piles. Largest hammer used for East Bay Project was 1,254,000 ft/lb Menck MHU 1700T impact hammer on 8 ft diameter steel piles. (Wilson (Lundberg), Christopherson et al., 2002)

Project	Attenuation Values	PSI	dB re 1µPa at pile	dB re1µPa (95 m from pile)	Reduction from No Mitigation at 100m (dB)
Vancouver, BC	No Mitigation	22	223	203[1]	N/A
	Unconfined Air Bubble Curtain	3	206	186[1]	17
East Bay Project	No Mitigation			197	N/A
	Unconfined Air Bubble Curtain			197	0
	Confined Air Bubble Curtain – Fabric curtain with air turned on			175	22
	Confined Air Bubble Curtain – Fabric curtain only with air turned off			184	13

[1] Calculated and assumes 20 dB loss through geometric spreading.

CONSTRUCTION OF LARGE DRILLED SHAFTS THE 2ND ANNUAL MIKE O'NEILL LECTURE

Dan Brown P.E., Ph.D., Dept. of Civil Engineering, Auburn University, AL, USA

Improvements in construction equipment and techniques in recent years have made possible the use of drilled shaft foundations in diameters and lengths not previously considered practical or feasible. Many highway bridge and other structures are now routinely founded on drilled shafts which are 8 to 12 feet in diameter and extending over 200 feet in depth below grade. There are unique challenges associated with constructing such large and deep cast-in-place foundations and engineers should be aware of the special needs associated with site investigation, construction specifications, material requirements, and quality assurance. This paper outlines a number of special considerations for these foundations, along with strategies that may be employed to improve the reliability and quality of large drilled shaft foundations.

INTRODUCTION

Large diameter drilled shafts are becoming increasingly popular on major bridge projects due to increased availability of drilling equipment and skilled contractors and inherent advantages of high capacity shafts in supporting axial and lateral loads. Shaft diameters of up to 4 m (13 ft) and lengths of up to 80 m (260 ft) are no longer unusual. These shafts pose exceptional challenges for construction because of the difficulties in excavating shafts of such size and because of the requirement for underwater placement of large volumes of concrete through dense reinforcing cages.

It is important that engineers involved in such projects be aware of the special challenges associated with construction so that designs can be developed which enhance reliability and minimize risk. In addition, engineers with responsibility for quality control and quality assurance on the project must be fully aware of the critical aspects of foundation construction. The use of design/build procurement for many large bridge projects can foster cooperative effort between design and construction professionals and typically requires engineers to proactively consider the important aspects of risk, schedule, and quality assurance in deep foundation construction.

This paper provides an overview of some important considerations in the construction of large diameter and deep drilled shaft foundations, with an emphasis on bridge projects. These considerations include:

- Excavation techniques suited to this type of construction
- Aspects of site geotechnical investigations important for construction
- Design of reinforcement for constructability
- Concrete placement techniques
- Concrete mix design

EXCAVATION TECHNIQUES

The high load demands which drive the size and depth of drilled shaft foundations on major bridge projects also tend to drive the construction into deep and hard bearing strata. The depths associated with high capacity foundations often include the need to penetrate through layers of rock or rock-like material which may contain boulders and/or cobbles, may be difficult to excavate, or may have special concerns for stability of the excavation during the extended time required to complete the excavation.

Other than the typical tools and equipment used for conventional drilled shaft excavation, large and deep excavations are often accomplished with an increased use of:

- Permanent casing
- Temporary casing installed using oscillators or rotators
- Reverse circulation drilling
- Combinations of coring, drop chisels and hammergrab tools in lieu of augers

With shaft excavations in excess of 8 ft diameter, the use of permanent casing is usually very desirable from a constructability standpoint. Permanent casing is particularly useful in forming the shaft through water and penetrating soft shallow strata which may be unstable. Attempts to remove large diameter casing in these shallow depths adds time to an already lengthy construction process in which the concrete must remain fluid and introduces additional risk.

Large diameter permanent casing is most effectively installed in advance of drilling and most often installed using vibratory hammers, although large offshore-type impact hammers have also been used (Figure 1). If a large hammer is required to install the casing, extraction of a casing would require an even greater force due to the time-dependent setup of the soil resistance in side shear (so leave it in place!). In some cases, the installation of a deep permanent steel pipe followed by excavation below may be considered as a type of steel pipe / drilled shaft composite pile. The axial resistance within the depth of permanent casing can be significant in proportion to the overall axial resistance of the shaft and may be included in the design.

Temporary casing to the full length of the shaft excavation may be used when the risk of excavation collapse is significant. For large and deep drilled shaft excavations, full length temporary casing is most effectively installed using hydraulic oscillator or rotator equipment, in advance of the excavation (Figure 2). The casing installed with this equipment is typically high strength steel, often double-wall, with flush fitting joints between segments. Segmental casing is used to achieve the great depths required. The development of this type of equipment has been instrumental in advancing construction of large deep shafts, because of the large torque and lifting forces that can be generated. In many cases, the thrust applied during removal of the casing requires substantial pile foundations to be installed in support of a template.



Figure 1: Installation of Permanent Casing



Figure 2: Oscillator Equipment for Installation of Segmental Casing

Another reason for using casing is the time required for completion of large deep shafts, which could be a concern if bentonite drilling fluid were used and the exposure time must be limited. Many specifications call for limiting the exposure time to a maximum of four hours for an open hole with bentonite slurry because of concerns relating to filter cake buildup and subsequent reduction in side shear capacity. The minimum length of time required to complete bottom cleaning operations, place rebar, and start concrete placement in a large shaft can easily exceed this limit.

Reverse circulation drilling techniques are often used to advance shaft excavations to great depth. With reverse circulation drilling (Figure 3), drilling fluid (usually water) is circulated by lifting the fluid through the center of the drill string, usually with an air-lift pumping system, and with fluid resupplied by pumping into the top of the shaft excavation from an external reservoir. Cuttings are removed from the base of the excavation by the circulating drilling fluid, which evacuates the material below the cutter head.

An advantage of reverse circulation drilling is that the tool does not need to be cycled in and out of the hole to excavate the soil or rock as would be the case with conventional augers, and for shaft excavations at great depth this advantage can result in improved productivity. However, the time required for setup on each hole is significant.

Other tools often utilized on large, deep shafts include percussion tools such as drop chisels or hammergrabs. With large diameter excavations in hard material, chisels can assist in breaking up boulders or large rock fragments left after coring with core barrels or within segmental casing. A hammergrab tool can be more effective at removing large objects within the excavation than rotary drilling equipment. It is worth noting that the base of the excavation will not be as flat and level as would be accomplished using conventional rotary drilling equipment. However, effective bottom of hole cleanout can be accomplished using airlift tools or downhole pumping.



Figure 3: Reverse Circulation Drilling Equipment



Figure 4: Chisel (left), Hammergrab (right)

GEOTECHNICAL SITE INVESTIGATION

Large drilled shaft projects require particular attention to construction issues during the geotechnical site investigation. In addition to the normal design parameters, critical information related to construction includes:

- Rock characterization and compressive strength
- Groundwater and potential for artesian conditions during construction
- Boulders or cobbles
- Sequence of construction operations and potential effects

The author is aware of several cases in which characterization of rock was limited to properties solely for design intent to the exclusion of

construction considerations, and costly differing site condition claims were the result. Proper sequencing of construction operations can also be critical, especially when there may be multiple contracts on a major project. For example, there is potential for lost ground around the shaft excavation due to cobbles and boulders and such soil movements can affect nearby operations or existing structures. Pile driving vibrations or vibrations from other sources can interfere with stability of shaft excavations.

One potential method of dealing with uncertainty in subsurface conditions on major projects is the use of a Geotechnical Baseline Report (GBR). This approach has been used on tunneling projects with success for years and has potential to improve our methods for defining conditions for bidding purposes on drilled shaft projects. A GBR is issued to specifically define geotechnical conditions as a baseline for bidding so that contractors can more fairly include "contingency" costs in their bid. Vague or exculpatory language is avoided in a GBR so that the basis for each bid is the same. Conditions that are more adverse than defined in the GBR (for example, more than 20 hours spent removing obstructions or boulders) are paid on a unit price basis. The use of a GBR has the potential to reduce the costly litigation associated with differing site conditions and improve the potential for true partnering on major drilled shaft projects.

DESIGN OF REINFORCEMENT FOR CONSTRUCTABILITY

Large, heavy reinforcing cages pose construction challenges of lifting, splicing, and placing the cage, and also from the standpoint of concrete flow through the cage. Multiple cranes, multiple pickup points or "tipping frames" may be required to lift the cage, as illustrated in Figure 5. Very long cages may need to be spliced while suspended over the hole, thus greatly increasing the exposure time during which the hole is open without agitation as discussed previously. Extremely congested reinforcing cages pose an impediment to concrete flow and can lead to entrapment of debris or low strength concrete outside the cage.

Some of the key components that can facilitate constructability are:

- Bundle the rebar to increase openings through the cage
- Avoid tight spacing in transverse reinforcing (spirals or hoops) by bundling the bars
- Avoid the use of multiple cages, which pose an extremely difficult condition for concrete placement underwater
- Utilize the permanent steel liner to reduce the longitudinal reinforcement and to provide confinement so that the transverse reinforcement is reduced.

The issue of utilizing the permanent steel liner for structural design has tremendous potential to improve constructability. In addition, the use of a permanent steel liner for bending stresses can provide a foundation with excellent strength and ductility in flexure for extreme event loads such as seismic or vessel impact forces. When reasonably cleaned using a wire brush or hydro-jet on the interior of the casing after drilling, good bond at the steel/concrete interface can be achieved. The confinement provided by the steel liner eliminates the need for tightly spaced spirals or hoops.



Figure 5: Lifting of Large Reinforcing Cages

The data presented on Figure 6 illustrate a comparison between two 8 ft diameter drilled shafts subjected to cyclic lateral load testing for the Cooper River Bridge in Charleston, SC (Brown and Camp, 2002). The more flexible shaft C-3 was constructed using a temporary casing that was removed prior to testing while shaft C-1 included a permanent casing of 1 inch wall thickness. Shaft C-1 displaced less than half as much at similar load and had significant additional strength in bending when shaft C-3 was at yield. Other than the casing, both shafts were reinforced similarly. The casing for shaft C-1 was installed with a vibratory hammer prior to drilling and no special cleaning tools were used.

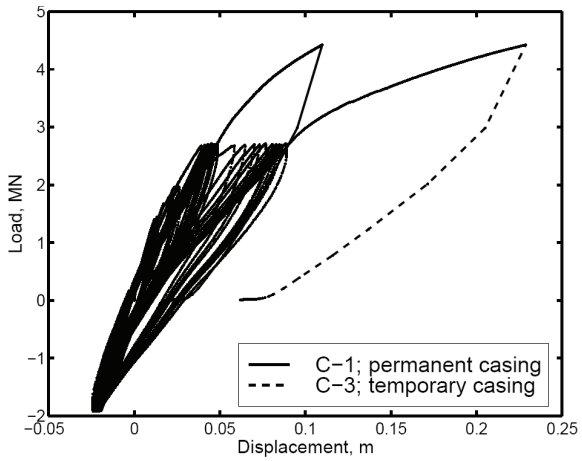


Figure 6: Comparison of Lateral Response of Two Drilled Shafts

CONCRETE PLACEMENT TECHNIQUES

Critical issues relating to underwater placement in large or deep drilled shafts include the initiation of flow through the tremie and control of concrete during casing removal. Gravity tremie placement is preferred over sealed pump line systems for deep shafts, although pumping into the top of the gravity tremie provides an excellent delivery system. A sealed pump line in a very deep shaft can result in negative pressures within the line that can lead to segregation and blockage within the line (Yao and Bittner, 2007). For very deep shafts, the use of an open segmental tremie is generally required; a sealed tremie with a closed end plate would be so buoyant and long that control of the empty tremie is difficult.

With an open tremie pipe, the initial charge of concrete is separated from the fluid in the pipe using a plug. The tremie plug will be compressed under very high pressures at depth and should maintain a sufficient width to keep concrete from bypassing the plug.

Even more critical than the plug, is the rate and volume of concrete delivery in the initial concrete charge to the tremie. With the extremely long tremie and large shaft diameter, many cubic yards of concrete may be required to achieve a head of concrete in the shaft above the bottom of the tremie. If a slug of concrete is discharged into the tremie without continuous resupply of concrete or control of the flow from the bottom, the inertia of this initial slug of concrete can

result in a very low head of concrete inside the tremie which would result in a breach as the water or slurry flows back into the tremie. This breach can be avoided if the tremie operator can hold the tremie within a few inches of the bottom so as to control the flow from the tremie and maintain a head of concrete within the tremie that exceeds the water head in the shaft, as illustrated in Figure 7. It is important that concrete delivery at this initial stage be provided rapidly and continuously, if possible.

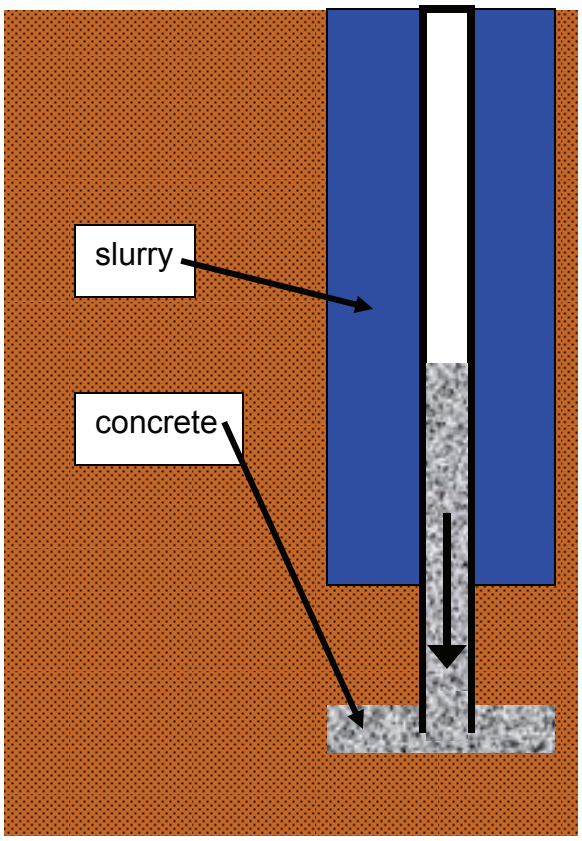


Figure 7: Initiation of Concrete Placement with Gravity Tremie

Concrete placement into a deep temporary casing also requires careful control of concrete volume during casing extraction. If there was difficulty in achieving a seal around the base of the casing during drilling, it is quite possible that some soil loss can occur around the outside of the casing with a resulting void. When the casing is extracted, the volume of concrete required to fill a void may result in a precipitous drop in the concrete level within the casing as shown in Figure 8. In a similar manner to the tremie discussed previously (the temporary casing might be thought of as a very large diameter tremie), a drop in head of concrete within the casing can lead to a breach of the seal below the casing or tremie, if a tremie is used inside the temporary casing.

Note that the withdrawal of a temporary casing from inside a permanent casing is subject to the same concerns regarding maintenance of a head of concrete within the inner temporary casing; water or slurry is typically present in the annular space between the two casings and must be displaced from the bottom up by the concrete.

THE NEED FOR HIGH PERFORMANCE DRILLED SHAFT CONCRETE

The most critical performance requirements for concrete are related to workability and thus the concept of "high performance" material emphasizes the construction aspects of the mixture in addition to hardened properties required to meet structural design requirements. Important components of a good mixture design and installation plan include requirements for workability for the duration of the concrete placement operations, passing ability, resistance to bleeding, and low heat of hydration.

In order to flow laterally from the discharge point and fill the shaft without entrapment of drilling fluids or laitance from the underwater surface of the fluid concrete, the concrete must flow smoothly through the reinforcing cage under its own buoyant weight without "piling up" near the tremie. A mixture with the desired workability will not result in more than a few inches of difference in height between the top of the concrete surface near the tremie and the concrete on the outside of the reinforcement as shown on Figure 9. The inability of the concrete to flow laterally can lead to entrapment of laitance (the contaminated concrete on the top of the rising column of concrete) and encapsulation of pockets of low strength as described by Brown (2004). Yao and Gerwick (2004) describe the desirability of underwater concrete to flow laterally in a "bulged" flow pattern with a relatively flat, smooth top surface rather than as a "layered" flow pattern which can

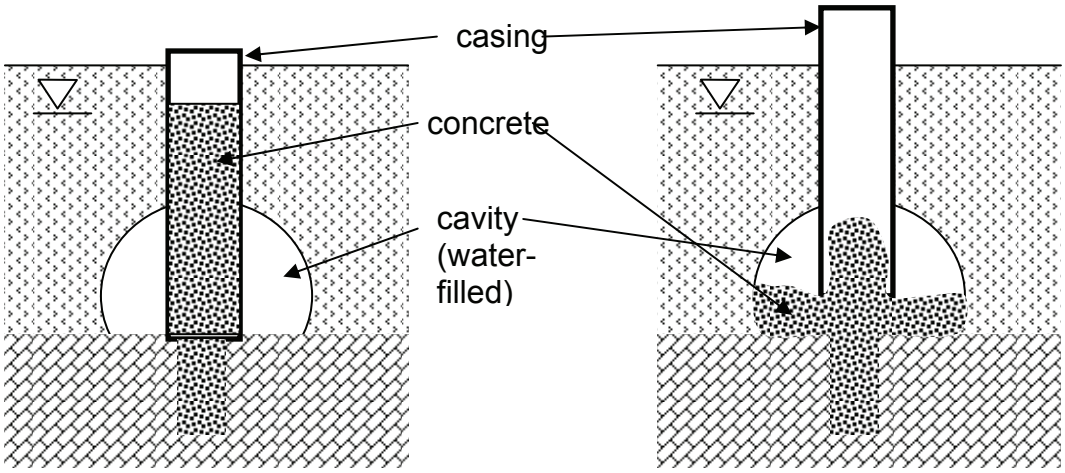
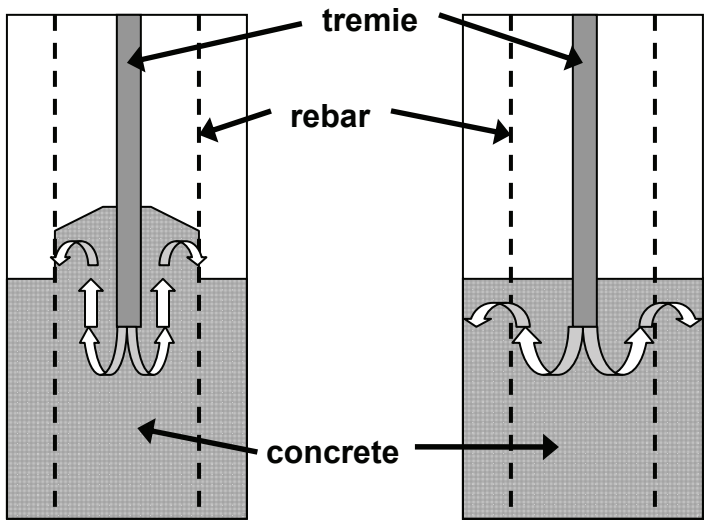


Figure 8: Loss of concrete into cavity during casing extraction (Brown, 2004)



Concrete with inadequate workability

Concrete with good workability and filling ability

Figure 9: Concrete Flow in Under Tremie Placement

result in steeply sloped and rugged top surface that increase the exposure of concrete surfaces to water.

Workable concrete for tremie placement in drilled shafts must be a flowable, cohesive, self consolidating mixture that is easily placed without external vibration. Although the use of the term “self-consolidating concrete” or SCC has been used in recent years with reference to mixtures with ultra workability in conventional concrete applications, drilled shaft concrete has always been intended as a self consolidating mixture. Traditionally, drilled shafts have been constructed using slump as the sole indication of workability. Alternative methods to describe workability may have application in large diameter drilled shafts.

Concrete slump ranging from 175 to 225 mm (7 to 9 inches) has been found to provide adequate workability for drilled shafts up to 2.5 m (8 ft) in diameter if the reinforcing cage has openings not less than 150 mm (6 inches). For mixtures requiring greater workability, the use of slump flow and/or the L-box (or J-Ring) tests may be more suitable for assessing the properties of the fresh concrete. The slump flow is a simple test performed with a conventional slump cone, but measurements are performed on the diameter of the resulting fluid concrete mixture rather than the height of the cone. Based on some initial field trials of drilled shaft construction using SCC-type mixtures (Brown et al. 2005), slump flow requirements in the range of 450 to 600 mm (18 to 24 inches) appear suitable for drilled shaft construction.

Concrete mixtures can be designed with high workability by using suitable aggregates and gradation and the proper dosage of water reducing admixtures. Rounded gravel aggregate sources are preferred over crushed stone, and coarse aggregates with a No. 67 or No. 78 gradation are preferred over a No. 57 in terms of workability. In general, an increase in the sand content in proportion to coarse aggregate will provide increased workability and passing ability with less tendency for segregation; a sand to total aggregate ratio (by volume) from 0.44 to 0.50 has been found to work well in drilled shaft mixtures. Water reducing admixtures in current use include polycarboxylate-based materials, which are preferred over the older naphthalene-based water reducers that have the potential to produce a “flash set”.

For large diameter shafts which can often require 300 to 500 m^3 (400 to 650 yd^3) of tremie-placed underwater concrete, retention of workability is critical. The dosage of retarding or hydration control admixtures must be selected to ensure that the concrete retains adequate workability to allow the tremie placement to be completed. Loss of workability will lead to difficulties in maintaining flow through the tremie, with attendant flaws in the shaft. It must be noted that hydration control is highly temperature dependent.

Difficulties with tremie placement associated with loss of workability are illustrated from a project record of over-water placement of concrete on a bridge project, shown on Figure 10. In this particular instance, there were difficulties and delays in loading the delivery barge (denoted as “traveling hopper”) and the mixture had sufficient retarder to maintain workability for only about 4 to 5 hours. Approximately 5 ½ hours after the first concrete was batched, the concrete became stuck in the tremie and the crane operator had difficulty lifting the tremie (which then suffered a failure of the rigging). When the tremie was finally pulled free, concrete was unable to flow freely from the tremie and flow was resumed only after jigging the tremie up and down. Subsequent integrity test results revealed poor quality concrete at the elevation corresponding to this event and expensive shaft repairs were required.

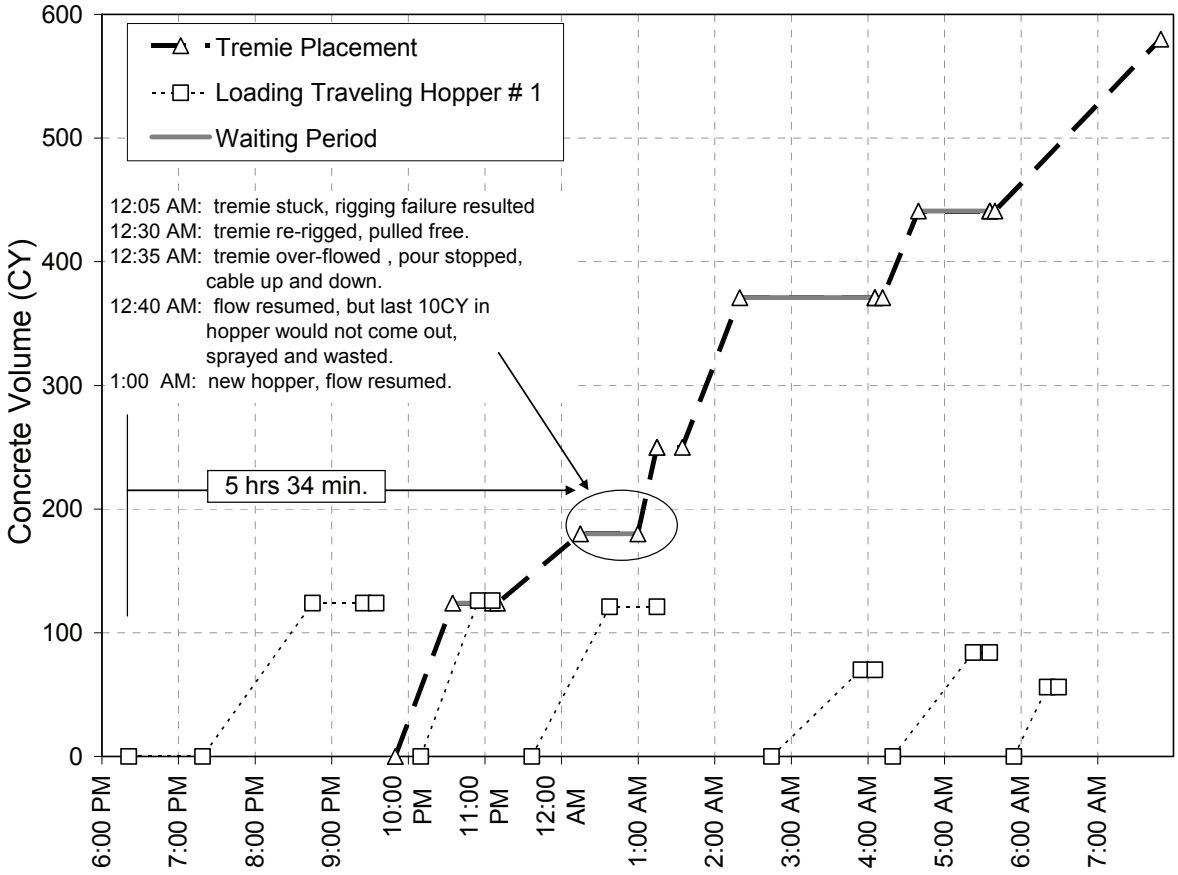


Figure 10: Placement Difficulties Associated with Loss of Concrete Workability

For drilled shafts with such high workability requirements, a mixture with low bleeding is necessary. Mixture characteristics relating to bleeding are also closely related to those affecting segregation, and a concrete mixture with a very high workability requirement is more susceptible to bleeding and/or segregation concerns. Ground conditions also play a role; low permeability cohesive soils are more conducive to bleeding concerns than sandy soils which allow excess water in the mixture to escape. The worst conditions for bleeding occur when there is a long steel casing that prevents excess water in the concrete from escaping into the surrounding soil.

Low bleeding can be obtained by using more cementitious materials and by using viscosity-modifying admixtures (aka, anti-washout admixtures). ASTM C 232 is an available test method to assess potential bleeding in a concrete mixture, and drilled shaft concrete should exhibit little to no bleeding in this test. This test method is unable to subject the concrete to high pressure conditions present in deep shafts, however. Considerations of workability dictate that there is water in a mixture that exceeds the amount of water needed to hydrate the cementitious materials. Reduction in the water-to-cementitious materials ratio will reduce bleeding, but mixtures that are exceptionally high in cement content can have other problems related to heat of hydration and set time. The total cementitious content can be increased without increasing net portland cement content by using more fly ash or ground-granulated blast furnace (GGBF) slag. Viscosity modifying admixtures (VMA) can be effective at binding up free water prior to setting of the concrete.

When high dosages of fly ash or GGBF slag are used, the strength development will be slower when compared to mixtures with only Portland cement. However, when cured, these mixtures may exhibit higher long-term strengths. In these cases it is advisable to test the specified compressive strength at 56 or 91 days in lieu of the normal 28 day specified strength for conventional concrete.

Control of temperature is important for drilled shaft concrete in order to control setting time and the heat of hydration. Excessive concrete placement temperatures will accelerate the rate of hydration significantly and reduce the concrete's workability. This effect is nonlinear and rate of hydration increases dramatically with temperature in excess of 70°F. The measurements presented on Figure 11 demonstrate the effect of initial temperature on the heat generated within the concrete as a function of time. This generated heat produces more rapid setting in the mixture and a significantly higher heat of hydration in mass concrete.

The data from Figure 11 demonstrate the benefits of controlling the fresh concrete placement temperature in terms of controlling heat of hydration. Temperature controls at the batch plant can be achieved by substituting some of the mixing water with ice, or with liquid nitrogen thermal probes that are used to cool the concrete in the truck.

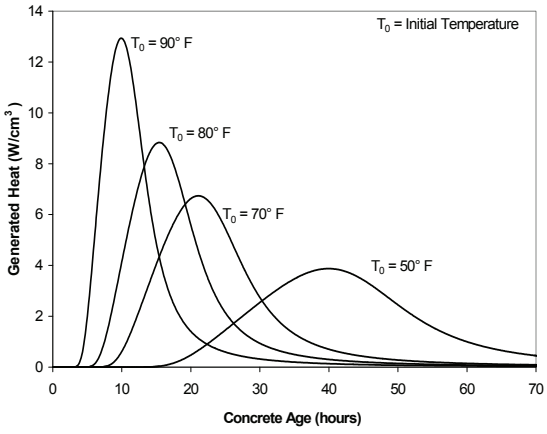


Figure 11: The effect of different initial mixture temperatures on the temperature development during adiabatic conditions (Schindler 2002)

The use of Type II cement and high dosages of either Class F fly ash or GGBF slag are often the best options to control heat of hydration. Concrete mixtures with high dosages of fly ash or GGBF slag will tend to generate less heat of hydration and are also less prone to delayed ettringite formation (DEF); temperatures up to about 178°F can be tolerated without significant concerns of DEF.

SUMMARY

Large diameter and very deep drilled shafts require special efforts during construction to ensure reliability. Excavation techniques often differ from conventional shaft drilling techniques because of the size and depth and vulnerability to difficult subsurface conditions. Geotechnical investigations must be conducted in such a way as to address construction issues because of the costs and risks involved in construction. Reinforcement should be designed to improve constructability, and the use of permanent steel liners as an integral part of the structural design of the foundation is encouraged. The special concrete requirements for this application should be considered, and the author proposes that the concept of "high performance concrete" should be applied to drilled shaft mixtures to incorporate critical performance requirements related to workability. Specific performance requirements that are particular to drilled shaft applications are described, including workability for the duration of the placement operation, passing ability, resistance to bleeding, and low heat of hydration. Perhaps the most important guideline is that each drilled shaft project should have a specific mixture developed to meet the requirements for that project.

ACKNOWLEDGEMENTS

The author gratefully acknowledges the contributions of Dr. Anton Schindler of Auburn University for his help with concrete mix characteristics, and to Malcolm Drilling Co. and Treviicos for many of the photographs of equipment and tools used in this paper. Finally, the author would like to express his gratitude to the late Mike O'Neill, in whose honor this paper is presented, for his many years of patient mentoring on this and many other subjects of foundation engineering.

REFERENCES

Brown, D., (2004). "Zen and the Art of Drilled Shaft Construction," *GeoSupport 2004*, ASCE, GSP 124, pp. 19-33.

Brown, D. A. and Camp, W.M., 2002. "Lateral Load Testing Program for the Cooper River Bridge, Charleston, SC" Geotechnical Special Publication No. 116, ASCE, pp. 95-109.

Brown, D. and Schindler, A. 2007. "High Performance Concrete and Drilled Shaft Construction" paper accepted for publication, Geotechnical Special Publication, ASCE, 11p.

Brown, D., Schindler, A., Bailey, J., Goldberg, A., Camp, W., and Holley, D. 2007. "Evaluation of Self-Consolidating Concrete for Drilled Shaft Applications at the Lumber River Bridge Project, South Carolina" paper accepted for publication, Transportation Research Record.

Mullins, G. (2006). Personal communication.

Schindler, A.K. (2002). "Concrete Hydration, Temperature Development, and Setting at Early-Ages," Ph.D. Dissertation, The University of Texas at Austin, Texas.

Schindler A.K., and Folliard K.J. (2005). "Heat of hydration models for cementitious materials," *ACI Materials Journal*, Vol. 102, No. 1, 2005, pp. 24-33.

Yao, S. and Bittner, R. (2007). "Underwater Concrete in Drilled Shafts: The Key Issues and Case Histories," paper accepted for publication, Geotechnical Special Publication, ASCE, 11p.

Yao, S. and Gerwick, B. (2004). "Underwater Concrete," *Concrete Int'l*, Feb., pp. 77-82.

DESIGN OF THE DRILLED SHAFT FOUNDATIONS FOR THE COOPER RIVER BRIDGE

Liang Shen, PE, Ben C. Gerwick, Inc. San Francisco, CA
Osama Safaqah, PhD, Ben C. Gerwick, Inc. San Francisco, CA
Robert B. Bittner, PE, Ben C. Gerwick, Inc, San Francisco, CA

The Cooper River Bridge, the longest cable-stayed bridge in North America, replaces two existing bridges along U.S. Highway 17 and connects the City of Charleston and the town of Mount Pleasant, South Carolina. Two diamond shaped towers support the 1,546 ft long main span over Cooper River and allows for a 1000 ft wide navigation channel. The Charleston high-level approach is 4351 ft long and provides a 250 ft wide navigation channel for Town Creek, while the Mount Pleasant high-level approach is 2,090 ft long. Due to the high seismicity in the region, potential vessel impact, and hurricanes, large lateral loads are expected. From various types of foundations, 10-foot diameter drilled shafts were selected for their high capacity against vertical and lateral loadings. The shafts are founded on a stiff to very stiff lightly cemented calcareous sandy clay or sandy silt layer, called Cooper Marl, which underlies the coastal sediments of the interbedded clays and sands. A group of 11 shafts supports each main tower, while a rock island protects it from vessel collision. A group of 4 to 8 shafts foundations support the other piers of the main span unit. A pair of shafts supports the High Level Approach piers. The shaft tip elevations vary from 120 ft to 230 ft below water line. An elaborate geotechnical investigation was conducted on the site, including a load test program on full-scale shafts under axial and lateral loads. The results of the tests were used to calibrate the lateral and axial soil resistance. The objective of this paper is to present the different aspects of the bridge foundation design.

INTRODUCTION

The new Cooper River Bridge, stretching approximately 3 miles, connects the city of Charleston and the town of Mount Pleasant along Highway 17 in South Carolina. As shown in Figure 1, the bridge crosses the Town Creek and Cooper River channels while passing through Drum Island and is currently the longest cable stay bridge (with a main span length of 1,546 ft) in North America. The wide main span allows for both widening of the navigation channel to 1,000 ft and deepening to accommodate larger vessels. The bridge carries a total of eight lanes of traffic and a shared pedestrian-bicycle lane. Officially opened for traffic on July 16, 2005, the Cooper River Bridge replaces the Grace Bridge, completed in 1929, and the newer 3-lane Pearlman Bridge, completed in 1965.

This $632 million design-build project includes a main span unit bridge structure, high-level approaches, low-level approaches, ramps and interchanges on both sides of the crossing. The contract was awarded to Palmetto Bridge Constructors, a joint venture of Tidewater Skanska and HBG Flatiron by South Carolina Department of Transportation, on July 2nd, 2001. The design team consisted of Parsons Brinkerhoff as the design manager and designer of the main span superstructure, Buckland and Taylor as designer for the superstructure of the high-level approaches, and Ben C. Gerwick, Inc. (BCG) as designer for the foundations of the main span unit and high level approaches, the main pier artificial protection islands, and vessel collision risk analysis.

SITE CHARACTERIZATION AND SUBSURFACE CONDITIONS

Major site investigations were carried out in 1993, 1999 and 2000. These investigations included soil test boring, lab index testing, consolidation testing, and tri-axial shear

testing. The last investigation, in 2000, was part of the design-build contract. All together, 148 soil test borings and 63 CPT soundings, ranging in depth from 20m to 107m, have been made in the proximity of the bridge. Figure 2 shows the subsurface conditions established by these investigations along the bridge alignment. An in-depth discussion and summary of site characterization and subsurface conditions for the bridge site was presented by Camp (2004).



Figure 1: Cooper River Bridge Site Plan

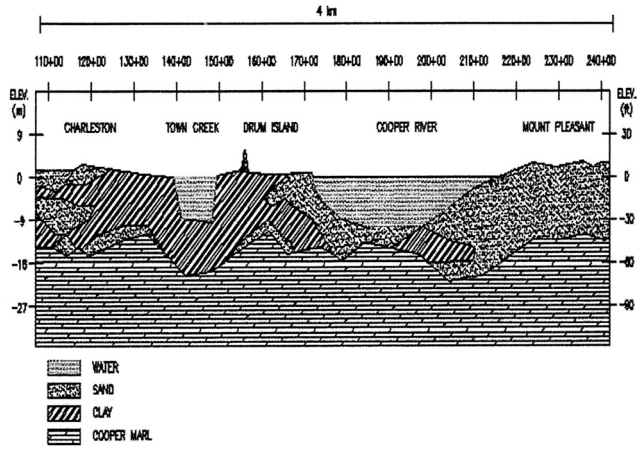


Figure 2: Generalized subsurface conditions

Most of the bridge alignment crosses over water or low-lying tidal, salt marshes. At the Town Creek and Cooper River channels, the mudline extends down to El. –56 ft and –45 ft, respectively. On the Charleston side, the upper soil strata consists of soft to medium stiff silty clay to sandy clay with an undrained shear strength (Su) in the range of 200 to 700 psf. At Drum Island, an active dredge disposal site, the upper soil consists of 25 ft of clayey sand dredge spoil underlain by a soft to medium stiff clay stratum with Su in the range of 200 to 800 psf. At both the Charleston shoreline and Drum Island, there are very soft clayey marsh deposits up to 35 ft thick. On the Mt. Pleasant side, the upper deposits consist of loose to dense sand with SPT blow counts ranging from 0 to 58. Cooper Marl, a cemented calcareous stiff to hard silty clay and clayey silt underlays these recent deposits.

The surface of the Cooper Marl is at an elevation –42 ft to –55 ft mean sea level, but at Town Creek it is as deep as –77 ft. Throughout the entire site the Cooper Marl is about 350 ft deep. This formation is highly plastic with OCR from about 3 to 6. It has a fines content of 75 to 90%, a calcium carbonate content, which is a measure of the remains of microscopic marine organisms, of 60 to 80%, and a clay fraction of 20%. The effective friction angle of the formation is about 43 to 46 degrees with a relatively high void ratio of 1 to 2.0 and a virgin compression index (Cc) of 0.6 to 0.8. The undrained shear strength (Su) is high with average values of 2.2 to 5 ksf and reaching 20 ksf below elevation –170 ft. The average liquidity index (LI), plasticity index (PI), and water content are 68%, 34%, and 48%, respectively.

FOUNDATION CONFIGURATIONS

The New Cooper River Bridge is a cable-stay bridge with a main span of 1,546 ft. The bridge has the longest cable-stay span in North America, which offers a 1,000 ft wide navigation channel and a vertical clearance of 186 ft. The approximately three-mile-long bridge, including the main span unit (with a 1,546 ft main span, two 650 ft side spans, and two 225 ft anchor spans for a total suspended span length of 3,296 ft, see Figure 3), the east and west high level approaches, ramps, and interchanges, were designed and constructed in four years.

The Cooper River Bridge is designed to withstand very large axial and lateral loads due to the region's high seismicity and hurricanes. To achieve a large lateral capacity, the bridge is supported by drilled shafts ranging from 8 to 10 ft in diameter. Each drilled shaft has a permanent 10'-6" diameter,

0.75” thick steel casing embedded a minimum of 5 ft into the Cooper Marl. The advantages of these drilled shafts include providing large axial and lateral capacities, minimizing the number of substructure units, and cost-effective installation.

Main Span Tower Foundations

Each main tower foundation consists of eleven 10 ft diameter drilled shafts, and an 80 ft x 110 ft cap with a depth varying from 15 ft to 18 ft. Rock fill islands that extend from the marl surface to elevation of +12 ft protect the main tower foundations from ship impact by rock fill islands (see Figure 4).

The rock islands surrounding the foundations serve three purposes. The first is to protect the bridge towers from ship collision, which is a concern due to the large amount of freight traffic along the waterway. The second is to provide full embedment for the drilled shafts to resist lateral loads. The third is to facilitate construction of the large concrete pile caps above the waterline.

Main Span Anchor Piers and End Piers

The dimensions and configuration of the anchor piers (Pier 2W, 2E) and end piers (Pier 3W, 3E) are shown in Figures 5 and 6. Pier 2W consists of two columns sitting on a group of eight 10 ft diameter drilled shafts with a cap of triangular ends capable of withstanding a 16,500 kip ship impact load. The cap is 12 ft thick. A 14 ft x 48 ft hollow space in the middle of the cap serves to reduce the weight of the cap. Each drilled shaft supports about 915 kips of the cap weight. Piers 2E, 3W, and 3E also consist of two columns sitting on a group of four 10 ft diameter drilled shafts with a rectangular shaped cap that is capable of withstanding a 7,800 kip ship impact load. The cap is 12 ft thick at the ends (connecting the column and shafts) and tapers to 8 ft in the middle. The cap is also hollow in the middle to reduce weight. For these caps, each drilled shaft will support about 1,160 kips of the cap weight. All the caps have a top elevation of El +7.77 ft

High Level Approach Piers

Typical high level approach piers are two column bents. Each pier column is supported by an enlarged single drilled shaft (Caltrans refers to this type of foundation as a Type II Pile Shaft). Collision struts are provided at waterline between the columns for all water piers (see Figure 7).

SHAFT Axial Load Testing

An extensive load testing program was performed to evaluate the axial and lateral resistance of the drilled shaft foundation (Camp, et al., 2002). The first phase pre-construction load testing took place in the fall of 2000 at three sites: Charleston, Mount Pleasant and Drum Island. This test program included Osterberg load cell tests and Statnamic tests for evaluating both axial capacity and lateral resistance. The test shafts were installed by various methods including wet methods (with bentonite slurry, polymer slurry or plain freshwater as drilling fluid) and a dry excavation method. The test shafts (12 in total) had diameters of 6 and 8 ft, and tip elevations around El. -100 and -150 ft. Two second phase construction stage load tests were performed at each of the two main piers to provide further information for the design of the deeper shafts required at these piers. For practical reasons, 5-ft diameter test shafts were selected and the resulting test data were extrapolated and modified for use in the design of the larger diameter production shafts (Castelli, 2004). The test shafts at the east and west main piers extended to El. -219.2 ft and El. -216.0 ft, respectively. Each test shaft included two levels (at El. –150 ft and approximately 4 ft above the base of the shafts) of Osterberg load cells, with each level consisting of three 21-in diameter load cells with a combined maximum load capacity of 6,000 kips.

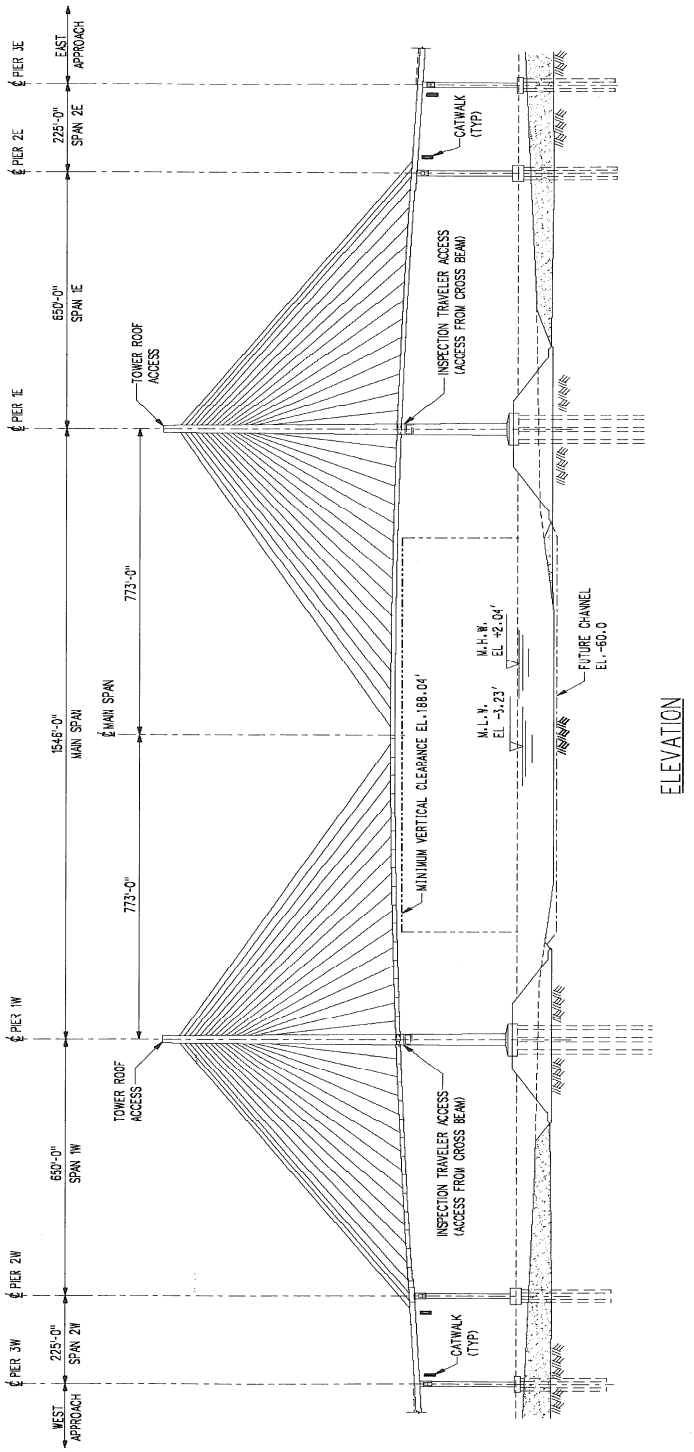
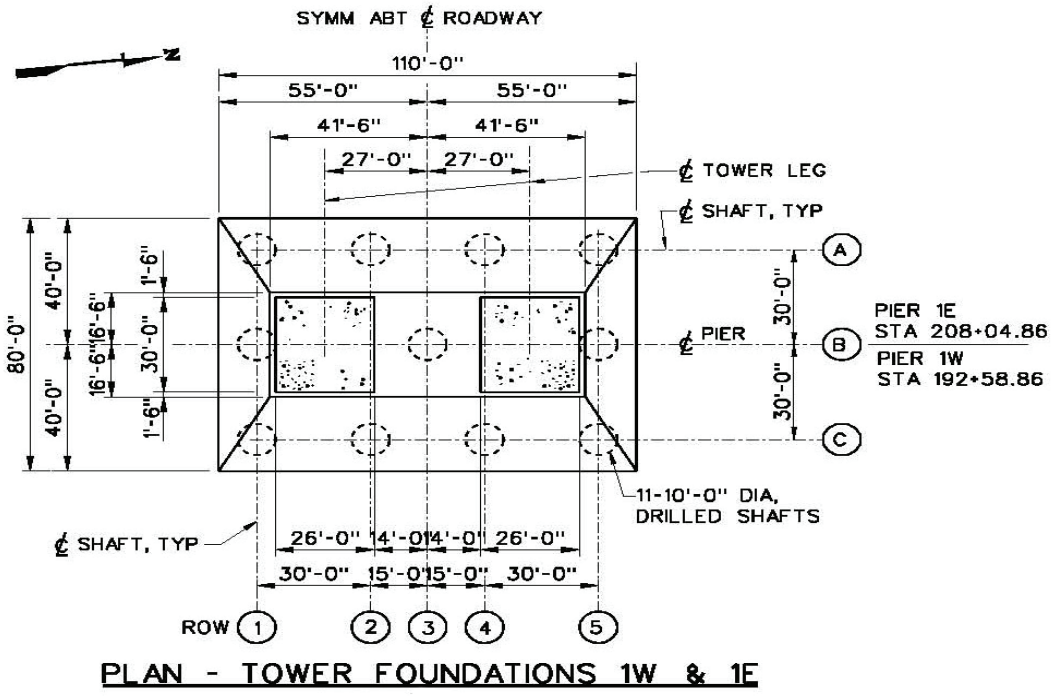
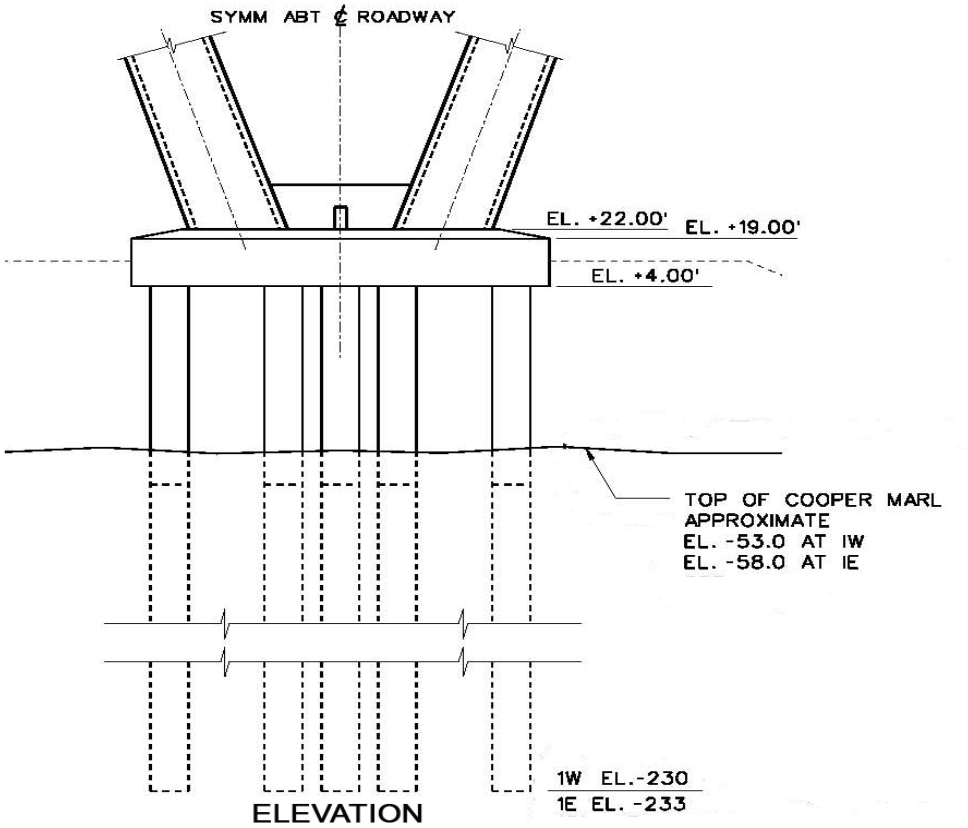


Figure 3: Main Span Unit – New Cooper River Bridge



PLAN - TOWER FOUNDATIONS 1W & 1E



ELEVATION

Figure 4: Main tower foundation

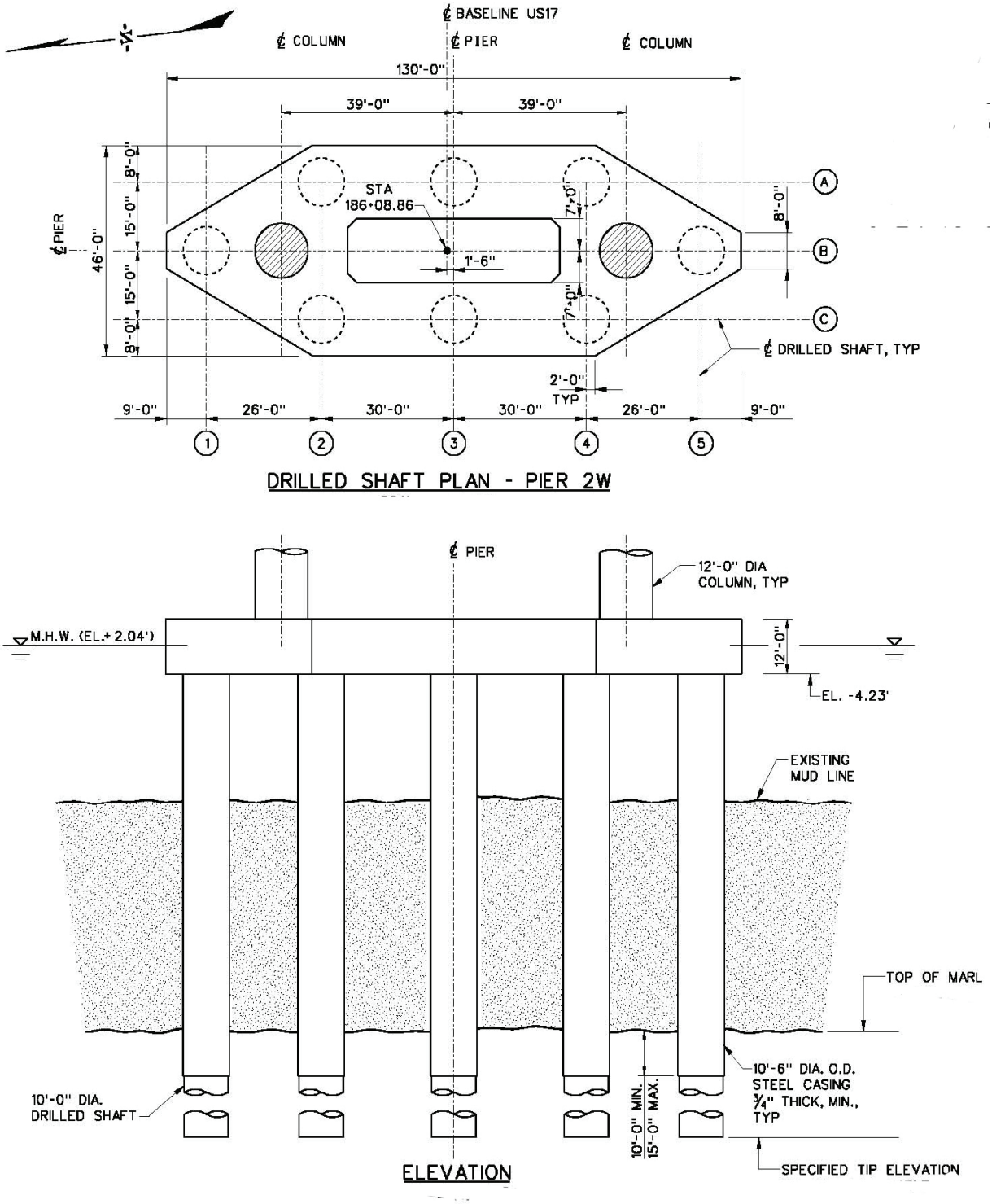


Figure 5: Pier 2W foundation

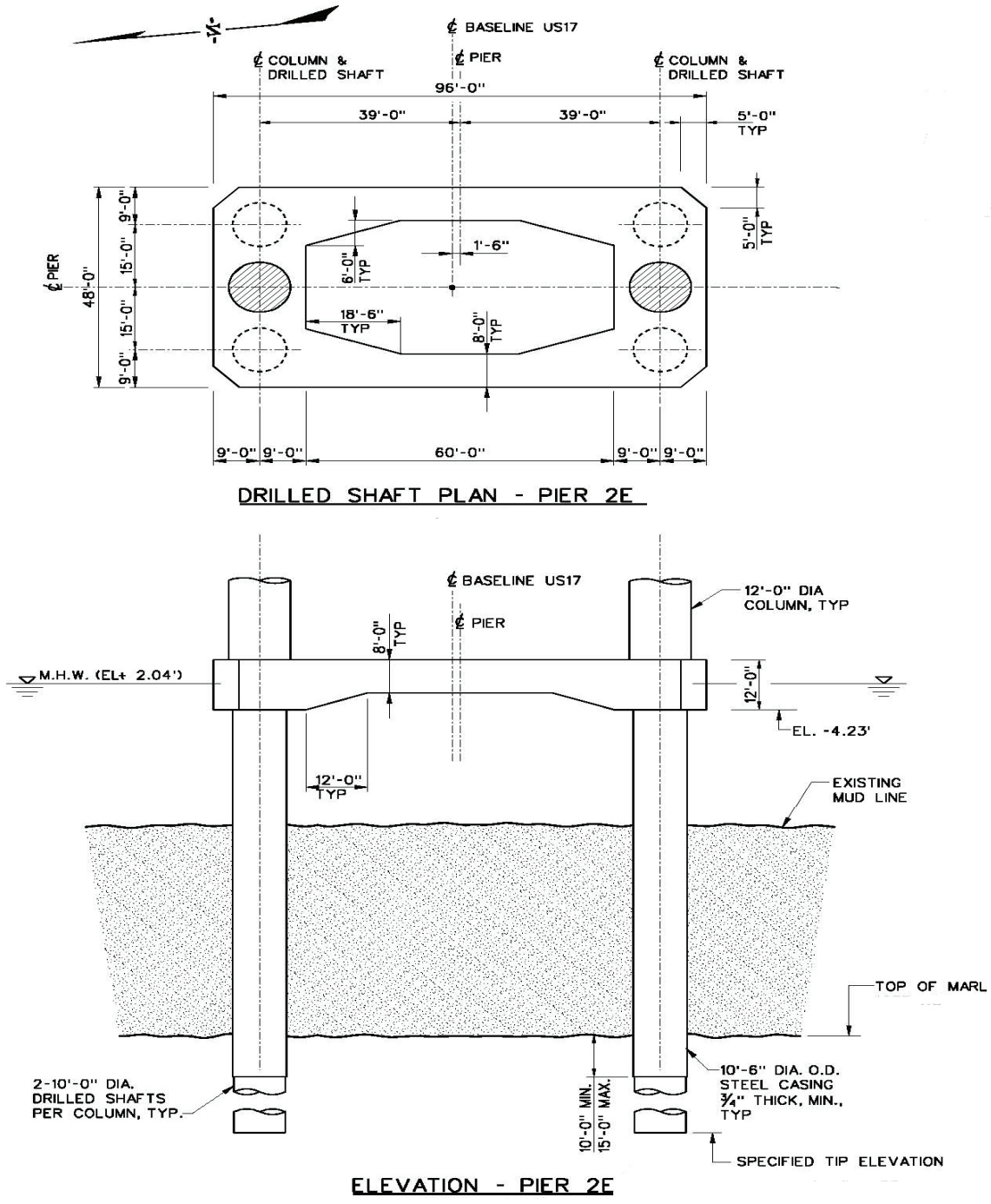


Figure 6: Piers 2E, 3W and 3E foundations

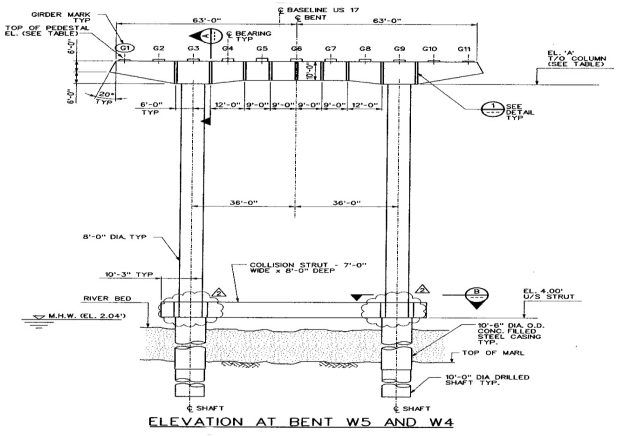


Figure 7: Typical high level approach foundation

Tables 1 and 2 summarize the pre-construction and construction stage axial shaft test results in the Marl formation.

Table 1: Summary of pre-construction axial shaft test results in Cooper Marl

Drilled Shaft Axial Resistance	Range (Ksf)	Average (ksf)
Ult. Unit Side Friction (cased)	-	1.3
Ult. Unit Side Friction (cased)	3.5 to 4.1	3.8
Ult. Unit End Bearing (at El. -100')	43 to 61	54
Ult. Unit End Bearing (at El. -150')	59 to 80	71

Table 2: Summary of contract axial shaft test results in Cooper Marl

Drilled Shaft Axial Resistance	Range (ksf)	Average (ksf)
Ult. unit side friction (cased)	-	1.25
Ult. unit side friction (uncased above El. -150')	3.65 to 3.99	3.8
Ult. unit side friction (uncased below El. -150')	5.24 (before ultimate reached)	5.24
Ult. end bearing at El. -216'	119 (at 3" Settlement)	119

SHAFT LATERAL LOAD TESTING

After completion of the axial load tests, a total of twelve drilled shafts were subjected to lateral loading at the three test sites. The Charleston site is characterized by 50 to 65 ft of soft clays and organic clays overlying the Cooper Marl. The Mt. Pleasant site is characterized by 50 ft of liquefiable loose sand overlying the Cooper Marl. The Drum Island site is characterized by 30 ft of loose to dense sand overlying the Cooper Marl. Figure 8 shows the soil profile at the three lateral load test sites. Shafts were tested to provide measures of soil response under lateral loading with the following variations (Brown, et al; 2002): (1) shafts with and without permanent steel casings, (2) cyclic loading in both sand and soft clays, (3) lateral loading at a high rate of displacement, (4) lateral loading using the split cylinder technique with embedded O-cells, and (5) test shafts in sand subject to blast-induced liquefaction. Cyclic lateral tests, inertial (statnamic) load tests, and split cylinder tests were performed. Detailed descriptions and summary of these lateral load tests were presented by Brown (Brown et al 2002).

The soil response of the Cooper Marl Formation was most important in design of the bridge foundations. In order to measure soil resistance vs. displacement relationships to significant displacement values, the split cylinder test was performed. This technique was first attempted by O'Neil (O'Neill 1997). With the split cylinder test, the soil resistance

vs. displacement relation is observed and used to generate p-y curves for design. The results of the two split cylinder tests are presented in Figure 9. On the same figure, a computed p-y curve using the Reese's criterion for stiff clay below free water, with the following soil properties: c = 30 psi, k = 500 pci, ε_{50} = 0.005, matches the test results very closely up to a displacement of around 0.04 m (1.6 in).

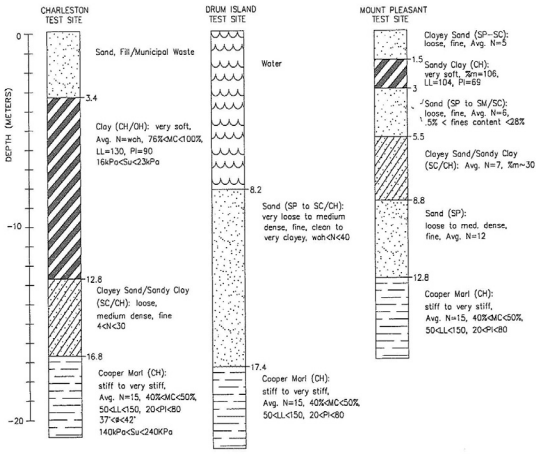


Figure 8: General soil conditions at lateral load test locations

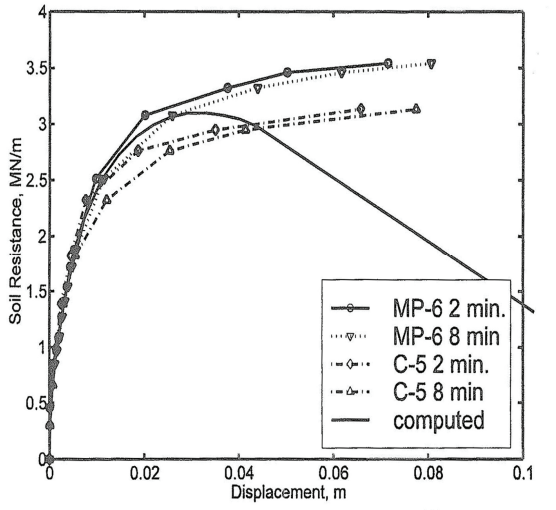


Figure 9: p-y curves from split cylinder test

Major technical conclusions from the lateral testing program include (Brown, et al, 2002):

- permanent casing has a substantial beneficial effect on the structural capacity of a large diameter shaft in bending
- cyclic degradation of the Charleston soft clays was relatively small
- rate of loading effects for 1st cycle dynamic loading of 8 ft diameter shafts in Charleston soft clays were represented by a viscous damping ratio of around 55%
- derived static response captured from inertial lateral loading using the statnamic device was almost identical to static response measured using conventional lateral tests
- split cylinder tests suggest that the Reese p-y criterion for stiff clay below water models the initial static response of the Cooper Marl fairly well
- blast-induced liquefaction effects on Mt. Pleasant sands were characterized using p-y curves for sand with R_u values of 0.7 to 0.85
- the higher R_u value is suggested by the higher rate of loading associated with the rapid inertial lateral loading test; the lower R_u value is associated with the relatively slow cyclic loading and may be influenced by dissipation of pore pressures with time after blasting.

DRILLED SHAFTS AXIAL RESISTANCE DESIGN

In the axial design of the drilled shafts, only combined friction and end bearing in the Marl formation were considered. Friction was neglected at the bottom of the shaft for a length of one shaft diameter to account for strains developed in the marl due to loads applied at the base of the shaft. Shaft load tests confirmed a ultimate friction value of 1.3 ksf within the cased section of the shaft, and an average ultimate friction of 3.8 ksf below the casing within the marl above EL. -150 ft. Therefore, these values were used for the design of all of the drilled shafts except for shafts with a tip elevation above EL. -100 ft and the section of shafts below EL. -150 ft at the main piers.

Based on the pre-construction and construction stage load test results and foundation settlement considerations, the following unit friction and end bearing values were developed for use in designing the axial resistance of all the pier shafts:

Ultimate friction resistance within the cased depth:	**1.3 ksf** *
Ultimate friction resistance in marl, above El. –150:	3.8 ksf
Residual friction resistance in marl, above El. –150:	3.2 ksf
Ultimate friction resistance in marl, below El. –150:	5.8 ksf
Residual friction resistance in marl, below El. –150:	4.9 ksf
End bearing resistance (at 3-inch base settlement):	½ x 119 ksf = 59.5 ksf
End bearing resistance (at 6-inch base settlement):	½ x 130 ksf = 65 ksf

* The ultimate friction value used along the cased length of shaft for determining shaft penetration was reduced to 0.65 ksf (one-half of the value shown) to account for anticipated disturbance to the marl due to installation of the contractor's proposed template support piles in close proximity to the drilled shafts.

Design Factor of Safety

Except at the main piers, factors of safety of 2.0 and 3.0 were applied to the ultimate friction and end bearing resistance values, respectively, for AASHTO Group I loads to account for displacement compatibility at the sides and base of the shaft. At the main piers, compression of the marl bearing stratum and related settlement of the drilled shafts due to the weight of the rockfill island resulted in about 4 inches of settlement at the shaft base. Therefore, for the main piers, a factor of safety of 2.0 was used for both friction and end bearing since displacement compatibility was not an issue. In addition to the above criteria, the design required a minimum factor of safety of 1.3, assuming no end bearing resistance. This later requirement ensures that the shafts have adequate capacity in the unlikely event that undetected problems during construction jeopardize the end bearing resistance.

For AASHTO Group II through VI loads, the factors of safety for friction and end bearing were decreased by 25 to 30 percent, consistent with the AASHTO overstress allowances for these load combinations. For seismic compression loads (2,500 year earthquake), a factor of safety of 1.1 was applied to friction resistance, and a factor of safety of 1.0 was applied to end bearing, consistent with AASHTO guidelines. For seismic tension loads, a factor of safety of 1.5 was applied to friction resistance.

The shaft axial resistance design was carried out by Parsons Brinckerhoff.

Downdrag Loads Induced by Rockfill Island Settlements at Piers 1W and 1E

The weight of the rockfill islands at Piers 1W and 1E will cause settlements of the marl and drilled shaft foundations. Settlements of the rockfill island include immediate settlement due to deformation and elastic compression (estimated to be 5 inches), and long-term consolidation settlement (estimated to be 10 inches).

Due to the settlement of the rockfill islands, the rockfill will settle relative to the drilled shafts, inducing a down drag load to the drilled shafts. At the Piers 1W and 1E islands, these down drag loads are estimated to be 750 kips and 850 kips, respectively, on each drilled shaft. Settlement of the marl relative to the drilled shafts will result in increased settlement of the drilled shafts, and development of down drag forces on the shafts. Along the shaft axis, a "neutral point" will develop that represents the point of zero relative displacement between the drilled shaft and the surrounding marl bearing stratum. For equilibrium, the structure loads and down drag loads above the neutral point will be resisted by a combination of end bearing resistance at the base of the shaft and positive side friction below the neutral point.

The foundation settlement (i.e., the settlement of the top of the drilled shafts after drilled shaft cap construction) was estimated by: (1)

determining the elevation of the neutral point along the shaft axis using the unit friction and end bearing resistance values determined from the load tests, (2) determining the settlement of the marl at the level of the neutral point, (3) setting the settlement of the drilled shaft at the neutral point equal to the settlement of the marl at this same level, and (4) adding the elastic shortening of the drilled shaft above the neutral point to the settlement at the neutral point to estimate the top of shaft settlement. Following the above procedure, the foundation settlement was estimated to be approximately 4 inches at both Piers 1W and 1E.

At Pier 1W, the neutral point was estimated to be at El. –116, and the corresponding down drag load from the marl above this level was estimated to be 6,300 kips. At Pier 1E, the neutral point was estimated to be at approximately El. –120, and the corresponding down drag load from the marl above this level was estimated to be 6,200 kips.

The un-factored design axial loads at Piers 1W and 1E are:

• AASHTO Group I:	11,000 kips
• AASHTO Groups II through VI:	14,500 kips
• Seismic Load (from time history analyses):	19,000 (compression) kips
	5,655 (tension) kips

Considering the above design parameters and loads, the penetration of the shafts are governed by the Group I loads and the final design tip elevations for Piers 1W and 1E are -230 ft and -233 ft, respectively.

For axial design of the shafts, only combined friction and end bearing in the Marl formation were considered. In addition, friction was neglected at the bottom of the shaft for a length of 1 shaft diameter.

DRILLED SHAFT LATERAL RESISTANCE DESIGN

The foundation lateral resistance design is dominated by seismic loads; therefore, this paper focuses on the seismic design aspect of the foundations.

The Cooper River Bridge is located in one of the most seismically active regions in the eastern United States. The largest recorded earthquake in the area occurred near Charleston on August 31, 1886 with an estimated moment magnitude of 7.3. Much of the seismicity in this region is related to reactivation of buried faults and sutures under horizontal compressive stress field in the east-northeast direction. Descriptions and discussions of local and regional geologic/seismotectonic setting, earthquake source characterization and paleoliquefaction seismicity data are summarized in Ref. G5, Ref. G19 and Ref. G31 of Supplemental Criteria for Seismic Design for U.S. 17 Cooper River Bridge.

A two-level earthquake design approach was developed by SCDOT, FHWA and the Seismic Review Panel for this project. The higher level performance criteria cover project Critical Access Path (CAP) structure which included the main spans over the Cooper River, high level approaches, low level approaches, one ramp entering and exiting the bridge on the Charleston side and one ramp entering and exiting the bridge on the Mount Pleasant side.

The Safety Evaluation Earthquake (SEE) is defined as an earthquake event that has a return period of 2,500 years. The design earthquake moment magnitude and the source-to-site distance for the SEE are taken as Mw = 7.25 and R = 33 km, respectively. For the SEE, all structures are designed to maintain life safety and prevent major failure. The CAP structures are designed to respond with repairable damage and non-CAP structures may suffer significant non-repairable damage. For the foundations, all structure elements are designed to remain essentially elastic under SEE event and also designed as capacity protected elements to ensure that damage wouldn't occur in the foundation elements.

The Functional Evaluation Earthquake (FEE) is defined as an earthquake event that has a

return period of 500 years. The design earthquake moment magnitude and the source-to-site distance for the FEE are taken as Mw = 6.5 and R = 45 km, respectively. At the FEE, the CAP structures are designed to respond in essentially an elastic manner (minimal damage). All CAP structures will remain fully operational during and after the FEE. The Non-CAP structures are designed to respond with limited damage, with any damage that does occur being accessible and readily repairable. For the foundations, all structure elements are designed to remain elastic under FEE event.

Site specific ground motion hazard analysis was conducted to develop the design response spectra. The two levels of earthquake considered were the FEE and the SEE. The design horizontal acceleration response spectra on the outcrop at the base of Cooper Marl are presented in Figure 10. The vertical acceleration response spectra were taken as about 80% of the horizontal spectra. As indicated in the figure, the ground shaking intensity for the 2,500–year SEE event is significantly higher than that for the 500-year FEE event, with the SEE to FEE peak ground acceleration (PGA) ratio exceeding 6 and the spectral acceleration ratio exceeding 10 for the period equal to 0.75 sec and shorter. As a result, the design of the Cooper River Bridge is governed by the 2,500-year SEE.

Equivalent linear one-dimensional site response SHAKE analysis (Schnabel et al. 1972) was performed primarily to (1) account for the site amplification effect due to the presence of Cooper Marl and recent deposits, (2) provide design spectra for the preliminary response spectral analysis, and (3) provide ground motion time histories for inelastic time histories analysis.

Three sets of ground motion time histories were developed for the safety evaluation earthquake (ICEC, 2000). For the FEE, one set of ground motion time histories was developed. Table 3 lists the seed acceleration time histories and the PGA, PGV, and PGD values of the resulted response-spectrum-compatible bedrock time histories.

Table 3: Response-Spectrum-Compatible and Seed Time Histories

	Source and M_w of Seed Time Histories	Response-Spectrum-Compatible Time Histories		
		PGA (g)	PGV (in/ sec)	PGD (in)
SEE	Joshua-Tree, 1992 Landers Earthquake, M_w = 7.3	0.66	26	15
	Cerro-Prieto, 1979 Imperial Valley Earthquake, M_w = 6.5	0.65	22	18
	Tabas,1978 earthquake in Iran, M_w = 7.4	0.65	25	16
FEE	Carson-Catskill, 1978 Whittier Narrows Earthquake, M_w = 5.9	0.11	2.9	1.5

Main Span Unit Foundations

The substructures of the main span unit include two main piers (1W and 1E), two anchor piers (2W and 2E) and two end piers (3W and 3E). Response spectrum analysis (GTStrudl) was utilized to perform the preliminary seismic design of these main span unit foundations. The final seismic design was based on the results of full inelastic time history analyses, using the computer program ADINA, which considers spatial variation ground motion time histories to account for wave-passage effects, wave scattering / incoherency effects and local site response effects. Two loading effects were considered in the design of drilled shafts and caps: (1) the inertial effect from the structure, and (2) the kinematic effect from the ground displacements. The kinematic coupled soil-structure interaction effect is accounted for by using nonlinear hysteretic p-y springs, t-z and q-z springs along the drilled shafts while the drilled shafts were modeled as moment curvature elements. The parameters used to derive the nonlinear p-y springs are presented in the Table 4. Figure 11 illustrates the

modeling of spatially varying ground motions (varying in elevation as well as in horizontal direction) that were applied to the support ends of the nonlinear springs to account for the kinematic interaction effects.

From the above analyses results, it was concluded that the plastic moment at the bottom of the column mainly affects the axial forces in the drilled shafts. On the other hand, the moment and shear forces in the drilled shafts are mainly caused by the inertia forces of drilled shaft cap and are not affected by the plastic moment at the bottom of the column.

Table 4: Soil Parameters Used to Define Nonlinear p-y Springs

Soil Type	Friction Angle	Cohesion C (psi)	50% Strain ϵ50	Sub-grade K (pci)	Lique Faction p-multiplier *
Loose to Medium Sand (Reese Model)	30 –34	-	-	20 – 40	0.15 – 0.25
Dense Sand (Reese Model)	36 –38	-	-	60 - 90	-
Soft to Firm Clay (Matlock Model)	-	2 – 7	0.01 – 0.02	-	-
Cooper Marl (Stiff Clay w/ Water)	-	30	0.005	500	-

*The p-multiplier was used to represent the residual strength/stiffness of liquefied loose to medium sand.

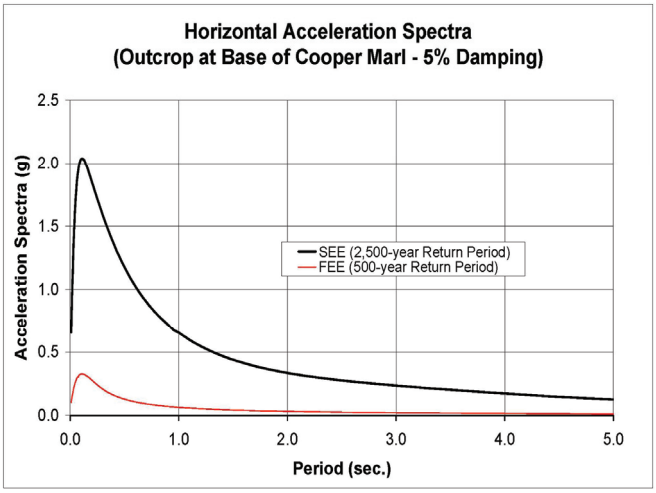


Figure 10: Outcrop horizontal response spectra

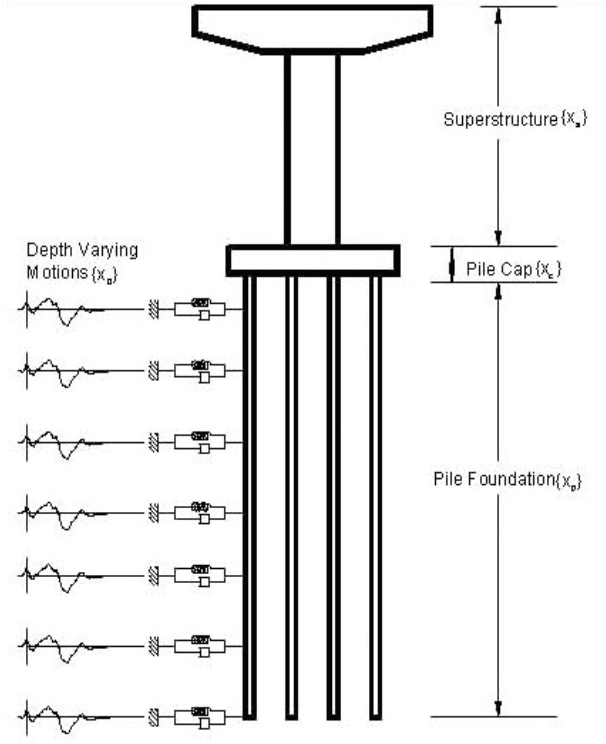


Figure 11: Modeling of kinematic interaction with spatially varying ground motions

BCG developed a computer program for the design of drilled shafts subjected to concurrent loads (axial load combined with flexural bending, and axial load combined with shear forces) that were derived from the elastic and nonlinear time histories results. This program calculates the required longitudinal reinforcement with the assumption that plane section remains plane after the application of loadings and other design assumptions in Section 8.16.2 of AASHTO Standard Specifications. By using this program, the drilled shaft design considers concurrent axial load and flexural bending combination directly retrieved from analysis results of each interval of the time histories. The design cross sections are about 5ft to 10ft along the drilled shafts per GTStrudl and ADNIA models. In addition, the program calculated the required shear strength provided by transverse reinforcement (Vs) at each interval of the time history considering the concurrent axial load effect on the shear strength of concrete.

The drilled shaft caps were designed using the 3-dimensional strut and tie method. In this strut and tie model, the concurrent time history response reactions (axial loads, biaxial bendings and shears) at the top of the drilled shafts were considered to determine the required tie forces and the compressive stress of the struts. For the moment-resisting connections between the members (column/drilled shaft cap and drilled shaft cap/drilled shaft), required amount of horizontal and vertical joint shear reinforcement was determined based on the magnitude of principal tension stress in the joint. BCG also develop a computer program for the cap design which calculated the 3-dimensional strut and tie forces and principal tensile stresses per concurrent time history result at the bottom of the columns and the top of the drilled shafts.

High Level Approaches Foundation

The foundations for the high level approaches (drilled shafts) were design based on the response spectrum analysis and pushover analysis results and the stress and strain demands were confirmed per final ADINA nonlinear time history analysis (similar with the main span unit nonlinear time history models). Along the high level approaches, each pier column is supported by a single drilled shaft. The drilled shaft segment above the mud-line was included in the global model; while the portion of the drilled shaft below the mudline was represented by a 6x6 equivalent stiffness matrix and mass matrix. This modeling technique was found to be very effective in addressing plastic hinging formed at a location above the shaft/column interface, and is a compromise between the stiffness matrix model and the complete model approaches.

Analyses were conducted for SEE seismic loads (Group VII) and non-seismic loads, Groups I, through VI and VIII). In addition, Group VII loads also include results from the transverse and longitudinal pushover analysis. For each drilled shaft, the analyses were conducted for two scour-related conditions: the 50% of the 500-year scour and the non-scour condition.

The computer program LPILE (Ensoft Inc.) was used to compute the drilled shaft 6x6 stiffness matrix at mud-line, also the deflection, shear, bending moment and soil response with respect to depth. The program uses the p-y method in an iterative procedure to model the nonlinear soil response and to analyze the soil-shaft interaction behavior under lateral loading.

BCG developed a computer program for the design of the high level approach drilled shafts. The features of this program are: (1) directly retrieved the LPILE analyses output (shear and bending moment versus depth), (2) calculated the drilled shaft axial load distributions by using the axial loads at the top of the drilled shaft along with its self-weight and skin friction, (3) calculated the required longitudinal reinforcement with was the assumption that plane section remains plane after the application of loading and other design assumptions in Section 8.16.2 of standard specifications of AASHTO, and (4) calculated the required shear strength provided by transverse reinforcement (Vs) while considering the concurrent axial load effect on the shear strength of concrete.

Due to the large design earthquake magnitude (M_w = 7.25), it was determined that all loose to medium dense sand deposits on the Mt. Pleasant side (Piers 5E to 10E) could potentially liquefy under the SEE event (PGA=0.65g). The foundations were designed to accommodate

both the direct seismic loading due to vibration and the loadings induced by lateral spreading. It is considered appropriate to design for vibration and lateral spreading in a decoupled manner as the peak acceleration of the structure typically happens before full liquefaction develops, and therefore, before significant soil movement begins.

In the vibration case, the foundation design considered the following: (1) vertical support of soil above the Cooper Marl was ignored, (2) down-drag forces were added to the design load, and (3) lateral resistance of liquefied soil was reduced to its residual strength and is modeled in LPILE with a p-multiplier of 0.15 to 0.25 (see Table 7.2). Also, liquefaction-induced lateral spreading was considered in the design of the drilled shafts on the Mt. Pleasant side with a continuous layer of liquefiable sand.

In order to estimate the magnitude of lateral spreading, Youd's empirical procedure was used for the SEE (M=7.5, R=30 km) and FEE (M=6.5, R=45 km) events (Youd, et al's 1999). Using an average liquefiable thickness of 40 ft, with an $(N1)_{60}$ less than 15, and an average gradient of 2%, lateral displacements on the order of 3 ft for the SEE and 1 to 2 inches for the FEE were calculated.

For the effects of lateral spreading on the drilled shaft design, two scenarios of spreading conditions were considered: (1) soil flow around the drilled shaft - liquefied soil without crust, see Figure 12, and (2) spreading that displaces foundation with soil – liquefied soil with crust (see Figure 13). For scenario 1, an LPILE analysis was performed by prescribing a 3-ft ground displacement profile within the upper 40 ft of the soil, pushing toward a 10-ft diameter drilled shaft via the p-y spring, and modeling the residual strength of the liquefied sand by applying a p-multiplier of 0.15 to 0.3. The calculated maximum deflection at the top of the shaft is just a little more than an inch and it was concluded that the spread movement has no impact during the SEE event in this case. For scenario 2, it was assumed that a 10 ft thick non-liquefied soil crust rides on the top of the liquefied layer. Similar LPILE analysis was performed and concluded that, for a 5-ft diameter shaft, the deflection at the top of shaft would exceed 30 inches, and for 8-ft diameter shaft, the deflection at the top of shaft would be about 5.5 inches and the response of superstructure to the foundation deflection is considered acceptable. These analyses demonstrate the advantages of using large-diameter drilled shafts in potentially liquefiable soils. The maximum pile deflection caused by lateral spreading was reduced, which eliminated the need for additional liquefaction mitigation. Also, the response of the structure to the foundation deflection as a result of lateral spreading was found to be acceptable.

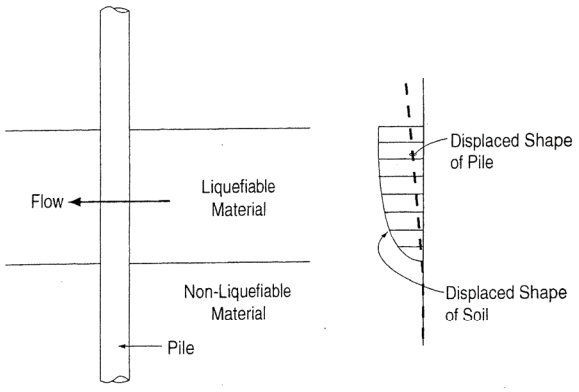


Figure 12: Soil Flow around shaft - liquefied soil without crust

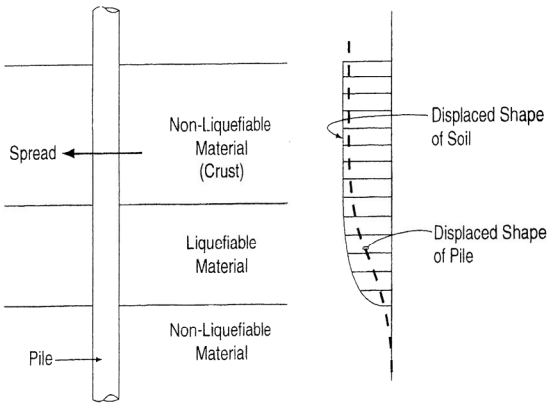


Figure 13: Spreading that displaces foundation with soil – liquefied soil with crust

ACKNOWLEDGEMENT

The client for the Cooper River Bridge project is the South Carolina Department of Transportation. The design-build team, Palmetto Bridge Constructor, was led by Skanska USA, Inc. and Tidewater Construction Company, in partnership with HBG Constructors, Inc. and Flatiron Structures Company. Design was led by Parsons Brinckerhoff.

REFERENCES

American Association of State Highway and Transportation Officials (1999). AASHTO Standard Specifications for Highway Bridges, Sixteenth Edition, 1999 Interim Revisions.

Applied Technology Council (1996). ATC-32, Improved Seismic Design Criteria for California Bridges: Provisional Recommendations.

Brown, D.A. (1999). "An Experiment with Statnamic Lateral Loading of a Drilled Shaft," Proceedings, OTRC'99 Conf., Austin, TX, ASCE GSP No. 88, pp. 309-318.

Brown, D.A., and Camp, W.M. III (2002). "Lateral Load Testing Program for the Cooper River Bridge, Charleston, SC," Proceedings of the International Deep Foundations Congress 2002, Orlando, FL, GSP 116, Vol. 1, pp. 95-109.

Camp, W.M. III, Brown, D.A., and Mayne, P.W. (2002). "Construction Method Effects on Axial Drilled Shaft Performance," Proceedings of the International Deep Foundations Congress 2002, Orlando, FL, GSP 116, Vol. 2, pp. 193-208.

Camp, W.M., (2004). "Site Characterization and Subsurface Conditions for the Cooper River Bridge," Geo-Trans Conference, Geo-Institute of ASCE, Los Angeles Vol. 1, pp. 347-360.

Castelli, Raymond J. (2004). "Design of Drilled Shaft Foundations for the Cooper River Bridge," Geo-Trans Conference, Geo-Institute of ASCE, Los Angeles. Vol. 1, pp. 334-346.

ICEC Inc. (2000). Final Report: Cooper River Bridges Replacement Project – Ground Motion Time Histories, Prepared for Parsons Brinckerhoff Quade & Douglas, Inc. and South Carolina Department of Transportation, 2000.

Lam, I. P, and Martin, G. R. (1986). Seismic Design of Highway Bridge Foundations – Vol. II, Design Procedures and Guidelines, Report No. FHWA-RD
86-102.

O'Neill, M. W., Brown, D. A., Townsend, F. C., and Abar, N. (1997). "Innovative Load Testing of Deep Foundations," Transportation Research Record 1569, Transportation Research Board, Washington, DC, pp.17-25.

Power, M.S., Wells, D.L., Youngs, R.R., and Chiou, B.S.J. (2004). "Design Ground Motions for Cooper River Bridge, Charleston, South Carolina," Geo-Trans Conference, Geo-Institute of ASCE, Los Angeles. Vol. 1, pp. 369-380.

Safaqah, O., "Design of Cooper River Bridge Foundations,: DFI Marine Foundation Seminar, New York, pp 89-98.

S&ME, Inc. (2000). "Phase II Geotechnical Data Summary Report-Cooper River Bridge Replacement Project, Charleston, SC," Report Submitted to Sverdrup Civil, Inc., New York, NY.

South Carolina Department of Transportation (2000). Supplement Criteria for Seismic Design for U.S. 17 Cooper River Bridge, Charleston, South Carolina.

Wang, J-N., Mesa, L., and Sizemore, J. (2004). "Seismic Design of Cooper River Bridge," GeoTrans Conference, Geo-Institute of ASCE, Los Angeles. Vol. 1, pp. 381-392.

Youd, T.L., Hansen, C.M., and Barlett, S.F. (1997). "Revised MLR Equations for Predicting Lateral Spread Displacement, Proceedings of the 7th U.S.-Japan Workshop on Earthquake Resistant Design of Lifeline Facility and Countermeasures Against Soil Liquefaction, August, 15-17, Seattle.

DESIGN AND CONSTRUCTION OF THE SUTONG BRIDGE FOUNDATIONS

Robert B. Bittner, Ben C. Gerwick, Inc. San Francisco CA, USA
Dr. Osama Safaqah, Ben C. Gerwick, Inc. San Francisco CA, USA
Xigang Zhang, Highway Planning and Design Institute, China
Ole Juul Jensen, Ole Rud Hansen, COWI A/S, Lyngby, Denmark

The Sutong Bridge across the lower Yangtze River in China will have, when completed, the longest span (1,088 m) and the highest towers (306 m) of any cable stayed span in the world. The foundations for this record setting span will also be record setting. They are located in water depths exceeding 30 m with maximum flows exceeding 3 m/sec. The soil at the site of the main pylons consists of layers of silty sands and silty clays extending to bed rock at 270 m below river elevation. This paper describes the innovative methods used by the team of foundation designers and constructors to support this record setting bridge at this very challenging site. This paper covers three specific topics related to the foundations of the Sutong Bridge:

- Design and construction of the 131 drilled shaft (2.8/2.5 m diameter and 114/117 m long) under each of the two main pylons, including the post-grouting of all drilled shaft tips.
- Design and construction of the scour protection for the two main pylons,
- Construction methods used to construct the waterline pile caps (113.8 m by 48.1 m by 13.3 m deep) under each pylon.

INTRODUCTION

Detailed design of the Sutong Bridge was performed by The Design Group of Sutong Project. Construction management of the entire project is being performed by the Jiangsu Provincial Sutong Bridge Construction Commanding Department (CCD). COWI A/S and Ben C. Gerwick, Inc. served as special consultants to CCD during design and construction of the bridge.

The width of the Yangtze River at the bridge site is approximately 6 km and the total length of the Sutong Bridge is approximately 8 km. The site conditions for the main towers are extremely challenging. The northern pylon, Pier 4, is located in about 30 m water depth and the southern pylon, Pier 5, is located in about 16 m water depth. The river is subject to both high fresh water run off volumes and tidal effects, creating currents exceeding 3.0 m/sec in the extreme conditions. Maximum potential wave heights at the site exceed 3.5 m. The river is alluvial and subject to rapid changes in bottom contours due to high erosion and deposition rates. The river bed at the northern pylon consists of sandy materials and at the southern pylon the bed material is mainly silty loam and silty clay. These site characteristics create a condition where the river bottom will immediately respond to the introduction of any structure such as a bridge pier or pylon. Hydraulic model studies for the bridge, performed by the Nanjing Hydraulic Research Institute, predicted up to 29 m of scour (100 year return period) at the south pylon with a caisson foundation and up to 24 m of scour (300 year return period) at the same location for a large diameter pile foundation solution (Jensen, 2004).

Bed rock is located at approximately 240 m below the river bottom. The soils in the upper 240 m consists of layered sediments of fine sand , course sand, silty sands and gravels with occasional layers of clay.

The river is the main waterway to the entire Yangtze Basin with heavy barge traffic and up to 50,000-t container ships in the main navigation channel.



Figure 1: Sutong Bridge – 1,088 m Main Span

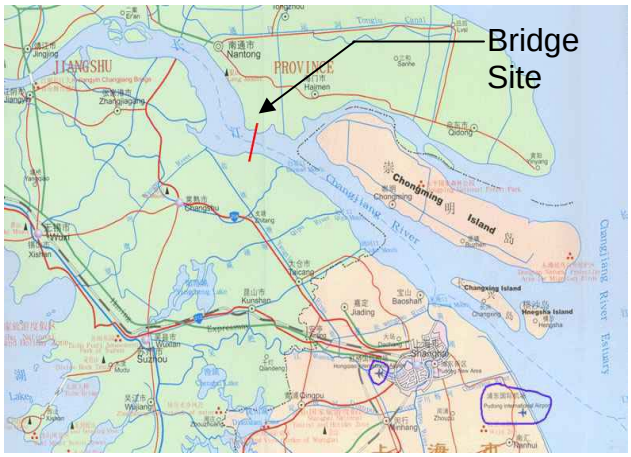


Figure 2: Bridge Location



Figure 3: Sutong Bridge

FOUNDATION DESIGN

The foundation for each A-shaped pylon consists of 131 drilled shafts, 2.8/2.5 m in diameter. See Figure 4 for layout of the pile cap and drilled shafts at each pylon. The drilled shafts are capped by a 13 m deep dumbbell-shaped pile cap with plan dimensions of 113.8 m by 48.1 m.



Figure 4: Pylon Foundation

The bottom of the cap tremie seal is positioned at Elev. -10.0 m, approximately 12.0 m below mean sea level. The drilled shaft casings are 2.8 m diameter with a wall thickness of 25 mm. See Figure 5. The permanent casings extend from Elev. -7.0 to Elev. -53. The drilled shafts beyond the casing tip are 2.5 m diameter and extend to a design tip elevation of -124 at Pier 4 and -121 at Pier 5. Post grouting of the drill shaft tips was performed to increase the total ultimate capacity.



Figure 5: 2.8 m Dia. Drill Casing

The ultimate load capacity of the drilled shafts was confirmed by four offshore load tests, two at Pier 5, the south pylon, and two at the approach piers. The two tests at Pier 5 confirmed an ultimate capacity of 92 MN (20,700 kips). Testing was performed using the Osterberg Cell Method. Test pile SZ5 was tested twice, before and after tip grouting, to give an indication of the increased capacity obtained through tip grouting. The tests indicated that the bearing capacity of the drilled shaft was increased by 20% or 15 MN (3,375 kips) by the tip grouting. The load deformation curve after grouting showed a much more rigid behavior than before grouting. This result demonstrated that the tip grouting had a positive effect on not only the tip but also on the side friction on the lower portion of the pile.

DRILLED SHAFT DESIGN

Drilled shaft design methods have traditionally relied on mobilizing skin friction along the shaft length to resist service axial loads. End bearing, if not discounted, is usually significantly reduced and mainly employed to satisfy extreme load conditions or safety factor requirements. This is mainly due to the concept of strain incompatibility since ultimate end bearing is mobilized at a shaft displacement two or three orders of magnitudes larger than the displacement required to mobilize ultimate skin friction. This is especially true for larger diameter shafts. Moreover, the displacement needed to mobilize significant end bearing is likely to be larger than estimated due to drilling-induced soil disturbance at the tip of the shaft and debris remaining after cleanout. As a result, developments in drilled shaft construction technology have been mainly focused on increasing shaft diameter or shaft length in order to increase shaft axial capacity.

An effective alternate technique that can be used to increase shaft axial capacity is post-grouting of drilled shaft tips. This technique, although introduced four decades ago, has not been widely used in the US despite its significant potential for cost saving and improvement of quality control of drilled shaft construction. This technique works by effectively preloading and densifying the soil and any remaining debris under the tip of the shaft by pressure grout delivered by a system of pipes pre-attached to the reinforcement cage of the shaft. As a result, larger end bearing capacity can be mobilized at the tolerable displacement limit, thus increasing overall shaft capacity without having to increase its length or diameter.

DRILLED SHAFT AXIAL CAPACITY

The maximum demand axial shaft load was determined to be 44.0 MN for the pylon foundation. With an adopted design safety factor of 2.0, the design axial load capacity of the pylon shaft should therefore be at least 88.0 MN.

The Chinese codes which applied to this project determine the ultimate axial capacity of the drilled shaft as the minimum of: 1) the load at which the shaft settlement is 80 mm, 2) the load at which creep is 0.2 mm per hour at the end of 24 hr load application, and 3) the load at which there is a dramatic and sudden change in the load versus displacement curve.

The soils at the pylon site consist mainly of firm to stiff CL clay extending to elevation -45 m followed by layers of medium to very dense fine to coarse sands and silty sands with occasional loam layers. Bedrock is located at approximately 240 m below riverbed. Based on the soil conditions, and the estimated skin friction of a 2.5 m diameter shaft, the design team decided that a shaft tip elevation of -124 m at the northern pylon and -121 m at the southern pylon would be sufficient if a significant percentage of end bearing could be relied on. To achieve this while meeting the settlement and creep criteria, and to minimize the detrimental impact of drilling-induced soil disturbance and remaining debris at the bottom of the drilled hole, post-grouting of the shaft tips was selected as the most economical solution. Also, a 2.8 m diameter permanent steel casing was selected to extend to an average elevation of -53 m to maintain hole stability and to increase lateral stiffness of the foundation in the upper clay layers.

DRILLED SHAFT CONSTRUCTION

Due to the high river currents, all drilled shaft construction was performed from a steel platform constructed over the top of the pier site. In addition, an upstream mooring platform (13 m by 44 m) and a downstream batch plant platform (39 m by 44 m) were constructed immediately adjacent to the main platform. See Figure 6.



Figure 6: Batch Plant Platform

The top elevation of the drill platform was +7 m, approximately 3 m above high water. The main platform was used as both a template to drive the 131 drill shaft casings and to provide a work deck for the drill units. Casings at the northern pylon were driven to grade with a vibratory hammer and at the southern pylon a diesel hammer was used. See Figure 7. After installation of each drilled shaft casing, bracing was added to tie each casing into the work deck, and thereby add rigidity to the entire work deck.



Figure 7: Casing Installation Hammer

Drilling was performed with 8 rotary-drill units positioned on the top of the work deck. Drill bits varied depending on the formations encountered. See Figures 8 and 9. A bentonite slurry with a minimum positive head of 3 m was used to maintain drill hole stability. Both drilling and concreting operation were conducted simultaneously on the platforms. A minimum concrete strength of 5 MPa (725 psi) was required in an adjacent drilled shaft before drilling was allowed. The post tip grouting operation was also performed concurrently with these operations. However, the grouting operations maintained a minimum distance of 50 m from drilling and concrete placement operations in order to avoid hole-instability problems from elevated pore water pressure created by the grouting operation.



Figure 8: 2.5 m Dia. Drill Bit



Figure 9: Drill Bit Exiting Hole

The reinforcing cages were fabricated in four sections and coupled together with threaded mechanical connectors on the work deck over the top of the casings prior to lowering them into the drill hole. See Figure 10. Concrete was placed with a tremie pipe centered in the drill hole.



Figure 10: Reinforcing Cage Installation

Concrete was supplied by a batch plant with a capacity of 100 cubic meters per hour, positioned on the downstream platform. Cement and aggregates were delivered to the platform by barges moored directly to the downstream platform.

Post grouting of the drilled shaft tips was performed with 4 loop-shaped pipes pre-attached to the reinforcing cage. The bottom of each loop turned at the bottom of the cage and extended into the interior of the drill shaft approximately 50 cm. Grout exited the pipes through 6 holes, 8 mm in diameter, drilled in the underside of each loop. A one-way valve was created by encasing the loop in a bicycle tire. To ensure that the system was not plugged during the concrete placement operation, clean water was pumped through the system under pressure to confirm open access to the surrounding tip area. Post grouting was performed with neat cement grout.

POST-GROUTING OF DRILLED SHAFT TIPS

Post-grouting of drilled shaft tips is usually conducted using two techniques; the flat jack, or the sleeve-port (also called tube-a-manchette). In the first technique, grout is delivered by tubes attached to the rebar cage to a steel plate with a rubber membrane underneath at the tip of the shaft. In the second technique, which was used in this project, grout is delivered to the tip through loop-shaped pipes which are pre-attached to the rebar cage. For this project, six tubes were used. The bottom of each pipe, at the tip of the shaft, has a U-shape and extends approximately 50 cm into the interior of the shaft, as shown in Figure 11. Grout was discharged through eight holes 8 mm in diameter in the underside of each U-shaped pipe, which was encased by a bicycle tire to act as a tight fitting rubber sleeve creating a one-way valve. The advantage of this system is that it allows clean water to be pumped under pressure to ensure that the system is not plugged during concrete placement operations, and confirms that an open access to the shaft tip area is maintained.

The major issues in post-grouting of shaft tips, other than the design of the grout delivery system, are to determine the grout pressure and grout quantity. The work of Mullins et al (2006) shows that the level of grout pressure is the most important factor affecting the gain in end bearing and the stiffness in its load-displacement relationship. Another secondary factor is the time period of application of grout pressure. In this project, grouting operations have been controlled by both grout quantity and grout pressure. The project criteria require the grout pressure to reach the targeted level for at least five minutes, and the grout quantity to be at least 80% of the design value. Obviously, since grout pressure acting on the shaft tip is resisted by the shaft skin friction, the maximum grout pressure, and therefore the maximum achievable enhancement in end bearing, is governed by the ultimate skin friction resistance. This also means that the process of post-grouting of shaft tips will cause an upward movement in the shaft as the soil-shaft interface is strained. Therefore, field measurements of the uplift movement of the top of the shaft when related to the applied grout pressure can provide valuable information to verify the axial capacity of production shafts. For the Sutong Bridge, the skin friction of the pylon shafts was estimated as 64 MN; therefore, for a 2.5 m diameter shaft, the estimated maximum grout pressure that can be applied at the shaft tip was 13 MPa plus the buoyant weight of the shaft. Practically, a lower grout pressure was used since the maximum pressure that can be applied in the field was 7 MPa.

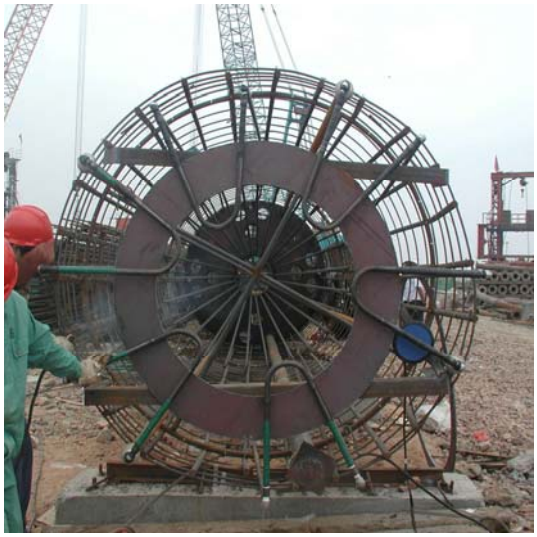


Figure 11: U-Shaped Grouting Pipes at the Shaft Tip

In addition to the upper limit governed by ultimate skin friction, the grout pressure should exceed the hydrostatic pressure at the shaft tip. The project criteria adopted the following method to determine the minimum operating pump pressure:

$$P_g = P_w + \xi \sum_i \gamma_i L_i \qquad (1)$$

where P_g and P_w are the pump and hydrostatic pressures at the shaft tip level, respectively, and γ_i and L_i are the effective unit weight and thickness of each layer (i) above the shaft tip, respectively. ζ is an empirical coefficient for grout resistance, which is a function of the type of soil material at the shaft tip. For sands, ζ ranges from 1.5 to 3.0. Therefore, the estimated minimum operating grout pump pressure in this project was 3 MPa.

Based on the estimated upper and lower grout pressure limits and the required gain in end bearing to meet the design safety factor, the design team decided to use a grout pressure of 5 MPa, which was subject to verification by field tests. Although not used during the design phase of this project, one can estimate the gain in end bearing as a function of the applied grout pressure and shaft settlement using the recent work of Mullins et al (2006), which suggests the following equation:

$$TCM = 0.713(GPI)(\%D^{0.364}) + \frac{\%D}{0.4(\%D) + 3.0} \qquad (2)$$

where %D is the shaft settlement as a percentage of its diameter D, TCM (tip capacity multiplier) is the ratio between the end bearing at a %D settlement to the end bearing at a settlement equal to 5% shaft diameter. GPI (grout pressure index) is the ratio of the applied grout pressure to the ungrouted end bearing at a settlement of 5%D. The ungrouted end bearing at a settlement of 5%D was estimated as 3.5 MPa for the pylon shafts. Therefore, for an applied grout pressure of 5 MPa, i.e. GPI of 1.43, the estimated TCM from this approach for 1%D, 3%D, and 5%D settlement is 1.3, 2.2, and 2.8, which correspond to an allowable end bearing capacity of 4.6, 7.7, and 9.8 MPa, respectively. Therefore, if this approach was used during the design phase of the project it would also indicate that a 5 MPa grout pressure would be sufficient to obtain at least 25 MN in end bearing while meeting the project settlement requirement of 80 mm. The design end bearing of 25 MPa was the end bearing targeted to obtain an ultimate axial shaft capacity with safety factor of 2.0.

The design grout quantity was estimated as 100 kN based on the porosity and grout penetration ratio of the soil at the shaft tip. Consideration was also given to the grout going upward around the pile shaft.

O-CELL TESTS WITH POST-GROUTING OF SHAFT TIPS

To measure and verify the skin friction and end bearing capacities of the design shafts, several on-shore and offshore shafts were tested. The results presented herein are from an O-cell test on an offshore shaft constructed at the southern pylon site which was loaded before and after grouting.

The 2.5 m diameter test shaft had a tip elevation of -121 m with a 2.8 m diameter 25 mm thick permanent steel casing with a tip elevation of -53 m, as shown in Figure 12. Six U-shaped grout pipes were attached to the shaft reinforcement cage as shown in Figure 11. O-cells were placed at two levels. The upper level was 28 m above the shaft tip with two 870 mm diameter O-cells and a total nominal ultimate load of 55 MN, while the lower level was 1.5 m above the shaft tip with two 660 mm diameter O-cells and a total nominal ultimate load of 32 MN. Four LVWDTs (Linear Vibrating Wire Displacement Transducers) were installed at each O-Cell level. Eight (8) levels of vibrating wire strain gauges and four telltales were used as shown in Figure 12. The test was conducted by LOADTEST Singapore office. The soil profile at the test site consists of layers of

gray silty CL clay down to elevation – 53.5 m overlying layers of fine to coarse sands that extend well below the shaft tip elevation.

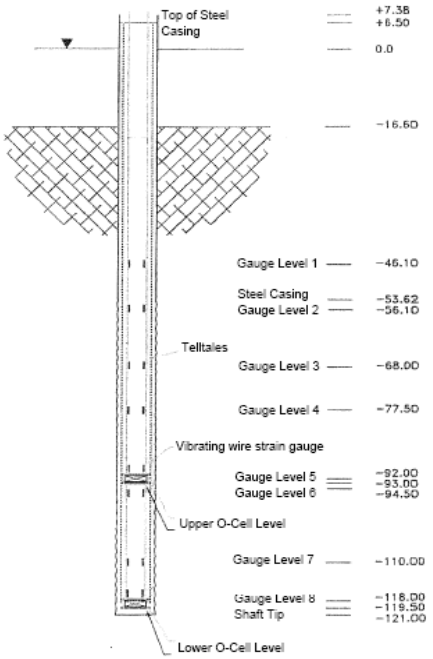


Figure 12: Test Shaft Layout and Instrumentation

The test was conducted in two phases; before and after grouting of the shaft tip. The first phase consisted of a one-stage load test. In this phase the lower O-cells were pressurized in 17 loading increments, each 0.9 to 1.0 MN and lasting 30 minutes, while the upper O-cells were kept closed. As shown in Figure 13 and summarized in Table 1, at the end of the 17th increment, the total lower O-cells load was about 16.5 MN with a total expansion of 93 mm, mostly from end bearing settlement, which is larger than the 80 mm limit required by the project design criteria. At the end of the first phase tests, the shaft was unloaded in 5 increments.

The second phase of the test was conducted 5 days after grouting of the shaft tip. The grouting process was conducted in three cycles to help achieve a uniform treatment of the soil at the shaft tip. In each cycle, the grout pressure was increased in equal increments to the design level, while the grout quantity was distributed equally in the straight grout pipes. In the first cycle 50% of the neat cement grout quantity was extruded, followed by pressure washing the grout pipes with clear water. After at least 1.5 hours of waiting, 30% of the grout quantity was extruded after which the grout pipes were pressure washed again with water. After at least 3.5 hours of waiting, the third cycle was completed by extruding the remaining 20% of the grout quantity. In the first and second cycles, there was more emphasis on controlling the grout quantity, while in the third cycle more emphasis was put on controlling the grout pressure.

Two main stages of load tests were conducted in the second phase. In the first stage the lower level O-cells were pressurized in 28 loading increments, each 0.9 to 1.0 MN, while the upper level O-cells were kept closed to assess the improvement in end bearing after grouting. As shown in Figure 13, after the final loading increment, an end bearing load of 27 MN was achieved with 44 mm tip settlement (1.8%D), while for a 1%D settlement, the measured end bearing capacity after shaft tip grouting was 5.3 MPa, which agrees well with the value predicted by the Mullins et al (2006) approach. This level of gain in end bearing was satisfactory and showed that the process of post-grouting of shaft tips can be reliably depended on to obtain the required design axial load capacity of the shafts while meeting the project settlement limit and eliminating the risk associated with drilling-induced soil disturbance and remaining debris at the tip of the shaft.

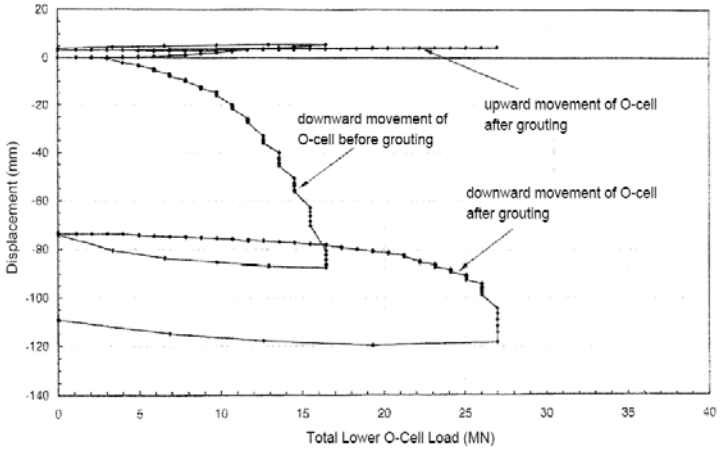


Figure 13: Load-Displacement Curves Before and After Post-Grouting of Shaft Tip from Stage 1

To measure the skin friction response along the shaft after grouting, a second stage of loading was conducted as part of the second phase of the test. This time, the upper level O-cells were pressurized in 1.6 to 1.7 MN load increments while the lower level O-cells were unlocked. The test was stopped when the upper shaft segment ultimate skin friction was reached after moving 106 mm upward, but

before reaching the ultimate skin friction of the lower segment, as shown in Figure 14. From this test, it can also be noticed that the lower 28 m long shaft segment close to grouted tip has a much stiffer skin friction load-displacement response than the upper 77 m segment. This is also evident from the load distribution curves based on strain gauges measurements, shown in Figure 15.

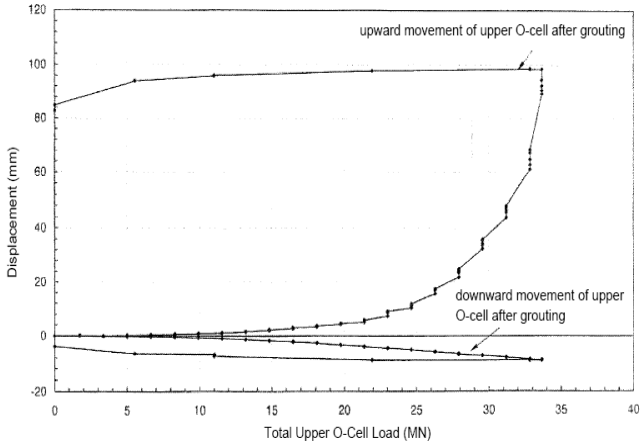


Figure 14: Load-Displacement Curves After Post-Grouting of Shaft Tip from Stage 2

Table 1: A Summary of O-cell Tests Procedure and Results Before and After Grouting

Stage	Loading Level		Upper Level O-Cells			Lower Level O-Cells		
			Max Load (MN)	O-cell Hydraulic System	Total Expansion (mm)	Max Load (MN)	O-cell Hydraulic System	Total Expansion (mm)
Before Grouting	1L-1 to 1L-17		0	Closed	-1.7	16.5	Pressure	+93.0
After Grouting	1	2L-1 to 2L-28	0	Closed	-1.4	27.0	Pressure	+118.5
	2	3L-1 to 3L-21	33.7	Pressure	+106.0	0	Free	+113.7

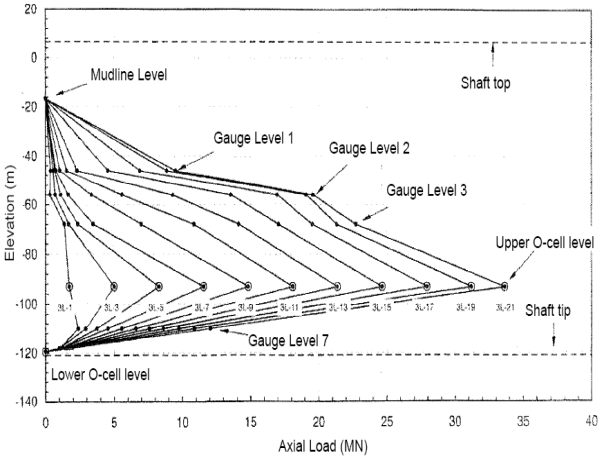


Figure 15: Shaft Load Distribution Curve from Stage 2 Using Strain Gauge Data

SCOUR PROTECTION

The conceptual scour design for the two main piers was performed by COWI A/S, Denmark. The detail design was performed by Jiangsu Provincial Communication, Planning & Design Institute. Hydraulic studies and surveys were performed by Nanjing Hydraulic Research Institute.

The hydraulic design parameters for the scour protection were a combination of the current, water level and in some cases, waves acting at the same time. See Figure 16.



Figure 16: 3 m/sec Currents at Pylon

The pile group width perpendicular to the river current is 48 m and the length is about 112 m. The hydraulic model tests showed the extension of the scour around the structure to be essentially equal in all four directions, approximately 60 m.

The ideas presented for scour protection were developed based on COWI's experience in combination with their understanding of the very difficult conditions in Yangtze River with deep water, high currents and high sediment transport.

The major problem associated with the scour protection was its construction. The scour protection in itself had to be made in a way that it was not too difficult to construct, and also, that it would prevent scour during construction. It was assessed that if the bridge piers were made without prior scour protection, the development of scour will be so rapid that it would be difficult to construct the scour protection later on and the bed level would have eroded to such a low lever, that the advantage of the existing bed levels would have disappeared.

Therefore, the scour protection as presented in Figure A-7 in the Appendix was designed in such a way as to allow for construction of piles through the center of the temporary scour protection and then later on the final scour protection could be introduced.

In addition, due to the very high flow velocities and high sediment transport, the adopted scour protection scheme would need to be relatively simple and robust and not require very accurate dredging levels before placing of the material in the scour protection.

It was also desirable to construct the protection in smaller sections that together would constitute the total protection. The final protection should also be robust and be able to function with unavoidable inaccuracies.

With these objectives in mind, the designers refrained from the use of large prefabricated mattresses, gabions or large bamboo/willow mattresses. Such solutions could be used but would be difficult to handle and place in the very high currents prevailing at the site.

The principal ideas for the scour protection of the pylons of the Sutong Bridge included the use of three distinct areas or zones.

(1) The Central Area or Inner Zone

This zone includes the central area where the bridge piles for the main pylons and temporary structures are present.

The area extends 20 m away from the structures. In this area, the river bed would be temporarily protected by use of layers (3 nos.) of sand-filled geotextile bags. See Figure 17.



Figure 17: Filling Geotextile Bags

The idea behind this concept is that by this action, the river bed will be protected but it will still be possible to bore the piles through the protection. After completion of the piling, the final protection was constructed with a filter layer of quarry-run and minimum 2 layers of armour stones (rock).

(2) Outer Area

Beyond the inner zone, the Outer Area is situated. It extends about 40 m further out from the Central Area. The scour protection consists of one layer of sand bags covered with a layer of quarry-run on top of which was placed the same type of rock armour as for the central area.

(3) The Falling Apron Area

Outside the Central and Outer Area is the Falling Apron Area. Its width varies according to an estimate of the scour depth and the width was set at 1.5 times the actual maximum expected scour depth. The material in this area consists of quarry-run on top of which layers of quarry stones were dumped.

During construction of the Falling Apron Area, it was decided to dump a layer of sand bags at this area as well because extensive scour was occurring.

The concept of the falling apron has been used in many countries for river training structures where the scour is expected to reach to a level significantly below the level at which the structure is or can be built.

Table 2: Stone and Sand Bag Sizes for the Scour Protection Material at the North and South Pylon

Item	Location	Density [t/m^3]	d_{50} [m]	
			North Pylon	South Pylon
Stones	Inner Area	2.65	0.40	0.50
Sand Bags		2.00	0.50	0.60
Stones	Outer Area	2.65	0.30	0.40
Sand Bags		2.00	0.30	0.40
Stones	Falling Apron	2.65	0.30	0.40
Stones at Slope		2.65	0.40	0.60

The principle is that the material in the falling apron will launch itself down the scoured slope that will thereby stabilize itself.

Table 2 shows the stone sizes of the scour protection for the North and South Pylon. The table also shows sizes of sand bags, which were exposed in the temporary protection during construction and were later on covered with stone material.

For practical considerations, the same size of bags were adopted all over and the same stone size for the outer area and falling apron. The actual sand bags used were of size: 1.6 m x1.6 m x 0.6 m.

Extensive surveys were performed during construction using multi-beam echo sounder in order to control and verify the amount of materials dumped. The dumping of material was performed using a grid with 28 x 26 cells for the North Pylon and 16 x 16 cells for the South Pylon.

With respect to the armor stones, it was essential that the structural integrity be obtained. Therefore, it was crucial that 2 layers of armor stones are present in all areas. In layer thickness, this corresponds to 1.0 m for the Central Area and the Outer Area. For the inner section of the Falling Apron Area, it corresponds to 1.2 m thickness.

The scour protection is a flexible structure that will be subject to some displacement of material. Especially the Falling Apron will be moving during launching when scour occurs at its edges. Therefore a detailed monitoring program was prepared covering the entire bridge alignment.

The solution adopted, with sand bags and stone layers dumped from the water surface, was found to be the most feasible under the given difficult circumstances with water depth up to 30 m, high currents and zero visibility. The future erosion at the edges of the protection will be prevented from progressing close to the bridge piers by the use of the Falling Apron concept for the outer edge of the scour protection.

See Figures A-6 and A-7 in the Appendix for further details of the scour protection system

PILE CAP CONSTRUCTION

The 13.3 m deep pile cap for each pylon is positioned at the water line with the bottom at Elev. -7.0 m and the top at + 6.3 m. The caps were constructed by first building a double-walled steel caisson in-the-wet, directly above final location. The 1.8/2.0 m thick double wall or perimeter wall was constructed as a watertight compartment and served four basic functions. See Figure 18.



Figure 18: 2 m Thick Caisson Perimeter Wall

It first served as the perimeter stiffening frame that gave the caisson its rigidity during lowering operations. Secondly it served as the buoyancy tanks to minimize the deadweight of the caisson as it was lowered into the water and down to final grade at Elev. -10.0 m. Third, it served as a temporary cofferdam and exterior permanent form for the casting of the pile cap. And finally, the perimeter wall acted as a permanent ship-impact protection fender during the service life of the bridge. The perimeter wall was filled with concrete below Elev. –1.0 m.

The first caisson (North Pylon) when initially constructed was 118 m by 52.4 m in plan, 7 m high, and weighed approximately 3050 tonnes. See Appendix Figure A-3. The bottom of the caisson was a steel plate stiffened by steel trusses that spanned the full width of the caisson and tied into the perimeter walls. The bottom deck of the caisson started out at approximately Elev. +6.0 and was lowered in three basic stages to Elev. -10.0. The first stage lowered the caisson approximately 5 m, at which point the caisson was floating under its own buoyancy. At the end of this stage, the lowering was stopped and the perimeter walls were increased to a height of 18 m and the lowering was completed in two stages to final grade by partial flooding of the cofferdam.

The lowering operation was performed with 16 strand jacks, DL-S418 (See Figures 19 and 20.) supplied and operated by Dorman Long Technology, Ltd. For the layout of strand jacks see Appendix Figure A-4.



Figure 19: Typical Strand Jack at Pylon 5



Figure 20: Strand Jack Model DL-S418 & Reaction Frames Inside Caisson at Pylon 4

All 16 jacks were spaced along the perimeter wall of the caisson and sat on support frames positioned over the top of the exterior drill shaft casings. Each jack had a safe working load of 418 tonnes, thus providing a safety factor of 2.2. The entire caisson was quite stiff and relative movements of only 10 mm between adjacent jacking points created a 35% differential loading. The entire lowering operation was controlled with a Dorman Long P40 computer control system which provided communications between jacks, power-pack and control computer. The lowering operation was performed with strokes of 200 mm and a stroke range of only 5 mm to ensure stable balanced loads between jacks.



Figure 21: Pylong 5 Caisson Being Lowered

Once the 13 m high caisson reached final grade at Elev. -10.0, the caisson was locked in position and the annulus between the drilled shaft casings and the steel plate of the caisson bottom deck was sealed. A 3.0 m deep tremie concrete seal was then placed over the entire bottom area of the caisson except for the 2 m wide exterior wall. After the tremie seal attained specified strength, the caisson was dewatered (See Figure 22) and the rest of the pile cap was constructed in the dry. See Figure 23.



Figure 22: Dewatered Cofferdam and Top of Tremie Seal

For the second caisson (South Pylon), the entire caisson was assembled full height and weighed approximately 5,800 tonnes. This caisson was lowered by a strand jacking system from Tonji University to a self-floating condition, and final grade was reached by partial flooding of the exterior perimeter walls. Once at final grade, the tremie seal was placed and the rest of the South Pylon was constructed in the dry. Both lowering operations worked well and everything went smoothly.



Figure 23: Completion of Pile Cap in the Dry at Pylon 4

CONCLUSION

The foundation design and construction team on the Sutong Bridge have succeeded in constructing foundations for a world record setting bridge at a very challenging site on the lower Yangtze River. The design team, working in conjunction with their construction counterparts, developed innovative holistic solutions that addressed the very rigorous requirements of the structural design while remaining fully constructible under extremely difficult conditions

Post-grouting of shaft tips was found to be an effective and economical procedure that was implemented to increase the axial capacity of the drilled shaft foundation of the Sutong Bridge in China. By preloading and compaction of the soil and any remaining debris at the shaft tips, the end bearing capacity can be significantly increased and reliably depended on. This was validated in O-cell tests conducted on shafts before and after tip grouting. Another advantage of post-grouting of shaft tips is the ability to check the axial capacity of each production shaft through measurement of grout pressure and upward movement of the top of the shaft.

ACKNOWLEDGEMENT

The authors wish to thank the Jiangsu Provincial Sutong Bridge Construction Commanding Department for the opportunity to assist them on this very challenging bridge project.

References:

JENSEN, O. J., AND TRUELSEN, C., 2004, Scour Assessment & Conceptual Design of Scour Protection for Sutong Bridge, P.R. China.

APPENDIX

1. Figure A-1 Main Span Side Elevation
2. Figure A-2 Pylon Details
3. Figure A-3 Main Pylon Caisson Details
4. Figure A-4 Caisson Lowering System
5. Figure A-5 Perimeter Wall Completion
6. Figure A-6 Scour Protection Details at Main Pylons
7. Figure A-7 Scour Protection Plan

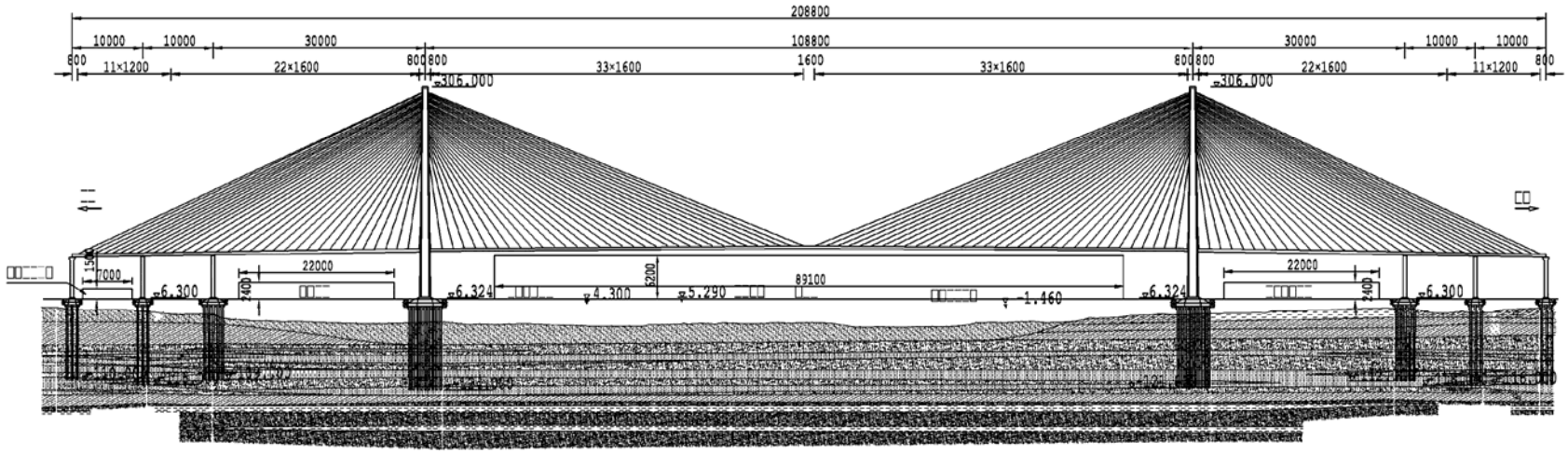


Figure A-1: Main Span Side Elevation

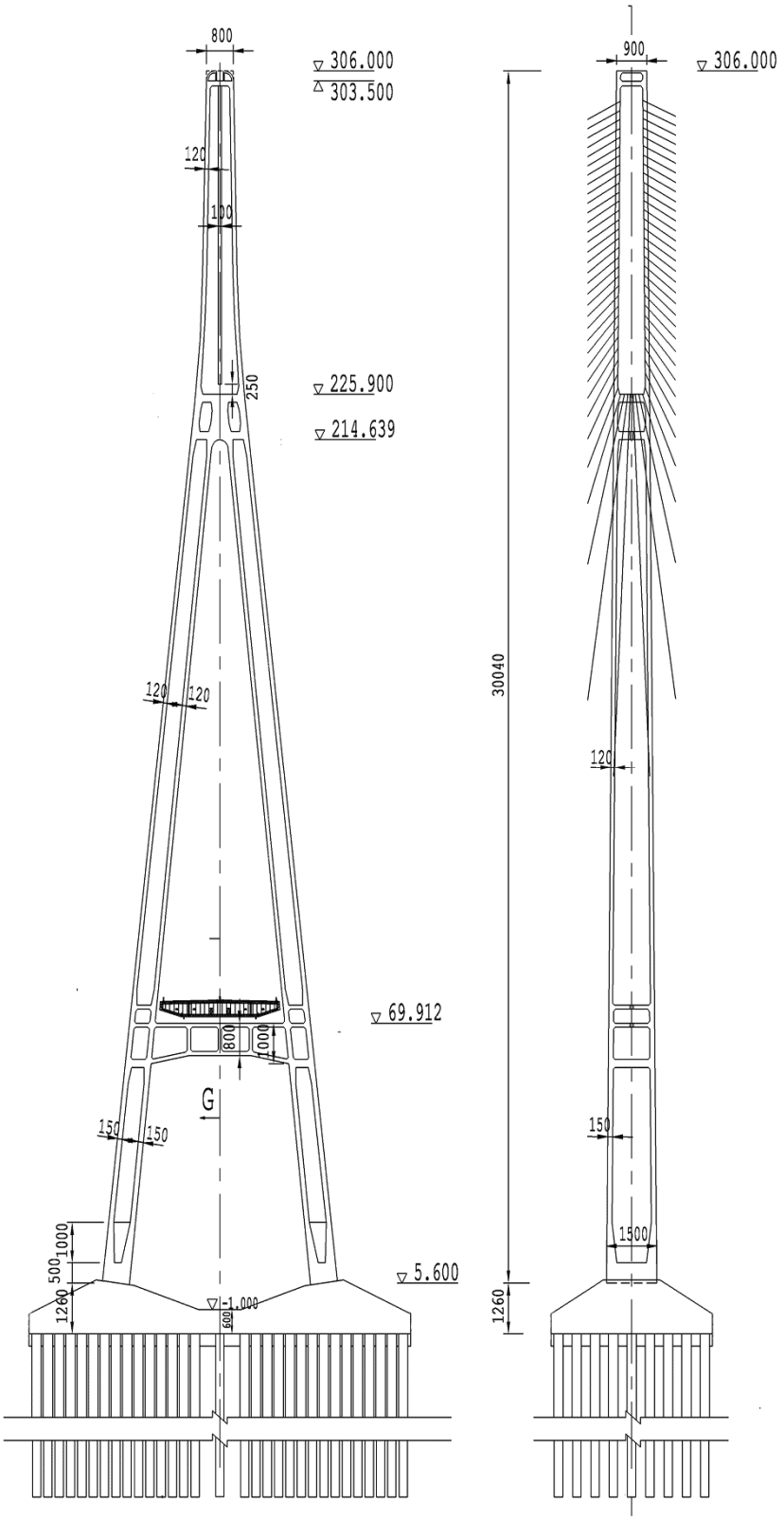


Figure A-2: Pylon Details

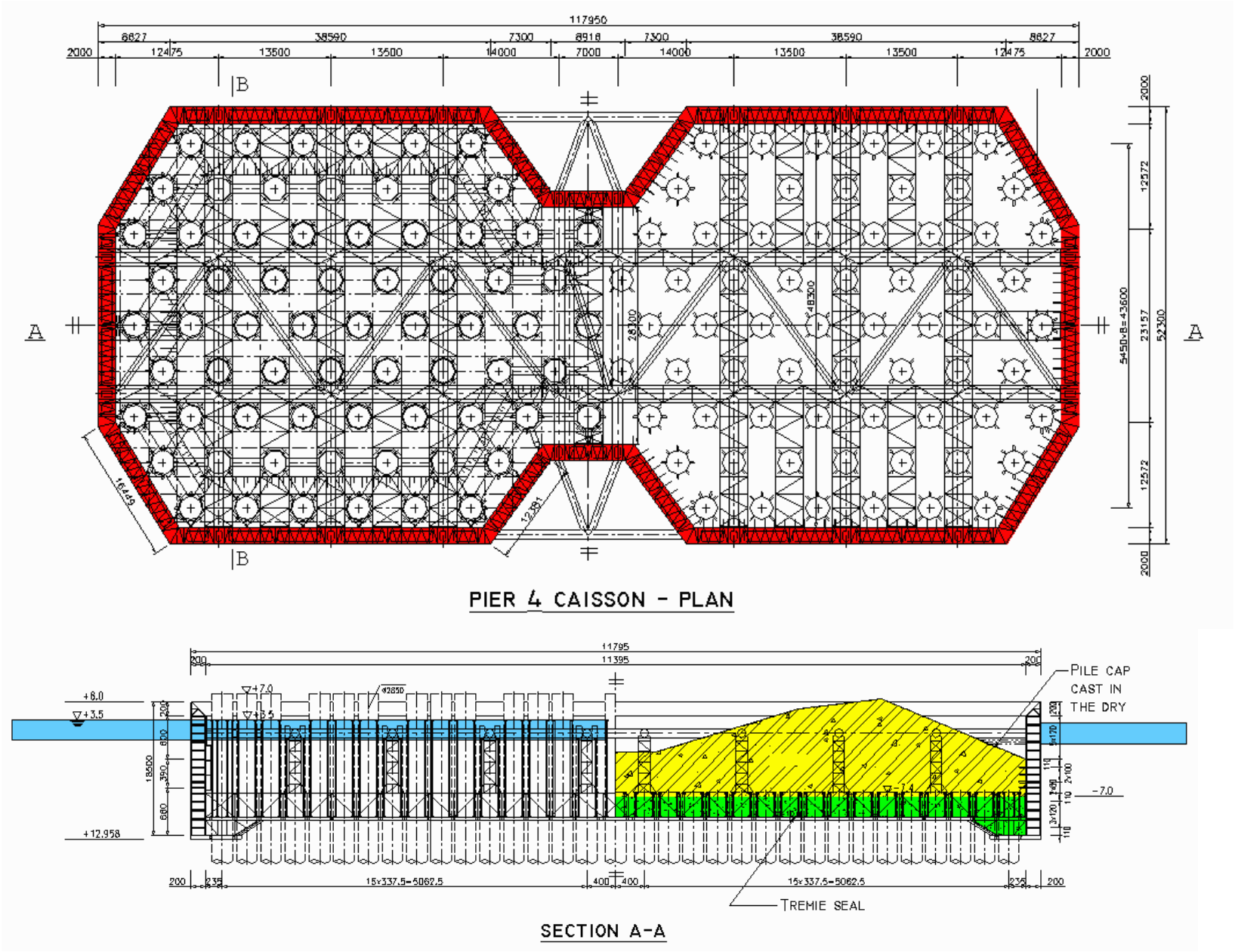


Figure A-3: Main Pylon Caisson Details

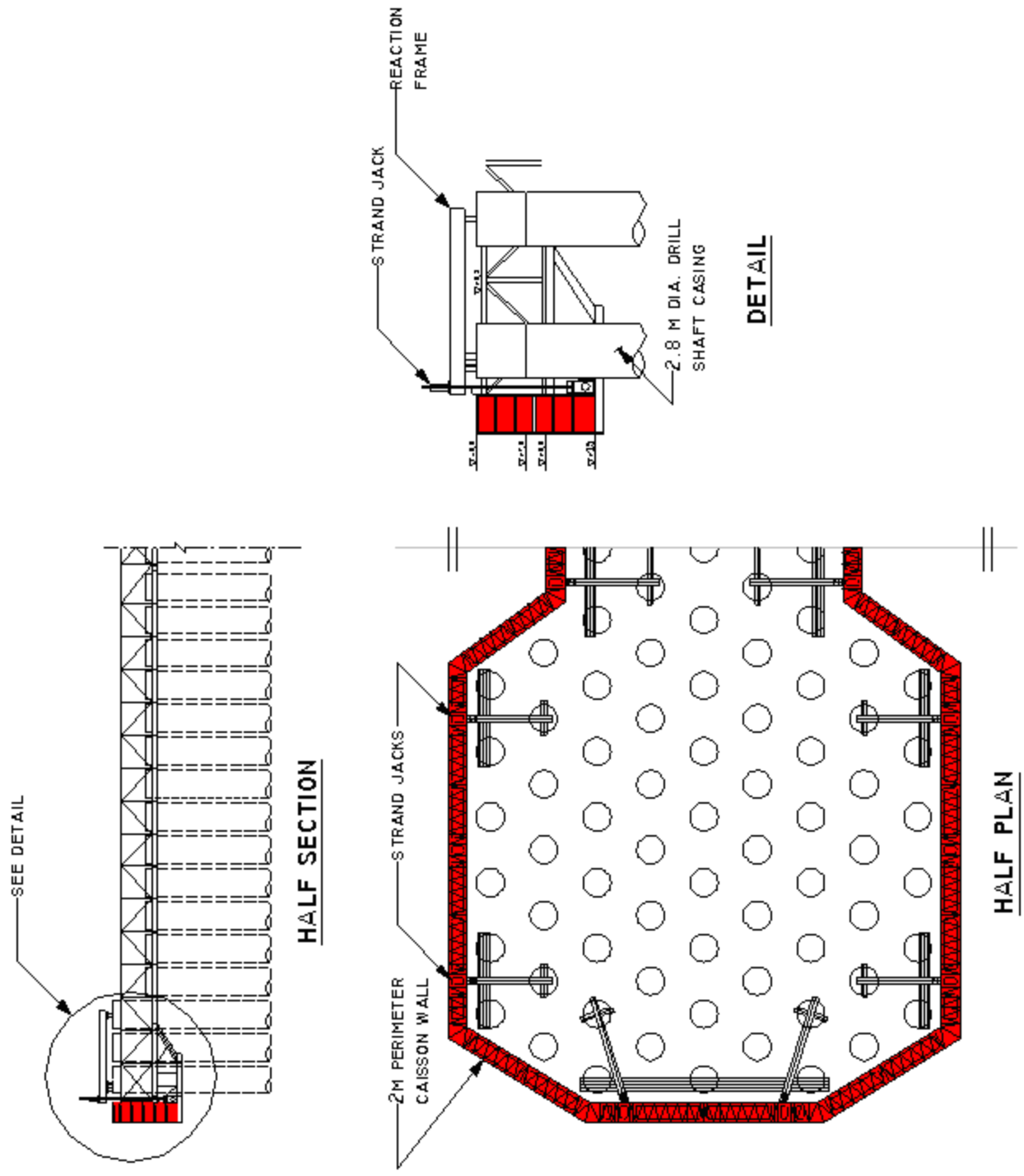


Figure A-4: Caisson Lowering System – Stage 1

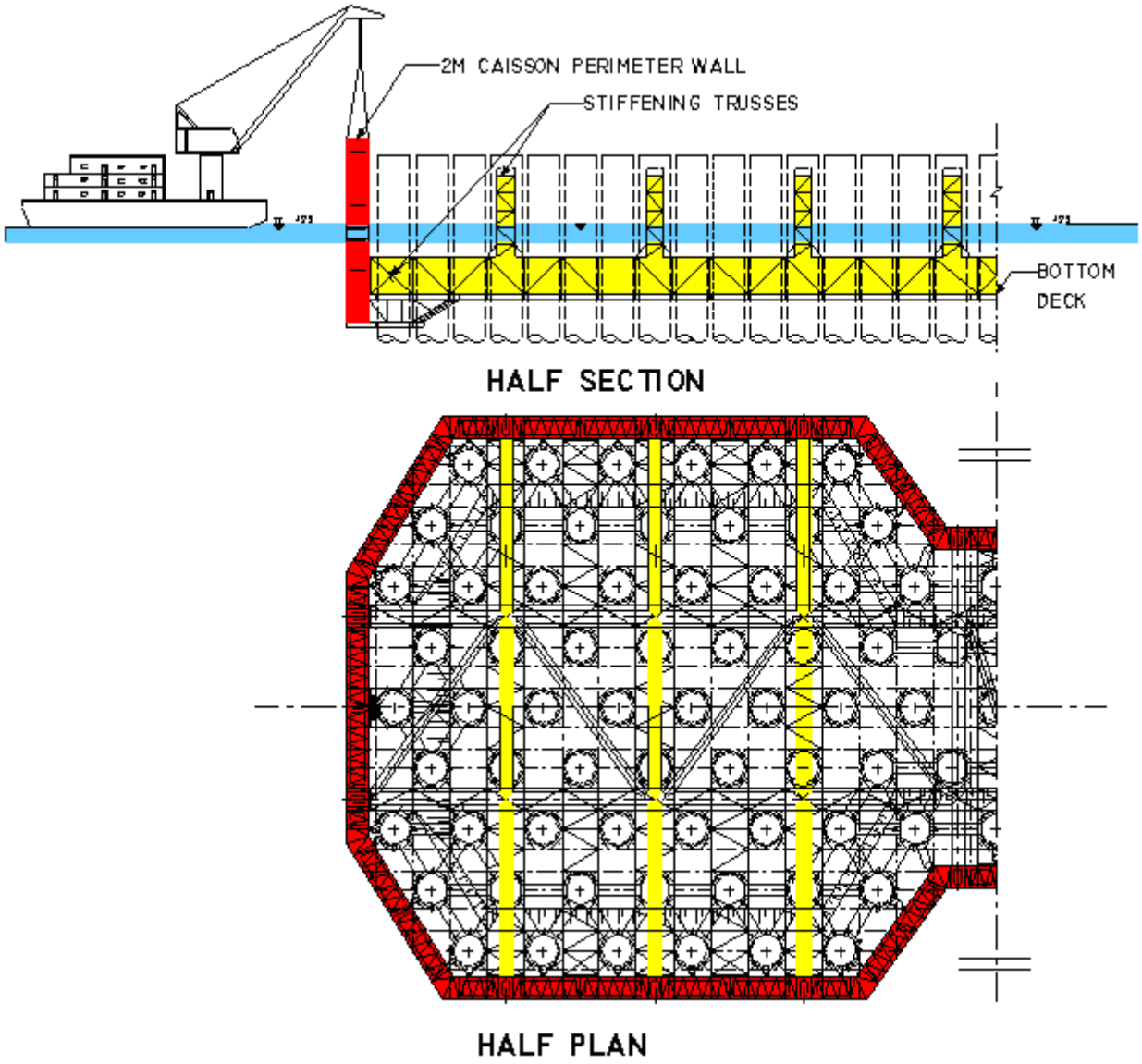


Figure A-5: Perimeter Wall Completion

Figure A-6: Scour Protection Details at Main Pylons

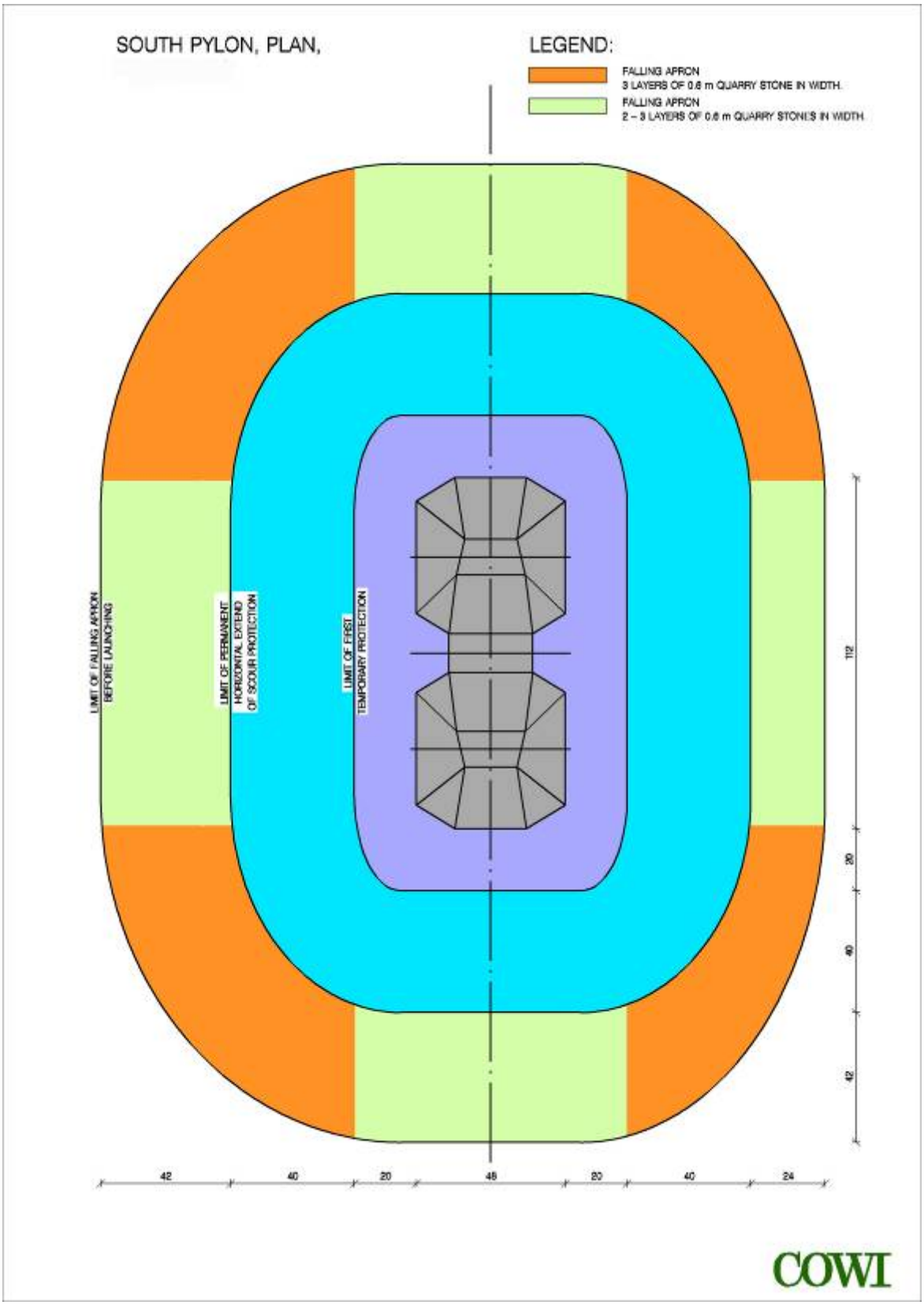


Figure A-7: Scour Protection Plan

LARGE DIAMETER SHAFTS – YOUGHIOGHENY RESERVOIR BRIDGE

Paul J. Lewis, P.E., Gannett Fleming, Inc., Harrisburg, PA, USA
David R. Scherer, P.E., Gannett Fleming, Inc., Harrisburg, PA, USA

Estimation of the axial side shear resistance of drilled shaft rock sockets is directly related to the unconfined compressive strength of the bedrock. Commonly, the mean unconfined compressive strength value is calculated from a range of laboratory test results and is used to estimate the side shear of the bedrock. This paper presents the results from a full scale axial load test performed on an 8.5-feet-diameter drilled shaft rock socket, and compares measured side shear values to estimated values for two different rock strata. Measured side shear values correlated well with the design value calculated for the "strong" rock stratum, but did not correlate well with the design value calculated for the "weak" rock stratum. The mean unconfined compressive strength was used to calculate the side shear in both strata, but review of the laboratory data indicates that this value may not have been appropriate for the weak stratum due to a large variation in the laboratory test results. Also included in this paper is a discussion of the subsurface conditions, the laboratory test results, and the methodology used to design the drilled shaft rock sockets for axial and lateral resistance.

INTRODUCTION

The project involves replacement of the existing structure that carries S.R. 0040 over the Youghiogheny Reservoir in Fayette and Somerset Counties, Pennsylvania. A Site Location Map is included as Figure 1. District 12-0 of the Pennsylvania Department of Transportation (PENNDOT) retained HDR Engineering, Inc. to design and prepare contract drawings for this conventional design/bid/build project. G.A. & F.C. Wagman, Inc. elected to bid an alternate structure and was awarded the contract. Subsequently, G.A. & F.C. Wagman, Inc. retained Gannett Fleming, Inc. to design and prepare the construction drawings for the alternate structure.

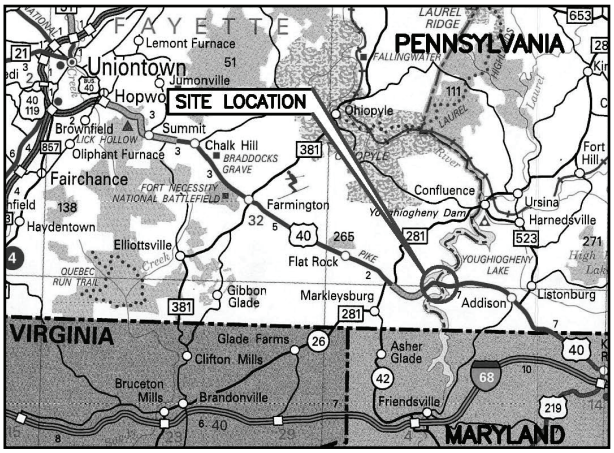


Figure 1: Site Location Map

The existing structure that carries S.R. 0040 over the Youghiogheny Reservoir is a 15 span bridge consisting of 9 simple spans of steel truss with floor beams and stringers, 1 simple span of rolled steel I-beams, and 5 spans of continuous rolled steel I-beams. Construction of this bridge began in 1939 concurrent with construction of a United States Army Corps of Engineers (USACE) dam downstream. Construction was halted in 1941 due to the need for steel for military operations during World War II. Bridge construction resumed in the mid 1940's and was completed in 1948. Since this structure was constructed prior to flooding the river valley, spread footings founded on relatively shallow bedrock were used to support the piers and west abutment. The east abutment was supported on 14-inch diameter steel concrete-filled pipe piles driven through the approach fill.

The replacement structure is an 8-span continuous steel girder bridge and has a total length of 1,730 feet. It is located immediately north (downstream) of the existing bridge. The foundations include driven H-piles to support both abutments and drilled shaft pier bents. Each pier bent consists of two 9-feet-diameter drilled shafts with 8.5-feet-diameter rock sockets. The total lengths of the drilled shafts range from approximately 50 to 130 feet. The shafts were constructed by Case Foundation Company.

SITE GEOLOGY

General Geology

The bridge is located in the Allegheny Mountain Section of the Appalachian Plateaus Physiographic Province. The Allegheny Mountain Section typically consists of broad, rounded ridges separated by broad valleys. The ridges occur on the crests of anticlines that have been eroded enough to expose the very resistant rocks that form the crests of the ridges. The valleys are broad, undulating surfaces with shallow to deep stream incision. The topography in the area of the bridge is rugged and the minor streams are entrenched in deep, steep-sided valleys.

Stratigraphy

The bridge is underlain by Pennsylvanian aged bedrock. The east and west abutments are founded in the Glenshaw Formation of the Conemaugh Group. A key marker bed, the Upper Freeport Coal, was encountered in the borings drilled in the valley floor. This marker bed delineates the overlying Glenshaw Formation from the Freeport Formation of the Allegheny Group below. These formations consist of alternating layers of shale, siltstone, sandstone, limestone, minor coals and clay. Marine limestone and shales are abundant in the Glenshaw Formation. Shaulis (1994) indicates that the Brush Creek coal and marine zone interval of the Glenshaw formation is exposed at the water level of the Youghiogheny River in the area of the western abutment of the bridge.

Structural Geology

The eastern portion of Fayette County and the western portion of Somerset County lie in the Appalachian Plateau where the bedrock has been deformed into broad open folds. The great open folds of the Allegheny Mountain section have amplitudes of as much as 3,000 feet. The general trend of the folds is in a northeast-southwest direction. The Youghiogheny Reservoir Bridge is situated between the Laurel Hills anticline and the Johnstown syncline. The Laurel Hills anticline is approximately 4.4 miles to the west of the west bridge abutment. The Johnstown syncline is a rather broad-bottomed structure located approximately 0.7 miles east of the east bridge abutment.

SUBSURFACE CONDITIONS

Numerous borings were performed to investigate the subsurface conditions at the project site. Fifty-four borings were performed under the direction of HDR Engineering, Inc., and fifteen borings were performed under the direction of Gannett Fleming, Inc. Soil samples were obtained with a 2-inch outside diameter split-spoon and a 140-pound hammer. Rock coring was performed with NX, NQ2 and HQ core barrels with split inner barrels. Both land and barge borings were required. The information obtained from the borings was generally consistent throughout the project site.

The borings conducted under the direction of Gannett Fleming, Inc., designated GF-1 through GF-15, were performed to investigate the subsurface conditions at the proposed pier locations for the alternate 8 span structure. A generalized subsurface profile developed from these borings is shown in Figure 2. A detailed discussion of the subsurface conditions encountered in these borings is included below.

Pier 1

Borings GF-1 and GF-2 were drilled at Pier 1. The ground surface elevation ranged from 1426.4 feet to 1418.9 feet. The overburden thickness varied between 5.0 feet and 7.5 feet. Bedrock was encountered in these borings at elevations ranging from 1418.9 feet to 1413.9 feet. Rock core recoveries in the borings were typically 100%, and were not less than 83%. An upper stratum of medium hard, fine-grained, silty sandstone varying in thickness from 5.9 feet to 9.0 feet was encountered in the borings. The rock quality designation (RQD) of this stratum ranged from 0% to 89%. Hard, coarse-grained sandstone was encountered in the borings at approximately Elevation 1408 feet. The RQD for this stratum ranged from 97% to 99%.

Piers 2 through 5

Borings GF-3 through GF-8 were drilled at Piers 2, 3 and 5. Borings NP6-1 and NP6-2, which were drilled under the direction of HDR, were located at Pier 4. The ground surface elevation at these borings ranged from approximately

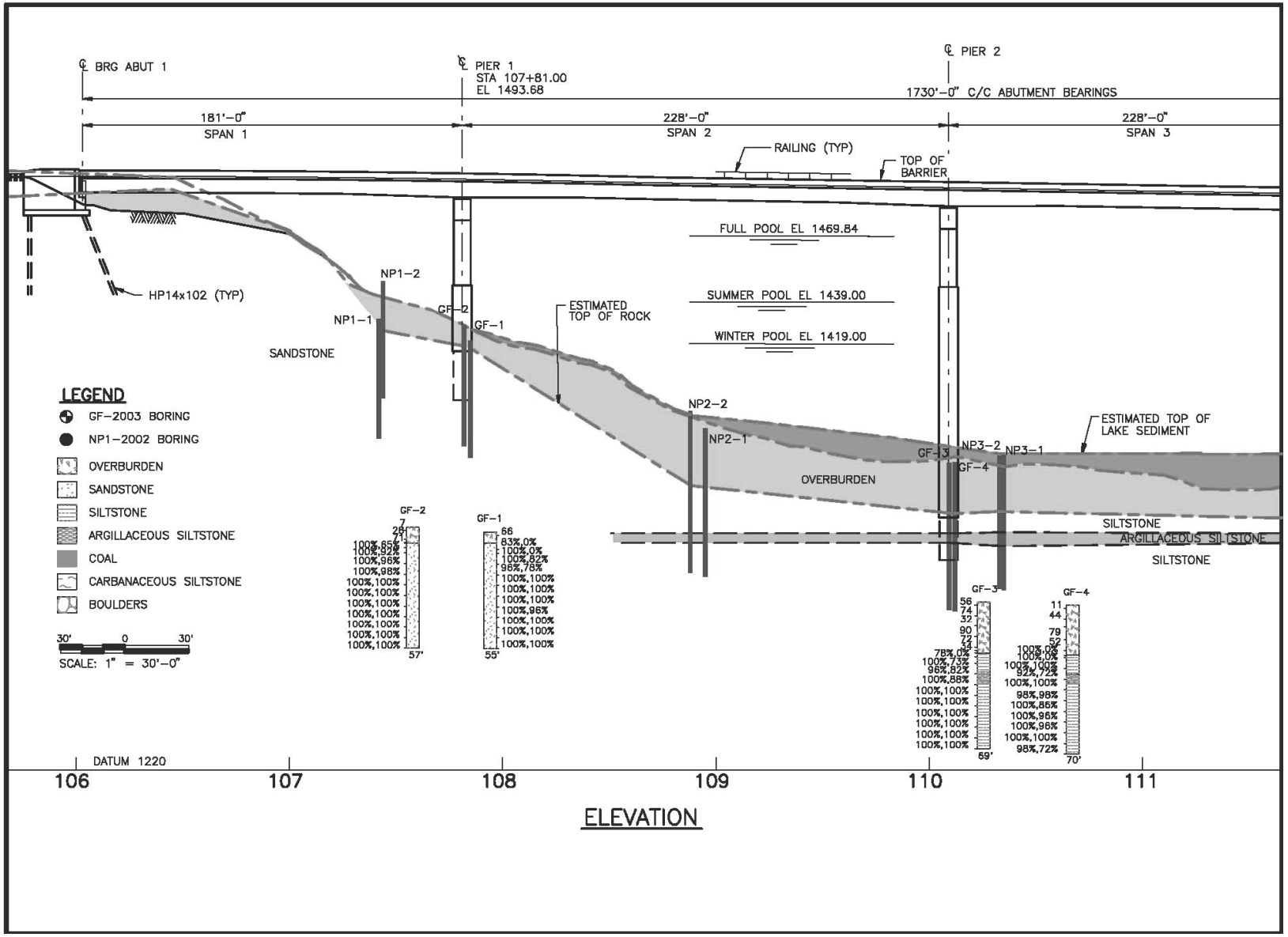


Figure 2: Subsurface Profile along the Youghiogheny Reservoir Bridge (sheet 1 of 3).

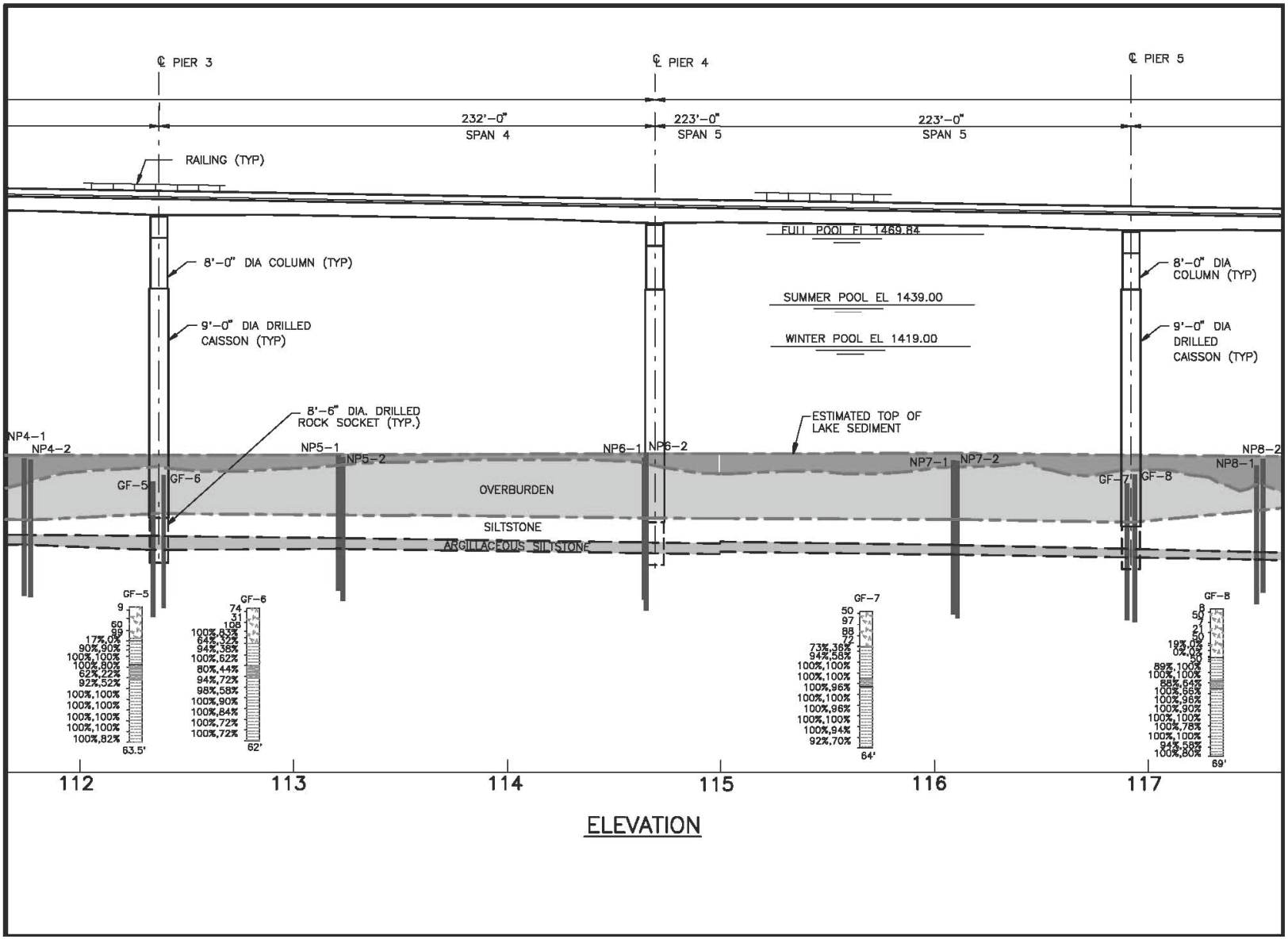


Figure 2: Subsurface Profile along the Youghiogheny Reservoir Bridge (sheet 2 of 3).

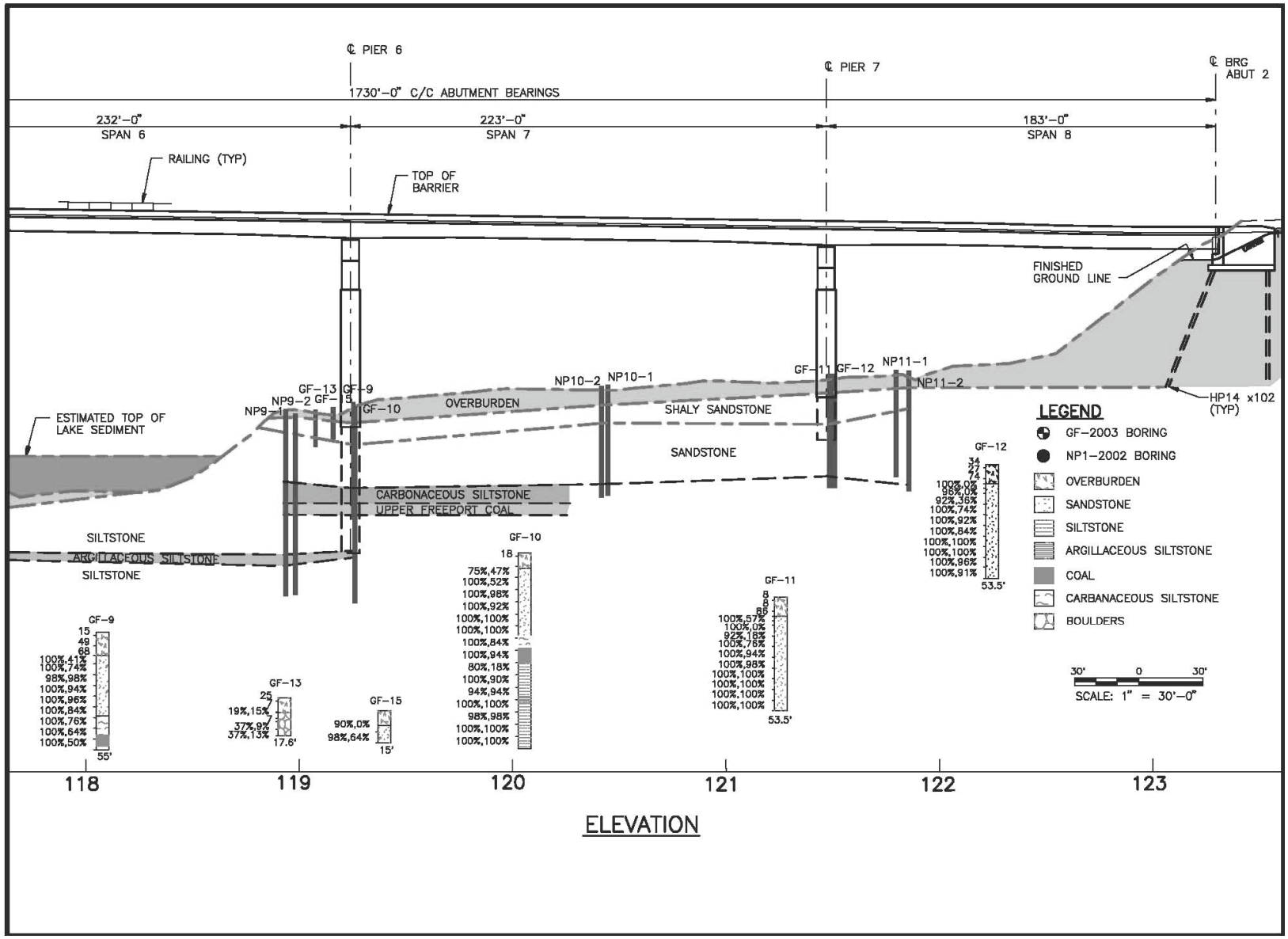


Figure 3: Subsurface Profile along the Youghiogheny Reservoir Bridge (sheet 3 of 3).

1367 feet to 1363 feet. The overburden thickness was approximately 30 feet and included up to approximately 10 feet of very loose silt (lake sediment). Bedrock was encountered in these borings at elevations ranging from 1339.7 feet to 1332.5 feet. Three rock strata were typically encountered in these borings. Rock core recoveries in the strata were typically greater than 90%. The upper stratum was generally described as medium to hard, sandy siltstone. The thickness of this layer ranged from 8.9 feet to 14.6 feet, and its RQD ranged from 51% to 85%. A relatively thin stratum of soft to medium hard argillaceous siltstone was encountered below the upper siltstone stratum. The thickness of this layer ranged from 3.7 feet to 6.7 feet, and its RQD ranged from 16% to 92%. A lower stratum of siltstone was encountered beneath the argillaceous stratum. This lower stratum was generally described as medium to hard sandy and shaly siltstone with occurrences of carbonaceous siltstone. The thickness of this layer ranged from 21.8 feet to 33.4 feet and its RQD ranged from 75% to 99%.

Pier 6

Borings GF-9 and GF-10 were drilled at Pier 6. The ground surface elevation at these borings ranged from 1393.3 feet to 1391.0 feet. The thickness of the overburden in these borings varied between 6.4 feet and 10.9 feet. Bedrock was encountered at elevations ranging from 1384.6 feet to 1382.4 feet. Rock core recoveries in the borings were typically 100%. The upper rock stratum encountered in the borings was described as hard sandstone and ranged in thickness from 28.3 feet to 32.9 feet. The RQD of this stratum ranged from 83% to 85%. Beneath this stratum a medium hard, carbonaceous siltstone stratum was encountered. This layer varied in thickness from 5.1 feet to 9.0 feet, and its RQD was 84%. The Upper Freeport Coal, ranging in thickness from 5.2 feet to 6.1 feet, was encountered beneath the carbonaceous siltstone. Beneath the coal very soft to medium hard argillaceous siltstone was encountered. This stratum was 6.5-feet-thick and had an RQD of 69%. Medium hard to hard siltstone, which had an RQD of 100% was generally encountered in the remainder of Boring GF-10. A very soft interbed of argillaceous siltstone with an RQD of 97% was encountered from a depth to 67.5 feet to 70.7 feet

Pier 7

Borings GF-11 and GF-12 were drilled at Pier 7. The ground surface elevation at both of these borings was 1406.4 feet. The overburden in these borings had a thickness of 8.9 feet, and bedrock was encountered at Elevation 1397.5 feet. Rock core recoveries in the borings were generally 100%. The upper rock stratum encountered in the borings was described as medium hard, fine-grained, silty sandstone. The thickness of this stratum ranged from 5.5 feet to 9.0 feet, and its RQD ranged from 0% to 23%. Hard, coarse-grained sandstone was encountered below the upper rock stratum. The thickness of this stratum ranged from 33.4 feet to 35.6 feet, and its RQD ranged from 86% to 94%. Boring GF-11 was terminated in the coarse-grained sandstone. Boring GF-12 encountered a 5.6-feet-thick layer of medium hard, carbonaceous siltstone in the bottom of the boring, and its RQD was 89%.

CHARACTERIZATION OF ROCK STRATA

As indicated in the Foundation Report for the as-designed structure prepared by HDR Engineering, Inc., the rock types encountered at the proposed piers were geologically grouped into two formations or units. The upper unit, which provides foundation support for Piers 1, 6 (North) and 7, is the Mahoning Sandstone Formation. The lower unit, which provides foundation support for Piers 2 through 5 and Pier 6 (South), is the Freeport Formation. Furthermore, these units were subdivided to distinguish between rock strata with “slight” variations and are summarized below in Table 1.

Table 1: Summary of Rock Strata

Formation	Rock Unit	Rock Type	Pier
Mahoning Sandstone	B1	Shaly Sandstone	6 (North) & 7
	B2	Sandstone	1, 6 (North) & 7
Freeport	C1 & C3	Upper & Lower Siltstone	2 thru 5 & 6 (South)
	C2	Argillaceous Siltstone	2 thru 5 & 6 (South)

Information recorded from the rock core samples, which were obtained during the subsurface investigations directed by Gannett Fleming, Inc. and HDR Engineering, Inc., included RQD and discontinuity measurements. The discontinuity measurements characterize the condition and spacing of discontinuities and are used in the determination of rock mass rating (RMR). Average values were calculated for individual rock units at each pier. Tables 2, 3 and 4 below summarize these average RQD values, discontinuity ratings and RMR values, respectively.

Table 2: Summary of Average Rock Quality Designation (RQD) Values

Rock Type	Rock Unit	Average Rock Quality Designation (RQD) Values				
		# of Values	Min. (%)	Max. (%)	Mean (%)	Std. Dev. (%)
Shaly Sandstone	B1	5	10	63	42	20
Sandstone	B2	7	92	98	96	3
Upper & Lower Siltstone	C1 & C3	25	60	100	84	13
Argillaceous Siltstone	C2	12	30	99	71	20

Table 3: Summary of Average Discontinuity Values

Rock Type	Rock Unit	Average Discontinuity Values				
		# of Values	Min.	Max.	Mean	Std. Dev.
Shaly Sandstone	B1	5	17	19	18	1
Sandstone	B2	7	19	21	20	1
Upper & Lower Siltstone	C1 & C3	25	17	23	21	1
Argillaceous Siltstone	C2	12	14	21	18	2

Table 4: Summary of Average Rock Mass Rating (RMR) Values

Rock Type	Rock Unit	Average Rock Mass Rating (RMR) Values				
		# of Values	Min.	Max.	Mean	Std. Dev.
Shaly Sandstone	B1	5	44	59	53	6
Sandstone	B2	7	72	75	74	1
Upper & Lower Siltstone	C1 & C3	25	56	70	65	4
Argillaceous Siltstone	C2	12	47	67	58	6

Compressive Strength of Rock Strata

Approximately 100 rock core samples obtained from the borings drilled at the project site were tested in the laboratory to estimate the unconfined compressive strength of the bedrock. The majority of the tests were performed in accordance with ASTM D 2938, "Unconfined Compressive Strength of Intact Rock Core Specimens". Some samples were tested in accordance with ASTM D 5731, "Determination of the Point Load Strength Index of Rock". Based on the results of these tests, the unconfined compressive strength of the rock strata were estimated for the calculation of axial and lateral resistances of the drilled shaft rock sockets. Table 5 below summarizes the results of the laboratory tests, and graphical presentations of the data are included in Figures 3 and 4.

Table 5: Rock Compressive Strength Test Results

Rock Type	Rock Unit	Rock Compressive Strength Test Results				
		# of Tests	Min. (psi)	Max. (psi)	Mean (psi)	Std. Dev. (psi)
Shaly Sandstone	B1	17	2,680	7,830	4,831	1,452
Sandstone	B2	22	6,279	15,910	11,295	2,869
Upper & Lower Siltstone	C1/C3	34	1,340	7,642	3,785	1,543
Argillaceous Siltstone	C2	21	55	3,353	938	931

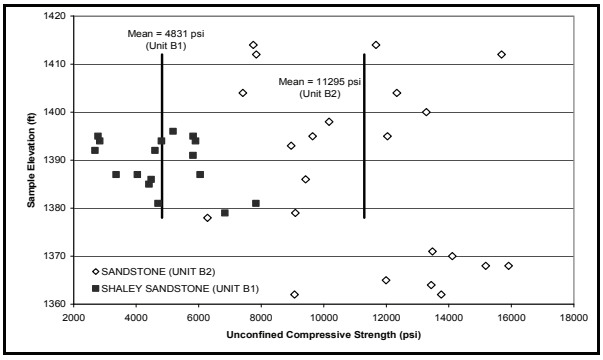


Figure 3: Laboratory Unconfined Compression Test Results (Rock Unit B)

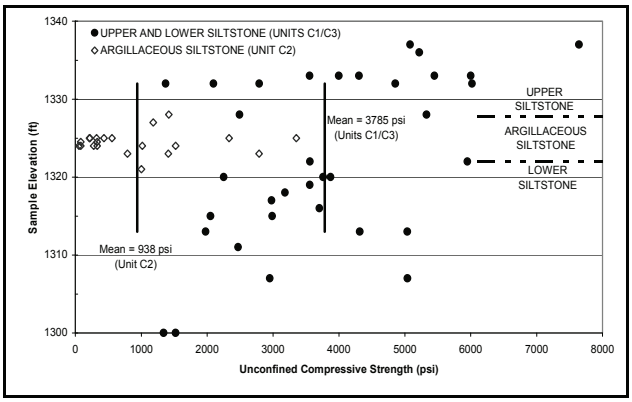


Figure 4: Laboratory Unconfined Compression Test Results (Rock Unit C)

AXIAL AND LATERAL DESIGN METHODOLOGIES

Rock Socket Axial Side Resistance

AASHTO's *LRFD Bridge Design Specifications* were used for the calculation of the axial side resistance of the 8.5-feet-diameter drilled shaft rock sockets utilized at the piers. As indicated in AASHTO Section C10.8.3.5, the side resistance of shafts socketed into rock is based on the lower value of unconfined compressive strength of the bedrock and drilled shaft concrete. Based on a design concrete compressive strength of 3,500 psi, the compressive strength of concrete controlled the calculation of side resistance for Rock Units B1, B2, C1 and C3. However, Rock Unit C2 had a mean compressive strength value (i.e., 938 psi) lower than the concrete, and therefore, controlled the calculation of side resistance in this rock unit.

The ultimate unit side resistance (q_s) of the rock units was calculated using AASHTO Equation C10.8.3.5-5, $q_s=0.67(q_u)^{0.5}$, where q_u is the lesser of the unconfined compressive strength of the rock or concrete. Note that this equation applies to unconfined compressive strengths greater than 20 tsf (278 psi). Ultimate unit side resistance values (q_s) were 10.6 tsf for Rock Units B1, B2, C1 and C3, and 5.7 tsf for Rock Unit C2. In accordance with PENNDOT's *Design Manual, Part 4* (DM-4), Table 10.5.5-3, the ultimate unit side resistance was multiplied by a resistance factor of 0.55 to obtain the factored unit side resistance (q_{sr}). Factored unit side resistances (q_{sr}) were 5.8 tsf for Rock Units B1, B2, C1 and C3, and 3.1 tsf for Rock Unit C2. The factored axial resistance of the rock sockets was calculated by multiplying the factored unit side resistance (q_{sr}) by the surface area of the drilled shaft rock socket. In accordance with DM-4, Section C.10.8.5.3, rock zones/stratum with an RQD less than 20% were neglected in the calculation of side resistance. The side resistance from the overlying soils was also neglected.

The calculations indicated that rock socket lengths ranging from 12 to 24 feet were required to provide adequate axial resistance. The large variation in the length of the calculated rock sockets can be attributed to three factors. One factor was the magnitude of the factored axial design load, which varied at the pier bents from approximately 4,000 kips to 4,700 kips. Another factor that impacted the rock socket lengths was the variable presence and thickness of rock strata with RQD<20%, which were neglected in the calculations for axial support. A third factor was the presence and thickness of Rock Unit C2 (argillaceous siltstone), which had a lower unit side resistance than the other rock units.

Drilled Shaft Settlement

AASHTO's design methods were also used to calculate settlement of the drilled shafts. AASHTO Section C10.8.3.5 indicates that the axial compression load on a shaft socketed into rock typically is carried solely in side resistance until a total shaft settlement on the order of 0.4 inch occurs. At this displacement, the ultimate side resistance is mobilized and slip occurs between the concrete and rock. As a result of this slip, any additional load is transferred to the tip and side resistance reduces to zero. Therefore, calculations were performed to estimate settlement of the rock sockets to determine whether axial loads would be supported by either side or tip resistance. Calculations indicated that settlement at each drilled shaft would not exceed 0.4 inch; therefore, the rock sockets were designed assuming axial resistance would be provided solely by side resistance with no contribution from tip resistance.

Rock Socket Lateral Resistance

The computer program COM624P was used to analyze the lateral load capacity of the drilled shaft rock sockets. The "fence posting"

approach was used as discussed in the COM624P manual. Using the free-head option in the program, various lengths of the rock sockets were input for each design loading condition. A plot of top deflection versus rock socket length was created from the results of the computer analyses. The rock socket length required to provide lateral resistance was estimated by choosing a point on the curve where an increase in the rock socket length provided little reduction in deflection at the top of the rock socket. Based on engineering judgment, a minimum rock socket length of 20 feet was required in order to have an embedment of at least 2 to 3 shaft diameters, irregardless of the results of the COM624P results.

The lateral analyses were performed using service loads and moments multiplied by a factor of two. As determined by the structural engineer, axial and shear loads and a moment were applied at the top of the rock socket. Cyclic loading was used to model repeated loadings from wind and traffic (not seismic), and lateral resistance from soils overlying bedrock was neglected. Load-deflection (p-y) curve options included in the COM624P program were utilized to model the soil-structure interaction in the analyses. The "vuggy limestone" p-y curves were used for the majority of the rock sockets. However, "stiff clay below the water table" p-y curves were used at Pier 1 and Pier 6 (South) due to sloping bedrock adjacent to the rock sockets. The vuggy limestone curves did not appear to adequately account for the sloping rock condition. Parameters used for all rock units included an internal angle of friction of 0 degrees, a cohesion of 10% of the design unconfined compressive strength, a modulus of subgrade reaction of 2,000 pci, and a saturated unit weight of 0.0536 pci. E_{50} values ranged from 0.001 for Rock Units B1 and B2 to 0.003 for Rock Unit C2. Based on the results of the COM624P analyses plots of rock socket length versus deflection were developed for each design case as shown below in Figure 5.

Recommended Rock Socket Lengths

Recommended rock socket lengths were determined based on the results of the axial and lateral analyses. Lateral resistance controlled the rock socket lengths for all the drilled shafts except Pier 3 (North). This rock socket was controlled by axial resistance because approximately 7 feet of the rock socket was neglected for axial resistance due to the presence of low (<20%) RQD rock. The majority of the drilled shaft rock sockets were 20 feet in length, and the longest recommended rock socket length was 28 feet.

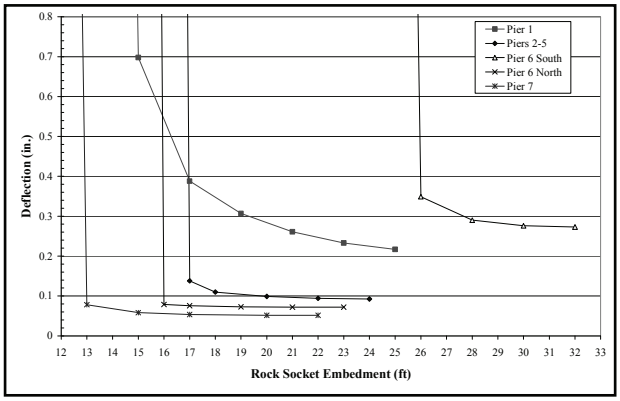


Figure 5: COM624P Results of Deflection versus Rock Socket Length

FULL SCALE AXIAL LOAD TEST

A 133-foot-long technique shaft was constructed to the north of Pier 5 prior to construction of the production shafts. The technique shaft and its rock socket had the same diameters as the production shafts. As presented in the 2004 report, an axial load test was performed by LOADTEST, Inc. on the technique shaft to verify the design side shear values and production drilled shaft lengths. Three 34-inch diameter Osterberg load cells located approximately 2 feet above the rock socket tip were used for the load test. The shaft was instrumented with Linear Vibrating Wire Displacement Transducers and telltales to measure displacement, and with vibrating wire strain gauges to measure side shear load transfer. Load increments were applied using the "Quick Load Test Method for Individual Piles" per ASTM D 1143.

Load Test Results

The maximum bi-directional load applied to the shaft was approximately 12,000 kips. At this maximum load 1.3 inches of displacement was measured above the O-cells, and 2.2 inches of settlement was measured below the O-cells. At these noted displacements an average unit side shear of 10.75 tsf was calculated for the rock above the O-cells, and a maximum applied end

bearing pressure of 98.25 tsf was calculated. LOADTEST, Inc. developed an equivalent top load curve from the test results. Based on this curve a top loading of approximately 5,600 kips would result in approximately 0.25 inch of settlement, and a top loading of approximately 10,200 kips would result in approximately 0.5 inch of settlement. Note that these settlements include elastic compression over the unsupported section of the shaft from the top of the drilled shaft to the top of rock, which exceeded 100 feet for this load test.

Comparison of Rock Side Shear Values (Design vs Load Test)

Unit side shear values used during the design phase were compared to values measured with strain gauges during the load test. These gauges were positioned in the three rock units (i.e., C1, C2, and C3) penetrated by the rock socket of the technique drilled shaft. The drilled shaft rock sockets for Piers 2, 3, 4, 5 and 6 (South) are founded in these rock units. Based on the results of the load test, the measured ultimate unit side shear values corresponding to 0.4 inch of deflection were approximately 1.5 tsf for Rock Unit C2 (i.e., argillaceous siltstone) and 10 tsf for Rock Units C1 and C3 (i.e., upper and lower siltstone). The ultimate unit side shear value used during design for Rock Units C1 and C3 was 10.6 tsf, which corresponds well with the 10 tsf value measured from the load test. However, the ultimate unit side shear value used during design for Rock Unit C2 was 5.7 tsf, which is nearly four times greater than the 1.5 tsf value measured from the load test.

CONCLUSIONS

As indicated above, ultimate unit side shear values measured during the load test correlated well with the design unit side shear value used for Rock Units C1 and C3 (upper and lower siltstone), but did not correlate well with the design unit side shear value used for Rock Unit C2 (argillaceous siltstone). The design unit side shear values (q_s) were based solely on the mean unconfined compressive strength (q_u) of the rock units using the equation $q_s=0.67(q_u)^{0.5}$.

The design unit side shear value for Rock Units C1 and C3 was controlled by the unconfined compressive strength of the concrete (3,500 psi), since the mean value from the unconfined compression tests on the rock samples was higher (3,785 psi). A review of the unconfined compressive strength test data presented previously in Table 5 indicates that the standard deviation for Rock Units C1 and C3 is 1,543 psi, which is approximately 40% of the mean value. Additionally, Figure 4 indicates that approximately 60% of the samples tested had unconfined compressive strengths greater than that of the design strength of the concrete. Conversely, the design unit side shear value for Rock Unit C2 was controlled by its mean unconfined compressive strength (938 psi). Table 5 indicates that the standard deviation for this rock unit is 931 psi, or approximately equal to the mean value, and Figure 4 indicates that approximately 60% of the samples tested had unconfined compressive strengths less than that of the mean value. This review of the unconfined compressive strength test results indicates that Rock Unit C2 values are more variable than Rock Units C1 and C3. Therefore, it is reasonable that the measured and design side shear values for Rock Units C1 and C3 more closely matched compared to the values for Rock Unit C2.

The unconfined compressive strength of Rock Unit C2 (argillaceous siltstone) was estimated based on the unit side shear value of 1.5 tsf measured during the load test. Using the equation $q_s=0.67(q_u)^{0.5}$, an unconfined compressive strength of 70 psi was back-calculated. This strength is less than the minimum value of 278 psi recommended for use with this equation. Therefore, using the equation $q_s=0.15(q_u)$, which is recommended by AASHTO for this range of unconfined compressive strengths, the back-calculated unconfined compressive strength is approximately 140 psi. This value is roughly 7 times lower than the mean unconfined compressive strength value from laboratory test results for Rock Unit C2; however, 3 of the 21 rock core samples tested from this rock unit had values lower than 140 psi. Although this low unconfined compressive strength value may not be representative of the rock strength at other drilled shaft locations, it is probable that this value is indicative of the rock strength at the technique shaft location.

In summary, the rock units encountered at the Youghiogheny bridge replacement site had fairly consistent unconfined compressive strength values, and the values were generally equal to or greater than the design strength of the

concrete. Thus, selection of design unconfined compressive strength values was not critical since it did not control the design. However, one rock unit was considerably weaker in strength, and laboratory unconfined compressive strength results varied dramatically. The mean compressive strength value for this rock unit was used for axial design of the drilled shaft rock sockets, but measured side shear values from a full scale load test indicated that this design value was extremely high, at least at the load test shaft location. This difference between design and measured values had little impact on this project. Minimal resistance was anticipated from this rock unit during design because this rock unit was thin, and the design unit side shear value of this rock unit was nearly half that of the other rock units. Furthermore, lateral capacity typically controlled the drilled shaft rock socket length, so additional side resistance was available at most locations without increasing rock socket lengths. Nevertheless, the selection of design values for calculating side shear resistance of drilled shaft rock sockets requires careful consideration of the range of the laboratory test values as well as the sensitivity of these values with respect to calculated rock socket lengths, particularly at sites where weak rock is encountered.

REFERENCES

American Association of Highway And Transportation Officials, 1998, AASHTO LRFD Bridge Design Specifications, 2nd Edition.

American Society of Testing And Materials, 2004, Standards on Disc, Volumes 4.08 Soil and Rock (I) and 4.09 Soil and Rock (II), ASTM International.

Commonwealth of Pennsylvania, Department of Transportation, April 2000, Design Manual Part 4, with revisions to April 2001.

Flint, N.K., 1965, Geology and Mineral Resources of Southern Somerset County, Pennsylvania, County Report C56A, Commonwealth of Pennsylvania, Bureau of Topographic and Geologic Survey.

Gannett Fleming, Inc., November 2003, Addendum to Structure Foundation Geotechnical Report, S.R. 0040 over Youghiogheny Reservoir, prepared for PENNDOT District 12-0.

HDR Engineering, Inc., April 2003, Final Geotechnical Engineering Report for Foundation Submission, Youghiogheny Dam Bridge Replacement, prepared for PENNDOT District 12-0.

Hickok, W.O. and Moyer, F.T., 1971 (reprinted 1973), Geology and Mineral Resources of Fayette County, Pennsylvania, County Report 26, Pennsylvania Geological Survey, Fourth Series.

Loadtest, Inc., May 12, 2004, Report on Drilled Shaft Load Testing (Osterberg Method), prepared for Case Foundation Company.

Shaulis, J.R., 1985, Coal Resources of Fayette County, Pennsylvania, Part 1. Coal Crop Lines, Mined-out Areas, and Structure Contours, Mineral Resource Report 91, Part 1, Pennsylvania Geological Survey, Fourth Series.

Shaulis J.R., 1994, Hooked on the Rocks: Exploring the Geology of the Youghiogheny River Lake-A Boating Field Trip, Pennsylvania Geology Volume 25, No. 2, Commonwealth of Pennsylvania, Bureau of Topographic and Geologic Survey.

U.S. Department Of Transportation, Federal Highway Administration, August 1993, COM624P-Laterally Loaded Pile Analysis Program for the Microcomputer, Version 2.0, Publication No. FHWA-SA-91-048.

DRILLED SHAFT FOUNDATIONS FOR THE FLOAT-IN DAM ON THE MONONGAHELA RIVER AT BRADDOCK, PA

Robert B. Bittner, P.E., Ben C. Gerwick, Inc., San Francisco, CA, USA
William R. Miles, P.E., Bergmann Associates, Rochester, NY, USA

The new gated dam on the Monongahela River at Braddock, Pennsylvania, was built for the US Army Corps of Engineers using an innovative "In-the-Wet" technology. A key feature of this technology involves construction of the foundations through the water and later mating the completed structure or a shell of the structure to the pre-installed foundation. This paper presents a description of the structure, its foundation, construction sequence and design details required to successfully implement this technology.

INTRODUCTION

Locks and dams in the United States have historically been built by blocking off large sections of the river with circular-sheet-pile cells; dewatering the area surrounded by the cells; and then proceeding with foundations followed by the superstructure. After completing one segment of structure, the area enclosed by cells is again flooded, the circular cells are moved and another section of the river is dewatered to allow a continuation of construction on the adjacent sections. This process is continued for multiple cycles until the entire lock or dam is completed. (See Figure 1 for an example of this type of construction.)



Figure 1: Conventional Cofferdam Construction

This method has been successful in the past, but suffers from a number of draw- backs:

- The large temporary cofferdams are expensive to build and remove;
- They restrict river flow and impact navigation (This is especially true when replacing an existing navigation structure.);
- Drying up extensive areas of the river bottom requires construction and operation of large expensive dewatering systems;
- If the structure is located on ground that contains contaminates, dewatering can spread contaminates in the ground and create a need for treatment of the water once collected by the dewatering system.
- The large temporary cofferdams are typically in place for 2 or more years and are subject to overtopping and flooding of the work area during periods of high water.

An alternative to this approach is a method referred to as "float-in" or "in-the-wet" construction that involves constructing the foundation for the structure through the water and then floating in or lifting in a shell of the structure and mating it to the pre-installed foundation. This technique has been in use for centuries. Early examples include float-in caissons used to build breakwaters and quay walls. Over the last 100 years, 125 immersed tube tunnels have been built around the world using this technique. It has been used to build paper mills up the Amazon River, power plants on the Mississippi River and large off-shore gravity base structures in the North Sea and Arctic Ocean.

The Pittsburgh District of the US Army Corps of Engineers in an effort to develop alternate and more cost effective construction methods for their navigation structure on the inland waterways of the US selected this method of construction for replacement of Dam 2 on the Monongahela River, eleven miles upstream from Pittsburgh at Braddock, Pennsylvania. See Figure 2 for an aerial view of the dam site. The Corps developed the initial concepts and

then selected a team consisting of Ben C. Gerwick, Inc of San Francisco, Bergmann Associates of Rochester, New York, and D'Appolonia of Pittsburgh, Pennsylvania, to perform the detailed design of the new 720-foot long navigation dam.



Figure 2: Braddock Dam Site

See Figure 3 for a location map of Braddock Dam.

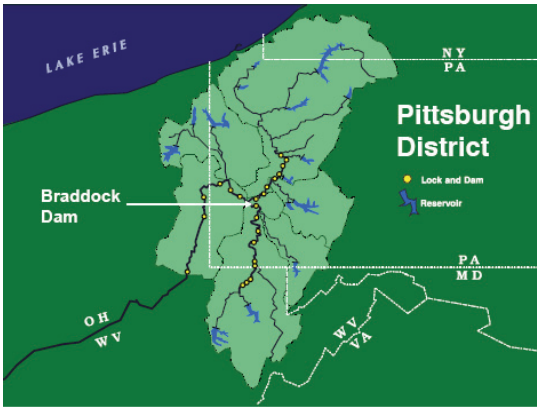


Figure 3: Location of Braddock Dam

The Corps initial "In-the-Wet" concepts envisioned using off-site prefabrication of thin concrete shells (or segments). The segments were to be built on a large barge in a two-level casting basin, or in a drydock, floated into final position over pre-installed foundations, and then locked onto the foundations by underbase grouting and infilling of the segments with tremie concrete. These concepts offered several advantages over conventional "In-the-Dry" construction:

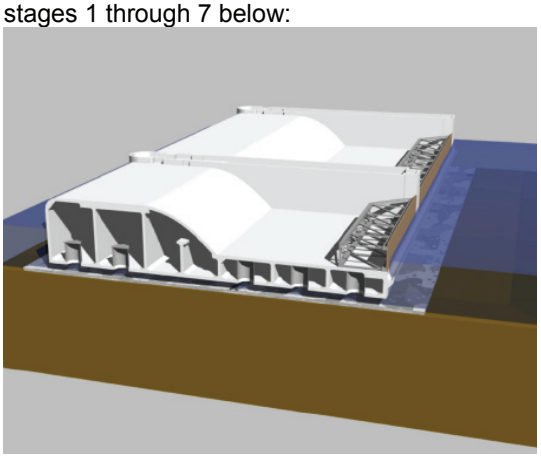
- Less disruption to river navigation and river flow;
- Lower cost of construction through the elimination of conventional large sheet pile cofferdams and site dewatering;
- Shorter construction time by allowing concurrent construction of dam segments and dam foundations;
- Less environmental impact by reducing dredging and eliminating site dewatering;
- Higher quality by allowing the use of precast concrete produced in a controlled on-shore environment.

The final design developed by the Gerwick-Bergmann-D'Appolonia team was constructed by a joint venture of JA Jones and Traylor Bros. The final structure consisted of two large prefabricated concrete segments that were floated into place, and set-down on a pre-constructed foundation. The float-in section of the new dam was a 600-ft long by 104.5-ft by 42-ft high structure with four gate bays and one fixed-crest weir bay. The final "In-the-Wet" design called for breaking the dam into two segments of 333-ft and 265-ft. The segments were constructed as closed bottom boxes in a two level casting basin. The exterior walls, bottom and top slabs of the boxes were 12-in thick and the interior walls were 10 and 12-in thick. The bottom slabs were post-tensioned and contained recesses to allow the pre-installed foundation to penetrate the bottom of the slab during set-down of the segments.

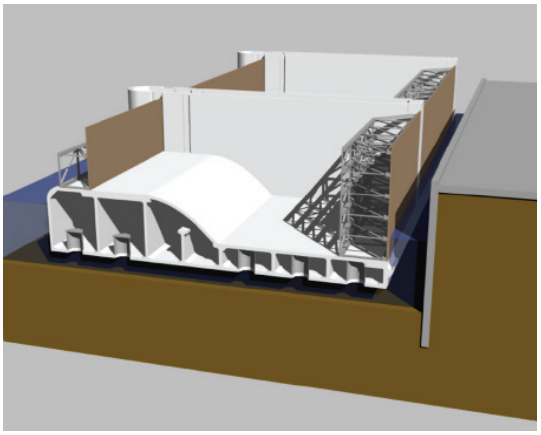
As each segment was completed, it was launched by flooding the basin and then towed to the outfitting pier two miles upstream of the dam site for final outfitting. The dam segments were then floated downstream to the dam site and positioned over the foundation caissons with a mooring system mounted on top of each dam segment. The foundation system consisted of sheet-pile cut-off walls upstream and downstream, H-piles below the tailrace area and 72 inch diameter drilled shafts installed in a pre-excavated area upstream of the existing dam. Each segment was ballasted down onto 6 landing shafts and leveled with flat jacks installed within the piers of the float-in dam segments. The under-base was then grouted, and 8-ft of tremie concrete was placed in the segment compartments. Each compartment within each segment was then dewatered and the remainder of the dam including tainter gates was completed in the dry. After all cells within a given segment had been filled with concrete, the dam segment was locked on to the tops of the drilled shafts by grouting the pile-top annulus.

SEQUENCE OF CONSTRUCTION

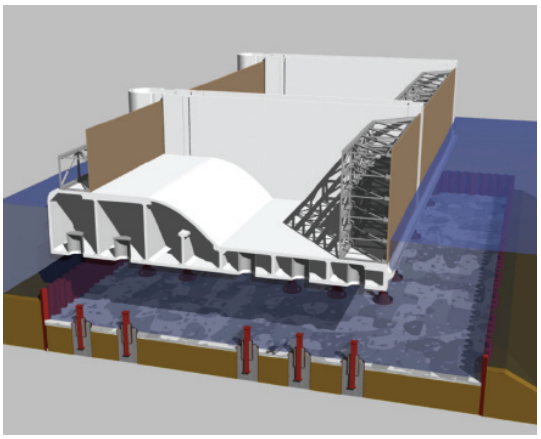
Construction of the dam was carried out in seven stages. See construction sequence stages 1 through 7 below:



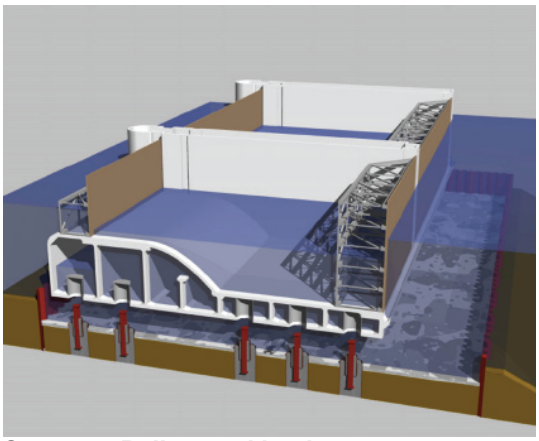
Stage 1 – Cast segment in two level casing basin.



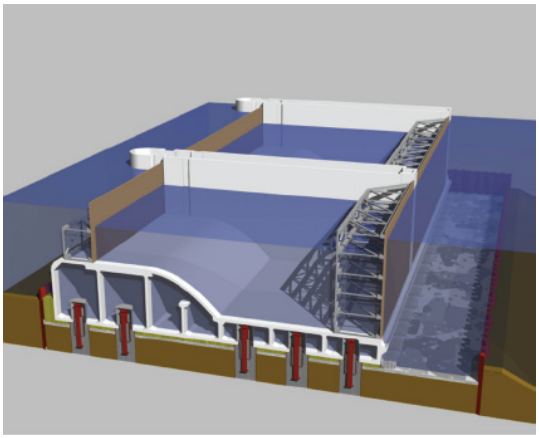
Stage 2 – Launch and tow segment to outfitting pier.



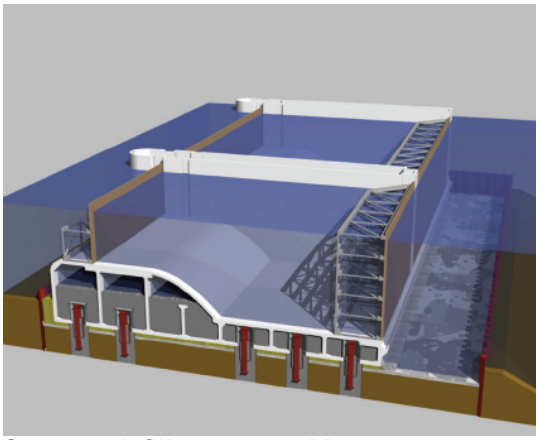
Stage 3 – Position segment over pre-installed foundations.



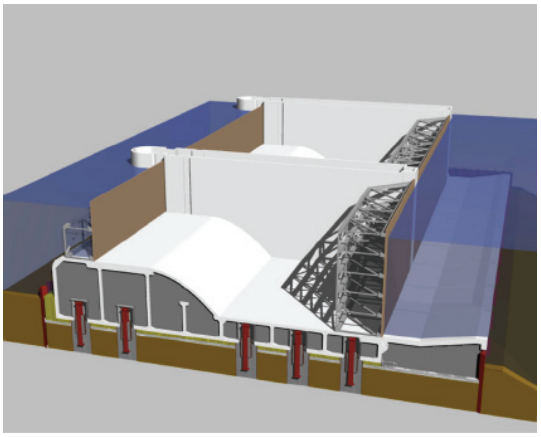
Stage 4 – Ballast and land segment.



Stage 5 – Underbase grout segment.



Stage 6 – Infill segment with concrete.



Stage 7 – Complete segment infill, grout pile tops, dewater bays, and install tailrace panels.

FIRST STAGE EXCAVATION AND BOTTOM PREPARATION

Dredging was performed in two stages. The first stage of pre-excavation for the dam foundation was performed below the footprint of the dam and consisted of excavation the river bed to El. 690, from the existing lock river wall to the left bank abutment toe in a strip about 140 feet wide. The depth of the excavation ranged from 14 feet to 32 feet across this reach. The excavation was inclined up the existing river bed grade at a slope of 1 on 10 upstream and 1 on 5 downstream to El. 702. Dredged materials were transported by barge to the upstream disposal site.

CUT-OFF WALLS

After pre-excavation, steel sheet piling were installed to provide both upstream and downstream cut-off walls and to serve as retaining walls for various stages of work on the dam. A prerequisite pile driving program was used to determine the elevation of rock to which sheets were to be driven. Sheets were ordered to accurate lengths once these elevations were determined. The upstream cut-off wall, located 3-ft from the upstream face of the future dam, was installed first. This 600-ft long wall was installed in two stages using a barge mounted pile driver. The first stage involved installation of 75-ft long H-piles on a 19-ft spacing. These H-piles were driven to the top of rock and were outfitted with pre-installed interlocks welded to one flange. At completion of driving, the top of the H-piles and the interlocks extended above water and provided a guide for installation of 18-ft wide sheet pile wall panels between the H-piles. The sheets were driven to final grade, approximately 29-ft under water, and thereby eliminated the need for divers to cut the sheets off under water.

The downstream cut-off wall was then installed in a similar manner. The downstream cut-off wall consists of a structural system of 24-inch diameter pipe piles and sheet piles. Pipe piles were used rather than H-piles because the pipes supported the downstream end of the precast tailrace panels, and this wall system was required to resist the loads imposed by the retained alluvium when the downstream face of the wall was excavated to rock for installation of scour protection. The pipe piles were first driven and a 6-ft deep reinforced concrete rock socket was installed in each pile tip. The sheet piles were connected to the pipe piles by a special interlock section that was pre-welded to each side of the pipe pile prior to driving.

SECOND STAGE EXCAVATION, BOTTOM PREPARATION, DAM FOUNDATION SYSTEM

With the cut-off walls in place, the area between the walls was excavated an additional 8 ft to El. 682, and a 12 inch layer of 1.5 inch stone placed and levelled. Eighty nine drilled shafts were used to support the dam piers and gate sills. Two rows of H-piles on 8-ft spacing driven to the claystone rock layer were used to support the dam tailrace. The tops of the H-piles extended up into the first tremie concrete poor below the tailrace slabs.

DRILLED SHAFT FOUNDATIONS

The base of the dam is at El. 683.7 ft which is about 38 ft below the normal pool level and 15 ft below the existing riverbed. The stratigraphy below the dam consists of approximately 16 ft of alluvium comprised of sandy gravel (GM) to silty sand with gravel (SM). Below this layer is soft to medium hard clay shale and claystone down to El. 658 ft. Medium hard to hard siltstone is encountered between El. 658 ft and 626 ft. The drilled shafts for the dam were founded in this layer. The average unconfined compressive strength of the clayshale is 840 psi and the siltstone 3600 psi. Two test shafts where installed and loaded both laterally and vertically. See Figure 4 for a stratigraphic

section of the river bottom relative to the river bottom and the drilled shafts.

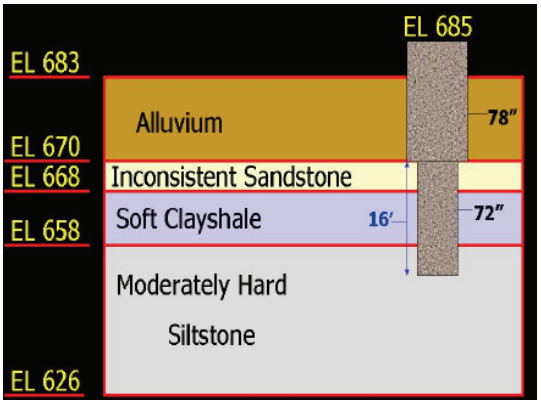


Figure 4: General Geologic Section

See Figure 5 for a layout of the 89 drilled shafts under the dam.

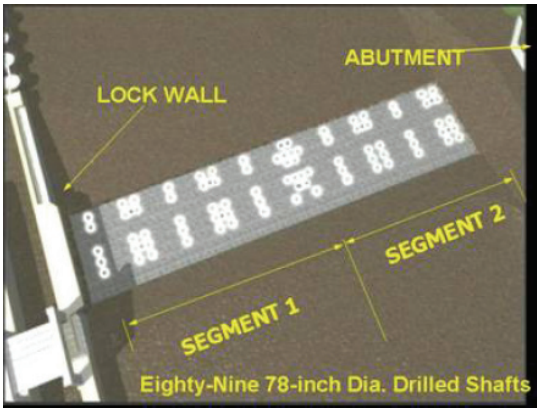


Figure 5: Layout of pre-installed drilled shafts

Two types of drilled shafts were installed under the main body of the dam:

- Six set-down drilled shafts under each of the floating-in dam segments provided initial support of the float-in dam segments at set-down;
- Seventy seven foundation drilled shafts provided long-term support of the completed dam.

See Figure 6 for a schematic of the two drill shaft types.

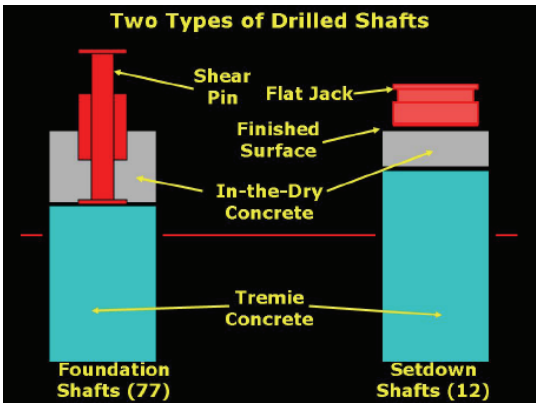


Figure 6: Two types of drilled shafts

All drilled shafts were step-tapered with a 72" diameter rock socket drilled through a 78" diameter permanent steel casing. Permanent casings were driven and seated into the top of the claystone rock layer. Drilling removed all material from within the casing and the 72" diameter rock socket were then drilled roughly 6 feet into the lower siltstone rock layer.

All drilled shafts were positioned using a four-legged two-level template. The fixed lower template was installed first to a tolerance of +/- 12 inches, and the sliding upper level template was set and fixed into position to a tolerance of +/- ¼ inch. Casings were then installed and barge mounted equipment performed the drilling. After the drilled shafts were thoroughly cleaned out, a steel reinforcing cage was installed, and the shaft was filled with tremie concrete to an elevation approximately 6 ft below the bottom of the future dam.

After the tremie concrete attained sufficient strength, the casings were dewatered and latent concrete was manually removed in-the dry. A tension-anchor/shear-pin assembly consisting of a 14" steel wide flange tension anchor and 36 inch diameter pipe shear pin was then installed and fixed in position by concrete placed in the dry. The top of each casing was then cut-off to a vertical tolerance of +/- ¼ inch using a temporary circular cofferdam that was installed over the top of the drilled shaft casing and sealed to the outside face of the casing below the cut-off point using inflatable rubber seals. The annulus between the casing and the temporary cofferdam was then dewatered and the drill casing was cut off in-the-dry from the inside the casing.

The 12 Set-down drilled shafts were generally constructed in a similar manner to the

foundation drilled shafts. However, instead of installing a tension-anchor/shear-pin assembly, a levelled grout surface was constructed at the bottom elevation of the dam. A tolerance of +/- 1/8th inch was obtained by milling the top surface of the drilled shaft concrete. The casing was then cut-off underwater using the same technique described above.

PRECAST SHELL FABRICATION, LAUNCH TRANSPORT AND OUTFITTING

While the dam foundations were under construction, the two float-in dam segments were constructed at a two level casting basin located at a 15-acre site 27 miles downstream from Braddock on the Ohio River. The two level casting basin allowed the segments to be cast on an upper level, a few feet above normal pool elevation in a protected area behind an earthen berm.

See Figure 7 for an aerial view of the casting basin and launch site at Leetsdale, PA.

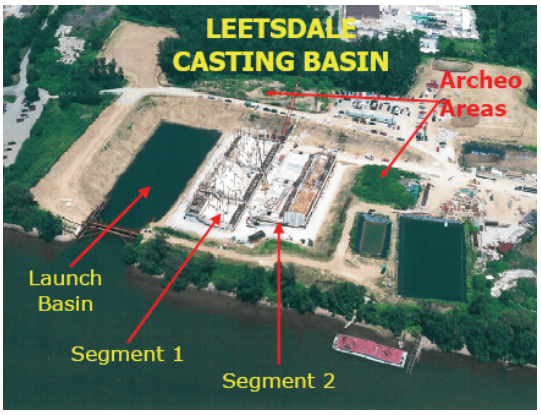


Figure 7: Cast and launch site

The total 600-ft length of float-in dam was divided into two segments. The 333-ft long Segment 1 weighed approximately 12,000 tons and the 265-ft long Segment 2 weighed approximately 10,000 tons. The float-in segment included: the gate sills, a portion of the stilling basin, and the pier bases up to El. 726.0. Segment No. 1 included the fixed weir bay, the water quality bay and one of the standard gate bays while Segment No. 2 included two standard gate bays. All bays were 110' wide. The joint between Segments 1 and 2 occurred at Pier 3, which made it 11 feet wider than adjoining piers to facilities this connection.

The walls and diaphragms of the float-in segments were precast panels. The top and bottom slabs were cast-in-place concrete. The largest individual precast wall panels were 21 feet by 30 feet and weighed approximately 80 tons. All wall panels were tied together with cast-in-place closure pours positioned at the intersection points of the walls. Sixty-inch diameter corrugated sleeves were cast into the bottom of the dam segments over the connection points to the tension-anchor/shear-pin assemblies installed in the tops of the drilled shafts. After erection of the wall panels, installation of post-tensioning ducts and bottom recess sleeves, the bottom slab was cast in place. See Figure 8 for a view of the erected precast wall panels and corrugated recess sleeves used to provide connection to the drilled shaft tension-anchor/shear-pin assemblies.



Figure 8: Precast wall panels and bottom recess sleeves

When the precast dam segment was ready for launch, the upper and lower basins were flooded to a common water level and the segments were floated one at a time over the lower basin. The water level in the lower basin was then returned to the outside river elevation, the exit sheet-pile wall was removed and the segment was towed out of the casting facility. The segments were completed to a partial stage such that the maximum draft of the segments did not exceed 11 feet. Segments were transported from the off-site assembly location to the project site for additional outfitting prior to set-down. All handling and transport were by towboats.

Each segment with a draft of approximately 11 feet was then towed to the outfitting site upstream of the dam site. Transport of the segment was performed using a primary tow boat and guided as necessary by a snubbing tow. The segments were transported through

two locks on the Ohio River, past the city of Pittsburgh, and up the Monongahela to a site upriver of the Braddock Dam site. See Figure 9 for a view of the Segment No. 1 under tow.



Figure 9: Dam segment No.1 towed up the Ohio past Pittsburgh

Once a segment arrived at the outfitting site, it was moored to the outfitting pier. The outfitting pier consisted of a system of circular sheet pile cells and arcs, and included a 15-ft high braced fendering system to keep the segment on the face of the pier during high water.

Each segment was completed and readied for set-down at the outfitting pier. The piers of each delivered segment were extended approximately 21 feet. Temporary bulkheads for immersion were added both upstream and downstream on each gate and weir bay. Additional permanent concrete ballast, ballast piping and portions of the mooring and alignment equipment were also added. Work platforms and vertical tremie pipes for post-set-down underbase and concrete infilling operations were installed. Once completely outfitted, each segment had a draft of approximately 14 feet. Additional water ballast was added as necessary to trim the segment before transport to the project site.

POSITIONING AND GUIDANCE SYSTEMS

After completion of outfitting on a given segment, it was maneuvered down river by a primary tow boat and guided by a snubbing tow boat. After positioning close to the set-down site, 8 mooring lines from winches mounted on top of the segments were connected to the drilled-shaft anchors pre-installed upstream of the dam site. The segment was then rotated transverse to the current, winched downstream, and then positioned directly over the top of the prepared foundation. The segment was then aligned with two horn guides located on the face of the river wall. See Figure 10 for an aerial view of Segment No. 1 being positioned at the dam site.



Figure 10: Segment No. 1 being positioned at site

BALLAST SYSTEMS

After each outfitted segment was maneuvered into position, it was ballasted onto its 6 set-down drilled shafts. Water was first added to the interior compartments of the segment and as the segment sank deeper into the water, ballast water was added to the individual bays. As ballasting progressed, all interior tanks were continuously sounded to monitor free surface effects and maintain hydrodynamic stability of the segment at all times.

By adding ballast water to the gate bays and using the horn guides, mooring lines and land based survey control for guidance, each segment was accurately lowered into position and the tension-anchor/shear-pin assemblies were threaded into the hollow recesses built into the bottom floor of the dam segments. Ballast water was then fed into the dry piers until the hydraulic jacks register the required initial loading. See Figure 11 for a view of the ballast system positioned on top of Segment No. 1 during float-in.



Figure 11: Segment No. 1 with ballast system on the top deck

A hydraulic ram on the downstream corner of the Segment 1, adjacent to the lock wall and in conjunction with the mooring lines, was used to align the segment on its longitudinal axis.

SEGMENT LEVELING SYSTEM

Each segment was landed on 6 set-down drilled shafts. These drilled shafts were laid out to provide two support points on the longitudinal centerline of each dam pier. In order to provide even support and level the segment to the specified tolerances, two hydraulic pistons were built into each pier. When a given dam segment was properly aligned and landed, the 6 pistons were directly aligned over the top of the 6 set-down drilled shafts. The pistons were 36" diameter steel pipe sections with end caps and were built into the floor of the pier, flush with the bottom of the dam segment. The pistons were fitted with rubber seals to prevent water leakage and their sides were greased prior to placing the bottom slab concrete. A pair of 36" diameter, 1000 ton capacity flat-jack was stacked on top of each piston and the upper surface of the flat-jack was in direct contact with a concrete reaction beam spanning the 12-ft width of the pier shell. The 6 flat-jacks were connected into three hydraulic circuits to provide a three-point support system for each segment.

Once a segment was levelled to the specified tolerance, the flat jacks were "locked-off" and the hydraulic fluid in the jacks was replaced with a high strength 2-part resin.

UNDERBASE GROUTING

Following set-down, the 12-inch deep void area between the underside of the dam segment and the preleveled, stone-covered river bottom was filled with grout to eliminate flow below the dam. To make the underbase grout placement more manageable, the area under the segment were divided into five 70-foot wide transverse strips by using inflatable grout bags pre-attached to the underside of the float-in segment prior to set-down. Both transverse and downstream bags were used. First, the space between the upstream cut-off wall and the dam was sealed to stop flow beneath the segment. Then each 70 foot wide strip was filled with grout using the vertical grout pipes installed at the outfitting pier. Typically, each grouting area contained six rows of 8-inch diameter grout pipes spaced at a maximum of 21-ft on center. Underbase grouting was started at the downstream row of grout pipes and continue upstream until the space below the dam was completely filled. Grouting was stopped when grout filled the 8-ft high by 3-ft wide vertical gap between the dam shell and the upstream cut-off wall.

STRUCTURE INFILL

Once all the underbase grouted had attained minimum strength, the dam was infilled with concrete which acted compositely with the hollow segment. Thirty two compartments in Segment 1 were filled with concrete in a two stage operation. The first stage placement consisted of filling the bottom 8 feet of each compartment continuously with tremie concrete while the segment was fully flooded. The second stage placement was placed in-the-dry after the first stage tremie concrete had cured and the compartment had been dewatered. Typically, each compartment had one or two 10 inch tremie pipes. The downstream compartments also had 8 inch evacuation pipes in each corner.

After infilling was completed, the dam segment was "locked" onto the foundation drilled shafts by pumping a sand/cement grout into the hollow recesses surrounding the tension-anchor/shear-pin assemblies.

PIER COMPLETION TAILRACE CONSTRUCTION AND GATE INSTALLATION

The upper portion of the dam piers between El 726 and El 765 was placed in-the-dry after the float-in dam segment were set-down and filled with concrete. This portion of the dam piers was completed with a combination of precast concrete and conventional cast-in-place concrete.

Trunnion girders were attached to the downstream face of each of the five piers for support of the four tainter gates, the trunnion girders were constructed of cast-in-place concrete.

While the piers were being constructed, the dam's tailrace was constructed in-the-wet. The tailrace was built utilizing precast panels that were 30'-6" wide by 20'-0" long by 15" thick. The upstream end of the panels was supported on a ledge cast in to the downstream edge of the dam segments and the downstream end of the panels was supported on the row of previously installed 24" diameter pipe piles, which were integral with the downstream cut-off wall. The area below the tailrace panels was filled with tremie concrete to create a mass concrete tailrace section supported by the previously installed H-pile foundation system.

Following the completion of the pier and tailrace structures and prior to installation of the left closure weir, the 220-t tainter gates were installed by floating in the assembled gates one at a time on the deck of a barge. Once the gate was located in its final position, the two hydraulic operation cylinders were installed. The cylinders were connected to each end of the tainter gate and to the cylinder girders which are anchored to the upper pier structure.

See Figure 12 for a schematic of the completed dam.

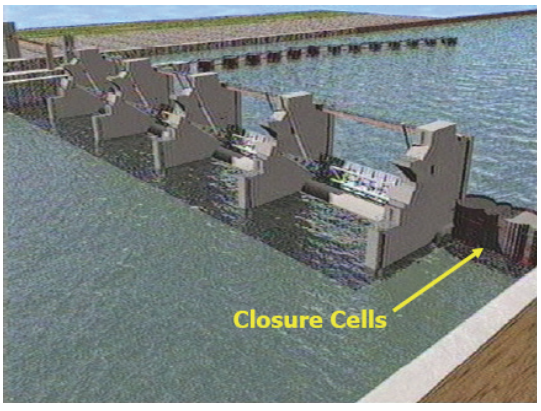


Figure 12: Schematic diagram of the complete dam and closure cells

CONCLUSION

The new Braddock was designed and constructed using "Float-in" technology. The project was the first use of this technology by the U.S. Army Corps of Engineers and was the largest float-in navigation structure built in the United States. The successful and economical first time adaptation of this technology to the design and construction of navigation structures has demonstrated the applicability of this technology to other inland waterway projects within the United States and offers the potential of revolutionizing the future construction of navigation projects within the Corps of Engineers.

REFERENCES

Ben C. Gerwick, Inc., 1995. Upper Mississippi River - Illinois Waterway System Navigation Study: Innovative Lock Concept Review.

Bergmann Associates and Ben C. Gerwick JV for the USACE Nashville District, 2003. Engineering Report on the Downstream Cofferdam in the Kentucky Lock Addition Project.

Bergmann Associates, Ben C. Gerwick, Inc. D'appolonia, Geosci, et al., 1998. Design of New Gated Dam for Innovative In-the-Wet Construction, Braddock Locks and Dam, Monongahela River.

Bergmann Associates., 3D Animated Video, 44 minutes, January 1999, (also part of the Construction Contract Documents).

Hegazy, Y.A., Cushing, A.G., and Lewis, C.J., 2004. Driven Pile Capacity in Clay and Drilled Shaft Capacity in Rock From Field Load Tests, Fifth International Conference on Case Histories in Geotechnical Engineering, New York, NY.

Miles, W.R., and Karaffa, W. In-the-Wet Construction of a New Gated Dam Braddock Locks and Dam, Monongahela River, PA.

DESIGN AND CONSTRUCTION OF THE RION ANTIRION BRIDGE FOUNDATIONS

Alain Pecker, Géodynamique & Structure, Bagneux, France

The choice of a design concept for a bridge foundation is guided by various factors; several of these factors are indeed of technical origin, like the environmental conditions in a broad sense, but others non technical factors may also have a profound impact on the final design concept. The foundations solutions adopted for the Rion Antirion bridge are described and an attempt is made to pinpoint the major factors that have guided the final choices. The Rion Antirion bridge is exemplar in that respect: the foundation concept combines the simplicity of capacity design, the conceptual facility of construction and enhances the foundation safety. The design of these foundations was a very challenging task which required full cooperation and close interaction with all the parties involved: concessionaire, contractor, designers and design checker.

INTRODUCTION

The Rion-Antirion bridge project is a BOT contract granted by the Greek Government to a consortium led by the French company Vinci Construction (formerly Dumez-GTM). It is located in Greece, near Patras, will constitute a fixed link between the Peloponese and the Continent across the western end of the gulf of Corinth and is intended to replace an existing ferry system (Figure 1). The solution adopted for this bridge is a multiple spans cable stayed bridge with four main piers; the three central spans are 560 m long each and are extended by two adjacent spans (one on each side) 286 m long. The total length of the bridge, with the approach viaducts, is approximately 2.9 kilometers (Figure 2). The call for tender was launched in 1992, the contract, awarded to the consortium in 1996, took effect in December 1997. Construction started in 1998 and has been completed in summer 2004 and opened to traffic on the 11th of August, five months ahead of schedule.

The bridge has to be designed for severe environmental conditions (e.g., Teyssandier et al. 2000; Teyssandier 2002): weak alluvium deposits, high water depth, highly seismic area, possible occurrence of large tectonic displacements. Very early in the design process it turned out that design was mainly controlled by the seismic demand imposed to the foundations.

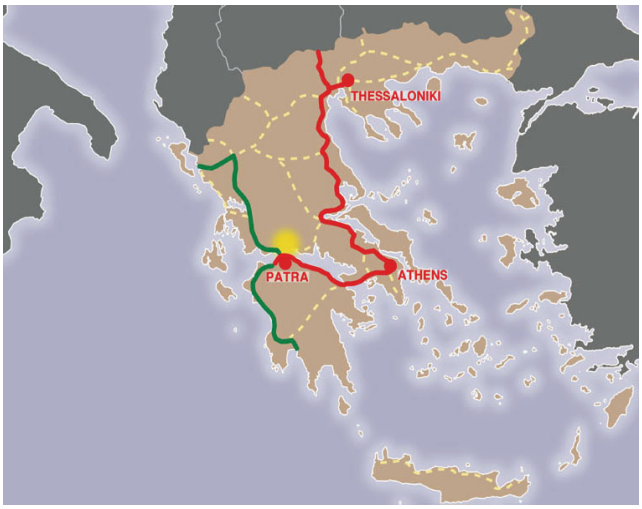


Figure 1: Location of the bridge

In order to alleviate potential damage to the structure due to the above adverse conditions and to carry the large earthquake forces brought to the foundation (shear force of the order of 500 MN and overturning moment of the order of 18 000 MNm for a vertical buoyant pier weight of 750 MN), an innovative foundation concept was finally adopted which consists of a gravity caisson (90 m in diameter at the sea bed level) resting on top of the reinforced natural ground (Combault et al. 2000). The ground reinforcement is composed of steel tubular pipes, 2 m in diameter, 20 mm thick,

25 to 30 m long driven at a grid of 7 m x 7 m below and outside the foundation, covering a circular area of approximately 8 000 m^2. The total number of inclusions under each foundation is of the order of 150 to 200. In addition, the safety of the foundation is greatly enhanced by interposing a gravel bed layer, 2.8 m thick, on top of the inclusions just below the foundation raft with no structural connection between the raft and the inclusions heads. This concept (inclusions plus gravel layer), in addition to minimizing the hazards related to differential settlements, enforces a capacity design philosophy in the seismic foundation design, (Pecker 1998).

In the following we will focus on the foundations of the main bridge, because the foundations of the approach viaducts (pile foundations) do not deserve much comments.

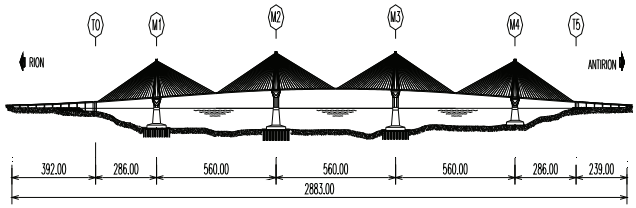


Figure 2: Bridge elevation

GEOLOGICAL AND GEOTECHNICAL ENVIRONMENT

The site has been subjected to extensive offshore soil investigations performed either from floating barges or from a ship, controlled with a dynamic positioning system; these investigations included cored boreholes, static Cone Penetration Tests with pore pressure measurements (CPTU), Standard Penetration tests (SPT), vane tests and dilatometer tests, seismic cone tests and sampling of intact soil samples for laboratory testing. All the borings reached depths ranging from 60 m to 100 m below the sea bed. Under each of the main bridge pier three continuous boreholes, three CPTU, two seismic cones, one SPT/dilatometer boring have been drilled. Approximately 300 samples have been retrieved and subjected to advanced laboratory testing. Based on the results of these investigations representative soil profiles have been defined at the locations of the main bridge piers and ranges of soil mechanical characteristics have been derived.

The water depth in the middle of the strait reaches 65 m. The soil profile consists of weak alluvial strata deposited in alternate layers, with individual thickness of a few meters, of silty sands, sandy clays and medium plasticity clays. In the top hundred meters investigated by the soil survey, the clay, or silty clay, layers predominate (Figure 3). No bedrock was encountered during the investigations and based on geological studies and geophysical surveys its depth is believed to be greater than 500 m.

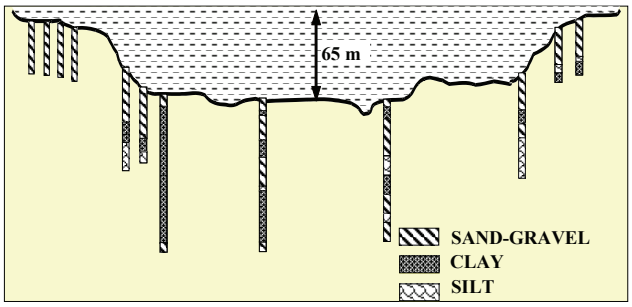


Figure 3: Soil profile

The mechanical characteristics of the offshore layers are rather poor with undrained shear strengths of the cohesive strata increasing slowly with depth from approximately 30-50 kN/m^2 at the sea bed level to 80-100 kN/m^2 at 50 m depth (Figure 4). A major difference occurs in the cohesionless strata: some of these layers are prone to significant pore pressure buildup, even possibly to liquefaction, under the design earthquake. Accordingly, the undrained strengths of the cohesionless layers are taken equal either to their cyclic undrained shear strengths or to their residual strengths.

Based on the results of the laboratory one dimensional compressibility tests and of correlations with CPT results or with the undrained shear strengths, a slight overconsolidation, of the order of 150 kN/m^2, of the upper strata was evidenced.

The shear wave velocities are also small, increasing from 100-150 m/s at the ground surface to 350-400 m/s at 100 m depth (Figure 5).

It is worth noting that for design, as shown in Figures 4 and 5, two sets of soil characteristics have been used instead of a single set based on characteristic values; this decision is guided by the fundamental necessity to maintain

compatibility in the whole seismic design process: the seismic demand is calculated assuming one set of properties (successively lower bound and upper bound) and the foundation capacity is checked with the associated strengths (respectively lower bound and upper bound); the capacity is never checked with low properties when the forces are calculated with high properties and vice versa. In addition, given the large foundation dimensions, special attention has been paid to the spatial variability of the soil properties across anyone foundation; this variability may have an impact on the differential settlement and tilt of a pylon. Figure 6 gives an example of the variability of the cone point resistance across a foundation, variability which is obviously reflected by variability in the shear strength and compressibility of the soil strata.

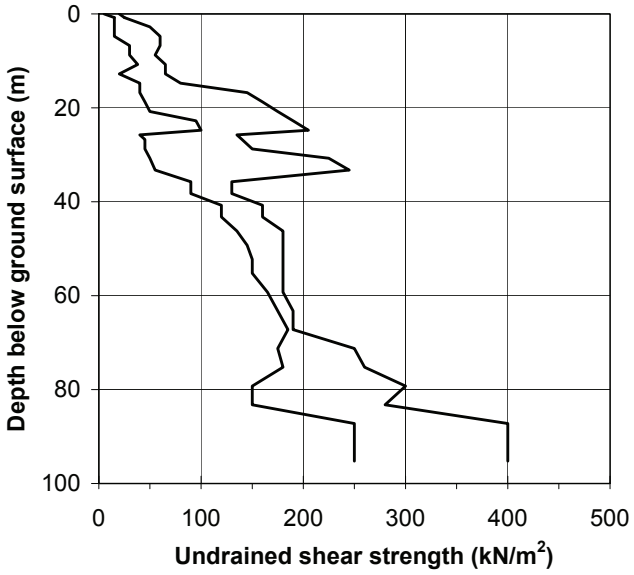


Figure 4: Undrained shear strength

ENVIRONMENTAL CONDITIONS

The environmental conditions are defined by three major possible events likely to occur during the bridge life time: ship impact on a main bridge pier, occurrence of a major earthquake in the vicinity of the bridge, long term tectonic movements.

Ship impact

The hazard represented by this impact corresponds to 160 000 Mg tanker hitting one pier at a speed of 16 knots (8.2 m/s). This impact induces an horizontal shear force of 480 MN acting at 70 m above the foundation level; at the foundation level the
corresponding forces are: shear force of 480 MN and overturning moment of 34 000 MNm.

Earthquake event

The bridge is located in one of the most seismic area in Europe. In the past 35 years three earthquakes exceeding 6.5 on the Richter scale have occurred in the Gulf of Corinth. The 1995 Aigion earthquake took place less than 30 km east of the site. Figure 7 presents the epicenters of the major earthquakes felt in the Gulf of Corinth along with the major tectonic faults. The contract fixed for the design motion a return period of 2 000 years. A comprehensive seismic hazard analysis has defined the governing event as a 7.0 surface wave magnitude earthquake originating on the Psathopyrgos fault (shown with an arrow in Figure 7) only 8.5 km east of the site (circle in Figure 7).

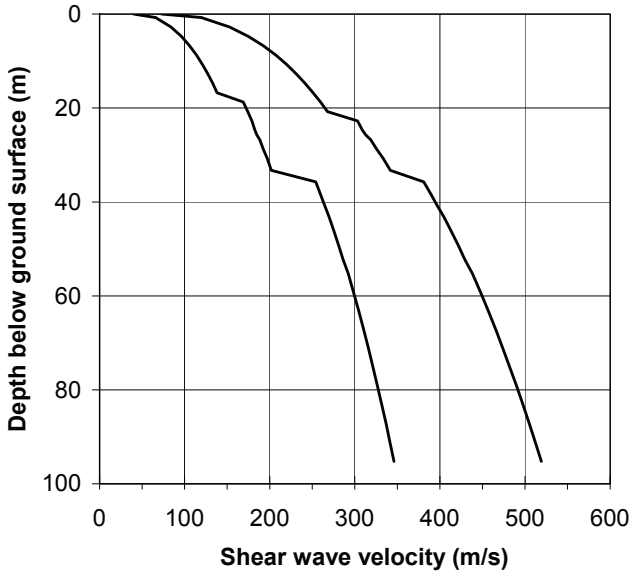


Figure 5: Shear wave velocity

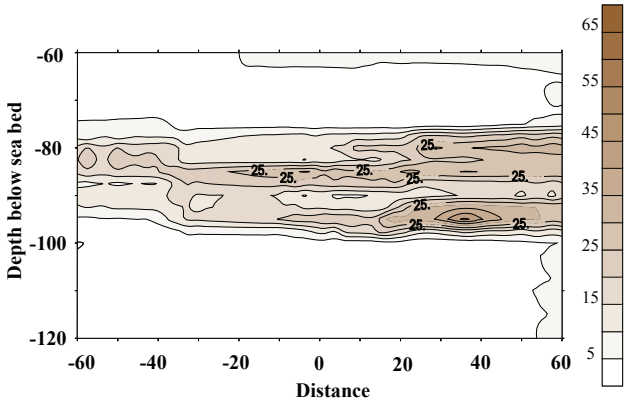


Figure 6: Spatial variability of cone point resistance across Pier M3

In recognition of the influence of the soil characteristics on the ground surface motion, the design response spectrum at the sea bed elevation is defined from specific site response analyses based on the actual soil characteristics and on the design rock motion defined by the seismic hazard analysis. The 5% damped response spectrum is shown in Figure 8: the peak ground acceleration is equal to 0.5g, the plateau at 1.2 g is extending from 0.2 s to 1.1 s and at 2 s the spectral acceleration is still high, equal to 0.62 g.

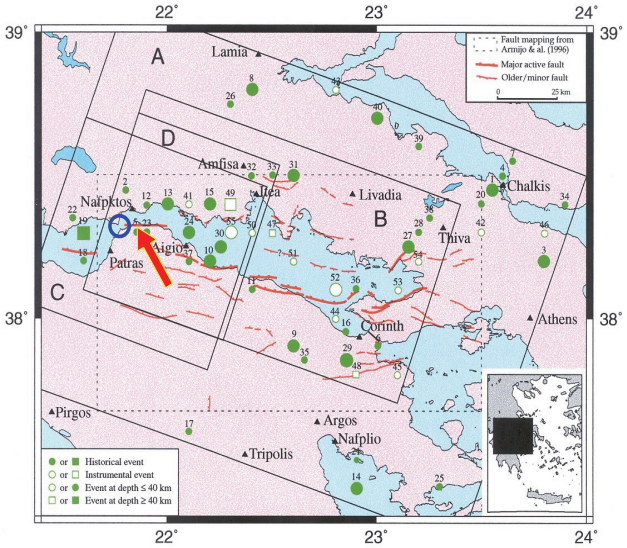


Figure 7: Locations of major earthquakes

Tectonic movements

The seismic threat arises from the prehistoric drift in the earth's crust that shifted the Peloponese away from mainland Greece. The peninsula continues to move away from the mainland by a few millimeters each year. As a result the bridge must accommodate a 2 m differential tectonic displacement in any direction and between any two piers.

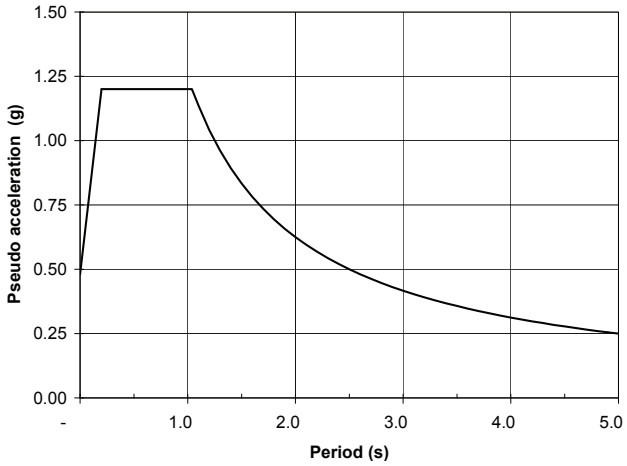


Figure 8: Design ground surface response spectrum

MAIN BRIDGE FOUNDATIONS

Very soon during the design stage it appeared that the foundations design will be a major issue. On the one hand, the unfavorable geotechnical conditions with no competent layer at shallow depth, the large water depth, typical of depths currently encountered in offshore engineering and the high seismic environment represent a combination of challenging tasks. It was also realized that the earthquake demand will govern the concept and dimensioning of the foundations. On the other hand, the time allowed for design turned out to be a key factor: thanks to the contractor who decided to anticipate the difficulties, the design studies started one year ahead of the official effective date. Advantage was taken of this time lapse to fully investigate alternative foundation solutions, to develop and to validate the innovative concept that was finally implemented. The amount of time spent initially for the development of the design concept was worthwhile and resulted in a substantial saving for the foundation. In addition, the close cooperation that existed from the beginning within the design team between structural and geotechnical engineers, between the design team and the construction team on one hand, and between the design team and the design checker on the other hand, was a key to the success.

Investigated foundation solutions

After a careful examination of all the environmental factors listed above, no solution seems to dominate. Several solutions were investigated: piled foundation, caisson foundation, surface foundation. Piles were quickly abandoned for two reasons: the difficulty to realize the structural connection between the slab and the piles in a deep water depth, and the rather poor behavior of floating piles in seismic areas as observed in Mexico city during the 1985 Michoacan earthquake. Caissons foundations were hazardous due to the presence of a gravel layer at the ground surface (Figure 3), which may induce some difficulties during penetration of the caisson. Surface foundation was clearly impossible in view of the poor foundation bearing capacity and of the high anticipated settlements. However, it was quickly realized that surface foundation was the only viable alternative from a construction point of view: construction techniques used for offshore gravity base structures are well proven and could easily be implemented for the Rion-Antirion bridge.

The problem posed by the poor soil conditions still remains to be solved. Soil improvement is required in order to ensure an adequate bearing capacity and to limit the settlements to acceptable values for the superstructure. Several techniques were contemplated from soil dredging and backfilling (soil substitution), to in situ treatment with stone columns, grouted stone columns, lime columns. The need for a significant high shear resistance of the improved soil and for a good quality control of the achieved treatment led to the use of driven steel pipes, a technique derived from offshore engineering, to reinforce the soil beneath the foundations. To prevent any confusion with piles foundations, which behave differently than steel pipes, those are named *inclusions*.

Adopted foundation concept: description and functioning

In order to alleviate potential damage to the structure due to the adverse environmental conditions and to carry the large earthquake forces brought to the foundation (shear force of the order of 500 MN and overturning moment of the order of 18 000 MNm for a vertical buoyant pier weight of 750 MN), the innovative foundation design concept finally adopted (Figure 9) consists of a gravity caisson (90 m in diameter at the sea bed level) resting on top of the reinforced natural ground (Teyssandier 2002, Teyssandier 2003). The ground reinforcement (Figure 10) is composed of steel tubular pipes, 2 m in diameter, 20 mm thick, 25 to 30 m long driven at a grid of 7 m x 7 m below and outside the foundation covering a circular area of approximately 8 000 m^2 The total number of inclusions under each foundation is therefore of the order of 150 to 200. In addition, as shown below, the safety of the foundation is greatly enhanced by interposing a gravel bed layer, 2.8 m thick, on top of the inclusions just below the foundation raft with no structural connection between the raft and the inclusions heads (Figure 10). The reinforcement scheme is implemented under three of the four piers: M1, M2 and M3. Under pier M4, which rests on a 20 m thick gravel layer, soil reinforcement is not required and the caisson rests directly on a 1 m thick ballast layer without inclusions.

The concept (inclusions plus gravel layer) enforces a capacity design philosophy in the foundation design (Pecker 1998). The gravel layer is equivalent to the "plastic hinge" where inelastic deformation and energy dissipation take place and the "overstrength" is provided by the ground reinforcement which prevents the development of deep seated failure mechanisms involving rotational failure modes of the foundation. These rotational failure modes would be very detrimental to the high rise pylon (230 m). If the design seismic forces were exceeded the "failure" mode would be pure sliding at the gravel-foundation interface; this "failure mechanism" can be accommodated by the bridge, which is designed for much larger tectonic displacements than the permanent seismically induced ones. The concept is also somehow similar to a base isolation system with a limitation of the forces transmitted to the superstructure whenever sliding occurs.

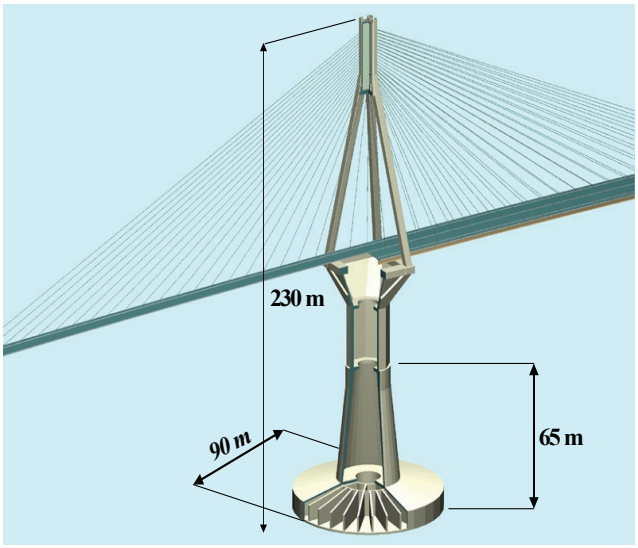


Figure 9: View of one pylon of the Rion-Antirion bridge

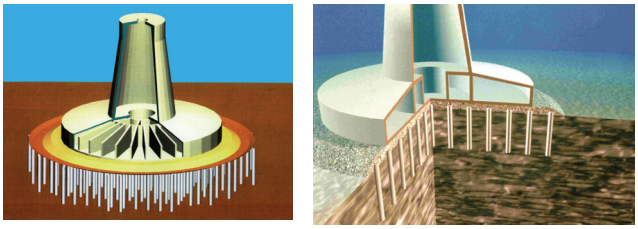


Figure 10: Foundation reinforcement

JUSTIFICATION OF THE FOUNDATIONS

The foundations have to be designed with respect to static loads (dead loads, live loads and tectonic differential movements) and with respect to dynamic loads (ship impact and earthquake). With regards to the static loads, the main issue is the settlements evaluation: absolute settlement and differential settlements inducing tilt, to which the 230 m high pylon is very sensitive. With regards to the earthquake loads, several problems have to be solved: evaluation of the *seismic demand*, i.e. the forces transmitted to the foundation during an earthquake, and check of the *foundation capacity*, i.e. calculation of the ultimate bearing capacity and earthquake induced permanent displacements.

Static loads

The immediate settlement of the foundation is not a major concern since approximately 80% of the total permanent load (750 MN) is brought by the pier below the deck level. More important are the consolidation settlements of the clay strata which induces differed settlements. The settlements are computed with the classical one dimensional consolidation theory but the stress distribution in the soil is computed from a three dimensional finite element analysis in which the inclusions are modeled. It is found that the total load is shared between the inclusions for approximately 35 to 45 % and the soil for the remaining 55 to 65 %. The average total settlement varies from 17 cm to 28 cm for Piers M1 to M3. For Pier M4 the computed settlement is much smaller, of the order of 2 cm. The figures given above are the maximum settlements predicted before construction; they were computed assuming the most conservative soil characteristics, neglecting for instance the slight overconsolidation of the upper strata. Consolidation settlements were estimated to last for 6 to 8 months after completion of the pier.

The differential settlements are evaluated on the basis of the spatial variability of the compressibility characteristics assessed from the variability of the point cone resistances (Figure 6). The computed foundation tilts range from $7.\ 10^{-4}$ to $1.8\ 10^{-3}$ radians, smaller than those that would have been computed without inclusions: the inclusions homogenize the soil properties in the top 25 m and transfer part of the loads to the deeper, stiffer, strata.

Although the previous figures were acceptable, it was decided, in order to increase the safety of the structure, to preload the pier during construction. This preloading was achieved by filling the central part of the cone pier (Figure 9) with water during construction to a total weight slightly larger than the final pier weight. Deballasting was carried out as construction proceeded, maintaining the total weight approximately at its final value. The beneficial effect of this preloading is readily apparent in Figure 11, which shows the recorded settlement and applied load versus time during construction. The final settlement amounts to 8 cm as compared to 22 cm originally anticipated, and occurred more rapidly. This is clearly a beneficial effect of the overconsolidation, as back calculations have shown. More important the foundation tilts are almost negligible, less than $3\ 10^{-4}$.

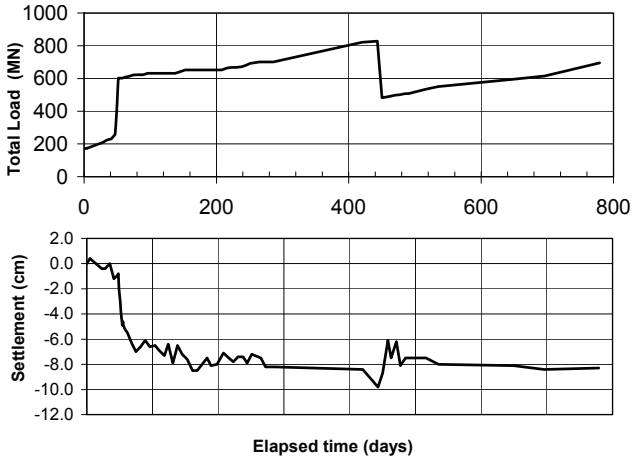


Figure 11: Settlement versus time – Pier M3

Seismic loads

The evaluation of the seismic behavior of the foundation requires that the seismic demand and the seismic capacity be calculated. However, as for any seismic design, it is important to first define the required performance of the structure. For the Rion Antirion bridge this performance criterion was clearly stated in the technical specifications: "The foundation performance under seismic loading is checked on the basis of induced displacements and rotations being acceptable for ensuring reusability of the bridge after the seismic event". In other words, it is accepted that the foundation experiences permanent displacements after a seismic event, provided the induced displacements remain limited and do not impede future use of the bridge. Full advantage of this allowance was taken in the definition of the design concept: sliding of the pier on the gravel layer is possible (and tolerated) but rotational mode of failures are prevented (and forbidden).

Seismic capacity

Because of the innovative concept and therefore of its lack of precedence in seismic areas, its justification calls for the development of new design tools and extensive validation. A very efficient three stages process was implemented to this end:

- Development of design tools based on a limit analysis theory to estimate the ultimate capacity of the foundation system and to define the inclusions layout: length and spacing. As any limit analysis method, this tool cannot give any indication on the induced displacements and rotations.
- Verification of the final layout with a non linear two, or three, dimensional finite element analysis. These analyses provide non only a check of the ultimate capacity but also the non linear stress strain behavior of the foundation that will be included in the structural model for the seismic calculations of the bridge.
- Experimental verification of the design tools developed in step 1 with centrifuge model tests.

As shown below all three approaches give results which are within ±15% of each other, which increases the confidence in the analyses performed for design.

The design tools are based on the Yield Design theory (Salençon 1983), further extended to reinforced earth media, (de Buhan and Salençon 1990). The kinematic approach of the Yield Design theory applied to mechanisms of the type shown in Figure 12, (Pecker and Salençon 1999), permits the determination, for a wrench of forces (N vertical force, V horizontal force and M overturning moment) applied to the foundation, of the sets of allowable loads; this set defines in the loading space parameters a bounding surface with an equation:

$$\Phi(N,V,M)=0 \qquad (1)$$

Any set of loads located within the bounding surface can be safely supported by the foundation, whereas any set located outside corresponds to an unsafe situation, at least for permanently imposed loads.

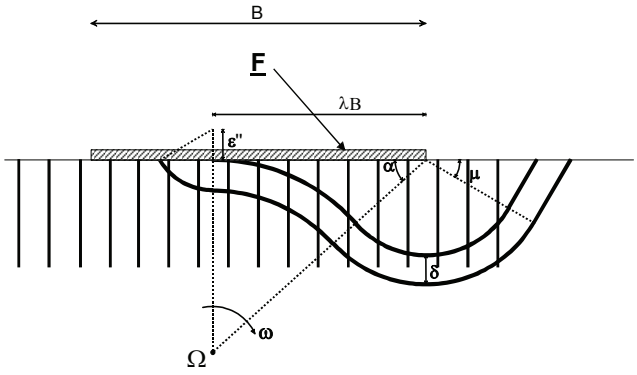


Figure 12: Kinematic mechanism

Figure 13 presents a cross section of the bounding surface by a plane N=constant, corresponding to the vertical weight of one pier. Two domains are represented in the figure: the smallest one correspond to the soil without the inclusions, the largest one to the soil reinforced with the inclusions. The increase in capacity due to the inclusions is obvious and allows the foundation to support significantly larger loads (V and M). Furthermore, the vertical ascending branch on the bounding surface, on the right of the figure, corresponds to sliding at the soil-foundation interface in the gravel bed layer. When moving on the bounding surface from the point (M=0, V=560 MN), sliding at the interface is the governing failure mechanism until the overturning moment reaches a value of approximately 20 000 MN; for larger values of the overturning moment, rotational mechanisms tend to be the governing mechanisms and the maximum allowable horizontal force decreases. The height of the vertical segment, corresponding to a sliding mechanism, is controlled by the inclusions layout and can therefore be adjusted as necessary. The design philosophy is based on that feature: for a structure like the pylon with a response governed by the fundamental mode, there is proportionality between M and V, the coefficient of proportionality being equal to the height of the center of gravity above the foundation. When V increases the point representative of the loads moves in the plane of Figure 13 along a straight line passing through the origin, assuming that the vertical force is constant; it eventually reaches the bounding surface defining foundation failure.

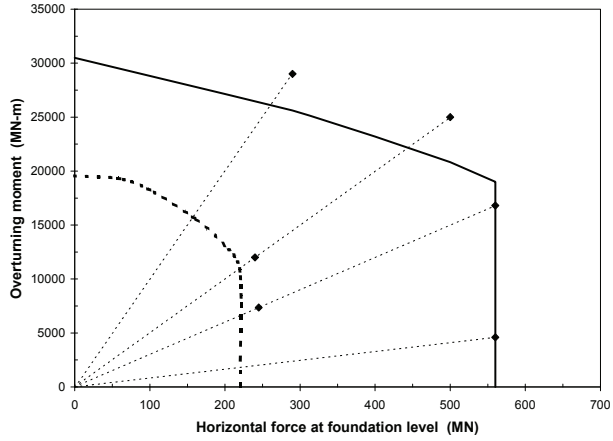


Figure 13: Cross section of the bounding surface: Doted line without inclusions; solid line with inclusions

The inclusions layout is then determined in a way such that this point be located on the vertical ascending branch of the bounding surface.

The previous analysis provides the ultimate capacity of the foundation but no information on the displacements developed at that stage. These displacements are calculated from a non linear finite element analysis. Most of the calculations are performed with a 2D model, but some additional checks are made with a 3D model. For those calculations, the parameters entering the non linear elastoplastic soil constitutive model are determined from the laboratory tests carried out on the undisturbed soil samples; interface elements with limiting shear resistance and zero tensile capacity are introduced between, on one hand, each inclusion and the soil and, on the other hand, the raft and the soil. These models are loaded to failure under increasing monotonic loads such that M/V=constant (Figure 14). Results are compared to those obtained from the Yield Design theory in Figure 13; a very good agreement is achieved with differences of the order of ±12% for all the calculations made for the project. However, it is worth noting that the finite element analyses, because of the large computer time demand, could not have been used to make the preliminary design; the Yield Design theory is, in that respect, a more efficient tool: to establish the full cross section of the bounding surface represented in Figure 10 requires only 10 to 15 minutes on a PC; a non linear finite element analysis, i.e. a single point of the curve, requires more than 4 hours of computing in 2D and 15 hours in 3D on a workstation with 4 parallel processors.

This totally innovative concept, at least in seismic areas, clearly calls for extensive theoretical analyses and experimental validation. As sophisticated as they can be, the theoretical and numerical tools do not have the capacity for modeling all the details of the behavior of this complex scheme during an earthquake. Centrifuge model tests were therefore undertaken with a three-fold objective:

- To validate the theoretical predictions of the ultimate bearing capacity of the foundation under monotonically increasing shear force and overturning moment,
- To identify the failure mechanism of the foundation under these combined loads,
- To assess the behavior of the foundation under various cyclic load paths.

Four tests have been performed in the 200 g-ton geotechnical centrifuge at the LCPC Nantes center, (Pecker and Garnier 1999). It is designed to carry a 2000 kg payload to 100 g accelerations, the bucket surface is at a radius of 5.5 m and the platform has a working space of 1.4 m by 1.1 m. All tests have been carried out at 100 g on models at a scale of 1/100. The dimensions of the corresponding prototype are as follows:

- radius of the circular footing: B_f = 30 m,
- inclusions length and diameter: L = 8.5 m and B=0.67 m,
- Wall thickness t = 6.7 mm (steel), Stiffness EI = 158 MN.m^2,
- Thickness of the ballast layer: 1.2 m.

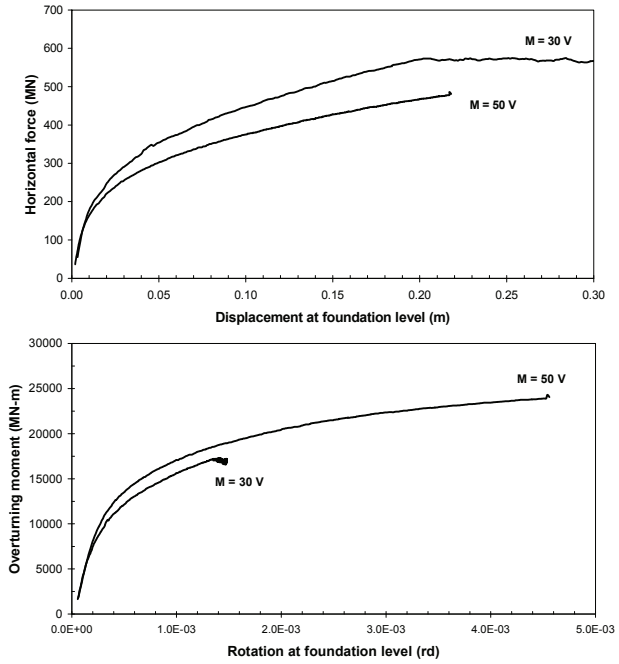


Figure 14: Finite element analyses: force-displacement curves

The soil material has been sampled at the location of pier N17 of the Antirion approach viaduct and sent to the laboratory where it was reconsolidated prior to the tests to reproduce the in situ shear strength profile. The loads applied to the foundation consist of a constant vertical force and of a cyclic shear force and overturning moment; at the end of the tests the specimens are loaded to failure under monotonically increasing loads with a constant ratio M/V. The main findings of the test are summarized in Figure 15 which compares the theoretical predictions of the failure loads (class A prediction according to the terminology introduced by Whitman) to the measured failure loads. Disregarding the preliminary tests that were carried out with another equipment (CESTA centrifuge in Bordeaux), all four tests yield values within ±15% of the predictions obtained with the Yield Design theory.

The centrifuge tests not only provide the ultimate loads but also valuable information on factors that either could not be easily apprehended by the analysis or need experimental verification. Of primary interest is the fact that, even under several cycles of loading at amplitudes representing 75% of the failure load, the foundation system does not degrade; no tendency for increased displacement with the number of cycles is noted. The equivalent damping ratios calculated from the hysteresis loops recorded during the tests are significant with values as high as 20%; it is interesting to note that these values have been confirmed by numerical analyses and can be attributed, to a large extent, to the presence of the inclusions (Dobry et al. 2003). Finally, a more quantitative information is given by the failure mechanisms observed in the centrifuge, which compare favorably either with the mechanisms assumed a priori in the Yield Design theory (Figure 12), or with those computed from the non linear finite element analyses (Figure 16).

The approach explained above takes care of the justification of the inclusions. Another important issue is the behavior of the gravel bed layer; a fundamental requirement for this layer is to exhibit a well defined and controlled shear resistance, which defines the ultimate capacity for the sliding modes of failure. This requirement can only be achieved if no pore pressure buildup occurs in the layer during the earthquake; the development of any excess pore pressure means that the shear resistance is governed by the soil undrained cyclic shear strength, a parameter highly variable and difficult to assess with accuracy. The grain size distribution of the gravel bed layer (10-80 mm) is therefore chosen to ensure a fully drained behavior (Pecker and *al* 2001). Furthermore, the friction coefficient between the slab and the gravel has been measured on site with friction tests using a concrete block pushed on top of the gravel bed layer; a rather stable value (0.53 to 0.57) has been measured for that coefficient.

Seismic demand

For the seismic analyses it is mandatory to take into account soil structure interaction, which is obviously significant given the soft soil conditions and large pier mass. In the state of practice, the action of the underlying soil is represented with the so-called impedance functions, the simplified version of them consisting, for each degree of freedom, of constant springs and dashpots. In the calculation of these springs and dashpots the soil modulus is calibrated on the free field strains, neglecting any further non linearity developed in the vicinity of the foundation (Pecker and Pender 2000). Such an approach may be inadequate because it implicitly assumes that the forces generated on the foundation are independent of its yielding. Therefore there is some inconsistency in checking the foundation capacity for those forces. Recent studies, (e.g., Paoluci 1997, Pedretti 1998, Cremer et al. 2001, Cremer et al. 2002), throw some light on this assumption and clearly show that close to the ultimate capacity it is no longer valid. This is typically the situation faced for the foundation of the Rion-Antirion bridge. Therefore it was decided to implement a more realistic approach which closely reflects the physics of the interaction. Since numerous parametric studies are necessary for the design, a dynamic non linear soil finite element model is not the proper tool.

In the same spirit as the impedance functions, the action of the soil (and inclusions) below the foundation slab is represented by what is called a macro-element (Cremer and *al* 2001, Cremer and *al* 2002). The concept of macro-element is based on a partitioning of the soil foundation into (Figure 17):

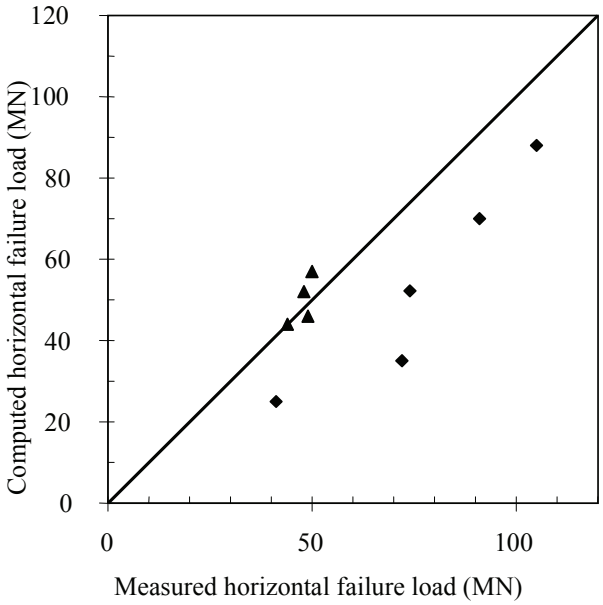


Figure 15: Computed versus measured failure loads in the centrifuge tests: Preliminary tests (diamonds); final tests (triangles)

- A near field in which all the non linearities linked to the interaction between the soil, the inclusions and the slab are lumped; these non linearities are geometrical ones (sliding, uplift of the foundation) or material ones (soil yielding). The energy dissipation is of hysteretic nature.
- A far field in which the non linearities are governed by the propagation of the seismic waves; the energy dissipation is essentially of a viscous type.

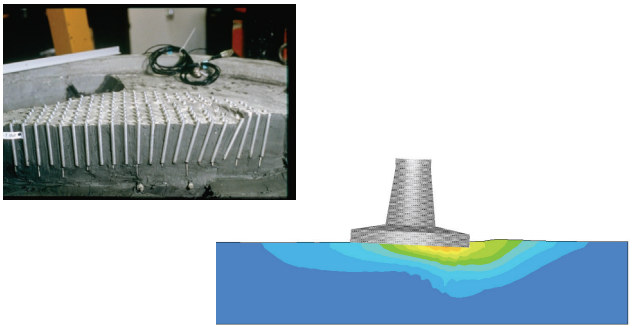


Figure 16: Failure mechanisms: centrifuge test (upper left), FE analysis (lower right)

In its more complete form the macro-element model couples all the degrees of freedom (vertical displacement, horizontal displacement and rotation) (Cremer et al. 2001). For the design studies of the bridge a simplified version of it, in which the degrees of freedom are uncoupled, is used. Conceptually this element can be represented by the rheological model shown at the bottom of Figure 17; it consists of an assemblage of springs and Coulomb sliders for the near field and of a spring and a dashpot for the far field. One such model is connected in each direction at the base of the structural model; the parameters defining the rheological model are calibrated on the monotonic force-displacement and moment-rotation curves computed from the non linear static finite element analyses (Figure 14). For unloading-reloading a Masing type behavior is assumed; the validity of this assumption is backed up by the results of the centrifuge tests (Pecker and Garnier 1999) and of cyclic finite element analyses (Dobry et al. 2003). The adequacy of the macro-element to correctly account for the complex non linear soil structure interaction is checked by comparison with few dynamic non linear finite element analyses including a spatial modeling of the foundation soil and inclusions.

Figure 18 compares the overturning moment at the foundation elevation calculated with both models; a very good agreement is achieved, not only in terms of amplitudes but also in terms of phases.

This model has been subsequently used by the structural design team for all the seismic analyses of the bridge. It allows for the calculations of the cyclic and permanent earthquake displacements; Figure 19 shows the displacement of the foundation center (bottom) and the variation of the forces in the (N-V) plane (top); sliding in the gravel bed layer occurs at those time steps when $V = N \tan\phi$.

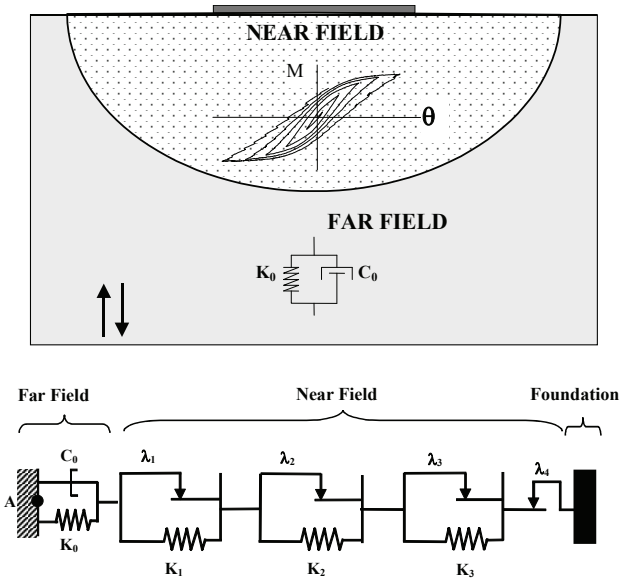


Figure 17: Macro element for soil structure interaction

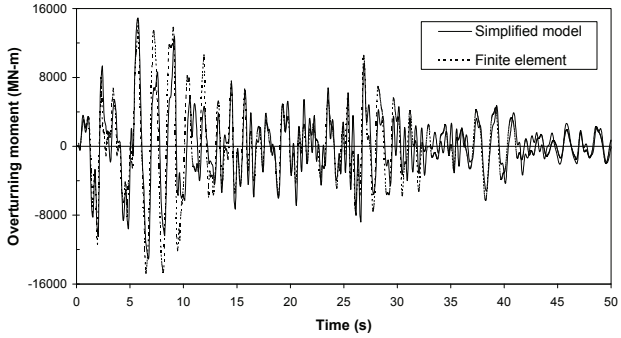


Figure 18: Time history of foundation overturning moment

CONSTRUCTION METHODS

The construction methods for the foundations, described in details by Teyssandier (2002 and 2003), are those commonly used for the construction of offshore concrete gravity base structures:

- construction of the foundation footings in a dry dock up to a height of 15 m in order to provide sufficient buoyancy;
- towing and mooring of these footings at a wet dock site;
- construction of the conical part of the foundations at the wet dock site;
- towing and immersion of the foundations at its final position.

However some features of this project make the construction process of its foundations quite exceptional.

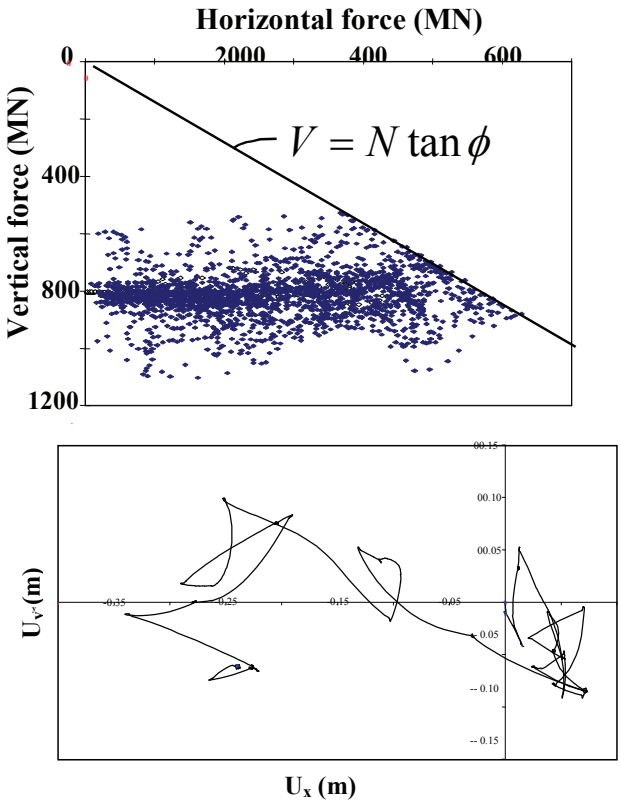


Figure 19: Time history of foundation displacement
Top – variation of forces in the (N-V) plane
Bottom - displacement of foundation center

The dry dock has been established near the site. It was 200 m long, 100 m wide, 14m deep, and could accommodate the simultaneous construction of two foundations. It had an unusual closure system: the first foundation was built behind the protection of a dyke, but once towed out, the second foundation, the construction of which had already started, was floated to the front place and used as a dock gate.

Dredging the seabed, driving of inclusions, placing and levelling the gravel layer on the top, with a water depth reaching 65 m, was a major marine operation which necessitated special equipment and procedures. In fact, a tension-leg barge has been custom-made, based on the well known concept of tension-leg platforms but used for the first time for movable equipment.

This concept was based on active vertical anchorage to dead weights lying on the seabed (Figure 20). The tension in these vertical anchor lines was adjusted in order to give the required stability to the barge with respect to sea movements and loads handled by the crane fixed on its deck. By increasing the tension in the anchor lines, the buoyancy of the barge allowed the anchor weights to be lifted from the seabed, then the barge, including its weights, could be floated away to a new position.

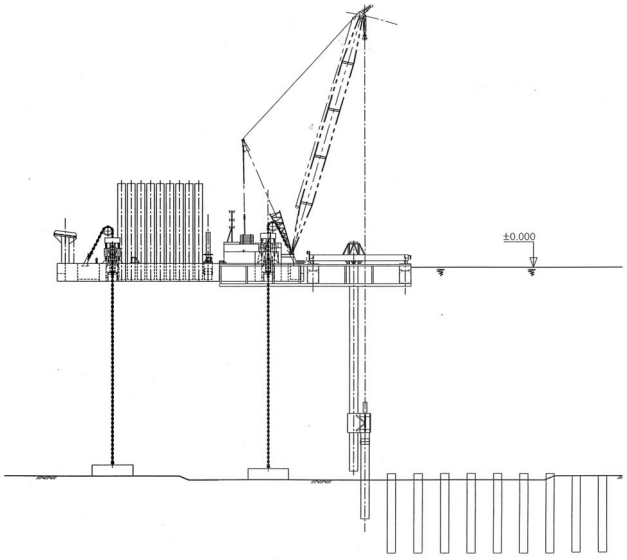


Figure 20: Tension-leg barge

As already stated, once completed the foundations are towed then sunk at their final position. Compartments created in the footings by the radial beams can be used to control tilt by differential ballasting. Then the foundations are filled with water to accelerate settlements. This pre-loading was maintained during pier shaft and pier head construction, thus allowing a correction for potential differential settlements before erecting pylons.

The deck of the main bridge is erected using the balance cantilever technique, with prefabricated deck elements 12 m long comprising also their concrete slab (another unusual feature).

ACKNOWLEDGMENTS

The development of this original foundation concept was made possible thanks to the full cooperation between all the parties involved in the project: the Concessionaire (Gefyra SA), the Contractor (Gefyra Kinopraxia), the Design JV and the Design Checker (Buckland & Taylor Ltd). The author is indebted to Mr. Teyssandier from Gefyra SA, Mr De Maublanc and Morand from Gefyra Kinopraxia, Mr Tourtois from the Design JV and Dr. Taylor for their long term collaboration and confidence. He also wishes to specially thank Dr Peck, Dr. Dobry and Dr Gohl, consultants to the Checker, for their invaluable contribution through their constant willingness to help him clarify and develop the concept.
More information on the project can be found on the web site www.gefyra.gr.

REFERENCES

Combault, J., Morand, P., Pecker, A. (2000). "Structural response of the Rion Antirion Bridge." *Proc. of the 12th World Conf. on Earthq. Eng.*, Auckland, Australia.

Cremer, C., Pecker, A., Davenne L. (2001). "Cyclic macro-element for soil structure interaction - Material and geometrical non linearities." *Num. Methods in Geomech.*, 25, 1257-1284.

Cremer, C., Pecker, A., Davenne L. (2002). "Modelling of non linear dynamic behaviour of a shallow strip foundation with macro-element." *J. of Earthq. Eng.*, 6(2), 175-212.

de Buhan, P., Salençon, J. (1990). "Yield strength of reinforced soils as anisotropic media." *in Yielding, Damage and Failure of Anisotropic Solids;* EGF5, Mechanical Engineering Publications, London.

Dobry, T., Abdoun, T., O'Rourke, T.D., Goh, S.H. (2003). "Single piles in lateral spreads: Field bending moment evaluation". *J. Geotech. and Geoenv. Eng.,* ASCE, 129(110), 879-889.

Dobry, R., Pecker, A., Mavroeidis, G., Zeghal, M., Gohl, B., Yang, D. (2003). "Damping/Global Energy Balance in FE Model of Bridge Foundation Lateral Response." *J. of Soil Dynamics and Earthq. Eng*., 23(6), 483-495.

Paolucci, R. (1997). "Simplified evaluation of earthquake induced permanent displacement of shallow foundations." *J. of Earthq. Eng.*, 1(3), 563-579.

Pecker, A. (1998). "Capacity Design Principles For Shallow Foundations In Seismic Areas." *Proc. 11th European. Conf.. on Earthq. Eng.,* A.A. Balkema Publishing.

Pecker, A., Salençon, J. (1999). "Ground Reinforcement In Seismic Area." *Proc. of the XI Panamerican Conf. on Soil Mech. and Geotech. Eng.*, Iguasu, 799-808.

Pecker, A., Garnier, J. (1999). "Use of Centrifuge Tests for the Validation of Innovative Concepts in Foundation Engineering." *Proc. 2nd Int. Conf. on Earthq. Geotech. Eng.*, Lisbon, 433-439.

Pecker, A., Pender, M.J. (2000). "Earthquake resistant design of foundations : new construction." *GeoEng2000* , 1, 313-332.

Pecker, A., Prevost, J.H., Dormieux, L. (2001). "Analysis of pore pressure generation and dissipation in cohesionless materials during seismic loading." *J. of Earthq. Eng.*, 5(4), 441-464.

Pedretti, S. (1998). "Nonlinear seismic soil-foundation interaction: analysis and modeling method." PhD Thesis, Politecnico di Milano, Milan.

Salençon, J. (1983). "Introduction to the yield design theory." *European Journal of Mechanics A/Solids* 9(5), 477-500.

Teyssandier, J.P., Combault, J., Pecker, A. (2000). "Rion Antirion: le pont qui défie les séismes." *La Recherche*, 334, 42-46.

Teyssandier, J.P. (2002). "Corinthian Crossing." Civil Engineering, 72(10), 43 -49.

Teyssandier, J.P. (2003). "The Rion-Antirion bridge, Design and construction." *ACI International Conference on Seismic Bridge Design and Retrofit*. La Jolla, California.

CONSTRUCTION OF THE MAIN TOWER PIER CAISSONS FOR THE GREENVILLE BRIDGE IN MISSISSIPPI

F. Keith Jacobson P.E., Massman Construction Co., Kansas City, MO, USA

To be involved in the construction of a deep dredged caisson for a major bridge pier is one of the most rewarding and professionally challenging experiences one can have in the bridge construction business. That experience was doubled in the construction of the two deep dredged caissons for the Highway 82 Bridge over the Mississippi River near Greenville, Mississippi. The challenges and the construction risks associated with constructing these two dredged caisson pier foundations highlight the construction engineering innovation associated with major bridge pier construction.

The 1,378-foot Main Span of the Highway 82 Bridge makes it the longest cable stayed bridge span over the inland rivers of the United States. The main piers for this bridge are supported on two dredged caissons measuring 80-feet by 122-feet in plan, founding 200-feet and 170-feet below the river surface. The challenges of constructing these caisson structures, sinking them through 70-feet of water to the river bottom and then excavating and further sinking them to the founding grade without exceeding the design tolerances, were enormous.

The construction engineering opportunities for innovation included major breakwater structures to create a friendly environment in 11 ft/sec currents, the first time use of Articulated Concrete Mattresses for river bottom scour control, unique air dome design to maximize the buoyancy of the caisson structure while floating, a caisson guide system to assure positive control and positioning of the caisson during the initial sinking phases, and a comprehensive sinking plan to assure maximum control and minimum risk. Many of the innovative solutions to the construction challenges on this bridge will be incorporated into future caisson construction projects on the lower Mississippi River.

INTRODUCTION

On July 27, 2001 the Joint Venture of Massman Construction Co, of Kansas City, Missouri and Traylor Bros., Inc., of Evansville Indiana, was awarded the $110,826,530.00 construction contract by the Mississippi Department of Transportation (MDOT) to construct the new Highway 82 Cable Stay Replacement Bridge across the Mississippi River near Greenville, Mississippi. This bridge is currently the longest cable stayed bridge across the inland waterways and the second longest cable stay bridge span in the United States. The bridge is significant because of its record setting 1,378-foot Main Span and because of its location in the Mississippi River System.

The new Highway 82 Bridge replaces the existing Highway 82 truss span highway bridge which has the dubious honor of being the “most hit bridge” on the Mississippi River by barge tows. The “honor” is the result of the placement of the original bridge in 1938; the narrow main span and the changing hydrology of the Mississippi River, combined with the growth in the size of the barge tows plying the river. Modern barge tows made up of thirty barges measuring 210-foot wide by 975-foot long weighing as much as 60,000 tons have an extremely difficult time navigating the upstream river bend and aligning themselves to transit the existing 850-foot main span in 11 ft/sec river currents. All too frequently the transit is not successful and a barge tow strikes one of the existing main piers and breaks up, resulting in loss of cargo and barges. The economic loss to navigation and the narrow bridge roadway made it economically desirable to replace the bridge with a new structure which would no longer impede navigation or restrict highway traffic.

HNTB (Howard-Needles-Tammen & Bergendoff) was engaged by the Mississippi Department of Transportation in partnership with the Arkansas Department of Transportation to design the replacement bridge for the existing Highway 82 Bridge. The design package was divided into three construction packages which were to be let by the MDOT as traditional Bid-Build projects. The first of those packages was for the main river crossing which consists of a single, 4-lane, 100-foot wide, cable stayed bridge structure with two main tower piers and two flanking anchor piers. The anchor piers were designed as drill shaft supported spread footings located on the existing river batture above the normal river stage. The two main span tower piers were designed as deep caisson supported foundations. The caisson structures were designed with foot-prints of 80-feet by 122-feet and founding at depths of 200-feet and 170-feet below the normal river stage Elevation of 25-feet. The completed towers for the main piers rise to an Elevation of 499-feet, resulting in total tower pier heights of 602-feet for Pier 37 and 574-feet for Pier 38 above each caisson's founding elevation.

The new bridge is located 0.6 miles downstream of the existing bridge. See Figure 1. This location was chosen for its favorable river alignment and acceptable subsurface geology.



Figure 1: Location of New Bridge relative to Old Bridge

HISTORY

The original Highway 82 Bridge crossing the Mississippi River at Greenville, Mississippi was started in December 1938 and completed in June 1940. The original designers were Ash-Howard-Needles & Tammen the parent of HNTB the designer of the new bridge. The contractor for the four river piers of the original bridge was Massman Construction Co., the sponsoring partner of the Massman-Traylor joint venture constructing the new bridge. The four river piers constructed by Massman on the original bridge, were founded on deep caisson structures.

CAISSON CONSTRUCTION OVERVIEW

The designers made the initial determination that the preferred foundation type for the main tower piers would be deep caisson foundations setting on competent soils well below the maximum anticipated scour profile resulting from the presence of the new piers. The designers sized the caisson structures; the foot-print dimensions, the lower caisson heights, the upper caisson or lower pier heights. They also established the distribution block dimensions, and the final pier and tower design. The designers performed their constructability review and determined that the caisson foundations as designed could be built.

The final details for the caisson construction and the means and methods to be employed to successfully and accurately install the caisson structures were contractually placed on the contractor. The owner and designer by contract required the contractor to have recent successful deep caisson construction experience.

The construction of deep caisson foundations is not a new process or art. Caisson foundations have been in existence since Roman times. There is no standard caisson structure nor is there a caisson for every situation. Caisson structures must be designed and detailed for the site specific geologic and hydrologic conditions. The contractor tailors the design to his abilities, experience, equipment and personnel in sinking large caisson structures.

Notwithstanding the unique and site specific characteristics of each caisson structure, at least six construction hurdles must be overcome to successfully construct a deep caisson. These six are: the decision on the best method of construction; the creation of a tolerable work environment in the immediate vicinity of the caisson construction operations; the means of controlling river bed scour; the type of air domes to provide buoyancy when utilizing a floating caisson; the caisson guide system; and development of a comprehensive caisson sinking plan.

METHODS OF CAISSON CONSTRUCTION

As stated earlier caissons are site specific foundation structures. The methods for constructing caissons are also site specific. The most critical of the site specific characteristics is the normal depth of water at the sinking site and the range or fluctuation of the water level during the period of caisson construction. In shallow water depths temporary sand island structures can be built which create an artificial island above normal water level. A cutting shoe can be assembled on this island and the caisson constructed in the dry and sunk by open excavation and sequentially increasing the caisson structure height.

In greater water depths a temporary submerged sand island structure can be constructed as a stand alone structure or within a box cofferdam. A cutting shoe and low steel caisson structure can be assembled which would allow the top of the steel structure to extend above the normal water surface. The caisson sinking procedure would be the same as with a sand island in which the caisson is sequentially sunk by open excavation and the caisson structure height increased.

For the Greenville Bridge site, sand islands or submerged sand islands were not acceptable alternatives due to the normal depth of water, the extreme range of water depths during sinking, and the high river velocities. The normal river depth at Pier 37 and Pier 38 was 70-feet. The range of depths went from 60-feet to over 90-feet during high river stages. The unobstructed river velocities ranged from 4 ft/sec to 11 ft/sec. The best alternative was to construct a floating caisson structure which could be lowered to the river bottom in a controlled manner, while still retaining positive buoyancy at touch-down. Once firmly on the river bottom the caisson would be modified by the removal of the air domes and sunk further to its founding elevation by sequential open excavation and further caisson structure construction.

The challenge was how to design a caisson structure which is light enough or buoyant enough to float and control its position until it drafts 70-feet of water, at touch down, and still be heavy enough in its final configuration to be able to be sunk through all the soil strata encountered between the river bottom and the founding grade. The answers to this and other construction issues will be addressed in the following discussion of construction hurdles.

MAJOR BREAKWATER

Once the determination has been made for the type of caisson construction, the next critical hurdle to be addressed is the creation of a tolerable work environment within the river for the caisson construction. In the case of the Greenville Bridge caisson construction this hurdle was made more difficult by the schedule driven decision to build both the Pier 37 and Pier 38 caissons in the river in the same time frame.

Working in the lower Mississippi River is not for the faint at heart nor is it a place to start one's construction engineering journey. Experience has shown that the Mississippi River is not inert but rather a dynamic force of great strength, authority, history and intentions. While the river has seemingly been tamed it is only willing to tolerate intrusions upon its space for a limited time. Failure to recognize these characteristics of the river is to invite calamity, failure, frustration and disappointment. However, if one utilizes their given talents, acquired education, practical experience and collaborative efforts to choose appropriate courses of action for working within the river one can be assured of reasonably predictable results. The best one can hope for is that "Old Man River" tolerates their presence.

A tolerable environment in the river for the caisson construction is a location that is free of the current loading caused by the river and a river bottom that stays at a predictable elevation. The first part of creating this environment is establishing a work zone free from the current effects of the river. This is essential because the size of the caisson structure while floating would be uncontrollable in current and could not be safely or accurately positioned at its design location.

To create a tolerable environment within the river for the caisson necessitated the construction of a major steel and sheet pile structure to deflect the river and create an acceptable backwater in which to locate and sink the caissons. Because of the earlier decision to construct both caisson structures during the same time frame, it also became necessary to construct two breakwater

structures. Each breakwater structure was determined to be “V” shaped with a downstream wing dimension of 100-feet. This wing dimension for two breakwaters would result in a 200-foot restriction within a 2600-foot wide river at normal river stage. It became readily apparent that the size of these obstructions would create new river hydraulics affecting current patterns, scour profiles, higher than normal velocities and significant eddies in and around the breakwaters and caisson construction.

Because of this unique engineering problem we engaged T.Y. Lin International to design and detail the breakwater structures for the river stage and loading conditions that would be experienced. T.Y Lin in turn contracted with WEST Consultants, Inc. to model the river hydraulics for the condition with and without the breakwater structures to determine the velocities, flow patterns, anticipated scour zones and to make recommendations on the forces to be resisted by the breakwaters.

The result of this design effort was the detailing of what might be the largest temporary breakwater structures constructed in the Mississippi River for bridge pier construction. Each breakwater was designed as a “V” shaped structure with its apex facing upstream into the current. Each wing of the “V” was 70-feet long with the distance between the downstream wings 100-feet. The breakwaters were set in 70-feet of water at normal river stage and were designed to be overtopped when the river rose to 90-feet of depth. The structures were supported by seven 60-inch steel pipe piling driven 60-feet into the river bed. The pile at the apex of the breakwater was anchored to resist the large tensile force developed by the structure overturning moment. See Figure 2.

The installed breakwaters produced river velocities approaching 27 ft/sec off their down stream corners. This velocity in turn created navigation issues and added additional scour considerations that had to be overcome. Once installed the breakwaters safely served their



Figure 2: Breakwater Structure and Caisson Guide System

purpose of creating a tolerable environment in which to position, construct and sink the two caisson structures.

UNIQUE SCOUR PROTECTION

All construction activities within the river create changes in the river hydraulics which in turn affect the scour profiles of the river bottom. The influence on scour is most evident in the construction of caisson structures, particularly floating caissons. The greatest localized scour effect occurs when the caisson structure approaches the river bottom and the river current velocities increase as they pass around and under the caisson. This increase in velocity suspends and transports river bottom materials and creates large scour holes moving the river bottom away from where it was expected to be when starting the caisson construction process.

For caisson construction, the way to address the scour issue is by installing scour protection on the river bottom. This scour protection has traditionally and historically been accomplished by sinking large woven willow mattresses ballasted with rip rap. These mattresses often measure 300-feet by 400-feet in plan dimension and are made up of cut willow trees woven together in fascines with wire rope cable. The willow mattress construction in recent caisson projects has been replaced by woven dimensional lumber. This substitution was necessitated by the limitation of harvestable willows and the relative economy of dimensional lumber.

The contract plans for the Greenville Bridge project required river bottom scour protection and suggested that either ballasted woven willow mattresses or dimensional lumber mattresses could be used for scour protection. Because it had been over a decade since a contractor had woven a scour mattress and because of the high cost of labor and materials and the antiquated method of weaving and sinking mattresses in deep water depths and high current velocities; it was decided that there had to be a better way of accomplishing this work. Many modern alternatives were considered and ultimately it was decided that the United States Army Corps of Engineers (USACE) were the true experts in performing scour protection in the Mississippi River. The challenge became how to involve the USACE with its vast experience and unmatched equipment to provide the scour protection required for this project. Through careful negotiation and identifying individuals within Massman/Traylor, the USACE and the MDOT, who believed they could partner to accomplish something new that benefited all, a team was assembled to overcome the contractual hurdles. The result was that MDOT would contract with the USACE to install an Articulated Concrete Mattress on the river bottom in the vicinity of the two caisson piers. The cost of the installation would be offset by a Value Engineering Change between Massman/Traylor and the MDOT.

Once all the contract changes were negotiated and executed, the USACE mobilized its equipment, materials and personnel. The scour protection for both piers was then installed in three days time. This time frame could not be matched by a traditional woven mattress installation. See Figure 3.

CAISSON AIR DOME DESIGN

Earlier it was said that the best alternative for the construction of the caissons on the Greenville Bridge was to construct a floating caisson structure which could be sunk to the river bottom while still retaining positive buoyancy at touch down. It was also stated: “The challenge was how to design a caisson structure which is light enough or buoyant enough to float and control its position until it drafts 70-feet of water, at touch down, and still be heavy enough in its final configuration to be able to be sunk through all the soil strata encountered between the river bottom and the founding grade.” This problem is unique to every floating caisson and is ultimately resolved by the caisson contractor since it is his means, methods and experience that must be applied to the problem.

The Greenville Bridge caissons designed by HNTB were adequate for their intended purpose but small from the aspect of buoyancy and heavy for sinking weight. A caisson must remain buoyant during the entire floating phase of construction until the caisson is safely setting on the river bottom. During this phase the caisson structure acts like an open top barge or floating vessel; that is its dry weight must be less than the weight of the volume of water being displaced. The buoyancy calculations takes into account the dry weight of all the caisson



Figure 3: USACE Laying an Articulated Concrete Mattress at Pier 37

structure, usually concrete, including that which is above the river surface. It is the contractor's sequence of constructing the steel caisson cutting edge and initial steel extensions with the sequence of placing reinforcing steel and concrete in the outer caisson walls and the interior concrete surrounding the dredge wells that allows the contractor to design for positive buoyancy at any stage of construction.

Buoyancy is made possible by constructing a temporary floor or bottom in the caisson. The type and location of the caisson floor provides the contractor with the means of adjusting or compensating for variations in the buoyancy of the caisson during construction. When the caisson floor or bottom is used to trap and control the volume of air between the lowest extreme of the caisson cutting edge and the floor it is known as an "air dome". The amount of trapped air directly affects the caisson buoyancy and helps to offset added caisson concrete weight during construction. Controlling the trapped air allows the contractor to control the caisson touchdown on the river bottom and the release of the trapped air enables the caisson to set down hard in its proper location before the dredging operations begin.

In the case of the Greenville Bridge caissons, the caisson dimensions did not allow for air domes to be constructed within the circular dredge wells or at the transition of the working chamber and dredge well, as is done in many floating caissons. For the Greenville caissons to be constructed as floating caissons another air dome system had to be developed and implemented. After many attempts to develop the optimal caisson details and to maximize the caisson buoyancy, it was decided that a half-cylinder air dome needed to be designed and constructed as a part of the working chamber. The working chamber dimensions dictated that the half-cylinder air dome would need to be 18′-0″ by 14′-10″ in plan dimension and have a dome height of 5′-2″, rolled to a 7′-9″ radius. In addition the maximum pressure on the dome during the floating caisson sinking phase would be 40-psi. See Figure 4.



Figure 4: Caisson Cutting Edge showing the Half-cylinder Air Domes

To our knowledge, no half-cylinder air dome of this size had been used in a floating caisson prior to this time. Because this was such an integral part of the success of the caisson construction and because there was no way to test the integrity and capacity of the fabricated dome prior to its use, we engaged T.Y. Lin International to design and detail the half-cylinder air dome and perform a design check on our entire caisson cutting edge structure.

The caisson cutting edge fabrication and half-cylinder air dome installation was done by Corn Island Shipyards in Grandview, Indiana. Once the cutting edges were complete, they were towed to the project site where they were outfitted with the air dome piping and protection system. Concrete was then placed within the lower 7-feet of the cutting edge. At this point the caisson cutting edges were positioned in the slack water behind the breakwater structures ready to begin the sinking phase.

CAISSON GUIDE SYSTEM

The fifth major hurdle to be overcome in the caisson construction operation was the development of a caisson guide system to assure that the caisson would, when being sunk through 70-feet of water, land on the river bottom at the location intended.

To accomplish this control, two vertical guide piling were incorporated into the previously installed breakwater structure. Once the cutting edge was located behind the breakwater three additional vertical piling were driven at a predetermined location off the downstream face of the caisson structure. These three piling were then framed to form a rigid three pile cluster. The exact locations of the vertical guide piling was determined by survey and a mating fabricated guide was attached to the caisson cutting edge 12-feet above its bottom. Once installed this guide system assured that the caisson structure would descend to it's exact location on the river bottom, so long as the caisson construction operations controlled the lean and twist of the caisson above the guide. See Figure 2.

The caisson guide system worked as planned and the caissons rested on the river bottom at their planned locations.

COMPREHENSIVE SINKING PLAN

There are many hurdles to be overcome in the planning and construction of a river bridge caisson. While each of them is important none is quite as important as a comprehensive caisson sinking plan. The sinking plan is the visual representation of the detailed analysis of all of the activities related to the caisson construction and sinking phase. It becomes the "what to do and what to expect" guide during the sinking process and the specific order of activities or events that have been previously agreed upon by management, engineering and operations. The sinking plan is to be comprehensive and must include the exact order of construction, the accurate estimations of the constructed dry weight, accurate calculations of both caisson draft and freeboard in the floating phase, expected air dome pressures at all phases and the points for required air pressure adjustments. The sinking plan must include the point in the process when the caisson will touch down on the river bottom and an accurate estimation of the caisson penetration into the river bed when the air domes are removed. At the point of touch down and removal of the trapped air and steel air domes the amount of freeboard must be analyzed for the possible river stages which could over top the caisson. During the open dredging phase the sinking plan must also show the caisson skin friction for the various soil strata being encountered. See Figure 5).

A well developed and carefully executed sinking plan will assure reasonably predictable results. It also serves as a ready reference when any unforeseen problem occurs to quickly assess and analyze solutions to the encountered problem. There are huge risks in sinking caissons for river bridge piers. These risks can be minimized and often mitigated through the careful development of a comprehensive sinking plan.

SUMMARY AND CONCLUSIONS

To be involved in the construction of a deep dredged caisson for a major bridge pier is one of the most rewarding and professionally challenging experiences one can have in the bridge construction business. That experience is multiplied when all the engineering and construction is carefully thought out, properly planned, effectively communicated and diligently executed to the successful completion. The construction of the two main river tower piers for the new Highway 82 Bridge across the Mississippi River at Greenville, Mississippi was such an experience.

SKIRT SUCTION FOUNDATION
- APPLICATION TO STRAIT CROSSINGS -

Takashi SAITO[1], Yoichi YOSHIDA[2], Masato ITOH[3], Naoki MASUI[4]

Abstract

Since early 1970's skirt suction foundations (skirted foundation / bucket foundation) have been used as support for large fixed substructures or anchors for floating structures in offshore hydrocarbon development projects. In recent years skirt suction foundations are recognized as one of the solutions in foundations applicable to bridge substructures installed in waters, because skirt foundations have a wide variety of functions such as control of settlement during service life, less impact to environments during operation at installation site.

This paper introduces general features of skirt suction foundations, and then discusses design practice of them for the application to bridge substructures, with reference to experiments in both laboratory and field.

1. Introduction

Since 1970 offshore structures have employed skirt suction foundations (so called skirted foundations or bucket foundations). Skirt, hollow cylindrical concrete or steel walls, is penetrated into seabed soil to transmit loads to deeper and stronger strata. So far approx. 30 concrete gravity based structures with skirt have been installed in waters 50-300m deep and numerous cylindrical suction anchors and piles with 5-10m diameters installed in waters 100-2,000m deep. The skirt suction foundations utilize a hydrostatic pressure at any stages from fabrication and installation (such as skirt penetration) to service. Therefore, they require some water depth at the installation site.

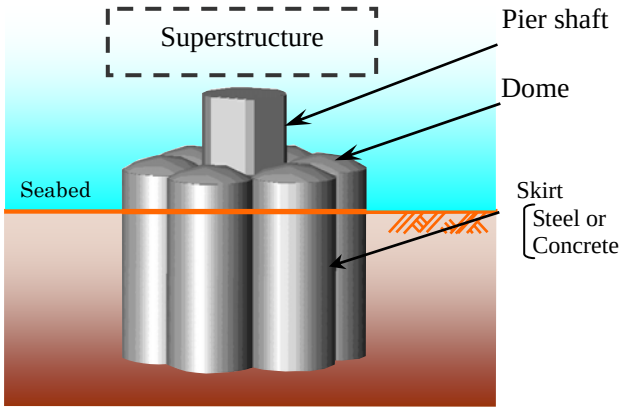


Fig.-1 Skirt Suction Foundation



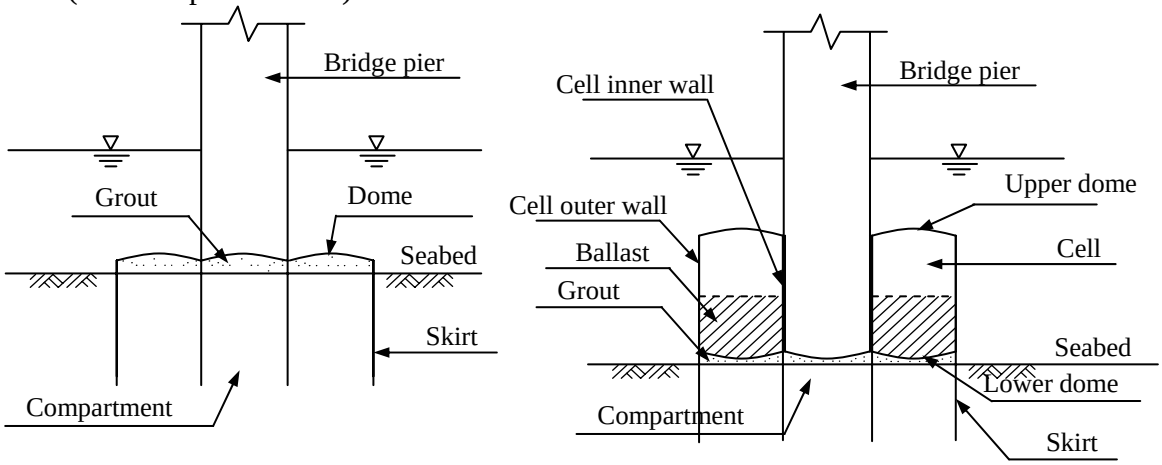
Fig.-2 Troll platform installed '95

[1] Collaboration Researcher, Structure Research Group, Public Works Research Institute, Japan
[2] Group Manager, Civil Engineering Technology Division, Obayashi Co., Japan
[3] Manager, Research Institute, Obayashi Co., Ltd., Japan
[4] Manager, Civil Engineering Technology Division, Obayashi Co., Ltd., Japan

2. Structural configuration

The skirt suction foundations for bridge substructures consist of cylindrical concrete walls (skirts) projecting down the dome, as shown in **Fig.3**. The diameter of the cylinder is normally 12-15m and wall thickness is 0.4-0.5m. The space in a cylinder is called “compartment”.

In case of large foundation for such as long span bridges installed in deep water the substructures are provided with cells on top of the lower dome to transmit the applied load (wt. of superstructure) to whole area of foundation.



[Typical foundation] [Large foundation with cells]

Fig.3 Structural configuration of skirt suction foundations

3. Suction effect

“Suction” provides increase or decrease in hydrostatic pressure by pumping water from and to skirt compartments. The following beneficial effects are expected by suction.

(1) Reduction of penetration resistance

During skirt penetration, pumping water provides an under-pressure in compartments and sets up seepage flow that reduces tip resistance together with internal friction. In case of sand or gravel strata, large suction degrades skirt tip resistance to approximately zero.

(2) Additional penetration force

If the water in compartments is evacuated, the downward load is provided by suction. This effect is applicable to both clay and sand.

(3) Leveling of structure

By adjusting hydrostatic pressure in compartments during skirt penetration, it is possible to control the inclination of structure due to heterogeneous soil condition or slope at sea bed. In extreme case pumped water into skirt compartment can raise the structure by an increased hydrostatic pressure.

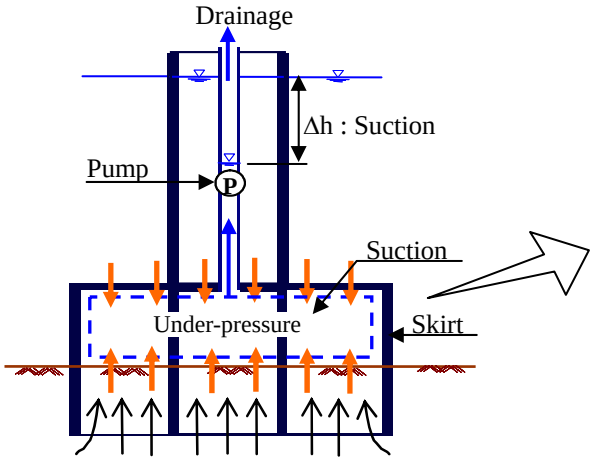


Fig.4 Seepage during suction installation

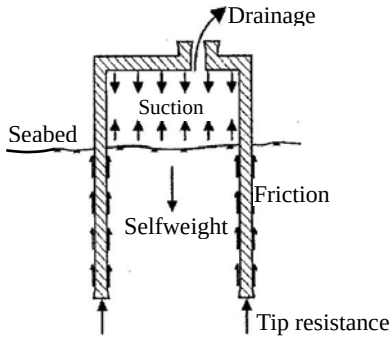
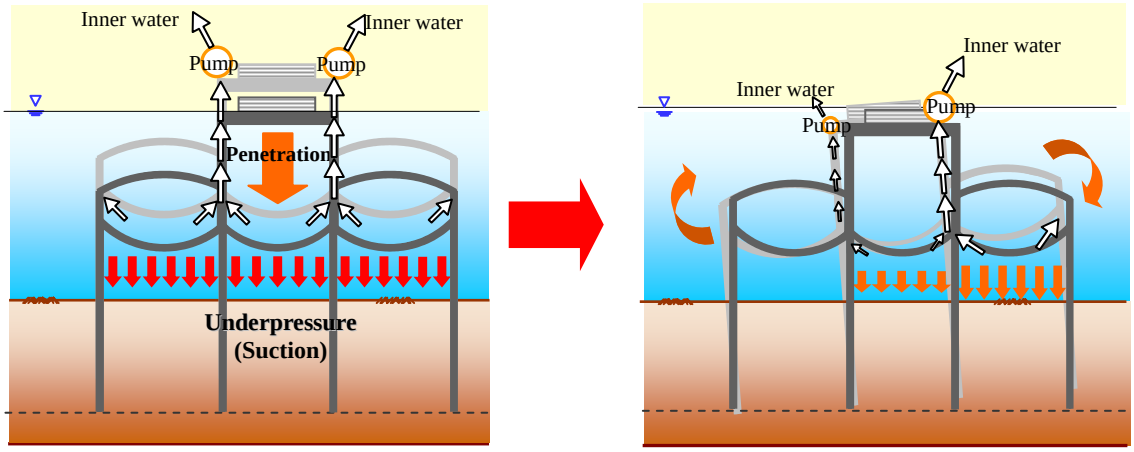


Fig.5 Force equilibrium during suction installation



[Penetration] [Leveling]

Fig.6 Penetration and leveling of foundation due to suction

The above effect is called "active suction". On the other hand "passive suction" effect is also expected. As reported in 20th BWS (2004), the existing research conducted at Public Works Research Institute (Japan) demonstrated that in foundations equipped with or without skirt passive suction is generated under the sealed baseplates in response to short term tension loads such as earthquake or storm. The findings of this research support significant tensile resistance of skirt suction foundations.

4. Application to bridge foundation

The skirt suction foundations for a bridge substructure expect the following effect over existing type of foundations.

(1) Reduction of settlement in service life (Preload effect)

During the skirt penetration and/or just after the installation of the foundation,

large vertical load induced by suction is applied to substructure. If the suction load is greater than the imposed load (such as weight of superstructure) after installation, the settlement during service can be reduced by some extent.

(2) Short construction period on site

The construction on site is only installation of foundations, because fabrication of skirts, domes and cells are conducted in dry docks and/or floating site (wet docks), if necessary, and foundations are towed to the site. Therefore considerably short occupancy of water at installation site is expected resulting in favorable effect on ship navigation and fishery.

(3) No soil improvement/dredging required

Foundation skirts have various function such as containing soft surface soils, compensating for seabed irregularities, reducing scour around foundation and transmitting load to bearing strata. Therefore no soil improvement and dredging is required in case of soft soil deposits and even in seabed slope. In addition, no noise and vibration is followed in the installation of skirt suction foundations. This means that skirt suction foundations are attractive to environments.

Water depth needs to be over 10m to utilize the above effects and skirt penetration is limited to cohesive soil, sand with a few gravels, or combination of those. Although the above limitation exists, possible bridge construction sites in Japan (Tokyo bay, Osaka bay and other shallow waters) have such a soil condition. Hence the skirt suction foundations are though to be applicable to substructure of the bridges in Japan.



［Center span : 500～600m］　　［Center span : 2,000～2,500m］

Fig.7　Application of skirt suction foundation to bridge substructure

5. Evaluation of performance as bridge foundation

It is necessary to satisfy various performances specified in "the Specifications for Bridges in Japan" to apply the skirt suction foundation to bridge substructures. In

addition, the following observation and experiment have been conducted to evaluate the typical performance of skirt suction foundations for bridge substructures.

(1) Leveling of foundation at penetration
(2) Preload effect by suction (Reduction of settlement)
(3) Seismic behaviour of foundation

The first two performances are explained in this paper.

5-1 In-site monitoring for penetration and leveling of foundation

First evaluation concerns the control of leveling of foundation. The offshore concrete structure shown in Fig.8 with the skirt 18m diameters and 5.0-5.5 height was installed with suction. It is required to protect the jetty from impact of ship out of control. The soil feature has the surficial soft clay of 3.5m thickness and medium dense sand below it. Photo1 shows that the structure was dry-towed by the heavy lift barge and lowered at the installation site.

The penetration of skirt is quite important process for this type of foundation. The skirt penetration should include the steep slope of the bearing strata. In order to overcome these obstacles, the penetration operation was divided into two process - skirt penetration and control of leveling. The former penetrated the skirt with suction until near the target depth and the lift barge assisted the operation throughout. The latter, without assistance from the lift barge, took the role of leveling of inclination and deeper penetration.

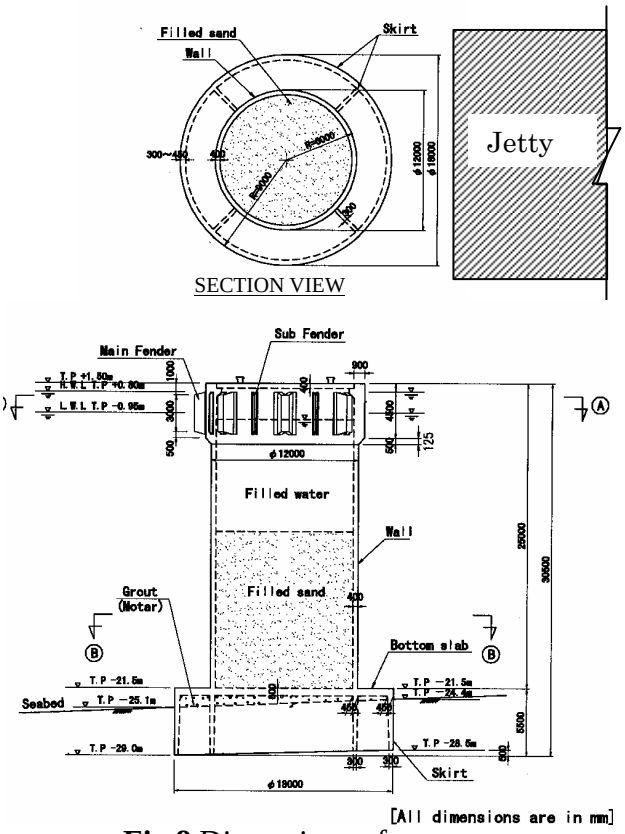


Fig.8 Dimensions of structure

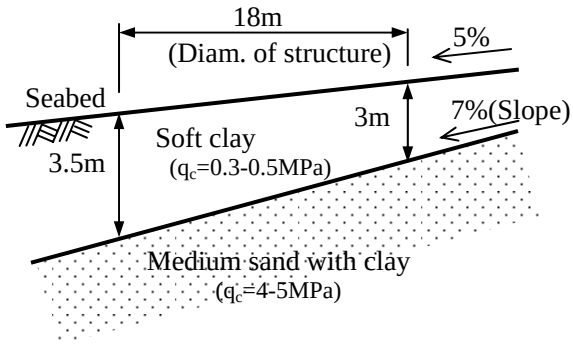


Fig.9 Soil strata



Photo1 View of protection just before skirt penetration

(1)Skirt penetration

After the accurate positioning the lift barge slowly lowered the structure until the skirt tip contact with subsoil, the touch-down. The very small penetration resistance was observed during the penetration in the surficial soft clay. However, the penetration resistance suddenly increased just after the penetration into the sand layer. The relation of penetration load with skirt tip depth is illustrated in **Fig.10**. The slope of the sand layer resulted in the inclination of 1.6 degree of the structure.

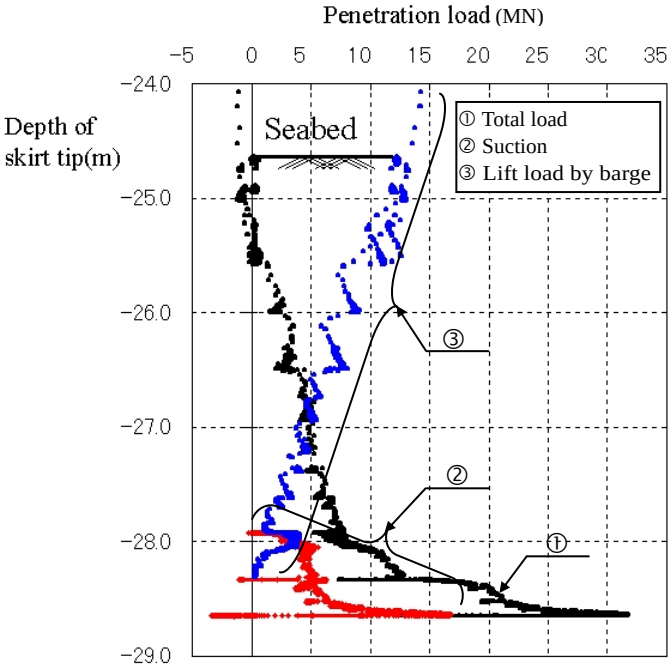


Fig.10 Penetration load vs skirt tip depth

(2) Control of inclination

By providing different suction for each skirt compartment, the inclination of the protection was well controlled. **Fig.11** shows that the suction of 10-15m water head (under-pressure) was applied to compartments②-⑤ and the reverse suction (over-pressure) of 15m head was given to compartment①. The inclination was adjusted within two hours; from 9am to 11am. The final installation was 0.3degree. No piping was observed, although these suction pressures were much higher than

those for boiling obtained from a conventional formula including soil weight and friction with wall.

Due to the impervious surficial clay the reduction in the vertical effective stress of the sand was negligible, which resulted in no reduction in tip penetration resistance in the sand.

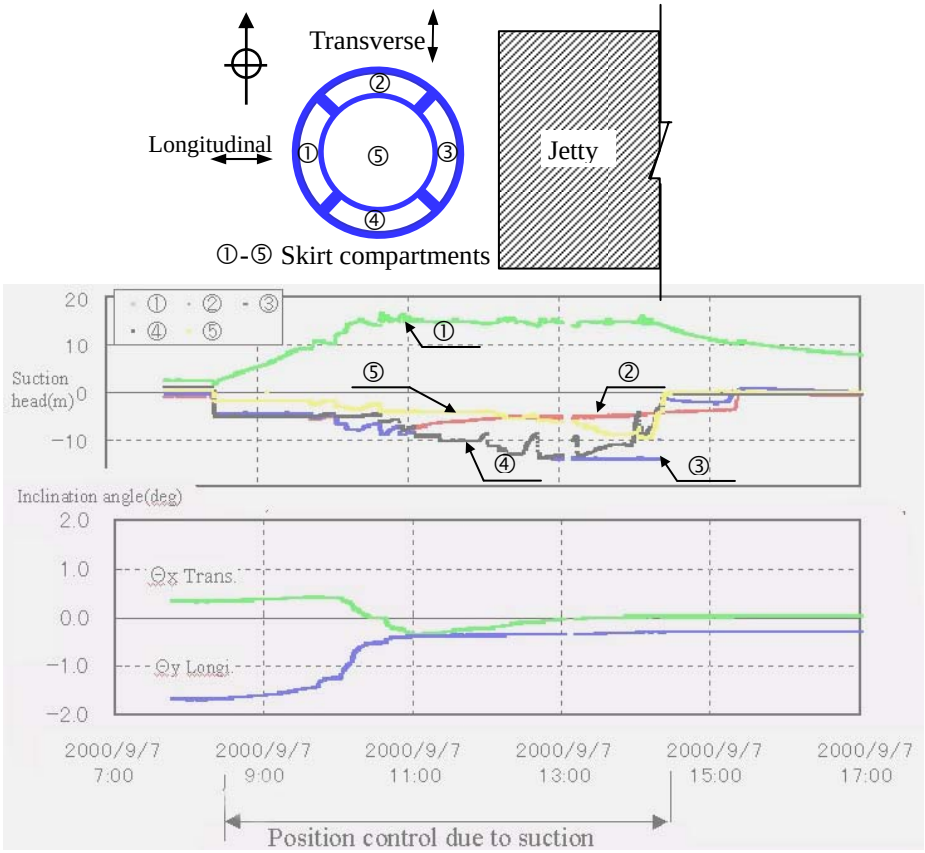


Fig.11 Control of inclination due to suction

5-2 Experimental evaluation of preload effect due to suction

Second evaluation relates to the preload effect, whose concept is illustrated in Fig.12. The penetration of skirt requires selfweight, ballast as well as suction (under pressure) of skirt compartments. If the load induced by suction (called “suction load”) is greater than the imposed load during the service, the settlement due to them could be considerably small as shown in **Fig.12**. Therefore, the suction is applied during installation and removed after it and the suction load is termed as “preload”. However, the effect of preload due to suction is not well understood, because the suction is not externally applied load but internal action and the effective stress in the surficial soil is temporarily reduced. The experiment using a centrifuge apparatus was executed to verify the effects of preload for skirt suction foundation. Details of the experiment are explained below.

(1) Purpose

The experimental approach investigates the difference in the preload effect between internal load due to suction and external load due to jacking.

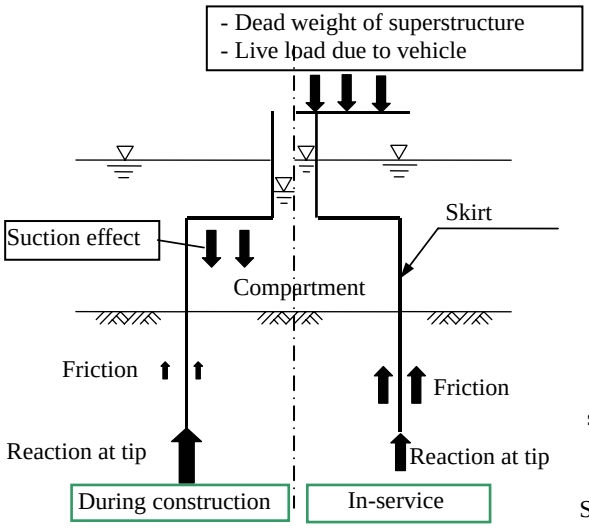


Fig. 12 Concept of "Preload" due to suction

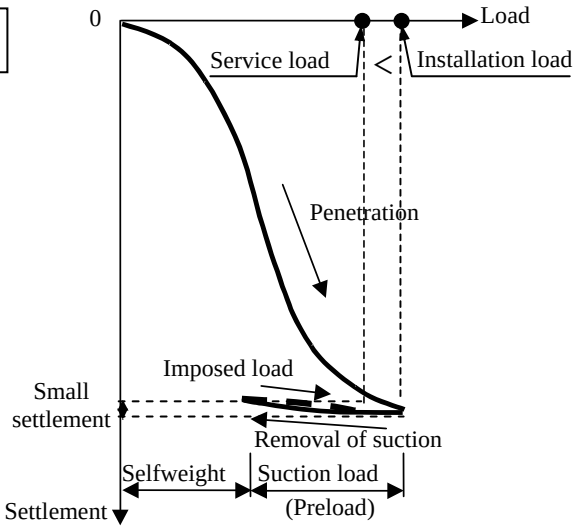


Fig. 13 Schematic description of preload effect

(2) Apparatus

The centrifuge scale model has been employed here. The centrifuge apparatus shown in **Fig.14** has the boom radius of 7.01m, table space of 2.2 x 2.2m and maximum acceleration of 120g.

The apparatus of the experiment on the table is shown in **Fig.15**. The filled sand in the container of 800mm diameter is fully saturated and has 550mm depth. The water depth is 250mm. The test specimen made of plastic has single skirt compartment with diameter of 150mm and wall thickness of 8mm and it was penetrated into the depth of 200mm under an atmospheric pressure. Then the acceleration was applied up to 30g and the further penetration was conducted with the rate of 1.3mm/min. The water pressure in the skirt compartment was controlled by the adjustment of water level of the tank through monitoring the pore pressure gauge installed in both the tank and the skirt compartment.

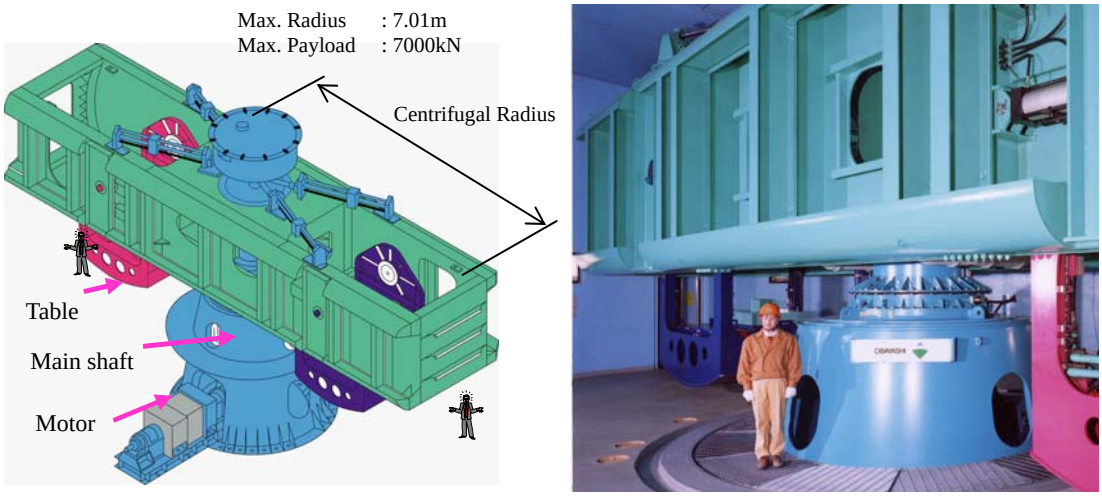


Fig. 14 Centrifuge facility for experiment

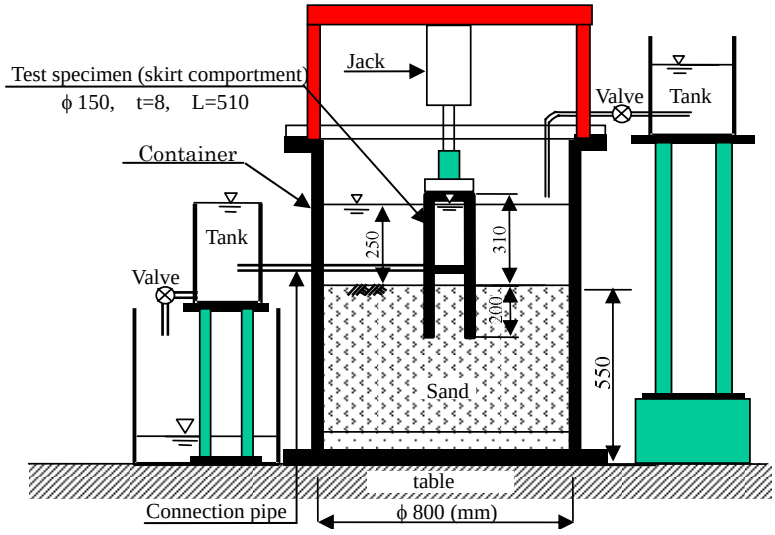


Fig.15 Apparatus and scale model of experiment on table

(3) Results and discussion

The test cases are shown in **Fig.16**. Case-2 expects the reduction in penetration resistance as well as the suction load.

Case-1 Penetration by jacking

Case-2 Penetration by suction together with jacking

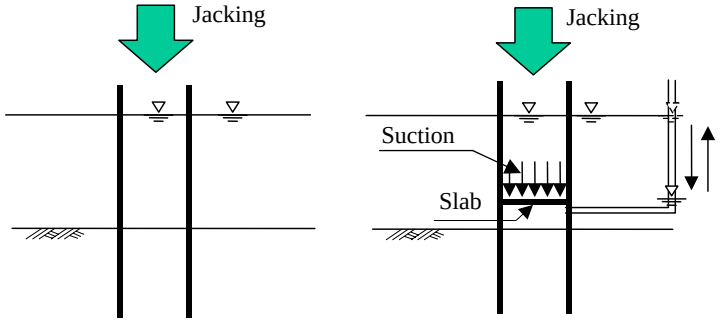


Fig.16 Test cases for preload effect

The load-settlement curve of Case-1 shown in **Fig.17** demonstrates that the reload after unload shows almost no settlement at the penetration depth both of 6.3m and 7.3m. It is found that the preload effect due to jacking was clearly observed. **Fig.18** shows the load-settlement curve in Case-2 where the penetration load up to the depth of 6.3m was applied by the jacking, then the suction was included until 6.8m depth, and the further penetration load was induced by jacking after removal of suction. The unloading and reloading was conducted at the skirt tip depth of 6.8m.

When the suction was applied during the penetration, **Fig.18** shows that smaller imposed load (5KN) in Case-2 than that in Case-1 is enough to penetrate the skirt until the depth of 6.8m due to the upward water flows induced by suction load of 0.7KN.

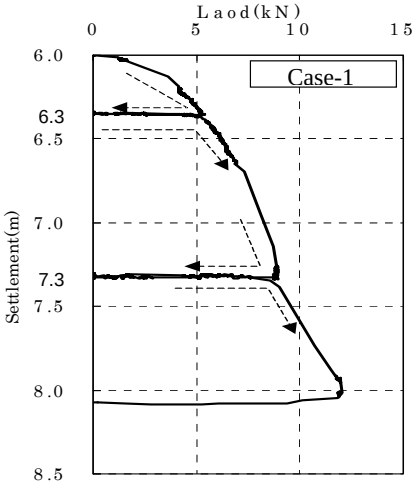


Fig.17 Load-settlement curve of jack preloading

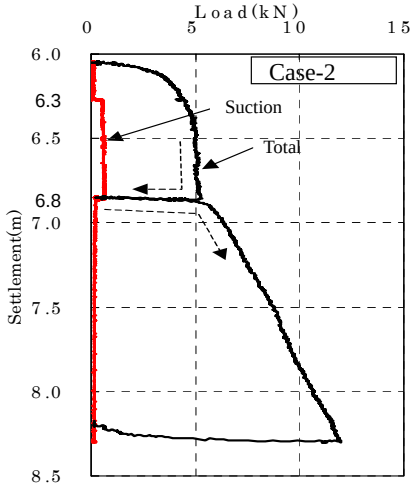


Fig.18 Load-settlement curve of suction preloading

After the removal of suction load at the depth of 6.8m the reloading was applied by jacking and the load – settlement curve shows that the settlement by the reloading until the preload (5kN) was nil just same as Case-1 due to the preload effect.

However, the penetration resistance at the same depth in Case-1 and –2 has a little difference because it might depend upon the load hysteresis during penetration.

An additional experiment has been conducted to verify the preload effect due to suction. This second experiment Case-3 employed the same apparatus as shown in **Fig.15** but different scale model illustrated in **Photo2**, whose dimensions are as follows.



Photo2 Additional scale model for experiment for preload in Case-3

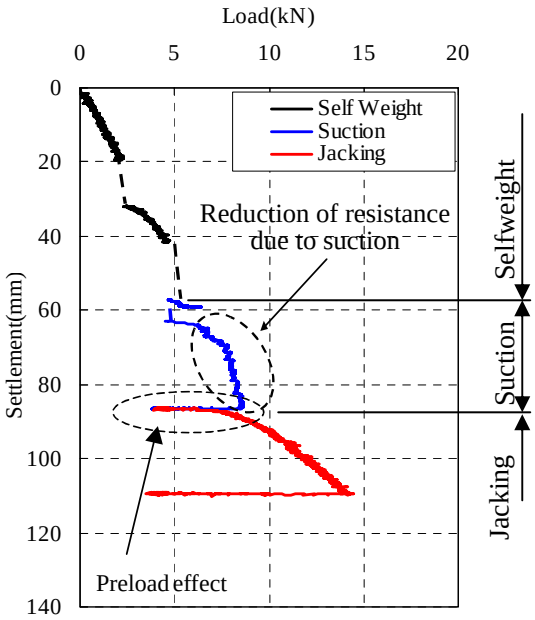


Fig.19 Load-settlement curve of Case-3

Diameter of outer compartment	ϕ_0	=370mm
Diameter of inner compartment	ϕ_I	=150mm
Height	h	=250mm
Wall thickness of compartment	t	=4mm

The test specimen was penetrated by suction and then reloaded by jacking as before. The result in **Fig.19** illustrates the load-settlement curve of both penetration and reloading. Until the depth of 60mm the applied penetration load was only the selfweight, and then the suction was imposed to reduce the penetration resistance up to the depth of 85mm. After the removal of suction the reload was imposed by jacking. The preload effect was clearly observed because of no significant settlement during reloading. Further the jacking beyond the hysteresis load (8kN) highly increased the penetration resistance which approached the load – settlement curve due to external loads.

Conclusions

The following performance of skirt suction foundations as a bridge substructure was observed by experiments in the field and laboratory.

(1)The offshore structure with skirt foundation was successfully installed. The position of a structure was well controlled by suction during and just after the skirt penetration. The installation accuracy was 0.5% of inclination, without soil improvement or dredging.
(2)Preload effect by suction was well observed, because the reloading by jacking up to the preload induced by suction showed no significant settlement of the foundation.
(3)Not only the above performances but also the tensile resistance due to seismic loading clearly shows high applicability of skirt suction foundation to bridge substructure installed in waters.

References

[1] Andersen, K.H. and Hans P.Jostad (2002): “Shear strength along outside wall of suction anchors in clay after installation”, Proceedings of 12 International Offshore and Polar Engineering Conference, 2002
[2] Audibert, J.M.E. et al (2003): “Suction caisson installation at Horn Mountain-A case history ”, Proceedings of 13 International Offshore and Polar Engineering Conference, 2003
[3] ERBRICH, CT. and TJETTA, TI. (1999): “Installation of Bucket Foundations and Suction Caissons in Sand – Geotechnical Performance”, Offshore Technology Conference, No.10990
[4] FUKUI, J, et al. (2004) "The Effect of Suction on the Foundations of Super Long Span Bridges During and Earthquake", 20th US-Japan Bridge Engineering Workshop
[5] HUSLID, C. (2001): “Full - Scale Monitoring of Troll A Concrete Platform: A

Huge Gravity - Based Structure", ISOPE, Vol. 2, pp. 647 - 654
[6] ITO, M., et al. (2002): "Centrifuge experiment for control of settlement of skirt suction foundation", JSCE 57th Annual Meeting, Vol. 3
[7] MASUI, N., et al. (2001): "Installation of Offshore Concrete Structures with Skirt Foundation", ISOPE, Vol.2, pp. 626-630
[8] MASUI, N., et al. (2002): "Review of penetration resistance based on in-situ monitoring", ISOPE, Vol.2, pp. 717-722
[9] MASUI, N. et al (2003): "Experimental evaluation of preload effect on skirt suction foundation", Proceedings of 13 International Offshore and Polar Engineering Conference, 2003
[10] MATSUDA, T. and HIGUCHI, S. (2002): "Development of the Large Geotechnical Centrifuge and Shaking Table of Obayashi", Proc., International Conference Physical Modeling in Geotechnics, pp. 63-68
[11] Tjelta,TI,Aas,PM,Hermstad,J,and Andenaes,E(1990): "The Skirt Piled Gulfaks C Platform Installation" Proc. 22nd Annual Offshore Technology Conference, pp 453-462.
[12] Zen, K. et al (2003): "Experimental and analytical studies on bearing capacity of suction foundation", Proceedings of 13 International Offshore and Polar Engineering Conference, 2003

NEW TACOMA NARROWS BRIDGE CAISSONS

R. Bruce Patterson, Kiewit Pacific Co., Vancouver, WA, USA

The New Tacoma Narrows Bridge is a classic suspension bridge founded on concrete caissons. Caisson construction was complicated by the proximity of the existing bridge piers, only sixty feet away. High capacity plate anchors were used successfully to moor the new caissons in currents as strong as seven knots during construction.

INTRODUCTION

The Tacoma Narrows project is a new suspension bridge parallel and adjacent to the existing bridge in Tacoma, Washington. The completed structure will be 5400 feet in length with a 2800 foot main span and two side spans of 1200 feet and 1400 feet. The design build project with Washington State DOT is a lump sum of $615 million and is a joint venture of Kiewit Pacific Co. and Bechtel Corporation.

The original Tacoma Narrows bridge was the famous “Galloping Gertie” that failed in 1940 and is familiar to many of us as a study in vibration and wind. Gertie fell into the water and is still present as a National Historic site.

CAISSON DESIGN

The two main towers are founded on reinforced concrete caissons 130 feet by 80 feet by 216 feet tall. The caissons are founded on very dense silty sand and penetrate the seabed approximately 62 feet. The outer wall of the caissons is four feet thick and the inner walls are three feet thick. The caissons are cellular structures with 15 shafts or dredge wells 22 by 22 feet open to the bottom. The dredge wells were fitted with temporary false bottoms or bulkheads at the tip to create a sealed, floating structure.

Construction of these relatively simple boxes was complicated by high currents up to seven knots in the narrows, the need to maintain a safe freeboard above the waterline during and after construction, the need to maintain a safe metacentric height for stability of the floating structure, and maintaining the correct position of the caissons in the water.

The caisson construction method is a classic bridge technique and was similar in many ways to the original caisson construction performed in the 30’s.



Photo 1: Cutting edge fabrication

CAISSON CONSTRUCTION SEQUENCE

The bottom 18 feet of the caissons started as a structural steel shell or cutting edge built by Todd Pacific Shipyards in Seattle, Washington. With the false bottoms installed the cutting edges were launched into the water and towed to the Port of Tacoma for outfitting.

Outfitting included forming and placing as much concrete as possible until the caissons drafted approximately 47 feet, the maximum allowable draft within the Port. Systems for handling air and pumping water were also installed. The first 60 feet above the cutting edge was sheathed with a .375” steel shell which served as an outside form and protected the freshly placed concrete from contact with the seawater. The shell also provided adequate freeboard during the early concrete placements.

After the outfitting stage was completed the caissons were towed to the Narrows and anchored in place – see details below.

On site concrete placement continued in ten foot lifts using jump forms on the outer wall and



Photo 2: Cutting edge floating with false bottoms installed

dredge well forms on the interior wall. The outer walls proceed ahead of the interior walls by as much as 70 feet to maintain stability and freeboard. Structural steel strut systems were used at two levels within the caissons to resist the hydrostatic forces on the exterior walls. The struts also provided access to the upper levels of the caisson interior and provided a convenient rebar template system.

CURRENT LOADING DESIGN AND RESEARCH

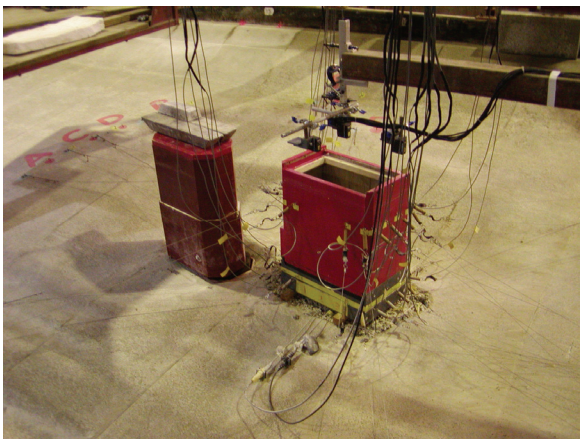


Photo 3: Scale model at Wallingford, England

A critical aspect of the design for the temporary mooring system was determination of the expected loads on the floating caissons. The situation was more complicated than the original caisson construction due to the presence of the adjacent existing piers. The mooring system had to hold the caissons clear of the existing bridge piers only sixty feet away and resist the current loading from the flood and ebb currents as well as the lateral loading during the flood caused by vortex shedding from the existing piers. Scale model testing was performed at a fluids lab in Wallingford, England using a model that mimicked the geometry and contours of the Narrows as well as the current conditions. Bechtel's fluids modeling group also performed computational fluids dynamics studies (CFD) to compare to the lab testing. The CFD and lab testing information was used as input to determine the optimum mooring system layout and the expected loads on the mooring system.

ANCHORS AND MOORING LINE DETAILS

The estimate was based on using sixteen temporary anchors at each caisson site. Anchors were to be large precast tubs weighing approximately three hundred tons and filled with rock. The plan was to attach each anchor to the caisson with a single line which would be jumped up as the construction progressed. Early in the planning stages it was determined that the loads were expected to be much higher than anticipated in the estimate and that two levels of mooring lines would be required to stabilize the caisson. We went to a total of 32 attachment points, sixteen upper and sixteen lower attachments on each caisson.

ANCHORS TYPE SELECTION

Seven different styles of anchors were evaluated during the early planning stages. Anchor types included several versions of gravity anchors resting on the seabed, buried systems that developed capacity by mobilizing the passive resistance of the soil and backfill, and "patent" anchors or high capacity commercial anchors similar to those used in some applications in the oil field industry. A unique alternative was the deeply embedded plate anchor. We looked at using a single anchor to carry loads from both the upper and lower mooring lines but the anchor would have had to have a working capacity of 1000 tons. Due to the high cost and schedule impacts of the various conventional anchors we were motivated to have a serious look at plate anchors. Plate anchors also had the advantage that they could be installed in the bottom at any orientation since the mooring chain came straight up off the anchor and loads

reaching the plate anchor itself were always vertical. Installation tolerance for position was quite generous – a 25' radius from the planned position in most cases – and we had little trouble installing the anchors within this tolerance. Another advantage of the plate anchor was increased redundancy – if one anchor failed we would loose one mooring line out of thirty two verses two out of thirty two if both upper and lower lines were attached to the same anchor.

Deeply embedded plate anchors have been in use by the U.S. Navy and in the oil patch for about 25 years. The Navy uses plate anchors for drydock moorings, fleet mooring applications, and recently for securing floating anti terrorist barriers. Historically, Navy plate anchors have had capacities of one hundred to three hundred tons although a few have been installed with up to 500 ton capacity. Some applications in the oil patch have used plate anchors for tension leg platforms with very high capacity over 1000 tons. Installation of 64 plate anchors with 500 ton capacity on one project at Tacoma Narrows was a first.

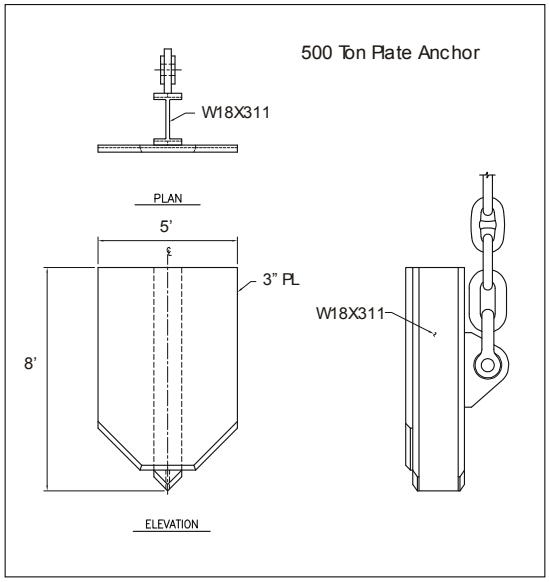


Figure 1: Plate anchor

Sixteen anchors were installed at a 300 foot radius from the center of the caisson and sixteen were installed at a 600 foot radius). All plate anchors consisted of heavy plate 5'X8'X3" thick with a W18X311 beam welded at the center of one side on the longitudinal axis. A 250 ton shackle was used to shackle the anchor to the anchor chain. Note that the shackle was operated at a reduced factor of safety of about 2.5 in this application. The inner circle of anchors was shackled to 3 ¾" Oil Rig Quality stud link anchor chain with a breaking strength of 1,750,000 pounds; the chain extended to within 50 feet of the caisson and was connected to the outboard adjusting tackle block with another 250 ton shackle. The outer circle of anchors was shackled to one shot (90') of 4" ORQ chain which was shackled to a 432' long bridge strand assembly made of 3 ½" diameter bridge strand. The inboard end of the strand was pinned to the outboard block on the upper adjusting tackle.

ANCHOR INSTALLATION

Site soils were dense to very dense sands and silty sands with some thin layers of cohesive clayey silts. Due to the very dense bottom material we elected to use aggressive jetting methods in addition to an APE 400 vibrohammer to get the anchors driven. All plate anchors were driven at least 50 feet into the seabed. We designed and fabricated a sixty foot "pogo stick" extension to fit between the hammer and the jaw, keeping the hammer clear of the seabed. The hammer was set up to run underwater to a depth of 250 feet (depth of the narrows varied from 60 to 200 feet in the area of the mooring systems). The pogo was made from a W14X342 beam with 3" thick plates heavily gusseted top and bottom and machined to fit the hammer and jaw bolt pattern. The jaw was a custom "compact" jaw machined from 14" thick plate and the jaw did fit within the footprint of the plate anchor assembly. Hydraulic cylinders and ports for the jaw hydraulics were all fitted internally into the 14" plate so there were no exposed hydraulic components in contact with the soil when the jaw was pushed into the ground.

The jet system included four Peerless jet pumps each with 1000 GPM @ 300 PSI capacity. The pumps were manifolded together and connected to four each, four inch jet hoses running to the top of the pogo stick. Five inch extra strong pipe was used to transmit the jet water down the pogo to nozzles on the plate anchor. The pipe was mounted in a compact fashion within the flanges of the W14. Minor plumbing and nozzles on the plate anchor itself were sacrificial and stayed with the plate anchor. We designed and machined double "O" ring slip couplers to connect the jet piping on the pogo to the give away piping on the anchor. We also provided a 2" air line for high pressure air to the tip of the

pogo for assistance in keeping the jetted material suspended during driving. The energy put out by this jet system was an awesome thing to behold!

In order to handle the anchor chain (about 15,000 lbs per 90' shot!) we provided an attachment point at the top of the pogo stick. After the plate anchor was gripped in the jaw and lowered overboard, the chain would be pulled up tight against the pogo and hung from the attachment point with a sling. The attachment was provided with a hydraulic cylinder release that was plumbed to the jaw circuit, ie when the jaw was released after the plate anchor was driven to tip, the cylinder would release the chain so the hammer and pogo could be pulled back out leaving the anchor and chain behind. The bitter end of the chain was hung from the edge of the flexifloat moonpool barge at the working end of the derrick. The entire hammer/pogo/plate anchor/chain package weighed in excess of 50 tons!

To stabilize the hammer package, two anchors were hung from the working end of the derrick down to the seabed. Chain tag lines were attached from the hammer to these down lines in order to stabilize the hammer package.

The driving sequence went as follows:

1. Position the derrick. The derrick was outfitted with differential GPS and the WINOPS system. With a GPS antenna on the boom tip we were able to position the plate anchor with sub meter accuracy in real time. In some cases for anchors right under the existing bridge GPS was compromised by poor radio signal strength and we used conventional survey methods.
2. Sound the depth at the anchor location to verify the topography shown on the drawings. Determine the desired tip elevation and prepare the sounding line for the hammer package.
3. Lower the two down lines from the working end of the derrick.
4. Stand the plate anchor on the moonpool float. The plate anchors had jet tubing and nozzles pre installed off the critical path.
5. Shackle the chain to the plate anchor, lay the chain out and dip the bitter end under the moonpool barge, secure the bitter end of the chain to the deck of the moonpool barge. For the chain/strand mooring lines we had a large spooler mounted on the deck of the moonpool barge to feed strand overboard as the plate anchor was lowered and driven.
6. Loft the hammer/pogo.
7. Connect the jet hoses, hammer hoses, and air hose.
8. Grip the jaw on the W18 plate anchor strongback beam, pick up the plate anchor and lower the package into the moonpool. A second crane line was used to handle the chain at this stage.
9. Pull the chain up tight against the pogo and hang from the attachment point.
10. Connect the tag lines from the hammer to the down lines. Connect the sounding line to the top of the hammer.
11. Start lowering the package and turn on the jets and the air. (We found that we did not need the air and got rid of the air compressor early.)
12. Start the hammer when the plate anchor nears the seabed.
13. Jet and drive the plate anchor into the seabed a minimum of fifty feet.
14. Release the jaw (chain attachment also releases), hoist the hammer to the surface and lay down on the barge.
15. Fleet to the storage float and hang the bitter end of the chain (or strand) on the storage float.
16. Move to the next plate anchor position.

Plate anchor driving went very well. As noted above, we found that we did not need the air so were able to cut the high pressure air compressor from the equipment spread. We typically ran all four jet pumps at full pressure but found that the system would work with three jet pumps with little impact on performance when one pump went down for a few days. We were able to drive most anchors very close to the plan position. Two anchors reached refusal on obstructions or scour protection rock at the seabed and had to be moved 15 to 20 feet to get down (still within the design position tolerance).

PLATE ANCHOR TESTING

The deck barge GC180 was mobilized for setting and pull testing the plate anchors. Note that the anchors are driven vertically and "toggle" or set when the load comes on the chain. Typically the anchors would move

upwards eight to twelve feet as they rotated to a near horizontal position. The design required a minimum of 37 feet of embedment after the anchors toggled. The pull test barge was fitted with a horizontal hoist system consisting of a stationary block at the stern and a traveling block that traveled in a beam guide system with 150 feet of travel. Twenty four parts of 1 ¼" wire were used for a rated capacity of 500 tons. The hoist system was equipped with a load cell and the barge had GPS for location. Two methods were used to test the inner circle of anchors, a horizontal pull or a vertical pull test. Five horizontal tests were done at caisson 11. For the horizontal test two anchor lines were pulled diagonally across the circle against each other to the full 500 ton working load. This required that we retrieve the chains from the storage floats and add chain to span across the circle. The horizontal method was time consuming but tested two anchors at a time. After the first ten anchors were tested successfully with the horizontal test we went to the vertical pull and pulled straight up with the pull test barge. The stationary block mounting was strengthened and we added a hefty roller on the opposite end of the barge where the chain came over. The vertical pull specified was 800 kips.
All tests were positive with the exception of two anchors. One anchor on caisson 12 suffered a failure of the padeye at the plate anchor. Analysis of the failed padeye found that it failed due to torsion likely caused by the chain being fouled below the padeye and thus causing an eccentric load on the padeye. One anchor at caisson 11 came up more than twenty feet but did hold the 800 kip test load. We elected to drive a replacement anchor for both of these cases. All outer anchors were proof loaded to the full 500 ton working load (in opposing pairs) after the upper tackle had been installed on the caisson and connected to the anchors.

It should be noted that the 800 kip vertical test is quite conservative. When plate anchors are loaded in the normal condition with the anchor chain horizontal or at a slight angle at the seabed, less than 50% of the load ever reaches the anchor itself. The chain will "burn in" to the seabed some distance and much of the load is taken up by the chain. Typically the upper 15 to 20 feet of chain assumes an arc in the seabed and at least twenty feet of chain above the anchor is vertical so that the load "seen" by the plate anchor is vertical.

ADJUSTING TACKLE

All mooring lines were connected to a sixteen part adjusting tackle at the caisson with the outboard block of the tackle at a nominal offset of fifty feet from the caisson. The outboard or traveling block was an eight sheave tandem block with four thirty inch sheaves and four twenty four inch sheaves. There were two inboard four sheave blocks mounted on the face of the caisson. Blocks on the upper tackle had a vertical separation of twenty feet and the lower blocks had a separation of ten feet. The 1 ¼" wire was dead ended on the upper four sheave block and the live end was led up the face of the caisson above the water line. Vertical separation of the inboard blocks helped spread the load on the caisson wall and kept the tackle from spinning up.

The lower blocks were pinned to fabricated padeyes bolted to the caisson with high strength bars. The upper blocks were pinned to a sliding beam system. The beams were W24X370's approximately 55 feet long and were fastened to the caisson with heavy duty clips bolted to the caisson at ten vertical foot centers. The slider system allowed us to "jump up" the upper mooring line by simply slacking off the tension in the tackle and hoisting on the top of the slider beam to pull it up ten feet. The beam was secured vertically by a latch mechanism that ratcheted onto the top of the slider beam clips. After the beam was moved up ten feet the line was retensioned to the specified preload. The live end of the lower tackle was secured to a padeye on the side of the adjacent slider beam clip above the water line. The live end of the upper tackle was secured to the top of the slider beam assembly.

The live end of each upper and lower tackle was stopped off with a Carpenter stopper. The Carpenter stopper was shackled to the caisson with a load cell shackle so we had a constant readout of the load in each tackle. All the load information was transmitted to the control room on caisson 11 so we had real time and archived information on the actual loads in the mooring system. All this information was displayed on the computer screen in the control room along with the real time position data from the GPS and tiltmeter instrumentation.

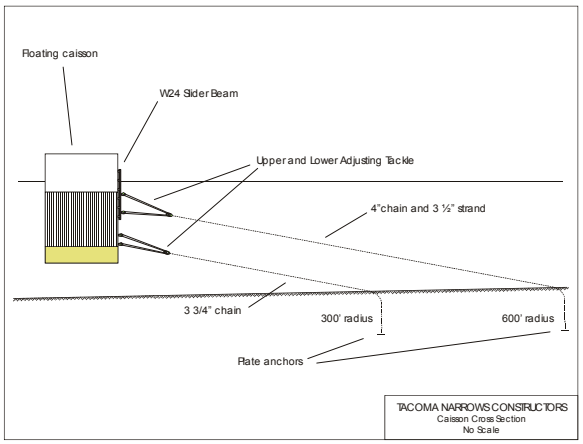


Figure 2: Caisson mooring system

TOWING AND MOORING THE CAISSONS

One of the key construction strategies was to build as much of the caissons as possible in the Port of Tacoma. This meant that we were faced with towing the caissons to the bridge site with a draft of 47 feet and a total weight of about 15,000 tons. Significant towing horsepower was required for the tow and to safely hold the caissons in position during flood and ebb currents while the initial connections were made to the mooring system.

Foss Maritime was selected as the towing subcontractor. Foss owns the largest tugs in the Pacific Northwest and was able to schedule their two large tractor tugs, the Lindsey Foss and the Garth Foss, for the two tows. Garth and Lindsey are sister ships with 8000 horsepower and "Voith" propulsion systems (The Voith drive system is capable of applying full thrust in any direction and this capability was a key to the success of the operation.). Both tugs are 155 feet long and have bollard pull of 174,000 pounds. In addition to the two large tractors we selected the Barbara Foss, 126 feet, 5,400 HP and the tractor tug Wedell Foss, 105 feet, 3,000 HP to assist.

A detailed plan was prepared for the tow and initial mooring hookup which included the following considerations:

1. Selection of optimum current "windows" or periods of relatively low current conditions that were favorable to the tow and mooring operation. Although the currents in the Narrows can be in excess of seven knots, there are periods of four or five days most months where the currents do not exceed three knots. Current meters were installed in the Narrows and we were able to verify that the current predictions available to us were reasonably close to those measured by the meters. A current of three knots was selected as the maximum operating condition for the tow and initial mooring work.
2. An analysis of the expected loads on the caisson during the tow and initial mooring connection. Zentech (Houston) provided guidance on the expected drag forces on the caisson during the tow and the work window. We used this information to size the tugs and the rigging. Zentech also provided guidance on the sequence for connecting the mooring system.
3. Tug selection and deployment of the tugs.
4. A chart of the tow route including way points and a timeline for reaching each way point.
5. A detailed hour by hour schedule for the tow and mooring system hookup. The schedule allowed three hours for "sea trials" in Commencement bay so we could verify the towing performance of the caisson and the tugs. The schedule included predicted currents each hour.
6. Detailed procedure drawings were prepared for each step of the operation (31 sheets). The drawings showed the expected velocity and direction of the current at the beginning and end of each step. The drawings also included procedure narrative for each step.
7. An organization chart. All personnel including superintendents, foremen, operators, riggers, and Foss' towmaster were included on the chart. Radio and cell phone information was also included on the organization chart.
8. A detailed risk analysis was prepared with "what if" scenarios and contingency plans to deal with the perceived risks.
9. Most important, a detailed hazard analysis was prepared.

Several meetings were held prior to the tow with all involved parties to review the above plan.

Twelve each, 100 ton capacity towing padeyes were installed on the caisson five feet above the waterline for towing and temporary mooring

connections. The two primary tugs (Garth and Lindsey) were made up to the head (Olympia) end of the caisson at the corners. A connection point was provided for the Barbara midships on the Olympia end although the Barbara was not used during the tow. The Wedell was made up to the tail end to help steer and control the yaw of the caisson. The primary tugs had enough bollard pull to tow and hold the caisson in the expected currents and the Barbara was deployed as a contingency vessel in case of a breakdown on one of the primary tugs. The tows proceeded exactly according to plan and the caissons towed fairly well at about two knots. The ten mile tow from the Port of Tacoma took approximately six hours.

PREPARATION FOR THE TOW

All sixteen lower mooring line tackles were pre installed on the caissons at the Port of Tacoma and laid out on two 34X110 "YFN" barges, one on each side of the caisson. Each YFN barge had four hydraulic spoolers for paying out and taking up slack in the 16 part 1 ¼" tackle. We also mobilized four "block floats" for use in supporting the 10,000 pound outboard blocks while the blocks were pulled out from the caisson to the vicinity of the plate anchor. The strategy was to perform as much preparation work as possible prior to the start of the tow so the moorings could be hooked up quickly. Of the sixteen moorings, we needed to hook up and tension eight (two in each corner of the caisson) prior to cutting the tugs loose.

In preparation for the arrival of the caisson two derricks were anchored out at the caisson site, one on each side. A "tailhold" was set up at the bridge site to moor the Seattle end of the caisson. The tailhold consisted of the GC 180 pull test barge previously described above. The stationary block at the stern of the GC180 was moored to the seabed with a chain bridle made of 3 ¼" anchor chain connected to two of the outer plate anchor chains with "dog-bone" plate shackles. The traveling block on the hoist was connected to the Seattle end of the caisson with a bridle made up of "Plasma" 10 inch synthetic line with a breaking strength of over 900,000 pounds. This tail-hold was quickly attached to the caisson and was able to hold it against the pull of the tugs on the Olympia end. This way we could quickly secure the caisson and adjust the position easily with the hoist on the barge.

ARRIVAL AND INITIAL MOORING CONNECTIONS

The tow arrived via the main channel a few minutes prior to high slack current. The tugs proceeded to tow the caisson under the bridge and past the previously deployed derrick barges. The Wedell then towed the caisson backwards between the two derricks "threading the needle" and held the caisson close to its final position while the crew connected the tail-hold line. Once the tail-hold was secure the primary tugs powered against it to hold the caisson steady against the ebb current. The tail-hold was designed to hold the caisson against the expected loads imposed by the flood currents.

The two derricks then commenced with connecting adjusting tackle to the previously installed mooring chains. The two Olympia end corners were connected first, then the two Seattle end corners, then one more line in each corner for a total of eight. Prior to cutting the tugs loose the eight mooring lines were pulled up to a few thousand pounds of initial tension. After the tugs left the derricks completed connecting all sixteen mooring lines.

In the weeks prior to the arrival of the caissons, the previously installed mooring chains were inspected. Chain from the inner circle (lower mooring system) and strand from the outer circle (upper mooring system) was drawn together in groups of six to eight lines on "storage floats" (30X40X7 Flexi floats) to keep the lines available and to keep them from becoming fouled. Due to various mishaps and strong currents some foul-ups did occur. Although we invested much time to check and clear fouled mooring lines, we discovered after the arrival of caisson 11 that the Northwest corner of the mooring system was badly spun up. This caused an expensive delay in completing the connection of the initial mooring lines and in allowing the tugs to leave. The three chains and one 3 ½" bridge strand were spun up together and had even picked up a section of beam from "Galloping Gertie".

To connect the adjusting tackle to the mooring chain the chain was retrieved from the storage float and pulled towards the caisson with the derrick, keeping enough slack out of the water to enable the crew to shackle the chain to the outboard block of the tackle. The tandem (outboard) block had previously been loaded

into the block float which supported it during the tackle connection. The block and float were then pulled out to the chain and the chain was shackled to the block. This sounds easy but the chain weighed 130 pounds per foot, the block weighed 10,000 pounds, and the shackle connecting block and chain weighed over 700 pounds! The block float was then removed and the block lowered into the water while the spooler took up slack. The crew would continue to take up slack until an initial tension of about 4000 pounds was attained on the live end of the tackle. After eight lines were connected and initially tensioned, slack was peeled off of the 1 ¼" wire spools, the wire was cut, and the next eight spools were loaded into the spoolers. Then the remainders of the mooring lines were connected.

A FEW PROBLEMS

We experienced considerable difficulty in pulling slack on the tackle and taking the slack back up without getting the tackle fouled up. Much of this was due to some close tolerances in the blocks. The clearance between the wire and the cheek plate bolts on the blocks was very tight and caused a lot of friction until some significant tension was put on the tackle. The high friction caused the inner parts of wire to take all the tension while the outer parts got slack and proceeded to foul up on everything. Also, every block had 6" angle handling "ears" sticking out at both ends that tended to foul wire at every opportunity. We soon learned to cut off the protruding ears. But for spinups and aggravating foul-ups on the blocks the tackle connection went according to plan.

Due to fouled chains, fouled tackle, and learning curve on the Tacoma side caisson (first tow) the last tug did not leave for several days. Things went much better on the second tow for the Gig Harbor side caisson and the time that the tugs were on site was reduced by half.

PREPARATION OF THE LANDING PADS

While caisson outfitting was taking place landing pads for the caissons were prepared in the narrows. The dredge "Seattle" excavated flat spots in the seabed at the caisson locations and placed a minimum of five feet of 24" minus rock as scour protection on the excavated flat spots. Scour protection rock was also placed around the existing bridge piers.

Rock for the landing pads was placed with a heavy, ten cubic yard capacity skip box which was lowered to within a few feet of the bottom and tipped. The rock was leveled by holding the loaded skip box at the top of pad elevation and sweeping back and forth. This method was adequate to achieve landing pads that were level within one foot of the desired elevation. Densification of the landing pad rock was not required.

ACCESS TO THE WORK



Photo 4: Access on existing bridge

To provide crew access and support for the concrete slick lines, a temporary walkway was installed from the beach to the existing piers on both sides of the narrows. The walkway was built within the truss on the existing bridge, just above the lower cord. Stairtower extended from the top of the existing pier up to the truss, approximately 150 feet. Steel bridges were fabricated to ramp from the top of the existing pier to the service derricks at each caisson. The derricks were fitted with structural towers extending forty feet up from the deck with stair towers and gangways to gain access to the caissons.

Two slicklines were installed on the walkways and extended vertically down adjacent to the stair towers and across to a concrete placing barge so that two pumps could be run for the large concrete placements. The concrete placing barge was fitted with two placing booms supported on towers to facilitate placement over the footprint of the caisson interior.

FORM SYSTEMS

Contractor's Engineers were selected as the form suppliers for caisson form systems. All forms were custom designed and fabricated steel forms. The exterior walls were poured in advance of the interior walls to add freeboard to the side of the caisson. Caisson buoyancy calculations were done to provide adequate freeboard to keep the formwork above the water line. Also, fresh concrete could not enter the saltwater until 10-days of cure had passed. The exterior formwork consisted of a cantilever form system for the inside and exterior face of the wall. The bottom of the form was secured to the wall with "pig-tail" anchors that were cast at top of a lift of concrete. Once the forms were jumped up, these pigtails supplied the anchorage point for the "she-bolts" to secure the forms to the walls. The form was aligned using pole braces around the exterior of the formwork.

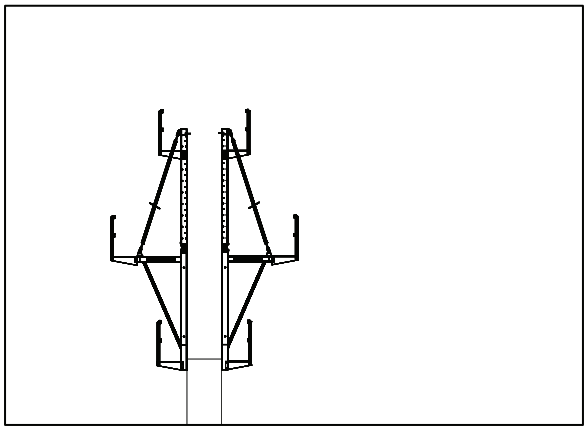


Figure 3: Exterior wall jump form schematic

The dredge well forms were modular, self stripping units supported by "chocks" that engaged into block-outs in the inner caisson walls. The forms used a release mechanism that pulled the form in when the form was picked with the crane so each form was stripped and reset with one pick. Forms for the exterior walls were cantilever jump forms supported on wiggle tails with vertical wales. The exterior form had three levels of scaffolding using the trailing scaffold for access to install the slider beam clips.

REINFORCEMENT

Rebar was prefabricated in panels and modules at our staging yard in the Port of Tacoma. Prefabricated sections were loaded onto barges with a 400 ton capacity Liebherr crawler crane and towed out to the caisson operation. RPM steel was the rebar subcontractor. The rebar mats were set in the caisson using the floating derricks. The two caissons contained 6,000 tons of rebar.

Above the exterior wall forms was the exterior wall rebar template (EWRT). The EWRT was a post and beam system that served as a rebar template and also gave us a place to run utilities, ballast water piping, and survey reference points.. The majority of the rebar was black bar while area around the splash zone and distribution cap is epoxy coated.

TOUCHDOWN

Touchdown is the art of landing caissons on the seabed within the desired tolerances, the first time. The Gig Harbor caisson touched down on 15 December 2003 followed by the Tacoma Caisson one month later. The team did a lot of planning for touchdown including the following considerations:

1. Understand the allowable tolerances for position, pitch, roll, and yaw. The specifications were fairly generous at Tacoma Narrows, allowing a three foot radius and an out of plumb tolerance of three feet over the height of the caissons at final tip elevation.
2. Establish a seabed landing target for position, tilt, and yaw that is realistic but also has a high probability of producing a caisson that is within tolerance when it has reached tip elevation. In our case we selected a two foot by two foot target and less than one degree of yaw, well within the specified tolerances at tip.
3. Minimize the potential for scour prior to and during the touchdown process. As a caisson nears the seabed the potential for scour increases as the current is accelerated under the caisson. We allowed for eight to ten feet of clearance between the cutting edge and the seabed at all times until the final touchdown operation. To maintain adequate clearance air was added to the false bottom spaces as ballast water

was pumped into the caissons. With air in the false bottoms touchdown could be initiated rapidly by blowing off the air.

4. Survey control planning was important. Three independent survey systems were used to position the caissons during touchdown. Differential GPS was used to monitor caisson position during construction and we had a real time readout of position, yaw, pitch, and roll for both caissons in the control room. The system received input from tiltmeters on the caissons and was able to compute the position of the tips of the caissons. (Note that we were not concerned about the position of the top of the caissons within a fairly liberal tilt tolerance but we had a tight tolerance on the position of the tip of the caissons at touchdown.) An independent check was performed using a total station instrument set up on the top of the existing pier. By shooting four points on top of a caisson the position of the tip could be computed. A third system consisted of long range vertical fan lasers on the shore and on the existing pier supplemented with "water levels" on the caissons to give an indication of pitch and roll. The three systems generated caisson positions consistently within acceptable tolerances.
5. A detailed plan was prepared for the air and water ballast systems. It was important to be able to blow off air quickly when the time came to set down. After touchdown, adequate pumping capacity was critical to keep the caissons "heavy" so they would stay on the bottom in a stable position during the flood tide and current. Bilge pumping capacity had to be adequate to discharge the ballast water quickly in case we had to lift off to reposition the caisson after touchdown. A pipe manifold was provided around the perimeter of each caisson so water could be added to any of the fifteen dredge wells as required.
6. Because of the scour depth constraints described in (3) above, we needed to rapidly lower the caisson to the seabed the final ten feet by blowing off air. Touchdown was planned to occur just prior to low slack current at approximately one knot ebb. Due to the rapid lowering, the mooring system would become somewhat slack during the final minutes. The motion of each caisson over a range of currents and tides was observed and adjustments to the mooring system were performed prior to touchdown to maximize the probability of landing within the target zone.

After the intensive planning effort, touchdown at Tacoma Narrows was somewhat of an anticlimax (as it should be!). Both caissons landed within a foot of the desired target and with less than half a degree of yaw. Note that it is possible to "steer" the caisson during the excavation operation but a sloppy touchdown can cause major headaches when trying to stay within tolerances during digging.

FALSE BOTTOM REMOVAL

After touchdown the remaining lifts of interior wall concrete were formed and placed up to the top of the previously placed exterior walls. Interior forms were removed and the caissons were flooded to ambient water elevation. Using a combination of spudding and underwater burning with divers, the half barrel shaped false bottoms were removed in preparation for caisson excavation.



Photo 5: Caisson excavation

CAISSON EXCAVATION

Early in the project the seabed at the caisson sites was prepared by excavating a flat spot and placing a five foot thick rock blanket on the "landing pad". The excavation also served to clear any obstructions on the seabed in the vicinity of the new caissons. The rock pad

provided a firm and level surface for landing the caissons and was designed to prevent scour prior to and during the touchdown operation.

As of this writing both caissons have been excavated to final tip elevation, the seal concrete has been placed, the distribution cap concrete has been poured, and work has started on the tower construction. Both caissons are well within the specified tolerances for position at less than one foot from dead center with an allowable position tolerance of three feet. Verticality of the caissons is optimum.



Photo 6: Caisson excavation

The clamshell dredge "Seattle" performed the excavation using a variety of clam buckets up to ten cubic yard capacity. There is a long history of caisson excavation techniques and lots of theory but some of the key points at Tacoma Narrows included:

1. Develop a detailed plan for the dredging. Understand the soils, study caisson sinking history, and write a plan.
2. Keep track of the excavation. Have some crew members with strong arms that can take lots of lead line soundings. Chart the soundings and the advance of the caisson. Provide access on top of the caisson for the sounding crew.
3. Do not overdig. Many caisson crises are caused by overdigging. Caissons advance by controlled bearing failure of the soil at the tapered exterior cutting edge. The failed soil is displaced into the interior of the dredgewell. Undermining the exterior walls usually results in excessive tilting of the caisson.
4. Do not take radical or drastic steps, be conservative.
5. Always track caisson position, tilt, and yaw. Constantly strive to achieve optimum position, tilt, and yaw. If you let down your guard, the caisson can rapidly get out of tolerance.

CONCLUSIONS

The New Tacoma Narrows Bridge caisson foundations are a contemporary example of a classic bridge foundation method. Although the equipment has changed, the techniques used in the new caisson construction were very similar to the original work.

Design and construction of the caissons was complicated by the proximity of the existing bridge piers. Considerable effort was required to assure the safety of both the new caissons and the existing bridge during construction. Using state of the art modeling methods to determine the current loads, an innovative mooring system was designed to hold the caisson securely in position. The 500 ton capacity plate anchors provided a very high quality and cost effective solution to the mooring problem.

REFERENCES

Forrest Ph.D., James, Taylor, Robert and Bowman, Lora., Design Guide for Pile-Driven Plate Anchors (Technical Report TR-2039-OCN); Naval Facilities Engineering Service Center, 1995.

Havers, John A. and Stubbs Jr., Frank W., Handbook of Heavy Construction; Section 28: Cofferdams and Caissons; Part D (Open Caissons by BEN C. GERWICK, JR.); McGraw-Hill 1971.

Hool, George A. and Kinne, W.S., Foundations, Abutments, and Footings; Section 3: Foundations; part 29; McGraw-Hill, 1943.

MOORING BRIDGE CAISSONS DURING CONSTRUCTION USING JETTED-IN DRIVEN PLATE ANCHORS

Osama A. Safaqah, Ph.D., Ben C. Gerwick, Inc. San Francisco, CA, USA
Marc Gerin, Ph.D., P.E. Ben C. Gerwick, Inc. San Francisco, CA, USA
Robert Bittner, P.E., Ben C. Gerwick, Inc. San Francisco, CA, USA

Driven plate anchors can be used to hold in place large bridge caissons during floating construction. Their small size and simple method of installation make them a very cost effective alternative to other direct-embedment, gravity, and drag anchors. The geotechnical design of plate anchors involves the anchor geometry, embedment, drivability, and proof testing. This paper describes the experience gained with plate anchors used during construction of the new Tacoma Narrows Bridge. For this project, the anchors had to be driven in dense to very dense sands, and had to resist large forces from 7-9 knot currents.

INTRODUCTION



Figure 1: Floating Caisson held in Position by Anchors

Driven plate anchors are conceptually very simple: as shown in Figure 2, plate anchors consist of a steel plate welded onto a section of structural steel beam to which a padeye is attached. As shown in Figure 3, the anchor is connected to a follower (H-Pile) by a hydraulic clamp and is driven vertically into the sea floor using an under-water hammer. After driving the anchor to the required depth, the follower is retrieved and the anchor is proof-tested. This will cause the anchor to rotate to the horizontal or "key in" thus developing maximum resistance to pull out (Figure 3).

Driven plate anchors are simple, inexpensive, quick to install and have a very high holding-capacity-to-weight ratio compared to other underwater anchor systems. This makes them very suitable for the temporary mooring of bridge caissons during their construction.



Figure 2: Driven Plate Anchor

The driven plate anchor design described in this paper was developed for the construction of the new Tacoma Narrows Bridge. The Narrows is a deep waterway located at the south end of Puget Sound, on the West coast of Washington State. The deepest point along the bridge alignment is about –67 m (–220 ft) elevation, and the tidal currents are very fast (7-9 knots) between tidal shifts. The new 1-mile long suspension bridge is supported by two main towers. These towers are founded on two 24x40 m (80x130 ft) caissons embedded 23 m (75 ft)

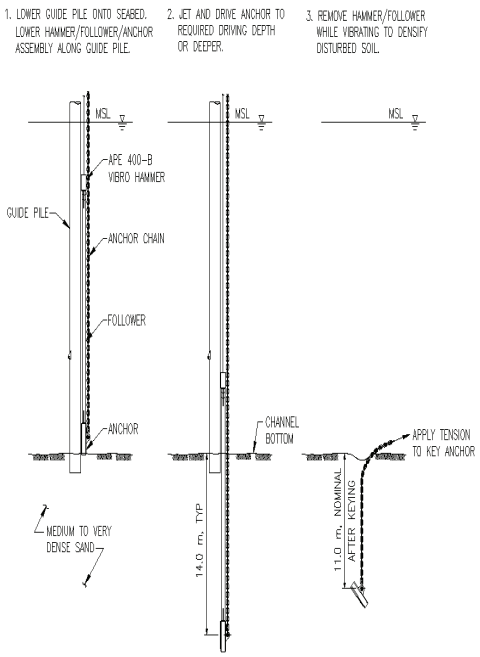


Figure 3a: Plate Anchor Concept and Installation Procedure

below the mudline in 40-46 m (130-150 ft) of water. The concrete caissons were constructed from a "raft" which was cast in a dry-dock, towed to the site and moored in place. The remaining concrete was cast-in-place in 3 m (10 ft) lifts. Until the bottom of the caissons reached the seabed, the floating caissons had to be moored in place.

The mooring system for the bridge caissons had to resist drag forces from up to 43.6 m (143 ft) of draft in 7-9 knots maximum tidal currents. Each caisson was moored by 16 lower anchors on a nominal 300-ft radius and 16 upper anchors on a nominal 600-ft radius. At the caisson end, the lower lines are attached approximately 7.6 m (25 ft) up from the bottom of each caisson and remain fixed during construction. The upper lines are initially installed approximately 18.3 m (60 ft) up from the bottom of each caisson. They are attached to a sliding beam, which is moved upward as the caisson is constructed. The lower mooring lines were 100 mm (4 in) diameter Oil-Rig-Quality stud-link chain and the upper lines were 95 mm (3.75 in) diameter bridge strand connected to one shot of 100 mm (4 in) chain. Each of the 64 mooring lines was attached to a driven plate anchor. See Figure 3b and 3c for schematic of anchor attachment to caisson.

GEOTECHNICAL DESIGN OF PLATE ANCHORS

Anchors can have either a "shallow" or a "deep" mode of failure depending on the embedment ratio (H/B, anchor depth to anchor smallest dimension), and the soil friction angle. In a "shallow" failure, the failure surfaces extend to the ground surface at small anchor displacements. This mode of failure results in the lowest anchor capacity. In a deep failure, failure starts locally around the anchor like bearing failure around a footing. Global failure takes place at large displacements with an inverted-pyramid-shaped rupture surface. This failure mode results in a much higher anchor capacity. Plate anchors are designed to develop a "deep" type of failure.

Plate anchor capacity in sands can be theoretically estimated using the following equation:

$$q_u = \gamma' H N_q^* \qquad (1)$$

where γ', H, and N_q^* are the effective unit weight of soil, embedment length, and anchor capacity factor, respectively. Obtaining a reasonably accurate estimate of N_q^* is the major task in designing plate anchors. This is because it depends on many factors including anchor orientation, embedment ratio, soil dilatancy, anchor roughness, soil angle of friction, and initial stress state. Further, the anchor installation method has an impact on the angle of friction and the stress state, which must be considered.

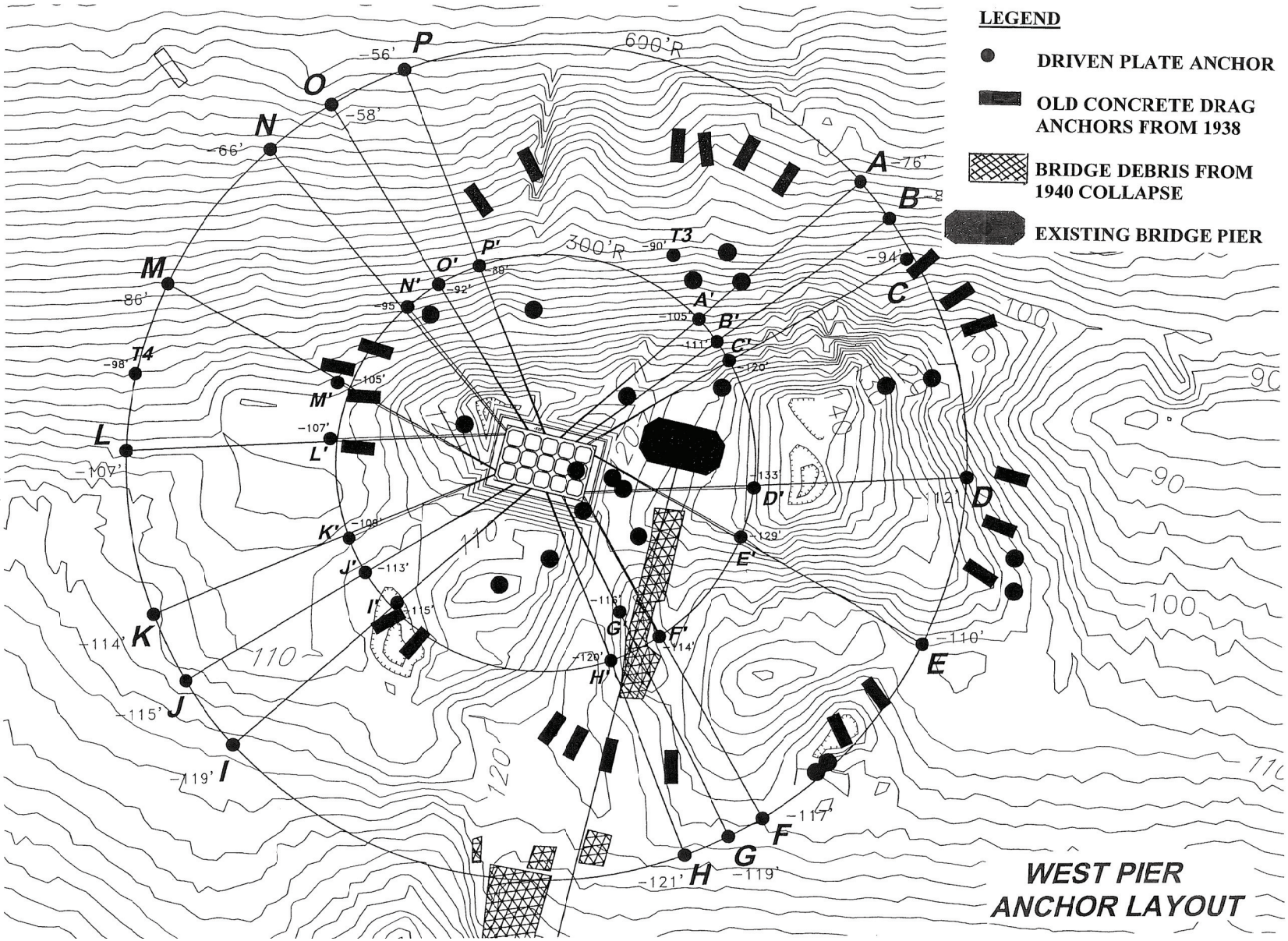


Figure 3 b: Plan View of Anchor Layout

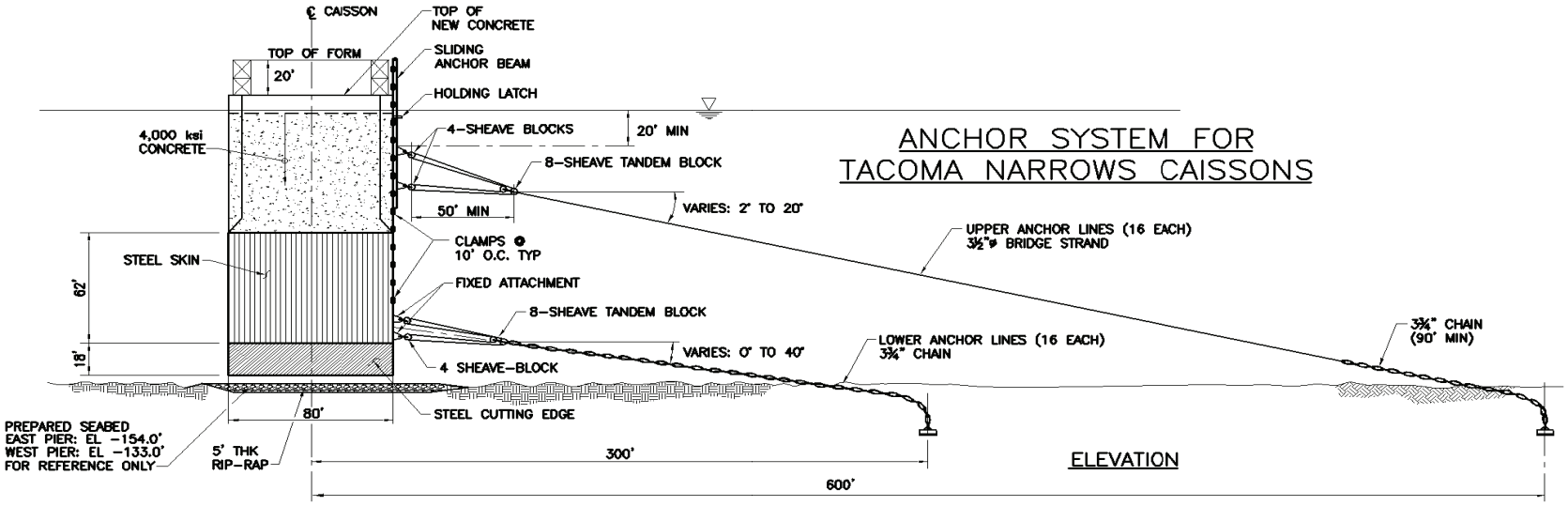


Figure 3c: Elevation- Anchor Attachment to Caisson

Many methods have been proposed to estimate N_q^*. Some are based on assumed failure mechanisms, some are based on small-scale centrifuge tests, and some are based on large-scale pull out tests. Unfortunately, N_q^* values estimated from these methods range from very conservative to very optimistic. The Majer (1955) method is based on a vertical slip failure surface and usually represents a lower, very conservative, limit on N_q^*. On the other hand, the Meyerhof and Adams (1968) method is based on a pyramid-shaped failure surface and results in upper estimates of N_q^*, however, these can be unconservative in dense sands. Other methods include Vesic (1972), based on the cavity expansion concept, and Vermeer and Sutjiadi (1985), which uses soil dilatancy to control the shape of the failure surface. A reasonable analytical method was proposed by Rowe and Davis (1982). They used two-dimensional finite element analyses with an elasto-plastic soil model to develop plate anchor design charts. Their model accounts for soil dilatancy, initial stress state and anchor roughness.

Perhaps the best approach to plate anchor design is one based on an empirical method calibrated with full-scale tests, and augmented with analytical analysis. The Navy design charts (Forrest et al., 1995) are well calibrated with full-scale field tests, and represent a good staring point. These charts relate the holding capacity factor (N_q^*) to the anchor embedment ratio, and the soil friction angle.

SITE CONDITIONS

At the West tower, the mudline elevation is about –36.6 m (–120 ft), and the upper 21 m (70 ft) of soil consists of very dense, gravelly sand and sandy gravel. At the East tower, the mudline elevation varies between –36.6 m and -48.8 m, and the upper 14 m (50 ft) of soil consists of medium dense to very dense gray silty fine sand.

Because of the dense soil conditions at the site, driving is aided by jetting ahead of the anchor. The jetting process will disturb the soil around the anchor reducing the friction angle, however, part of this loss can be recovered by using the vibro-hammer to compact the soil during retrieval of the follower. Table 1 shows the soil properties used in the design of the plate anchors.

TABLE 1: Soil properties used in the design of the plate anchors

Location (1)	Condition (2)	Friction Angle, ϕ (degrees) (3)	Buoyant Unit Weight, γ_b (kN/m^3) (4)
West Tower	Undisturbed	38 to 40	10.4
West Tower	After Jetting and Vibro-compaction	35	9.4
East Tower	Undisturbed	36 to 38	10.4
East Tower	After Jetting and Vibro-compaction	35	9.4

DESIGN AND INSTALLATION OF PLATE ANCHORS

The plate anchor dimensions and embedment depth were selected to provide a holding capacity of 4450 kN (1000 kip) at the mudline with a factor of safety of two. The chain embedded in the sand typically contributes at least 20% of the total capacity, therefore, the plate anchor itself was designed to provide 3560 kN (800 kip) capacity with a factor of safety of two. Using the Navy charts and the Rowe and Davis method, N_q^* was estimated at 20 (Other methods gave values ranging from 7 to 40). The analysis showed that an embedment ratio of 7 is needed to ensure a deep failure mode at this site.

The anchors consist of a 75 mm (3 in) thick steel plate 2.4 m x 1.5 m (8 ft x 5 ft) welded to an 2.4 m (8 ft) long piece of W18x311 structural steel beam (Figure 2). The driving end of the plate and beam are beveled at 45 degrees. A 75 mm (3 in) thick padeye welded onto the beam provides the attachment point for the 100 mm (4 in) stud-link chain.

For a plate width of 1.5 m (5 ft), the required embedment depth is 10.5 m (35 ft) after “keying-in”. The distance the anchor travels to rotate and key in is a function of the soil friction angle, proof load orientation, and the configuration and length of the anchor. Denser soils and smaller anchors require smaller keying distance. As a

rule of thumb, plate anchors in sands require 1.5 times their length to key in. Therefore, the minimum driving depth for the Tacoma Narrows anchors is 14.3 m (47 ft) below the mudline.

The anchors are installed using a 18.3 m (60 ft) follower (a W14x342 steel beam) with an APE 400 vibratory hammer mounted at the top, and a hydraulic clamp mounted at the bottom. Drivability analyses were used to select the hammer and to optimize the design to four water jets at 2400 kPa (350 psi) pressure. The water jets help loosen the sand making vibration more effective. A hydraulic clamp was used to hold the anchor during driving, instead of a passive attachment, to maximize the transfer of vibration from the follower to the anchor, See Figure 4. After delivering the anchor to the required depth, the follower was retrieved under vibration in stages of 1.5 – 3 m (5-10 ft) each lasting 2-3 minutes to densify the sand above.



Figure 4: Hook up of Jet Hoses and Vibratory Hammer to Anchor

To validate the design, two full-scale test anchors were installed and tested using the equipment designed for the production anchors. The tests indicated the installation system is capable of driving the anchors to the required depth in 20 to 40 minutes, and confirmed the 4450 kN (1000 kip) holding capacity. See Figure 5.



Figure 5: Installation of Anchors Using Water Jets

ANCHOR LOAD TESTING

Load testing the anchors is an integral part of the anchor installation. This causes the anchor to rotate and key in, thus positioning the anchor for maximum pull-out resistance, and minimizing any further displacement during operation. Load testing also verifies the anchor holding capacity. Load testing in sands can be carried out either vertically or horizontally since the anchor chain remains vertical throughout most of its embedded length. For this project, horizontal testing was used at first. Later on, vertical testing was used because it was faster.

With horizontal testing, two opposing anchors were pulled against each other using a loading mechanism on a barge located between the two. The chain from one anchor was fixed to the barge (the dead end), while the chain from the other anchor was connected to the end of a sliding block (the live end). The sliding block was connected to a winch via a 12-part block and tackle. First, tension was applied to remove any slack in the anchor chains; 220 to 310 kN (50 to 70 kips) was required. Then, tension was slowly increased until one anchor broke loose, causing the tension in the anchor chain to fall off, indicating the anchor is keying. The drop in tension on one side caused the barge to move away from the keying anchor. This helps identify which anchor is keying first. After that, the tension started to build up again until the second anchor broke loose and the tension fell off again. After both anchors keyed, the tension was increased until the proof load was reached. For this project, the proof load was set at 4000 kN

(900 kip), slightly less than 50% of the ultimate capacity of the anchor.

To reasonably estimate the keying distance of each anchor, and therefore the final embedment depth, the following data was recorded during the tests. *Line tension*, indicates when the anchors slip, and when the proof load is reached. *Amount of chain pulled in*, indicates the total keying length (sum of both anchors), and if an anchor is pulling out. *Barge movement,* is the movement along the line between the anchors needed to proportion the total amount of chain pulled in to each anchor. *Tidal elevation change*, needed to adjust the amount of chain pulled in to determine the final embedment depth. Figure 6 shows the data collected from one of these tests.

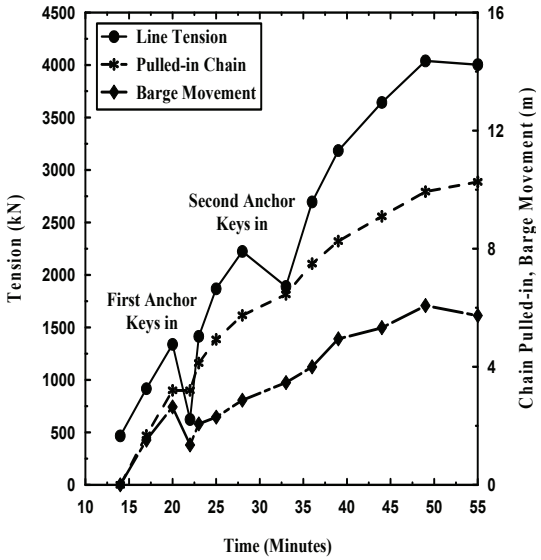


Figure 6: Horizontal Testing for Two plate Anchors

Vertical testing of one anchor at a time has proven more efficient because of the reduced maneuvering of the test barge, and simpler chain hook-up. With a vertical pull, there is less resistance from the chain embedded in the sand, thus the proof load can be reduced by about 20%. For this project, the vertical tests were conducted to a proof load of 3560 kN (800 kip). For these tests, the anchor chain ran over a roller installed on the end of the barge, and was then connected to the sliding end of the block and tackle. Counterweights were used to keep the barge relatively level during testing. Determining the final anchor embedment depth is simpler with vertical tests since all the chain pulled in comes from movement of the one anchor. Figure 7 shows the results from vertical testing of two anchors, which represent the range of keying behavior encountered in this project.

All anchors were successfully tested to at least 3560 kN (800 kip) with insignificant anchor movement at the final test load. Tests data indicate that the keying distance ranged from 2.0 to 7.3 m (6.5 to 24 ft), with most anchors keying in 3.0–3.7 m (10-12 ft) as predicted. Line tension at keying ranged from 890 to 1780 kPa (200 to 400 kips). Some anchors keyed-in suddenly while others keyed in gradually with little release of tension at each step. Differences in the keying behavior are attributed to variations in site conditions. Since the anchors are spread over a large area, soil conditions such as soil density and silt/clay content and the slope of the seabed vary from one location to another.

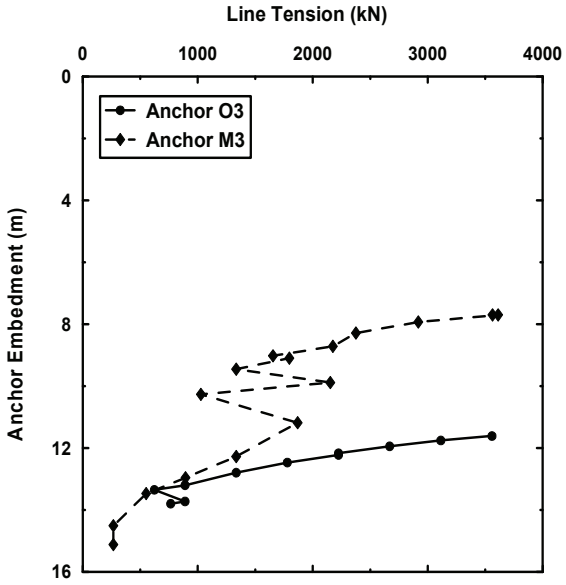


Figure 7: Vertical Testing of Plate Anchors

CONCLUSIONS

Driven plate anchors can be jetted in very dense sands to obtain high-holding-capacity anchors with significant cost savings over other anchor types. The challenge to the geotechnical engineer in such soil conditions is usually the prediction of anchor drivability, the effect of anchor installation on the keying behavior, and the final capacity of the anchor. The role of the

geotechnical engineer starts by characterizing the site conditions and reasonably predicting the design parameters of the soil. Then he can determine the anchor geometry and required embedment depth, assess the anchor drivability, and help design the installation and testing methods and equipment.

Jetted-in driven plate anchors with a design capacity of 4450 kN (1000 kip) were successfully used in the construction of the New Tacoma Narrows Bridge. They held in place the large concrete foundation caissons in the deep and fast waters of the Narrows.

REFERENCES

Dicken, E.A. (1988). "Uplift behavior of horizontal anchor plates in sands". *Journal of Geotechnical Engineering Division*, ASCE, 114 (11), 1300-1317.

Forrest, J., Taylor, R. and Bowman, L. (1995). "Design Guide for Pile-Driven Anchors". *Technical Report TR-2039-OCN*, Naval Facilities Engineering Service Center, Port Hueneme, California.

Majer, E.L. (1955). "Zur Berechnung von Zugfundamenten". *Osterreichische Bauzeitschrift*, 10(5), 85-90 (in German).

Meyerhof, G. G., and Adams, J. I. (1968). "The ultimate uplift capacity of foundations". *Canadian Geotechnical Journal*, 5(4), pp 225-244

Row, P. W., and Davis, E. H. (1982). "The behavior of anchor plates in sand". *Geotechnique*, 32(1), London, England, 25-41.

Vermeer, P. A., and Sutjiadi, W. (1985). "The uplift resistance of shallow embedded anchors". *Proceedings, 11th International Conference on Soil Mechanics and Foundation Engineering*, San Francisco, California, Vol. 3, 1635-1638.

Vesic, A. S. (1972). "Expansion of cavities in infinite soil mass". *Journal of Soil Mechanics and Foundation Engineering Division*, ASCE, 98 (SM3), 265-290.

CAISSON FOUNDATIONS FOR MISSISSIPPI RIVER BRIDGES IN THE NEW ORLEANS AREA

William B. Conway, P.E., Modjeski and Masters, Inc., New Orleans, LA, USA

This paper will describe the large caisson pier foundations for four of the bridges crossing the Mississippi River in the New Orleans area; and will discuss some of the unusual problems encountered during their sinking. Certain settlement phenomena experienced during their service life will also be related:

The four bridges in order of their construction:

The Huey P. Long Bridge, River Mile 106.1, completed in 1935
The Greater New Orleans Bridge No. 1, River Mile 96.0, completed in 1958
The Hale Boggs Bridge, River Mile 121.6, completed in 1983
The Greater New Orleans Bridge No. 2, River Mile 96.1, completed in 1988

Each of these bridges employed large open-dredged concrete caissons as foundations for one or more of the river piers, with the smallest being the 65ft by 102ft caissons for Piers I and II of the Huey P. Long Bridge and the largest being the 99ft by 214ft caisson for Pier II of the Greater New Orleans Bridge No. 2. The Huey P. Long caissons are founded in a dense fine sand at -170 while all of the other bridge caissons are founded in hard preconsolidated clay at elevations varying from -150 to -185.

The Huey P. Long Bridge is currently being widened without increasing the caisson foundations under any of the river piers; and the design reasoning that led to this decision is presented.

THE HUEY P. LONG BRIDGE

The Huey P. Long Bridge is a high-level, steel-truss structure carrying both railroad and vehicular traffic across the Mississippi River. Completed in 1935, it was the first bridge crossing the Mississippi River, south of Vicksburg. The bridge carries two railroad tracks within the through-truss main bridge and a narrow, 18 ft. wide, 2-lane roadway bracketed off each side of the through-truss structure. The bridge is 22,996 ft. long from railroad abutment to railroad abutment, and has a vertical navigation clearance of 135 ft. over high water river stage of +18.0.

The facility is owned by the New Orleans Public Belt Railroad Company, but the State of Louisiana, Department of Transportation and Development, has control and dominion over the vehicular roadways. Because of the limited capacity of the narrow roadways, the safety hazards experienced, and the substandard level of service offered, the LADOTD has embarked on a project to widen the existing bridge roadways to the greatest extent practical.

That project was begun in 1986 with a feasibility study of various widening schemes which resulted in a recommended scheme of widening the existing 18 ft. roadways to a new width of 43 feet, sufficient for 3 travel lanes in each direction. It has progressed through the intervening years in fits and starts (caused by sporadic funding) to the present day. The current status of the project is that:

Main River Crossing Substructure was let to Contract – March 2006

Railroad Modifications were let to Contract – July 2006

Main River Crossing Superstructure will be bid – May 2007

East and West Approaches to be let to Contract – August 2007

PROPOSED STRUCTURE

The project contemplates that the existing, essentially plain concrete piers of the river crossing unit will be bracketed out on each side to support a new steel truss. On the downstream side, a new truss will be erected parallel to and 50'-6" downstream of the existing downstream truss; and the same will be repeated on the upstream side. What is now a "single barrel" two-truss structure with 18 ft. roadways bracketed off each side will become a "three barrel" structure with a 43 ft. roadway contained within each of the two outboard "barrels."

The existing cantilevered floorbeam bracket supporting an 18 ft. roadway will be incorporated into and become part of the new roadway floorbeam spanning between the trusses forming each of the outboard barrels. Existing roadway stringers, sub-floorbeams, railing and roadway deck will be removed and discarded. They will be replaced with new roadway stringers spanning over the floorbeam and made continuous over 3 or 4 panel lengths supporting a reinforced concrete deck.

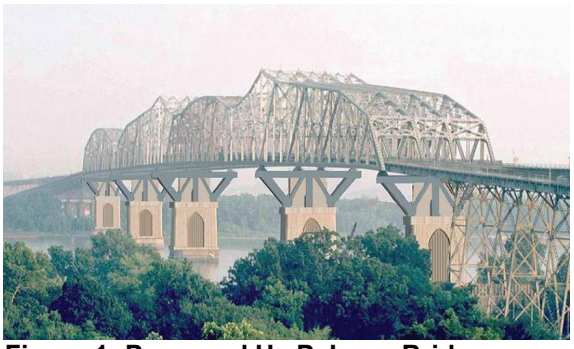


Figure 1: Proposed H. P. Long Bridge Widening

CAPACITY OF EXISTING CAISSON PIERS

The existing main piers of the river crossing unit are each supported on a concrete caisson measuring 65' x 102 ft., founded at a depth of about 170 feet below Mean Gulf Level. The founding elevations and caisson sizes were based on studies made in 1927 by Dr. Karl Terzaghi who recommended founding in a sand layer at that elevation using a net additional dead load pressure no greater than 5.5 tons per square foot. The caissons were sunk into the river bottom using open dredging in the classic sand island method of sinking. The substructure contractor, Siems-Helmers, Inc. had developed and used this method once before in constructing the piers of the Suisun Bay Bridge for the SPRR. The procedure consists of construction of a large island of sand enclosed in a steel shell at the site of each pier, with the caisson sunk through the sand by open dredging. Construction of the caisson takes place entirely above water level with the position of the cutting edge initially accurately located and readily controlled during sinking. After reaching the founding elevation, the cutting edge chamber and the lower portion of the dredge walls were cleaned and sealed with a tremie concrete plug to a depth of 20 ft. The upper portion of the wells remained unfilled, excepting water, to the caisson top which was set at -35.0 elevation.

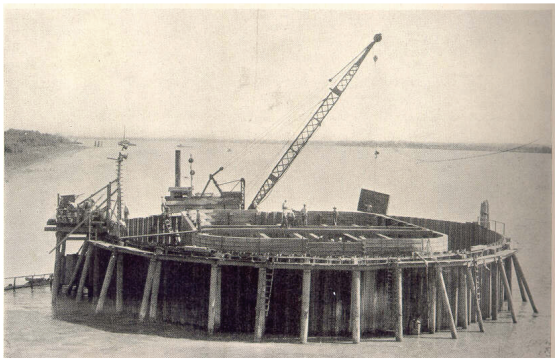


Figure 2: Sand Island – H. P. Long Bridge

At the time the main bridge piers were being built estimates were made of the settlements that could be expected through the life of the structure. For the two main piers, Piers I and II, the total settlement due to soil consolidation was estimated to be 5 ½", with some 4" estimated to take place during construction and 1 ½" after opening of the facility. In fact, 3 ¾" took place before the bridge opened in December 1935 and now, after 70+ years total settlement is measured at between 4" and 5" for Piers I and II.

The apparent lack of precision in this measured settlement is founded in a curious phenomenon: that the river piers of the bridge rise and fall in inverse relation to the river stage. i.e. As the river stage rises the piers settle and as the river stage falls the piers rise. The point of greatest settlement coincides with the time of the peak of high water. The range of pier movement is about 0.075 ft. or 7/8 inch for a 15 foot change in river stage. This occurrence has been studied, particularly by William P. Kimball, later Dean of the Thayer School of Engineering, with the

conclusion that while the river pier caissons are founded in sand, that sand is underlain by a thick layer of hard gray clay which is behaving perfectly elastically.

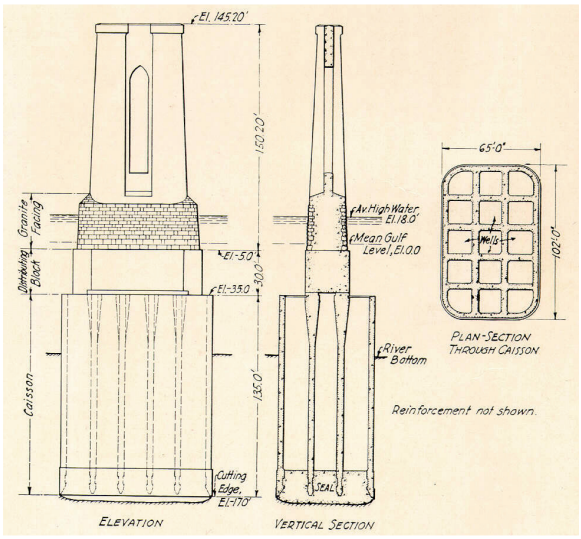


Figure 3: Pier II Caisson – H. P. Long Bridge

The proposed new widened structure will be supported on these same caisson piers, with no measures deemed necessary to increase or supplement the carrying capacity of those piers. i.e. It was determined that the existing caissons could carry the increased loads without distress and without excessive additional settlement. While the superstructure dead load applied at the top of a main pier, say Pier II, will more than double, increasing from 13,782 kips to an estimated 29,426 kips; and while the dead load at the top of the caisson distribution block will nearly double, increasing from 36,873 kips to 73,693 kips, the dead load at the bottom of the caisson will increase by less than 45%, increasing from about 80,335 kips to about 116,000 kips. This amount is computed without counting upon any effects of skin friction on the caisson vertical surfaces. With an embedded depth of 106 ft., a perimeter of 305 ft., and assuming a minimum cohesion of 0.5 k/sq. ft., the skin friction that could be mobilized is estimated to be 16,165 kips.

VERTICAL LOADS AND PRESSURES

Pier	Total Dead Load (Kips)	Total Live Load for E65 & H15 (Kips)	Base Area (Sq. Ft.)	Total Gross Dead Load Press. Tons/ Sq. Ft.	Embedded Depth of Caisson (Ft.)	Previously Existing Earth Press. at Pier Base Tons/ Sq. Ft.	Net Additional Dead Load Press. Tons/ Sq. Ft.
A	37,712	4,122	2,998	6.3	100	3.5	2.8
I	80,335	9,580	6,437	6.3	99	3.5	2.8
II	80,335	9,580	6,437	6.3	106	3.7	2.6
III	58,798	6,778	4,846	6.1	122	4.2	1.9
IV	58,078	5,571	4,846	6.0	131	4.6	1.4
V	27,374	3,949	5,550	2.5	45	1.6	0.9
B	14,580	3,541	(Pier B is founded on 594 timber piles)				
C	14,280	3,541	(Pier C is founded on 594 timber piles)				
D	10,402	2,478	(Pier D is founded on 368 timber piles)				

Figure 4: Foundation Loading – H. P. Long Bridge

The total gross dead load pressure for the existing bridge at the bottom of the Pier II caisson was estimated at 6.3 tons/sq. ft. Subtracting the previously existing soil pressure at that level, the net additional dead load pressure at the bottom of the Pier Ii caisson was computed to be 2.6 tons/sq. ft. For the proposed widened bridge, the comparable net additional dead load pressure would be 5.3 tons/sq. ft., somewhat below the Terzaghi recommended maximum of 5.5 tons/sq. ft. With mobilization of the conservatively assumed caisson skin friction, the net additional dead load pressure of the widened structure would reduce to about 4.1 tons/sq. ft. This additional dead load pressure at the caisson base is estimated to cause an additional settlement of 1.5 inches due to elastic compression in the supporting subsoils, with much of the settlement occurring within a few months of construction completion.

The additional settlement and the higher net additional dead load pressure were judged to be acceptable, with no strengthening or supplementing of the existing caissons needed.

GREATER NEW ORLEANS BRIDGE NO. 1

Greater New Orleans Bridge No. 1 is a high level cantilever-truss structure of 1575 ft. main span, carrying 4 lanes of highway traffic across the Mississippi River. At the time of its completion in 1958, it was the longest highway cantilever and third longest cantilever span of any type in the world, and it is still ranked 6th among the world's greatest cantilever-truss spans. The bridge Trusses are 64 ft. center to center and provide a vertical navigation clearance of 150 ft. over a mean high water elevation of +20.0.

Main Piers II and III are supported on deep open-dredged concrete caissons extending to founding in hard clay at elevation -182.5 for Pier II and at elevation -164.3 for Pier III. Based on several core borings to elevation -400 and extensive and comprehensive soil tests, these main bridge caissons were limited to a net additional dead load pressure of 2.5 tons per square foot. They are founded on a hard preconsolidated clay layer laid down during the Pleistocene epoch. While Pier 3 is located on the river batture in an area subject to flooding only by river stages above Elev. +10 and the caisson therefore was sunk in a land operation, Pier II is located in 70 ft. of water and was sunk in an open-dredged floating caisson operation. Dravo Corporation of Pittsburgh, PA was the construction contractor.



Figure 5: Willow Mattress Pier II – GNO 1

Prior to the Pier II caisson installation, a willow mattress was placed on the river bottom at the pier site so as to stabilize the river bottom during the sinking operation (and especially as the caisson cutting edge approaches the river bottom) as well as to afford long-term scour protection. The mattress, 300 ft. by 500 ft., was constructed of willow brush and saplings near Plaquemine, Louisiana some 90 miles upstream from New Orleans. The mattress was floated to the site and sunk to the bottom by placement of so-called "one-man-stone" until negative buoyancy was obtained. Additional rip rap was placed on the mattress to stabilize it and a sheet pile stall supported by 36" pipe piles was then constructed. The caisson steel cutting edge section 20 ft. in height was fabricated at Neville Island, Pittsburgh and towed 1900 miles to the site. Six inch tongue and groove timber sheeting braced with steel members was installed as a cofferdam extending the sides of the cutting edge section.

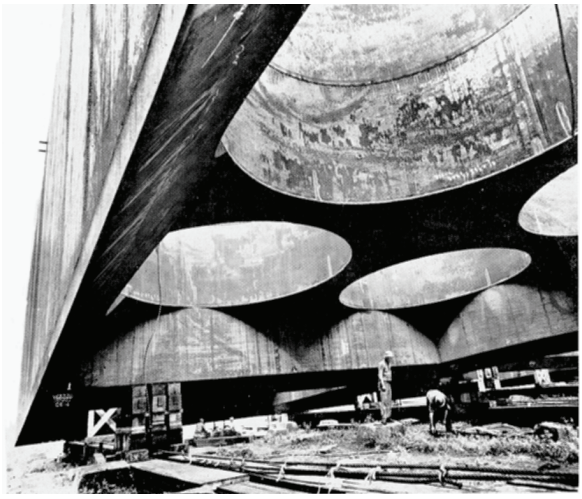


Figure 6: Steel cutting edge – Pier II – GNO 1

Sinking of the floating 88 ft. by 151 ft. caisson was accomplished by placing concrete in the void area and extending the outside cofferdam and dredge wall tubes as required to maintain freeboard. On landing on the mattress at elevation -70.0 a long chisel pointed I beam was used to cut cleanly through the mattress at the caisson perimeter. Mattress materials were dredged up through the dredge wells and the sinking commenced.

Sinking was accomplished by alternatively dredging river material through the wells and placing additional concrete lifts on the walls and dredge well tubes. The amount of concrete added depended on the weight needed to continue sinking while dredging. Insufficient weight would invite blow-ins of sandy layers while too much weight would crowd materials up into the dredge wells enough to result in loss of control of direction. In this caisson, the ratio of buoyant weight to skin friction area was such as to make the caisson sensitive to dredging with the result that the 33,000 ton base was landed with little trouble. In its 165 ft. vertical height the caisson was plumb within 1 ¼ in. and out-of-position by only 2 inches.

Caisson dredging was stopped at elevation -179.6, but there was some creep as preparations were made for the sealing operations. The cutting edges had been designed to divide the base into six separate seal sections. When the first seal was placed (in the east half of the center section) the caisson had crept to elevation -181.3 and when all seals had been completed some 60 days later the cutting edge had settled to -182.15. The

distribution block was then poured, the pier base constructed and concrete pier shafts constructed to a top-of-pier grillage elevation of +162.34 as of February 1957.

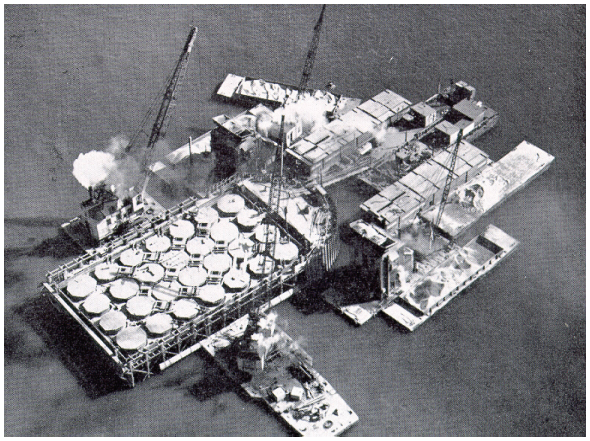


Figure 7: Caisson sinking – Pier II – GNO 1

The Pier II caisson has performed entirely satisfactorily with little further vertical settlement through the years. However, an unusual horizontal movement of Piers II and III has been experienced. By 1975 we had become concerned by a phenomenon that was occurring on the bridge, involving an apparent increase in the horizontal distance between the tops of Piers II and III. Based on a comparison of expansion joint openings, expansion bearing leans and false chord openings for the years between 1958 (when the bridge opened) and 1975 it became apparent that the horizontal distance between Piers II and III (the 1575'-3" main span) had increased some 6 to 7 inches. A review of the annual readings indicated a rate of increase approximating 3/8 inches per year. The piers were not rotating, but remained plumb, so that one plausible explanation was that the deep clay layer upon which the pier caissons were founded, was behaving plastically and very slowly extruding away from the river due to the additional weight of floodwater engendered by our civilization's levee system. Another explanation might be based on the recent awareness of shallow geologic faulting in the New Orleans area.

The solution, not dependent on the explanation, has been to accommodate the movement by periodically resetting expansion joints, expansion bearings, dummy chord pins and the like. If the movements continue into the future at the same rate such adjustments to the articulating truss joints will have to continue to be periodically made.

THE HALE BOGGS BRIDGE

The Hale Boggs Bridge is a high-level, cable-stayed, box girder bridge crossing the Mississippi River near Luling, Louisiana. At the time of its completion in 1983, the 1222 ft. main span was the longest cable-stayed span in North America. The structure afforded a minimum 133 ft. of vertical clearance over high water elevation of +22.4, a nominal waterway width of 1200 ft with steel A-frame towers extending from the base at elevation +50.0 to a top at elevation +405.0. These towers were designed to resist a hurricane wind of 150 MPH with a gust factor of 30%. The legs of the towers are spaced 125 ft. apart at the base with a 25 ft. by 20 ft. cellular section, and taper to a 12.5 ft. by 12 ft. section spaced 57 ft. apart at the top.

The main bridge consists of a box girder and deck structure designed to be continuous over five spans (260; 495; 1235; 495; 260') for a total length of 2745 ft. This structure is supported on 6 piers; 1 S and 1 on the West bank and 2, 3, 4 and 1N in the river. Piers 2, 3 and 4 are caisson supported piers with the caissons founded in the same dense pre-consolidated clay layer referred to earlier at the Greater New Orleans Bridge No. 1 site. Piers 1S, 1 and 1N are pile supported piers. Massman Construction Company was the substructure contractor.

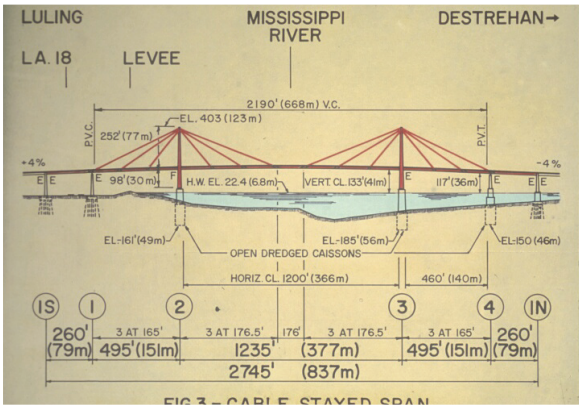


Figure 8: Schematic elevation – Hale Boggs Bridge

Although this bridge predates the AASHTO Guidelines for vessel collision the possibility of such extreme events was considered in the design of the bridge substructure. Piers 2 and 3, which flank the main navigation channel, were

designed to resist the impact of a 40,000 DWT ship traveling at 14 ft. per second. The impact force was estimated to be in the order of 60,000 kips. Further, the top of the pier base was set at elevation +50.0 and the width was set at 31 ft. to prevent vessel bow overhang from reaching the steel cellular tower legs. Pier reinforcing at the upstream nose was detailed with 12 inches of concrete cover so as to prevent exposure from the spalling caused by barge collisions. No fender was provided to protect Piers 2 and 3. Rather, timber rubbing strakes were mounted on the channel face of each pier as anti-sparking devices to protect vessels from fire.

Pier 2 is supported on an open-dredged concrete caisson measuring 64'-6" by 201'-0" with 30 dredge wells, 16'-6" in diameter, arranged in a 3 by 10 configuration. The caisson is founded at elevation -168.0 with a top of distribution block at elevation -40.0. A reinforced concrete pier base or plinth extending to a grillage plate at elevation +53, and a steel A-frame tower to elevation +405 are supported on the caisson. Pier 3 is comprised of a somewhat larger open-dredged concrete caisson measuring 84'-0" by 201'-0" with 40 dredge wells, 16"-6" in diameter, arranged in a 4 by 10 configuration. This caisson is founded at elevation -185.0 with the top of distribution block at elevation -40.0. A similar concrete plinth and A-frame tower are carried by the Pier 3 caisson. Pier 4 is a smaller open-dredged concrete caisson measuring 64"-6" by 103"-6" with 15 dredge wells, 16"-6" diameter, arranged in a 3 by 5 configuration. The caisson is founded at elevation -150.0 with the top of distribution block at elevation -39.0. A similar but smaller concrete plinth extends from the top of distribution block to elevation +50.0, with a two column concrete bent then extending to a bearing seat at elevation +133.5.



Figure 9: Caisson sinking – Piers 3 and 4 – Hale Boggs Bridge

These three caissons were sunk by open-dredging and were then sealed with a 15 ft. thick tremie concrete seal after reaching approved founding elevations. The caissons for Piers 3 and 4 reached founding within specified tolerance, but Pier 2 did not. That pier caisson, adjacent to the west bank levee and being sunk through a sloping river bank, moved or "walked" riverward during sinking a total of 13 feet, well beyond reasonable tolerances.



Figure 10: Follower Cofferdam Pier 2 – Hale Boggs Bridge

The cause of this movement has never been positively determined but it was probably caused by the fact that the caisson was being sunk in a "heavy" state, where the perimeter skin friction was always exceeded and the clay soils under the cutting edge chamber were being forced some distance up into the dredge wells in order to mobilize enough additional skin friction to hold the caisson weight. Such a condition renders a caisson very difficult to control and combined with the unbalanced side pressure from the sloping riverbank allowed the caisson to "walk" towards the river.

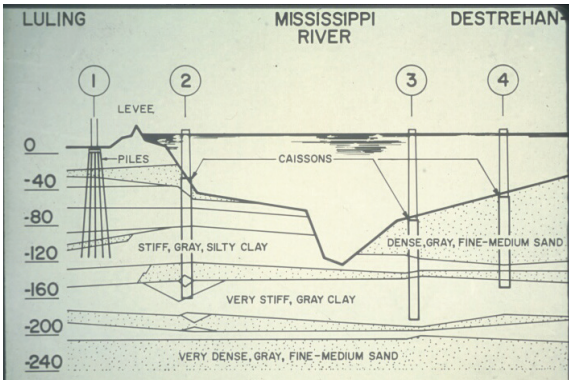


Figure 11: Soil profile – Hale Boggs Bridge

The Pier 2 caisson, however, never got seriously out-of-plumb during its walking episode. When founding elevation was reached enough skin friction had developed that the cutting edge chamber could be cleaned out and a tremie concrete seal poured into that chamber. Subsequent lateral movement and vertical settlements were carefully monitored and found to be essentially non-existent, such that the caisson could be accepted as a satisfactory base for Pier 2 and its A-frame tower.

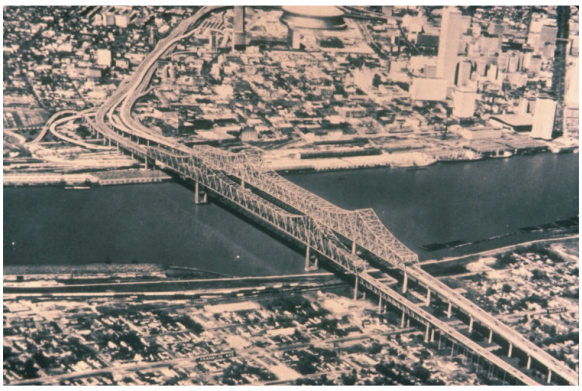


Figure 12: Pier 2 – Hale Boggs Bridge

To compensate for the 13 ft. of movement, however, the cable-stayed superstructure had to be modified. The main span was reduced from 1235 ft. to 1222 ft. with the adjacent span on the west bank side increased a like amount to 508 ft. Thus the final span layout for the three spans from Pier 1 to Pier 4 is 508 ft., 1222 ft., 495 ft. Appropriate minor modifications in roadway grade and span details were made in order to maintain structure symmetry insofar as possible.

GREATER NEW ORLEANS BRIDGE NO. 2

In September of 1978 the US Coast Guard, after a long period of environmental impact investigation, issued a permit for construction of a new bridge as a parallel crossing to the existing 1958 vintage Greater New Orleans Bridge. The old bridge was then routinely carrying 95,000 vehicles per day, with peaks in excess of 100,000 vpd, and it was clear that an additional crossing was needed. The concept was that a new wider structure in the same corridor would form a one-way couplet with the



older bridge, more than doubling river crossing capacity.

Figure 13: GNO Bridges 1 and 2

The new bridge, designated GNO Bridge No. 2 was located 400 ft. downstream and parallel to the existing bridge with the main bridge pier locations and truss generally aligning with the existing structure. The span lengths of the new bridge were set to be identical to the nominal as-designed span lengths of the existing bridge. However, since it was known from previous studies (as related previously) that the existing river piers of Bridge No. 1 had migrated steadily away from each other, with the main span distance increasing by about 7 inches, only new Pier II was set exactly opposite its old bridge counterpart.

The new bridge had its trusses spaced at 102 ft. center to center, affording a 94 ft. gutter to gutter dimension.

A 60 ft. roadway to be striped for four 12 ft. lanes with shoulders, a 2 ft. median, and a 32 ft. transitway, designed for light rail loading but initially set up for bus transit, were provided. Because the wider new structure has a deeper floorbeam and requires a deeper bottom chord than the old, and in order to maintain the existing navigation clearance, the roadway Profile Grade Line was set at PVI elevation of +194.0, 5.90 ft. higher than that of the existing bridge.



Figure 14: Pier II Caisson – GNO No. 2

Pier II, the only caisson-supported pier, is located some 560 ft. off the New Orleans wharf bulkhead line in approximately 70 ft. of water. The caisson measured 99 ft. by 214 ft. with thirty-six 20 ft. diameter dredge wells arranged in a 4 by 9 configuration. It is the largest caisson placed in the Mississippi River and one of the largest ever placed. The contractor was the Joint Venture of Massman-Johnson-James.



Figure 15: Pier II Caisson with Follower

The river bottom was protected against scour by placement of a 300 ft. by 400 ft. long willow mattress, located so as to overlap the adjacent bridge's willow mattress by 60 ft. Although no scour had occurred during construction of the adjacent bridge it was considered prudent, due to proximity of the new caisson to the existing pier and possible scour beneath the cutting edge just prior to reaching the river bottom, to provide such protection.

The caisson was designed to be founded within the Pleistocene clay at the same -180.0 elevation as the adjacent existing pier. The maximum gross dead load pressure on the caisson base was computed to be 5.15 tons/sq. ft. with a net additional dead load pressure of 2.26 tons/sq. ft. Total buoyant weight carried on the 21,286 sq. ft. caisson base is about 218,200 kips, while the comparable weight carried on the adjacent old bridge Pier II caisson was about 134,200 kips. Because of the 400 ft. separation, the pressure bulbs of the adjacent caissons were felt not to overlap or interact.

The caisson was made of two sections, the lower portion, 4 wells wide, to extend from the -180 founding elevation to elevation -72 at approximate river bottom, with an upper narrower portion 2 wells wide and 7 wells long, to extend from elevation -72.0 to elevation -15.0. The caisson was capped with a 10 ft. thick distribution block on which was constructed a concrete pier subshaft or plinth extending to elevation +30.0.

Following completion of this GNO No. 2 project, it was found that the new bridge Pier II had no measurable effect on the elevations of the adjacent bridge Pier II; but that both piers rose and fell a small amount inversely to the stage of the river, i.e. with a high river stage pier elevations are lowered and with a low river stage the elevations rebound. The order of magnitude of the fluctuations in pier elevations is 1-1/8 inches, about what had been previously experienced on the Huey P. Long Bridge.

GENERAL COMMENTS

Open dredged concrete caissons have proven to be satisfactory and appropriate for underwater bridge pier foundation in the deeper portions of the Mississippi River. While not inexpensive to construct (a cost of $30m to $40m) they offer certain desirable features. Some of these are:

- The ability to provide stable, strong foundations in the relatively soft alluvial soils found in the New Orleans area.
- The ability, because of their size and mass, to satisfactorily resist (so far) vessel collisions by large deep draft ships in the Mississippi River.
- The ability to be safely constructed in deep water with strong currents, without requiring workmen to be at risk underwater for any significant time.

OPEN WELL CAISSONS OF A 1917 RAILROAD BRIDGE:
HOW 19TH CENTURY CONSTRUCTION CAN INFLUENCE 21ST CENTURY CONSTRUCTION

Alan D. Fisher, PE, Cianbro Corporation, Portland, Maine, USA

Amtrak made a decision to replace an aging bascule bridge with a vertical lift bridge for their crossing of the Thames River in New London, Connecticut. The new lift bridge occupies the same alignment and shares the same foundations as the bascule span. During construction the deep foundation caisson supporting the bascule span settled and tilted. Investigation into possible reasons revealed interesting historical facts, both of the construction of the innovative open well caisson foundations and of the state-of-the-art in tremie concrete placing methods in use at the turn of the century. This paper describes both of these topics.

Foreword

In October 2005, when Amtrak began it's project of replacing the movable span across the Thames River in New London, Connecticut, no one knew how much the foundation construction problems of nearly a century earlier would impact the work of today. In July of 2006, it was determined that the foundation supporting the bascule span had begun a slow tilt to the south. This was the impetus for investigating the history of the original foundation construction and through that the technology that existed at the time for doing such work.

Background

Amtrak owns very little of the trackage and structures over which it operates. The northeast corridor between New Haven and Boston is an exception. Amtrak owns and maintains four movable bridges which had been built originally for the New York, New Haven and Hartford Railroad. The Thames River Bridge, in place in 2005, was built in 1918 to replace the first railroad crossing of the Thames which had been built in 1889. This first bridge needed to be replaced relatively soon after its construction because the westernmost pier had begun to settle soon after construction. (1)

The Thames River Bridge is comprised of five through truss spans (A, B, C, D and E) with lengths of 190', 330', 210', 330' & 330' respectively, (Fig. 1). The central span, Span C, is a Strauss Heel Trunnion Bascule. The piers are labeled west to east as 1, 2, 3 and 4. The substructure work in the 2005 construction contract was to enlarge Piers 2 and 3 by installing four drilled piles adjacent to the south end of each pier and connecting the new piles to the piers with enlarged pier caps. Pier 2 is the most heavily loaded pier as it supports half of Span B and all of Span C, about 7000 kips of dead load and 4500 kips of live load.

Bascule bridges are very large precision mechanisms, imagine a motorcycle transmission the size of a house. Even though they are huge, they still must maintain tolerances in the thousandths of inches and unexpected movements of even a quarter of an inch can prevent them from operating properly. Given the need to maintain such precise relationships between the operating parts, one can understand Amtrak's concern when it was discovered that Pier 2 had begun to slowly tilt to the south at the rate of a quarter of an inch per month. It was determined that the removal of an obstruction during the drilled pile installation in April 2006 and the seating of the drilled piles in June 2006 had restarted lateral movements of Pier 2 which harked back to the days of the original construction. Everyone's attention was now focused on why this was occurring and how it could be halted. This paper deals with the why, the author leaves it to others to describe the how.

Discovery

The unexpected movement of Pier 2 initiated a search for information. One area of interest was what could be learned from historical sources. The contract drawings for the 2005 bridge replacement project contained no information on

the existing foundation construction below elevation -20 as the new pier cap construction was entirely above elevation +5. An appendix to the 2005 contract documents contained a collection of original 1917 construction drawings. One of these 1917 vintage drawings was an "as-built" of the existing Pier 2 foundation from elevation -20 up, (Fig. 2). Elevation -20 was given as the top of the caisson below the Pier 2 concrete pier. A single, tiny, note near the bottom of the sheet read "Bottom of foundation El. -131.6±".

A 1941 edition of Jacoby and Davis' Foundation of Bridges and Buildings, (2) was also found to contain information and a drawing of the foundation under Pier 2, (Fig. 3). This drawing was included in the book to illustrate an example of an open well caisson. It shows the arrangement of the timber framing and the concrete cutting shoe. The details of the concrete pier portion of the substructure indicate that this drawing was developed prior to actual construction. Significantly, this drawing differs from the 1917 "as-built" drawing in that the top of the caisson is shown to be at elevation -32, not -20. Here again a small note near the bottom of the drawing gives the bottom of the caisson as "El. -142.0±". Apparently something had caused the caisson advancement to be halted 12 feet above its original design depth.

Firsthand accounts of the 1917 construction

Two journal articles describing the substructure construction were found in a search of the literature from the time of the construction, one during and the other after the caisson construction. The first article was from Engineering News magazine (3) and apparently was written by a reporter. The second article was from Engineering and Contracting magazine (4) and was written by James W. Rollins, a partner in Holbrook, Cabot and Rollins, the company which constructed the substructure.

The Engineering News article describes the construction process for the four piers as follows. The foundations for Piers 1, 2, and 3 were to be constructed as open well caissons extending down and into a known sand and gravel layer. Pier 1 was to go to elevation -110 and Piers 2 and 3 were to go to elevation -140. Pier 4 was to be built on shafts excavated under pneumatic pressure down to elevation -96. This further confirms that the bottom of the caisson for Pier 2 was intended to reach elevation -140.

The construction process for each of the open well caissons, as described in the journal articles, was well thought out. The conditions to be overcome involved a water depth of about 50 feet, then 80 feet of soft silts and clay to the start of the sand and gravel strata. Rock was believed to be 30 to 60 feet further down depending on the location, but it was anticipated that advancing the caissons completely through the sand and gravel would not be necessary.

Each caisson was built starting with a 13 foot tall concrete cutting shoe. Above the cutting shoe the caisson was constructed using repeating levels of 12 x 12 timbers up to where a regular timber framed cofferdam was used to complete the foundation, (Fig. 4). The timber caisson was arranged to provide for eight, 8 foot by 12 foot, solid sided dredging wells. These wells descended through the caisson to the top of the concrete shoe which served as the transition zone where the eight rectangular wells each opened up to 20 feet by 25 feet so that they encompassed the entire bottom of the caisson.

The concrete cutting shoe was formed and placed in a drydock and was provided with a removable bottom so that the shoe and a portion of the timber caisson could be assembled in the drydock and then floated out to deeper water. Once in location, additional layers of timber were added until the caisson was tall enough to reach the surface when sunk at its permanent location. After this additional timber was added, the temporary bottom was removed and the caisson sunk into the river sediment by adding stone and concrete to the spaces adjoining the dredging wells. The caisson was then advanced to its final grade by dredging the material out from under the caisson using an orange peel bucket through the dredging wells, and while the timber work was carried on above to keep the top of the caisson out of the water.

The spaces in the caisson, between the dredging wells, were filled with more stone and concrete as the caisson was sunk down. Once the caisson was bottomed at the desired elevation the dredging wells were to be filled to elevation -60 with concrete using a 15 inch tremie pipe. This meant a very deep tremie placement even by the standards of today. After the tremie concrete had set, the dredging wells

were to be dewatered and the balance of the well concreted in the dry. The pier concrete would then be placed on top of the caisson within a typical rectangular timber cofferdam.

At the time the Engineering News article was written, the caisson for Pier 1 had been completed and concreted with a bottom elevation of -96 and work had progressed on Pier 2 with the bottom of the caisson at about elevation -100. Two statements in the article are worthy of note for their foretelling of problems to come: "*No difficulty was found in keeping the piers vertical and in position. ... The dredging was so controlled as to correct any error of the level or, when necessary, produce a slant in one direction or another to force the pier over into line if it was found to be off line slightly.*" The second statement is even more foreboding: "*Some boulders have been found in the upper portion of the gravel stratum and the sand directly above it. They give a certain amount of trouble at times by tendency to collect, the buckets dredging out mainly the smaller stuff until more or less of a layer or pocket of larger stone has formed, which interferes with digging.*"

Construction Methods of the Period

As we gathered information about the construction methods employed we began to appreciate how innovative this substructure was for its time. We discovered that the deep open well caisson was a new concept at the time and that the methods for placing concrete that deep under water were also just being developed. We recognized how difficult it would be today to build this caisson and place concrete 130 feet under water and how it was possible that we would have trouble being successful.

The use of open well caissons for deep foundations was just beginning at the start of the 20th century. Pneumatic caissons had been employed in the United States since James Eads first used them for the St. Louis Bridge across the Mississippi in 1869. At the end of the 19th century the maximum practical depth for a pneumatic caisson was 110 feet. The need for deeper foundations drove the development of open well caissons. The first documented use of an open well caisson in the United States was for the Poughkeepsie Bridge across the Hudson River in 1888 (5). The bottom of the deepest pier was 134 feet below high water. Although the constructors of the Poughkeepsie Bridge employed the open well caisson construction process, they did not use concrete to fill the caisson using "gravel" instead, (Reference 5, page 269). Apparently the stone fill and the timber were sufficient to support the structure above.

The open well caisson method was utilized several times, both in the USA and in other countries, after the Poughkeepsie Bridge and prior to the Thames River Bridge. Only a few were of the depth that the Thames River Bridge was attempting. The Fraser River Bridge, constructed in 1904, advanced open well caissons down to 135 feet below water level and employed tremie concrete as the fill material. The Willamette River Bridge, constructed in 1911, used open well caissons down to 151 feet below high water. The Thames River Bridge, while not the first to use open well caissons, was certainly an ambitious use of a new approach to a difficult problem.

Sub-Aqueous Concrete

Prior to the adoption of the tremie method, underwater concrete was referred to as "sub-aqueous concrete". The successful placing of sub-aqueous concrete was known by some to be possible, if proper techniques were used, by the middle of the nineteenth century. Hasley (6) writes of using bottom dump buckets in 1883, (Fig. 5). Shield (7) noted the use of "tripping bags" in 1892, (Fig. 6). Gillette and Hill (8) described the use of paper and fabric bags for placing sub-aqueous concrete.

Although some knew in the mid-1800's that poor quality sub-aqueous concrete was caused by poor placing technique, by the early 1900's this cause had gained widespread understanding. Baker (9) in 1905 wrote "*When concrete is deposited in water, a pulpy gelatinous fluid is washed from the cement and rises to the surface. This causes the water to assume a milky hue; hence the term laitance, which French engineers apply to this substance.*" This description was echoed by other writers of the period, after which the issue disappeared from newer texts on the subject.

The first documented use of a "tremie" pipe for placing sub-aqueous concrete was for the Boucicault Bridge across the Saone River, France in 1893 (10). The technique appears to have quickly been accepted as the preferred

method of placing sub-aqueous concrete as "sub-aqueous concrete" disappeared from the lexicon, being replaced by "tremie concrete" as the generic term for all concrete placed under water. Taylor (11) in 1907 extensively quotes the Chief Engineer for the Charlestown Bridge in Boston on good and bad practices for placing the substructure concrete for that bridge with the use of a tremie pipe, (Fig. 7). That description is too long to be quoted verbatim in this paper, but is as true today as it was a hundred years ago.

Construction at Thames River

When the Engineering News article was written in March of 1917, the project had completed the first pier caisson which was bottomed at elevation -96. The tremie placement required the use of a 106 foot long tremie pipe, a length that would be a challenge today to control. Pier 2 was at -100 and going down per plan and one can only imagine that the anticipated elevation of -140 was going to require a very long tremie pipe.

The source of the history of the Thames River Bridge construction now relies on that of James Rollins report written in 1920. "*Pier 2 took an ugly slant when about 100 feet down and it took a lot of "jockeying" of the crib, using a jet, excavating in the necessary pockets, and loading others with concrete and stone, until finally the crib was sunk to grade and straightened up, with the result that it was about 2 feet out of position*."

"*When we got the caissons down to a foundation satisfactory to the engineers, we began to fill up the dredging pockets, which were 8 ft. by 12 ft. in section and 130 feet deep. We deposited the concrete through a 12 in. tremie up to -60, and then pumped the water out and finished the concrete in the wells in the dry.*" No explanation is given as to why the caissons were stopped ten feet higher than they had originally planned. It is today's writer's opinion that the collection of boulders at the bottom of the dredging wells, noted in the Engineering News article, had become too much to get by.

Rollins continues with a description of the results of the tremie concrete placement: "*When we pumped the water out of the first dredging wells we found to our dismay about 8 feet of laitance on the top of the concrete*." The total height of the tremie being 70 feet, 8 feet of laitance indicates that their tremie placement was not successful He continues by writing that they excavated the laitance out, but no mention is made of any attempt to repair the tremie concrete below. They may have reasoned that there was a sufficient amount of timber in the caisson to support the pier without concrete in the dredge wells or that the material placed inside the pockets between the dredge wells would suffice. Whatever the reason, the net effect was that the most solid load path for the pier loads above went through the cutting shoe at the base of the caisson.

Recent Construction

The installation of drilled piles near the Pier 2 caisson in 2006 appears to have disturbed something below the concrete caisson cutting shoe, restarting a movement process which had come to an equilibrium state. It is known that Pier 2 had tilted west 6 inches and sunk 1 inch between the time of its original construction and 1980 when a major bridge rehabilitation program was performed. The installation of drilled piles at Pier 3 in 2006 did not result in any similar significant movement.

Borings performed after movement began confirmed that in some of the dredge wells the material which had been placed by the tremie method was largely washed of cement and consisted primarily of large aggregate. It was also found that the tremie concrete was intact over virtually its full extent in other of the dredge wells. It can be concluded that the original constructors eventually learned how to make a very deep tremie placement successfully.

Summary

Just because a structure has been in place for 100 years doesn't mean it was made right in the first place. When they say "they don't build them like they used to" it is sometimes a good thing. That being said, the people who took on the challenge of building foundations for a bridge that will last in excess of 100 years have succeeded. Rollins words say it well: "*Everybody worked for the best interest of the job: no pet schemes or new theories were tried out, for we all realized that we had a most difficult problem, which was a new one for all of us, and that it needed thought, brains and the most diligent attention, in order to be carried through with success.*"

References

1. New York, New Haven and Hartford Railroad, Groton Bridge (Thames River), Historic American Buildings Survey (HAER No. CT-25), US Department of the Interior, Philadelphia, Pennsylvania, 1978

2. Foundation of Bridges and Buildings, Jacoby and Davis, 3rd Edition, 1941, McGraw-Hill, New York

3. Deep Dredging Piers and Multiple Pneumatic Pier on the Thames River, Engineering News, Volume 77 Number 11, March 15, 1917

4. Methods of Constructing Substructure of Thames River Railroad Bridge, James W. Rollins, Engineering and Contracting, Volume 54, July 28, 1920

5. Foundation of Bridges and Buildings, Henry Jacoby and Rolland Davis, 1st Edition, 1914, McGraw-Hill, New York

6. Railway Masonry and Bridge Foundations, James Hasley, 1883, The Railway Age Publishing Company, Chicago

7.Principles and Practice of Harbour Construction, William Shield, 1895, Longmans, Green & Company, New York

8. Concrete Construction – Methods and Costs, Halbert Gillette and Charles Hill, 1st Edition, 1908, Myron C. Clark Publishing Company, New York

9. A Treatise on Masonry Construction, Ira Baker, 9th Edition, 1905, John Wiley and Sons, New York

10. The Cofferdam Process for Piers, Charles Evans Fowler, 1st Edition, 1898, John Wiley and Sons, New York

11. Concrete – Plain and Reinforced, Frederick Taylor and Sanford Thompson, 1st Edition, 1907, John Wiley and Sons, New York



Figure 1 – Thames River Railroad Bridge in foreground – Spans A, B and C – Piers 1, 2 and 3

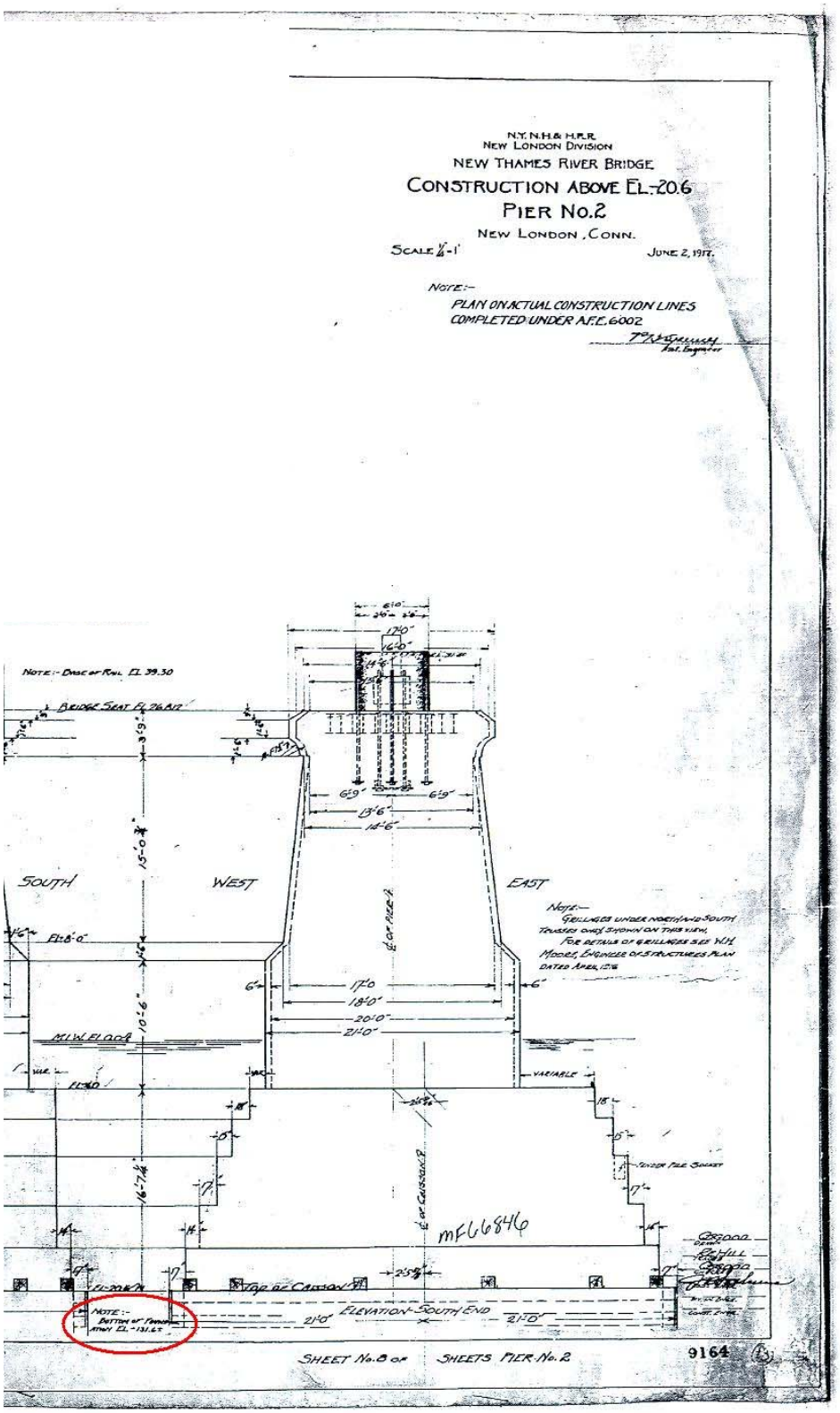


Figure 2 – As-built dimensions of Pier 2

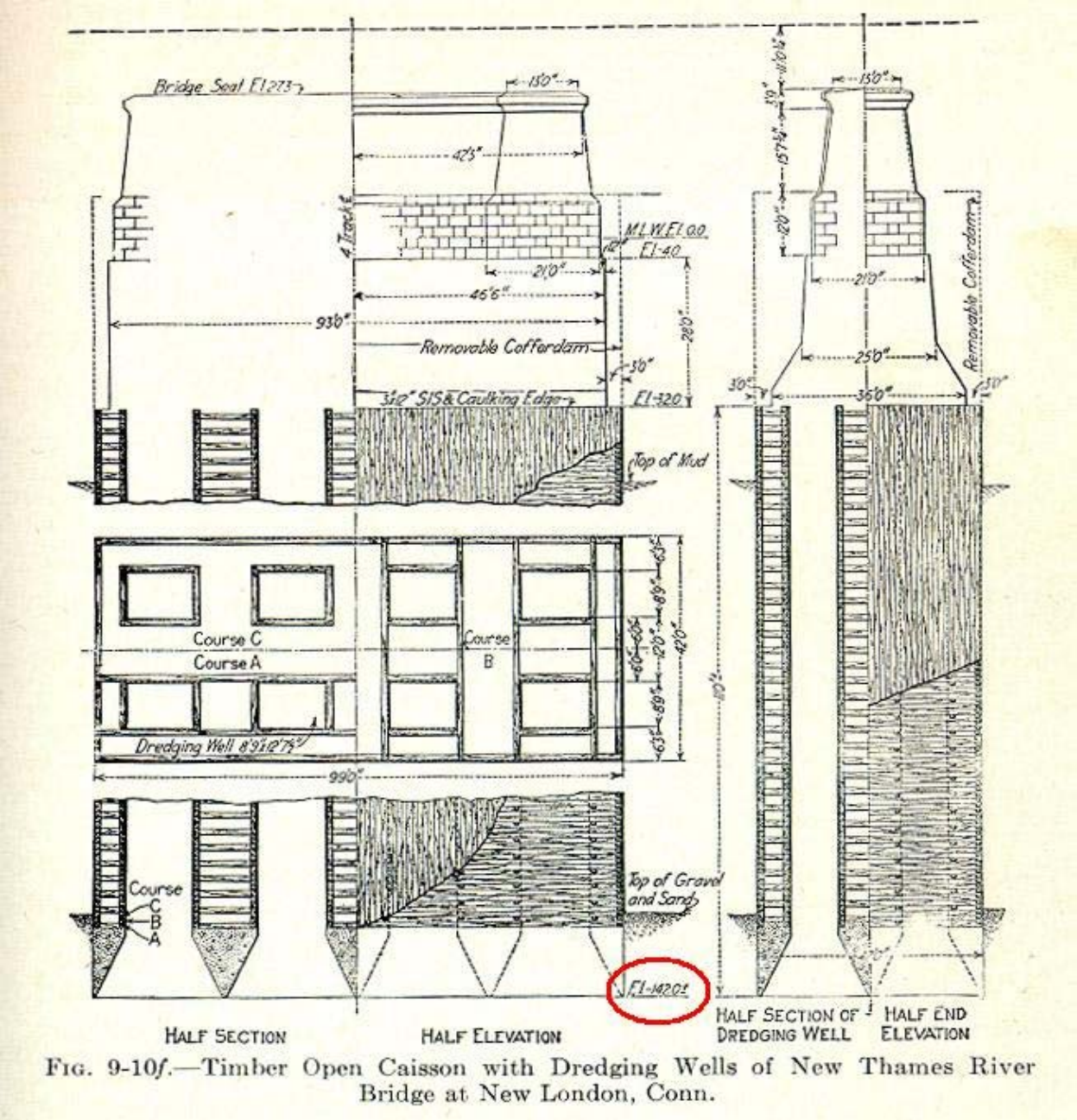


FIG. 9-10*f*.—Timber Open Caisson with Dredging Wells of New Thames River Bridge at New London, Conn.

Figure 3 - Planned construction drawing for Pier 2 open well caisson

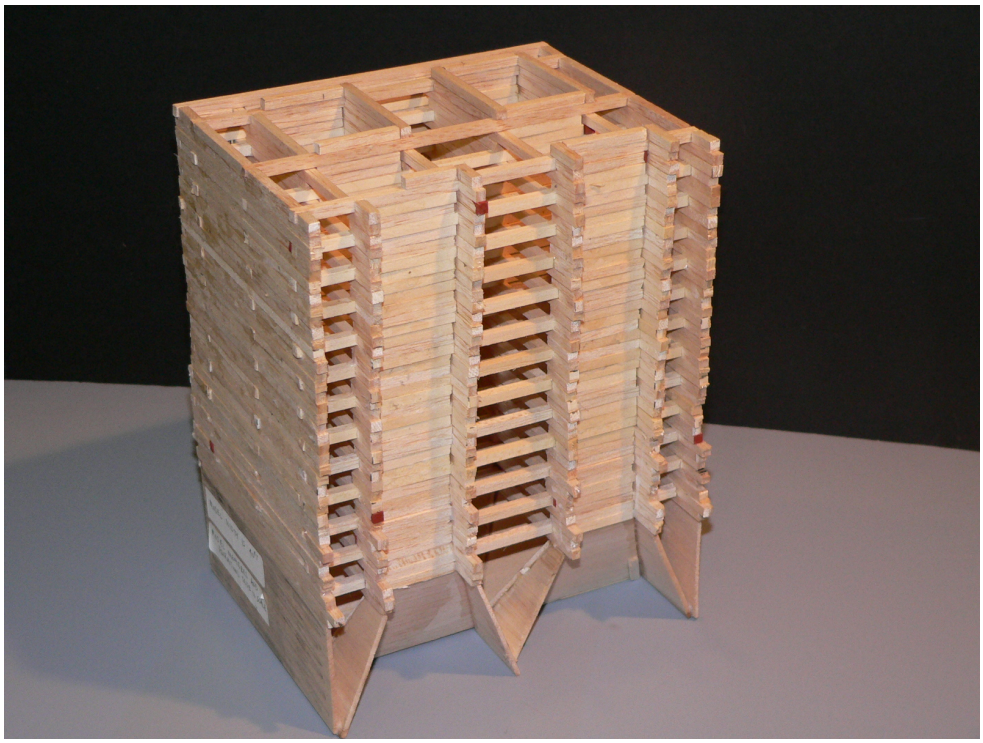


Figure 4 – Model of the caisson – represents caisson from El -130 to El -80, full width, 1/3 full length

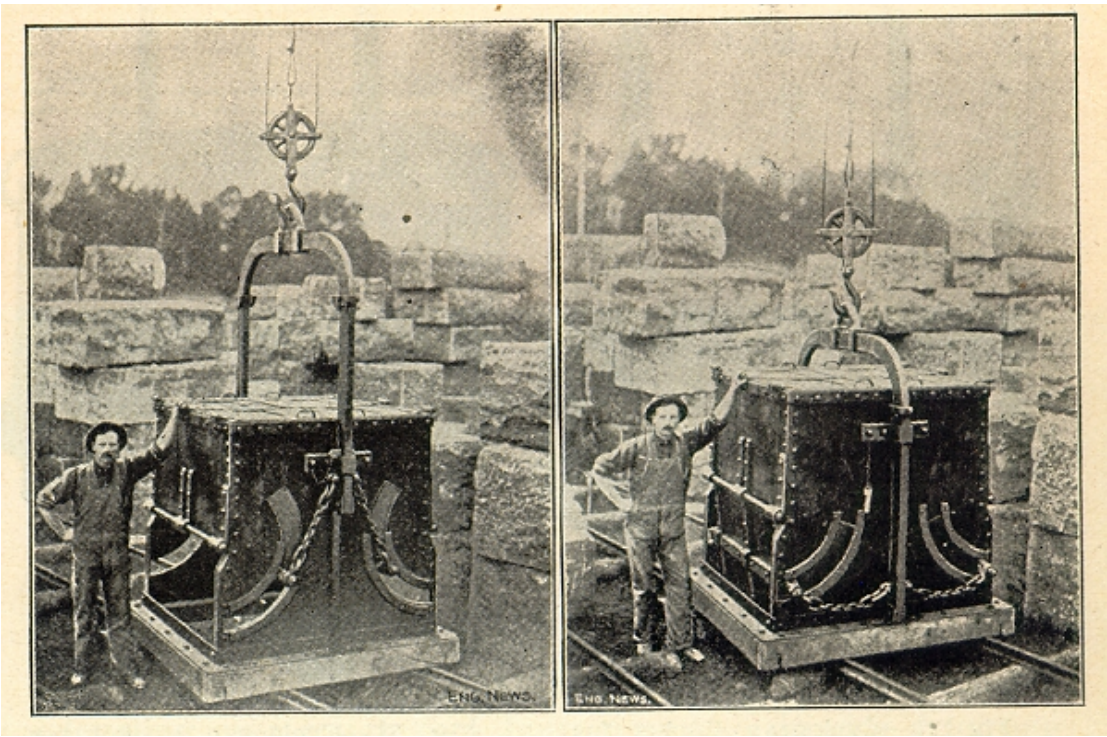


Figure 5 – Bottom dump bucket - closed and open

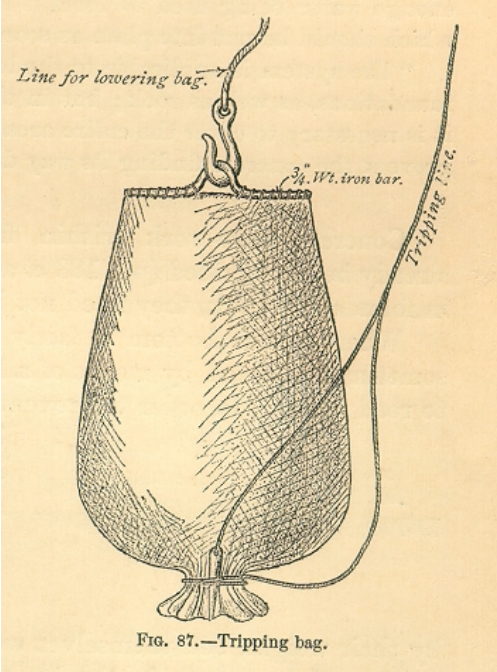


FIG. 87.—Tripping bag.

Figure 6 – Tripping bag for sub-aqueous concrete placement

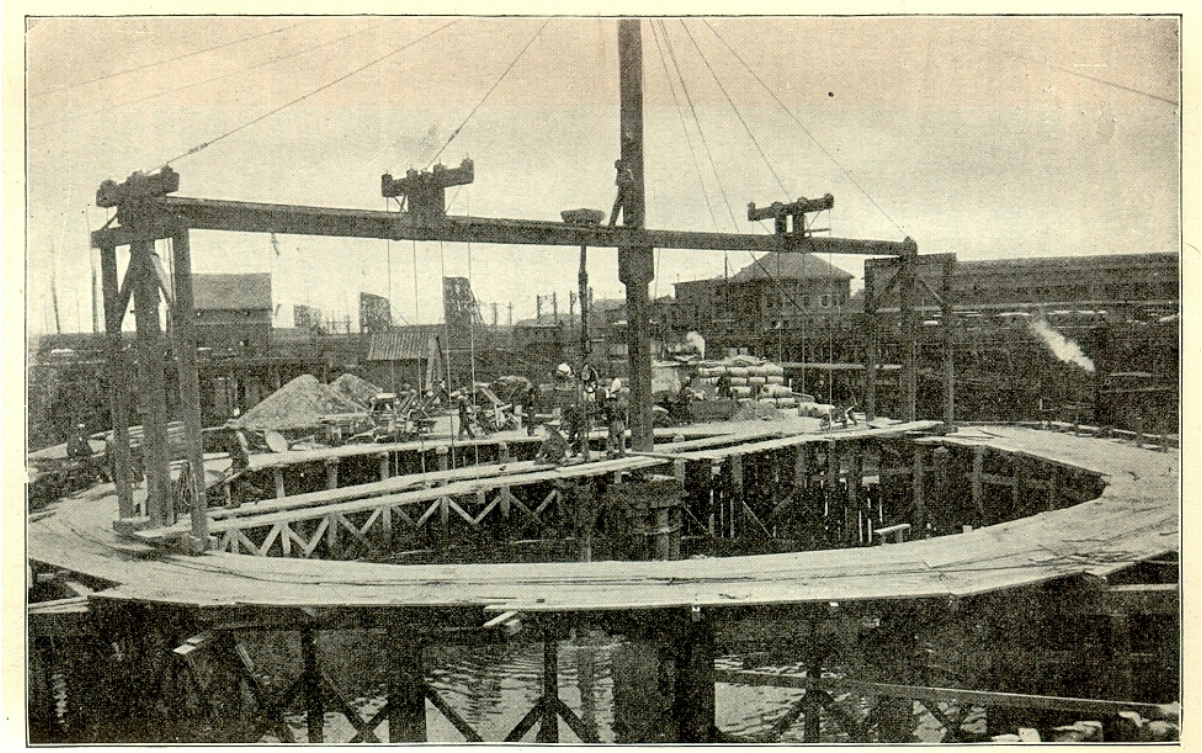

FIG. 106.—Depositing Concrete of Draw Foundation Pier, Charlestown Bridge. (*See p.* 361.)

Figure 7 – Tremie placement at the Charlestown Bridge – Boston, Massachusetts 1898

Figure Credits

1. Photograph of the Thames River Bridge, Fisher, 1998

2. Construction Drawing, New York, New Haven and Hartford Railroad, 1917

3. Foundation of Bridges and Buildings, Henry Jacoby and Rolland Davis, 3rd Edition, 1941, McGraw-Hill, New York

4. Photograph of a model of an open well caisson, Fisher, 2006

5. Concrete Construction – Methods and Costs, Halbert Gillette and Charles Hill, 1st Edition, 1908, Myron C. Clark Publishing Company, New York

6. Principles and Practice of Harbour Construction, William Shield, 1895, Longmans, Green & Company, New York

7. Concrete – Plain and Reinforced, Frederick Taylor and Sanford Thompson, 1st Edition, 1907, John Wiley and Sons, New York

8. Concrete Construction – Methods and Costs, Halbert Gillette and Charles Hill, 1st Edition, 1908, Myron C. Clark Publishing Company, New York

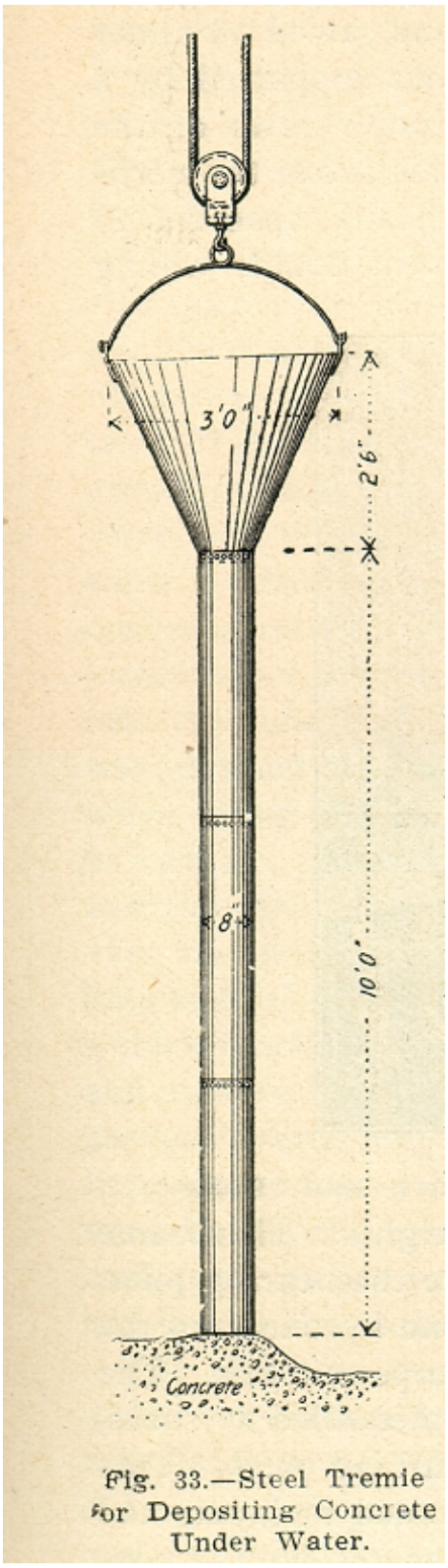


Fig. 33.—Steel Tremie for Depositing Concrete Under Water.

Figure 8 – Tremie pipe design

MARINE FOUNDATIONS OF BRIDGES IN THE NORTHEASTERN USA

James S. Graham, P.E., Norwalk Marine Contractors, Norwalk, CT, USA
Joel Moskowitz, P.E., Mueser Rutledge Consulting Engineers, New York, NY, USA

Marine design and construction methods are presented on the caisson foundations for the tower piers at the Brooklyn, Ben Franklin, Delaware Memorial 1st, Tappan Zee, Walt Whitman, Throgs Neck, Verrazano Narrows, Delaware Memorial 2nd, and Newport Bridges. All of the bridges are founded on caissons, bearing on bedrock, soil, or piling. Caissons at the Tappan Zee Bridge are partially supported by piling and partially by buoyant forces. General subsurface conditions for each are provided.

The purpose of this paper is inform engineers how bridge foundations using caissons were built over major waterways in the Northeastern USA in the past, anticipating a surge of new bridge construction in the near future.

INTRODUCTION

This paper was based largely on Dr. James P. Gould's Kapp Memorial Lecture given in March, 1982 at the ASCE Metropolitan Section wherein he summarized geotechnical and structural data for five fall line bridges in the Northeastern USA. His lecture was mainly focused on the soil and rock conditions at each bridge site, and the resulting bridge tower and anchor settlements. This paper expands his original work to describe the construction methods used for the tower foundation caissons on bridges in the Northeastern USA.

"FOUNDATIONS OF THE GREAT BRIDGES"

Jim Gould spent most of his professional career at Mueser Rutledge Consulting Engineers and, the majority of his work was in the Northeast Corridor, extending from Washington DC, through New York City to Boston. The focus of his 1982 Kapp lecture was the geological considerations for five major suspension bridges at or near the fall line, the boundary between shallow bedrock and thickening sediments. All of the bridges were the suspension type, similar to the Brooklyn Bridge.

Perhaps the most interesting feature in Jim's lecture was, regardless of the founding level, the net bearing pressure on the base of the tower foundations was four to six tons per square foot (tsf). The largest settlement observed was seven inches at the Brooklyn-side tower of the Verrazano-Narrows bridge. The basic data from his lecture were summarized in the attached Table 1.

BROOKLYN BRIDGE – 1870 TO 1883

John Roebling had no experience with caisson construction, but his son, Colonel Washington Roebling, spent nearly a year in Europe studying the successful use of similar foundations. One caisson job Washington Roebling studied was the 15 by 75 ft. pneumatic caissons that were used by H. Loeffler to sink the piers for a railroad bridge over the Pregel River at Konigsberg in East Prussia. William J. McAlpine, President of the American Society of Engineers, was on Roebling's board of experts and could vouch for the concept since he had built a six ft. diameter iron caisson.

The subsurface profile at the Manhattan approach comprises schist and gneiss of the Manhattan Formation below Elev. -140 the surface of which was eroded by glaciation. Above rock lies a thin layer of glacial till, overlain by predominantly granular glacial outwash and recent river deposits and fill. The Manhattan tower is founded at Elev. -78 "…on a very hard material overlying gneiss rock…" (1945, City of New York). The Manhattan anchorage is at about Elev. 0 founded on outwash deposits.

Bedrock at the Brooklyn approach is believed to be between Elev. -65 and Elev. -100 overlain by basal till and hardpan, glacial lake deposits, compact outwash sand and fill. The Brooklyn tower is founded at Elev. -45 on "…trap boulders packed closely together and cemented…" The Brooklyn anchorage is founded at about Elev. 0 on compact till and outwash. Both anchorages are on timber grillages.

Roebling's tower caissons were 102 by 172 by 22 ft. high made of 12 inch square dense Southern pine laid in solid courses crossing each other, fastened with through–bolts. The sides were 8 ft. thick at the top, tapering down to 8 inches at the iron– bottom edge. The caissons had six timbers cross partitions 4 ft. thick. The interior of the caisson was lined with boiler iron. Access to the bottom was through air-locks. Excavated soil was removed through water-locks.

The caissons were constructed nearby and floated into position inside a three-sided timber pile enclosure, and sunk by placing 7 to 10 ton square blocks of granite facing with blue limestone in the middle, laid in uniform layers in hydraulic cement. Lowering the caisson was accomplished by removing a portion of the pine blocks from beneath the inside partitions. The remaining wood blocks compress, gradually lowering the caisson about one inch. After reaching the founding levels at 45 ft. on the Brooklyn side and 78 ft on the Manhattan side, the voids in the caissons were filled with solid hydraulic concrete, and the tower piers were constructed. (Figures 1 & 2)

Several years ago, Jim Graham inspected the base of the Manhattan anchor as a guest of Ammann & Whitney. The grillage of 14 inch square timbers had always been below the ground water level and in perfect condition. In the mid 1990's groundwater was lowered temporarily for a nearby project. The grillage was again inspected and found in excellent condition. There was about 6 inches of concrete between every timber. The Brooklyn anchorage was not as fortunate as the water level had been lowered by wells for air conditioning purposes, and the timber grillage was decaying and had to be repaired.

BEN FRANKLIN – 1922 TO 1926

The Delaware River Port Authority hired a local engineering firm led by Ralph Modjeski to design the Ben Franklin Bridge. The contractors were Keystone State Construction and Holbrook, Cabot & Rollins, a joint venture. Daniel E. Moran, founder of Mueser Rutledge Consulting Engineers was the consulting engineer for foundations. The bridge was positioned below the "fall line" where the Delaware River bends northwest towards rocky upland, between Philadelphia and Camden. The base of primary weathering, micaceous schist bedrock, was located 60 to 65 ft. below sea level in Philadelphia and 85 to 105 ft. below sea level in Camden.

The tower sites were dredged to 40 ft. and the caissons constructed of 12 by 12 inch timbers in the shell carried on an all-steel working chamber, totaling 70 by 143 ft., 40 ft. high, were sunk by placing 12 ft. of concrete over the roof of the working chamber. Like the Brooklyn Bridge, men working under air pressure, excavated the soil and rock from beneath the caisson. The caisson design by Moran provided for walls that were self-supporting, a widely recognized advance that eliminated cumbersome cross-ties and braces. The average rate of sinking was 6-1/2 inches per day for the Philadelphia caisson which was sealed at 58 ft. when the air pressure was 28 lb. per sq. in.; the Camden caisson sank at 15 inches per day to 82 ft. when the air pressure was 34 lb. per sq. in. The working chamber was filled with concrete and, after the air was taken off, the void below the roof was filled with grout. (Figure 3). The foundation was completed without a single fatality and only a small number of minor injuries.

DELAWARE MEMORIAL (1ST) – 1948 TO 1952

Othmar Ammann designed the first Delaware Memorial Bridge with Howard, Needles, Tamman & Bergendoff, the construction manager. Merritt-Chapman & Scott was the contractor on the suspension bridge piers and six approach piers; Conduit and Foundation Co. built the 20 Delaware land approach piers and the west abutment; and Lewis and Bowman did the 15 New Jersey approach piers and abutment. The geotechnical consultant was Moran Proctor Freeman and Mueser. Bedrock was about 500 to 600 ft. deep below coastal plain sediments.

Subsurface conditions generally comprise a series of irregular beds of compacted sands and hard clays of the Raritan and Magothy Cretaceous age formations. River bottom deposits of soft clays or loose sand extend to about 80 feet below Delaware River level.

The tower piers and west anchorage were built by the open-dredge caisson method sunk from fendered 68 ft. sand islands and pinned with dolphins. The caisson on the Delaware side

caisson was 95 by 221 ft with a 13 ft. high cutting edge girder; the caisson on the New Jersey side was 99 by 225 ft. Four longitudinal and 11 transverse square spaces contained the 60 lowest rings of 15 ft. diameter dredge wells. The caissons were prefabricated in a New Jersey shipyard, towed downriver and sunk to 116 feet on the Delaware side and 87 ft. on the New Jersey side.

The caissons were sunk by clam-shelling from dredge wells to barges. The bottom of the caissons were sounded with inverted mushroom-type weights and cleaned out with a 12 inch vertical rotating pipe feeding 4-inch pipes drawn down to 1-1/2 inch nozzles with 350 psi water pressure. Floating concrete mix plants placed a tremie seal in the bottom of the caisson. The soil bearing pressure for the towers was 8.3 tsf. (Figure 4)

TAPPAN ZEE – 1952 TO 1956

The engineering firm of Madigan-Hyland designed and oversaw construction of the Tappan Zee Bridge over the Hudson River at Tarrytown. Spanning the Hudson River at its widest point, the 3,000 foot bridge consists of a cantilever span 138 feet above water and a truss span. The riverbed of the Hudson River consisted of layers of silt with bedrock more than 300 ft.; too deep for conventional caisson construction. There is believed to be a relatively thin layer of glacial till overlying bedrock. The till is overlain by as much as 140 feet or more of glacial lake sediments of alternating thin layers of fine sand, silt and clay. Up to 40 feet of fluvial sand sits atop the glacial lake deposits and is in turn overlain by river bottom organic sediments.
The two main towers were supported by concrete caissons 100 by 190 ft., 40 ft. high, with exterior walls 34 to 45 inches thick. The caissons were constructed 10 miles away, barged to the jobsite, floated into position within a fender system, filled with water and sunk 45 ft. atop a previously placed 5 ft. thick layer of sand and gravel. Open wells lined with corrugated, galvanized iron were built to run vertically through the compartmentalized walls of the caissons. 33,400 LF of concrete filled steel pipe piles, 30 inch diameter and some 270 f. long, were driven through the open wells to bedrock some 270 ft. below, and then encased with concrete within the walls of the caisson.

Eight of the underwater concrete caissons, which support about 70 percent of the bridge's dead weight, were partially supported by the steel piles driven to rock, and partially by a "buoyant" force that stores pressurized air within small compartments. Two pumps, with 60 and 300-gallon-per-minute capacity pump water out of the 8 to 24 compartments in the caissons to achieve the desired buoyancy. The pumps were required to maintain buoyancy for the 50 year life expectancy of the bridge.

The western causeway portion of the Tappan Zee Bridge was constructed of floating concrete caissons partially supported by 1,602,200 LF of untreated timber piles. When the piles were designed, attack from marine borers was minimized by pollution of the Hudson River.

The Tappan Zee is in brackish tidal waters and pollution has been decreased by the Clean Water Act, allowing marine borers to re-enter the Hudson River. The borers will attack any untreated timber piling exposed above the mud line, possibly causing a reduction of structural capacity in the causeway portion of the bridge. (Figures 5 & 6) Studies are underway for a replacement river crossing or an upgrade to include seismic retrofit.

WALT WHITMAN – 1953 TO 1957

Designed by Modjeski & Masters and Amman & Whitney, the Walt Whitman Bridge spans the Delaware River south of Philadelphia. Bedrock was 150 to 220 ft. deep on the Philadelphia side and about 250 ft. on the Gloucester side. At the towers there was about 40 ft. of fill and silt underlain by sand and gravel with a layer of over-consolidated clay-sand-gravel mix 90 ft. deep 45 ft thick and on the Philadelphia side and 25 ft thick 85 ft. deep on the Gloucester side. Shearing strength of the clay averaged 4,000 psf. Founding loads were 4.5 tons per sq. ft.

The two tower piers foundations were sunk through sand peninsulas. Each tower was founded on a rectangular open dredged caisson, 64 by 174 ft. with 27 dredging wells of 15 ft. 4 inch diameter. Caissons were designed by Moran, Proctor, Mueser and Rutledge for the Fehlhaber Corporation. The towers were sunk to 105 ft. on the Philadelphia side and 74 ft. on the Gloucester side. The lower chambers of the caissons were sealed with 15 ft. of tremie

concrete. The dredging wells were left filled with water and sealed at the top of the caisson at Elev. -14 by a concrete distributing block. Pier shafts are granite faced. (Figure 7)

THROGS NECK – 1957 TO 1961

Othmar Ammann designed the Throgs Neck Bridge to span between the Bronx and Queens where the East River connects with Long Island Sound. Merritt Chapman & Scott built the towers; Fehlhaber Corporation constructed the Bronx anchorage; J. Rich Steers and Frederick Snare did the Queens anchorage. Bedrock was 150 to 220 ft. deep overlain by decomposed rock, sand, clay, and glacial deposits. The tower pier foundations were cast-in place concrete caissons with a steel cutting shoe sunk to 135 ft. on the Bronx side and 147 ft. in Queens; the anchorages were open dredge well caissons constructed on sand islands sunk to 68 feet in the Bronx and 135 feet in Queens.

The tower caissons were steel 75 by 162 ft. by 13 ft. high double wall with 36 digging wells 14 ft. in diameter. Water depth at the piers was 60 ft. in the Bronx and 80 ft. in Queens. Rows of 4 steel pipe piles, 18 and 20 inch diameter, spaced at 13 ft. o.c., with the outer 2 battered 1:5, were used as a fender enclosure for the tower caissons. Inside the pipe piles, 14-inch H-Piles were driven 75 ft. into the soil.

Lifts of skin plates, digging wells, and trussed cross-bracing were 16 to 34 ft. high and took 100 men, 30 Miller welding machines, 10 days to complete. A concrete plant mounted on a barge supplied both tower caissons. There were 40 tremie pipes on top of the caisson, 40 ft. long, and 18 inch diameter. An average day's pour was about 1,000 cubic yards of concrete. It took 3 or 4 days to complete a lift. Two 50-ton derricks mounted on each caisson with 2-1/2 yd clamshells excavated the soil beneath the caissons. The allowable tolerance was 1 ft. in either direction. After reaching founding depth, a 15 ft. thick tremie seal was placed to close off the bottom of the caissons.

Caissons for the anchorages were sunk using the sand island method. Steers-Snare dredged 14,000 yd of river mud and silt on the Queens anchorage then backfilled with sand to 30 ft. below water level. Cellular steel cofferdams were driven, an additional 10 ft. of sand placed, and a 3-stage dewatering system installed. The 146 by 226 ft. caisson with 77 digging wells 16 ft. diameter was placed inside the cofferdam. After 5 lifts of concrete each 5 ft. thick, 4 cranes excavated material from the digging wells. (Figure 8)

VERRAZANO NARROWS – 1960 TO 1964

The Verrazano Narrows bridge was designed by Othmar Ammann to span between Brooklyn and Staten Island. Bedrock was at 180 to 300 ft. The tower foundations were built by a joint venture of J. Rich Steers and Frederich Snare using cast-in place concrete caisson foundations 129 by 229 ft. The Staten Island caisson was designed to go 127 ft. but only went 105 ft.; the Brooklyn caisson was designed to go 197 ft. but only went 170 ft. (The contractor took test borings below the cofferdam to prove that better than assumed soil conditions existed at shallower depths.)

Prior to construction, 31 test borings were performed to a maximum depth of 354 ft. A total of 19 consolidation tests were performed at the Port Authority and Columbia University under the supervision of Professor Donald M. Burmister. The tests indicated that a deep organic clay layer on the Staten Island side had been pre-stressed by ice cover to about 8.0 tons per sq. ft. where as the average overburden stress was only 3.4 tsf. Hence, bridge tower settlement for foundations placed above were considered to be within tolerable limits. An organic layer at Brooklyn tower was normally consolidated and was unsuitable for support of the tower.

The Staten Island caisson was located 300 ft. off shore in 18 to 35 ft. of water. To create an artificial sand island, a cellular cofferdam with 16 cells, 49 ft. in diameter was driven by a MKT 10B-3 using sheets 40 to 55 ft. long and a template supported by timber pile spuds. Sand was placed within the cofferdam to 10 ft. below the water surface and the site dewatered. The Brooklyn caisson was partially on land, so the contractor used a combination of cells and Z 32 piling with tie-rods and deaden anchors.

A steel cutting edge was delivered to the sand islands in 37 to 49 ft. sections and assembled. There were 66 rectangular dredging wells, 17 by 17 ft. Concrete was placed in 10 ft. high lifts using 3000 psi concrete in the bottom 43 ft and 2,500 psi above, at a rate of 940 to 1,730 cu yd

per day for 5 to 6 days. Clamshell buckets, 1-1/2 to 2 cu yd, worked 24 hours per day 7 days a week to excavate soil from beneath the caisson. An orange peel was used for hard soil conditions. Jet pipes embedded at intervals in the wells pointing 30 degrees upward aided the excavation.

At the founding elevation, a combination of jetting with a 6-inch vertical rotating pipe with two 2-1/2 inch nozzles and an air lift removed soil from beneath the bottom of the caissons. The air lift was a vacuum on a 12-inch diameter pipe with air bubbles injected near the bottom. The lower density of the aerated water caused the soil and water to rise at a fast rate. Cleaning the dredging chamber took 6 days in Staten Island and 7 days in Brooklyn. Divers were used to examine the dredging chamber for cleanliness.

Finally, concrete was placed onto the dredging chamber and wells using a tremie kept several feet into the wet concrete to minimize salt water intrusion that causes laitance (wet concrete never hardens if intruded with salt water). Consideration was given to the horizontal flow of concrete in water at a ratio of 10 : 1.

The caissons were placed to a maximum horizontal deviation of 7-1/2 inches, within the specified allowable of 12 inches. The Brooklyn tower has settled 7 inches; the Staten Island tower has settled 4-1/2 inches. (Figure 9)

DELAWARE MEMORIAL (2ND) – 1964 TO 1968

The second Delaware Memorial bridge is parallel to and very similar to the earlier bridge. The four traffic lanes are one foot wider than the original. West tower and anchorages were supported by H-Piles 14 x 117 driven within a cofferdam to pile tips at 120 to 130 ft. below sea level. The east anchor was constructed within a cofferdam excavated to 65 feet below sea level. A 30 foot thick tremie concrete plus was placed.

NEWPORT BRIDGE, R.I. - 1965 TO 1969

Parsons Brinckerhoff Quade and Douglas, Alfred Hedefine, Partner-in Charge, designed the Newport to Jamestown Bridge and Perini Corporation was the foundation contractor.

Because the water depth was excessive for conventional caissons at the two main towers, piles were designed to support a caisson (or footing), located at the bay bottom, to support hollow rectangular piers at each tower.

The east tower was located where there was 100 ft. of water and 230 ft. of silty sand over hard shale bedrock. The west tower water depth was 140 ft. with 80 ft. of overburden over bedrock at 220 ft. Soil above bedrock was very dense silty clay with fine sand lenses.

Scour was not considered a problem as an estimated bottom (134 ft.) velocity of 4.5 fps during a hurricane surge at high tide was less than the 5.1 fps minimum velocity required to produce scour with flow parallel to the pier.

The bay bottom was dredged for 20 ft. for the east and west towers. For the east tower, 512 friction piles, H-14 x 89 at 4 ft. o.c., 80 ton design capacity, were driven with a MKT S14 underwater hammer to 6-inch horizontal deviation. Divers cut-off the piles using electric oxygen torches. The divers used a Westinghouse saturation diving bell and could cut 15 piles in a 6 hours day. On the west pier, 327 end-bearing 70 ft. long H-14 x 102 steel piles were driven on a 4 x 5 ft. grid to end–bearing on rock at 135 ton design capacity.

To guide the caisson into position, eight 36-inch diameter piles were driven to 5 ft. below the bottom of the footing depth, cleaned out, then 14 inch H-Piles were driven inside and fixed in-place with expanding grout.

The 68 by 134 by 30 to 32 ft. high caissons with the necessary reinforcing bars and eight 42-inch diameter guide pipes were floated into position and set on top of the H-Piles to El. -162 using a 500 ton capacity floating derrick with twin booms. The hollow tower piers consisted of four 14-ft. diameter shafts, 22.7 x 88 ft on centers interconnected by 4ft. thick walls. The caissons and piers were filled with tremie poured concrete. (Figure 10)

CONCLUSIONS

Foundations for most of the large bridges in the Northeastern USA were based on the caisson method used for the Brooklyn Bridge. In 1867, John Roebling sent his son, Colonel Washington Roebling, to Europe to study the successful use of caissons for bridge foundations. (The word caisson was derived from the French word for a drawer.) The Europeans had developed a

system of using a timber structure that resembled an upside down drawer placed into a river bottom and sunk by placing heavy stones on top and removing the soil from below by hand-digging with men in a chamber illuminated by gas lights. Water was kept out of the caisson by keeping the inside air pressure equal to the outside water pressure. The foundations for the Ben Franklin, Delaware Memorial, Tappan Zee, Walt Whitman, Throgs Neck, Verrazano Narrows, and Newport bridges followed the example of the Brooklyn Bridge as each was built on a caisson foundation, but with variations based on improved construction technology and differing site conditions.

Only a handful of engineers were selected to design most of the major bridges in the Northeastern USA; John and Washington Roebling, Ralph Modjeski, Othmar Ammann, and Frank Masters were in this select group. The engineering firms, Ammann and Whitney, Modjeski and Masters, etc., had to develop a core design and construction group specializing in tower caissons and anchoring foundations

.

The latest designs use machines to excavate soil from beneath the caissons. Steel or concrete is used instead of timber and stone. Equipment positioned above the water is used to remove the soil below the caisson. Where dense soil or bedrock is too deep to economically sink a caisson, piling has been used to support a partially sunk caisson.

The 50 year old Tappan Zee is the most unusual of all the bridge foundations, as floating caissons are anchored on piles and pumps are used inside the caissons to maintain buoyancy. Untreated timber piles are supporting the floating caissons on the western causeway portion of the Tappan Zee.

Bridges of the future will probably be of cable-stayed design, especially since they eliminate the need for expensive anchorages but the need for towers in deep water perpetuate the need for deep caissons and cofferdams. The use of labor intensive pneumatic caissons is for all intents and purposes extinct and open dredge cells are the method of choice.

REFERENCES

ENR Staff, *Crossing the Delaware from Delaware,* Engineering News-Record, Volume v 144, Issue n 3, Jan19,1950, p36-38

Eastern Roads, *Tappan Zee Bridge, Historic Overview,* with numerous references including: Westchester County, Hugh R. Pomeroy, Joseph C. Ingram, ASCE, The Bergen Record, New York Post, Mark Kuelwicz, John Vargo, Vollmer Associates, The Times Herald,The New York Times, The Journal News, The Albney Times-Union, etc.

Two Methods to Sink Big Bridge Caissons, Construction Methods and Equipment, January 1959, p127-130

Brumer, Milton, and Hansen, C.W., *Development and Design of the Walt Whitman Bridge*, Journal of the Structural Division, Proceedings of the ASCE, July, 1956

Carswell, Charles, *Sinking Pneumatic and Open Caisson Foundations for Philadelphia-Camden Bridge,* Engineering News-Record, Volume 94, No. 23, June 4, 1925, p920-926

Gould, James P. *Foundations of the Great Bridges,* ASCE, Metropolitan Section, March 1982 Kapp Lecture

Grey, Nomar, Decancq, H. George, *Verrazano – Narrows Bridge: Construction of Tower Foundations and Anchorage*s, Journal of the Construction Division, Proceedings of the ASCE, March, 1966, p 95-117

Hedefine, Alfred and Silano, Louis G., *Newport Bridge Foundations*, Civil Engineering, ASCE, October, 1968

Just, Leo H., Levy, Ira G., Obrcian, Vladimir, *Verrazano – Narrows Bridge: Design of Tower Foundations and Anchorages*, ASCE Structural Engineering Conference and Annual Meeting, Preprint 121. October 19-23, 1964

Janberg, Nicolas, *Walt Whitman Bridge*, Structural, Historical Overview 1998-2005

Vogel, Robert M., *Designing the Brooklyn Bridge*, Annals of the New York Academy of Sciences, Volume v 424, May 1984, p 3-39, [Department of Public Works City of New York Brooklyn Bridge Technical Survey, Final Report, 1945]

Table 1: Summary of Basic Data, Five Fall Line Bridges, by Dr. James P. Gould

SUMMARY OF BASIC DATA, FIVE FALL LINE BRIDGES

BRIDGE NAME, LOCATION & SIZE	CONSTRUCTION DATES	COST IN MILLION FOUND/BRIDGE	GENERAL GEOLOGY	DATA OF MAIN FOUNDATIONS	SETTLEMENT DATA
BEN FRANKLIN BRIDGE, DELAWARE RIVER, PHIL. 1750 FT. MAIN SPAN, 126 FT. DECK WIDTH	1922-1926	7/16 (44%)	BEDROCK-50 TO -100 BENEATH THIN COASTAL PLAIN AND PLEISTOCENE RIVER SAND AND GRAVEL	TOWER PIERS FROM WOODEN FLOATING CAISSONS SUNK WITH AIR PRESSURE: 28 PSI AT PHIL, TO -61;34 PSI AT CAMDEN TO -85, ANCHORAGES IN OPEN DREDGE WELL CAISSONS, TO -63 AND -104, BEARING ON BEDROCK AVERAGE 6.4 TSF.	PROBABLY VERY SMALL
WALT WHITMAN BRIDGE, DELAWARE RIVER, S.PHIL. 2000 FT. MAIN SPAN, 90 FT. DECK WDITH	1953-1957	10/31 (32%)	BEDROCK -160 to -220 BENEATH THICK SERIES OF RARITAN CLAY AND SAND. THICK PLEISTOCENE SAND & GRAVEL ABOVE.	TOWER PIERS OF OPEN DREDGE WELL CAISSON SUNK THRU SAND PENINSULAS, TO -105 PHIL, -74 IN GLOUCESTER. ANCHORAGES PLACED IN DRY LAND EXCAVATIONS INTO PLEISTOCENE SAND, -70 PHIL, -52 GLOUCESTER, BEARING AT 4.5 TSF TOWERS, 3.5 TSF ANCHORS.	TOWERS: 1" TO 1 1/2" ANCHORS: 1/2" TO 1".
THROGS NECK BRIDGE, BRONX TO QUEENS 1800 FT. MAIN SPAN, 93 FT. DECK WIDTH	1957-1961	25/51 (49%)	BEDROCK -150 TO -220 OVER-LAIN BY DECOMPOSED ROCK, LLOYD SAND, RARITAN CLAY IN QUEENS, GLACIAL DEPOSITS, THROUGHOUT BELOW DEEP THROUGH IN LI SOUND	TOWER PIERS OF FLOATING STEEL CAISSONS TO -135 BRONX, -147 QUEENS. ANCHORAGES IN OPEN DREDGE WELL CAISSONS ON SAND ISLANDS WITHIN CELL WALLS, TO -68 BRONX -135 QUEENS. BEARING ALL AT 4 TO 4.5 TSF.	QUEENS TOWER & ANCHOR: LESS THAN 1" BRONX TOWER & ANCHOR 3/4" TO 1 1/2"
DELAWARE MEMORIAL (FIRST BRIDGE) DELAWARE RIVER BELOW WILMINGTON 2150 FT. MAIN SPAN 61 FT. DECK WIDTH	1948-1952	13/26 (50%)	DEEP CRETACEOUS STRATA OVER BEDROCK AT -500 TO -600. MAGOTHY ABOVE RARITAN CLAYS IN BORINGS. THIN LAYER OF PLEISTOCENE SAND AND GRAVEL BENEATH MUD.	STEEL FLOATING CAISSONS FOR TOWERS TO -87 AND -116 AND WEST ANCHOR TO -93. EAST ANCHOR BUILT WITHIN COFFERDAM WITH RECORD TREMIE TO -69. ALL BEARING WITH SHORT PENETRATION IN MAGOTHY AT 4 TO 4.5 TSF.	ALL 3 1/2" EXCEPT WEST TOWER - 4 1/2"
DELAWARE MEMORIAL (SECOND BRIDGE) DELAWARE RIVER 2150 FT. MAIN SPAN, 61 FT. DECK WIDTH	1964-1968	17/39 (43%)		WEST ANCHOR AND TOWERS ON 14 BP 117 DRIVEN WITHIN COFFERDAM TO TIPS AT -130 AND -120. 10' THICK TREMIE PLACED ON PILES. EAST ANCHOR EXCAVATED IN COFFERDAM TO -65, 30' THICK TREMIE.	TOWER LESS THAN 1". WEST ANCHOR 1 1/2". EAST ANCHOR 2 1/2"
VERRAZANO-NARROWS BRIDG, STATEN ISLAND TO BROOKLYN, N.Y. 4260 FT. MAIN SPAN, 103 FT. DECK WIDTH	1960-1964	40/143 (28%)	GLACIAL DEPOSITS ON BOTH SHORES AND IN NARROWS, FOLLOWED BY GARDINERS CLAY, SOME RARITAIN AND LLOYD IN BROOKLYN. ROCK -180 TO -300.	TOWER PIERS ON OPEN DREDGE WELL CAISSONS ON SAND ISLANDS, TO -105 STATEN ISLAND, -170 BROOKLYN. ANCHORAGES IN DRY EXCAVATIONS ON LAND, +6 ON STATEN ISLAND, -20 IN BROOKLYN. TOWER BEARING AT 5 AND 6 TSF, ANCHORS AT 4 TO 5 TSF.	BKLYN TOWER = 7", SI. TOWER = 4 1/2". ANCHORS: 4 1/2" TO 5 1/2"

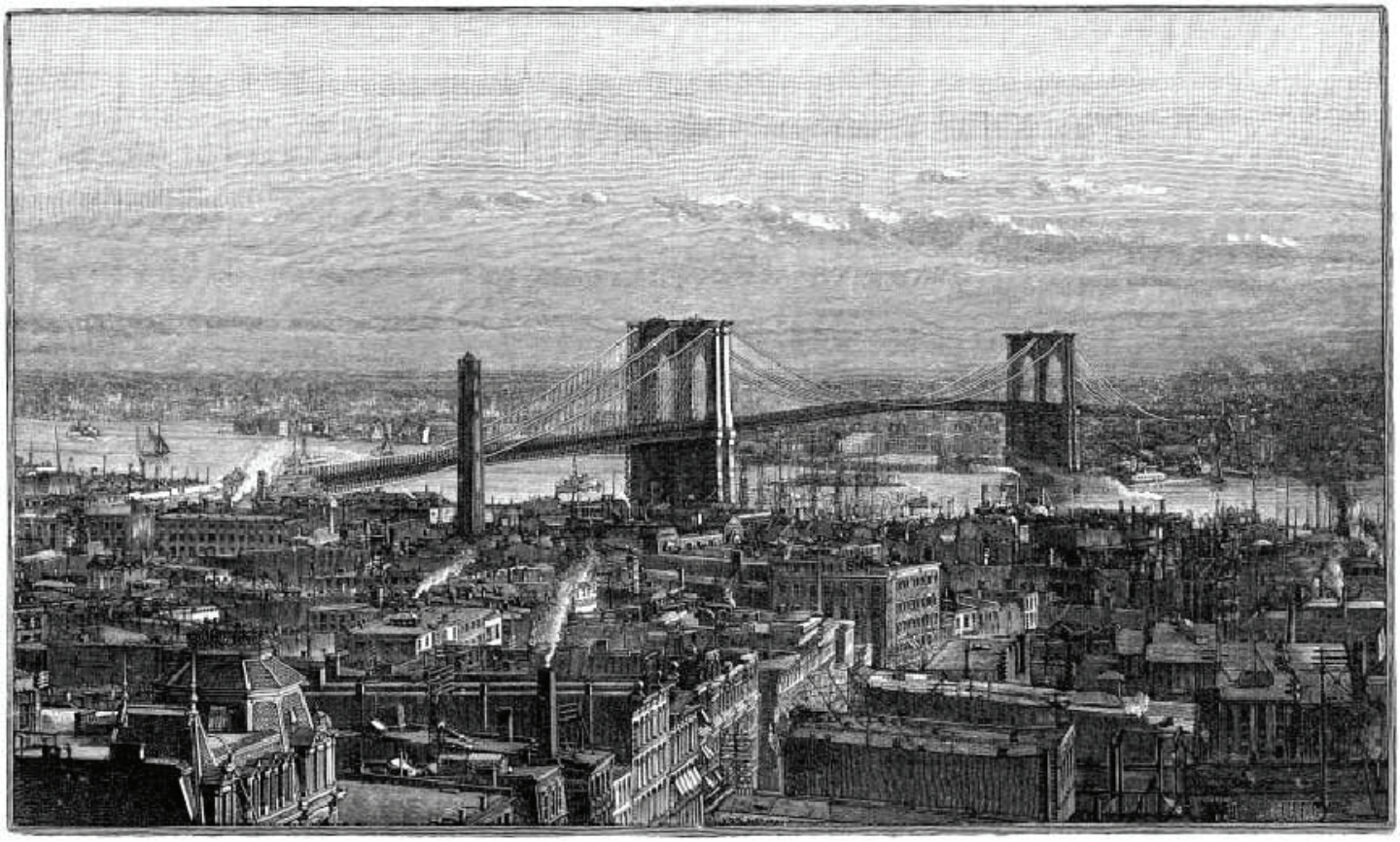


Figure 1: View of the Brooklyn Bridge from New York *www.catskillarchive.com/rrextra/bbstory.html*

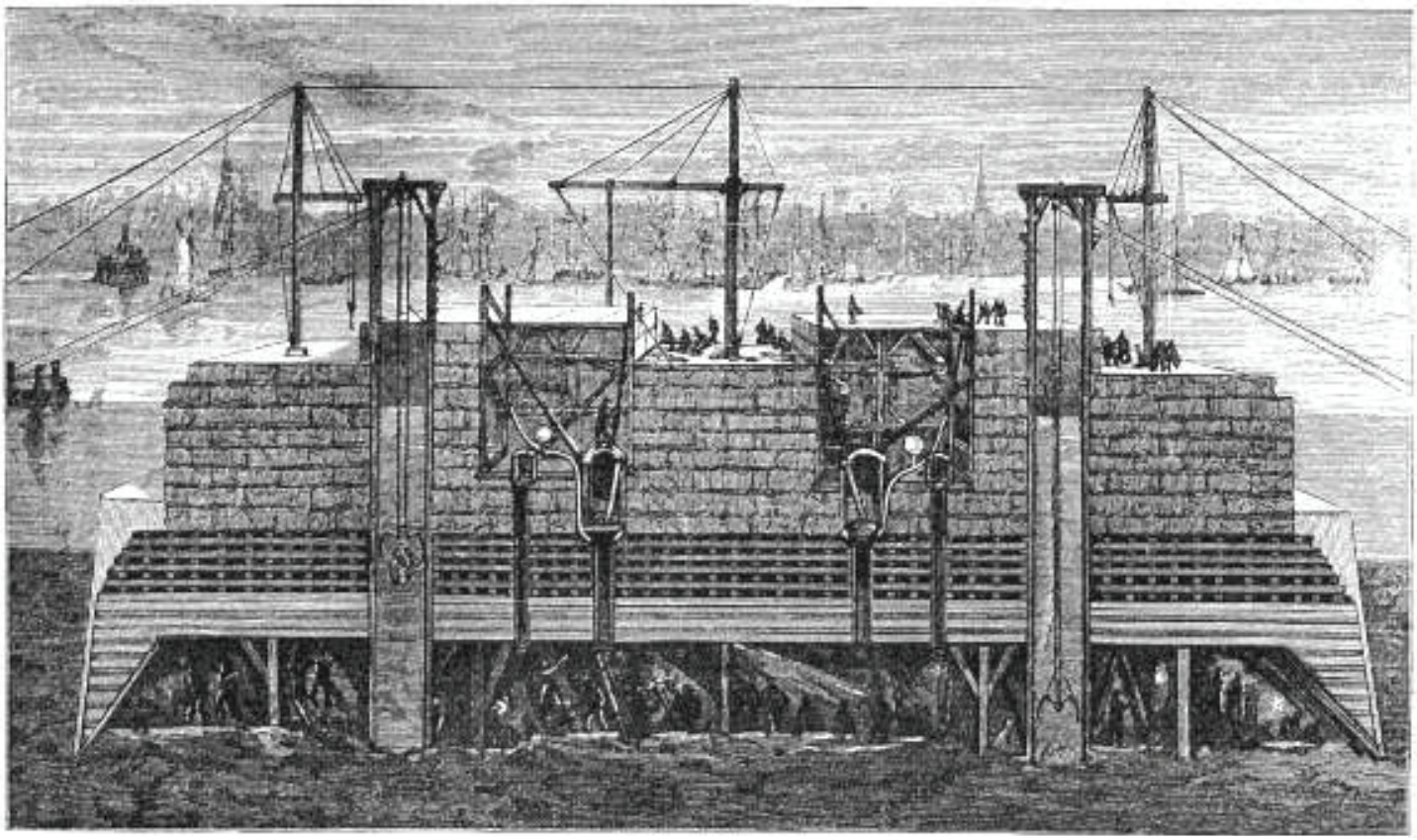


Figure 2: **Brooklyn Bridge Pneumatic Caisson**
www.catskillarchive.com/rrextra/bbstory.html

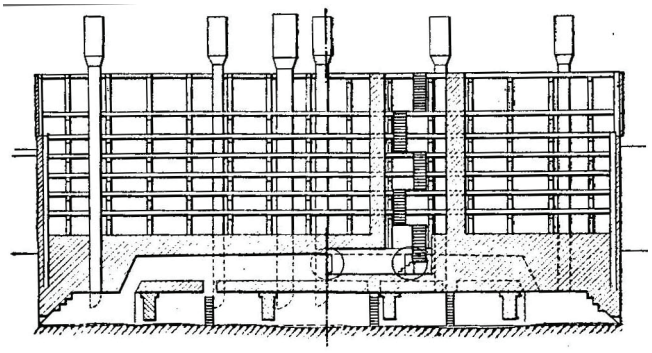


Figure 3: Pneumatic Caisson for Main Pier of the Ben Franklin Bridge (*ENR, 1925)*

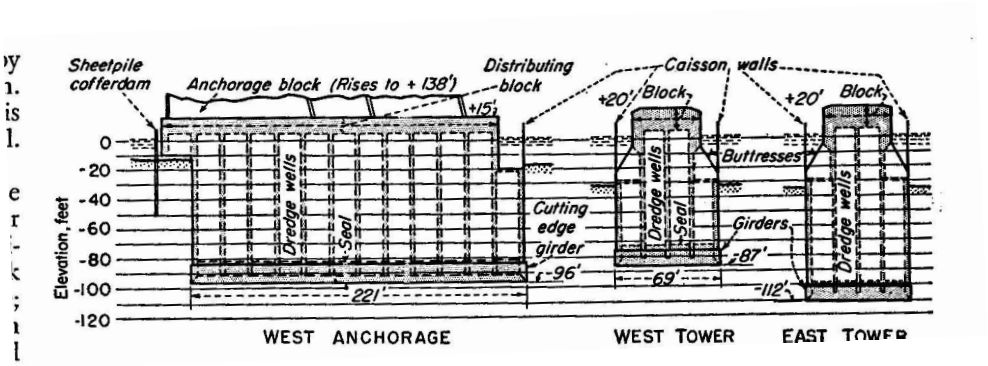


Figure 4: Open-dredged caissons for the Delaware Memorial Bridge (*ENR, 1950)*



Figure 5: Historic Overview of Tappan Zee Bridge *www.nycroads.com/crossings/tappan-zee*

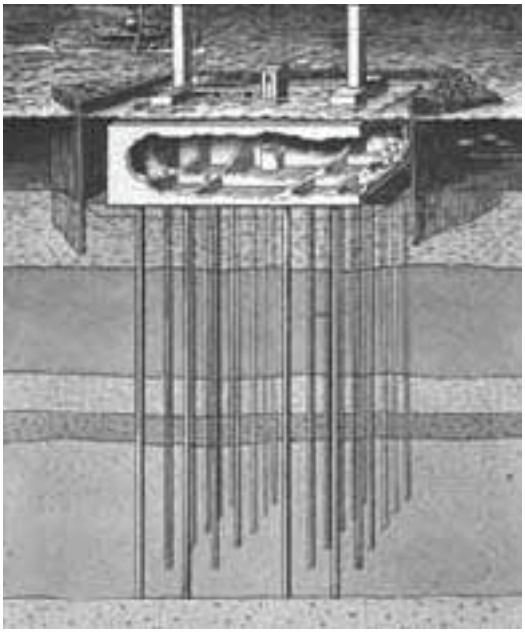


Figure 6: Floating Caisson at Tappan Zee Bridge

www.nycroads.com/crossings/tappan-zee

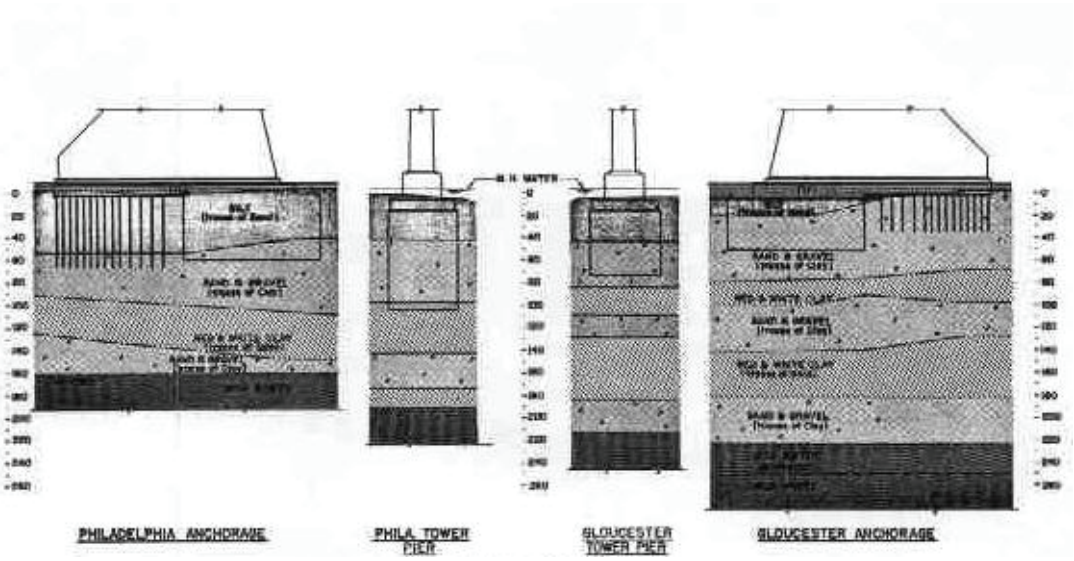


Figure 7: Walt Whitman Bridge Stratification of Foundling Materials (*ASCE, 1956)*

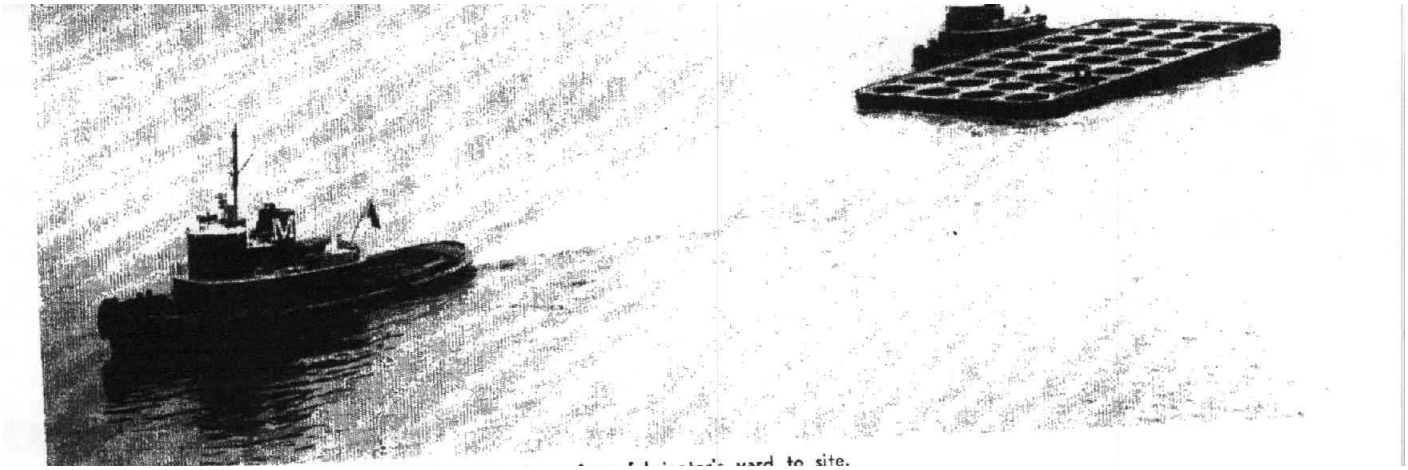


Figure 8: Tug Pulls Caisson to Throgs Neck Bridge (*Construction Methods and Equipment, 1959)*

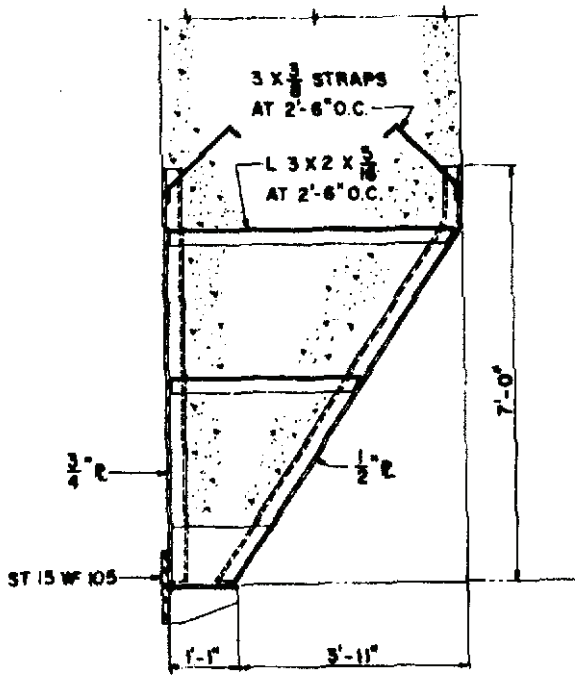


Figure 9: Exterior Cutting Edge of Caisson at Verrazano-Narrows Bridge
(*Nomar et al, ASCE, 1966)*

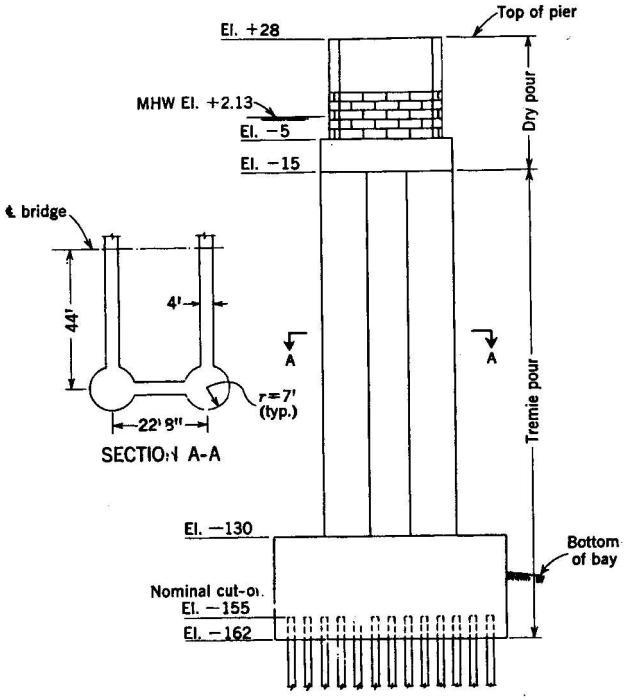


Figure 10: Newport Bridge Tower - Pier 1W
(Hedefine and Silano, ASCE, 1968)

WOODROW WILSON BRIDGE COFFERDAMS

Roderic A. Ellman, Jr., P.E., Mueser Rutledge Consulting Engineers, New York, NY, USA
Jim X. Zhang, Ph.D., P.E., Tidewater Skanska, Inc., Norfolk, VA, USA
Bill Spence, P.E., Tidewater Skanska, Inc., Norfolk, VA, USA

The new Woodrow Wilson Bridge (WWB) will replace the existing bridge over the Potomac River to connect Alexandria, Virginia to Prince Georges County, Maryland. The new WWB will extend approximately 1.1 miles across the river, with a 367-ft long bascule span in the main river channel where the water depth is about 36 ft. The subsurface soil profile consists of up to 50 ft of a soft organic silty clay layer that is very vulnerable to scour, underlain by a deep deposit of hard sandy clay. Foundation construction in the Potomac River required the use of cofferdams to allow structural concrete work to be performed in the dry.

This paper will the present the types of cofferdams used to construct the foundations for the WWB replacement project. The bridge is primarily comprised of fixed spans in relatively shallow water and a bascule span over a navigation channel in relatively deep water. Foundation construction included the installation of 48" to 72" open end steel pipe piles and cast-in-place concrete pile caps. To achieve the desired bridge appearance, pile caps were required to extend below the water surface and below the existing river bottom in shallow water locations. Conventional steel sheet pile cofferdams with tremie concrete seal were used to construct fixed span, shallow water piers. Selection of deep water bascule span foundation cofferdams was governed by several factors including contraction scour, environmental considerations and cost. Potomac River cofferdams, i.e., relatively shallow depth cofferdams that are supported by the foundation piling were selected. This cofferdam system provided a shallow profile which minimized contraction scour and the amount of filling in the river. Design issues include load selection and cofferdam stability in very soft alluvial soils. Construction issues include erection sequence, tremie concrete mix design and placement procedures.

INTRODUCTION

The Woodrow Wilson Memorial Bridge is the only Potomac River crossing in the southern half of the Washington Metropolitan area (Figure 1) to connect Alexandria, Virginia to Prince Georges County, Maryland.

Consisting of fixed spans and a movable (bascule) span, it carries the Capital Beltway (I-495), which is part of I-95, the main north-south interstate route on the East Coast. Approximately 1.1-mile long, a new bridge has been designed for HS25 loads consisting of six lanes for local traffic, four lanes for express traffic, and two HOV lanes. Provisions are made for future replacement of the HOV lanes with rail. The bascule span is 367-ft long in the main river channel where the water depth is about 36 ft, with 174 ft wide navigation channel. In 1998, Maryland State Highway Administration awarded Parsons Transportation Group (PTG) the design and construction support services of the new bridge. Mueser Rutledge Consulting Engineers (MRCE) performed the foundation design.

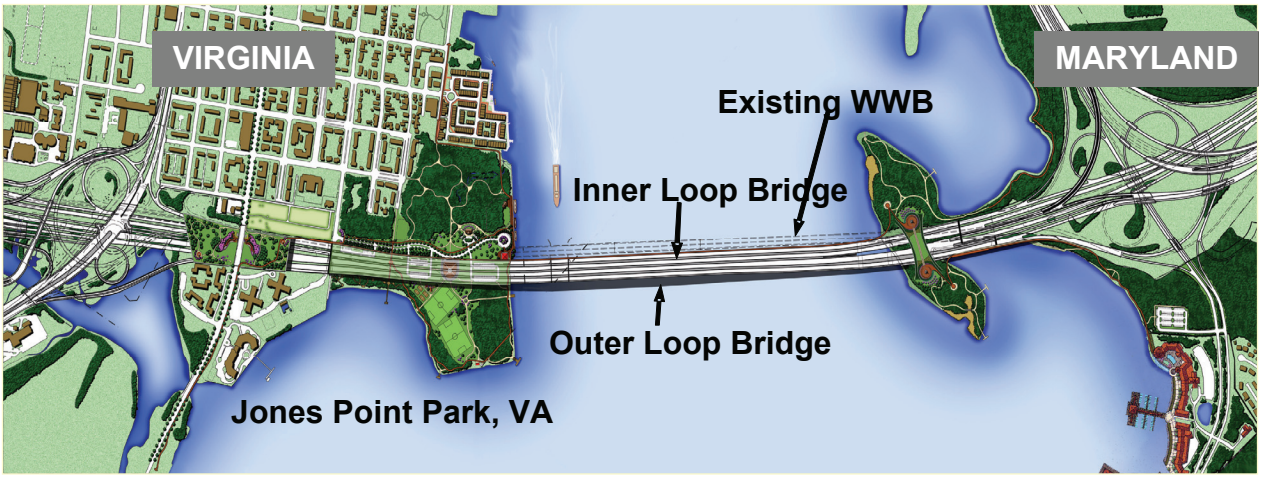


Figure 1: Woodrow Wilson Bridge Site

The joint venture of Tidewater Skanska, Inc., Kiewit Construction Company, and The Clark Construction Group, Inc. (TKC) was the low bidder for the foundation contract at approximately $125 million and was awarded the Notice to Proceed on May 17, 2001. The foundation contract included seventeen (Outer Loop) piers south of the existing bridge, eleven in the Potomac River and six in Jones Point Park in Alexandria, Virginia. Two of the eleven river piers will support the bascule span and are located in relatively deep water. The other nine river piers support fixed spans and are located in relatively shallow water. This paper will the present the types of cofferdams used to construct the foundations for the WWB replacement project.

SUBSURFACE CONDITIONS

The generalized strata encountered include man-made fills, alluvium, interbedded granular and fine-grained materials which could represent either the Terrace or Potomac Group strata (or both), underlain by very stiff to hard Potomac Group Clays, extending to the depths of penetration (See Figure 2).

Based upon the subsurface conditions, the length of the project area can be divided into the following three (3) design sections.

Section 1: Virginia Approach - Virginia Shore

Section 2: Virginia Shore, across the Main Navigation Channel to Mid-River

Section 3: Mid-River, across the Secondary Channel to the Maryland Shore

Section 1 Virginia Approach – Virginia Shore

The borings indicate the Virginia Shore portion of the site to be overlain by materials placed by man (fill). These materials extend to depths of 10 feet, and consist of sandy silt, silty sand, and crushed stone and include heterogeneous components, such as bricks, organic debris, concrete, and pieces of metal.

The fill materials are underlain by a 10 to 20 foot layer of Alluvial deposits that are generally composed of fine-grained and consist of silt, clayey silt, and sandy silt. Extensive lenses of silty sands were also encountered throughout this layer. The SPT results are generally between 4 and 10 blows per foot, but range as high as 18 to 22 blows per foot in several samples.

The Alluvial deposits are underlain by a 20 to 30 foot layer of Terrace deposits that are generally composed of coarse to fine sands, with variable portions of gravel and silty and clayey fines, sandy and clayey silts. Localized pockets of fine to coarse gravel and cobbles are also present. These materials range from medium dense or medium stiff nearer the surface to very stiff or dense at the base of the unit. The SPT values range from as low as 2 to 10 in the weaker zones nearer the surface, to values greater than 100 blows per foot at greater depths. It is noted that the very high SPT results are generally associated with the presence of a gravel component.

The Terrace deposits are underlain by the Potomac clays below approximate Elevation –50 in the western portion and dipping to approximate Elevation –83 near the Potomac River shoreline. The materials consist exclusively of hard to very

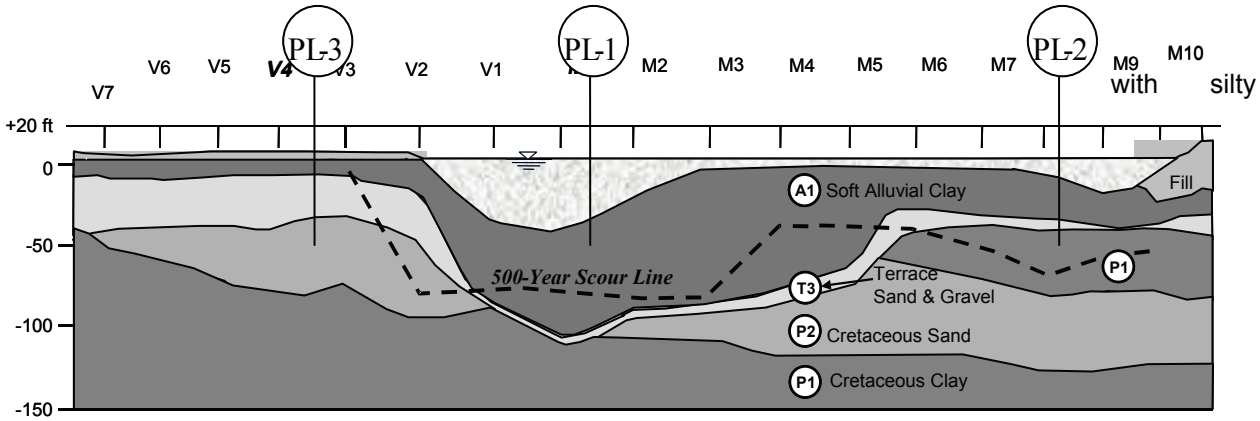


Figure 2: Soil and estimated scour profile, bridge pier locations, and pile load test locations

hard clays with SPT values exceeding 50 blows per foot.

Section 2 Virginia shore, across the Main Channel to Mid-River

Below the 2 to 30 feet of water in the portion of the river from the Virginia shore, across the main navigation channel to mid-river, the river bottom consists of 50 to 80 feet of Alluvial deposits that are comprised of clayey silts, silt or silty clay. Lenses of silty medium to fine sand occur throughout the strata. SPT results indicate very soft consistencies, with the sampler advancing under the weight of the drill rods (WOR) up to 10 blows per foot.

The Alluvial deposits are underlain by 5 to 10 feet of Terrace deposits that are comprised of clayey sands and gravels. The minimal thickness of the Terrace deposits and the significant depth of Alluvium in this portion of the river is a result of erosion of the Terrace deposits over time and the replacement of the lost Terrace deposits with Alluvium. The Terrace deposits exhibit SPT blow counts between 26 and 95 blows per foot.

The Terrace deposits are underlain by the Potomac clays below approximate El. –90 on the western edge of the main navigation channel and dipping to approximate El. –100 near the eastern edge. The materials consist exclusively of hard to very hard clays, with SPT values in excess of 50 blows per foot.

Section 3 Mid-River, across the Secondary Channel to the Maryland shore

Below the 2 to 20 feet of water in the portion of the river from mid-river, across the secondary navigation channel to the Maryland shore, the river bottom consists of 20 to 50 feet of Alluvial deposits that are comprised of clay or silty clay, and clayey fine sand, and clayey silt. The consistency of these materials is also very soft, with the large majority of the SPT results being WOR or WHO, and blow counts, where applicable, of 5 or less.

The Alluvial deposits are underlain by 5 to 20 feet of Terrace deposits that are comprised of interbedded sands and gravels, clayey and/or silty sands and sandy or clayey silts with the sandy materials predominating. The blow counts indicate the strata to be dense to very dense or very stiff to hard, and exhibit SPT values of 14 in the shallower zones and increasing to greater than 100 blows per foot with depth.

The Terrace deposits are underlain by the Potomac Group below approximate Elevation –40. The Potomac Group along Maryland side of the river consists of 20 to 40 feet of Potomac Clay underlain by 40 to 50 feet of Potomac Sands and Gravels, in turn underlain by a second layer of Potomac Clay. The clays exhibit hard to very hard consistencies with SPT values generally exceeding 50. The sands exhibit dense to very dense relative densities with SPT values generally exceeding 30.

BRIDGE FOUNDATIONS

Foundation design and selection followed a design phase testing program and optimization study which resulted in cost effective, constructable foundations. Foundation construction included the use of 24” concrete piles on land, the use of 48” to 66” open end steel pipe piles for fixed spans in the river and 72” open end steel pipe piles for the bascule span. A general plan and elevation is shown in Figure 3.

Foundations for the Virginia approach spans consist of 24” square pre-stressed, pre-cast concrete piles with 10’ thick cast-in-place concrete

pile caps (See Figure 4). Excavation depths varied but most of these foundations were installed in open cut excavations. Scour considerations for Pier V2 adjacent to the river required the use of 54" diameter open end steel pipe. The V2 cast-in-place pile caps were 11' thick.

Foundations for the Maryland approach spans included 66", 54" and 48" diameter open end steel pipe piles with nine to eleven foot thick cast-in-place concrete pile caps. The pile caps are located below river level and extend below the mud line (See Figure 5). Bascule span foundations include 72" diameter open end steel pipe piles with 16' thick cast-in-place pile caps. These caps also extend below river level (See Figure 6).

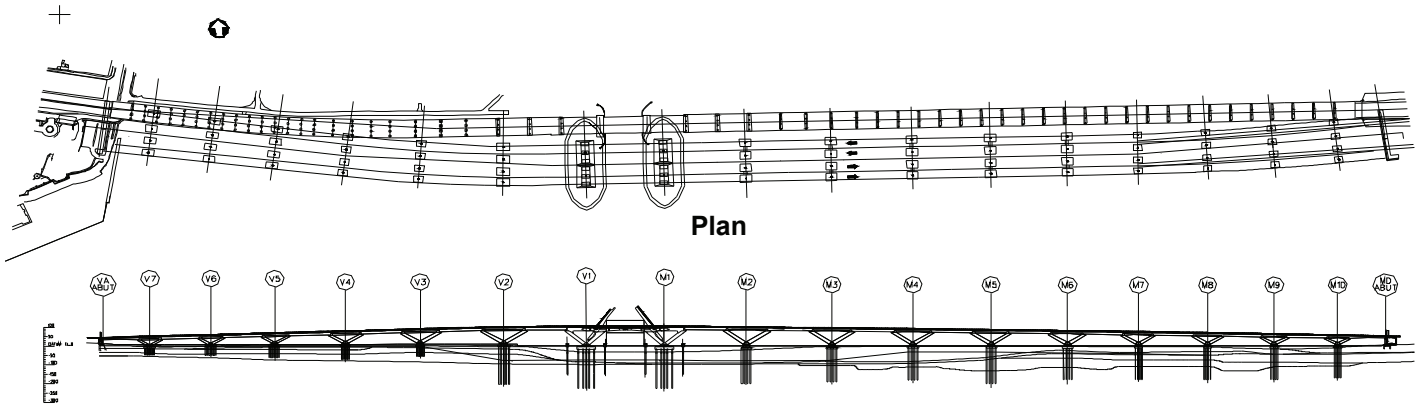


Figure 3: Woodrow Wilson Bridge – Plan and Elevation

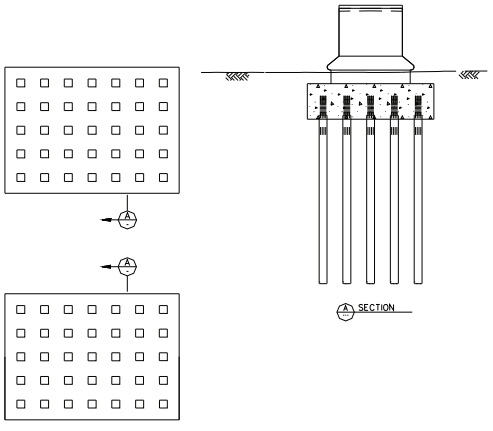


Figure 4: Typical Virginia Pier (Land Pier)

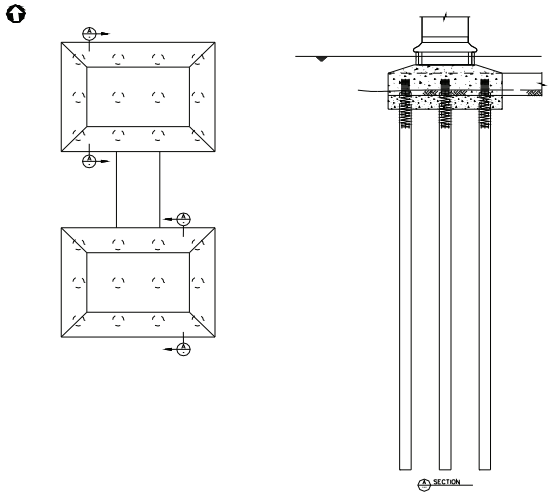


Figure 5: Typical Maryland Pier (River Pier)

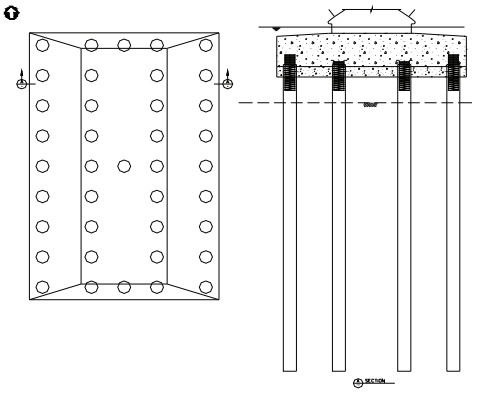


Figure 6: Typical Bascule Pier (River Pier)

COFFERDAM DESIGN

To permit construction of the cast-in-place pile caps in the dry, and to accommodate removal of soil, interlocking steel sheet pile cofferdams were required.

Water depths at the Maryland approach piers are generally shallow and dredging was required to permit access of floating construction equipment. Conventional steel sheet pile cofferdams with tremie concrete seal slabs and one level of internal steel bracing were used to construct these foundations (See Figure 7). While the design of the cofferdams was left to the contractor, Contract documents required the tops of the sheet piles to extend five feet above mean high water to prevent overtopping by vessel wakes. AZ-13 sheet piles were selected by the contractor.

To resist hydrostatic uplift pressures during unwatering a tremie concrete seal was required. The tremie slab was designed to span between the steel pipe piles and relied on sufficient bond between the tremie concrete and steel piles to resist the uplift forces. To enhance the bond stress, steel shear rings were added to the outside of the steel pipe piles. The tremie slab thickness was nominally five feet.

One level of internal steel bracing (perimeter wale with corner braces) was used to brace the side walls. The bracing was located above the river level and acted as a template to guide the sheet piles. Corner bracing was positioned to clear the foundation piling.

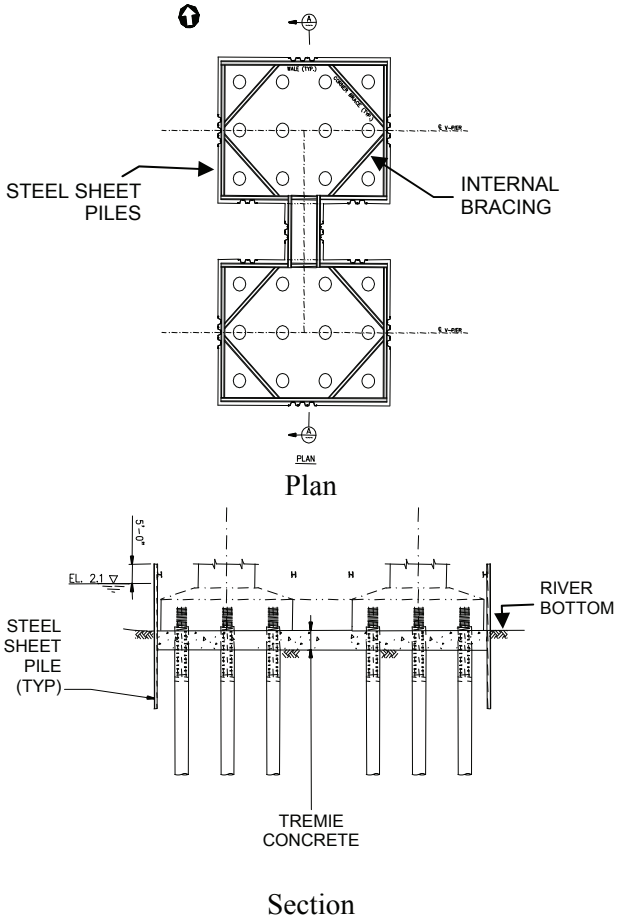


Figure 7: Shallow Water Cofferdams Plan & Section

Due to the very soft consistency of the recent river sediments there was some concern by the contractor about placement of the tremie concrete including possible mixing of the concrete with the river mud, thereby reducing its strength; concern with the ability of the soft sediment to support the weight of the tremie that could result in excessive overage in tremie concrete quantities and possible consolidation of the soft sediments under the weight of wet tremie concrete. To mitigate these effects it was considered to place precast concrete planks on the excavated subgrade to help distribute the weight of the tremie concrete during initial placement. It turned out that the planks were not needed and the tremie was placed directly on subgrade.

Bascule span foundations are located in relatively deep water adjacent to the main navigation

channel. This channel was originally formed during the last period of glacial activity and has filled with approximately 50 feet of recent soft alluvial sediment. Due to the predicted high volume design flows under the 100 year flood, the relatively narrow channel cross section and the soft river sediments, the channel section was found to be very susceptible to contraction scour. Full length sheet pile cofferdams would tend to decrease the channel cross section and increase contraction scour that could affect the performance of the bascule foundations. The solution was to utilize "Potomac River" cofferdams. These cofferdams are supported on the bridge foundation piling thereby reducing their overall depth, maintaining the channel cross section and minimizing the potential for contraction scour during a flood event.

Contract documents indicated a schematic design for the "Potomac River" cofferdams utilizing friction collars attached to the foundation piles supporting a soffit frame with precast planks to initially support the weight of the tremie concrete. Side walls were also precast concrete and internally braced to resist full hydrostatic pressures. The tremie concrete slab was designed to resist hydrostatic uplift forces and to carry the weight of the wet pile cap concrete. This design required much of the cofferdam frame to be constructed underwater (See Figures 8a & 8b).

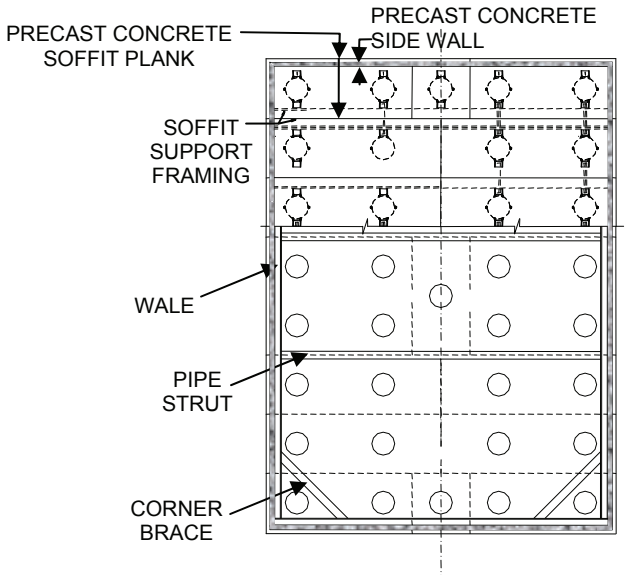


Figure 8a: Potomac Cofferdam on Friction Collars-Plan

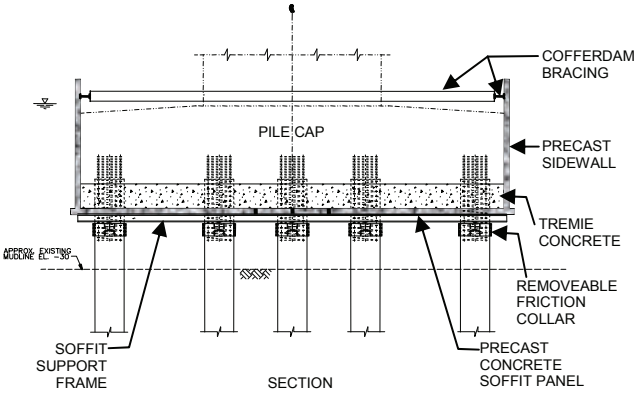


Figure 8b: Potomac Cofferdam on Friction Collars-Section

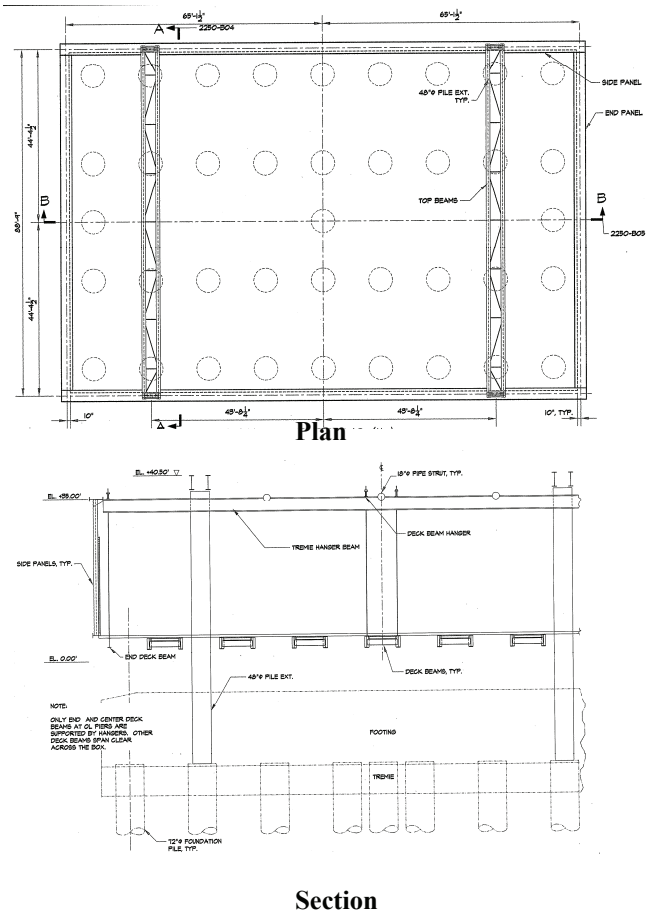


Figure 9: Potomac Cofferdam Supported on Pile Extensions Plan & Section

To minimize the amount of underwater construction the design was modified by the contractor such that the cofferdam frame was hung from hanger beams supported on pipe extensions fitted to the foundation piling (See Figure 9). The hanger beams were design to support the weight of the cofferdam empty, allowing most of the cofferdam to be constructed in the dry. Cofferdam side walls were constructed of steel sheet piles and bridge deck forms were used for the floor (See Figure 10). After the cofferdam was constructed, it was lowered into final position and hung from a lower hanger beam assembly designed to support the weight of the cofferdam and tremie concrete (See Figure 11). Once in final position, divers sealed any remaining openings and tremie concrete placed. Tremie thickness was approximately six to seven feet which was required to resist hydrostatic uplift and to support the weight of the wet cast-in-place concrete pile cap (See Figure 12).

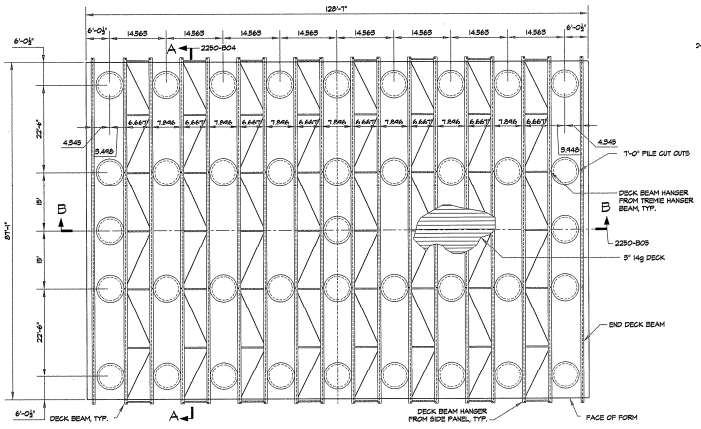


Figure 10: Potomac Cofferdam Deck Beams

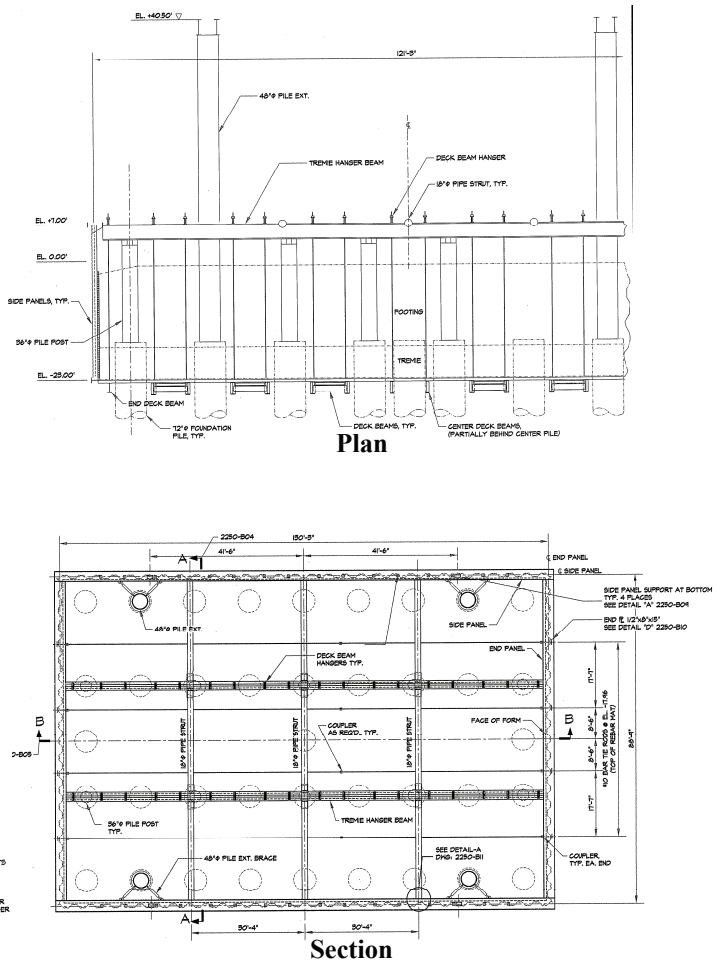


Figure 11: Cofferdam Box Lowered for Tremie Pour Plan & Section

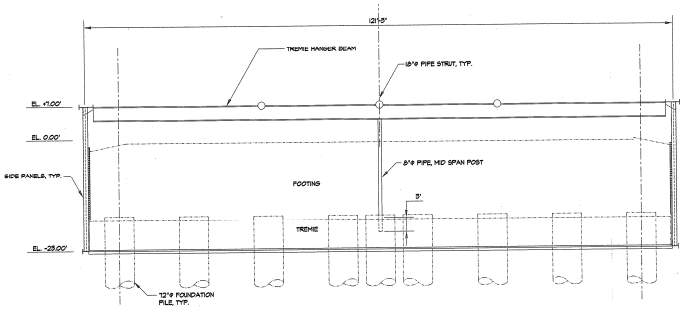


Figure 12: Dewatered Cofferdam

CONCLUSIONS

Cofferdams are typically required to construct bridge foundations in riverine or high ground water environs where construction work must be performed in the dry. Cofferdam design must consider:

1. The external forces acting upon it including hydrostatic, wind, wave, current and impacts from vessels if necessary, and the characteristics of the supporting soils, to provide a safe and dry working area for the permanent structure.

2. How will cofferdam stability be affected by unwatering. This typically includes a check of basal stability. Uplift pressures are typically handled by use of tremie concrete seal slabs.

3. Constructability must be addressed with regard to ease of installation, installation sequence, temporary construction stage loadings and installation equipment.

4. Effects of cofferdam construction on the permanent structure. As was the case for the Wilson Bridge, conventional cofferdams would have potentially increased contraction scour at the bascule foundations. To limit this effect, "Potomac River Cofferdams" were used to allow minimal restriction to the river flow.

ACKNOWLEDGMENTS

The new Woodrow Wilson Bridge is a joint project of Federal Highway Administration (FHWA), Maryland State Highway Administration (MSHA), and Virginia Department of Transportation (VDOT).

The project was designed and managed by Parsons Transportation Group PTG). The contribution of Dr. Serafim G. Arzoumanidis of PTG, Project Manager for the new bridge, was instrumental in establishing the overall design approach and coordinating all team members.

Other consultants involved in the geotechnical and seismic aspects of the project were:

- Potomac Crossing Consultants (Parsons Brinkerhoff, URS Greiner & Rummel, Klepper & Kahl).
- Contract BR-2 was awarded to the Joint Venture Tidewater/Skanska, Kiewit Construction and Clark Construction (TKC). Their work was performed on schedule and within budget.

FLOAT-IN COFFERDAMS

Robert B. Bittner, P.E., President, Ben C. Gerwick, Inc., San Francisco, CA, USA

Large diameter piles (2 to 3 m diameter, both driven and drilled) are being used more frequently by designers of bridge foundations. The use of these large piles allows the pile cap to be positioned off the bottom but usually still below water. Conventional cofferdams as shown in Figure 1 below are not suited to this type of pile cap. However, float-in cofferdams offer a viable alternative. This paper describes the float-in cofferdam system, its initial development for use on the Bath-Woolwich Bridge in Maine and its most recent application on the new Carquinez Bridge in California.

INTRODUCTION

Cofferdams are temporary structures used in the construction of bridge piers and other marine structures. Their primary purpose is to hold out water and unstable soil from the construction area, and thereby, allow in-the-dry construction of the permanent structure below the water line and quite often below the mud line. Typically, cofferdams consist of long interlocking steel sheet piles driven through water into the bottom of the waterway. The sheet piles form temporary exterior walls which are typically braced internally with wales and struts. The bottom of the cofferdam is typically sealed with tremie concrete or an impervious clay layer if one exists. This type of cofferdam is typically used for structures positioned at or below the mud line.

The cost of the cofferdam can represent a significant percentage of the total cost for constructing the underwater structure. At extreme depths, the cost of the cofferdam can exceed the cost of structure being built in the cofferdam. In addition, there are practical limits to the depth to which conventional cofferdams can be used. As an example, sheet piles over 30 m in length are extremely difficult to transport and handle during installation.

However, designers of marine structures are tending to use larger and larger diameter piles, both drilled shafts and driven piles. Designers are finding that piles in the range of 2 to 3 m diameter are more efficient than a high number of smaller piles. These larger piles with their higher stiffness make it possible from a design standpoint to position the pile cap at any point in the water column rather than at or below the midline as required with the use of smaller piles. In most cases, the pile-top structures are not positioned completely out of the water because of aesthetics and concern with splash-zone corrosion at the pile to pile cap connection. Therefore, the bottom of the pile cap is typically located at least a meter below low water line. For this type of off-the-bottom pile top structure, conventional bottom founded cofferdams may not be the best solutions.

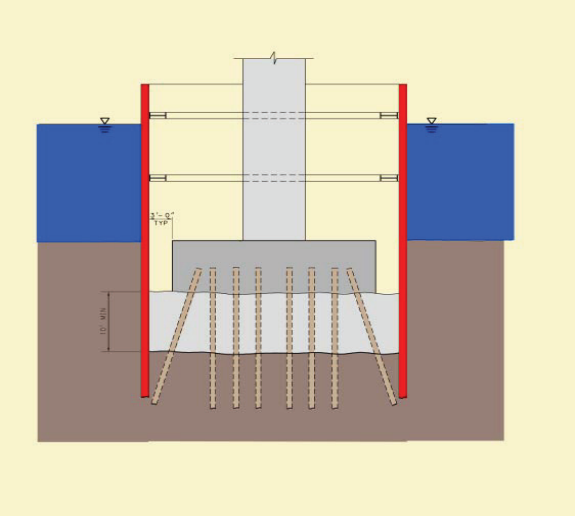


Figure 1: Conventional braced cofferdam

FLOAT-IN COFFERDAM CONCEPT

The float-in cofferdam concept has been developed to specifically address the construction requirements for pile-top marine structures positioned below water but up off the bottom of the waterway. This concept is perhaps best described by its sequence of construction (See Figures 2 through 8 for a plan view of a typical float-in cofferdam and construction sequence):

1. Piles or drilled shaft casings are installed through the water. Following completion of the pile installation, they are cut off underwater.
2. Concurrent with pile installation, a thin shell of the structure is pre-fabricated at an off-site location. This thin shell (and follower cofferdam if needed) is referred to as the float-in cofferdam.
3. Following completion of fabrication, the float-in cofferdam is launched and towed to the installation site.
4. Once at site, the float-in cofferdam is lowered down on to the pre-installed piles.
5. A seal is then formed between the piles and the bottom of the float-in cofferdam, and grout (or tremie concrete) is placed to lock the float-in cofferdam to the piles.
6. The float-in cofferdam is then dewatered.
7. All remaining work is then completed in-the-dry similar to a conventional cofferdam. This includes completion of reinforcement and concrete placement in the piles or drilled shafts, and placing reinforcement and concrete for the cap and pier shaft.
8. After completion of the shaft, if a follower cofferdam was used, the cofferdam area is re-flooded and the follower cofferdam is removed for re-use on the next pier.

The float-in cofferdam method of underwater construction offers the following significant advantages over conventional cofferdams:

- It can be used in essentially any water depth where the unsupported permanent foundation piles can serve their intended function. This is in comparison to conventional bottom-founded sheet pile cofferdam systems that are limited by the efficient lengths that standard sheet piles can be rolled, shipped and handled at the site.

- It offers the potential advantage of a reduced construction schedule by allowing the pile installation work to commence immediately rather than wait until the cofferdam has been designed, sheet piles ordered, bracing frames fabricated and cofferdams installed. This is a significant time advantage in that pile installation work is typically on the critical path and is the most common cause of delay on a marine construction project. Time is of course required to design, build and launch the float-in cofferdam. But all of this work can be performed concurrent with the pile installation work.

- This cofferdam method can offer significant cost savings by:

  1) eliminating or reducing the length of sheet piles,
  2) eliminating the conventional tremie seal that is used to resist hydrostatic uplift,

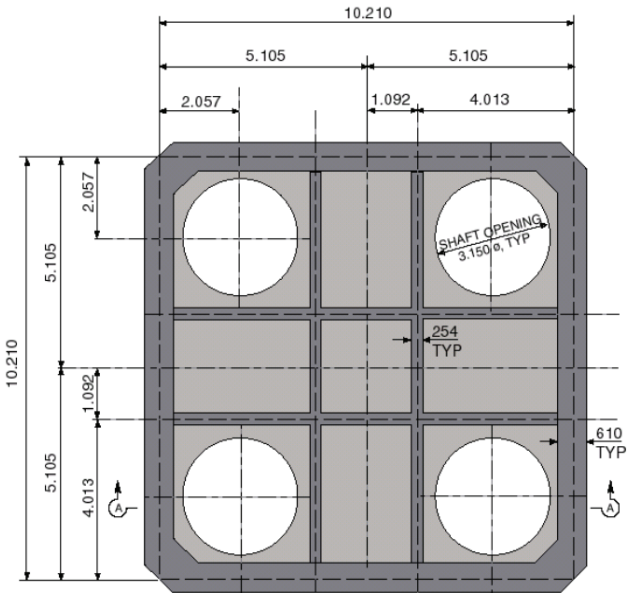


Figure 2: Plan at top of precast pile shell

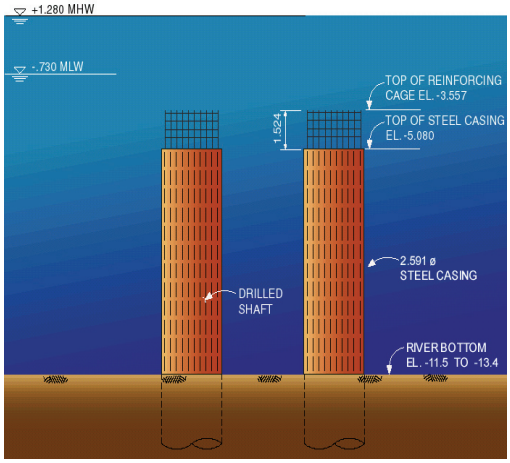


Figure 3: Stage 1 – Pile

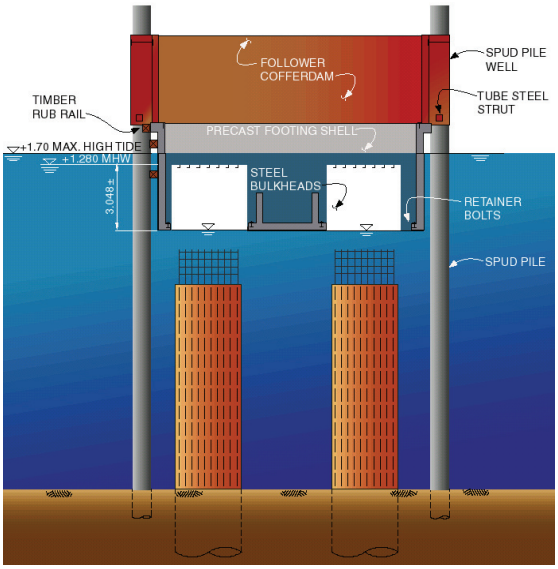


Figure 4: Stage 2 – Launch and position float-in cofferdam

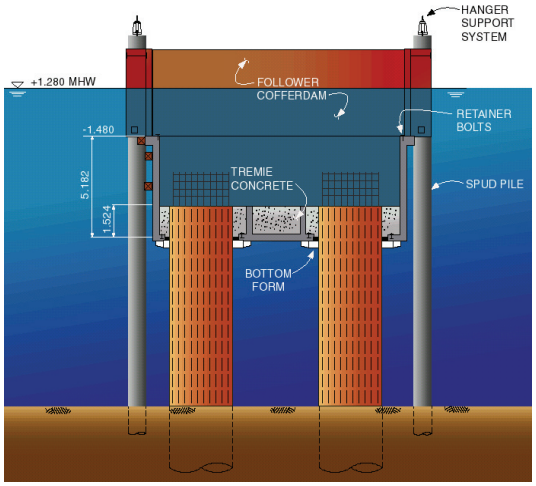


Figure 5: Stage 3 – Land cofferdam, seal pile connection and place tremie concrete

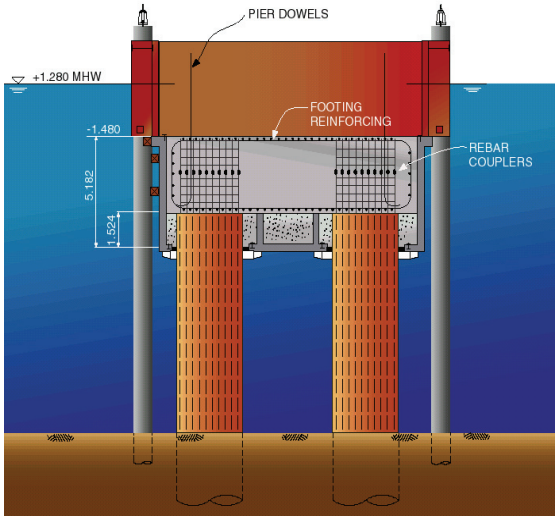


Figure 6: Stage 4 – Dewater cofferdam and construct pile cap

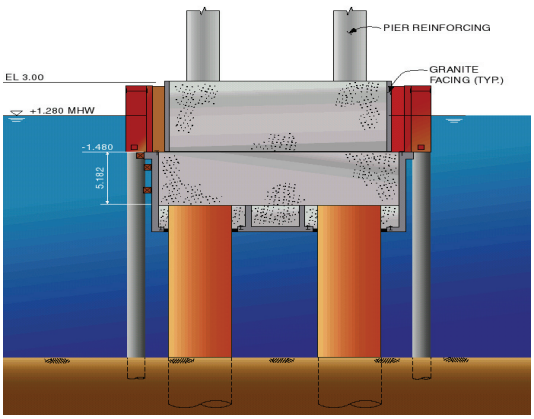


Figure 7: Stage 5 – Construct pier shaft

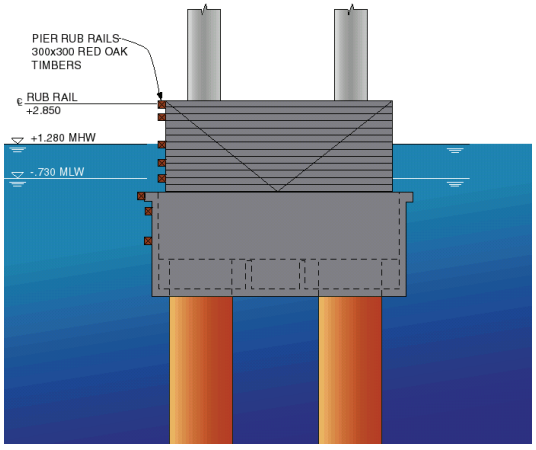


Figure 8: Stage 6 – Strip follower

3) allowing the pile cap fabrication operation to be performed more efficiently at a centrally located fabrication site on shore or at dock side rather than at multiple in-water cofferdam locations, and
4) allowing for more competitive pricing for material and labor by enlarging the geographical area over which the shells can be fabricated.

These cost savings are offset to some degree by the cost of the offsite fabrication and launch facility; however these are usually less than the cost associated with the savings listed above.

- It can reduce construction risk by minimizing the amount of time that the work is exposed to severe whether and fluctuating water levels. In addition, the critical operations such as float-in, positioning and landing can be timed to fit optimum weather and water level conditions.
- It can provided higher quality for the underwater concrete by allowing the exterior of the pile cap to be precast on shore in ideal conditions under tighter quality control.
- From a design point, this system allows elimination of the conventional tremie concrete seal. This reduces dead weight of the structure, and in areas of seismic risk, significantly reduces seismic loadings as well.

FLOAT-IN COFFERDAM FEATURES

The float-in cofferdam concept has the following typical features:

- **Off-site prefabrication –** A thin steel or concrete shell which forms the exterior of the pile cap is pre-fabricated in a dry dock or on the deck of a barge with the barge positioned at dock side to allow construction support from a shore based crane. (See Figures 2 and 4 for details of the float-in pile-cap shell used on the Bath-Woolwich Bridge.) This offsite fabrication is typically performed at a central location that allows an efficient flow of materials and effective monitoring for quality control. If the construction site is affected by severe weather conditions, it may be preferable to locate the fabrication facility indoors where higher labor efficiency can be obtained. Additionally, selection of the fabrication site should take into consideration the method of launching. (See launch method below for specific details.)

- **Temporary bulkheads** – Temporary bulkheads are typically steel ribbed elements used to close off openings in the shell structure, making the shell water tight and allowing it to float after launch. These bulkheads are typically salvaged and re-used on following caps. The bulkheads are typically bolted in place and use compressible neoprene or rubber seals at the mating surfaces to maintain water tightness. (See Figures 23 and 24 for a view of the temporary bulkheads used on the Carquinez Bridge float-in cofferdams.)

- **Pile-top bulkheads** – Pile-top bulkheads can be classified as a special type of temporary bulkhead. They are inverted open-bottomed cans that are centered directly over the top of the circular openings in the bottom of the pre-fabricated shells. They allow the foundation piles to penetrate up into the interior of the shell while maintaining the watertight integrity of the float-in cofferdam. (See Figures 10 and 22 for examples of pile-top bulkheads used on the Bath-Woolwich and Carquinez bridges respectively.) These blockouts are of course watertight except for the open bottom and can act as individual ballast compartments if compressed air hoses are attached to each compartment. By regulating the air pressure in each pile-top blockout, it is possible to level or trim the float-in cofferdam during launch and transport. (See Figure 12 for a view of the air piping used on the Bath-Woolwich Bridge.)

- **Follower steel cofferdams** – Follower cofferdams are required for pile-top structures that are positioned completely under water. Follower cofferdams extend the height of the prefabricated shell walls sufficiently to allow the pile cap to be lowered to final grade without allowing water to overtop the cofferdam. These are typically stripped at completion of the pier and re-used on following piers. (See Figures 14, 15 and 18 for pictures of the follower cofferdam used on the Bath-Woolwich Bridge.) These follower cofferdams are very similar to conventional sheet pile cofferdams. They

have the same type of internal bracing consisting of steel wale frames and struts. The walls of the follower cofferdams can be steel ribbed panels, corrugated panels or even conventional steel sheet piles. All three types typically terminate in a flat bottom plate that bolts directly to the top of the pile-cap shell structure.

- **Concurrent foundation and pile-cap shell construction** – The float-in cofferdam method of construction allows installation of foundation piles to run concurrently with fabrication of the pile-cap shell. This feature allows for a shorter construction schedule compared to conventional pier construction.

- **Temporary pile-top cofferdams for underwater cut off of piles** – In order to float-in over the pre-installed piles, it is necessary to cut the permanent piles off to grade under water. This can be performed with divers, however it is expensive and risky to do so. It is preferable to cut the piles off in-the-dry using a temporary cofferdam that slips down around the permanent pile and seals to the side of the pile, thus allowing the annulus between the outer cofferdam and the exterior wall of the pile to be dewatered. Once the interior of the pile and the annulus have been dewatered above the cut off point, a worker is lowered into the interior of the pile, and the pile is cut off to precise grade. An alternate method which can be used when the drill casings are torqued into position is to use drilled shaft casings that have a reverse torque disconnect built into the wall of the casing. The disconnect point is pre-determined at each pile location, and each casings is fabricated with a disconnect at a pre-planned location. This method was used on the drilled shafts for the Bath-Woolwich Bridge.

- **Cofferdam launch method** – There are many different potential ways to launch the float-in cofferdams. The launch method is usually tied to the method and location of the shell fabrication or casting. If the shell is fabricated in a dry dock, launching is performed by flooding the dry dock and exiting through a removable gate at the entrance to the dry dock. If the shell is cast on the deck of a flat-deck barge, it is typically launched by ballasting the barge out from under the shell and allowing the shell to float free. If this method is used, special consideration needs to be given to maintaining stability of the barge during all ballasting operation. The stability analysis for the launch operations should be performed and monitored by an engineer experienced at performing stability calculations or by a naval architect. The stability can be controlled by setting one end of the barge down on a pre-leveled bottom or by attaching wing-tanks to the barge in order to provide sufficient water plane during all stages of launch. If the shell is light enough and heavy lift equipment is available, the shell can be lifted off and set in the water. (For an example of this method, see Figure 11 for a photo of the float-in pile-cap shell being lifted off the deck of the casting barge at the Bath Ship Yard. If launch ways are available close to the installation site, they cap provide an alternate launch method.

- **Method of transport** – Tugs are typically used to assist the floating cofferdams during their transit to the installation site.

- **Positioning and guidance system** – Positioning and guidance systems are needed during the mating of the float-in cofferdam to the pre-installed foundation piles. These are particularly important when the tops of the foundation piles are several meters below water and out of site. These systems include mooring lines, anchors, and tapered guide structures to direct the cofferdam onto the permanent support piles.

- **Temporary ballast system** – In order to sink the prefabricated pile-cap shell down to the cut-off piles, it is necessary to partially flood the cofferdam. During the sinking operation the cofferdam should be maintained relatively level. This requires an ability to add water to different areas of the pile-cap shell. The ballast system performs this function.

- **Temporary support system** – In order to land the float-in cofferdam on the cut- off piles, a means of load transfer must be developed to carry the partial dead weight of the cofferdam. The required capacity for the system is relatively low and is only temporary until it is replaced by the tremie or grout closure pour. (See Figures 19 and 20 for details of the temporary support beam,

shown in yellow, used as the temporary landing support on the Carquinez Bridge.)

- **Bottom sealing system** – After landing of the float-in cofferdam, the foundation piles typically penetrate up into the bottom of the pre-fabricated pile- cap shell, and a grout or concrete placement is made in the bottom of the shell to lock the shell to the foundation piles. In order to place the grout or tremie concrete, it is first necessary to seal the bottom of the annulus between the outside wall of the pile and the hole in the bottom of the pre-fabricated shell. This seal does not have to resist the total hydrostatic head at that point but only the buoyant head of a few feet of the grout or tremie concrete. (See Figure 20 for details of the temporary sealing system used on the Carquinez Bridge.)

- **Grout or tremie closure** – The grout or tremie concrete placement is the primary sealing system to allow dewatering of the float-in cofferdam. It is also the primary load transfer element to resist the uplift buoyancy of the cofferdam after the cofferdam is dewatered and to support any net downward load immediately after placement of the first lift of concrete in the pile-cap shell. (See Figure 5 for a schematic of the tremie concrete closure that was used on the Bath-Woolwich Bridge float-in cofferdams.)

SPECIFIC CONSIDERATIONS IN THE DESIGN OF FLOAT-IN COFFERDAMS

Tolerances – The float-in cofferdam method requires the mating of the float-in cofferdam to the top of the pre-installed piles. In order for this mating to succeed without punching a hole in the bottom of the float-in cofferdam, it is essential that the pile be properly located within a specified tolerance.

Piles installed from floating equipment on anchor lines or spuds can typically meet installation tolerances of +/- 15 cm horizontally at the surface of the water and 1% in verticality. Piles installed through a bottom founded template can be installed to a tolerance of typically 6 cm at the surface of the water and 0.5% verticality. These tolerances need to be taken into account when designing the net clearance of the openings in the bottom of the float-in cofferdam relative to outside diameter of the pile. These clearances need to be large enough to take into account possible misalignment of the piles while maintaining the structural integrity of the bottom slab and providing a void space that can be effectively sealed off for grouting or tremie placement.

The cut-off tolerance of the piles under water using a pile top cofferdam for access is typically about +/- 3 mm. This tolerance may be necessary if the support bearing on landing is directly onto the pile cut-off surface. However an alternate way of leveling the float-in cofferdams after landing is to use flat-jacks attached at the bearing points in the float-in cofferdam. These jacks should be plumbed together to allow a three point landing system.

Water Tightness – During launch, transport and positioning of the pile-top cofferdams it is essential that the inflow of water into the cofferdam be controlled at all times. The joints between the float-in pile top structure and water tight bulkheads, follower cofferdam and pile top blockouts are all typically fitted with strips of compressible neoprene or rubber. These continuous strips are typically 5 to 8 cm wide and 1 cm thick. The durometer of the seal should be approximately 40 to 60. Compression of the sealing strip is provided by bolts on a typically about 30 cm. The strips should be positioned to compress with application of increased bolt tension and increased hydrostatic load on the outside of the cofferdam.

If conventional steel sheet piles are used for the follower cofferdam, the interlocks should be treated with hydrophilic strips prior to attachment to the float-in cofferdam.

If ballasting operations during sit-down operations require internal bulkheads to maintain stability, the water tightness of these bulkheads is essential and should be treated with the same level of importance as exterior bulkheads. Leaking interior bulkheads can cause loss of stability during ballasting operations and result in loss of the floating pile-cap shell.

Draft Limitations – There may be several factors that will limit the allowable draft of the float-in cofferdam at launch. These may include the depth of dry dock where the float-in cofferdam is being fabricated, the depth of the navigation channel leading to the installation site

and finally, the cut-off elevation of the foundation piles at the installation site. If excessive draft is a problem, there are several potential ways of minimizing the draft:

- Decrease the thickness of the concrete walls and bottom slab.
- Use lightweight or semi-lightweight concrete for the shell.
- Blow all water out of the open-bottom pile top bulkheads.
- Attach supplemental buoyancy tanks.

Floating Stability – A floating stability check should be performed for all stages of launch, transport, positioning and landing of the float-in cofferdam. This is performed using standard naval architecture principles for calculation of meta-centric height and reserve stability. These calculations may show that a float-in cofferdam is unstable during the set-down or landing operation when water is pumped into the cofferdam in order to increase draft. This typically occurs when water is allowed to freely flow from one side of the cofferdam to another. This sloshing can create an unstable situation and is referred to as excessive free-surface effect. The standard way of reducing the free-surface effect is to partition the interior of the cofferdam with watertight bulkheads. If interior bulkheads are necessary their water tightness is critical to the stability of the cofferdam and tests should be conducted on their watertightness prior to launch of the float-in cofferdam.

Installation Stresses – The float-in cofferdam should be designed for all stages of launch, transport, positioning and landing as well as buoyancy forces and full hydrostatic forces that develop when the cofferdam is sealed off and dewatered. In a typical installation sequence for a float-in cofferdam, the vertical loading on the temporary support system will reverse during the course of construction. Upon landing on the foundation piles, the support system must support the partial dead weight of the float-in cofferdam. Once the grout or tremie concrete seal has been placed, cured and the interior of the cofferdam dewatered, the support system must then be able to resist the full upward buoyancy force of the float-in cofferdam. During placement of the first lift of footing concrete, the support system must resist the net difference between the buoyancy and the dead weight of the first lift.

EXAMPLES

Bath-Woolwich Bridge

Ben C. Gerwick, Inc. (BCG) of San Francisco working for Flatiron Structures Company of Longmont, Colorado designed the floating cofferdam system used on the Bath-Woolwich Bridge across the Kennebec River at Bath, Maine. The Maine Department of Transportation awarded the design-construct contract for the 1,000 m long four lane bridge to Flatiron Structures Company (FSC) and Figg Engineers in August of 1997, and shortly thereafter, FSC contracted with BCG to design a cofferdam system for the six main river piers.

Figg's design for the six main river piers called for two size footings: 10.9 m by 9.9 m by 3.6 m deep supported by four 2.44 m diameter steel cylinder piles socketed into rock and 9.6 m by 9.6 m by 3.6 m deep supported by three piles of the same size. The typical footings had a 2.7 m deep tremie seal and was located in 13 m of water with the top of the footing about 1.4 m below mean tide. This cap design significantly reduced the water depth at which the footing were to be constructed, however, it created the problem of how to construct an underwater footing suspended 6 m above the river bottom.

In order to address this problem and reduce the amount of work in the river, BCG proposed the use of a floating cofferdam system (See plan view in Figure 2 and sequence of construction shown in Figures 3 through 8):

• Pre-install the drilled shafts using a two stage template.

• Construct a precast pile-cap shell on shore and attach a reusable temporary steel follower cofferdam.

• Launch the cofferdam and tow it to the bridge site.

• Position the cofferdam over the drilled shafts and fix it in position with four spud piles.

• Lower the cofferdam down over the pre-installed drilled shafts with jacks located on top of the spud piles.

• Lock the pile-cap shell to the drilled shafts by placing a 1.3 m deep tremie seal.

• Dewater the cofferdam and complete the pile cap and pier shaft in the dry.

• Flood and remove the follower cofferdam for reuse on the next pier.

The floating cofferdam system and the above sequence substantially reduced in-water work and improved quality control by transferring the work to an offsite dock location. The system also saved 4 months in the construction of the foundations by allowing the drilled shaft installation to start immediately after contract award and to proceed concurrently with fabrication of the floating cofferdams.

The final design for the precast pile-cap shell was a 5.182 m deep box with 288 mm thick walls and bottom slab.

The typical precast box weighed 340 tons and was cast on the deck of a barge at dock side.



Figure 9: Casting pile-cap shell on deck of barge, Bath-Woolwich Bridge

(See Figure 9.) Two 4.267 m high steel followers were constructed of interlocking steel sheet piles and assembled on the deck of another barge. Two local shipyard cranes were used to lift the precast pile-cap shells off the deck of the casting barge and into the water. (See Figure 11.) The precast shell was then leveled by using compressed air to vary the water level in the open bottomed 3 m diameter pile top block outs. (See Figure 12.) Once the segment was afloat and trimmed, one of the steel followers was lifted into position on top of the precast pile-cap shell and bolted to the top lip of the shell. (See Figure 14) The floating cofferdam was then towed into position over the top of the preinstalled piles (See Figure 13) and locked in horizontal position with four 1 m diameter spud piles driven through the pockets, attached to the corners of the cofferdam. (See Figure 15)

One of the keys to the successful use of this technique was the installation tolerances of the 2.44 m diameter drilled shafts. The drilled shafts had to be installed to a relatively tight tolerance or the holes in the bottom of the pre-cast shell would not have matched the layout of the pre-installed piles. For the Bath-Woolwich Bridge, the inside diameter of the holes in the bottom of the pile-cap shell was 3.15 m. This provided a pile clearance of 355 mm. The drilled shafts where successfully installed to a horizontal

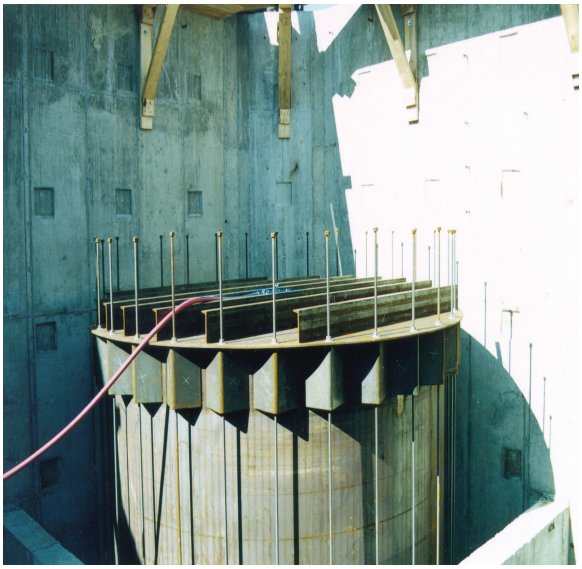


Figure 10: Pile-top bulkhead inside precast shell, Bath-Woolwich Bridge

tolerance of +/- 150 mm at the point of cut off, 5 m below mean water elevation. This tolerance was obtained by using a two piece template. The bottom steel frame was positioned with anchor winches to a tolerance of +/- 300 mm and fixed in vertical and horizontal position with four 1 m diameter spud piles. The upper guide slides on top of the bottom frame and were positioned to a tolerance of +/- 50 mm before it was fixed to the lower frame. The drill casing was then stabbed through a guide sleeve attached to the top guide.

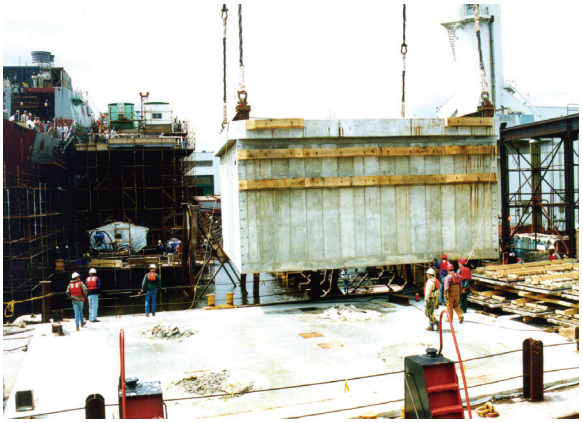


Figure 11: Lifting pile-cap shell off deck barge, Bath-Woolwich Bridge

A second key to the successful installation was the initial temporary underwater connection between the float-in cofferdam and the pre-installed drilled shafts. This connection was made with a 1.22 m deep tremie seal, and the vertical load was transferred through bond of the tremie seal to the sides of the drilled shaft casing. This bond was sufficient to resist the buoyancy of the dewatered float-in cofferdam at high tide and allowed placement of the pile cap reinforcing steel and first concrete lift in the dry. (See Figures 16 and 17.) When the footing concrete was being placed in the pile-cap shell, and the tide was out, the vertical loading was reversed, and the bond supported the dead load of the fresh concrete. The allowable bond stress between the tremie concrete and the drilled shaft casing was calculated using the American Petroleum Institute (API) Code RP 2A, Recommended Practice for Planning, Designing and Constructing Fixed Offshore Platforms.



Figure 12: Hooking up air lines to pile-top bulkheads, Bath-Woolwich Bridge



Figure 13: Pre-installation of drilled shafts using two-stage template to set casings, Bath-Woolwich Bridge



Figure 14: Mating follower cofferdam to pile-cap shell, Bath-Woolwich Bridge

With this type of support system, if additional

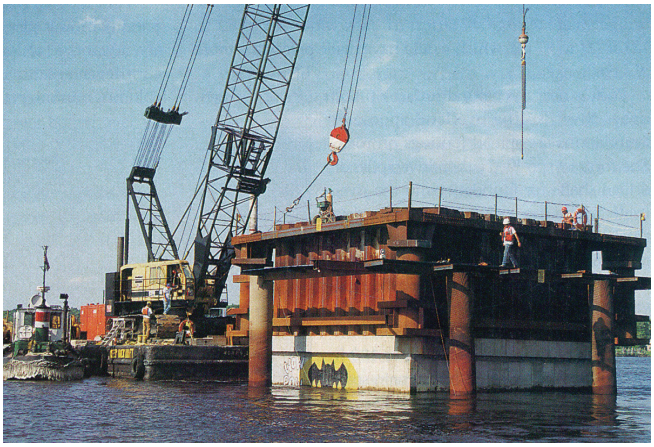


Figure 15: Positioning and lowering float-in cofferdam, Bath-Woolwich Bridge

capacity is required, the bond area can be increased by deepening the tremie placement or the allowable bond stress be increased by adding weld beads to the outside of the casing in the zone of tremie concrete.

Following completion of the pile cap, the pier shaft was completed to a point above the high water line and the follower cofferdam was stripped. (See Figure 18)

New Carquinez Bridge

The contract for the new bridge was awarded in early 2000 to a joint venture between FCI Constructors and Cleveland Bridge California, (FCI/CBC). Ben C. Gerwick, Inc. was selected by FCI/CBC to modify Caltran's float-in cofferdam concept and further reduce the amount of onsite work.



Figure 16: Dewatering float-in cofferdam, Bath-Woolwich Bridge

The foundation design for the new bridge required six 3 m diameter drilled shafts under each of the four main tower legs. Because of the very high lateral stiffness of these piles, it was possible to elevate the four tower footing blocks - 5.4 m deep and 18 m by 20 m in plan - up off the bottom of the strait. At the north tower, the footing block is positioned 30 m off the bottom with the lower edge of the footing at 2.34 m below mean sea level. The original design by Caltrans was to cast the footing shells offsite, float them to the bridge and land them on pre-installed erection frames, or falsework. The footing shells were to be used as temporary cofferdams and as templates for the installation of drill shaft casings.



Figure 17: Placing pile-cap reinforcement, Bath-Woolwich Bridge



Figure 18: Stripping follower cofferdam from completed pier shaft, Bath-Woolwich Bridge

BCG modified this concept by designing a temporary support system that allowed the float-in cofferdams to be landed directly on the pre-installed drill shaft casings. (See Figures 19 and 20 for details of the temporary support system, shown in yellow.) This modified design offered

significant advantages. First, it allowed drilled shaft installation, an activity which was on the critical path, to begin sooner, by allowing casing installation to start before the float-in cofferdams had been completed. Secondly, the modifications meant that the construction schedule was shortened by allowing casing installation to run independently of and concurrently with cofferdam fabrication.

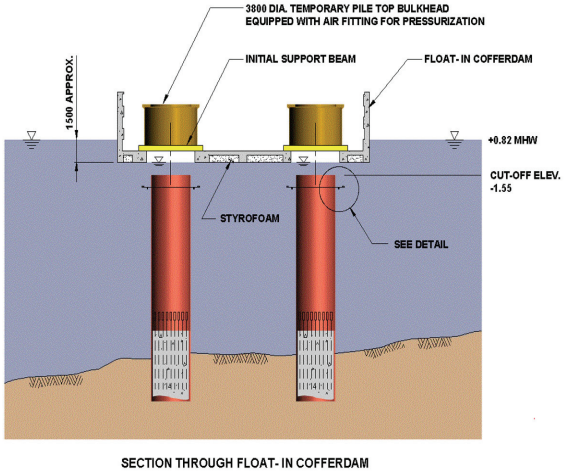


Figure 19: Float-in cofferdam concept for Carquinez Bridge

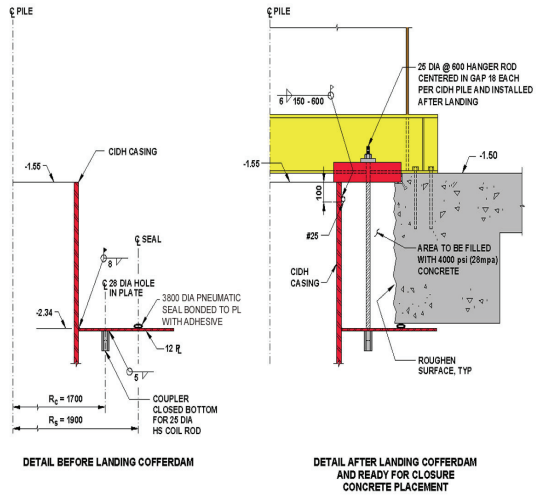


Figure 20: Pile-top details for Carquinez Bridge

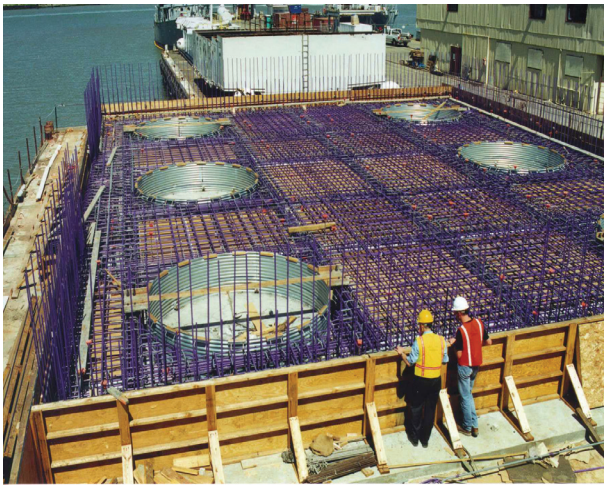


Figure 21: Casting float-in cofferdam on deck of launch barge, Carquinez Bridge



Figure 22: Completed float-in cofferdam with pile-top bulkheads on deck of launch barge, Carquinez Bridge

Construction cost was reduced by completely eliminating the need for erection frame or temporary falsework support for the float-in cofferdam and infill concrete, and risk was also reduced as a result of decreasing exposure time of a partially completed cofferdam and footing to storm conditions.

Cofferdams and connecting ties were cast on a flat-deck barge, 22 m wide by 76 m long and 4.6 m deep, which was positioned at the dockside within reach of a shore-based crane. (See Figures 21, 22 and 23) The surface of the barge was prepared by casting a 15 cm concrete slab to provide a level and smooth casting surface. In order to ensure that the cofferdams would lift off the barge at launch, the

surface of the casting slab was sprayed with a bond breaker that created a polished surface. As an added precaution, water pressure was applied to the contact surface between the top of the slab and the underside of the cofferdams. This was performed about a week after casting and before the six 3.8 m diameter pile top blockouts were flooded with a head of 3 m for launching. Complete release from the casting bed was confirmed when water seeped out at the perimeter of the cofferdam.

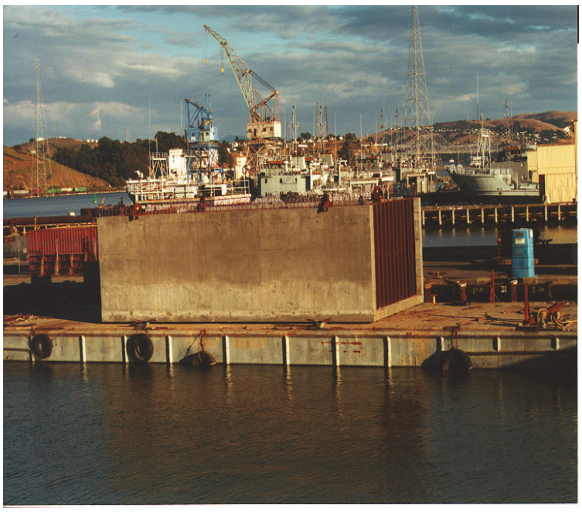


Figure 23: Completed precast shell of link-beam on deck of barge, Carquinez Bridge

For the launch operation, a site was selected in the Carquinez Strait approximately 2-km upstream from the bridge. The primary criteria were that the site should have a level bottom and a water depth at low tide of about 6.7 m. The barge was towed to the site and positioned alongside a derrick barge on anchors. In order to maintain sufficient stability of the casting barge and cofferdams during the launch, the barge was ballasted down one end at a time. The stern of the barge was first set down on to the bottom during low tide, and then, as the tide turned, the bow was gradually ballasted down allowing the cofferdams to float free one at a time.

Following launch, each cofferdam was towed to the dockside and stored afloat until the drilled shafts at the first tower were completed. (See Figure 24)

The modified design incorporated a number of features essential to the success of the project: First, the cut-off elevation of the drilled shaft casings was set at 1.55 m below mean sea level,



Figure 24: Float-in cofferdams floating in storage at dock side after launch, Carquinez Bridge

it was therefore necessary to limit the draught of the float-in cofferdams to 2 m. This was accomplished by following modifications:

- the wall thickness of the float-in cofferdam was decreased,
- semi-lightweight concrete with a specific gravity of 2 was used,
- Styrofoam blocks were used to form the bottom ribs of the cofferdam, and finally,
- each pile-top block-out in the bottom slab (located over the top of each pile position) was capped with airtight 3.8 m diameter steel cylinder and the water was forced out of the pile compartments with compressed air.

Secondly, Caltrans set the horizontal positioning tolerance for the 3 m diameter drill shaft casings at +/- 150 mm, but site conditions including water depths of up to 32 m and tidal currents up to 3 m/s made meeting these criteria difficult. In order to meet the specified tolerances under these conditions, a steel guide template with four spud piles was installed at the south tower and a template attached to the pile driving barge was used on the north tower. As an added precaution against fit-up problems during landing of the cofferdams, the size of the blockouts in the bottom of the float-in cofferdams was increased to 3.66 m. This provided a

theoretical clearance around the pre-installed drilled shafts of 330 mm.

Third, the system for cutting off the drilled shafts under water included a 4.5 m diameter cylindrical cofferdam that fitted over the top of the drilled shaft. The cofferdam sealed to the casing at about 1 m below cut-off elevation by means of an inflatable rubber O-ring that fit inside a circular recess at the bottom of the cofferdam. Following inflation of the seal, the cofferdam was dewatered and the drilled shaft casing was cut off in the dry to a precise elevation. This cut-off cofferdam also allowed access for welding a steel ring to the exterior of the casing; the ring was used to provide the watertight seal between the float-in cofferdam and the drilled shaft casings. It also provided the necessary shear resistance for the support of the cofferdam during the concrete infill operation. (See Figures 19 and 20 for details of the bottom seal.)

Fourth, high tidal currents in the Carquinez Strait meant there was only about an hour of slack tide during which the cofferdams could be landed. Hence it was necessary to install a guide system to allow rapid positioning and landing. Because the water was more than 32 m deep, the guide system was attached directly to the 3 m diameter drilled shaft casings. The guides were L-shaped wide flange brackets attached to the casing just below the landing support bracket and extended above high tide so they could be used for visual positioning of the cofferdams. (See Figure 25)



Figure 25: Positioning and landing float-in cofferdam at N. Tower, Carquinez Bridge

The 4.5 m diameter cylindrical cofferdam allowed the tops of the casings to be cut off to a precise elevation. This provided an excellent bearing surface for the landing of the cofferdams. Caltrans' initial design showed the top of the casing protruding through the 3.2 m diameter holes in the bottom of the cofferdam and cut off flush with the bottom floor of the precast cofferdam. Landing support was provided by steel beams spanning across four of the bottom slab openings and bolted flush to the floor of the precast cofferdam. The actual bearing surface was the top edge of the drilled shaft casing and the underside of the steel beam. (See Figures 19 and 20 for details of the bearing surface.)



Figure 26: Landed float-in cofferdam and accessing seals through through pile-top bulkheads, Carquinez Bridge

In order to dewater the cofferdam it was necessary to create a watertight seal between the six drilled shaft casings and oversized holes in the bottom of the cofferdam. This was accomplished by pre-welding doughnut-shaped steel rings – 12 mm thick by 700 mm wide - to the casings just below the cut-off elevation, at the finished bottom elevation of the cofferdam. These plates were attached in-the-dry by using the same 4.5 m diameter cofferdam used for casing cut-off.

At the outer edge of the steel doughnut, an inflatable O-ring was bonded to the plate. As the void space around each casing was dewatered the hydrostatic pressure pushed up on the bottom of the steel plates and the rubber O-rings provided the necessary seal. In areas where the



Figure 27: Float-in cofferdams and link-beam shell in place, ready for placement of reinforcing steel, Carquinez Bridge



Figure 28: Placing reinforcing cages in drilled shafts at Carquinez Bridge

seal did not seal properly, vertical hanger bolts were available to pull the 12 mm plate tight to the bottom of the cofferdam and compress the seal. (See Figure 20 for details of the seal.)

The initial support system for landing the cofferdams was simple and allowed a quick landing, but it was directly in the path of both the vertical extension of the drilled shaft reinforcement and the horizontal reinforcement in the bottom footing mat, hence it had to be replaced before the reinforcement could be installed.

Final support was provided by placing infill concrete in the void spaces between the 3 m diameter drilled shaft casings and the oversized 3.6 m diameter holes in the bottom of the float-in cofferdam. (See Figure 20 for a detail of the void space.) The 3.8 m diameter cans positioned over the top of each hole provided access to this area and the seal system described above allowed the cans to be dewatered and the infill concrete to be placed in-the-dry. (See Figure 27, showing removal of the lids of the pile top bulkheads.) Hanger rods 25 mm in diameter and spaced at 600 mm along the center of the void space provided shear reinforcement and the fillet weld connecting the 12 mm plate to the drilled shaft casing provided the necessary shear resistance.

After the concrete in the void space had reached the specified strength, the entire cofferdam was dewatered, the 3.8 m diameter cans were removed from each drilled shaft location, and the initial support beams were removed. At this point the area over the top of each drilled shaft casing was free and open for extending the drilled shaft vertical reinforcement up into the footing, and installation of the footing bottom reinforcement mat. (See Figure 28 for a view of the cleared area inside the float-in cofferdam.)

CONCLUSION

The successful use of the float-in cofferdam system on two major bridges has demonstrated the effectiveness of this method for constructing pile-caps in deep water where the caps are located below water but elevated off the bottom.

REFERENCES

Anderson, H. V.: Underwater Construction Using Cofferdams

Bittner, R. B.: Tapping Technology, BRIDGE design & engineering, Issue No. 14, First Quarter 1999, pp. 40-41.

Bittner, R. B. : Fast-track float-in, BRIDGE design & engineering, Issue No. 24, Third Quarter 2001, pp. 38-40.

Ratay, R. T.: Handbook of Temporary Structures in Construction, Chapter 7, by Ben C. Gerwick, Jr.

Stubb, F. W., Jr.: Handbook of Heavy Construction, 3rd Edition, Chapter 23, Cofferdams and Caissons, by Ben C. Gerwick, Jr.

FINITE ELEMENT ANALYSES AND COFFERDAM EXCAVATIONS

Dimitrios C. Konstantakos, Mueser Rutledge Consulting Engineers, New York, NY, USA

Cofferdam excavations have traditionally been designed with classical design methods that involve direct computations of active or apparent earth pressures. However in contrast to finite element methods, traditional analyses can not account for full soil-structure interaction. Because of their complexity, numerical analyses are performed almost exclusively by computers. Recent theoretical and computer advancements have made the use of the finite element method much more user-friendly and affordable. General information about the basics of the finite element method in geotechnical engineering and for cofferdam excavations is presented. While knowledge of all intricate theoretical and computational details is not needed, the designer should at a minimum be aware of the most important aspects of soil modeling. Most importantly, the designer must have sufficient experience to be able to judge the relative "correctness" of vast numerical results produced by today's software programs. Hence, the human factor is an irreplaceable component of finite element computations.

INTRODUCTION

Cofferdams are enclosed temporary excavations that retain soil and water outside of a construction site. Marine cofferdams typically provide temporary excavation support for construction of bridge piers or other structures that have to be founded a considerable depth below water. In the majority of cases, marine cofferdams comprise a system of joining steel sheet piles braced by steel members.

Cofferdam excavations have been in use for a long time. In most projects, cofferdams have been designed with conventional analysis methods, where the soil pressure distribution is based on limit equilibrium theory (active – passive) or on empirical pressure distributions (Peck 1969 and others). In the typical classical design approach, separate analyses are required for:

a. Cantilever staged excavation.
b. Excavation with a single bracing level.
c. Multi-level-braced excavation.
d. Rotational instability.
e. Basal instability.
f. Surface settlement assessment.

Hence, the major disadvantage of "classical" approaches is that the relation between soil pressures, wall-soil displacements, and sequential construction staging can not be captured. Here lies the "beauty" of finite element methods. Today, finite element methods can unify most aspects of staged construction of cofferdam excavations into a single analysis.

Literally, the finite element method is a divide and conquer approach to solving engineering problems. This is achieved by descretizing the soil continuum and structural elements in basic elements where a known mathematical framework can be applied to assure force equilibrium and displacement consistency. While performing such calculations and setting the proper finite element mathematical framework with hand calculations is possible, the task would be so daunting that an engineer could well spend his entire career solving one problem! Hence, finite element problems have been traditionally solved with the aid of a computer. Recent advancements in computer technology and geotechnical modeling have made the use of finite elements a very effective method for analyzing cofferdam excavations.

While in the majority of cofferdams it is not necessary to conduct finite element analyses, it would be beneficial to perform analyses in projects that require or involve any of the following:

a. Accurate determination of lateral and vertical soil and wall displacements.
b. Construction adjacent to sensitive structures.
c. Basal stability in soft clays.
d. Accurate groundwater modeling.
e. Unbalanced soil loading conditions.

f. Complicated soil profile and site conditions.
g. Consideration of construction staging effects.
h. Full accountability of construction staging.
i. Consolidation effects.
j. Considerable excavation depth (40 ft or more)
k. Three dimensional effects

It would be impossible and impractical to cover every aspect of geotechnical finite element modeling in this publication. Hence, the author aims to provide the reader with a basic understanding and a general approach of how finite element theory can be used to analyze cofferdam excavations.

FINITE ELEMENT BASICS

The finite element method is a general systematic computational procedure for approximately solving problems in physics and engineering. The term finite element method was coined in the late 1950s to define the method for computer- based structural analyses.

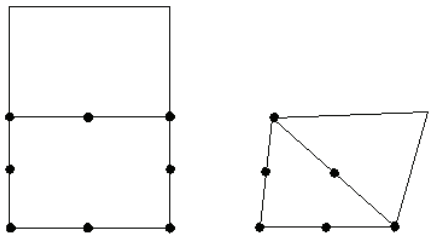


Figure 1: Rectangular and triangular finite elements

In geotechnical engineering, the finite element method involves dividing the soil and structures into discrete elements that are easier to analyze. Then, material properties and behavior are described by a set of predefined models. Equilibrium and energy numerical approximations are then used to simplify the analysis and satisfy all necessary conditions for equilibrium. Thus by the nature of the method, it is unavoidable that all FE analyses will contain a certain degree of numerical error.

$$\begin{bmatrix} \varepsilon_{xx} \\ \varepsilon_{yy} \\ \varepsilon_{zz} \\ \gamma_{xx} \\ \gamma_{yy} \\ \gamma_{zz} \end{bmatrix} = \frac{1}{E} \begin{bmatrix} 1 & -v & -v & 0 & 0 & 0 \\ -v & 1 & -v & 0 & 0 & 0 \\ -v & -v & 1 & 0 & 0 & 0 \\ 0 & 0 & 0 & 2(1+v) & 0 & 0 \\ 0 & 0 & 0 & 0 & 2(1+v) & 0 \\ 0 & 0 & 0 & 0 & 0 & 2(1+v) \end{bmatrix} \begin{bmatrix} \sigma'_{xx} \\ \sigma'_{yy} \\ \sigma'_{zz} \\ \sigma'_{xy} \\ \sigma'_{yz} \\ \sigma'_{zx} \end{bmatrix}$$

E= Young's modulus v= Poisson's ratio
σ'_{xx}= Effective stress

Figure 2: Typical Matrix Equilibrium Set Up.

The most used types of discretized elements are rectangular and triangular elements as shown in Figure 1. The governing equilibrium equations are always performed in matrix operations as demonstrated in Figure 2. However, for more complicated element types the matrix equations can become extremely complicated and time consuming. While matrix operations are daunting to most engineers (including the author), the beauty of recent software developments is that the end user never has to deal with the intricate details of each step by step matrix operation. Thus, research centers and major finite element software organizations have effectively taken the computational burden off the shoulders of practicing engineers. However, at a minimum, a user should be aware of the general manner in which the finite element method is applied by the software program he or she decides to use because in this day and age, it is almost unimaginable for anybody to attempt solving a finite element problem by hand computations.

SOIL BEHAVIOR & STIFFNESS MODELING

One of the major challenges in geotechnical engineering and soil structure interaction is the "true" modeling of soil behavior. In this continuing effort, many researchers have proposed various soil models. Soil models basically comprise mathematical frameworks that relate parameters such as elasticity, stress, displacement, time, failure criteria, and stress history. Most idealized soil behavior can be described by a response included in Figure 3. Most soil models used in finite element analyses generally fall under or combine some of the following categories:

I. Linear elastic soil behavior (strain increases linearly with stress).
II. Linearly elastic-perfectly plastic (strain increases linearly with stress until yielding occurs. Beyond yielding, stress remains the same at increasing strain levels i.e. plastic behavior). These models offer a simple idealization of soil behavior; however, they may not capture correctly displacements near yielding.
III. Non linear models with strain hardening or strain softening behavior. Almost all soil models used in practice can not capture strain softening behavior.
IV. Time dependent features for consolidation and creep. Secondary displacements associated with long term soil creep may have to be considered when modeling soft clays. Soil creep and consolidation are typically not significant issues in temporary works such as

cofferdam excavations that are constructed within a short time span.

V. Different loading and unloading behavior. Overconsolidated soils are typically stiffer when loaded or unloaded to smaller stress levels than the maximum soil stress state experienced in the past. In this region, soils are slightly stiffer in the unloading mode than in the loading mode (Figure 3). All soil models known to the author that include unloading behavior, model both loading and unloading response as linear (in the unloaded region). This behavior is a good approximation when the load is not cycled between two stress levels a significant number of times. Unfortunately, no rational framework has been developed to properly model plastic soil straining from load cycling.

VI.

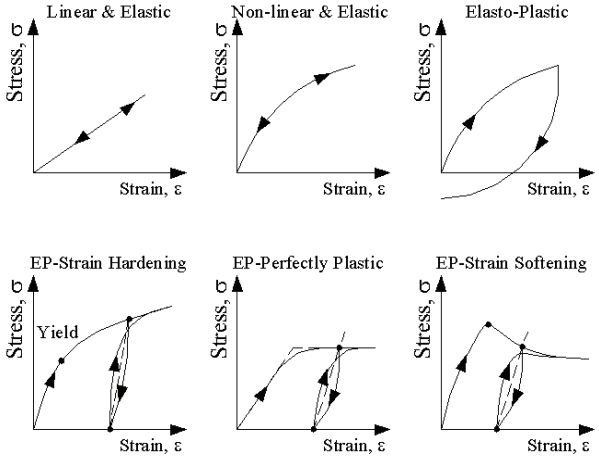


Figure 3: Idealized Modes of Elastic Soil Behavior (Whittle, 2005)

SOIL STRENGTH

An equally important aspect of capturing soil behavior is defining proper failure and yielding criteria. Natural soils Figure considerably more complicated yielding behavior than engineering materials such as steel. Traditionally, soil strength has been described by a cohesive strength and an internal frictional angle (Mohr, 1772). Depending on the soil type, soil strength is strongly on the rate of loading (or unloading). For purely frictional soils (sands) the rate of loadings has almost no effect (with the exception of intense earthquakes).

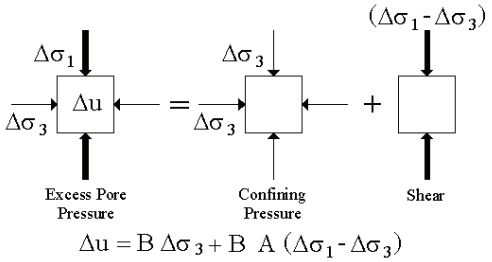


Figure 4: Pore Pressure Parameters (Skempton, 1951)

On the other hand, clays display different strength for short and long term loadings. The short term loading strength behavior is also routinely referred to as “undrained” strength behavior, and has been described by Skempton (1951) and others (Figure 4). Because of its low porosity and internal crystal electrical ionization forces, a clay soil does not allow pore water to easily escape (i.e. drain) when it experiences a “fast” load change. As a result and because water is practically incompressible, excess internal pore pressures develop that resist applied load changes. Hence, initially there is little change in effective stress while the total stress level has changed.

Clay strength is also influenced by the direction of loading (or loading mode). Naturally, clays Figure greater undrained strength in compression than in tension. When basal movements are involved, clays may be compressed, sheared, and stretched as shown in Figure 5. Unfortunately, this strength anisotropy may not be properly captured by a single set of parameters for most soil models. If anisotropy plays a significant role, then one may have to specify different soil strengths for the same soil layer that describe the different loading mode strengths. Unified advanced soil models such as the MIT-E3 soil model can account for soil anisotropy (Whittle & Kavvadas, 1994).

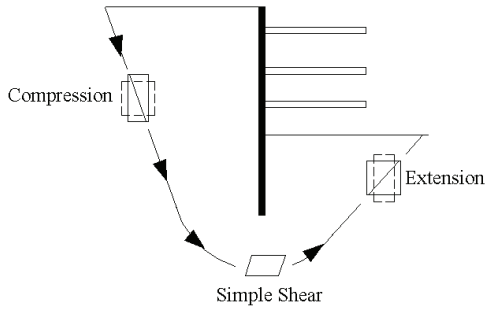


Figure 5: Modes of soil behavior in an excavation with basal movements.

GEOTECHNICAL SAFETY FACTORS

Traditionally, basal and rotational stability safety factors have been defined as the ratio of resisting over driving forces. In finite element methods such safety factor definitions do not have much meaning. Instead, a more meaningful safety factor can be obtained by the ratio of available shear strength over the shear strength that is required to reach failure. Finite element codes can be achieve this task automatically by successively decreasing the friction angle and cohesion of soil materials until failure is obtained. Then the geotechnical safety factor can be described as:

$$Safety\ Factor = \frac{Available\ Strength}{Strength\ at\ Failure}$$

TYPICAL ADVANCED SOIL MODELS

Capturing the "true" soil behavior is a significant challenge. While simple linear-elastic-perfectly plastic models can produce reasonable first order results, a more realistic response can be obtained by simulating soil as a non-linear material. In this respect, two of the most commonly advanced soil models used in practice are:

a) Hyperbolic Soil Model by Duncan & Chang (1970), (called DC model).
b) Hardening Soil Model by Vermeer (1978), Schanz (1998), (called HS model).

Both models use a reference confining pressure to define soil stiffness, however, whereas the DC model uses the atmospheric pressure as a reference (100 kPa, 2.04 ksf), in the HS model the reference confining pressure is a variable. The models are also similar in that they use hyperbolic shear stress-strain formulations (Figure 6). One of the differences between the two models, is that the DC model is defined by the initial stiffness E_i while the HS model uses the secant modulus E_{50} (at 50% of the ultimate stress level). The two stiffness parameters can easily be correlated to each other. A further similarity between the two soil models is they both simulate unloading and reloading with a linearly elastic stiffness response (E_{ur}). In cofferdam excavations, the unloading/reloading modulus is a very important parameter since soils are unloaded laterally and vertically. In this respect, the linear modeling of the unloading/reloading behavior predicts slightly greater unloading and reloading strains.

While both models use a hyperbolic loading response, the HS model can capture volume changes associated with dilation during shearing that the DC soil model can not account for. This is achieved by hardening of the yield surface in

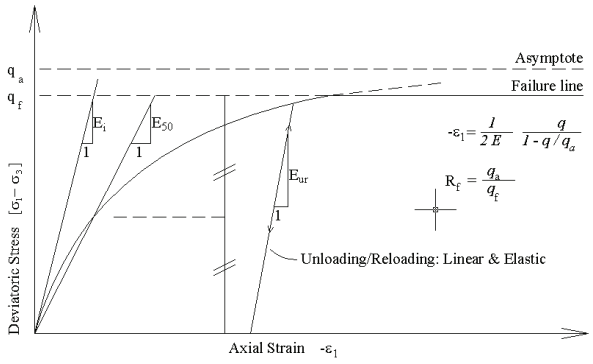


Figure 6: Hyperbolic Stress Strain Modeling

association with a flow rule that relates volumetric strains to shear strain together with the ultimate dilation angle. The theoretical background is based on the critical state mechanics concept of the constant volume frictional angle that predicts shear resistance at large strains. Strain hardening can also occur during compression loading as shown in Figure 7. The cap surface essentially defines a set of stress path combinations beyond which a soil would experience a loading response (for HS & DC models this would be a hyperbolic behavior). If the stress path retracts within the cap then the behavior will be controlled by the unload/reload response of the soil model (in HS & DC this is a linear elastic response). Beyond the current maximum state of stress experienced by a soil, when compression is increased and the stress path remains within the Mohr-coulomb failure line, the cap expands typically as shown in Figure 7. For both the HS and DC models this cap surface is described by the equation of an ellipse.

While the HC and DC models are considered advanced soil models, they both share similar shortcomings. Most significantly, strain softening behavior at very large strains is not captured by any of the two models. Another limitation is that the cyclic loading plastic strains (repeated unloading/reloading between two similar stress conditions) can not be captured.

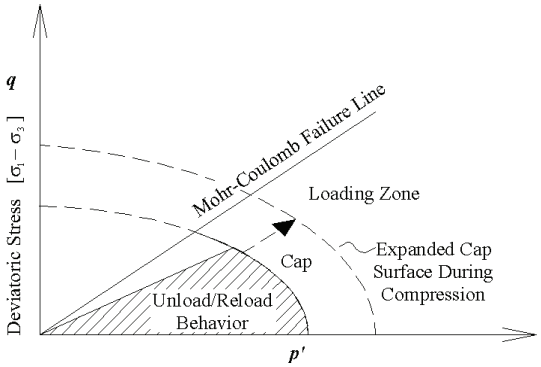


Figure 7: Cap Surface

SOIL TESTS & FINITE ELEMENT PARAMETER SELECTION

Selecting appropriate engineering properties of soil materials for finite element analyses can be as challenging as performing finite element computations by hand. As designers, we are confronted with a number of parameters that have to be selected. Adding to complexity, soil properties are variable even in laboratory tests and a number of factors can influence test results one way or the other. As a result, considerable judgment is required in selecting appropriate stiffness, strength, and engineering soil parameters.

While there is no single best way to estimate soil parameters, a combination of in-situ and laboratory tests generally provides data to estimate most desired parameters. Table 1 provides a list in-situ and laboratory soil tests that can be used to estimate specific engineering soil parameters. From a quick view of Table 1 one realizes that there is no single test that can cover all soil properties. However, one should use caution with the standard penetration test (SPT). Engineering properties estimated with SPT tests are highly speculative and should not be relied upon.

Cone Penetration Tests (CPT) offer a more viable way to obtain engineering parameters, especially when results are calibrated against laboratory tests. CPT can be especially useful in sands that are difficult to sample and test in their natural state without disturbance. For sands, stiffness parameters for sands can be estimated from published charts as shown in Figure 8. It is the author's opinion that a good balance of cone penetration tests and laboratory triaxial shear tests is the best way to estimate soil properties. The author is aware of sites where more than 200 borings with SPT tests have been completed over the last 60 years and no proper soil tests ever been conducted! When there are no available soil test data then parameters can be estimated from available published information. In this case, performing sensitivity analyses with varying strengths and stiffness scenarios is probably a very good idea.

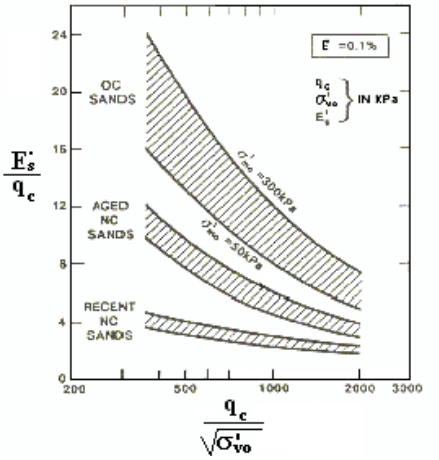


Figure 8: Estimation of secant modulus of elasticity for sands from cone penetration tests (PLAXIS B.V., 2003)

As discussed before, cohesive soil Figure time-dependent response. For undrained loading, the modulus can be described by either the undrained Young's modulus E_u or the shear modulus G. The shear modulus actually describes the soil "skeleton" response, so it is independent of drainage conditions, all other factors being equal (Kulhawy & Mayne, 1990). Duncan and Buchignani (1976) have compiled a very useful chart for estimating the ratio of undrained secant modulus to undrained shear strength of overconsolidated clays (Figure 9).

In cofferdams soil is primarily unloaded as the excavation progresses. Thus when hyperbolic soil models are used, the predicted behavior is controlled by the linear reload-unload modulus of elasticity (E_{ur}). As a first order estimate E_{ur} can be taken as three to four times the secant modulus of elasticity E_{50} for sands, and as three to five times E_{50} for normally consolidated clays. Over-consolidated clays typically have greater ratios of E_{ur}/E_{50}. E_{ur} should be estimated directly from test data when possible.

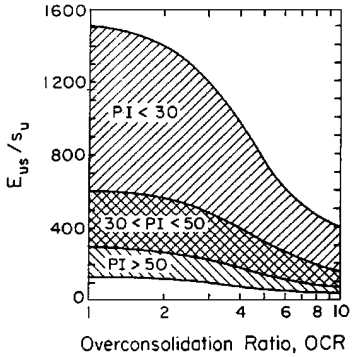


Figure 9: Generalized Undrained Modulus Ratio versus OCR and PI (Duncan & Buchignani, 1976)

Table 1: Matrix relating model parameters to soil investigation, (CUR 195, 2000)

Soil investigation tests / Parameters	Cone (piezo) Penetration tests	Dissipation tests during CPT	Pumping test	CPM-tests, Menard test	In-situ Vane test	Dilatometer test	Standard Penetration test	Oedometer test unload reload	Triaxial tests: Unconfined Undrained	Triaxial tests: Consolidated Undrained Standard	Triaxial tests: Consolidated Undrained Extension	Triaxial tests: Consolidated Undrained Compression	Triaxial tests: Consolidated Undrained unloading	Triaxial tests: Consolidated Drained tests	Direct and simple shear tests	Classification tests	Torvane tests	Sieving	Constant and falling head	Unit weight (wet and dry)
γ_{dry}	X			X		X	X									√				√
$\gamma_{wet\ (saturated)}$	X			X		X	X									√				√
k_x	X	X	√	X				X										X	√	
k_y	X	X	√	X				X										X	√	
c_k			√					X											X	
e_{init}								X								√		X		
e_{min}																√		X		
e_{max}																√		X		
E_{ref}	X			X		X	X	X		√	√	√	√	√	X	X				
G_{ref}	X			√		X	X	X		X	X	X	X	X	√	X				
E_{oed}	X			X		X	X	√		X		X		X	X	X				
E_{50}^{ref}						X	X	X		√		√		√						
E_{oed}^{ref}						X	X	√												
E_{ur}^{ref}				√							√		√	√						
power (m)										√				√						
R_f										√	√	√	√							
λ^*	X							√								X				
κ^*								√								X				
μ^*								√								X				
K_o^{nc}	X			√		X														
OCR	X			X		X		√								X				
POP								√												
ν				X						√		√		√						
ν_{ur}				X							√		√							
c'	X				√	X			√	√	√	√	√	√	√	X	√			
φ'	X			X		X				√	√	√	√	√	√	X	X	X		X
ψ	X			X						X	X	X	X	√						
max. tensile strength										X			√	X						

√ Means that the model parameter can directly be evaluated from the test.
X Means that the model parameter can be estimated through correlations.

FINITE ELEMENT MODELING STRATEGY

Formulating an appropriate modeling strategy is essential in generating a finite element model that "reasonably" captures the behavior of a cofferdam excavation. In this respect the GIGO principle applies to all finite element simulations (good input = good output). A good modeling strategy should include some of the following steps:

I. Finite element model layout: Drawing a model simplifies the thinking process and sometimes may reveal mechanisms of failure or other considerations that have to be taken into account. In general, models should extend at least two to three times the excavation depth (or wall depth) beyond the excavation. When basal instability is an issue, the model depth should extend to a stiff boundary (such as bedrock) and include all clay layers that contribute to basal movements.
II. Soil parameters: Appropriate selection of soil strength and stiffness parameters from laboratory or in-situ tests as described in the previous section. When soil tests are absent then parameters can be estimated from published literature as first order estimates.
III. Construction staging: Finite element models of cofferdam excavations should accurately model construction staging by including all stages and construction activities affecting results. Typically, all multi-prop excavations should include a cantilever stage and then subsequent installation of bracing and further excavation until final subgrade is reached. When excavations in clay are modeled, it may be more appropriate to consider construction times between stages in the analysis. In some cases it may be prudent to include ground modifying effects such as jet grout installation and soil loses where appropriate.
IV. 2D vs. 3D: Although the main focus of this paper is on two dimensional analyses, three dimensional effects can be considerable in cofferdam excavations of limited width. While in engineering practice three dimensional effects are typically ignored, one may be able to obtain more economical designs if such effects are included. However, despite the increase in computational power 3D analyses can still be very time consuming.
V. Engineering judgment: Ironically, one of the most important aspects of finite element analyses is the human factor. Once an analysis has been performed, results must be criticized with considerable judgment by a qualified engineer with experience in actual excavation behavior. Performing sensitivity analyses also yields valuable insight. It is always useful to compare finite element results against conventional design methods. In this respect, performing a conventional design bounds the problem and gives indications of expected finite element results.

CASE STUDY ANALYZED WITH FINITE ELEMENTS

A useful case study is presented in this section. The cofferdam studied was constructed within the reservoir pool of the Martin Manatee dam in Manatee, Florida. The dam is 23 ft high earth filled dam with a soil-cement face. A new intake structure was to be constructed 5 ft from the tail of the dam. This involved the construction of a 58 ft long by 39 ft wide cofferdam with the subgrade nearly 40 ft below maximum water pool elevation (Figures 10, 11). Ground movements caused by excavation and fill placement had to be minimized in order to avoid breaching the dam and causing failure. Support of excavation was provided by three levels of stacked internal bracing that were slid into their design elevations. Excavation was performed in the wet and dewatering took place only after the base slab had been poured and gained sufficient strength.

Soils at the site consist of cemented sands and a softer clay layer at 20 ft below subgrade. Available soil information did not include any laboratory strength tests on the soft clay layer. Hence, soil stiffness parameters had to be estimated using cone penetration data performed on a nearby site using published information (Figure 8). A summary of estimated soil properties is available in Table 2.

Table 2: Typical Finite Element Parameters

	LF	Dam	IA	IB	II	III	IC	IV	V	Unit
-	Light Fill				Sand Layers			Soft Clay	Stiff-Clay	
Note:	DR	DR	DR	DR	DR	DR	DR	U	U	-
γ_{dry}	60	120	115	115	120	115	120	105	120	pcf
γ_{wet}	90	120	115	115	120	115	120	105	120	pcf
E_{ref}	700	600	500	650	1500	150	400	70	600	ksf
p_{ref}	2.0	2.0	0.5	1.8	1.1	2.0	2.0	2.0	2.0	ksf
c_{ref}	-	-	-	-	-	-		400	1600	psf
Φ	40	34	35	35	40	30	36	-	-	Deg.
R	0.8	0.8	0.8	0.8	0.8	0.8	0.8	0.8	0.8	-

DR: Drained behaviour
U: Undrained brhaviour

A typical FE model can be seen in Figure 12. Initial models indicated lateral soil movements in excess of 1.0 inch towards the excavation. Predicted settlements were even greater due to rip rap being placed on top of the existing dam behind the sheeting. While it was recognized that the problem was inherently three dimensional, the owner was

very risk averse. As a result, full three dimensional effects were not incorporated into the finite element analyses. Contract documents required a minimum rotational safety factor of 1.5. Finite element models showed that replacing the proposed rip rap with a light fill (LF in Figure 12) would significantly minimize predicted wall and soil movements and increase geotechnical safety factors. In addition, battered piles were utilized to further minimize lateral soil displacements after final backfilling behind the cofferdam.

During construction, the dam was intensively monitored with a number of settlement monitoring points and inclinometers. Practically no soil movements were registered from inclinometers. Predicted lateral sheet pile movements after the base slab had been poured and the cofferdam dewatered were in the order to 0.5 inches. This discrepancy in predictions and measurements can be attributed mainly to three factors: a) three dimensional soil behavior was ignored, b) Sand cementation was ignored, and c) the soft clay layer in all likelihood is not continuous and is interbedded with sand and silt. Figure 13 shows predicted horizontal and basal soil movements with estimated lateral displacements in the order of 0.5 inches.



Figure 10: Cofferdam during construction

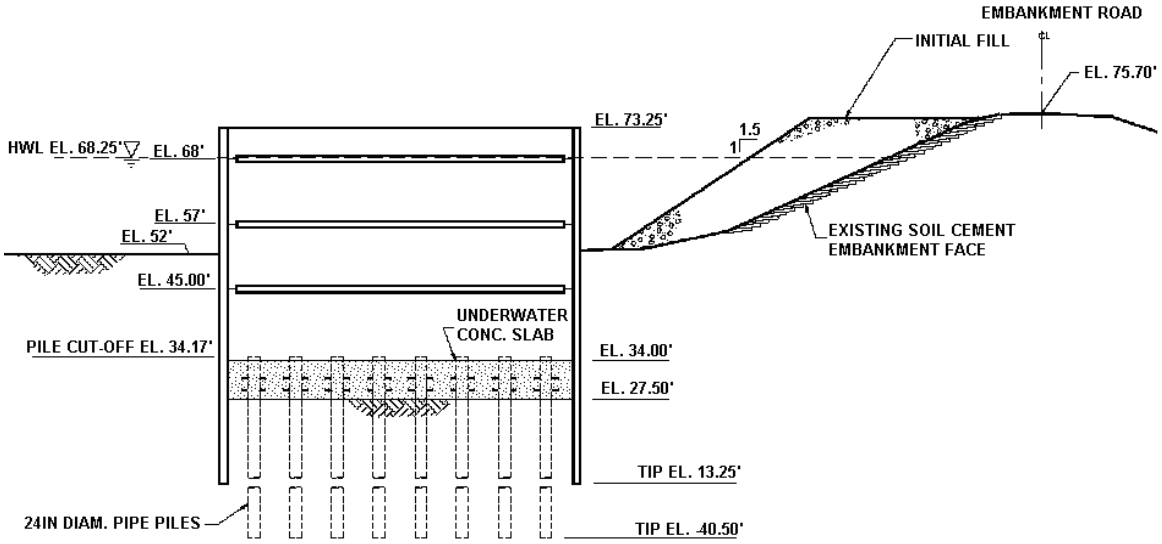


Figure 11: Section of cofferdam excavation

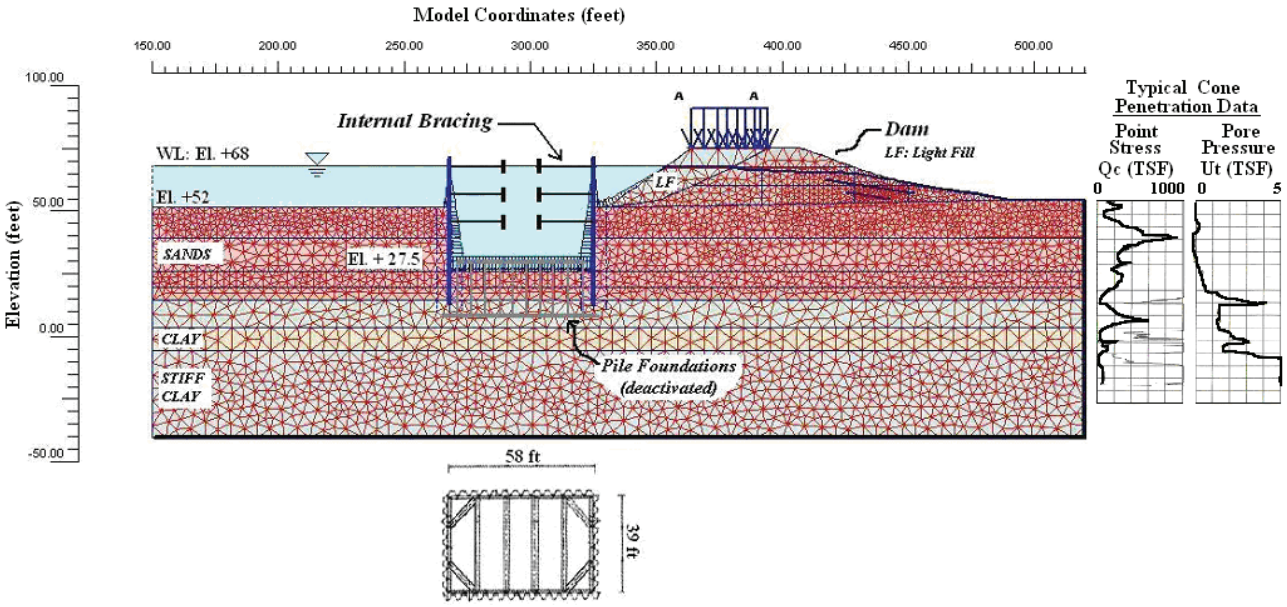


Figure 12: Finite element model at final subgrade

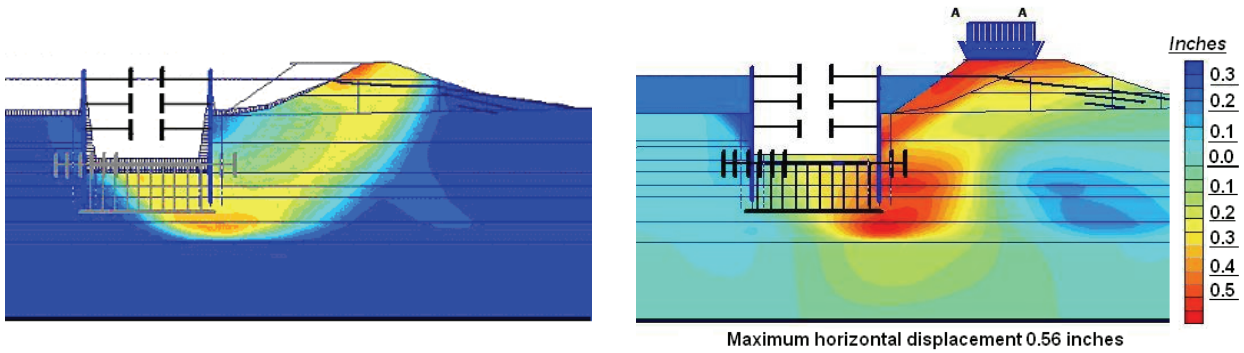


Figure 13: Basal failure mode and predicted soil displacements with 2D finite element analysis.

FUTURE AND CONCLUSIONS

While significant progress and achievements have been made in the field of geotechnical finite element mechanics, further advancements are necessary. On the practical side, as computational power increases it is expected that three dimensional software programs will be come increasingly popular and more affordable. On the theory, further research is required to formulate models that capture soil softening, and hysteretic cyclic unload-reload behavior. The continuation of benchmarking efforts is essential to the acceptance and modification of finite element methods in geotechnical engineering.

Not all aspects of finite element modeling have been covered in this article. Numerous publications discuss practical and theoretical aspects in much greater detail. The author encourages the interested reader to further investigate as many relating publications as possible. One should keep in mind that there is no single answer to geotechnical problems and especially finite element analyses. It is almost certain that two different analysts will in all likelihood produce two different results for the same problem. Hence, human judgment is by far the most important aspect of finite element analyses of cofferdam excavations.

REFERENCES

Brinkergreve, R.B.J., Vermeer. P.A., “PLAXIS – Finite Element Code for Soil and Rock Analyses”, 1998, Users Manual – Version 7 for Windows 95/NT. A.A. Balkema, Rotterdam, The Netherlands

PLAXIS, B.V., “PLAXIS Bulletin No. 13”, January 2003, Plaxis B.V., The Netherlands

CUR 195, “Backgrounds on Numerical Modelling of Geotechnical Constructions”, Part 3, Centre for Civil Engineering Research and Codes, April 2000, CUR, Gouda, The Netherlands

Duncan, J.M. and Chang, C. –Y., “Nonlinear Analysis of Stress and Strain in Soils”, Journal of the Soil Mechanics and Foundations Division, ASCE, Vol. 96, No. SM5, Sept. 1970, pp. 1629-1653

Duncan, J.M. and Buchignani, A. L., “An Engineering Manual for Settlement Studies”, Department of Civil Engineering, University of California, Berkley, June 1976, 94p.

Kulhawy, F.H. and Mayne, P. W., “Manual on Estimating Soil Properties for Foundation Design”, Cornell University, 1990, Geotechnical Engineering Group, EL-6800, Research Project 1493-6

Peck, R.B., “Deep Excavations and Tunneling in Soft Ground”, 1969, 7th ICSMFE, State-of-Art Volume, pp. 225-290

Schanz, T., “A Constitutive Model for Hard Soils”, 1998, The Geotechnics of Hard Soils – Soft Rocks Vol II, Balkema, Rotterdam, The Netherlands, pp. 861-868.

Skempton, A.W., "The Bearing Capacity of Clays", 1951, Proc. Building Research Congress, vol. 1, pp. 180-189.

Vermeer, P.A., “A Double Hardening Model for Sand”, 1978, Géotechnique 28, No.4, 413 - 433

Whittle, A.J., “Computational Geotechnics; New York, January 2005”, 2005, Plaxis Course Material, New York, NY.

Whittle, A.J., Kavvadas, M.J., “Formulation of MIT-E3 Constitutive Model for Overconsolidated Clays”, January 1994, Journal of Geotechnical Engineering, Vol. 120, No. 1, pp. 173-198

COOPERATIVE EFFORT OVERCOMES PROBLEMS WITH PIER AND COFFERDAM CONSTRUCTION CAUSED BY ROCK SLOPE

Herbert F. "Buck" Darling, III, Herbert F. Darling, Inc., Williamsville, NY
Richard J. Hartman, Hartman Engineering, Clarence, NY

A bridge replacement project in Rochester, NY, encountered difficulties when it was determined that rock below one pier was sloping downward toward the river at an angle of 42 degrees versus anticipated 12 degrees. Cofferdam design and construction became very difficult. The unanticipated subsurface conditions delayed the project by eighteen months and increased the cofferdam cost by almost $3.0 million ($US) when direct costs and associated delays were taken into account. The initial approach after discovery of the problem was to use the same type pier design and modify the cofferdam accordingly. This resulted in a cofferdam 12 meters (39.4 feet) deep on the shore side and 18 meters (59.0 feet) deep on the water side. The design used a master pile system to attain required wall strength and used rock anchors to prevent the cofferdam from moving toward the river. The pier foundation was then redesigned by the owner using revised seismic parameters. The original stepped footing carved into rock was replaced by caissons socketed into the rock beneath a large tremie concrete placement. The revised pier and cofferdam designs caused a shift from a mostly land based cofferdam, excavation, and rock removal project into an almost entirely water based cofferdam, caisson drilling, and tremie construction project. These design changes resulted in a reliable, safe, and unusual cofferdam and construction method. All of this was accomplished within a very narrow worksite with a railroad on one side, and the river with its public and commercial freighter traffic on the other. In addition, the existing two-leaf drawbridge was to be maintained in place which put further limitations on the water borne equipment. The engineering and construction considerations, problems, and solutions related to these cofferdams and pier foundations are presented.

History

The Stutson Street Bridge over the Genesee River in Rochester, NY was built in 1917 as a double leaf bascule bridge. It provided access to both sides of the river while allowing recreational and commercial boat traffic. Having reached the end of its service life, and due to the fact that commercial freighter traffic and cruise traffic were still using that portion of the river, a new lift bridge was required to replace the existing one. In July of 2000, the Monroe County Department of Transportation (MCDOT) in conjunction with the New York State Department of Transportation (NYSDOT), which provided the conceptual design and which would provide construction oversight, let out for bid the contract documents for what would become the new Colonel Patrick O'Rorke Bridge. The bridge was so named in honor of a local Civil War hero. The design of the new bridge called for two abutments and four piers, and two of the piers would require cofferdams in the river. The two abutments were to be supported by HP305x79 (HP12x53) piles. Pier 1, located in the river, was to be founded on rock. Piers 2 through 4 were to be supported by HP356x174 (HP14x117) piles, with Pier 2 also a river pier. Herbert F. Darling, Inc., (HFD) elected to bid the piling portions of the project as the piling subcontractor.

Early on in the bidding process, it was apparent that one of the two river piers, Pier 1, would not be of normal construction. Pier 2 was constructed using standard methods; it utililzed an H-pile foundation, a large tremie concrete placement inside a typical cofferdam, all designed in accordance with the original bid documents. Pier 2 was located only 50 meters (164.0 feet) face to face from Pier 1 which was founded on rock at approximately 15 meters (49.2 feet) depth. Pier 2 required HP356x174 (HP14x117) piles 27 meters (88.6 feet) long to reach rock. Pier 1,

however, was to be especially difficult because of differential water and soil depths to rock across the cofferdam width, the large size of the pier, the need to excavate contaminated river sediments to rock, and to also excavate rock underwater to a stepped pattern. As a result of these perceived difficulties, Hartman Engineering was retained as the cofferdam design consultant to provide pre-bid and post-bid consultation for methods and means of river cofferdam construction. As early as the middle stages of the bidding process, there were concerns regarding elevations of the rock at Pier 1, but nothing specific could be determined with the available information. A soil boring location plan is shown in Figure 1.

A cofferdam design was then discussed and bid, based upon the assumption that conditions would be as presented in the contract bid documents. That is, that a rectangular steel sheet piling cofferdam with multiple rows of bracing would be founded on rock believed to slope at approximately 12 degrees across the width of the cell. This cofferdam would allow excavation of the river sediments and excavation of the stepped foundation in the rock.

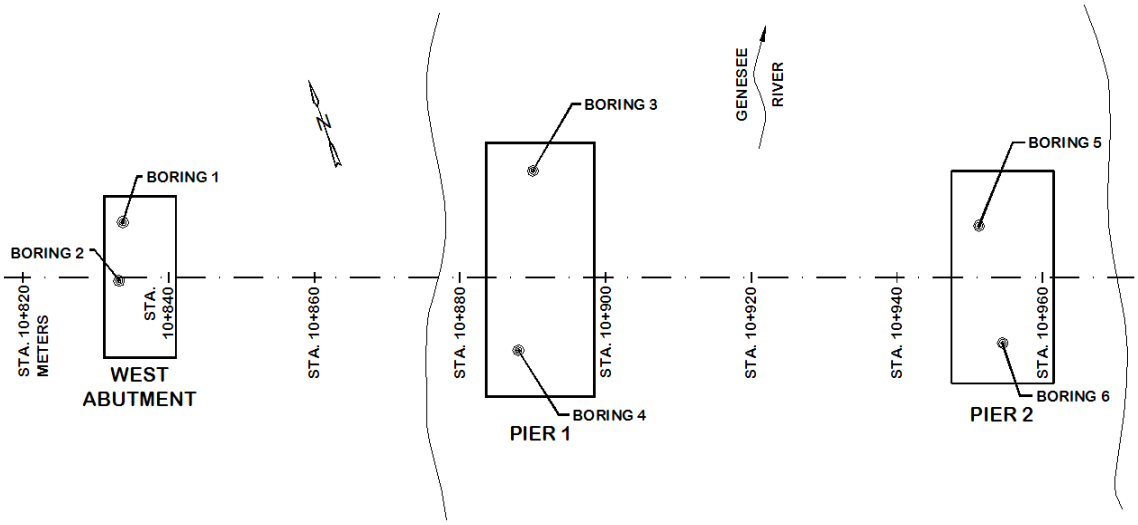


Figure 1 – Boring Location Plan

The bid estimate was completed and bids submitted to the owner on July 24, 2000. Crane Hogan Structural Systems of Rochester, NY, was the apparent low bidder. MCDOT officially awarded the general contract, and a groundbreaking was held on September 27, 2000. Shortly after that, the general contractor awarded a subcontract in the amount of $4.2 million dollars ($US) to the piling subcontractor to perform minor water side demolition work, bearing pile, fender pile, and fender timber installation, drilled shafts for river dolphins anchoring the fender system, river cofferdam installation, and cofferdam excavation work. After the subcontract was finalized, the cofferdam design consultant was formally retained by the piling subcontractor to perform design work for the two piers located in the Genesee River.

Cofferdam Designed for Anticipated Conditions

The original pier design required construction of a cofferdam with plan dimensions approximately 14 meters by 35 meters (45.9 feet by 114.8 feet). Rock was anticipated to slope approximately 12 degrees, or 3 meters (9.8 feet), toward the river across the width of the cofferdam and 5 degrees, or 3 meters (9.8 feet), along the length of the cofferdam; thus, across a diagonal connecting opposite corners of the

cofferdam, the maximum anticipated change of elevation of the rock was 6 meters (19.7 feet). The soil surface was level along the cofferdam length but sloped at approximately 12 degrees, similar to the rock, across the cofferdam. The foundation design called for 24 rectangular flat areas to be excavated into the rock, all at different elevations. The rock at the site is known to be shale at the elevations involved in the construction. The cofferdam designed for anticipated conditions is shown in Figure 2. The components are standard materials consisting of Z-shape sheet piling, pipe struts, and W-section wales. A tremie concrete seal was to be placed on the excavated rock and would extend upward to the elevation of the bottom of the pier foundation.

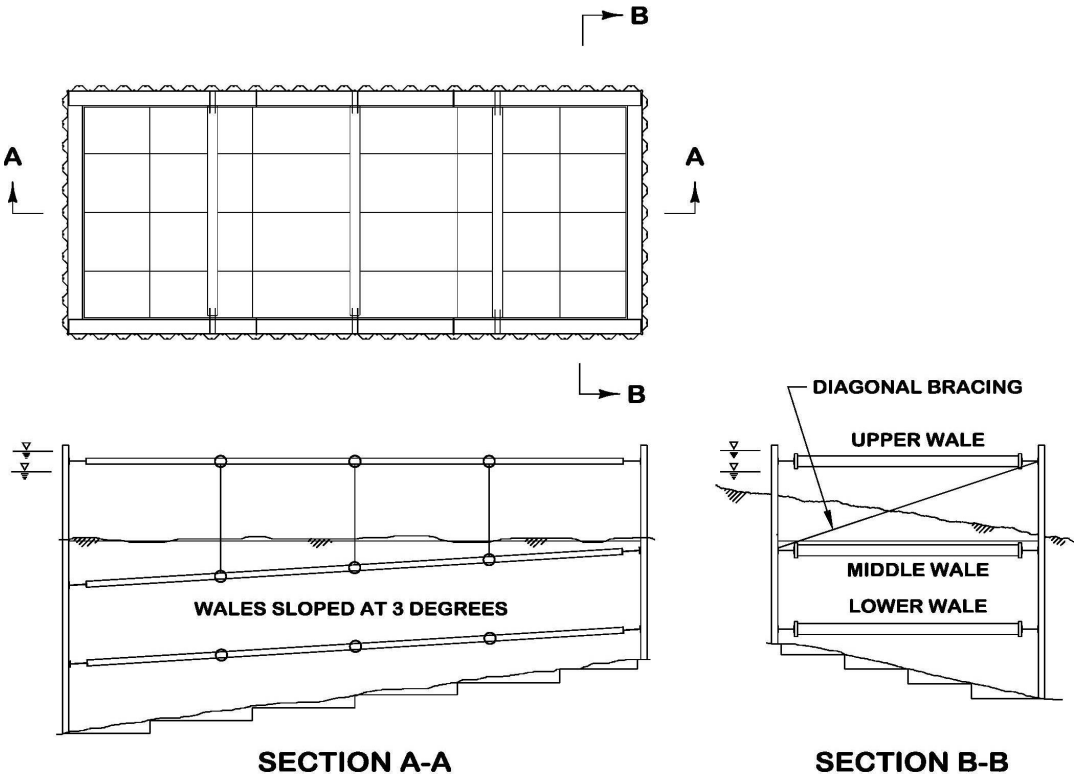


Figure 2 – Anticipated Cofferdam

Design and construction of the cofferdam presented technical challenges resulting primarily from the changes in elevation of the soil and rock. Due to the soil slope, diagonal bracing was required between the 1st (upper) wale level and the 2nd (middle) wale level in order to prevent movement of the 1st level of bracing toward the water. Due to the rock slope, the 2nd wale level and 3rd (lowest) wale level were required to slope approximately 3 degrees parallel to the cofferdam length in order to remain above the highest rock and still control sheet piling spans at the locations where the rock was lowest.

Construction was anticipated to proceed along conventional lines. The three levels of bracing would be pre-fabricated, stacked together, and set in location on spud piles (piles driven to support the dead loads of the bracing prior to attachment to the sheet piles). Sheet piling would be set and driven around the perimeter. Excavation of soil would proceed until the 2nd and 3rd levels of bracing, still stacked together, could be lowered so that the 2nd level was in final position. Diagonals and posts would be installed between the 1st and 2nd bracing levels. Then soil would be excavated as necessary to allow the 3rd level to be

lowered into final position. After lowering the 3rd level, the remaining soil would be excavated. When the soil excavation was completed, the rock would be excavated to form the 24 rectangles required for the foundation.

Provisions were made in the design for normal variations in rock elevation. The elevation of the bottom of each sheet pile would be monitored; this would ensure that the occurrence of gaps between the sheet piling and rock would be detected, and they could then be closed. In addition, if sheet piles extended deeper than anticipated, toe pins cut from steel rod would be set into holes drilled in the rock to restrain the bottom of the sheet piling.

From a constructability standpoint, this conventional type design would presumably have few difficulties associated with it. It would be possible to install the sheet piling from land, and the bracing could be installed in pieces sufficiently small and of appropriate weight for the crane to handle and eventually lower into place. Excavation would be incrementally performed and the bracing elements sequentially lowered to their proper positions. In summary, it would be a normal cofferdam installation utilizing typical, readily available materials and construction methods.

The Start of Cofferdam Construction

With the early phases of the general contractor's work on the project proceeding on schedule and knowing that the river piers were in the critical path, the piling subcontractor began the submittal process for all its required work. In order to purchase sheet piling necessary for Pier 1 installation, more accurate elevation data was required to determine the proper lengths. The piling subcontractor wished to perform a probing program utilizing a long H pile and a vibratory hammer along specific section lines in order to determine the rock elevations.

Unfortunately, no work was allowed in the river until November 15th in order to protect spawning salmon, trout, and steelhead. On September 13, 2000, and again on October 26, the piling contractor requested special permission of the owner to enter the water to perform the probing, citing the need to complete the cofferdam design and order the sheet piles to allow cofferdam construction to start on the first unrestricted day in the river. Access was denied. The New York Department of State had jurisdiction over all other regulating bodies involved in the construction process. After repeated requests and negotiation, permission was granted to access the water in order to perform the probing.

Preliminary probing began November 21st, and the data showed a much steeper rock slope at Pier 1 than had been anticipated. Formal written notice of the changed condition was forwarded to the general contractor for transmission to the owner. This notice was written to include the opinion that major delays and cost increases were likely due to the unexpectedly steep rock slope.

In the meantime, mobilization of a crew and equipment to the site occurred on November 14th in preparation for the first non-restricted water work date of November 16th. The first order of business was to build a new docking structure for trans-loading materials and docking of water equipment. Then work would begin on the Pier 2 cofferdam template and sheet piling. This would allow the unexpectedly more complicated design of the cofferdam for Pier 1 to be undertaken with the least disturbance possible to the overall project schedule.

Discovery of Unanticipated Rock Conditions

The piling subcontractor conducted a program to map the top elevation of the soil and rock in the vicinity of the cofferdam location. Soil elevations were established using a weighted tape and rock elevations were determined using an H-Pile probe driven with a vibratory hammer. Soil elevations were found to be essentially as anticipated. However, the top surface of the rock sloped toward the river, or across the cofferdam, much steeper than anticipated. The originally anticipated 12 degree slope was found to be 42 degrees, resulting in 13 meters (42.7 feet) of elevation change across the 14 meter (45.9 feet) cofferdam

width. Rock slope along the cofferdam length was found to be approximately 5 degrees, resulting in 3 meter (9.8 feet) elevation change along the length; this was consistent with the previous data. However, the change from 12 degree to 42 degree slope across the cofferdam width presented major problems. Whereas the anticipated difference in rock elevation diagonally across the cofferdam was 6 meters (19.7 feet), it was now 16 meters (52.5 feet).

After the probing established that the elevation of the rock surface was much different than anticipated, borings were taken and soil samples and rock cores were collected. Soil was confirmed to be a typical mixture of sand and silt. Rock cores confirmed that the rock was shale but examination of the rock and experimentation with it established that the rock was very poor quality; it lost all its strength when disturbed, and it would disintegrate into particles if placed in water and slightly agitated. These rock properties presented additional major difficulties for both design and construction.

Deep Cofferdam with Rock Excavation

Meetings were then conducted among the owner, contractors, and the contractors' consultants in order to determine the best solution to the problems. The owner wished to maintain the same type of pier foundation, i.e., a tremie concrete seal placed on top of horizontal rectangular platforms excavated into the rock; the number of rectangles was reduced to 8 from the original 24. Figure 3 shows the primary features of the cofferdam system designed for the deep excavation. The design presented numerous challenges and construction was anticipated to be very difficult.

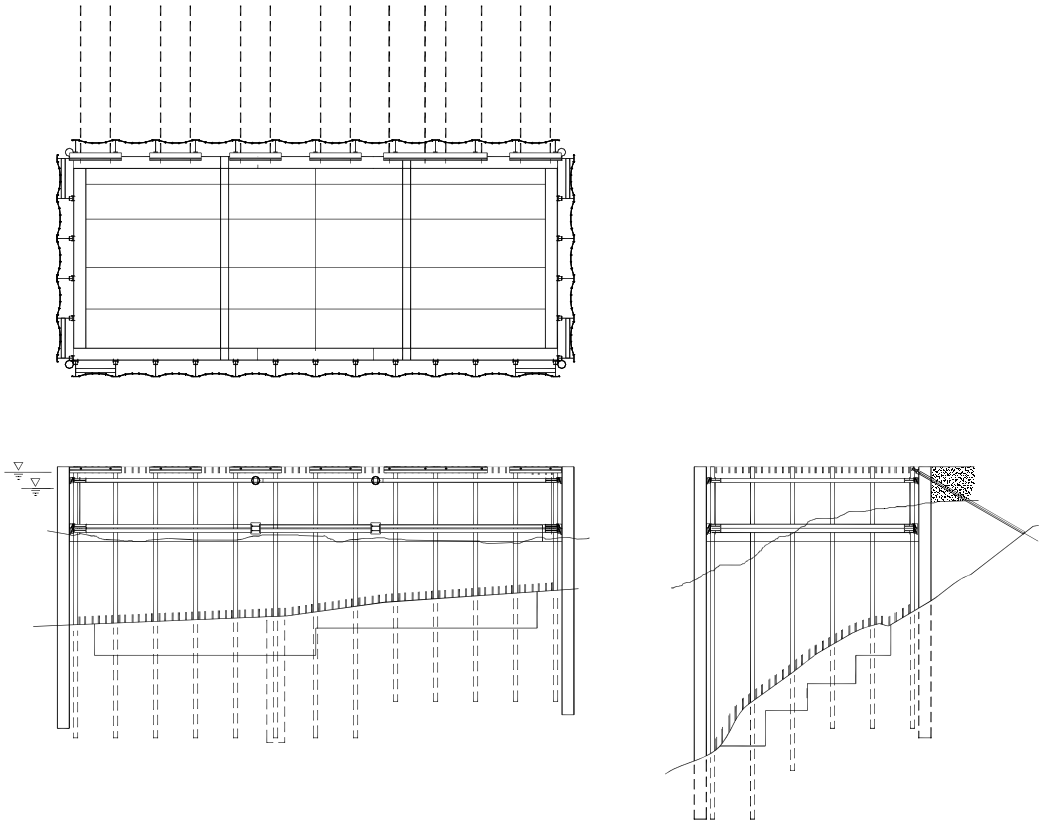


Figure 3 – Deep Cofferdam with Rock Excavation

An obvious problem was the long spans, up to 16 meters (52.5 feet), to which the walls were subjected. They required a wall with strength greater than can be provided by conventional sheet piling. There were two options. One was a master pile system, which utilizes W section master piles with flat sheet piles (PS type) between the master piles. The other was a combination wall system which utilizes W section master piles with Z-shape piles between. In both cases the master piles would be W36

Another problem was that the very steep rock slope resulted in a large unbalanced force applied to the cofferdam. The method selected to resist the unbalanced force was a set of 14 rock anchors installed along the wall on the land side. As shown in Figure 3, soil would be placed between the cofferdam and shore in order to provide passive resistance to allow testing and loading of the rock anchors.

From a construction standpoint, this design represented an increase in complexity over the initial design. A routine land based installation became a complicated water based operation. Constructability and material availability were becoming major issues. The schedule was slipping away, so no materials could be used that would require long lead times. This system would require a large amount of pre-fabrication to allow bracing installation below water by divers. In order for this installation process to be planned and to allow for tolerance in placement of the drilled piles, wales were designed to be smaller than the inside dimensions of the sheet piles by 0.3 meters (1.0 feet). In order to then fill in this gap, thus effectively blocking the wale to the pile, special upper and lower steel wedge blocks would be fabricated. Special plates designed to hang from the outside face of the wale would be fabricated with a sloping face toward the master pile to accept the wedges, all of which could be handled by a diver.

Because of the steeply sloping rock only two rows of bracing could fit into the rock excavation geometry. As a result of this, the lower wale now consisted of double W920x271 (W36x182) beams. The finished row of bracing was so heavy that the crane sections and would be set into holes drilled into the rock. The master pile system with flat sheets was selected for two reasons. First, a larger distance could be used between master piles, thus reducing the number of master piles and the number of holes that must be drilled for rock sockets. Second, the piling subcontractor was concerned about the difficulties associated with alignment of the master piles and considered that the system using flat web sheet piles provided more flexibility.
could not be used to lower it into final position. Thus, a mechanical system utilizing hydraulic cylinders, threaded rods, nuts, and plates was designed for hanging the wale above the water, and later, lowering the bottom wale into place.

The selected master piles were W920x201 (W36x135) and W920x253 (W36x170) sections with cover plates welded to one flange, and a specially bent PS27.5 flat sheet pile welded to the other flange. The size and weight of the material was increasing significantly. The weight of these materials would become unmanageable given the availability of standard equipment. The drill rig to install the master piles would have to be mounted on a barge in order to access all the master pile locations. Finally, the sheer enormity of the drilling task led to schedule concerns. There were a total of 38 holes that would need to be drilled. Paradoxically, and in accordance with previous experience, the very rock that could not be counted upon to carry the design loads of the pier once exposed to water would likely be very difficult to drill in-situ. This could lead to accuracy problems in the placement of the piles. The piling subcontractor was also concerned that there would not be sufficient room for error in being able to install the flat web sheet piles between the master piles given the uncertainty of the master pile final locations.

Revised System Using Drilled Shafts to Support the Pier

Considering the multiple difficulties associated with the deep cofferdam, the owner elected to modify the design of the pier foundation. Extensive work was required for redesigning the pier in order to resolve difficulties associated with the rock

slope and seismic considerations. The redesigned pier and resulting cofferdam system as constructed are shown in Photograph 1 and Figure 4.



Photograph 1 – Cofferdam for Pier 1 and Completed Pier 2

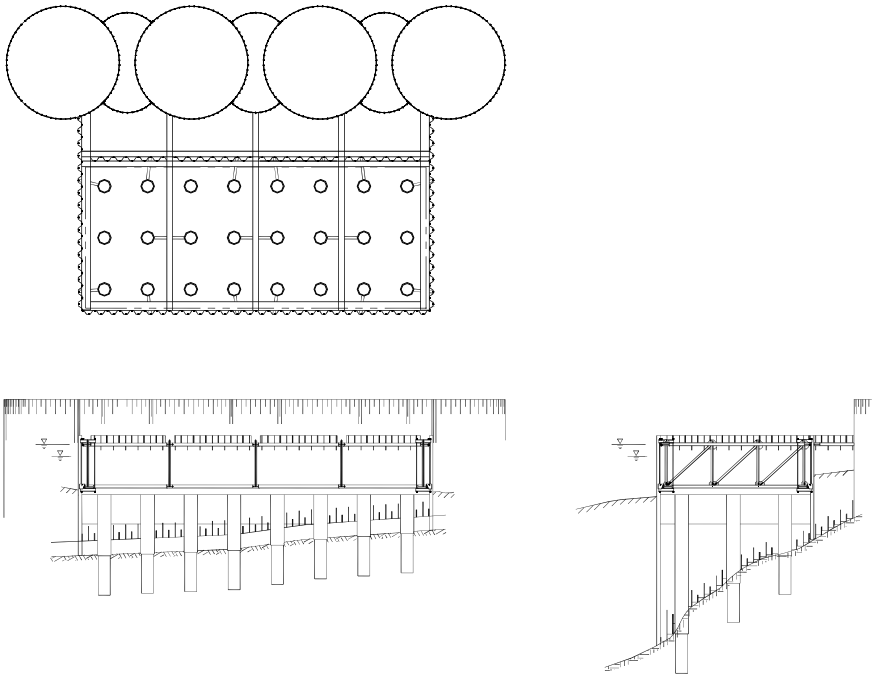


Figure 4 – As Built Cofferdam with Drilled Shafts

The cofferdam design and construction both faced challenges but the system was much safer for construction personnel, primarily divers, and the pier foundation was much more reliable. In overall concept, the pier is supported on 24 drilled shafts, and a tremie seal was installed to allow dry construction of the pier footing. Horizontal restraint was still required to resist the unbalanced horizontal load. The revised design used circular cells and connecting arcs as anchorage and tension members connected the cofferdam to the cells. Use of the circular cells for anchorage was enhanced

because the load was reduced by excavating soil from the area between the cells and the rectangular cofferdam. The rock slope beneath the circular cells was less severe than beneath the pier and this mitigated concerns related to the cellular structures sliding on the rock.

The drilled shafts were installed at the same time as the cellular structures and prior to the cofferdam. The casings extending upward from the shafts supported the cofferdam bracing. Sheet piling was then installed on the cofferdam perimeter. In order to expedite installation of the bracing system and reduce associated diver work, an "unfolding" post and diagonal system was used between the two levels of bracing. After excavation had progressed sufficiently to allow positioning of the 2nd level of bracing, the 2nd level was lowered and the posts and diagonals "unfolded" into their design location. They were then secured by bolts installed by personnel standing on the upper brace level. Photograph 2 shows the cofferdam with the shaft casings and bracing system still in place. Photograph 3 shows the cofferdam after removal of the casings and the bracing system when the area is ready for construction of the pier footing.

Administrative and construction difficulties with the final design were numerous. Much care and consideration for constructability and material availability were incorporated into this final design. However, constructing the final product was still a challenge.



Photograph 2 – Cofferdam with Bracing in Place



Photograph 3 – Completed Cofferdam Ready for Pier Construction

As the final cofferdam design was completed, submitted and approved, arrangements were in process for creation of the mechanisms to pay for the changes. They resulted in an addition to the general contract in excess of ten million dollars. The original bid specifications contained an item for escrow of all bidding documents to be opened and used in just such a case. They would be used to determine the items originally included in the general contractors bid, and used as a starting point for assessing costs for new work if it became necessary. New items were created, old items deleted or modified, and coordination with other items were undertaken in order to account for previous and future impacts.

With the introduction of the drilled caissons into the footing design, the project changed from a land based operation to a water based installation using rented floats and contractor owned spud barges and tugboat. In addition, the river work was required to comply with the calendar restrictions placed on the project by regulating authorities.

One of the major problems was to ensure the location and dimensional accuracy with which the newly redesigned footing needed to be constructed. The caissons were required to be located accurately so that the cofferdam could be built around them to the correct size. Due to the large size of the cofferdam, even minor increases in size resulted in larger quantities for excavation, tremie concrete, and backfill. Conversely, there was no tolerance for having the cofferdam and tremie be smaller than designed. This led to great effort being

expended in the fabrication and placement of templates to ensure accurate location of the permanent casings for the caissons. Due to the extremely limited reach of the caisson equipment on the barge, only one row of casings could be vibrated into the soil at a time. After the casings were in place in the soil, the drilling subcontractor could clean them out and proceed with rock drilling. Casing installation and drilling were performed in very close quarters and that resulted in implications for safety. It was only after all of the caissons were installed that work on the steel sheet piling cofferdam could be started. The cofferdam portion of the work proceeded without significant difficulty.

Working on the water, there were to be no impacts to the use of the navigable channel during pier construction. There were numerous recreation vessels and two major commercial users of the river. This reach of the river is a primary access point for boat traffic to and from Lake Ontario. There was a dinner cruise ship and a commercial cement freighter that required full and unrestricted use of the channel. The size of the freighter and the narrowness of the channel made it necessary to completely clear the channel for its passage. A full hour was required to move all barges offline prior to the arrival of the ship. Then it took about another hour for the ship to clear. The piling subcontractor could then move back into position to work, but then would have to move again for the ship to go back out to the lake either the same day or the next depending on arrival time. The freighter returned every one to two weeks, sometimes more often. Total time lost was on the order of 3 to 6 hours of work per appearance depending upon the timing.

Once installation of the caissons and the steel sheet pile cofferdam were complete, excavation of river sediments and placement of the bracing were undertaken. Due to the depth of excavation, the water based operation, and the contaminated nature of the excavated materials, the excavation was performed by crane and clam bucket (the excavation of contaminated material would be a problem no matter which design was undertaken). Concerns for environmental problems during the disposal of the spoils became a concern. Thus, the excavated material was required to be transported by barge to a confined disposal facility operated by the U.S. Army Corps of Engineers in Buffalo, NY. The round trip including transit of the Welland Canal and unloading the contaminated spoils required 2 to 3 days, slowing the excavation process and causing large amounts of downtime for equipment and personnel both at the site and at the disposal facility. However, there was much labor intensive hand cleaning of the caisson casings, the in-bays of the sheet piling, and the top of rock that had to be performed by divers working in water with no visibility. Much of this was done during the delay time, thus reducing downtime charged to the owner.

After the first stage of excavation and cleaning operations were completed, bracing installation occurred in a manner very similar to that of the first redesign. The two rings were fabricated in place atop one another and sequentially lowered and blocked into place utilizing the wedge block procedure described previously. The final excavation, rock and casing cleaning, brace lowering and wedging operations were performed in stages.

Once all the excavation, bracing, and mud cleaning operations were complete, the truss posts and diagonals were secured. As described earlier, these were prefabricated as much as possible to allow them to be placed from above water elevation and “unfolded” into place. They were bolted to the upper level brace by workers in dry conditions. This was successful because of extensive planning and prefabrication.

Simultaneous with work on the water, a crew on shore installed the circular cells to be used as an anchor for the sheet pile cofferdam. As soon as the rear wall of the cofferdam and the circular cells were completed, the two were connected using HP sections as tension members.

Well before completion of the steel sheet pile cofferdam, circular cells, bracing and excavation, plans were being made for installation of the tremie concrete. This was a major operation due to its location.

The access for equipment behind the cellular structures consisted of a linear roadway, approximately 15 meters (49.5 feet) wide sandwiched between an operating railroad line and the circular cell structure. Space was required to set up the concrete pump, to maintain access for two concrete trucks at the pump, and to maintain room to stage at least two more trucks in the event they arrived early. Concrete was required to be delivered from two plants simultaneously in order to maintain anticipated production of the pump. The concrete suppliers could guarantee the production of their plants only if the tremie were placed during off hours. This was both to dedicate the plants to the project, and to reasonably assure no traffic delays for the transit trucks. Therefore, it was decided that the tremie installation would begin at the end of the normal first shift and go on through the night. Great effort was expended to ensure uniform and accurate top elevation of the tremie concrete. It was night time and there was no visibility through the 2.5 to 3.0 meter (8 to 10 feet) of water above the top of tremie elevation. Concern for the elevation of the top of the tremie concrete was a result of the lesson learned at the Pier 2 location at which the top of tremie was too high varying from 2 inches to 16 inches, thus requiring a massive expenditure of labor and equipment to grind, chip, and clean the top down to the proper elevation.

Upon completion of the tremie placement, all of the bracing was removed and the open cofferdam is shown in Photograph 3. This allowed construction of the pier footing and pier to take place in dry conditions. After the footing and pier stem were completed, the sheet piles were cut off at the top of tremie elevation by divers. The cutting and removal of the sheet pilling was a very slow operation. Limited or no visibility in the water caused incomplete cuts to go unnoticed until attempting to remove the pieces with the crane, resulting in re-cutting of the sheet piles.

Conclusion

A relatively straightforward job became a complex series of engineering and work tasks requiring great effort on the part of all parties associated with the project. A change in the geology underlying one pier of the bridge caused a massive redesign and construction effort.

Eighteen months passed from the start to the finish of the design and planning phases for Pier 1. This occurred because it was required that parties agree on what needed to be done, how it would be done, how much it would cost, who was going to pay for the increases, and what payment mechanisms would be put in place to pay $3.0 million design, construction, and delay cost overruns for the cofferdam. The general contractor incurred additional costs including delays, installation of the caissons, overruns on the disposal of excavated soil, and placement of additional tremie concrete. In total, the cost increase exceeded $10 million.

The redesign and construction required the combined effort of three design engineers, the general contractor, two subcontractors, and two departments of transportation. All parties were required to take into account constructability and material availability in order to complete the project in the fastest and safest manner possible.

Typical of subsurface work, none of the additional planning, construction, and cost is now apparent when viewing the bridge. But everyone involved knows the detail and effort required to complete the project and can be pleased with the final product. Without the cooperation and commitment of every participant, it would certainly have taken even longer and cost more.

INNOVATIVE COFFERDAMS USED ON THE I-205 COLUMBIA RIVER BRIDGE

Robert Bittner, P.E. Ben C. Gerwick, Inc. San Francisco, CA, USA

The following is a report on the development of two unique and separate cofferdam systems used in the construction of the marine foundations for the I-205 Columbia River Bridge at Portland, Oregon for the Oregon Department of Transportation. The first of these two systems utilized interlocking H-pile 100 ft long to form a cofferdam 145 ft by 58 ft in plan and 100 ft deep. The second system consisted of two immense bell shaped steel forms. The larger of the two forms was 83 ft by 66 ft in plan, 62 ft high and weighed 450 tons. This form was externally stiffened for a designed hydrostatic head of 54 ft. Both forms were designed, except for the top 14 ft, to be set and stripped in one solidly welded unit. The supporting geological formation for the bridge foundations is the Troutdale, a cemented sand and gravel. This formation is at the ground surface on the Washington Shore and slopes downward to a depth of 115 ft below normal high water at about mid-channel. In this area the Troutdale formation is covered with a layer of fine to medium sand 90 to 100 ft thick. It was the variable depth of the Troutdale which determined the two types of foundations and the corresponding to the two cofferdam systems.

INTERLOCKING H PILE SYSTEM

The first two piers off the Washington shore, Piers 12 and 13, flank the main 600-foot navigation channel. Both of these piers were designed to bear directly on the Troutdale. The design depth of the foundation at Pier 13 was 100 ft below normal high water. Because of this extreme depth, it was originally designed as a concrete caisson. After the notice of contract award, a study was made to determine the feasibility of using a cofferdam approach. Again, due to the extreme depth, conventional sheet piling were ruled out primarily because of the numerous levels of bracing which would have been required for the hydrostatic head of 62 ft at Pier 13.

Two alternate sheeting systems were evaluated. The first of these was an interlocking pipe pile system offering a section modulus as high as 469 cubic inches per foot of wall compared to the 46.3 cubic inches for the highest capacity Z sheet pile manufactured. The second system was Arbed interlocking H-pile system manufactured in Luxembourg which offered a section modulus as high as 555 cubic inches. The final selection was the Arbed HZ-600-LA sheet pile with a section modulus of 243 cubic inches. (See Figure 1.) These high strength sheets required only the seal and one wale support point to resist the designed hydrostatic head of 62 ft. The final design used two wale frames, but the purpose of the top frame was to provide support during threading and driving of the sheet pile and to carry the wall loadings as struts were removed on the main frame to allow continuation of the pier shaft. (See Figure 2.)

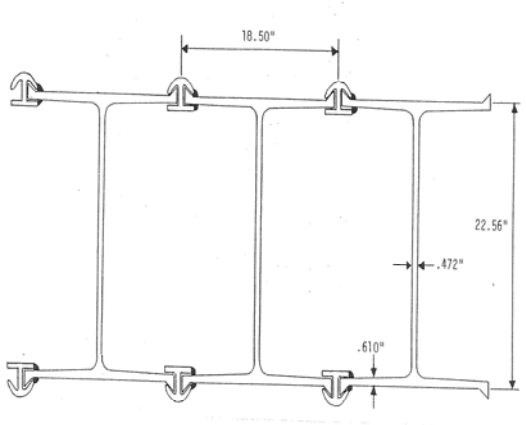


Figure 1: Arbed HZ 600 LA Sheet Piling System



Figure 2: Positioning Pier 12 Cofferdam Frame

An additional advantage of the interlocking H pile over conventional Z pile is the closed pocket formed by the interlocking flanges. These pockets when filled with a silty sand mixture not only increased the water tightness of the cofferdam walls, but also increased the total dead weight of the cofferdam by 2,450 tons. This increased weight allowed a corresponding decrease in the seal concrete volume by 1,250 cubic yards. In order to insure that this weight could be considered in the balance of forces on the seal, two steps were taken. First a concrete plug was inserted into each of the pockets and lowered down to the bottom of the pile where it wedged against the reinforced pile tips. This plug ensured that the weight of the sand fill was transferred to the sheet pile. The second step consisted of installing a vertical shear key on the inside face of each pile to insure the weight of the cofferdam and sand fill were transferred to the seal. The shear key was designed so that the seal could not move upward relative to the sheet pile, but the sheet pile could move upward relative to the seal. This allowed pulling of the sheet pile after the pier was completed.

The use of only one load carrying wale frame above the seal resulted in extremely high loadings on the lower wale frame. The wales consisted of double W-36 x 230 beams stitch welded along both flanges to form a box section 36 inches by 32 inches and carried a design loading of 26 tons per foot of wall. This section not only allowed utilization of conventional rolled shapes but provided a stable section against any rolling tendency during the driving of the sheet piles. The struts consisted of 30 inch diameter pipe with a wall thickness of .750 inch and carried a maximum design loading on the diagonal struts of 700 tons per strut. The entire bracing system when assembled weighed 350 tons, covered an area 145 ft by 59 ft and stood 24 ft high.

The initial step in the cofferdam construction after pre-assembly of the bracing frame, was to float the frame into position, and lift it clear of the barge using a 600 ton capacity catamaran gantry barge. With the bracing frame suspended by four load blocks, four 36-inch diameter spud piles were driven, and the load of the bracing frame was transferred to the piles. Threading and driving of sheet piles followed, using a Toymomenka VM2-25000A vibratory hammer. (See Figure 3.) The double interlocking system with an interlock threaded on each flange of the H-section created initial threading problems due to variations of ± ¼ inch in the flange spacing at the interlock. However, the sheets were finally threaded, and driving progressed in a clockwise direction around the cell, driving each sheet 10 to 15 ft before progressing to the next.

During the third driving cycle the ground had become so compacted ahead of the piles that further attempts at driving resulted in melting of the interlocks between the piles. The piles were finally taken to the Troutdale by using a combination air and water jet down one of the pockets a few pockets ahead of the pile being driven. The jet was allowed to penetrate below the tips of the H-piles and loosened the sand so effectively that whole sections of wall began dropping as the vibratory hammer was turned on.



Figure 3: Threading Sheet Pile at Pier 13



Figure 4: Internal Cofferdam Bracing at Pier 12

The remaining steps in the cofferdam construction were similar to conventional cofferdams except for the size. (See Figure 4.) The seal at Pier 13 as an example was 38 ft deep, required 11,500 cubic yards and took 72 hours to complete. Concrete for the seal pour was supplied by both a floating batch plant and a back up system of barge mounted concrete trucks. The floating batch plant was mounted on a barge 275 ft by 60 ft by 18 ft deep and equipped with a concrete plant capable of producing 180 cubic yards per hour. Mounted on the bow of the barge were two 5 in diameter concrete pumps equipped with 103-foot articulating booms. (See Figure 5, 6 and 7.)

Upon completion of the seal and footing, the shaft was poured in lifts of 10 ft up to the underside of the bottom struts. At that point, the bolts connecting the struts to the wale frame were removed and the cell was flooded to the surrounding river elevation. After allowing the disconnected struts to float to the surface, the cell was again unwatered to a point just below the last construction joint in the shaft, and the next lift on the shaft was completed. In this manner, the need for struts passing through the shaft was completely eliminated. This step was repeated on the top wale frame, as the shaft pour was completed to the underside of the top struts.

The transfer of the cofferdam frame from Pier 12 to Pier 13 involved increasing the plan dimensions of the cell by 4 ft. This was accomplished by bolting 24-inch by 24-inch timbers to the outside of the wale frame. Another change made at Pier 13 was the method of pouring the seal. At Pier 12, the pour started in the middle of the cofferdam and worked towards each end. At Pier 13, the seal was started with one end and progressed to the other. This second method with only one direction of flow resulted in a much more controllable seal pour and a more even surface on the completed seal.



Figure 5: Floating Batch Plant



Figure 6: Pouring Tremie Seal at Pier 13



Figure 7: Pouring Tremie Seal at Pier 12.



Figure 8: Setting Bell Pier Form and Reinforcing Cage

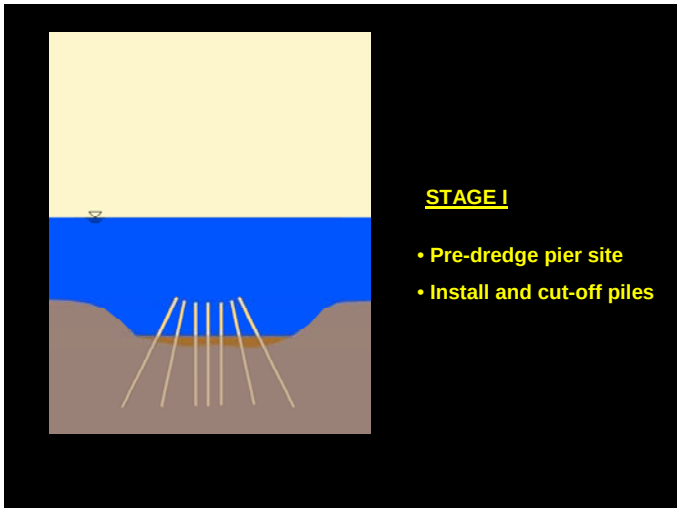
Bell Pier System

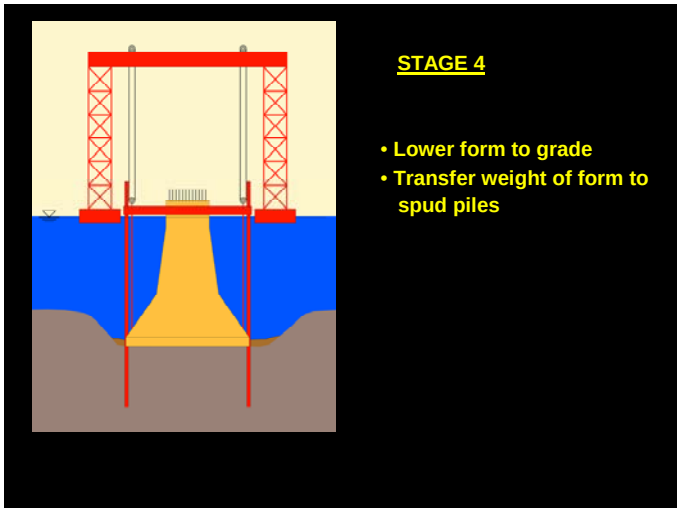
The second cofferdam system was used on the remaining 26 piers, double piers 14 through 26. The Troutdale formation at these piers varies from 105 to 115 ft below normal high water and is covered with a layer of dense to medium dense unconsolidated sands 90 to 110 ft thick. These piers were originally designed as pile supported precast bells. The original design called for setting a bottom precast segment in a pre-excavated hole. The bottom slab of this segment was to be blocked out and used as a template for driving the 50 to 100 H piles at each pier. Once the piles were driven, cut off, and the block outs grouted, three additional precast segments were to be stacked on top of the first. After sealing the joints between each segment, the interior of the bell was to be filled with tremie concrete. This method had been successfully used to construct the foundations for the Richmond-San Rafael Bridge.

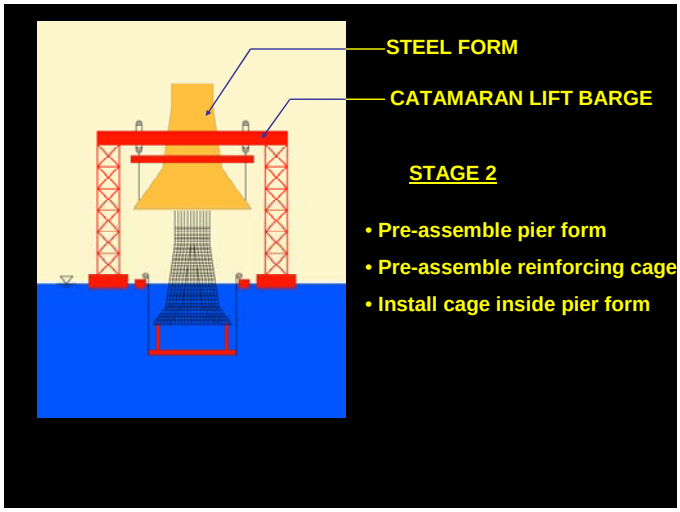
The revised method of construction proposed by the Contractor, provided essentially the same pier but arrived at by a different means.(See Figure 8.) The new concept was executed in six (6) stages illustrated in Figure 9. The pier site was first pre-excavated as originally designed. Piles were driven and cut off under water. Immediately after pile driving a steel form and reinforcing cage were positioned over the top of the piles and lowered to grade. The bottom 9 ft of the form was then filled with tremie concrete, sealing the bottom of the form and encasing the driven piles. After curing for about 60 hours, the interior of the form was unwatered allowing access to the top of seal. A reinforcing mat was placed on top of the seal and a void form 10 ft in diameter with reinforcing cage was set vertically inside the form. The next step was to place the remaining structural concrete from top of seal to a point 2 ft above normal high water. The final step was to stripe the form in one solid piece. These steps were the general concepts developed prior to bid opening. After notice of contract award, work began on converting the concepts into the reality of functional systems and equipment.

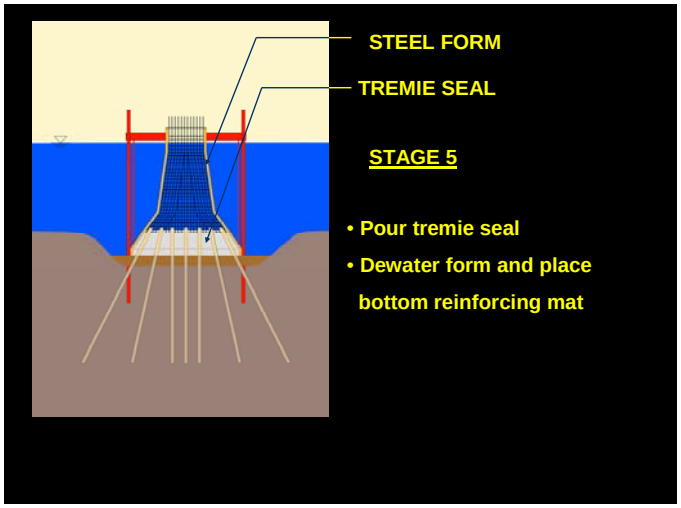
The forms were built as single piece cofferdam designed for a hydrostatic head of 54 ft without any internal bracing. The forms, unlike conventional cofferdams because of their sloping faces, were required to resist the hydrostatic loading in both the horizontal and vertical direction.

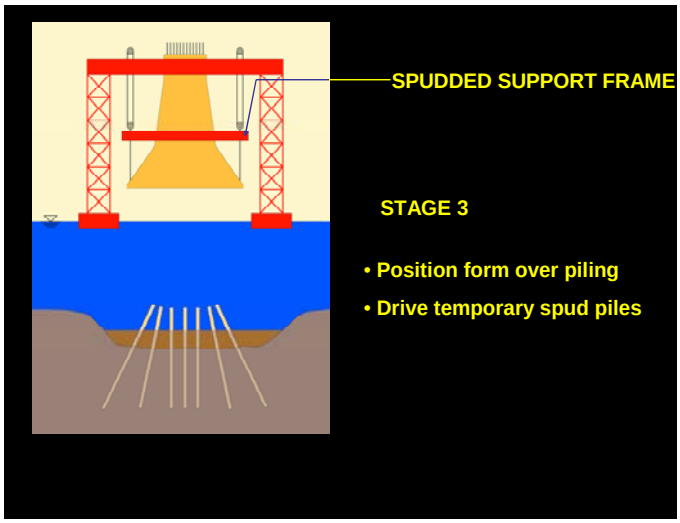
The skin of the forms was 3/8 inch plate stiffened with 8x4-inch vertical angles. The angels were in turn supported by eleven horizontal trusses up to 7 ft in depth, banked perpendicular to the sloping faces of the forms. These trusses formed rings circling the forms and were stabilized by twelve vertical trusses along the form perimeter. The larger of the two assembled forms was 83 ft by 66 ft in plan, stood 62 ft high, and weighed 450 tons including support frame. This weight plus the 100 tons of reinforcing cage and spud piling brought the total required lift to 550 tons.











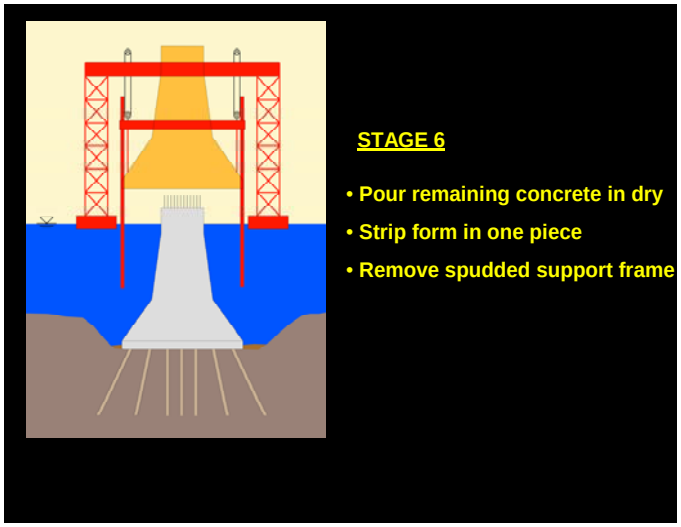


Figure 9: Sequence of Bell Pier Construction



Figure 10: Driven Batter Pile at Bell Pier



Figure 11: Positioning Reinforcing Cage under Small Form

The heavy lift requirements of the bell pier construction were met by designing of a 600-ton capacity catamaran gantry crane. (See Figure 11 and 12.) Support of the straddle lift gantry was provided by two barges 104 ft by 30 ft by 10 ft deep, one under each framed tower of the gantry. Vertical clearance under the cross beams was 80 ft off the water, and horizontal clearance between the barges was 74 ft.

Prior to setting the form it was first necessary to install a 72-foot high reinforcing cage inside the 62-foot high form. (See Figure 11). In order to eliminate the two week cage fabrication time from the pier construction cycle, it was necessary to pre-assemble the cage. This meant the bell shaped cage had to be installed from the bottom side of the form. Rather than build a gantry crane with a head clearance of over 130 ft, it was decided to sink the completed cage 40 ft below the river surface, and allow the floating gantry to position the form over the reinforcing cage. Once over the cage the form was lowered and the reinforcing cage raised to meet the form.

The sinking of the cage was performed by building the cage on a steel deck suspended between two pontoons. The steel deck was supported by four cables running to hydraulic winches mounted on the pontoons. The deck was also fitted with four vertical pipe columns which traveled through roller guides on the support pontoons. The purpose of the pipe and roller guides was to insure vertical alignment of the cage in the 3 ft per second river current.

After the cage was fitted up into the form, the reinforcing steel was secured to the face of the form with U-shaped clamps passing around the vertical bars and in turn bolted through the skin plate. The skin plate at these locations was backed with a water tight steel pocket to allow removal of the clips during the pouring of the structural concrete.

Before installation of the reinforcing cage and form, 50 to 100 H piles were driven into the pre-excavated pier site. The pile driving specifications required the piles to be positioned within a tolerance of ± 6 inches at a point approximately 40 ft below the river surface. This specification was met by installing an accurately placed template at a depth of 40 ft and by providing a highly accurate and stable pile driver at the surface. (See Figure 10.)

The template consisted of an adjustable pipe ring positioned two feet above the pile cut off point. The ring was supported by a trussed frame held in position by four 24-inch diameter spud piles. The template was positioned by triangulation from shore using two theodolites equipped with wild DI-35 Distomats.

The design of the pile driver insured accurate positioned capability by providing finite articulation of the leads without moving the barge. This was accomplished by using independent hydraulic drives and controls for each of the basic motions of the leads.

The next step consisted of positioning the form, reinforcing cage, and support frame over the required pier location, lowering the entire load 58 ft to the river bottom over the top of the pre-driven piles and finally, transferring the entire load from the floating gantry to the support frame and four 36-inch diameter spud piles. It was necessary to use the separate support frame to allow the floating gantry to work with both forms. The separate support frame also provided greater positioning accuracy and

stability during the seal pouring operation. The form was suspended from the support frame by four cables connected at mid-height on the form and was fixed into position by four arms jacketed to the support piles. These positioning arms were fitted with eight hydraulic rams which allowed the entire from to be repositioned within a one foot radius of its initial set position. This feature allowed a precise positioning of the form once the form had been transferred from the floating gantry to the pile supported frame.



Figure 12: Location Positioning Large Bell Pier Form and Support Frame

During the preliminary planning of the bell pier system, it was feared that as the form was lowered closer to the river bottom, the immense shape of the form would cause the river current to increase sharply at the lower edge of the form and progressively scour away the sand from below the form. To ensure that this did not happen, the pier site was over excavated 2 to 3 ft and a layer of 4-inch minus rock was placed. This rock layer also helped prevent contamination of the relatively thin tremie seal with the loose river bottom sand.

An additional precaution taken to ensure the integrity of the seal was the installation of a 2-foot deep cutting edge attached to the bottom of the form. It was essential that the outer edges of the form be sealed tight against any water flow. The potential for this flow existed because of possible unevenness of the river bottom and also because of the possibility of scour under the edge of the form. The cutting edge eliminated both of these concerns.

After the form was in position, a single centrally located tremie pipe was used to place the 9-foot deep 1,300-cubic yard seal. The rapid pour rate and on site batching capacity of the floating batch plant helped provide a free flowing tremie around the forest of H piles. (See Figure 13).

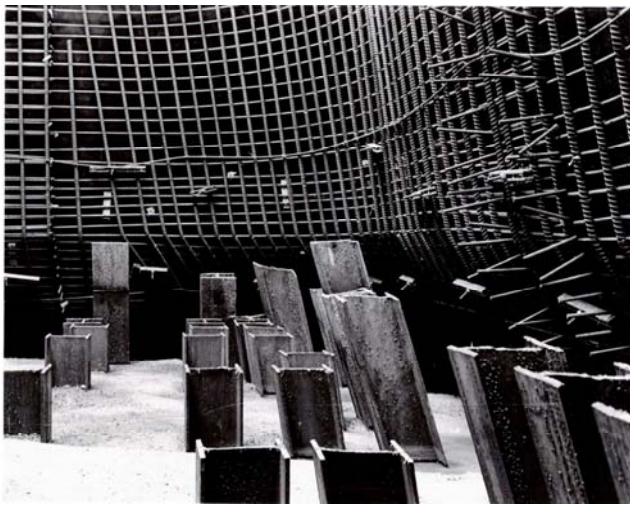


Figure 13: Dewatered Bell Pier and Top of Tremie Seal

After dewatering of the bell pier form and placing of the bottom reinforcing mat and void form, the remaining 2,000 cubic yards of structural concrete were placed in the dry.

The final stage in the sequence of pier construction was the removal of the bell pier form. The forms, except for their top 14 ft, were one solidly welded unit. The stripping step was the most critical of the entire bell pier operation. The bonded area of form to concrete was over 10,000 square feet.

From a deflection analysis, it was reasonable to expect the form to move away from the face of the completed pier. During the unwatered stage of construction, the form was deflected inward under a maximum hydrostatic pressure of approximately 3,000 pounds per square foot, and the only outward pressure during the casting operation was that created by the fresh concrete which, under a pour rate of 3 to 5 ft per hour, produced a maximum pressure of approximately 700 pounds per square foot. Once the pier was cast and water allowed to seep back between the steel skin and the concrete, the form was expected to rebounded from the initial deflection.

There were four basic steps taken to ensure that the form would come free of the pier. The first was to use a minimum sloping surface of 1 horizontal to 6 vertical. In order to meet this criteria, it was

necessary to isolate the top 14 ft of vertical form and allow this bonded area to break free separately. The second step was to grease the entire surface of the form with a special grease used in the launching of ships. This grease was reapplied after every pier casting. The third step was to provide 140 hydraulic ports on 8-foot centers over the interior face of the form. The purpose of these ports was to break the bond between the steel form surface and the face of the completed pier. This was accomplished by inducing water at a pressure of 80 psi into a smaller cylinder which jacked the face of the form away from the pier in a small localized area. At the same time, the pressurized water was allowed to fill the localized void and progressively enlarge the bond free surface. The fourth and final precaution was to provide excess lifting capacity over that required to lift the dead weight of the form. The floating gantry was designed for a maximum lift of 600 tons. The jacking system on top of the spud piles used for final grade adjustments of the form had a designed lift capacity of 600 tons, and finally two 800-ton jacks were available for setting on top of the completed pier for jacking against a reaction beam connected to the form. These three lifting systems had a combined capacity of 2,800 tons to lift a form and frame which had a maximum dead weight of only 450 tons.

On the first pier to be stripped, it became evident the excess lifting capacity would not be required. The form lifted free of the pier with less than 10 tons over the dead weight of the form. The following 25 piers in a like manner were stripped without the use of the excess lift capacity.

The 26 bell shaped piers were cast over a period of 18.5 months utilizing two bell pier forms. The average cycle time for each pier was 37 calendar days including all weather and mechanical delays. This relatively fast cycle time per pier was attributable in part to three factors. First, the installation time for reinforcing was separated from the cycle time for each pier by pre-fabricating the reinforcing cage. Secondly, the multitude of construction steps associated with conventional sheet pile cofferdams were replaced with the single step of the setting the form. And, finally, the steps of forming the footing and column were completely eliminated and the two concrete placing steps were combined into one.



Figure 14: Competed Foundations

construction time, the bell pier system offers the potential for substantial reductions in seal concrete volume. For the I-205 Columbia River Bridge, the bending strength of the seal determined the required seal thickness in the bell piers. For cofferdams with seals designed to provide dead weight against hydrostatic uplift of the whole cofferdam, the bell pier system can greatly reduce the required seal concrete by reducing the total uplift on the cofferdam. This can be accomplished because of the inward sloping faces of the bell pier cofferdam which reduces the cofferdam's displaced volume in water without reducing the cofferdam's base area or height.

The bell pier system also offers the potential for adaptability to greater water depths. The bell pier system has performed at a depth of 62 ft using a rectangular shaped form stiffened with heavy trusses. This same system could be used at depths in excess of 100 ft without the use of heavy stiffening trusses by designing the piers and cofferdam forms with circular across sections allowing the cofferdam walls to carry all hydrostatic loads in compression.

Conclusions

Both the interlocking H pile cofferdam system and the bell pier cofferdam system proved to be sound methods of pier construction. All 28 marine piers were safely constructed to required specification within the schedule 1,000 calendar days and within the owner's original estimate. Both systems offer the potential for savings on future marine foundation.

UNDERWATER CONCRETE IN DRILLED SHAFTS: THE KEY ISSUES AND CASE HISTORIES

Sam X. Yao, Ben C. Gerwick, Inc. San Francisco, CA, USA
Robert B. Bittner, Ben C. Gerwick, Inc. San Francisco, CA, USA

In construction of drilled shafts under water, placing concrete in the shafts is technically demanding and involves complex construction logistics. Past construction experience has demonstrated that high quality concrete can be placed in drilled shafts under water with a proper concrete mix and proper placement techniques. However, a significant number of failures have occurred which have resulted in excessive cost overruns and delays. These problems may have occurred because proper underwater concrete construction techniques have not been widely disseminated within the industry. This is a technical area where competent design and sound construction planning can achieve a significant reduction in both risk and cost. This paper will discuss some key technical issues in the concrete mix design, concrete production and placement for the drilled shaft construction. The paper also describes two lesson-learned case histories from drilled shaft construction projects.

INTRODUCTION

Placing concrete in the shafts is one of the most critical and complex operations that often determine success or failure of many drilled shaft construction projects. If the concrete is placed under water, the construction is even more technically demanding and involves complex construction logistics. A number of failures have occurred due to improper concrete mix or improper construction procedures. The following sections present some important technical issues that are frequently encountered in underwater construction of drilled shafts.

CONCRETE MIX DESIGN

Because concrete placed underwater is inherently susceptible to cement washout, laitance, segregation, cold joints, and water entrapment, it must possess some unique properties that are not otherwise required. The following list outlines the essential and unique requirements for concrete placed underwater:

Flowability: the concrete must be able to flow around and fully encase reinforcing steel bars. In practice, the interpretation of flowability is specific to the application for a given project. Therefore, the level of concrete flowability must be specifically defined and fully understood by all the parties involved in the design and construction for a given project.

Self-compaction: the concrete must consolidate itself under its own weight without entrapping any water and laitance. It should be pointed out that the self-weight of concrete is substantially reduced by its buoyancy in water. This differs from the so-called self-consolidating concrete normally placed in the dry.

Adequate cohesion: Cohesive concrete prevents segregation, excessive bleeding or cement wash-out. A high degree of cohesiveness in concrete improves homogeneity and strength of the underwater concrete. The required degree of concrete cohesion, however, depends on many variables for a specific project. For a given mixture, an increase in flowability tends to reduce cohesion and vice versa. Nevertheless, modern engineering practice has proven that proper mixture proportions can provide for highly flowable concrete with adequate cohesion characteristics.

Retention of workability: underwater concrete often entails transportation of a large quantity of

materials over distance, which may create logistic problems with regard to the time lapse between concrete mixing and concrete placement. In such cases, the concrete mixtures must be able to maintain all the desirable properties (such as flowability, cohesiveness, and self-compacting characteristics) over a reasonable work window.

Adequate in-place concrete strength: The mix design should account for some inevitable wash-out of cement by water during concrete placement, which leads to loss of in-place concrete strength. Commons measures to ensure the in-place concrete strength include use of a low water-to-cement ratio, typically below 0.45 and relatively high cementitious materials content, typically above 650 pounds per cubic yard of concrete. Use of silica fume and anti-washout admixtures is also very effective for increasing in-place concrete strength.

Concrete mixture proportioning is essentially a trial-and-error optimization process. The process should be guided by a set of governing variables and an understanding of how each variable affects the concrete. Based upon past experience and research (Yao, Berner, and Gerwick, 1999), the authors found that five key variables have the most significant effects on workability of underwater concrete:

A water-to-fines ratio of concrete: When the ratio is within an optimum range of 0.85 to 1.0 by volume, the concrete can be made to be very flowable by use of water-reducing agents, while still maintaining adequate cohesion to prevent segregation. The fines content is defined as the total amount of cementitious materials and aggregates finer than 100 μm.

Particle packing characteristics: The gradation, maximum size and proportions of coarse aggregates have critical influence on the concrete flowability. Coarse aggregates in tremie concrete are normally in the range of 50-55% of total aggregates. Maximum size of aggregates should be limited since large aggregates tend to increase the propensity for segregation of highly flowable concrete.

Composition and content of cementitious materials: Partial replacement of Portland cement with fly ash or ground granulated blast furnace slag improves the concrete workability and reduces the heat of hydration. Use of silica fume improves the anti-washout characteristic of the concrete.

When placing concrete under water or slurry through a prefabricated reinforcing steel cage, the clear spacing between steel bars should be at least 5 times the maximum nominal size of coarse aggregates in the concrete. This requirement greatly exceeds code requirements for spacing of bars in above water concrete placement, but is necessary for underwater concrete, because the driving force to produce concrete flow under water or slurry is reduced by half due to buoyancy.

Dispersion characteristics of solid particles in concrete: water-reducing and anti-washout admixtures can substantially enhance the performance of underwater concrete.

CONCRETE PRODUCTION, DELIVERY, AND PLACEMENT

Proper concrete production, supply, and placement are critical in achieving high quality concrete and cost-effective construction. The choice of a proper underwater concreting plan for a project has to be ultimately determined by site conditions, engineering requirements, availability of equipment and contractor's preference. Only general comments are given in this paper.

Good quality underwater concrete is obtained through a continuous placement at a constant placement rate. Any prolonged interruption in concrete placement imposes high risks for defective concrete. Efforts should be made to ensure adequate and continuous concrete supply to the placement. The location of a concrete batch plant is an important consideration in logistics planning and has a significant impact on construction cost, risk, and quality control. An on-site batch plant has the main advantage of providing more reliable control of the concrete workability at the point of placement, because the time between concrete batching and placing is relatively short. This option, however, requires a significant investment in equipment.

Alternatively, a batch plant may be located off the project site, and concrete is transported by transit mixers to the point of concrete placement near drilled shafts. This frequently creates

problems with regard to the time lapse between concrete mixing and concrete placement. When the construction logistics indicates the possibility of substantial time lapse between concrete mixing and placing, adequate considerations should be given in planning to ensure the concrete maintains the required properties (e.g., flowability and cohesiveness) at the point of placement. The required work window should take into account concrete delivery time, the duration for each placement, delay due to site access and potential interference of other onsite activities. Consideration should also be given to delays of concrete delivery due to traffic congestion and equipment breakdowns.

Once the concrete batch plant is selected, the effective mixing time is critical in determining the peak concrete production and placement rates. It is desirable to determine the mixing time in field mock-up tests taking into account the essential field variables. The mixing time should be such that all the concrete ingredients are fully dispersed and the concrete reaches the desired workablity.

The most common concrete placement methods in drilled shaft construction are the tremie method and pump method. These two methods function in fundamentally different manners. While tremie placement deposits concrete solely by gravity feed in an open-to-atmosphere system, the pump method utilizes surges of pump pressure to deliver concrete in a closed system. As a result, the technical requirements and inherent risks with the two methods are substantially different.

The tremie method is a way of placing underwater concrete by means of gravity flow. The tremie system basically consists of a rigid pipe suspended vertically through the water and a hopper fixed on top of the pipe to receive concrete. With the tremie method, there exists a “hydrostatic balance point” at which the gravity force inside the tremie is in equilibrium with the resistance to flow such as the hydrostatic pressure, the friction between the concrete and tremie wall, and the resistance of previously placed concrete. Thus, the concrete placement rate can be reliably controlled by the speed in which concrete is fed to the hopper. Although good quality concrete has been placed by both tremie method and pump method, past experience and studies have found that the tremie method encounters less construction problems than the pump method (Yao and Gerwick, 2004, and HERON, 1973). There are two main reasons for this phenomenon. The first is related to the concrete flow rate. When pumping concrete down directly to its deposit area, the pump pressure surges plus self-weight of the concrete are at times much greater than the hydrostatic balance head outside the pump line. Thus, the concrete exits the pump line at an uncontrollably high speed, causing significant disturbance to the concrete that has already been deposited. Secondly, a pump system is closed to the atmosphere. If concrete is being pumped down into deep water, concrete may fall at a rate faster than the pump output. As a result, a vacuum will be created in the pump line. The vacuum pressure so created will suck away the cement paste from aggregates, causing segregation of the concrete. American Concrete Institute provides recommendations as good practice for both the tremie placement method and the pump placement method for underwater concrete. The engineers and contractors need to be aware of the distinctions and different requirements between the two placement methods.

QUALITY CONTROL

Due to inaccessibility for inspection of underwater concrete placement, there is significant uncertainty with the quality and integrity of underwater concrete in drilled shafts. Strict enforcement of engineering requirements and quality control must be imposed for underwater concreting. Attention is directed to the following aspects of the underwater concrete in drilled shafts:

Bottom condition of drilled shafts - The bottom of the drilled shafts should be cleaned of sediments just prior to placement of underwater concrete.

Initial start of placement - The bottom of the tremie pipe should be sealed with a cap prior to installation in the drilled shaft casing. The tremie pipe should rest on the bottom of the drilled shaft. It should then be sounded to confirm that the pipe is dry prior to filling with tremie concrete. The pipe should then be lifted 4 to 6 inches to dislodge the cap and commence placement.

Conditions of the concrete delivery system (leakage, plug or spill over) - Before using a

tremie pipe, all the joints should be checked for possible leakage.

Concrete flowability at the points of placement, slump and slump flow.

The rate of concrete placement should ensure a continuous and smooth concrete flow within the drilled shafts.

The depth to the top tremie concrete surface at various locations - Continuous soundings at predetermined locations should be performed for every 5 foot concrete rise during the entire placement.

Persistent monitoring of all concreting operations including any start and completion of concrete placement, and embedment depth of the tips of tremie pipes in concrete. The tremie pipe should be clearly marked to indicate the depth of the tremie tip. Lateral movement of the tremie pipe should be avoided, and vertical movements of the tremie pipe fully controlled to prevent loss of the tremie seal at the bottom.

Frequent checking on the watertightness and tremie seal of the concrete delivery pipes - Any leakage or loss of tremie seal of the delivery pipes will certainly result in substantial concrete defects in the shafts.

Volume of concrete produced vs. volume of in-place concrete measured by sounding - If the in-place concrete volume measured by sounding is less than that produced and fed into the tremie, it is an underrun of concrete. If the in-place concrete volume is more than that fed into the tremie, it is an overrun of concrete. In general, underrun indicates a possibility of loss of concrete, possibly leaking through a skirt or cut-off wall. Overrun is indicative of serious segregation of the concrete. The segregation may be caused by a leaking joint in the tremie, or loss of the tremie seal. More than 5% deviation of the measured concrete volume from the theoretical value may be a cause for concern. If the deviation is more than 10%, the concrete placement should be halted and the cause be investigated.

Delays of concrete delivery and any construction joint in the shaft.

Confirmation - Cross –Sonic- Logging or similar means should be conducted to confirm that sound concrete has been attained.

CASE STUDIES

The most common concrete defects found in drilled shafts and their causes are summarized below.

Voids or lenses in concrete and excessive wash-out of cement due to loss of tremie pipe seal during tremie concrete placement;

Voids behind the steel cage due to loss of concrete workability during placement, or insufficient clearance between reinforcing steel.

Significant washout of concrete and trapping of water in concrete due to unbalanced concrete surface or placing concrete directly through water

Necking of the shaft due to cave-in of the soft zone of the ground (e.g., thick clay seams in rock);

Entrapment of debris in concrete due to insufficient bottom cleaning prior to concreting.

Case A. On a 19 km (12 miles) long below-grade railway trench project in California, over 9,000 reinforced concrete drilled shafts were constructed below the underwater as a part of the secant pile/retaining wall system. Underwater concrete was placed in these drilled shafts. After excavation of the railway tunnel, a large percentage of the exposed drilled shafts were found to have significant defects as follows:

The most common defects in the piles were vertical and horizontal grooves outside the reinforcing steel bars, especially the bundled vertical bars (Figure 1 and Figure 2). The grooves are often accompanied with sizable voids with entrapment of silt. These defects show the evidence of stiff concrete flow patterns and poor concrete consolidation in these areas. These defects typically occur when underwater concrete at the time of placement loses the capability of flowing around and fully encasing the reinforcing bars;



Figure 1: Defective concrete in drilled shafts

Most break-out and soil contaminated areas contained inferior concrete. Typical evidence of inferior concrete quality in these areas is lack of cement paste due to cement wash-out, concrete segregation, and lack of consolidation of the concrete;

Many break-out areas showed very poor bond of concrete to reinforcing bars. The poor bonding was due to stiff consistency of the concrete during placement, lack of concrete consolidation, and entrapment of silt;

It is evident that the defects were mainly due to the fact that the concrete lost its capability of flowing around and fully encasing the reinforcing cages during placements. In this case, a polycarboxilate-based high-range water reducing admixture was used without any set-retarding admixture or low-range water reducing admixture. It was not until the very end of the construction that a slump retention test was performed under the field condition. The field test indicated that the concrete experienced rapid slump loss in approximately 90 minutes



Figure 2: Concrete defect due to the lack of concrete flowability during concrete placement

after the initial batching and mixing, which is generally shorter than the time for delivering and placing the concrete in each drilled shaft. In the past, this type of defect was not uncommon in drilled shafts and reinforced concrete slurry walls.

Case B. A 2500 m long new bridge under construction in California has 17 bents within its main span. Each bent is supported on 8 or 9 shafts in a 3 by 3 grid. The drilled shafts consist of 2.2 m diameter rock sockets drilled into the rock below 2.5 m diameter concrete filled steel casings.

Due to an unforeseen geological problem on this project involving instability of the rock socket portion of the shaft, shaft construction was forced to adopt a rotated-casing method for drilling the rock socket that typically ranged from 50 to 100 m below the water surface. Use of the rotated-casing method solved the problem of cave-in during drilling, but completely changed concrete placement logistics. The tremie concrete would now be placed as the temporary rotated casing was being withdrawn. The rotated casing was 2.2 m diameter and fit inside the 2.5 m diameter permanent steel casing. Thus, there was an abrupt change in size of the concrete pour as the tip of the temporary rotating-casing passed the tip of the permanent casing. The concrete was now able to flow beyond the limits of the temporary casing which had been confining the concrete. As the concrete level dropped inside the temporary casing to fill the suddenly larger pile, mixing occurred with debris and slurry trapped between the temporary casing and the permanent casing

(see Figure 3). In some cases, further mixing also occurred as the soil at the tip of the permanent casing caved in. Although concrete overpour was implemented in an attempt to flush debris and laitance out of the permanent portion of the shaft, not all of the debris and laitance due to the mixing could be carried to the top of the tremie concrete. Both debris and laitance were entrapped inside the drilled concrete shaft.

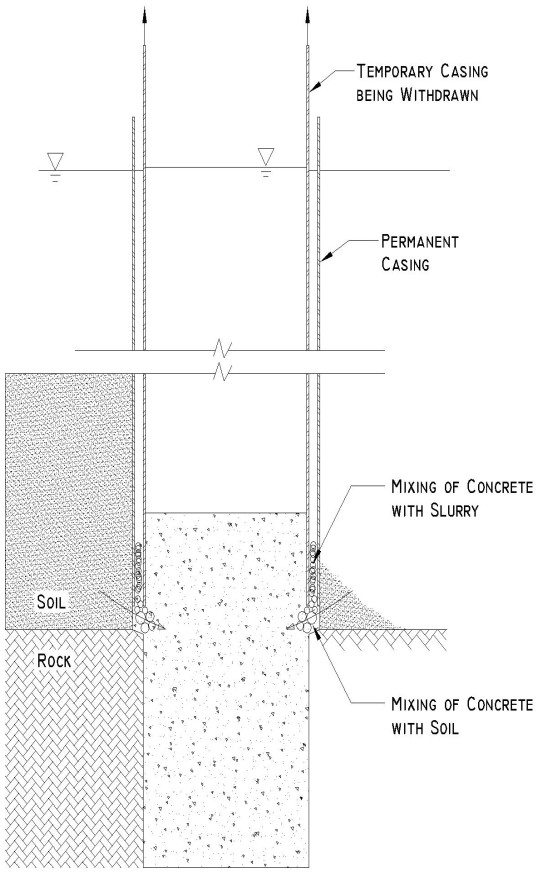


Figure 3: Schematic of mixing of concrete with slurry and soil during withdrawal of the temporary casing

Non-destructive tests (i.e., Gamma-Gamma Logging and Crosshole Sonic Logging) were performed on each shaft. The tests showed that the rock socket portion of the shaft were almost entirely free of anomalies. However, the portion of the tremie concrete inside the permanent casing contained numerous anomalous or defective zones. About 87 percent of the shafts required extensive mitigation of the concrete with significant cost and schedule overrun.

The key issue on this project was sudden enlargement of the drilled shaft cross section. When placing concrete through a withdrawing temporary casing, special attention should be paid to the zone of sudden changes in tremie concrete pour size. Efforts need to be made to minimize the mixing of concrete and slurry in these zones, including enforcing an adequate positive hydrostatic head of tremie concrete inside the casing, slow-down of raising the temporary casing passing these susceptible zones, and reducing tremie concrete placement to minimize washout. Furthermore, the concrete mix must be highly flowable and cohesive so that the laitance and debris would be pushed to the top of the tremie concrete.

CONCLUSIONS

High quality concrete can be placed underwater in drilled shafts. However, proper concrete mix and proper placement techniques are essential as well as performing effective non-destructive testing to confirm sound concrete.

REFERENCES

Netherlands Committee for Concrete Research, “Underwater Concrete”, HERON, 1973

ACI 304R-00, "Guide for Measuring, Mixing, Transporting, and Placing Concrete", Chapter 8 "Concrete Placed Under Water", American Concrete Institute, 2000

Yao, S.X., Berner, D.E., Gerwick, B.C., “Assessment of Underwater Concrete Technologies for In-the-Wet Construction of Navigation Structures”, U.S. Army Corps of Engineers Publication, *TR INP-SL-1*, 1999.

Yao, S. X., and Gerwick, B. C., “Underwater Concrete Part II: Proper Mixture Proportioning” and “Underwater Concrete Part III: Construction Issues”, *Concrete International*, February and March 2004.

SEAL SLAB PRESTRESSED PILE INTERFACE BOND FROM FULL-SCALE TESTING

Gray Mullins, Ruben Sosa, Rajan Sen and Moussa Issa, University of South Florida, Tampa, FL, USA

This paper presents experimental results from a study to assess the interface bond between a cast-in-place concrete seal slab and prestressed concrete piles in cofferdams. Three different seal slab placement conditions - fresh water, salt water and bentonite slurry - were evaluated and the results compared against controls where no fluid had to be displaced by the concrete. Normal pile surfaces were investigated. Additionally, the situation of "soil caked" piles was also investigated. Both model and full-scale tests were conducted. In the model tests, twenty eight 15 cm square prestressed sections were used with the embedment depth varied between d-2d, where d is the width of the pile. In the full-scale tests, 16 specimens were tested. The prestressed piles were 36 cm square with the embedment varied between 0.5d-2d. Four of the sixteen piles were cast with embedded gages located at the top, middle and bottom of the interface region.

The results showed that loads were transferred to the piles over an effective area, not the entire embedded depth. Significant bond stresses developed even for the worst placement condition. Recommendations are made for revising current values in specifications.

Keywords: seal slab, cofferdam, bond, concrete, bentonite, salt water, full-scale, prestressed, pile, foundation.

INTRODUCTION

Seal slabs are unreinforced concrete slabs cast inside cofferdams to prevent the intrusion of water and provide a dry working surface for subsequent construction (see Figure 1). Concreting is typically carried out by displacing water (or natural slurry in cases where the cofferdam supports the sides of an excavation) using a *tremie*. A tremie is essentially a funnel with a long pipe that places concrete directly on the bottom of the cofferdam. Because the concrete does not fall through the water, cement is not washed away and there is no segregation of coarse and fine aggregates. A series of tremie pipes are used to limit the flow of concrete in the horizontal direction and to prevent the build-up of excessive laitence[1].

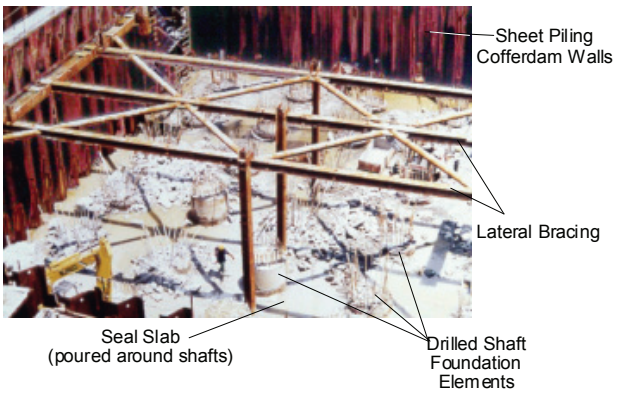


Figure 1: Seal Slab in Cofferdam Construction (Courtesy Georgia D.O.T.)

As the function of the seal slab is primarily to provide a dry working surface, its design is relatively unsophisticated. The slab depth is selected so that its weight balances the maximum uplift forces. Thus, a 10 m unbalanced head would require a 4 m thick seal slab since concrete density is approximately two and a half times that of water. Such a calculation neglects the frictional resistance that develops at the interfaces between the seal slab and foundation elements such as piles or drilled shafts.

The Florida Department of Transportation (FDOT) requires[2] the seal slab to cure for at least 72 hours before the standing water (or slurry) inside the cofferdam can be pumped out. At that time, the seal slab experiences full uplift pressure due to imbalance in hydrostatic pressure inside and outside of the cofferdam. Rational design therefore requires information on the interface shear corresponding to the 72-hour concrete strength. Unfortunately, no published data is available even though the earliest work on interface shear between two concrete surfaces was reported as far back as 1914[3].

In the absence of experimental data, specifications provide interface shear values that are of necessity conservative. For example, AASHTO[4] states that "*in seals, the bond between timber, steel or concrete piles and surrounding concrete may be assumed to be 10 psi*"(69 kPa). The1998, Florida Design Guidelines[5] limited the interface bond between the

seal slab and concrete piles to 276 kPa though it was only set at 34 kPa for steel piles. The larger values permitted in Florida may be due to the local experience associated with the large number of bridges crossing waterways, a relatively high water table, and the predominance of highly pervious cohesionless (sandy) soils that result in excavations quickly filling with inflowing ground water.

Recognizing that the allowable values were too low, in 1997 the Florida Department of Transportation issued a request for proposals (RFP) to assess this bond from full-scale tests. In January 1998, the University of South Florida commenced a two-year research program to investigate this problem. Although the goal of the study was to evaluate bond on the basis of full-scale tests, a 1/3rd scale pilot study was initially carried out to evaluate critical parameters and to develop an efficient method of testing. Following completion of this study, a limited number of full-scale tests were conducted to assess the interface seal slab/pile bond characteristics for prestressed concrete and steel piles and to recommend suitable values for design. This paper presents results relating to the seal slab / concrete interface bond. A companion paper provides the corresponding results for steel piles[6]. The complete experimental results as well as the comparative finite element modeling may be found elsewhere[7, 8].

RESEARCH SIGNIFICANCE

No studies have previously been carried out to evaluate the seal slab/concrete interface bond for conditions that may be directly used in design specifications. This study provides the first such experimental data from full-scale tests. Results of the study have already led to changes in the latest specifications.[9] Therein, the allowable stresses are greater permitting thinner seal slabs and bringing about significant savings in construction costs.

OBJECTIVES

The overall goal of the study was to recommend interface bond values for seal slab and piles that could be directly used in FDOT's design specifications. These values were to be based on full-scale tests on specimens prepared in accordance with current FDOT specifications for commonly encountered conditions. Variables examined were the pile embedment depth, pile surface, pile material (steel or concrete), and the type of fluid displaced by the concrete.

EXPERIMENTAL PROGRAM

A seal slab is subject to uplift pressures that are resisted in part by its weight and in part by shear resistance that develops at the pile/slab and sheetpile/slab interfaces as shown in Figure 2a. The same load transfer characteristics can be simulated by applying tensile loads to the pile and compressive loads to the seal slab (Figure 2b). In essence, the determination of the interface bond translated into conducting 'pull-out' tests on individual piles embedded in the seal slab; such an equivalent system was used in this study.

The reaction frame required to remove the piles from a seal slab had to meet multiple requirements of capacity, economy and portability. An adaptable design was also required to accommodate the differing connections for the steel and concrete pile specimens. Additionally, it needed to be integrated with electronic devices that permitted measurement of load and displacement.

A key parameter in the design of the test equipment was capacity. An upper limit could be determined on the basis of the ultimate tensile capacity of the prestressed pile. This depended on the pile size, concrete strength and the effective prestress. The greater the capacity, the larger and heavier the equipment, making testing that much more difficult (and expensive).

Uncertainties associated with bond strength predictions were addressed with a comprehensive pilot study using small-sized piles. A scale model study was carried out to develop an efficient testing method and also to identify critical parameters for the subsequent full-scale program. Brief details from both studies, a complete set of results, and their analysis are presented.

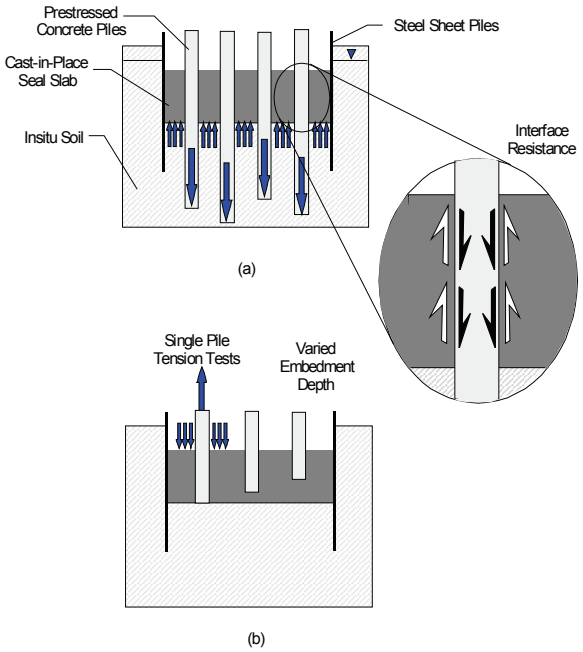


Figure 2: (a) Field Loading, (b) Uplift Load Simulation

PILOT STUDY

The pilot study simulated three different seal slab placement conditions involving (1) salt water (2) fresh water and (3) drilling fluid. Results were compared against the controls where no fluid was displaced by the concrete. One-third scale was selected since this allowed standard 45 cm prestressed piles to be exactly modeled[10]. Two different surface conditions - natural and soil-caked - were investigated.

Based on results of preliminary trials, the maximum interface bond between the two concrete surfaces was estimated to be about 1.7 MPa. This value was used to determine the maximum embedment depth that would not cause tension failure of the prestressed pile. As a result, three different embedment depths d, 1.5d and 2d (d is the side of the pile) were investigated. For each embedment depth, two specimens were tested, i.e. 24 tests were conducted (4 conditions x 3 embedment depths x 2 specimens). In addition, four soil-caked specimens were tested - one for each placement condition - for an embedment depth of 2d.

A total of 28 prestressed piles were tested. Square prestressed piles (1.22 m long, 15 cm wide) were fabricated at a commercial prestressing facility. During fabrication, 3.2 cm threaded Dywidag bars were embedded centroidally in the specimens to provide a convenient attachment for pulling the specimens (shown in Figures 3 and 4). Complete details may be found in the final report[7] .

Cofferdam Simulation

Four, 0.76 m high wood boxes with inside dimensions of 1.4 m x 1.4 m were fabricated to simulate the four excavation conditions. Plastic sheeting was used to make the boxes watertight. Wood templates were prepared so that the piles could be accurately positioned inside the form. The piles were spaced at 3 x pile size, i.e. the center to center distance was 0.45 m (3 x 0.15). The edge distance from the center line was 1.5d or 0.23 m.

As all the specimens were the same length and the seal slab the same thickness, the three different embedment depths of d, 1.5d and 2d were accommodated by varying the bonded and debonded lengths. For the 15 cm piles, this length varied between 15 (d) to 30 cm (2d). All bonded regions were at the bottom of the pile/seal slab. The debonded area was achieved by using bitumen covered with felt paper rapped in duct tape (Figure 3). A soil-caked surface was simulated by applying a paste consisting of a viscous mixture of the clay mineral kaolinite and water with a trowel. The clay had to be kept moist to prevent it from flaking off when it dried.

Three of the four simulated cofferdams were initially filled with either (1) fresh water, (2) 3% salt water, or (3) drilling fluid. The latter was made by mixing dry, high yield bentonite and fresh water to achieve slurry properties similar to those in the FDOT specifications. The final density achieved was 10 kN/m^3 with a pH of 8 and a viscosity of 37 seconds (Marsh Cone method). The fourth cofferdam was the control and was therefore not filled.

Seal Slab Placement

Class III seal concrete specified by FDOT[2] was used. This mix has 332 kg of cement/m^3, a water cement ratio of 0.51, and a specified 28 day strength of 21 MPa. The concrete was purchased from a ready-mix plant and was pumped through a 7.6 cm diameter hose. It was placed from the bottom upwards keeping the hose tip below the rising level of concrete. This is similar in placement and identical in effect to the tremie method. Figure 3 shows the fresh water cofferdam just after concreting with several inches of free water still present.

Pullout Frame

The frame designed for the 1/3rd scale pilot study is shown in Figure 4. It consists of two telescopic sections that react against each other via a stiffened beam and a hydraulic jack as shown. A standard nut was used to connect the free end of the Dywidag

rod in the prestressed pile to the base of the tension assembly. Although Figure 4 conceptually depicts the device assembly, the test procedure was streamlined by leaving it partially assembled between tests. The entire device weighed over 2.2 kN fully assembled and required an overhead chain hoist to assemble and/or move.

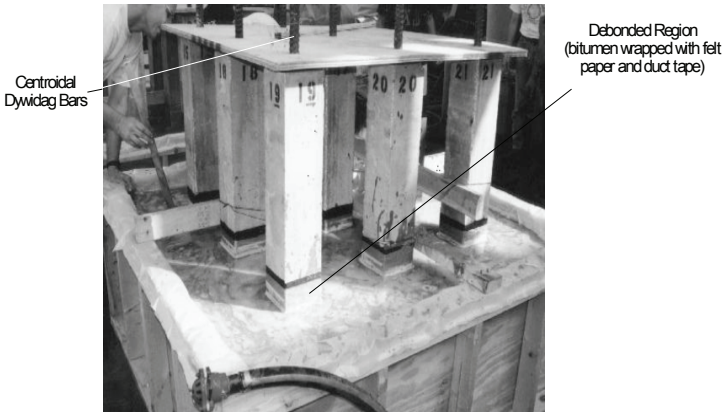


Figure 3: Pilot Study Simulated Cofferdam

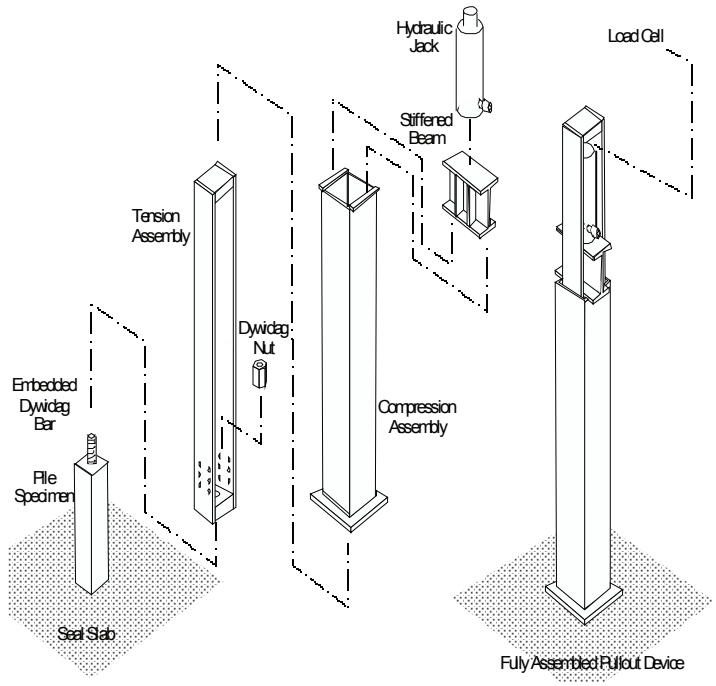


Figure 4: Pullout Equipment in Pilot Tests

Tension loads were measured using a load cell inserted between the top of the jack and the tension assembly. The stiffened beam transferred the load from the base of the jack to a built-up column section which in turn applied a uniform compressive stress to the seal slab.

Leveling

As the exposed surface of the seal slab was left uneven from the tremie placement method, a self-leveling grout pad had to be poured around each pile prior to testing. To further assist in the leveling process, a 12 mm steel bearing plate was placed on the grout immediately afterwards. Once the grout had time to cure (about 15 minutes), the tension assembly was connected to the pile and the compression assembly supported on the bearing plate.

Instrumentation

A Megadac data acquisition system by Optim Electronics Corporation was used for collecting and recording the test data generated. Loads were measured using a 100 tonne load cell and movement was monitored by two LVDTs. One of the LVDTs was magnetically attached to the compression assembly and positioned to record displacement with respect to an external reference beam. This registered any possible seal slab surface crushing or settlement occurring during testing. The other LVDT was attached to the tension assembly and referenced to the top of the compression assembly. This accounted for specimen movement, along with elastic deformation of the frame which was later accounted for in the data reduction.

Test Procedure

Tests were initiated after the seal slab had been cured for 72 hours. Concrete cylinders were periodically tested to monitor changes in compressive strength during the time it took to complete the tests. The frame was set in position and the pull-out test commenced. The tensile load was increased slowly using a manually operated toggle switch which intermittently engaged the power to a hydraulic pump. The load was increased slowly to reduce any possible dynamic stiffening of the system. Each specimen was displaced upward at least 2.5 cm.

PILOT STUDY RESULTS

A summary of the test results is presented in Table 1. This provides information from all 28 tests and contains details of the compressive strength, the failure load and the computed average bond stress. This was determined as the quotient of the measured failure load and the calculated surface area of the pile in contact with the seal slab. The following observations may be made:

1. Concrete strengths varied between 27-31 MPa over the duration of testing.
2. Significant bond stresses developed; the highest value obtained was 4.4 MPa (salt water/1.5d) and the lowest 0.2 MPa soil-caked control. Highest values were for salt water, followed closely by controls and fresh water.
3. Embedment depths above 1.5d led to lower average values (Table 1). This suggests that the bond stress distribution is non-uniform and instrumentation would be required to gain an understanding on the stress transfer.
4. Results for salt water and fresh water cofferdam conditions did not differ significantly.
5. The soil-caked condition did not affect interface bond except in the case of controls and bentonite slurry. For the salt water or fresh water condition, the soil caking was washed off by the water prior to the installation of the seal slab.

For the larger embedment depths, the prestressed concrete specimens cracked (see Figure 5).

This suggested that depths in excess of 1.5d may be inappropriate for the full-scale tests. Cracking of the seal slab was also observed during dismantling of the test set-up when the sides of the simulated cofferdam were removed. Figure 6 shows a load-slip plot obtained from the pilot study where the pullout capacity did not exceed the tensile capacity. Inspection of this plot indicates that there was continuous slip although minimal up to 50 kN (the elongation of the member was very small, L/AE≈0.015 mm/kN).

Table 1: Summary of Pilot Test Results

Type	Speci-men	f'c MPa	Bond Length	Pull out Load (kN)	Bond Stress (MPa)	Ave (MPa)
Control	C22	27	1d	377	3.9	3.8
	C23	27	1d	358	3.8	
	C24	27	1.5d	610	4.2	4.3
	C25	27	1.5d	632	4.3	
	C26	27	2d	630	3.3	3.3
	C27	27	2d	625	3.3	
Salt Water	C8	29	1d	398	4.1	4.1
	C9	29	1d	378	4.1	
	C10	29	1.5d	631	4.4	4.2
	C11	29	1.5d	591	4.1	
	C12	29	2d	651	3.3	3.4
	C13	29	2d	689	3.6	
Fresh Water	C15	29	1d	354	3.7	4.0
	C16	29	1d	417	4.3	
	C17	29	1.5d	620	4.3	4.1
	C18	29	1.5d	573	3.9	
	C19	29	2d	560	2.9	3.1
	C20	29	2d	622	3.2	
Ben-tonite	C1	29	1d	141	1.5	1.5
	C2	29	1d	149	1.5	
	C3	29	1.5d	557**	3.9	2.8
	C4	29	1.5d	237	1.6	
	C5	29	2d	206	1.1	1.9
	C6	29	2d	543**	2.8	
Soil-caked	Control	27	2d	39	0.2	
	Salt Water	31	2d	521	2.7	
	Fresh Water	31	2d	397	2.0	
	Ben-tonite	31	2d	49	0.3	

(** higher values are attributed to scouring action of the pumped concrete on piles closest to inflow)

FULL SCALE STUDY

The results of the pilot study were used to develop a program for full-scale tests. The principal changes were (1) elimination of the salt water condition (2) instrumentation of selected piles to allow evaluation of bond stress distribution with embedment depth and (3) restriction of the soil-caked surface to bentonite slurry placement. In view of the very high bond stresses that were obtained, the depth of embedment was limited to 1.5d excepting for bentonite where the maximum depth was increased to 2d. In addition, embedment depths of 0.5d were investigated for the control and fresh water placement conditions where the interface bond was expected to be very high.

With three different placement conditions (control, fresh water and bentonite), two different embedment depths (d, 1.5d or 2d) and two specimens per test, a total of 12 specimens were required. Four additional specimens were tested - one each for embedment depth of 0.5d (for the control and fresh water condition) and two for investigating the effect of soil caking for the bentonite slurry for an embedment depth of 1d. Thus, the controls and the fresh water condition each had five specimens with six specimens in the bentonite slurry condition.

The bond stresses obtained from the pilot study (Table 1) ranged from a low of 1.1 MPa (bentonite/2d) to a high of 4.3 MPa (control/1.5d). Because of these large values, 36 cm wide square prestressed piles were used in the full-scale tests. The length of each specimen was limited to 1.5 m.



Figure 5: Post-mortem Profile View of the Pilot Study Specimen During Dismantling

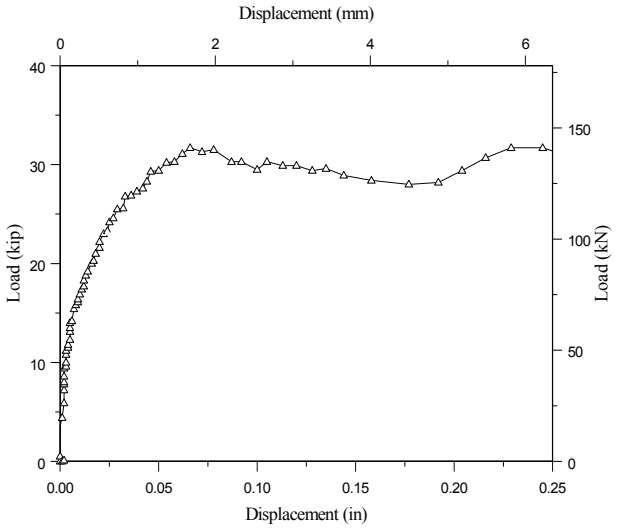


Figure 6: Load vs. Displacement – Specimen C1 (1d, bentonite.)

Unlike the pilot tests where a central Dywidag rod was integrally cast with the specimens, for the full-scale tests the strands were directly attached to the tension frame with prestressing chucks. To ensure that the piles would have a somewhat greater capacity, bigger 15mm strands were used instead of the standard 12.5 mm strands though they were stressed to provide the same effective prestress. The eight 15 mm strands gave an ultimate pulling capacity of 260 x 8 = 2.1 MN that exceeded the expected pullout load of the pile. This provided a margin of safety against sudden, dangerous tensile failure of the strands.

A total of eighteen specimens were cast at the same commercial prestressing yard. The spacing of the specimens inside the prestressing bed was adjusted so that each specimen had a 0.6 m length of strand projecting from the pulling end that served as a connection point to the pull-out frame. Additionally, four specimens were instrumented with embedded sister bar-type strain gages to allow the distribution of bond stresses to be assessed. Figure 7 shows three sister-bar strain gages which consist of a resistive foil strain gage bonded to a short length of 13 mm rebar. These were located at the bottom, middle and top of the bonded length of 1d (three specimens) or 2d (1 specimen) (Figure 7). Complete fabrication details may be found in the final report[7].

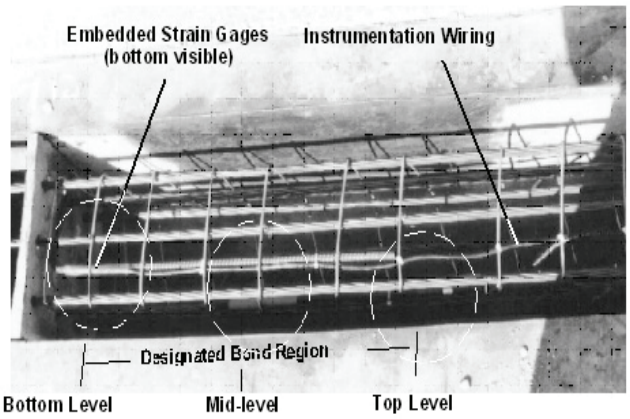


Figure 7: Prestressing Bed for Casting 36 cm Instrumented Piles

Simulated Cofferdam

Three cofferdams had to be constructed for the three conditions investigated. The dimensions of the cofferdams were determined by the number of piles and a 3d pile spacing (1.07 m) as in the pilot study. Thus, two of the cofferdams - fresh water and control - were identical in size, but the bentonite slurry-filled cofferdam was larger as it had more specimens.

The cofferdams were constructed using rented steel reinforced plywood box forms made by Symons Corporation, Des Plaines, IL. The forms were connected to form each cofferdam using wedge pins provided by the manufacturer. They were also externally braced using wooden stakes and internally braced with a wooden template that maintained the pile positions. Additionally, each cofferdam was lined with 0.15 mm plastic sheeting. This allowed for the forms to be watertight, preventing the loss of any construction fluid (water or bentonite slurry).

Specimen Support

Following the construction of the cofferdam, the specimens were accurately positioned on plywood pads to prevent damage to the plastic lining. Additionally, a polystyrene seal was placed between each concrete pile specimen and the wooden pad to prevent possible bonding between the cast-in-place seal concrete and the bottom of the pile. The specimens were vertically supported by a wooden framework that was secured to the Symons forms (Figure 8).

Debonded Surface

As in the pilot study, differing lengths (0.5d, 1d, 1.5d and 2d) of the pile surface were bonded or debonded. Debonding was achieved in the identical manner. The bonded concrete surfaces were left in their natural state excepting for the two specimens that were tested for the soil-caked condition. For this case, an adhesive clay soil, typically used for clay models by artists was used because it bonded better than the kaolinite paste tested in the pilot study.

The debonded length extended from the boundary of the bonded region to approximately 15 cm above the intended elevation of the finished surface of the seal slab. This included an additional 36 cm depth determined from finite element analysis to ensure uniform distribution of compressive loads to the seal slab (Figure 2b).

The bentonite slurry was made by mixing dry, high yield bentonite and fresh water. The mixing was accomplished through the use of a shear pump. Enough bentonite clay was added to achieve slurry properties similar to FDOT specifications. The final density achieved was 10.2 kN/m^3 with a viscosity of 40 seconds (Marsh Cone Method) and a pH of 8. Figure 8 shows the filling and completion of the bentonite slurry filled simulated cofferdam.



Figure 8: Overview of Cofferdam During Concreting

Seal Slab Placement

Seal concrete was placed using a concrete pump truck. The concrete was pumped through a 15 cm diameter hose. It was placed from the bottom upwards keeping the hose tip below the rising level of concrete. This procedure is identical to the tremie method commonly used in construction practice.

Testing Apparatus

Similar considerations of capacity, economy and portability dictated the design of the pullout frame. This design incorporated an available double-acting, 3 MN hydraulic jack, a 69 MPa hydraulic pump system, and could accommodate connections for both concrete and steel pile types. Additionally, it provided sufficient clearance for a 4MN loadcell as well as means to record pile displacement.

As with the pilot test, the reaction frame consisted of a tension and compression assembly. The tension assembly was connected directly to the pile using prestress chucks and supported by the hydraulic jack and load cell. The stiffened beam was integrated directly into the compression assembly which applied compressive loads to the seal slab. Fully assembled the device weighed 16 kN and was placed over each specimen with a straight mast industrial forklift (Figure 9). Additional information on the design and fabrication may be found elsewhere.[7]



Figure 9: Full-Scale Pullout Device

Test Setup

The test setup was similar to the pilot study and involved placement of a grout layer, assembly and connection of the hydraulic testing apparatus, attachment of the data acquisition system, and application of loading until failure. Given the requirement that testing be completed quickly following the 72 hour cure period, appropriate adjustments were made to expedite testing.

Leveling Grout Pad

Since concrete vibration is not used in seal slab construction due to possible aggregate segregation in the submerged environment, various degrees of surface roughness developed depending on the pour condition. The bentonite pour condition had the greatest degree of unevenness; the control had the least. The uneven surfaces were leveled using a thin layer of high strength grout that was placed directly over the seal slab (Figure 9). The grout was poured and finished two days after the placement of the CIP seal slab. Since the debonded portion of each pile specimen extended well above the CIP slab, there were no difficulties with possible bonding of the grout to the piles.

Frame Assembly

Although much heavier than the pilot study device, the full-scale pullout device was easier to use in that it could be left fully assembled between tests. This reduced the number of heavy lifts and expedited testing.

As the entire frame was lowered over the test specimen, the exposed prestressing strands were threaded through the holes in the base of the tension assembly. Standard prestressing chucks which incorporate wedge-type grips were secured on each strand. A 76 mm gap was maintained between the tension assembly and the top of the pile to permit removal of the prestressing chucks after testing. With the chucks in place, the frame was centered and the concrete pile tested.

Data Acquisition

As with the pilot study, the Megadac data acquisition system by the Optim Electronics Corporation was used for collecting and recording the test data generated by the pull-out testing. Along with the Megadac, a load cell and two electronic displacement gages (LVDTs) were used to monitor each pile specimen as it was tested. The load cell had a capacity of 4 MN. The electronic displacement gages had a 50 mm range. Additionally, strains were monitored in selected piles

that had been cast with embedded resistance-type sister bar strain gages (Figure 7). For the concrete specimens, one LVDT was magnetically attached to the bottom of the tension assembly and positioned to register displacement with respect to an external reference beam. The other LVDT recorded relative displacement between the tension assembly and the top of the pile specimen. This accounted for any possible slippage of the prestressing chucks.

Test Procedure

Once the set-up procedure was completed, the pull-out testing could be conducted. The tensile load was increased slowly using a manually operated toggle switch which intermittently engaged the power to the hydraulic pump. The load was increased slowly to reduce any possible dynamic stiffening of the system. Each specimen was displaced upward at least 25 mm to ensure that the bond interface had been displaced.

RESULTS

A summary of the test results is presented in Table 2. This provides information from all 16 tests and contains details of the compressive strength, failure load, and the computed average bond stress. Inspection of Table 2 shows that the bond stresses were quite high ranging between 4.5 MPa for 0.5d embedment in the controls to the lowest value of 1.1 MPa for one of the soil-caked bentonite specimens. Trends observed in the pilot tests were repeated: the average bond stresses decreased with increased embedment depth. For example, the average bond stress reduces from 2.7 MPa to 2.0 MPa for fresh water specimens embedded 1.0d and 1.5d, respectively.

Table 2: Summary of Full Scale Test Results

Type	Speci-men	f'c MPa	Bond Lgth	Pull out Load (kN)	Bond Stress (MPa)	Ave (MPa)
Control	C0.5	27	0.5d	1151	4.5	
	C1.0A	32	1d	1656	3.2	3.2
	C1.0B	32	1d	1580	3.1	
	C1.5A	32	1.5d	1584	2.1	2.4
	C.15B	32	1.5d	2020	2.6	
Fresh Water	W0.5	27	0.5d	892	3.5	
	W1.0A	27	1d	1358	2.7	2.7
	W1.0B	27	1d	1336	2.6	
	W1.5A	27	1.5d	1591	2.1	2.0
	W1.5B	27	1.5d	1527	2.0	
Ben-tonite	B1B	23	1d	1338	2.6	2.5
	B1D	23	1d	1274	2.5	
	B2A	23	2d	1625	1.6	1.5
	B2B	23	2d	1438	1.4	
Bento-nite	B1A	23	1d	931	1.8	1.5
(soil caked)	B1C	23	1d	570	1.1	

Variations in concrete strength over the duration of the test may also be noted. The lowest compressive strength was for the bentonite series (f'c = 23 MPa) and the highest for the controls (32 MPa). This was in part due to increase in strength over the seven day period it took to complete the testing. A typical load vs slip variation plot is shown for each cofferdam condition in Figures 10-12. As before, the plots show continuous displacement with increasing load; initially elastic and then plastic. While measurements included the effect of elongation of the 1.5 m long prestressed pile, calculations show that length increases were minimal even after the pile had cracked. Figure 10 shows no evidence of cracking (bentonite) whereas Figures 11 and 12 indicate pile cracking at 1044 and 955 kN, respectively. The cracking load was consistently smaller than expected due to the shortened transfer length near the end of the pile and the associated inability to develop effective prestress in the concrete. This was due to the relatively short length of the test piles. In actual construction where longer piles are used this would not be the case. Additionally, variations in cracking force in nearly identical specimens was attributed to indiscernible alignment errors during testing.

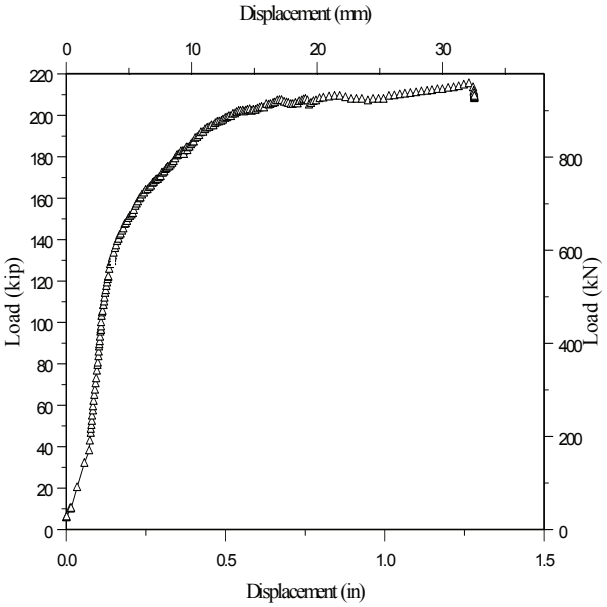


Figure 10: Load vs. Displacement - Specimen B1A (1d, bentonite, soil-caked)

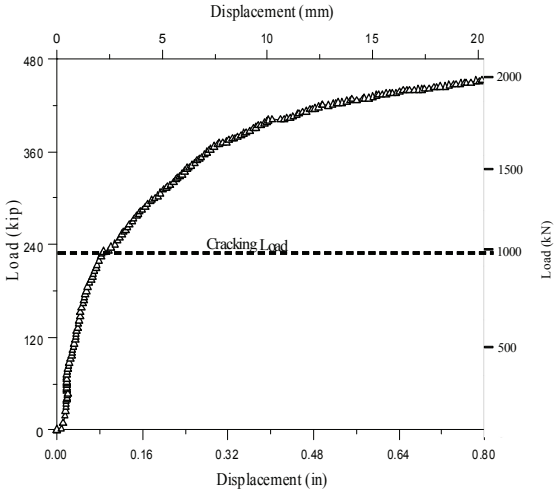


Figure 11: Load vs. Displacement - Specimen W1.5B (1.5d, water)

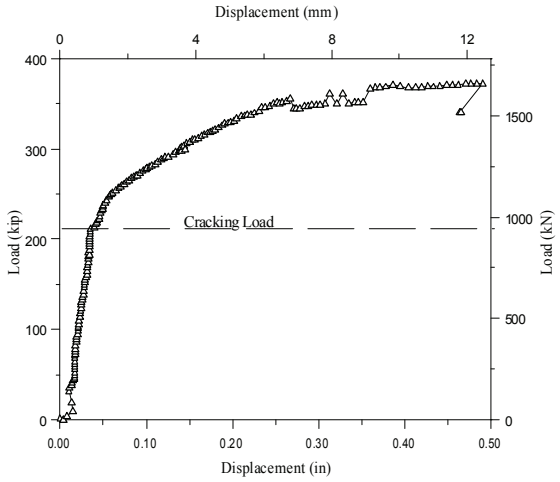


Figure 12: Load vs. Displacement - Specimen C1.0A (1d, control)

Strain Variation

The shear stress distribution within the bonded region of the pile was evaluated using embedded strain gages in four of the specimens: fresh water (1), control (1), and bentonite (2). The bond length was 1d for three of the specimens (one in each bed) and 2d for an additional specimen in the bentonite. The gages were located at the top, middle, and bottom of the bonded region. Figure 13 shows the axial strain at measured at three points along the bond interface during testing of one instrumented pile specimen. Additional results may be found in the final report[7].

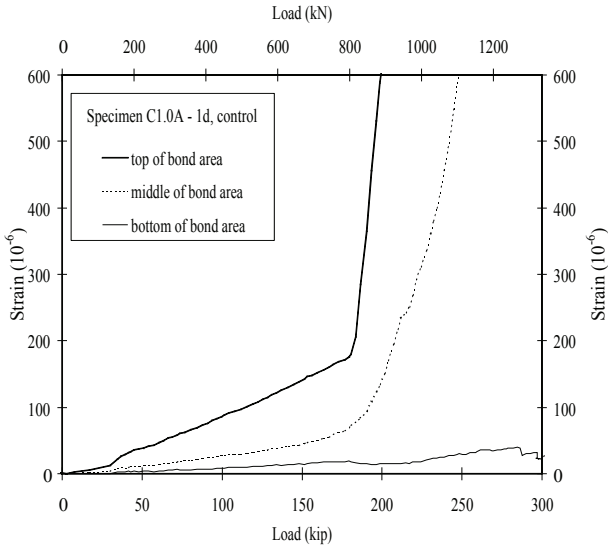


Figure 13: Change in Strain with Respect to Load for Specimen C1.0A (control, 1d Embedment)

The strains recorded at three levels (top, middle, and bottom of the bond interface) define two bonded layers (upper and lower) separated by the middle gage. The difference between the top and middle gage indicates the load carried by the upper layer. Likewise, the difference between the middle and bottom gage indicates the load carried by the lower bond layer. Inspection of this plot shows the load distribution stayed relatively constant up to the elastic limit of the upper bonded layer (2 MPa); at which time the load was gradually transferred to a lower layer. The top gage reading should linearly relate to the loadcell as there is no alternate load path between them. As expected, the gage at the bottom of the bond area registers near zero strains as no additional capacity can be developed below that level. The non-linear portion of the middle gage indicates the upper layer bond failing and transferring load to the lower layer. Sharp discontinuities are observed in the upper gages due to sudden cracking; whereas less severe strain changes are noticed in the middle gages as the cracked sections reach further into the seal slab.

The load distribution as measured by the strain gages indicates that the full bond length contributed to its capacity. However, peak bond capacities occurred at different locations and time from top to bottom in that the amount of slippage required to develop peak shear strength is small with respect to elastic elongation. This can also be deduced by evaluating the average bond strengths from Table 2 with respect to embedment (e.g. Average Control Values: 0.5d, 4.5 MPa; 1.0d, 3.2 MPa; and 1.5d, 2.4 MPa). As embedment decreases, bond strength approaches an upper limit proportional to the concrete strength as shown in Figure 14.

As in the pilot study, cracking was observed in both the prestressed piles and in the seal slab. Figure 15 shows a transverse tension crack just above the seal slab. Figure 16 shows a crack that formed in the seal slab originating from the corner of a pullout specimen. These conditions need to be addressed in design.

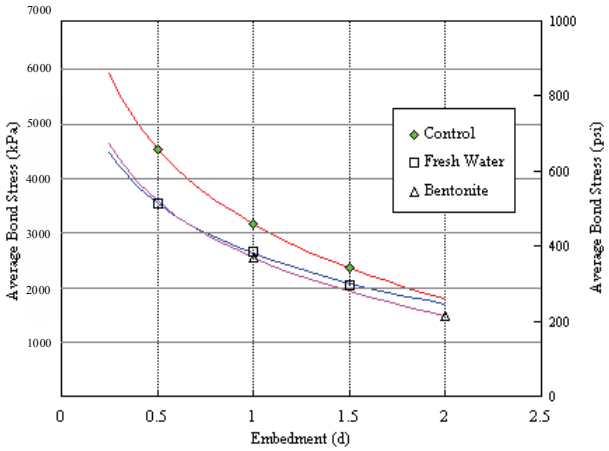


Figure 14: Average Bond Stress Variation with Embedment from Full-Scale



Figure 15: Pile Cracks During Loading



Figure 16: Seal Slab Cracks During Testing

CONCLUSIONS

This study presents results from an experimental study that investigated the interface bond stress that developed between seal concrete and prestressed piles in cofferdams. Two series of tests were conducted. In the first series, one-third scale models were fabricated and tested. Three variables were investigated (1) displacement of fresh water, salt water and bentonite slurry, (2) different pile surface conditions, and (3) varied embedment depths expressed as multiples of the pile width (d). In the second series, full-scale tests were conducted for only two conditions (fresh water and bentonite slurry) as well as varied embedment depths. In all cases, results were compared against controls where no fluid was displaced. Seal slabs were cast using concrete delivered by ready-mix plants that conformed to Class III concrete in current FDOT specifications[2]. The concrete was allowed to cure for 72 hours prior to testing as permitted by existing specifications.

The following conclusions may be drawn:

Bond stresses determined experimentally were significantly higher than set in current specifications. Average values obtained from the full-scale tests varied between 2.0-2.7 MPA for fresh water displacement and from 1.5-2.5 MPA for bentonite displacement. The lowest value obtained was 1.1 MPA for piles caked in soil and embedded in bentonite to a depth d.

Bond stress values from the full-scale tests were generally smaller than those for the model tests excepting for bentonite slurry (Tables 1 and 2).
Strain data indicated that regardless of the embedment depth, loads were transferred to the pile over an effective depth. For the specimens tested, this depth was the same as the size of the pile (d).
The bond between seal slab and piles caked with mud was largely unaffected when fresh water or salt water was displaced. These effects became important in controls or when bentonite slurry was displaced. This was because the caked soil was washed away by water currents that developed during concreting.

Prestressed piles and seal slabs developed cracks before the full pullout load was developed Thus, structural failure of the seal slab and/or the piles themselves should be considered in any rational design process.

RECOMMENDATIONS

The buoyancy force generated at the base of a seal slab can be withstood using a combination of both the bond strength formed between the pile and the cast-in-place concrete as well as its self weight. While using this bond to offset a portion of the upward load, the tensile force developed in the pile cannot be permitted to exceed its cracking strength. The bond capacity developed by an individual pile may be determined using the allowable bond stress, $f_{b,}$ listed in Table 3.

Table 3: Allowable Bond Stresses for Square Piles

Material	Condition	f_b (MPA)
Concrete	Salt or Fresh Water	2.1
	Bentonite	0.7

This stress (f b) may be assumed to act uniformly over an effective surface area, A_e given by:

$A_e = pD$ if $D < d$, or
$A_e = pd$ if $D > d$

given the pile width *d,* pile perimeter *p,* and the seal slab thickness *D*. This limits the effective bond length to 1.0d of the pile. Hence, the uplift capacity of the pile (P) is the lesser of the allowable bond

capacity (P sub a ~=~ f sub b A sub e), or the pile tensile strength (e.g. AASHTO (5.6.3.4.1-1)).

In the latest Florida Design Guidelines[9], allowable bond stress values have been increased from 40 psi (0.3 MPA) to 250 psi (1.7 MPA) based on the results that are presented in this paper.

ACKNOWLEDGMENTS

This investigation was carried out with the financial support of the Florida Department of Transportation. The authors especially acknowledge the contribution of Hayward Baker Inc. Tampa, FL in the full-scale testing as well as Rudy. Additional thanks are extended to Mr. Paul V. Liles, Jr. and the Georgia Department of Transportation for providing Figure 1. The opinions, findings and conclusions expressed in this publication are those of the writers and not necessarily those of the Florida Department of Transportation.

REFERENCES

1. Tomlinson, M.J. (1986). Foundation Design and Construction, 5th ed., Longman Scientific and Technical, Essex, England.
2. Standard Specifications for Road and Bridge Construction (1999). Florida Department of Transportation, State Specifications Office, Tallahassee, FL.
3. Johnson, L.J. and Nichols, J.R. (1914). "Shearing Strength of Construction Joints in Stems of Reinforced Concrete T-Beams as Shown by Tests," Transactions of the American Society of Civil Engineers, Dec., pp. 1499-1522
4. Standard Specifications for Highway Bridges 13th Edition (1983). American Association of State Highway and Transportation Officials, Washington, D.C., Section 4.3.4.6.2.
5. Structural Design Guidelines (1998). Florida Department of Transportation, Section 4.18, Topic No: 625-020-150c, July, p. 4-12, Tallahassee, FL.
6. Mullins, G., Sosa, R., Sen, R. and Issa, M. (2001). "Seal Slab/Steel Pile Interface Bond from Full-Scale Tests," Paper in preparation.
7. Mullins, G., Sosa, R. and Sen, R. (2000). "Seal Slab/Pile Interface Bond", *Final Report* submitted to Florida Department of Transportation, June, pp. 151.
8. Wu, Z (1999). "Studies of Bond of Cast-in-Place Concrete to Other Surfaces," MSCE Thesis, Department of Civil and Environmental Engineering, University of South Florida, Tampa, FL, August.
9. Structural Design Guidelines (2000). Florida Department of Transportation, Table 5.3, Tallahassee, FL.
10. Fischer, J., Mullins, G. and Sen, R. (2000). "Strength of Repaired Piles." *Final Report* submitted to Florida Department of Transportation.

SEAL SLAB / STEEL PILE INTERFACE BOND FROM FULL-SCALE TESTING

Gray Mullins, Ruben Sosa, Rajan Sen and Moussa Issa, University of South Florida, Tampa, FL, USA

This paper presents results from model and full-scale tests to assess the interface bond between a cast-in-place concrete seal slab and steel H-piles in cofferdams. Three different seal slab placement conditions - fresh water, salt water and bentonite slurry - were evaluated and the results compared against controls where no fluid was displaced by the concrete. Normal pile surfaces were investigated. Additionally, the situation of "soil caked" piles was also tested.

In the model tests, eight 15 cm deep, W6 x 15 sections were used for two different embedment depths of 1.5d and 2d, d being the depth of the section. In the full-scale tests, 16 specimens 35 cm deep (W14 x 90 sections) were tested with the embedment varied between 0.5d-2d. The results show that significant bond stresses developed even in the worst placement condition. Recommendations made for revising current values in specifications have already been implemented by the Florida Department of Transportation.

INTRODUCTION

Cofferdams are usually required in the construction of bridge foundations over waterways. Typically, a sheet pile enclosure is constructed in water and piles are driven as shown in Figure 1. A tremie concrete seal is then poured. When the seal has sufficiently cured, the cofferdam is dewatered and internal bracing installed. Thus, the seal allows the construction of the pier to be carried out under dry conditions.

As the function of the unreinforced seal slab is primarily to provide dry working conditions its design is quite simple. The seal thickness is essentially determined so that its weight balances the maximum uplift pressure since the allowable interface shear stresses are very small. Earlier AASHTO specifications[1] permitted interface shear stress values of 69 kPa (10 psi). However, these values were reduced to 34.5 kPa (5 psi) for steel interfaces in the Florida Design Guidelines[2]. Neither values are based on test data.

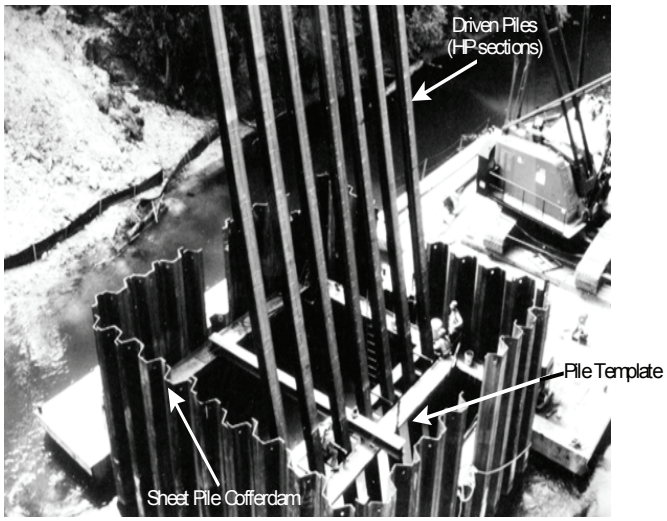


Figure 1: Sheet pile cofferdam with pile driving template. ***(Courtesy of Applied Foundation Testing)***

In 1997 the Florida Department of Transportation funded a study to evaluate interface bond from full-scale tests. This paper presents results relating to the seal slab /steel pile interface bond. A companion paper provides the corresponding results for prestressed piles[3]. The complete results from this study including finite element modeling may be found elsewhere[4,5].

RESEARCH SIGNIFICANCE

This study provides the first set of experimental results on the interface shear between steel piles and seal concrete slabs cast in accordance with construction specifications[6]. The results obtained have already led to increased allowable interface shear in the latest specifications.[7] This should result in reduced construction costs.

OBJECTIVES

The overall goal of the study was to recommend interface shear stress values for seal slab and piles that could be directly used in FDOT's design specifications. These values were to be based on full-scale tests conducted on specimens that had been prepared in accordance with current FDOT specifications[6] for conditions that were commonly encountered. Variables examined were the pile embedment depth, effect of pile surface, effect of the pile material (steel or concrete) and the type of fluid that was displaced by the concrete.

EXPERIMENTAL PROGRAM

The load transfer characteristics in seal slabs can be simulated by conducting pullout tests as illustrated in Figure 2 in which compressive loads are applied to the seal slab and tensile loads to the steel piles. Careful attention had to be paid to the experimental set-up so that tests could be carried out under field conditions. Small-scale bond tests were conducted to identify the maximum pullout lengths for a 1/3 scale pilot study. Results of the pilot study were used to subsequently refine the apparatus and procedures for the full-scale testing.

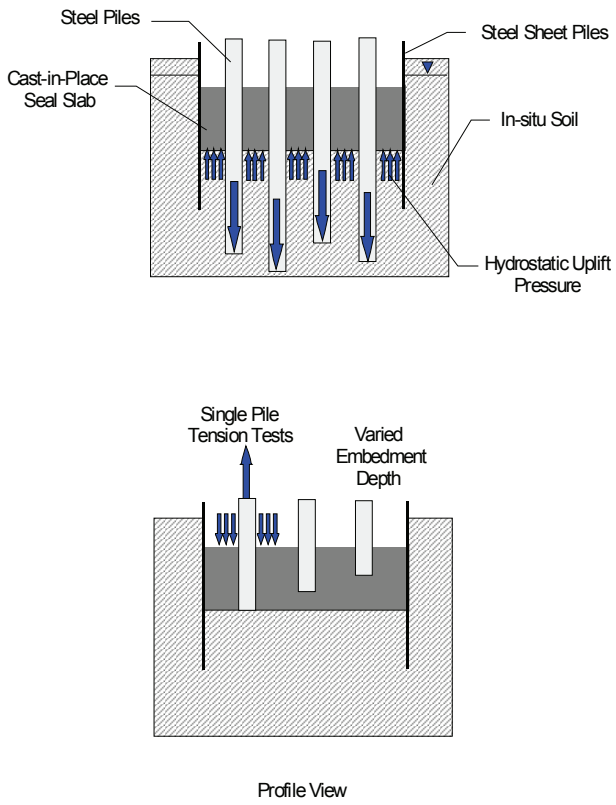


Figure 2: Simulation of loads

PILOT STUDY

The pilot study simulated three different seal slab placement conditions involving: (1) salt water, (2) fresh water, and (3) drilling fluid. These results were compared against controls where no fluid had to be displaced by the concrete. The 15 cm deep, wide flange sections were tested for two different embedment depths, 1.5d and 2d (d is the nominal pile size). Thereby a total of 8 model scale tests were conducted (4 conditions x 2 embedment depths).

The steel pile specimens were fabricated using a W 6 x 15 beam section made from A36 structural steel. Each steel pile was 0.91 m (36 inches) in length. On each pile, a line of three, 23.8 mm (15/16 inch) diameter holes were drilled into each flange to facilitate the twelve, 22 mm (7/8 inch) bolts required to provide the connection to a pullout apparatus.

Cofferdam Simulation

Four, 0.76 m high wood boxes with inside dimensions of 1.4 m x 1.4 m were fabricated to simulate the four placement conditions. Plastic sheeting was used to line and seal the boxes. Wood templates were used to properly position each pile within the simulated cofferdams. The piles were spaced at 3 x pile size, i.e. the center to center distance was 45 cm. The edge spacing from the center line to the box edge was 1.5d or 22.5 cm.

All piles were identical in length and tip elevation; however, the two different embedment depths of 1.5d and 2d were accommodated by varying the bonded and debonded lengths within the concrete. The bonded region (steel to seal slab) was provided at the bottom of the simulated cofferdam in all the specimens. For the 15 cm piles, the bonded length was either 22.5 cm (1.5d) or 30 cm (2d). Above this bonded length, the piles were debonded using a thick layer of bitumen (Figure 3) applied up to a height sufficiently above the anticipated upper surface of the seal slab. The overall slab thickness and debonded region was set such that the bitumen extended at least 1d below the upper seal slab surface for all specimens. This minimum debond length was intended to eliminate bearing stress concentrations based on finite element modeling.

Three of the four boxes were filled with either fresh water, 3% salt water or bentonite slurry (Figure 3). The latter was made by mixing dry, high yield bentonite and fresh water to achieve slurry properties similar to those in the FDOT specifications[6]. The final density achieved was 10 kN/m^3 (64 pcf) with a pH of 8 and a viscosity of 37 seconds (Marsh Cone method). The fourth box served as a control and was therefore not filled.

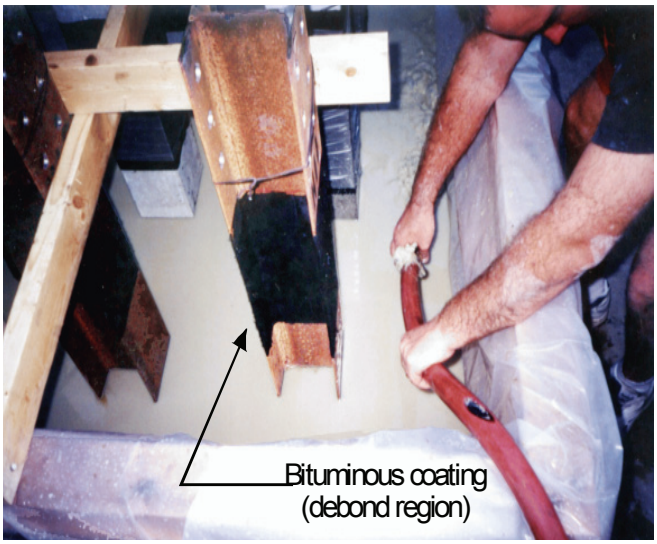


Figure 3: Drilling fluid pumped into simulated cofferdam

Seal Slab Placement

Class III seal concrete specified by FDOT[6] was used. The specified 28 day strength of the seal slab was 21MPa (3000 psi). This mix has 330 kg of cement / m^3 (560 lb of cement/cy) and a water cement ratio of 0.51. The concrete was purchased from a Readi-Mix plant and was pumped through a 76 mm (3 inch) diameter hose. The concrete was placed from the bottom upwards keeping the hose tip below the rising level of concrete. This is similar in placement and identical in effect to using a tremie pipe.

Pullout Frame

The pullout frame used is shown in Figure 4. It consists of two telescopic sections that react against each other via a stiffened beam and a hydraulic jack. The pile specimen was bolted to the tension assembly. The pullout frame weighed 2.2 kN fully assembled and required an overhead chain hoist to assemble and/or move. Tension loads were measured using a load cell positioned between the top of the jack and the tension assembly. The stiffened beam transferred load from the base of the jack to a built-up column section which in turn applied uniform compressive stress to the seal slab.

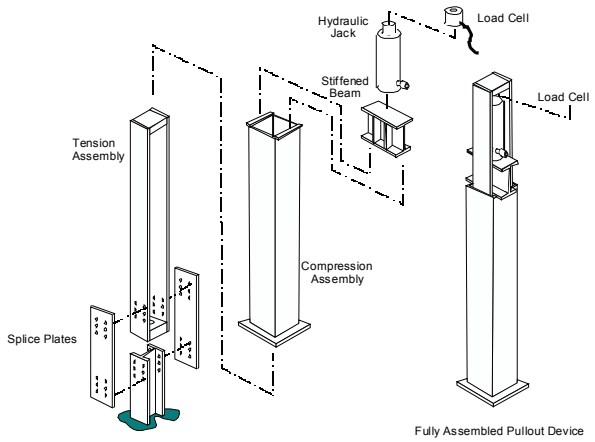


Figure 4: Model scale pullout equipment

Leveling

Before the pullout frame was installed, a grout pad was poured around each pile specimen using a high strength, fast curing, self-leveling grout. To further assist in this alignment process, a steel bearing plate was placed in the fresh grout and squared with respect to the longitudinal axis of the pile.

Instrumentation

A MEGADAC data acquisition system by Optim Electronics Corporation was used for monitoring and recording the test data generated. Loads were measured using a load cell and slip was monitored by two LVDTs. One of the LVDTs was magnetically attached to the compression assembly and positioned to record displacement with respect to an external reference beam. This registered any possible seal slab surface crushing or settlement that might occur during testing. The other LVDT was attached to the tension assembly and referenced to the top of the compression assembly. This recorded specimen movement as well as the compliance of the frame which was later accounted for in the data reduction.

Test Procedure

Pullout tests were commenced after the seal slab had been cured for 72 hours in accordance with FDOT requirements. Concrete cylinders were tested at periodic intervals to monitor the change in compressive strength. The tension assembly was bolted to the piles using 22 mm (7/8 inch) diameter bolts. Once the grout had time to cure (about 15 minutes), the compression assembly was lowered on to the bearing plate. The stiffened beam, along with the hydraulic jack, was then positioned between the compression section and the upper end of the tension assembly as shown in Figure 4.

With the specimens set-up, the pull-out test commenced. The tensile load was increased slowly using a manually operated toggle switch which intermittently engaged the power to the hydraulic pump. The load was increased slowly to reduce any possible dynamic stiffening of the system. Each specimen was displaced at least 25 mm.

RESULTS

A summary of the test results is presented in Table 1. This provides information from the 8 tests and contains details of the compressive strength, the failure load and the average bond stress. Over the duration of the tests, there was no change in the compressive strength.

Table 1: Summary of pilot test results

Type	Speci-men	f'c MPa	Bond Lgth	Bond Area (m2)	Pull out Load (kN)	Bond Stress (MPa)
Control	H41	31	1.5d	0.206	611	3.01
	H42	31	2d	0.274	720	2.66
Salt Water	H21	31	1.5d	0.206	744	3.66
	H22	31	2d	0.274	563	2.08
Fresh Water	H31	31	1.5d	0.206	336	1.66*
	H32	31	2d	0.274	620	2.29
Ben-tonite	H11	31	1.5d	0.206	320	1.58
	H12	31	2d	0.274	344	1.27

The following observations may be made:

Significant bond stresses were developed; the highest value obtained was 3.66 MPa (salt water/1.5d) and the lowest 1.27 MPa (bentonite/2d). Highest values varied with embedment depth. For 1.5d embedment, the highest was for salt water followed by controls and fresh water. For 2d, control values were highest followed by fresh water then salt water. The magnitude of the bond stress decreased with an increase in embedment depth. This suggests that the distribution of bond stress is non-uniform.

The results for bentonite slurry were surprisingly good. Indeed, for embedment depth of 1.5d, values obtained were comparable to that for fresh water.

Values for salt and fresh water are similar.

FULL SCALE STUDY

The pilot study provided important information on the magnitude of the interface steel/seal bond that could develop. The significant scatter in the results indicated the need to conduct additional tests. These findings led to refinements in the full-scale test program. The principal changes were: (1) elimination of the salt water condition - this was based on the results of more extensive tests carried out on prestressed piles[3], (2) consideration of the effect of soil-caked surface, and (3) increase in the number of specimens.

In view of the very high bond stresses that were obtained, the depth of embedment was limited to 1.5d excepting for bentonite where the maximum depth was increased to 2d. In addition, embedment depths of 0.5d were investigated for the control and fresh water placement conditions.

With three different placement conditions (control, fresh water and bentonite), two different embedment depths (d, 1.5d or 2d) and two specimens per test, a total of 12 specimens were required. Four additional specimens were tested - one each for embedment depth of 0.5d (for the control and fresh water condition) and two for investigating the effect of soil caking for the bentonite slurry for an embedment depth of 1d. Thus, the controls and the fresh water condition each had five specimens with six specimens for the bentonite slurry condition. These were identical to the conditions investigated for prestressed piles[3].

The depth (35 cm) and length of the steel piles was kept the same as that for the prestressed piles. As a result, 1.52 m long W14 x 90 sections made from A36 steel were used. Holes for 28.6 mm (1-1/8 inch) diameter bolts were drilled in each flange to connect the pile specimens to the tension assembly frame (Figure 5).

Simulated Cofferdam

Three cofferdams had to be constructed for the three conditions that were investigated. Two of these - fresh water and control - were identical in size. The bentonite slurry condition with the larger number of specimens was larger. The dimensions of the cofferdam were determined by specimens and edge distances that were kept the same 3d (1.06 m) as in the pilot study.

The cofferdams were constructed using rented steel reinforced plywood box forms connected to each other using wedge pins provided by the manufacturer. They were also externally braced using wooden stakes and a two-by-four framework. Additionally, each cofferdam was lined with 0.2mm (6 mil) plastic sheeting. This provided a water-tight barrier, preventing the loss of any construction fluid (water or bentonite slurry). Figure 5 shows one of the cofferdams just prior to filling with fluid.

Specimen Support

Following the construction of the cofferdam, the specimens were accurately positioned on plywood pads to prevent damage to the plastic lining. The specimens were vertically supported with a wooden two-by-four framework that was secured to the box forms (Figure 5).

Debonded Surface

As in the pilot study, differing lengths (0.5d, 1d, 1.5d and 2d) of the pile surface were bonded or debonded. Debonding was achieved in the identical manner as in the pilot study. The bonded steel surfaces were left in their natural state excepting for the two specimens that were tested for the soil-caked condition. For this case, an adhesive clay soil, typically used for clay models by artists was used because it bonded better than the kaolinite paste tested in

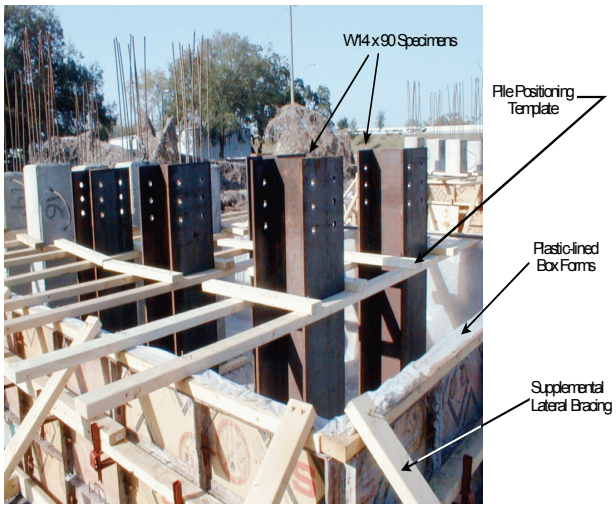


Figure 5: Steel Piles in simulated cofferdam (Prestressed piles were also tested in the same bed.)

the pilot study[3]. The debonded length extended from the boundary of the bonded region to approximately 15 cm above the intended elevation of the finished surface of the seal slab. This included an additional 35 cm length determined as needed by finite element analysis to ensure uniform distribution of compressive loads to the seal slab surrounding the bonded region.

Placement Conditions

One cofferdam was left dry prior to concrete placement (control); the second was filled with fresh water from a nearby potable source. The third was filled with bentonite slurry which was made by mixing dry, high yield bentonite and fresh water. The mixing was accomplished through the use of a shear pump. Enough bentonite clay was added to achieve slurry properties similar to FDOT specifications. The final density achieved was 10 kN/m^3 (65 pcf) with a viscosity of 40 seconds (Marsh Cone Method) and a pH of 8.

Seal Slab Placement

Seal concrete was placed using a concrete pump truck. The concrete was pumped through a 15 cm (6 in) diameter hose and was placed from the bottom upwards keeping the hose tip below the rising level of concrete. This is similar in placement and identical in effect to the tremie method.

Testing Apparatus

Identical considerations of capacity, economy and portability dictated the design of the pullout equipment. A steel reaction frame was designed to take advantage of an available double-acting, 2670 kN (300 ton) hydraulic jack which would be operated with a portable 69 MPa (10 ksi) hydraulic pump system. The frame required connection designs for both concrete and steel pile types. Additionally, the frame would need to be integrated with electronic devices to measure load and displacement.

As for the pilot test, the reaction frame consisted of a tension and compression assembly. The tension assembly was connected directly to the pile with two splice plates and housed the hydraulic jack and load cell. The compression assembly applied compressive loads to the seal slab. Figure 6 shows a photograph of the complete assembly being placed over a pile specimen. Additional information on the design and fabrication may be found elsewhere[4].

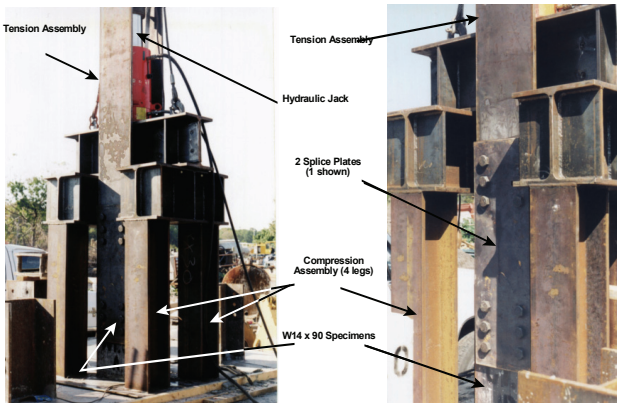


Figure 6: Full scale test apparatus

Test Procedure

The test setup and procedure was similar to the pilot study involving placing a grout layer, connecting the tension assembly to the pile, lowering the compression assembly on to the leveled grout surface, attach the appropriate instrumentation, and extract the specimens. However, some variations were adopted to expedite the testing procedure so less variation in concrete strength would be observed after the 72 hour FDOT curing period.

Since no concrete vibration or finishing is used in seal slab construction, various degrees of surface roughness developed in the submerged conditions. Instead of leveling the base of each pile individually, all cofferdams were leveled at the same time with a skim coat of grout batched from a single truck. The grout was poured and finished two days after the placement of the CIP seal slab without adding significant delay before testing could commence. The bentonite pour condition had the greatest degree of unevenness, whereas the control was more uniformly placed due to the visual input during its placement (although unfinished). Since the debonded portion of each pile specimen extended well above the CIP slab, there were no difficulties with possible bonding of the grout to the piles (Figure 7).

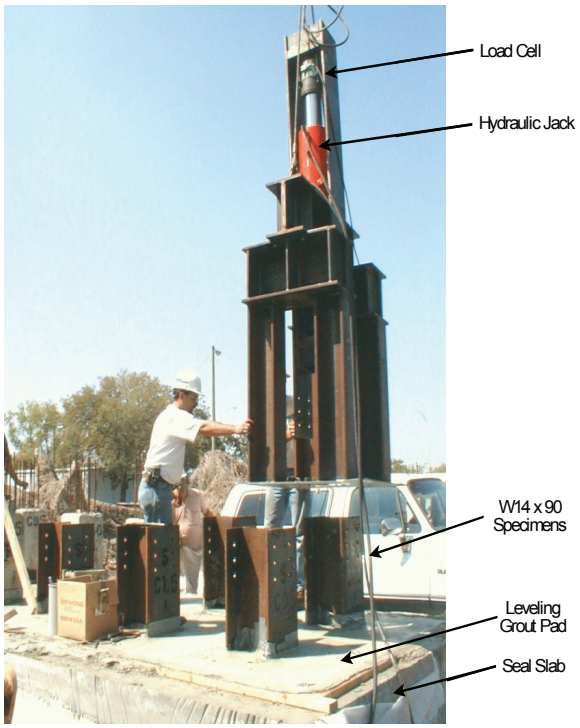


Figure 7: Full Scale pullout device suspended over test specimen

Although much larger than the model scale device, the pullout apparatus could be attached more quickly due to easy access of the splice plate bolts. It was also left fully assembled between tests. Instrumentation and data acquisition attached to the device was again similar to the model scale tests with the exception of the load cell capacity (2670 kN) which was sized to accommodate the increased loads. One of two displacement gages was magnetically attached to the pile and referenced to the top of the slab. The other gage was magnetically attached to the pile and referenced to an external reference beam to monitor global movements.

The tensile load was increased slowly using a manually operated toggle switch which intermittently engaged the power to the hydraulic pump. The load was increased slowly to reduce any possible dynamic stiffening of the system. Each specimen was displaced upward at least 25 mm to ensure that the bond capacity had been fully developed.

RESULTS

A summary of the test results is presented in Table 2. This provides information from all 16 tests and contains details of the compressive strength, the failure load, and the average bond stress. Inspection of Table 2 shows that the bond stresses were quite low compared to the pilot study. The highest value was 1.63 MPa (control/0.5d) and the lowest 0.50 MPa (bentonite/2d). However, trends observed in the pilot tests were repeated; the average bond stresses declined with increased embedment depth. For example, the average bond stress reduces from 1.31 MPa to 1.07 MPa for a fresh water embedment depth increase from d to 1.5d.

Table 2: Summary of full scale test results

Type (w)	Spec. (w)	f'c MPa	Bond Lgth (w)	Pull out Load kN	Bond Stress MPa	Ave MPa	Norm-alized MPa
Control	SC0.5	32	0.5d	618	1.63		
	SC1.0A	32	1d	1018	1.34	1.40	1.20
	SC1.0B	32	1d	1100	1.45		
	SC1.5A	32	1.5d	1140	1.00	1.02	0.88
	SC.15B	32	1.5d	1187	1.04		
Fresh Water	SW0.5	27.5	0.5d	438	1.15		
	SW1.0A	27.5	1d	1105	1.33	1.31	1.21
	SW1.0B	27.5	1d	975	1.29		
	SW1.5A	27.5	1.5d	1317	1.16	1.07	0.99
	SW1.5B	27.5	1.5d	1116	0.98		
Ben-tonite	SB1B	23.5	1d	874	1.15	0.88	0.88
	SB1D	23.5	1d	466	0.62		
	SB2A	23.5	2d	827	0.55	0.52	0.52
	SB2B	23.5	2d	767	0.50		
Ben-tonite (soil-caked)	SB1A	23.5	1d	629	0.83	0.91	0.91
	SB1C	23.5	1d	753	0.99		

Variations in concrete strength over the duration of the test may also be noted. The lowest compressive strength was for the bentonite series (f'c = 23.5 MPa) and the highest for the controls (32 MPa). The bond strength is normalized to a 23.5 MPa concrete strength in Table 2 by dividing the measured values by the percent increase in the square root of the concrete strength. For example the control values were normalized as follows:

$$1.20MPa = 1.40MPa\frac{\sqrt{23.5}}{\sqrt{32}}$$

Representative load vs displacement plots are shown for each of the simulated cofferdam conditions in Figures 8-10. Each graph also shows the effect of embedment depth on the pullout response for the various conditions. The control and freshwater environments showed similar results for normalized bond values of 1.20 MPa and 1.21 MPa, respectively. Likewise, the trends associated with the effects of embedment were comparable (Figures 8 and 9). The pullout capacity increased somewhat linearly with embedment depth up to 1d. This can be noted in both peak and residual values when comparing the 0.5d and 1d test results. With longer embedment depths (1.5d) little increase in average capacity was observed (10% in controls and 17% in water). This was also noted in Table 2 where average bond strengths decreased 18% (1.31 to 1.07 MPa) and 27% (1.40 to 1.02 MPa) in the water and control specimens, respectively for the same increased embedment depths. Figure 10 shows the pullout response of the piles cast in the bentonite slurry-filled cofferdam. Therein, several differences were introduced due to anticipated decreases in bond strength: (1) 0.5d embedment was not used, (2) the 1.5d was increased to 2d, and (3) soil caking was applied to some 1d specimens. The effects of embedment were similar in this set of tests as no significant additional pullout capacity was realized with the additional bond area from 1d to 2d embedment. This is supported by the moderate 19% average increase in pullout with a 100% increase in embedment (670 kN to 797kN). This decreased bond efficiency is further illustrated by the 41% decrease in the average bond strength in Table 2 (0.88 MPa to 0.52 MPa). The effect of soil caking was less significant than that of the embedment depth most probably due to the scouring action during the seal slab placement. In general, the bentonite condition produced larger variations in the measured bond values. However, the overall findings indicate that the bond between steel and seal slabs is significantly higher that specified in design codes.

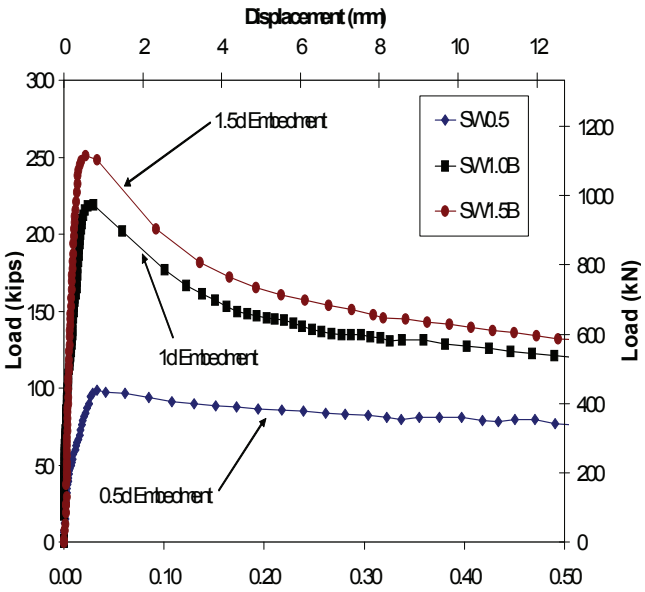


Figure 8: Water-filled cofferdam test results

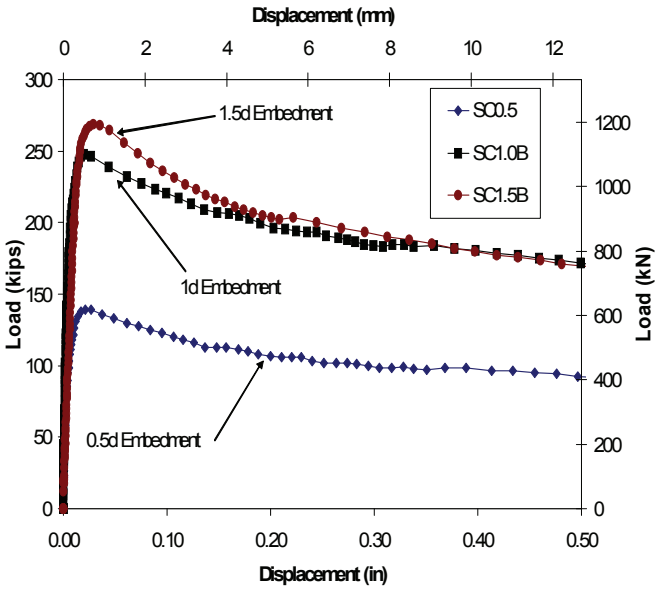


Figure 9: Control cofferdam test result

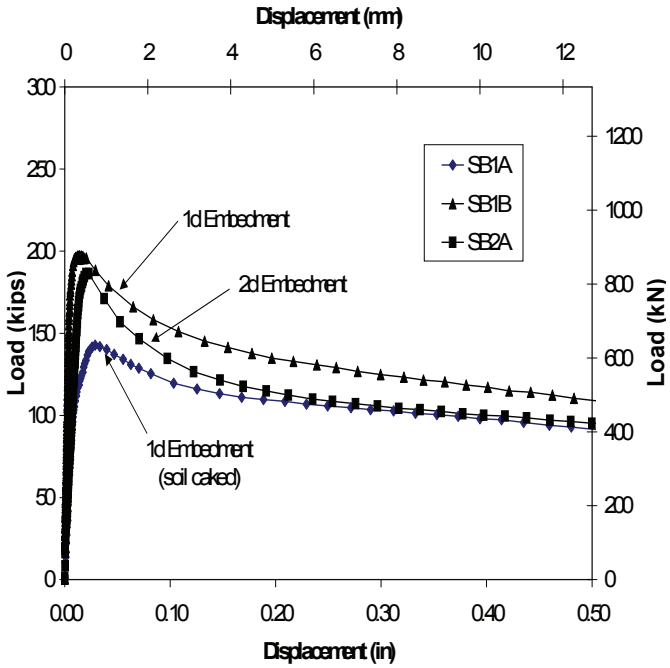


Figure 10: Bentonite slurry-filled cofferdam test result

DISCUSSION

The goal of the study was to determine the interface bond between steel piles and seal slabs that had been cast in accordance with existing construction specifications (concrete piles were also tested). As the FDOT specifications allow a 72 hour cure period for the seal slab, the need to develop a scheme that met the requirement for rapid testing without compromising the results was of critical importance. Pullout testing was used and several innovative measures adopted to expedite the testing process.

In the model study, 36 tests (28 concrete and 8 steel) were completed within 8 hours following the 72 hour cure period. During this time, no changes in concrete strength were observed. In the full-scale tests, greater time was required to complete the testing. An important constraint was access to heavy lifting equipment (and an operator) to move the pullout frame after every test. However, all 32 tests (16 concrete and 16 steel) were completed within 10 days of the casting of the seal slab. As concrete strengths

were evaluated throughout the test period, the relationship between the interface bond and concrete strength was used to normalize the bond values. Taking into consideration the totality of the study, the model and full-scale results provide a good indication of the magnitude of the interface bond that develops between the seal concrete and piles.

The results from the model tests gave higher bond values than those from the full-scale tests (see Tables 1 and 2). Similar trends were observed in the tests on the prestressed piles[3] though the differences were much smaller. This is most likely because the surfaces of the steel piles in the full-scale tests were smoother compared to those used in the model tests. In contrast, the concrete surfaces in both model and full-scale tests were similar.

As with prestressed piles, the results clearly indicate that the variation in the interface bond is non-linear since the pullout load was not proportional to the embedment depth. Unfortunately, this distribution could not be measured without introducing surficial anomalies due to instrumentation. However, in the concrete piles where strain gages could be embedded during casting this relationship could be ascertained[3]. The non-linearity in the interface shear distribution was indirectly incorporated in the proposed recommendation by defining an effective "embedment depth." Embedment in excess of this effective depth did not contribute significantly towards the total resistance (Figures 8 - 10).

CONCLUSIONS

This study presents results from an experimental study that attempted to determine the interface bond stress that developed between seal concrete and steel piles. Two series of tests were conducted. In the first series, a one-third scale model was fabricated and tested. Three different placement conditions were investigated - displacement of fresh water, salt water, and bentonite slurry for two different embedment depths. In the second series, full-scale tests were conducted for two different conditions - fresh water and bentonite slurry. In all cases, results were compared against controls where no fluid was displaced. Seal slabs were cast using concrete delivered by ready-mix plants and conformed to Class III concrete in current FDOT specifications. The concrete was allowed to cure for at least 72 hours prior to testing as permitted by existing specifications. The following conclusions may be drawn:

Bond stresses determined experimentally were significantly higher than set in current specifications. Average values obtained from the full-scale tests varied between 1.1-1.3 MPa for fresh water displacement and 0.5-0.9 MPa for bentonite displacement. The lowest value obtained was for piles embedded in bentonite cofferdam a depth 2d.

Bond strength varied with embedment depth as indicated by both the model and full scale test results. This implies that thicker seal slabs cannot develop full bond capacity simultaneously along the entire bonded area beyond a maximum length. Instead, they develop full capacity over shorter bonded lengths dependent on the concrete shear strain limit value with respect to the elongation of the pile. In this case it was shown that embedment depths in excess of 1d were ineffective in supplying additional pullout capacity.

The results of the study confirm the poorer interface bond for steel surfaces compared to concrete where 1d average values for water and bentonite conditions were 2.7 MPa and 2.5 MPa, respectively[4].

Variations between the model-scale and full-scale test results can be in part attributed to the surface roughness of the as-delivered steel piles. The model piles were partially oxidized, whereas the full-scale piles had never been exposed to an outdoor environment prior to placement. The recommended values are based on the full-scale test results which are therefore conservative.

RECOMMENDATIONS

Loads supported by the bond between seal concrete and steel piles (*section depth* d*, perimeter* p*, embedded depth* D *in seal slab*) may be determined from the allowable bond stress, $F_{b,}$ listed in Table 3. This stress may be assumed to be uniform over an effective area A_e given by:

$A_e = pD$ if $D < d$
$A_e = pd$ if $D > d$

Table 3 Allowable Bond Stresses:

Material	Condition	F_b (kPa)
Steel	Salt/Fresh Water	1000
	Bentonite	350

In the latest Florida Design Guidelines[7], allowable interface shear values have been greatly increased based on the findings presented in this paper.

ACKNOWLEDGMENTS

This investigation was carried out with the financial support of the Florida Department of Transportation. The authors especially acknowledge the contribution of Hayward Baker Inc. Tampa, FL in the full-scale testing as well as Rudy. However, the opinions, findings and conclusions expressed in this publication are those of the writers and not necessarily those of the Florida Department of Transportation.

REFERENCES

1. Standard Specifications for Highway Bridges 13th Edition, American Association of State Highway and Transportation Officials, Washington, D.C., 1983.

2. Structural Design Guidelines, Florida Department of Transportation, Section 4.18, Topic No: 625-020-150c, July, p. 4-12, Tallahassee, FL, 1998.

3. Mullins, G., Sosa, R., Sen, R. and Issa, M., "Seal Slab Prestressed Pile Interface Bond from Full-Scale Tests," ACI Stuctural Journal, Vol 98, No.5 Sept.- Oct., 2001, pp.743-751.

4. Mullins, G., Sosa, R. and Sen, R., "Seal Slab/Pile Interface Bond", *Final Report* submitted to Florida Department of Transportation, June, 2000, pp. 151.

5. Wu, Z., "Studies of Bond of Cast-in-Place Concrete to Other Surfaces," Master's Thesis, Department of Civil and Environmental Engineering, University of South Florida, Tampa, FL, August, 1999.

6. Standard Specifications for Road and Bridge Construction, Florida Department of Transportation, State Specifications Office, Tallahassee, FL, 1999.

7. Structural Design Guidelines, Florida Department of Transportation, Table 5.3, Tallahassee, FL, 2000.

UNDERWATER CONCRETE - MIX DESIGN AND CONSTRUCTION PRACTICES

Sam X. Yao, Ben C. Gerwick, Inc., San Francisco, CA, USA

The underwater concrete technology has historically evolved largely through a trial-and-error process of constructing marine works. Many outstanding examples exist of high quality concrete placed underwater. However, failures also occurred and led to excessive cost and/or schedule overruns. These failures were largely due to improper concrete mix design or improper placement. The problems may have occurred because proper underwater concrete construction techniques and experience have not been widely disseminated. This section focuses on technical issues of underwater concrete mix design, concrete production and placement, and quality control.

PROPER MIX DESIGN

The basics of proportioning underwater concrete are generally the same as those applicable to the conventional concrete. The general principles of mixture proportioning should follow the concrete industry guidelines (e.g., ACI 211.1). However, due to its special site conditions and peculiar placement methods, underwater concrete mixes must be further refined to meet the special requirements. The following address some special requirements pertaining to underwater concrete mix design.

Concrete placed underwater is inherently susceptible to cement washout, laitance, segregation, cold joints, and water entrapment. Thus, it must possess some unique workability characteristics that are otherwise not required for concrete. According to the definition of ACI 116R, workability of concrete is "that property of freshly mixed concrete or mortar that determines the ease with which it can be mixed, placed, consolidated, and finished to a homogeneous condition". In practice, the interpretation of workability is inevitably specific to applications in each project. Unless the level of concrete workability is specifically defined and fully understood by all the parties involved in the design and construction, underwater concreting will be exposed to risks of failure.

For underwater concrete, workability can be generally interpreted as three basic performance requirements as follows:

1. ***Flowability***: The concrete must be able to flow out easily underwater and completely fill the placement area without trapping water inside. At the presence of obstructs such as steel cages or piles, the concrete is required to flow around and fully encase the structural embedment. Consistency of concrete has been traditionally measured by the slump test. It works well for concretes with slump up to 150 mm (6 in). For flowable concrete, the slump flow test produces more consistent and reliable results. The slump flow is the average diameter of concrete spread in a slump test. Keep in mind that the required level of flowability can only be estimated approximately with slump flow test, because concrete flow is closely related to such construction variables as the rate of concrete placement, concrete pour size, flow distance, flow impedance by obstructs such as reinforcing steel. The dynamics of flowing concrete also has a significant impact on workability during placement.

2. ***Self-consolidation***: Since it is impractical to consolidate concrete underwater by mechanical vibration, the concrete must consolidate itself underwater. The primary driving force for spreading and consolidating concrete placed underwater is its own weight, which is substantially reduced by the buoyancy in water. Figure 1 illustrates the compressive strength of concrete as a function of its consistency (slump) and the degree of compaction on the basis of laboratory tests in air. It shows that at a slump above 150 mm (6 in), there is little difference in the compressive strength between compacted and uncompacted concrete. Underwater concrete, however, generally need a slump higher than 175 mm (7 in) in order to achieve self-consolidation under its own buoyant weight.

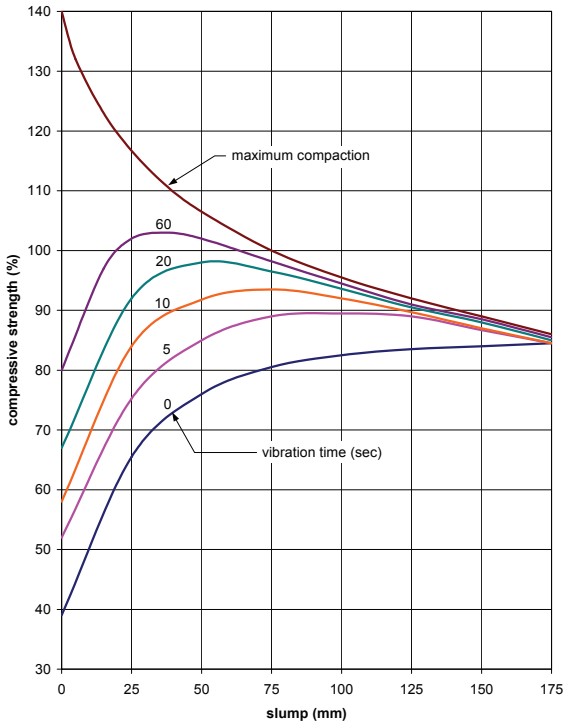


Figure 1: The compressive strength as a function of the degree of vibration and slump

3. ***Cohesion***: The concrete is required to remain cohesive underwater. The primary objective is to ensure the homogeneity and strength of underwater concrete by minimizing cement washout, segregation, and laitance. The desirable degree of cohesion for concrete, however, depends on many construction variables such as the thickness and configuration of concrete pours, concrete flow distance, and exposure to flowing water during placements. The cohesion of concrete is more difficult to quantify than its flowability. In theory, it is often described with two rheological parameters – yield stress and plastic viscosity. At present, however, a comprehensive knowledge base has not yet been established to quantitatively correlate the rheological parameters with concrete workability. In practice, the U.S. Army Corps of Engineers' washout test is widely used to measure the cohesion against cement washout in the U.S.

In addition to the three basic requirements above, many special applications impose even higher demand on workability. For example, underwater repair of a concrete slab may require self-leveling concrete, and placing concrete in flowing water requires high anti-washout characteristics for concrete mixes. In essence, it is important to understand that the workability requirement varies over a wide range, depending on specific applications. The mix design should be tailored for each application. As an example, Table 1 shows a range of workability requirements that are being used for various project applications.

Research indicates that the in-place concrete quality is closely related to the way that the concrete flows underwater. The importance of the concrete flow pattern has been recognized since the early part of last century. Further investigations revealed that concrete generally flows under water in one of the two distinct patterns. When concrete is highly flowable and cohesive, it tends to flow in a "bulged" flow pattern, i.e., newly placed concrete pushes previously placed concrete sideways, forming a successive series of bulges (Figure 2). It has been found that the bulged flow pattern tends to develop a relatively flat and smooth top surface with good in-place concrete quality. On the other hand, less flowable concrete flows in a "layered" pattern, i.e., newly placed concrete flows upward around the placement pipe and over the top of previously placed concrete (Figure 3). Apparently, this layered flow pattern exposes more concrete to water and is usually associated with a steep and rugged top surface with large quantities of laitance. It is indeed counterintuitive that, for the same cohesion, more flowable concrete is less susceptible to laitance formation due to its reduced exposure to water, but past experience and tests have verified this phenomenon.

Table 1: Typical Workability Requirements for Some Common Applications in Marine Foundations

Applications	Essential Requirements	Slump Flow Inch (mm)
Tremie seal for cofferdam	Infill in simple geometry Little obstruction to the flow	11 - 16 (280 – 400)
Drilled shafts	Reinforcing steel to obstruct the flow Short flow path	14 - 18 (350 – 450)
Reinforced concrete slurry walls or structures	Reinforcing steel to obstruct the flow Moderate to Long flow path	16 – 23 (400 – 580)
Reinforced tremie concrete slab with flat top surface	Reinforcing steel to obstruct the flow Long flow path Self-leveling concrete	23 - 27 (580 – 680)

In general, workability of concrete is linked to complex relationships among several variables, such as the water-to-fines ratio, cementious materials content, and chemical admixtures. Engineering judgment and experience are

necessary in evaluation of concrete workability for each application. The theoretical and practical aspects of these key variables are discussed below.

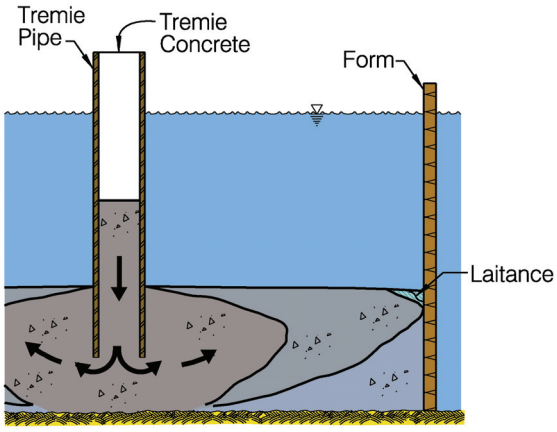


Figure 2: Flowable underwater concrete exhibits a "bulged" flow pattern

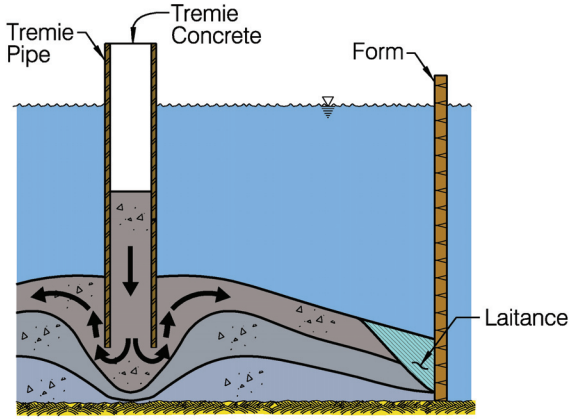


Figure 3: Less flowable underwater concrete exhibits a "layered" flow pattern

Underwater concrete mixtures typically contain cement content in the range of 360-500 kg/m^3 (600-840 lb/cy), which is generally higher than typical concrete placed in air. Past experience shows that rich cement content results in much better quality concrete placed underwater. For many years, it has been intuitively understood that the rich cement content tends to compensate for inevitable washout for underwater placements. Further studies indicate that high cement content is required for the workability of underwater concrete as well as the strength.

Workability of concrete is significantly affected by the amount and nature of water in concrete. The mixing water can be classified into free water and bound water (also known as "water demand"). Free water is the interstitial water existing between solid particles in concrete. It disperses and lubricates the solids to create fluidity and plasticity of concrete. Bound water is a result of chemical and physical binding of water by the solids. The chemical binding of water results from the chemical reactions of cement. As cement hydration progresses, more water is chemically bound in the hydrates and the free water gradually decreases. Loss of workability over time is a direct result of the loss of free water. The physical binding of water results from water absorption and surface tension of the solids. The larger the surface area of the solids, the higher the water demand. Since the fines count for more than 90% of the total surface area of the solids, bound water is nearly proportional to the fine content. Therefore, it is the water-to-fine ratio that determines the amounts of bound water, free water and workability of concrete. For underwater concrete, a water-to-fine ratio in the range of 0.85 to 1.0 by volume often provides a good balance between flowability and cohesion requirements.

A practical question is whether a portion of the cement content can be replaced with other fines without degrading the performance of underwater concrete. It is well known that a moderate increase in sand content tends to reduce cement washout in concrete placed underwater. It appears that the increased washout resistance is a direct result of an increase in fine content.

In recent years, underwater concrete construction have trended towards using ternary concrete mixtures that incorporate a proper combination of GGBF slag, fly ash and silica fume in concrete. Concretes containing up to 50% fly ash and 80% GGBF slags have been successfully used in mass tremie concrete pours. These field applications of high volume mineral binders have proven their beneficial effects on workability, durability, and control of the heat of hydration.

Silica fume plays a special role in underwater concrete mixture. Due to its high water-binding capability, silica fume is frequently added to underwater concrete as a "mineral-based" anti-washout admixture. In general, the net effects of silica fume are highly dose-dependent. At a relatively small dosage up to 6%, the microsilica particles in fresh concrete tend to attach to cement particles as a dispersion agent, which results in an improvement of concrete workability. When silica fume is added at higher dosages, microsilica particles start to flocculate among themselves, resulting in high water demand and less workability.

Limestone powder has been successfully used in underwater concrete as a supplement or replacement of cement by 10 to 20 percent. Finely

ground limestone powder has strong capability to bind water and enhance cohesion. In addition, limestone powder improves dispersion of cement particles in fresh concrete and bridges between cement hydrates. As a result, studies show that concrete mixtures containing limestone powder have high consistency, low bleeding, and low permeability. For many years, limestone powder has been widely used in Europe and Canada as a filler material in commercial cement. European cement standards allow up to 35% limestone to be added to commercial cement, provided that the limestone meets certain chemical purity requirements for use in concrete (e.g., $CaCO_3$ and clay contents). In the U.S., limestone powder that meets the criteria for use in concrete are abundant.

For a given concrete mixture, an increase in its flowability tends to reduce its cohesion to some extent and vice versa. In the past, the mix design for underwater concrete had to be a compromise between its flowabilitiy and cohesion. Before the 70s, for example, underwater construction traditionally limited concrete flow distance to 5 m (16 ft) and concrete slump to about 150 mm (6 in). These limitations seriously constrained advanced applications of underwater concrete. In recent years, development of high range water reducing admixtures (HRWR) and anti-washout admixtures (AWA) have had a revolutionary impact on the performance of underwater concrete. Underwater concrete can now achieve high flowability at a low water-cement ratio, and yet retain adequate cohesion to resist cement washout and segregation.

AWA is primarily composed of long chain saccharide polymers. When dissolved in water, the long chain molecules entangle to restrains mobility of free water. Viscosity of the solution consequently increases. Upon agitation, the polymer chains tend to disentangle and align with the shear flow. The faster the agitation, the lower the resistance is to the concrete flow. When the agitation stops, the AWA polymer chains entangle again and the solution returns to the original viscosity. This thixotropic effect of AWA has proven to be the key in placing high performance underwater concrete. Under the fully hydrated condition, AWA may not function properly in concrete unless HRWR is also present. It is postulated that cement particles must be fully dispersed before AWA can form the necessary bridging between them.

With increasing uses of chemical admixtures, underwater concreting requires special considerations for constructability. It is well known that HRWA may sometimes react adversely to cause rapid or erratic slump loss. Although some new HRWR admixtures, such as the polycarboxilate-based type, show potential benefits in preventing the rapid loss of workability, their net effects on various cements and concrete mixtures are variable and should in generally be verified through trial tests under field conditions.

When the construction logistics indicates the possibility of substantial time lapse between concrete mixing and placing, it is essential that flowability of the concrete at the point of placement be maintained above certain minimum criteria. The required work window should take into account of concrete delivery time, the duration for each placement, delay due to site access and potential interference of other onsite activities. On the other hand, overdosing set-retarding admixtures can produce an excessively prolonged delay of the set, which is especially pronounced when AWA and HRWR are added to concrete. Excessive retardation in combination of low ambient temperature during concrete curing can lead to excessive bleeding and irreparable damage to concrete strength.

Air-entraining admixtures (AEA) are often used to improve workability of concrete placed in air. This practice, however, may not be suitable for underwater concrete. The main concern is the stability of the entrained air in concrete placed under water. Past experience shows that the entrained air content depends on many job-site factors such as temperature, concrete delivery and placement, water depth, and compatibility with other admixtures. Since it is difficult to control these factors so as to produce uniform consistency under various field conditions, it is prudent to refrain from using AEA in underwater concrete unless the concrete will be subsequently exposed to freezing and thawing environments.

In principle, chemical admixtures should not be used to compensate for poor mixture proportions and poor materials quality. Only when the concrete proportions are optimized can chemical admixtures effectively improve the performance of concrete.

In summary, the mix design for underwater concrete must be performed with sound technical know-how and thorough considerations for specific project requirements, as any sizable defect due to improper mix design is likely to result in costly repair and less quality structures. The mix design is essentially an optimization process. The process should be guided by a set of governing variables and an understanding of how each variable affects the concrete performance.

CONCRETE PRODUCTION

Underwater concrete construction often entails transportation of a large quantity of materials over water. Location of a concrete batch plant is an important consideration in logistics planning and has significant implications in construction cost, risks, and quality control. The batch plant can be established either onshore or offshore, depending on the placement plan and site conditions. The offshore production option has main advantage of more reliable control of the concrete workability at the point of placement, because the time between concrete batching and placing is relatively short. However, this option could entail a significant investment in the equipment. An offshore concrete production facility commonly consists of a floating batch plant, a concrete conveyer, materials storage/delivery barges and facilities. Purchasing or leasing such a facility is justifiable only for the largest projects. Other concerns include logistics of materials supply and equipment maintenance. In general, it is difficult and costly to maintain consistent concrete materials quality on barges (e.g., the moisture and temperature). As materials in storage are consumed, the floating plant will list and trim. The batch scale must be supported in such a way that gives accurate weights despite the barge list and trim. In general, equipment breakdowns are likely and difficult to repair offshore. In order to ensure continuous placement of underwater concrete, consideration should be given to provision for redundant equipment supplies including the essential accessory items (such as barges, tug boat, and lighting), and key standby equipment (such as pumps and tremie pipes).

Alternatively, a batch plant may be set up on shore and the concrete is transported to the placement site by transit mixers or hoppers on barges. This often creates logistic problems with regard to the time lapse between concrete mixing and concrete placement. In any circumstance, the concrete mixes must be able to maintain all the required properties such as flowability, cohesiveness, and self-compacting characteristics over the work window. Underwater concrete construction of many bridge foundations frequently consider delivery of concrete on barges, often with a retarding admixture in the concrete, and then re-mixing after arrival at the site.

Use of a ready mix plant, with delivery by trucks to the shore, and then by pump line supported over the water, is another production/delivery method. This method was successfully used to place over 25,000 cy of tremie concrete during construction of the Braddock Dam. In construction of the Dame Point Bridge, however, the same scheme encountered some difficulties. The concrete mixture was pre-cooled by injection of liquid nitrogen at the mixing plant. But delays in delivery due to roadway traffic allowed the concrete warm up to near ambient temperature, resulting in extensive thermal cracks in the concrete mass. The lesson learned is that roadway traffic could unexpectedly interrupt concrete delivery. A near-shore plant should be required for this option.

Once the concrete batch and mixing plant is selected, the effective mixing time is critical in defining the peak concrete production and placement rates. It is desirable to determine the mixing time in field mock-up tests taking into account the essential field variables. The mixing time should be such that all the concrete ingredients are fully dispersed and the concrete reaches workable consistency.

CONCRETE PLACEMENT

Modern engineering practice has shown that proper placement method is critical in achieving high quality concrete and cost-effective construction. The choice of a proper underwater concreting plan for a project has to be ultimately determined by the site conditions, engineering requirements, availability of equipment, and cost.

Placement Rate

The rate of concrete placement is a critical parameter to the quality of in-place concrete, the form pressure, and the construction planning in general. High quality of underwater concrete is obtained through a continuous pour at a consistent placement rate. An interruption of concrete placement for a period to the concrete set time will result in a cold joint. Given the difficulties with underwater preparation of cold joints, cold joints generally degrade the quality of in-place underwater concrete. Thus, it is essential that concrete be continuously produced and delivered to the placement point at the required placement rate. It is also essential that the necessary quantities of materials can be supplied to the batch plant at the required rate. The logistical planning should include provision for alternative or redundant supplies, provision of all the accessory items, and standby key equipment.

Before chemical admixtures were widely used in concrete construction, underwater concrete mixtures generally had stiffer consistencies than the concretes used today. Consequently, concrete placed at a slow rate often had very uneven, steep surfaces and a non-homogeneous distribution of concrete mass. In practice, it was found that the rapid placement of concrete resulted in marked improvement in the tremie concrete quality. The technique of the rapid placement takes advantage of the dynamic energy of flowing concrete to overcome the lack of concrete flowability. With a highly flowable concrete mixture, the kinetic energy of the fast flowing concrete is not always required for placement of good quality concrete. Nevertheless, a smooth and continuous tremie placement is still essential for good quality concrete. In general, a placement rate of 0.75 to 2 ft concrete rise per hour or 50-100 yd^3/hr is common for modern concrete mixes, depending on the concrete pour size, placement method and sequence.

Placement Sequence

Planning a tremie placement sequence must be based upon the size and geometry of the placement area, the available concrete production and delivery capabilities, and the concrete mixture properties. There are two basic schemes to sequence a tremie placement. The first scheme is to feed concrete into several tremie pipes at about the same time. Thus, the concrete rises everywhere at approximately the same rate. In this case, the maximum concrete flow distance is approximately one half of the tremie spacing. This placement scheme is suitable for tremie placement in small areas. For relatively large concrete placement, however, this scheme demands very high, and sometimes impractical, concrete production capacity. Furthermore, cold joints can potentially form between two adjacent tremie pours as laitance accumulates at the boundaries. A practical method is to divide a large area into several smaller areas. Both walls of steel sheet piles and walls of precast concrete have been used. Within each confined area, the simultaneous placement scheme can be applied.

The second placement scheme is the advancing slope method. In the scheme, the placement starts at one location and progressively proceeds to cover the entire area. Only when the concrete at the tremie location arises to the required elevation and an adjacent tremie has immersed in concrete by at least 0.3 m (1 ft), the tremie placement will proceed to the adjacent tremie. The tremie concrete flows out with an advancing slope. The surface slope of tremie concrete usually ranges from 1:5 to 1:40, depending on the concrete flowability and the placement rate. Thus, the tremie placement advances from one end of the placement area to the other end, following an advancing slope of the tremie concrete. The main advantage of this method is that it imposes less demand on the concrete production capability than the first scheme. In addition, the scheme facilitates the removal of laitance. As the placement progresses from one side to another, most of the laitance is pushed to the front edge of the advancing slope and eventually collected at one end of the form. Then, the top of the hardened concrete can be jetted off and the suspended laitance be removed by air lifting or eduction. This method eliminates the potential cold joints between adjacent tremie pours.

In some large-scale concrete placements, a combination of the simultaneous placement and the advancing slope scheme is the most appropriate, i.e., concrete is simultaneously fed into a row of tremie pipes that proceed with an advancing slope. The objective of this approach is to achieve optimum balance between the required placement rate and the concrete production capability.

Placement Method

Underwater concreting is currently carried out by five basic placement methods. They are (a) the tremie method, (b) the pump method, (c) the hydrovalve method, (d) the buckets or skip method, and (e) the preplaced aggregates method. Among them, the most common placement methods are the tremie method and pump method. These two methods function in fundamentally different manners. While tremie placement deposits concrete solely by gravity feed in an open-to-atmosphere system, the pump method utilizes surges of pump pressure to deliver concrete in a closed system. As a result, the technical requirements and inherent risks with the two methods are substantially different.

The tremie method is a way of placing underwater concrete by means of gravity flow. The tremie system basically consists of a rigid pipe suspended vertically through the water and a hopper fixed on top of the pipe to receive concrete. With the tremie method, there exists a “hydrostatic balance point” at which the gravity force inside the tremie is in equilibrium with the resistance to flow such as the hydrostatic pressure, the friction between the concrete and tremie wall, and the resistance of previously placed concrete. Any concrete added above the hydraulic balance point will cause concrete to flow. The more concrete added above the point, the faster the concrete flow rate. Thus, the concrete flow rate can be reliably controlled by the speed in which concrete is fed to the hopper.

The tremie method has proven to be the most reliable way of placing high quality concrete. Its main advantage is that tremie concrete can be deposited in a continuous and controlled flow speed with little turbulence. If the concrete is carelessly dumped into the tremie, it defeats the purpose of the tremie method.

In order to minimize cement washout and laitance, the placement operation should cause as little disturbance to the concrete underwater as possible. Most of the disturbance occurs during starting and restarting of the placement, or due to loss of the seal, or by dragging the tremie horizontally while embedded in the concrete underwater. This requires that the tremie pipe be embedded in fresh concrete to a minimum depth of 0.7 m (2 ft). Vertical movement of the tremie pipe should be limited to that absolutely necessary. Horizontal movement of embedded tremie pipes should be generally prohibited.

There are two basic techniques to start tremie placement – the dry method and wet method. While the dry method utilizes an end cap to seals off a tremie pipe from the water entry, the wet method utilizes a moving plug to prevent the concrete from mixing with water. The plug fits tightly inside a tremie pipe. As concrete is fed into the tremie, the plug slides down under weight of the concrete and push out water in a piston-like action.

Although good quality concrete has been placed by both tremie method and pump method, past experience and further studies found that the quality of tremie concrete is generally superior to that of pumped concrete especially in deep water. There are two main reasons for this phenomenon. The first reason is related to the concrete flow rate. When pumping concrete down directly to its deposit area, the pump pressure surges plus self-weight of the concrete are at times much greater than the hydrostatic balance head outside the pump line. Thus, the concrete exits the pump line at an uncontrollably high speed, causing significant disturbance to the concrete that has already been deposited. Secondly, a pump system is closed to the atmosphere. If concrete is being pumped down into deep water, concrete may fall at a rate faster than the pump output. As a result, a vacuum will be created in the pump line. The vacuum pressure so created will suck away the cement paste from aggregates, causing segregation of the concrete.

Nevertheless, the pump method is an excellent way of placing underwater grout or concrete containing only pea gravels. In this case, a pump line has a small diameter and the ratio of the skin friction to concrete volume is high. The skin friction slows down the speed of concrete fall. It is a good practice to install an air vent over the top bend of the pump line so that the pump system is open the atmosphere and the grout flow is controlled by the hydrostatic equilibrium.

Concreting Around Obstructions

Excessive obstruction to flow, such as closely spaced reinforcing bars, would cause buildup and sudden overflow of concrete. This tends to create trapping laitance. It is a good practice to limit the maximum size of the aggregate to facilitate the concrete flow. A rule of thumb is to keep the clear spacing between bars at least 5 times the maximum size of coarse aggregates. This greatly exceeds some code provisions for concrete placed in air. But it is necessary, because the driving force to cause the concrete flow is reduced due to buoyancy of water.

Reinforcement or other obstructions should be detailed to facilitate the concrete flow. In general, large size steel bars are preferred to a large number of small bars. Bundled bars are preferred to single bars at closer spacing. Mechanical couplers are preferable to lap splices. On the other hand, flowing concrete can impart a significant force on the reinforcement. It is desirable to make the reinforcement into cages that are securely supported to the forms at multiple points.

Concrete Protection

Underwater concrete has an excellent curing environment. Normally, no special post-placement operation is required. However, underwater concrete needs adequate protection before it sets and gains adequate strength. For example, pile driving should not be performed near a concrete placement before concrete sets. Swift currents or waves can potentially erode fresh concrete. The fact that similar incidents occurred in construction of several bridge foundations (e.g., Tsing Ma Bridge in Hong Kong, Second Severn Bridge in England, Oresund Crossing in Denmark) shows there is a serious danger of erosion of fresh concrete by current and waves. Therefore, protective measures need to taken to shield the concrete from current and waves. There are several effective ways to seal the gap between the bottom of in-situ forms and an existing river bed or ocean floor. In the past, sand bags and grout bags have been placed by divers to seal the gap. Steel skirts and protective mats are often used in offshore construction. Another technique is to attach pleated curtains of heavy canvas around the in-situ forms to seal off the gap. A more elaborate technique is to use inflatable fabric grout bags. The bags are attached to the bottom of in-situ forms.

Once the forms are installed under water, grout is pumped into the bag to inflate the bags.

QUALITY CONTROL

Because of the poor visibility and difficult accessibility of underwater work, there is uncertainty with the quality and integrity of underwater concrete. Strict enforcement of engineering requirements and quality control is required for underwater concreting. In principle, on-site monitoring and quality control of underwater concrete placement should be mainly carried out above water. Under most circumstances, the effectiveness of divers' inspection is very limited due to the poor visibility. Divers walking on the concrete surface will create turbulance and laitance. Nevertheless, periodic inspection by divers should be made for such conditions as the seal of the precast form to the river bed.

The following five critical items need continuous monitoring throughout the concrete placement: (a) the rate of concrete placement, (b) the depth of concrete at various locations, (c) volume of concrete produced vs. volume of in-place concrete measured by sounding, (d) concrete delivery system (leakage, plug or spill over), (e) embedment depth of the tremie. Specific recommendations on quality control include the following items:

1. The workers should have been properly trained and supervised full time by an experienced foreman or engineer who is familiar with the requirements for good workmanship.

2. Contractor should conduct frequent testing of concrete from batch-to-batch and within a batch. Important tests include slump, slump flow, unit weight, temperature, and concrete compressive strength of concrete cylinders.

3. After the concrete hardens, cores should be taken to verify the quality of the in-place concrete. Locations of the coring should be determined by the project engineer after examining the concrete placement log.

4. Continuous soundings at predetermined and well-marked locations over the entire placement areas. All sounding data should be recorded on data sheets and submitted to the project engineer at the end of each shift. A typical sounding device is a plate connected onto a weighted line marked for easy reading. Alternatively, sonar depth finders may be used to constantly monitor the depth of concrete at specific locations. Underwater inspection or monitoring by divers without independent soundings is not recommended.

5. The concrete placement rate and sequence should be carefully monitored and controlled. The concrete level within the tremie should be frequently checked and compared with the sounding data. The concrete placement should ensure continuous flow of concrete

6. The volume of concrete produced and fed into the tremie should be compared with the volume of concrete theoretically required to complete the placement as determined by soundings. If the in-place concrete volume measured by sounding is less than that produced and fed into the tremie, it is an underrun of concrete. If the in-place concrete volume is more than that fed into the tremie, it is an overrun of concrete. In general, underrun indicates a possibility of loss of concrete, possibly leaking through a skirt or cut-off wall. Overrun is indicative of serious segregation of the concrete. The segregation may be caused by a leaking joint in the tremie, or loss of the tremie seal. Overrun or underrun of 3% or less is typical. Over 5% deviation should be investigated.

7. Careful monitoring of all concreting operations including any restart and completion of concrete placement. The tremie pipe should be clearly marked to indicate the depth of the tremie tip.

8. Periodic checking of concrete delivery and placement equipment. Before using a tremie pipe, all the joints should be checked for possible leakage.

9. Adequate contingency plans should be provided in the Contractor's quality assurance program. If the sounding data indicate an undesirable distribution of tremie concrete, the foreman will determine the need to adjust the placement rate or relocate the tremie according to the contingent plan.

CONCLUSIONS

Underwater concreting is often a critical component of the marine foundation construction. It is technically demanding, usually on the critical path of the project schedule, and involves complex construction logistics. Therefore, its significance in the project goes far beyond the concreting operations themselves. This is the area where sound design and competent construction planning can achieve a meaningful reduction in risk and cost.

MARINE FOUNDATION RETROFIT FOR THE RICHMOND – SAN RAFAEL BRIDGE

Patrick E. Durnal, Senior Engineer, Ben C. Gerwick, Inc. San Francisco, CA, USA
Henrik Dahl, Vice President, Ben C. Gerwick, Inc. San Francisco, CA, USA

A joint venture of Ben C. Gerwick Inc., Sverdrup (now Jacobs) and DMJM (now DMJM Harris) designed the $779 mill seismic upgrade of the Richmond - San Rafael Bridge over the San Pablo Bay in the San Francisco Bay Area and provided construction support to Caltrans. Construction of the marine foundation retrofit was completed by a joint venture of Tudor Saliba/Tidewater/Koch-Skanska and their subcontractors: Pomeroy Precast Construction, AGRA Foundations, Dutra Construction and Vortex Divers. Construction management and inspection was performed by Caltrans with support of various consultants.

MARINE FOUNDATION RETROFIT SCOPE

The retrofit design of the submerged foundations included:

- A total of 476 tension and compression micropiles (290-1140 kips) installed through cored holes through the underwater bells at 31 pier locations
- Fourteen 126/150/164 inch diameter CISS concrete shear piles (1160-2660 kips) installed through new precast concrete pile cap extensions. (See Figure 1.)
- Twelve CIDH shear piles (1060-2130 kips) with 150 inch diameter steel shells to top of bedrock and 30 ft long and 11 ft diameter rock socket installed through new precast concrete pile cap extensions.

The specified post bid test boring revealed deeper bedrock at one pier location allowing deletion of the rock socket. Thus 15 CISS and 11 CIDH shear piles were installed at 11 pier locations - 9 piers with 2 piles and 2 piers with 4 piles. Cut off elevations for the shear piles ranged from 46 ft to 60 ft below mean sea level and cut off for the micropiles was 8 ft to 46 ft below mean sea level. Almost all foundation retrofits required work under limited headroom conditions. Underwater construction connections required innovative design details and construction techniques for each pile type. The 11 piers had 22 precast concrete pile cap extensions were installed in pairs and connected by either tremie concrete closure pours or by large pipe struts. The precast pile cap extensions were strapped underwater using large steel bands wrapping around the belled piers with grouted annulus. The precast pile caps were founded with 14 inch diameter steel pipe piles, which were either support piles or seismic tension and compression piles. The seismic piles were connected in grouted corrugated steel pipe sleeves cast into the new concrete pile caps.

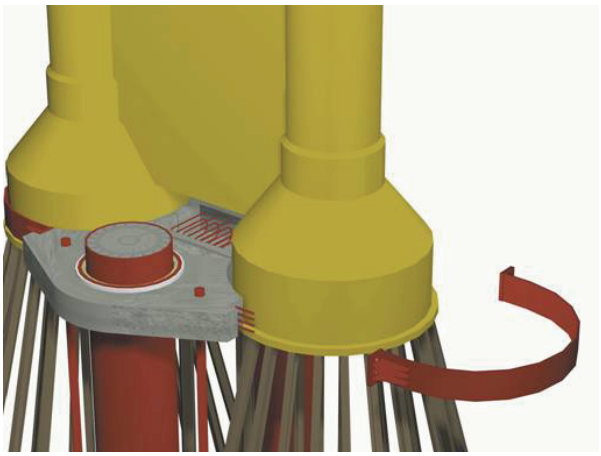


Figure 1: Bell Pier Retrofit with CISS Shear Piles

The West Trestle required complete replacement with bridge closure restricted from midnight to 5 am. This was accomplished by removing portions of the existing deck on each side of the viaducts and then installing new 66 inch diameter CIDH piles on each side of the roadways.

GOVERNING SUBSURFACE CONDITIONS

The depth of the San Francisco Bay to mudline varies from 30 ft to 60 ft below MSL along the bridge alignment. The total depth of soil profile

from mudline to top of the Franciscan Formation bedrock ranges from 15 ft to 200 ft. Micropiles were needed where the depth to bedrock was less than 80 ft, because the marine sediments do not provide enough capacity to the existing BP14x89 pile under the piers. The depth of the soils below the micropile footings varied from 9 ft to 114 ft. The depth of soils at the replacement viaduct for the 66 inch CIDH installation varied from 20 ft to 80 ft.

The upper 40 ft to 80 ft of soil consisted of very soft to medium stiff Young Bay Mud (YBM). In a few locations the YBM extended the full depth to bedrock. Often the bedrock was overlaid by thick alluvial deposits of medium dense to very dense sandy silt, sands and/or medium stiff to stiff clays.

The Franciscan Formation bedrock at this site consists of greywacke, sandstone and shale. The weathered top horizon was thin and grades into fresh medium soft to hard rock west of the main channel.

A steep carved ridge of very soft to soft intensely weathered greywacke was located east of the main channel. The high point was capped with over 65 ft highly fractured moderately hard to hard chert.

All the bedrock drilling of 12 inch micropile sockets, 5 ft and 11 ft CIDH sockets was stabilized using synthetic slurry, because the material in the rock seams and fractures was predominantly cohesive. But drilling micropiles in the highly fractured chert and at one of the shalely 11 ft socket CIDH locations at the east end of the bridge was problematic. Drilling through the chert was similar to drilling gravel with a few clay seams and the stand-up time of the fractured cohesive shale at one pier was only 2-3 days, not the 5-7 days it took to drill, set and pour most of those 11 ft rock sockets.

The bedrock surface was fairly well defined by the existing pile driving records and the infrequent new and older test borings. Jet probing had been used to reasonably define the original bridge BP14x89 pile procurement lengths.

The construction contract included an extensive test boring program, to assure that the proper shear pile CIDH steel shell lengths were purchased and to check the CISS locations that might have had shallower bedrock than anticipated. Borings were also installed at each micropile pier location to give the contractor the opportunity to design the bond lengths of the micropile 12 inch diameter rock sockets.

MICROPILE CONSTRUCTION

AGRA Foundations installed the micropiles with drill rigs that could core the bell piers with 13 inch diameter core barrels that were long enough to core straight through the 12-14 ft deep foundations. Strict horizontal tolerance control was maintained by rigid circular templates and conductor casing extensions to the top of the belled piers.



Figure 2: Micropile Drilling Operation

Each drilling template was designed to fit over recurring micropile layout conditions of similar diameters and configuration. (See Figures 2, 3 and 4.)

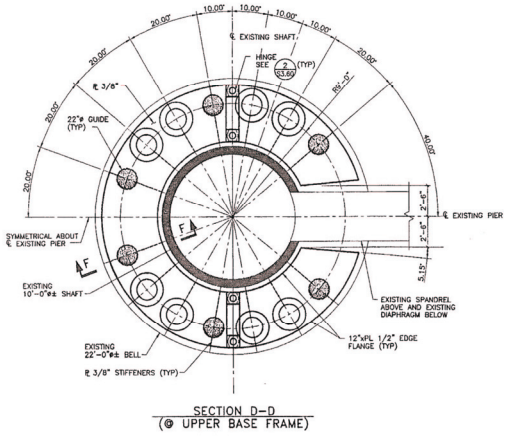


Figure 3: Micropile Template Plan

The battered and vertical existing BP14x89 piles were within inches of the cored hole locations. In some cases the templates were rotated to miss some of the existing piles, but inevitably some of the existing piles were partially cored. Out of the 476 piles shown on the plans, only 8 could not be installed due to obstructions. As the outcome of the hole coring was revealed, a criteria was developed for allowable cutting of existing piles. Some of the obstructed micropiles were re-analyzed and relocated, if possible.

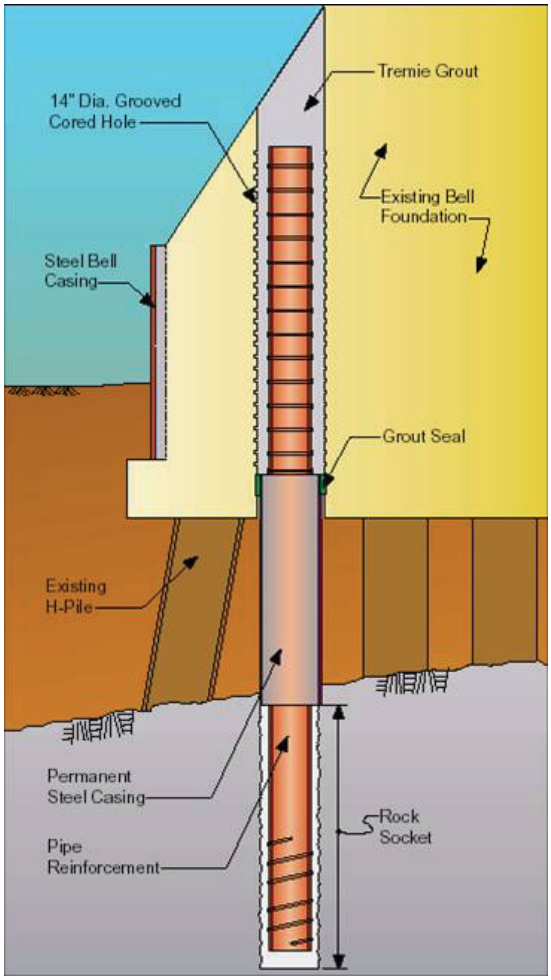


Figure 4: Micropile Section

The micropile testing used adjacent piles for reaction and two piles were tested at each of the 31 piers. Most of the piles met the elastic elongation criteria to the middle of a 38psi or group effect socket length, but a few did not. The bond stress range was increased due to an extension of the PP12.75”x0.5” casing to well below the top of bedrock. The increased the unbonded lengths caused more elastic deflection than our design criteria anticipated. The deeper casing length also a decrease in the bonded zone length and increased the bond stresses. The typical drill depth usually ended up at the specified minimum elevation due to group pull out. AGRA's resulting demand bond stresses ranged from 45 psi to 75 psi. To mitigate their design changes we directed the addition of a Williams #20 thread bar down the middle of the PP8.625x1.00 steel pipe reinforcement to reduce the increased

deflections. This mitigation worked very well in conjunction with re-analysis.

The upper horizon decomposed greywacke and shale did not cave in because it was cohesive. Pressure grouting this zone was considered but not implemented due to recommendations by outside consultants. We now have micropile experience in the same decomposed horizon indicting primary grouting under pressure is most beneficial in this weaker Franciscan rock zone.

At the micropile pier locations a reliable linear load transfer was developed in the 25-40 psi bond stress range. (See Figure 5.)

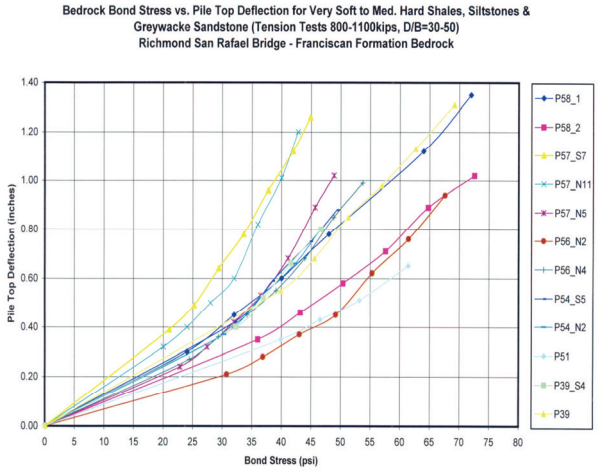


Figure 5: Bond Stress vs. Deflection

SHEAR PILE CISS/CIDH CONSTRUCTION

Shear piles were installed where the lateral shear forces exceeded the capacity of the existing BP14x89 foundation piles. Shear piles attached to the footings reduced the pier drift and seismic demand on the existing piles.

Pomeroy Construction prefabricated the precast pile caps and transported them to the site by barge. (See Figure 6.)



Figure 6: Main Span Precast Pile Cap

The retrofit included adding precast concrete pile caps and attaching them to the bell shaped bottom of the piers. Old fenders were removed to allow access and clearance for the heavy lift and setting procedures.

The precast pile cap extensions are supported by 14 inch pipe piles. The contractor used a Delmag D19-32 and swinging leads to drive the piles. (See Figure 7.)

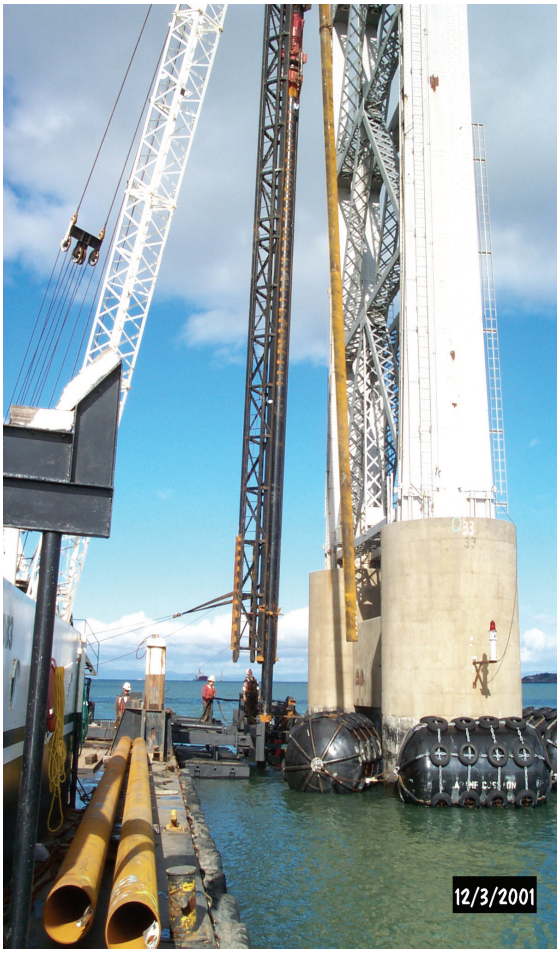


Figure 7: Installation of 14 inch pipe piles

Divers cut the 14 inch piles and inserted spudded bearing plate landing pads and shims to level the pile cap and transfer load to the piles. The precast caps were fitted with guide beams in order to be jacked together from each side. (See Figures 8 and 9) Heavy lift crane barges and lowering frames were used to set the shells.

The precast shells were bolted to the belled footing steel casing shells by divers. Tremie concrete was pumped into the closure pour pockets. The seismic 14 inch pipe piles had shear rings for connection in the pile cap and were driven through metal sleeves in the pile caps. This sleeved connection was sealed with plywood at the soffit by divers for the final placement of underwater neat cement grout.



Figure 8: Pile Cap on Barge with guide beam



Figure 9: Lowering Frame

The CIDH/CISS steel piles were pitched from horizontal to vertical and slowly lowered through the sleeves in the pile caps until they stopped in the marine sediments. (See Figure 10.)

An IHC S-500 hydro-hammer was placed on top of the large steel shells. (See Figure 11.) When the top of the shell was low enough, a follower or conductor casing was added to the top of the shells to prevent the hammer sleeve from hitting the pile caps and to allow cleanout of the piles and over pour of the tremie concrete.



Figure 10: Steel Pile Lowering



Figure 11: IHC S-500 on a Pile

Hammer grabs were used to cleanout the steel shells. A wire rope supported circular disk was fitted with wire rope brushes and rotated to clean the steel shell ID.

Slurry for drilling the CIDH sockets was premixed and stored in tanks on barges. The large CIDH sockets were drilled with a Seacore T40 pile top drill. Structural steel frames connected to the existing pier prevented conductor casing rotation and provided lateral support for the drilling oscillations. The roller cone drilling shield was equipped with a long shroud casing on top to protect the tooling from cave-ins and to increase the velocity of slurry flow along the sides of the 11 ft diameter sockets. The airlifted reverse circulation flow rates were high, so the roller cones were constantly cleaned free of cuttings. The drilling went well on all the sockets.

The CIDH piles had 60 ft rebar cages that doweled the steel shell to the rock sockets.

The tremie concrete pours took up to 8 hours and was placed using the gravity feed technique. Four mix designs were approved for the tremie concrete placement with retarder doses for 4, 6, 8 and 10 hour pours. The stand-up time for the rock socket placements was on the order of 5-7 days from start of drilling.

The holes remained stable for all but one pile. The unstable pile was backfilled. The hole was re-drilled, over-reamed and then filled with fiber reinforced tremie concrete. The over-reamed concrete plug was then drilled out and completed successfully.

Caltrans required cross-hole sonic testing of the sockets. A few anomalies were found in the 11 ft diameter CIDH shear pile sockets, however none of any consequence.

NEW 66 INCH CIDH CONSTRUCTION

Each of the 132 CIDH had 66 inch steel shells that were seated into bedrock to allow drilling of the 25 ft x 5 ft diameter rock sockets. The steel shell length to bedrock ranged from 30 ft to 135 ft below cut off elevation. The CIDH piles in between two viaducts were drilled out from a temporary trestle supported on 36 inch steel pipe piles. The work on the two outside rows of CIDH was performed completely from barges. (See Figures 12, 13 and 14.)

There were several pile locations with limited overhead conditions in the transition zone from two single viaducts to the double decked main spans. The 66 inch permanent steel shell installation was performed in sections using a



Figure 12: Drilling from Barge at Outer CIDH

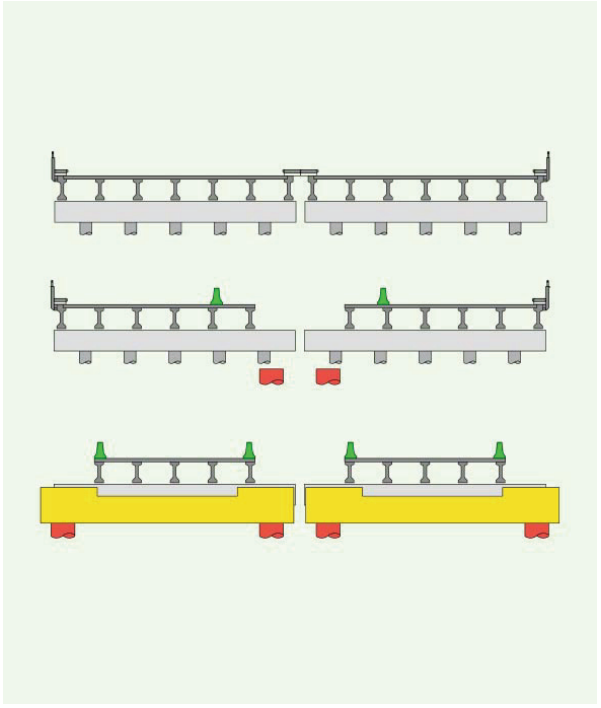


Figure 13: Provision for Drilling Access

casing oscillator and CJP butt welding of the sections. The sockets were excavated with a hammer grab and chisel and the reinforcing cages were lowered in short sections and spliced with mechanical couplers.

In zones of the alluvial sands over the greywacke bedrock, shell driving penetration resistance was masked and a few 66 inch shells were not adequately seated. Sand flowed like



Figure 14: 60 Inch Socket Casing and Oscillator

through an hour glass into the socket and then AGRA chose to use the oscillator to case the socket, after telescoping casing attempts did not work.

Tutor Saliba installed the majority of the steel shells using Delmag D80-12 and D100-13 diesel hammers. When driving resistance picked up on bedrock below bay mud the PP66x0.75 steel shells could be seated with a few hard blows and were undamaged. Where bedrock was overlain by dense sands at several locations driving the shells for seating into rock proved problematic, because it was difficult to determine when the rock was penetrated, since the blowcounts were already higher than normal, and there was no significant increase in penetration resistance. This situation resulted in overdriving the relatively thin walled steel shells and caused the bottom of the shells to bend inwards. When this happened AGRA was allowed to install smaller diameter sockets and/or they cored through the bent shell tips. The majority of the piles were installed without these problems.

Concrete was placed in two lifts. The socket and lower shell were filled with tremie concrete by the gravity feed method. The upper construction joint was green cut and then depending on scheduling, the hollow bent cap beams were barged under the existing bridge girders and set on the tops of the steel shells from both sides of the viaduct. Placement of dowel and bent cap rebar followed and then the final in-the-dry closure pour could take place. This construction facilitating design feature worked very well.

BEST PRACTICES: DREDGING AND DREDGED MATERIAL DISPOSAL

Raymond Sandiford, P.E., The Port Authority of New York and New Jersey, Newark, NJ, USA
Peter Dunlop, PhD., P.E., Gahagan & Bryant Associates, Inc., Wilmington, DE, USA

Dredging is a method commonly used to excavate subaqueous material. Dredging is usually associated with the maintenance of waterways and the creation of new ports facilities and channels; however it is also widely used in the mining and land reclamation industries. In addition, dredging has been used to remove contaminated sediments from waterways as a means of environmental remediation. In the past two decades, dredging activities have become highly regulated and publicly scrutinized. As such, new methods and technologies have evolved to transform what was a relatively "sloppy" practice into an "engineered" activity.

INTRODUCTION

As with most efforts, successful dredging projects start with proper planning. The volume, characterization and environmental testing of the material to be dredged is of paramount importance. Not only for the selection of dredging equipment, but also for properly characterizing the material for placement options and permitting. Selection of the dredging equipment may be dictated by environmental considerations rather than optimal dredging efficiency, and dredged material disposal may require innovative material re-use or disposal in confined environments. This document will discuss issues that typically arise with dredging projects.

WHAT IS DREDGING

Dredging is the removal and placement elsewhere of a full range of natural underwater materials - silts, clays, sands and rock formations. The major categorization of materials to be dredged today is whether they are contaminated or not. The term "sediment" is used herein to designate materials depositing in the waterways and ship berths at the present time. These sediments are often contaminated.

Also included with the dredged material is any debris that might be on or in the material to be dredged. There are numerous situations where dredging is the preferred means of material movement, including to:

- Deepen and maintain waterways, shipping channels, and ports.
- Create and maintain beaches.
- Excavate harbors and build docks, terminals and piers.
- Reclaim land.
- Restore aquatic and wetland habitats.
- Excavate pipeline, cable and tunnel trenches.
- Mine ores or aggregate.

Dredging is accomplished by either of two general methods. The oldest method of dredging is mechanical excavation, which is performed using equipment such as: backhoes, clamshells, grabs, dippers (formerly steam shovels), draglines, bucket ladders, and special function equipment. Mechanical dredges range in sizes from very small units to behemoths that can remove 260 cubic yards at a bite. The other widely used method is hydraulic dredging, which is performed using equipment such as: trailing suction hopper, cutter suction, plain suction (vacuum), dustpan, water injection, and bucket wheel suction. Hydraulic dredges also range from very small units to huge trailing suction hoppers that can dredge to 440 feet and carry 45,000 cubic yards. The reader is referred to a web site produced by the U.S. Army Corps of Engineers (USACE), which contains more detailed descriptions, illustrations and photographs of these various dredging methods:

http://www.usace.army.mil/inet/usace-docs/eng-manuals/em1110-2-5025/c-3.pdf

Herbich (2000) is also an excellent source of information.

PROJECT PLANNING

General

Prior to the 1970s there was only one permit required to perform dredging activities. This was the USACE permit in compliance with Section 10 of the Rivers and Harbors Act of 1899. With environmental awareness commencing in 1972, the number of permits and the complexity of the criteria have continued to expand. The various issues will be discussed in the following; however, the reader is cautioned that this is but a very brief introduction.

Permitting

Permitting requires a significant amount of time and is often the critical path in any dredging project. Permitting/compliance agencies include: federal (U.S. Army Corps of Engineers (USACE), Environmental Protection Agency (EPA), United States Fish & Wildlife (USF&W), National Marine Fisheries Service (NMFS), U.S. Coast Guard (USCG), Alcohol Tobacco and Firearms (ATF) - for blasting operations; state (DEC, etc.), and local (city agencies, community boards, fire departments, and citizen groups).

Federal Permitting Requirements

Dredging permits are issued by the USACE in conjunction with input from the EPA. A request is sent to the USACE with details of the planned dredging. This starts a process, which could entail Environmental Impact Statements (EIS), public hearings, issues of Essential Fish Habitat (EFH), mitigation for air and habitat impacts, and biological testing.

State Permitting Requirements

The states have developed permits to implement certain federal requirements as well as their own dredging requirements. These may consist of Coastal Zone Management (CZM), air mitigation – if the dredging site is in a non-compliance zone – and mitigation for loss of habitat.

City Permitting Requirements

City agencies have developed various requirements relating to dredging.

Testing Requirements

There are a number of investigations and tests required prior to commencing dredging. These could include:

Subsurface Investigations

Subsurface investigations are undertaken to characterize the materials to be dredged and to recover samples of the soils/rock for detailed chemical and biological testing.

Bathymetry – The depth of the water in areas to be dredged can be obtained by lead line sounding, single beam, or multi-beam methods. Today, most bathymetry is obtained by the multi-beam method.

Geophysical Investigations – Side scan sonar, reflection, and refraction are often used in conjunction with bathymetric surveys to obtain information on the character of the surficial soils/rock. Side scan sonar can identify areas of soft sediment (for contract delineation of "contaminated" sediment, areas of rock, and provides a picture of the character of the channel bottom including surficial debris).

Borings and Cone Penetration Tests – With the above geophysical data and historical information, borings can be planned to recover specific types of materials – sediment, soils, or rock. Cone Penetration Testing (CPT) is useful in providing continuous information with depth for sediments and soft soils.

Material Characterization

Soil and Rock Classification

The most important classification today is whether the sediments or soils are contaminated. In general this process entails a tiered investigation, examining the potential for the sediment or soil to have become contaminated. Recent sediment, which is currently depositing or has deposited since the industrial revolution (post anthropogenic), is clearly suspect, and is usually tested for chemistry and biological effects (see next section).

Another source of very useful data is the record of previous investigations and dredging experience. Areas of planned dredging activity have often been dredged in the recent past (not many new harbors have been developed recently).

Excavated rock is generally considered uncontaminated and used predominantly for the development of offshore ("artificial") reefs.

Pertinent Soil Properties

The soil properties of interest relate to their impact on the selection of dredging method and equipment. These include grain size, Standard Penetration Test blow counts (N), Cone Penetration Tests (CPT), specific gravity, strength, settling rate, consolidation, uniformity, bulking factor, and degree of cementation.

Pertinent Rock Properties

A major issue with rock is whether the rock can be dredged without drilling and blasting. Recent advances in cutter suction dredges have resulted in very massive cutter heads that can dredge certain rocks. Large backhoes and dipper dredges might also be able to dredge some rocks. A technique using underwater pile drivers fitted with chisels to break up the rock for dredging with mechanical dredges is gaining use (mechanical hammering not unlike jack-hammering).

Rock strength, Rock Quality Designator (RQD) and the number and character of joints are of interest. There have been some recent attempts to correlate these parameters with geophysical reflection techniques, allowing for complete characterization of materials in the area to be dredged.

Environmental Testing

The requirements for testing of materials to be dredged have evolved from the "London Dumping Convention" of 1972 which states that members will "take all practicable steps to prevent the pollution of the sea by the dumping of waste and other matter that is liable to create hazards to human health, to harm living resources and marine life."

These requirements are implemented in the U.S. through the Marine Protection, Research, and Sanctuaries Act (MPRSA). The EPA's Ocean Dumping Regulations implement the MPRSA. National guidance for the Ocean Dumping program was published by the EPA and the USACE in *Evaluation of Dredged Material Proposed for Ocean Disposal - Testing Manual (EPA and Corps, 1991)*, also called the "Green Book." The Corps, in consultation with the EPA, determines the suitability of dredged material proposed for ocean disposal under the criteria defined at 40 CFR 227.

Dredged materials proposed for discharge in waters of the U.S. are tested according to the *Inland Testing Manual (ITM) (EPA and Corps, 1998)*. The ITM is similar to and consistent with the Green Book.

Chemical Testing – Chemical testing of materials to be dredged is often required. Specific chemicals of concern are identified by regulatory agencies along with acceptable concentration levels. In general, chemical testing alone is not sufficient to exclude soils and sediments from biological testing.

Biological Testing – Biological testing provides information on the response of certain marine species. Testing requires two criteria to be complied with: toxicity to the species (acute or short term effects), and bioaccumulation in the tissue of the species (chronic or long term effects).

A major time constraint has developed due to the complexity of biological effects-based testing (i.e. quality assurance/quality control of field collected organisms), and the extremely refined detection limits for evaluation (chemical detection limits have decreased with time and are now as low as 1 part per trillion). It often takes up to a year to complete all aspects of biological sampling and testing, which may be too long for certain projects.

DREDGED MATERIAL DISPOSAL

The historic method of disposal of sediments has been by placing them in near-shore Confined Disposal Facilities (CDF's). These facilities consist of diked areas into which hydraulically dredged materials are pumped. The CDF's need to be large enough to allow the sediments to settle out before the water is discharged back into the waterway. Many of

these CDF's cover hundreds or thousands of acres. Certain areas of the country have relied on ocean disposal for dredged materials; however as the criteria for ocean disposal have become more stringent, less material is going to ocean disposal sites.

Ocean Dumping – Only "clean" materials are suitable for placement at ocean disposal sites. These sites are designated by the EPA and can consist of areas requiring remediation such as New York's Historic Area Remediation Site (HARS), areas providing replenishment of coastal sediments, and artificial reef sites for creation of fish habitat.

Upland Placement – This has been used for sediments unsuitable for ocean disposal. In general, the contaminated sediments are mixed with materials to reduce contaminant mobility, reduce moisture content, and to provide a more stable material (Solidification and Stabilization). Most upland placement consists of mixing the sediment with cement or lime, air-drying, and then compacting. This processed dredged material (PDM) has been used for parking lots, golf courses, and general site grading. Additives other than cement and lime – or related products – have been used; however, many of these are proprietary.

Confined Aquatic Disposal (CAD) – This entails the placement of contaminated sediment within a natural or manmade underwater depression followed, by capping with clean materials or by natural sedimentation. CAD's have been used in a number of places for confining contaminated sediments; however their acceptability appears to be decreasing.

Beneficial Re-use – This is the "constructive" use of dredged materials. There are many uses that dredged materials have fulfilled including beach nourishment, sand from channel mining, gravel sources, cement manufacturing, capping of contaminated areas in the ocean, landfill covers, and even brick or tile manufacturing. Specific uses obviously depend on the character of the material dredged and on the level of contamination.

Decontamination – This is being instituted in many areas as demonstration projects. The reader is referred to the following web site for additional discussion of decontamination: http://www.bnl.gov/wrdadcon

CONTRACTING

The major contracting decision is to select a contractor that has the experience and the equipment to perform the work to the expected level of quality. Other contract considerations include:

Permit Requirements – Permitting agencies often designate specific equipment, practices or performance monitoring requirements. These could include type of bucket, i.e. "environmental bucket" with horizontal cut, rubber seals and positive closure indication. There might also be a prohibition for hydraulic dredges, overflow from the scows, and hours of operation – particularly for drilling and blasting. All of the requirements imposed by the agencies must be clearly described in the contract documents so that there are no surprises to any of the parties and no fines imposed.

Disposal Method – Agencies may desire or designate a specific placement method or disposal location. These may include time of disposal (e.g. daylight only), time in the tide cycle (slack tide plus or minus 1 hour), and location (specific permitted upland sites, placement requirements based on chemistry, leaching, or geotechnical properties).

Form of Contract – Contracts are generally Unit Price but could be Lump Sum, or some combination thereof, depending on the degree of specificity in the documents and supporting data.

Unit Price – is preferable if there are unknowns such as the volume of contaminated sediment or rock. There could also be an hourly rate if "move-on-demand" orders are possible from the U.S. Coast Guard.

Lump Sum – is suitable if the character, area and volumes of all materials to be removed are well known, and if there are no potential for "changes" in any of the contract terms and conditions.

Pay Volume and Depth Tolerances - are a consideration in developing the contract

documents. There are many factors in specifying the volume of material to be removed and for which the contractor will be paid (pay volume). Seldom does the pay volume equal the actual volume removed.

As an example, the owner will not want to pay the dredger for any material removed that is of no benefit to the project. Contracts often include a minimum depth and a maximum pay depth. The maximum pay depth reflects the fact that to achieve the minimum depth requires dredging to a greater depth due to the type and size of the equipment, the accuracy of dredge control, irregularities that may be left on the bottom, desired storage volume for new sediment accumulating in channels, and berths to limit maintenance dredging to acceptable periodicity, as well as the accuracy of the post dredge surveys. In general, the pay depth is 1.5 to 2 feet deeper than the minimum depth. It is quite common to see very local pinnacles or high spots in the post-dredge surveys. These are difficult to remove by redredging the area. In fact, new pinnacles may develop if the dredge has spuds that push into the bottom. Dredgers often use drag bars to level these small pinnacle areas. The use, or potential use, of drag bars should be clearly understood by contractor, owner, and regulatory agencies.

Placing structures on a dredged bottom generally require depositing sand or gravel and screeding this fill to provide a uniform base for the structure rather than placing it directly on the as-dredged base. *Tavelero (2005)* shows that dredged depths can vary significantly (two standard deviations of 2 to over 4 feet) when dredging at depths of 40 to 50 feet).

In certain cases, the contracts may have a pay depth the same as the minimum excavation depth. In this case the dredger will add the cost of the over-depth dredging that is expected with his equipment into the unit price of the defined pay volume.

There have even been contracts in which there is a penalty to the dredging contractor for excavating deeper than 6 inches below the minimum channel depth. These types of contract issues require careful consideration because if the equipment for precise control is not available, bid prices will become very high, or contractors may not submit bids for the work.

Care must be exercised that all entities understand what is meant by terms such as “design depth”. The design depth to the USACE may bear little relationship to the actual contract dredged depth that could be 2 to 3.5 feet deeper for “safety” and over-depth factors. The same can occur at the berth where berth design depth may be less than the future dredging depth because of the over-depth issues discussed above, and for storage of sediment accumulating within the berth. This could have a significant impact on wharf design.

Another area where the issue of depths enters is in the sampling for environmental testing. Should sampling extend to the minimum dredging depth, the expected average dredged depth, or to maximum over-depth? And what are the issues if the dredger digs beyond the pay over-depth because of the equipment used or lack of precise control? All of these apparently minor issues can and have become major points of controversy.

Some of the companies within the contracting chain may have different volume calculation methods. For instance, upland processors are concerned only with the volume brought to be processed, i.e. cubic yards in the scow at his dock because each cubic yard requires additives, processing, and transport to final placement. The dredging contractor is usually paid by volume removed at the dredging site calculated from pre- and post- dredging surveys, and then only within the pay limits. Others, such as landfill operators, if the material goes to a landfill, bill on the basis of tons. Again, clarity of terms and pay bases is a ***must*** to prevent disputes.

Debris is another issue of concern. Metal, cable, tires, timbers, bolts, and even cars are often in the material to be dredged and must be accounted for in the contract documents.

Interferences

Channels and berth areas are often crossed by utilities (natural gas, electric, fuel, oil, communications). Many of these were installed long ago and the records may not exist. *It is imperative that a complete search be instituted prior to dredging.*

Facilities within the dredging area may also have been constructed in the past and subsequently abandoned without full removal, and without any record or documentation. These may consist of bridge abutments, abandoned pipelines, offloading facilities, and particularly piles and concrete pile foundations.

Risks

There are several other potential hazards that deserve mention.

There are risks of scow sinking, oil sheens appearing at dredging and disposal locations, misplaced material due to operator error or equipment malfunction; unexpected items such as piles and old pipelines, unexploded ordnance, endangered species, damage to existing structures from the large dredging equipment, damage or alleged damage from blasting operations, noise complaints and attendant required equipment modifications.

Monitoring/mitigation of some of these risks is provided by having USACE-licensed inspectors on the dredges, and during tow and disposal operations. In addition, real time monitoring of scow draft can indicate if material is being lost during transit. Risks may be limited by proper planning, detailed investigations, and effective communications among all the entities.

CONCLUDING REMARKS

Dredging practice has changed tremendously over the past two decades, from a “dig and dump” process to a regulated engineering and construction process, with much real time recording of events. This trend will continue.

The future challenges are to ensure clear communications and understanding among all the interested parties; about the present equipment capabilities, the real impacts of dredging and any potential or required improvements; to assure meaningful protection of the environment while still allowing contractor ingenuity, and providing safe and economical shipping.

REFERENCES

Herbich, John B., 2000, Handbook of Dredging Engineering, 2nd Edition.

Tavelero, John 2005, Presentation No. 21 at the Corps of Engineers East Coast Dredging Conference (USACE-ECDC).

http://www.usace.army.mil/inet/usace-docs/eng-manuals/em1110-2-5025/c-3.pdf

http://www.bnl.gov/wrdadcon

VESSEL COLLISION DESIGN - RISK ANALYSIS AND DEEP FOUNDATION ISSUES FOR BRIDGES OVER NAVIGABLE WATERWAYS

Michael A. Knott, P.E., Moffatt & Nichol, Richmond, VA, USA

Large lateral forces on bridge foundations due to extreme events such as vessel collisions, earthquakes, and wave forces on storm surges during hurricane events are often the controlling design condition for bridge foundations. A review of the American Association of State Highway and Transportation Officials (AASHTO) vessel collision analysis and design codes used in the United States for highway bridges will be presented. The paper includes the background and development of the *AASHTO Guide Specification and Commentary for Vessel Collision Design of Highway Bridges (1991)* and vessel collision provisions of the *AASHTO LRFD Bridge Design Specifications (3rd Edition 2004 and the approved 2005 Interims)*. Experience in using the AASHTO codes will be discussed and observations on the adequacy and gaps, comparison with the European Standard Code, and recommendations for immediate and long term needs will be presented.

BACKGROUND

General

Ship and barge collisions with bridges represent a growing and serious threat to public safety, port operations, motorist traffic patterns, and environmental protection in many cities throughout the world that are located in coastal areas and along inland waterways. In the 42-year period from 1960 to 2002, there have been 31 major bridge collapses worldwide due to ship or barge collision, with a total loss of life of 342 people.

The greatest loss of life occurred in 1983 when a passenger ship collided with a railroad bridge on the Volga River, Russia. One hundred and seventy six (176) were killed when the aberrant vessel attempted to transit through a side span of the massive bridge. Most of the deaths occurred when a packed movie theatre on the top deck of the passenger ship was sheared off by the low vertical clearance of the bridge superstructure's side span.

U.S. Accidents

Seventeen (17) of the bridge catastrophes discussed above occurred in the United States, including the 1980 collapse of the Sunshine Skyway Bridge crossing Tampa Bay, Florida, in which 1,300 feet of the main span collapsed and 35 lives were lost as a result of the collision by an empty 35,000 DWT (deadweight tonnage) bulk carrier.

One of the more publicized tragedies in the U.S. involved the 1993 collapse of a CSX Railroad Bridge across Bayou Canot near Mobile, Alabama. During dense fog, a barge tow became lost and entered a side channel of the Mobile River where it struck a railroad bridge causing a large displacement of the structure. The bridge collapsed a few minutes later when a fully loaded Amtrak passenger train attempted to cross the damaged structure. Forty seven (47) fatalities occurred as a result of the collapse and train derailment.

Recent bridge collapses in the U.S. include the Queen Isabella Bridge connecting South Padre Island to the Texas mainland, which was hit by a barge in September 2001 (8 fatalities); and the collapse of the I-40 Bridge over the Arkansas River near Webber Falls, Oklahoma, which was hit by a barge in May 2002 (13 fatalities).

It should be noted that there are numerous vessel collision accidents with bridges which cause damage that varies from very minor to significant damage, but do not necessarily result in collapse of the structure or loss of life. A recent USCG study (May 2003) of towing vessels and barge collisions with bridges located on the U.S. inland waterway system during the 10 year period from 1992 to 2001 revealed that

there were 2,692 accidents with bridges. Only 61 of these caused bridge damages in excess of $500,000 (1,702 caused very minor damage with no repair costs to the bridge), and there were no fatalities within the study period. The study concluded that 90% of the barge accidents were related to human performance (78% to pilot error and 12% to other operational factors). Only 5% were related to mechanical problems, and for the remaining 5% there was insufficient information to assign a cause.

Vessel collision accidents can also cause environmental damage to a waterway. An accident with a double-leaf bascule bridge occurred in Portland, Maine in September 1996 when a loaded tanker ship (560 feet in length and 85 feet wide) rammed the guide pile fender system of the existing Million Dollar Bridge over the Fore River. A large portion of the fender was destroyed; the flair of the ship's bow caused significant damage to one of the bascule leaves of the movable structure (causing closure of the bridge until repairs were made); and 170,000 gallons of fuel oil were spilled in the river due to a 30-foot-long hole ripped in the vessel hull by an underwater protrusion of the concrete support pier (a small step in the footing). Although the main cause of the accident was attributed to pilot error, a contributing factor was certainly the limited horizontal clearance of the navigation opening through the bridge (only 95 feet)

AASHTO GUIDE SPECIFICATION

General

The 1980 collapse of the Sunshine Skyway Bridge was a major turning point in awareness and increased concern for the safety of bridges crossing navigable waterways in the United States. Studies initiated as a result of this tragedy led to the 1988 pooled-fund research project sponsored by 11 states and the Federal Highway Administration (FHWA) which developed a proposed design code for use by bridge engineers in evaluating structures for vessel collision. This effort culminated in 1991 with the adoption of the *AASHTO Guide Specification and Commentary for Vessel Collision Design of Highway Bridges (1991).*

The AASHTO Guide Specification was based on lessons learned from historical bridge accidents; data available in the late 1980's from vessel collision studies conducted by various consulting firms for specific bridges, such as the Skyway Bridge (included were the initial planning studies of the Great Belt Bridge conducted in the 1970s, as well as other bridges worldwide); and the published research of a variety of authors in the technical literature. A particularly notable collection of state-of-the-art papers at the time was the proceedings of the *International Association for Bridge and Structural Engineering (IABSE) Colloquium on Ship Collision with Bridges and Off-shore Structures, Copenhagen, Denmark (IABSE 1983).*

For the first time in the U.S., the AASHTO specification enabled structural engineers to assess the risk of vessel collision with a bridge; calculate the disruption costs due to a catastrophic collapse of the structure; develop plans to minimize the risk of collision; and develop designs to protect the bridge and its motorists in the event of a collision. In addition to the planning and design of new bridges (its primary intent), the provisions and procedures of the Guide Specification could also be used to evaluate the risk of vessel collision to existing bridges, to assess their vulnerability to collision, and to develop retrofit pier protection measures if required.

Purpose

The AASHTO Guide Specification established design provisions for bridges crossing navigable waterways to minimize their susceptibility to damage from vessel collisions. The intent of the provisions is to provide bridge components with a “reasonable” resistance capacity against ship and barge collisions. In navigable waterway areas where collision by merchant vessels may be anticipated, the Guide Specification requires that bridge structures be designed to prevent collapse of the superstructure by considering the size and type of vessel fleet navigating the channel, available water depth, vessel speed, structure response, the risk of collision, and the importance classification of the bridge.

It should be noted that damage to the bridge (even failure of secondary structural members) is permitted by the code as long as the bridge deck carrying motorist traffic doesn't collapse (i.e., sufficient redundancy and alternate load paths exist in the remaining structure to prevent collapse of the superstructure).

Risk Analysis

The Guide Specification contains three alternative analysis methods for determining the design vessel and associated design impact loads for each bridge component in the structure in accordance with standard risk acceptance criteria.

Method I is a simple to use semi-deterministic procedure; Method II is a detailed risk analysis procedure; and Method III is a cost-effectiveness of risk reduction procedure (based on a classical benefit/cost analysis). The Guide Specification requires the use of Method II risk analysis for all bridges unless special circumstances exist as described in the code for the use of Methods I and III. Special circumstances for using Method I include shallow draft waterways where the marine traffic consists almost exclusively of barges; and for Method III include very wide waterways with many piers exposed to collision, as well as existing bridges to be retrofitted.

Method II of the AASHTO Guide Specification is a probability based risk analysis procedure for determining the appropriate vessel impact design loads for a bridge structure. Using Method II procedures, a mathematical risk model is used to estimate the annual frequency of bridge collapse based on the bridge pier/span geometry, ultimate resistance of the pier (or span), waterway characteristics, and the characteristics of the vessel fleet transiting the channel. The estimated risk of collapse is compared to standard acceptance criteria, and the bridge characteristics (span layout, pier strength, etc.) are adjusted until the acceptance criteria are satisfied. The Method II procedure is iterative in nature and is normally performed by specialized computer programs and spreadsheets.

Based on Method II, the risk of vessel collision with a bridge pier is computed using the following equation:

$$AF = (N)(PA)(PG)(PC) \quad (1.1)$$

where,

AF = annual frequency of bridge pier collapse;

N = annual number of vessels in the waterway which can strike the pier;

PA = probability of vessel aberrancy;

PG = geometric probability of a collision; and

PC = probability of collapse.

The annual frequency of collapse is computed for each individual pier in the waterway. The summation of the AF for each pier in the structure results in the annual frequency of collapse for the entire bridge. If required, the possibility of span collision can also be included in Equation 1.1.

Vessel Frequency, N

The number of vessels, N, passing under the bridge is determined based on the size (usually expressed in deadweight tonnage, DWT); type (such as tanker and cargo ships, deck and hopper barges, etc); and loading condition (empty, ballasted, partly loaded, or loaded) of the ship or barge tow. A vessel frequency distribution is initially developed for the navigation channel of the waterway. This distribution is then modified for each bridge pier location based on the available water depth at the pier and the draft of the ship or barge. Depending on waterway conditions, a differentiation between the number and loading condition of vessels transiting inbound and outbound may also be required.

Probability of Aberrancy, PA

The probability of aberrancy, PA, represents the statistical probability that a vessel will stray off course and threaten the bridge. Vessel aberrancy is usually a result of pilot error (representing 60%-90% of all accidents), adverse environmental conditions, or mechanical failure. Based on historical accident data, the AASHTO vessel collision specification recommends the following empirical relationship for estimating PA:

$$PA = BR(R_B)(R_C)(R_{XC})(R_D) \quad (1.2)$$

where,

BR = base rate for collisions (0.6x10-4 for ships, and 1.2x10-4 for barges);

R_B = correction factor for bridge location (based on whether the bridge is located in, or near, a bend/turn in the waterway, and the magnitude of the angle of the bend/turn);

R_C = correction factor for currents in the

waterway acting parallel to the vessel as its transiting the channel under the bridge;

R_{XC} = correction factor for cross currents acting perpendicular to the vessel; and

R_D = correction factor for vessel traffic density in the waterway (based on the frequency in which vessels meet, pass, or overtake each other in the immediate vicinity of the bridge)

Geometric Probability, PG

The geometric probability, PG, is the conditional probability that a vessel will hit a bridge pier given that it has lost control (i.e., it has become aberrant) in the vicinity of the bridge. Based on historical bridge collision data, a normal distribution is used to model the location of an aberrant vessel in the waterway. The standard deviation, σ, is set equal to the length overall (LOA) of the ship or barge tow, and is centered on the transit path that the vessel would typically take in passing under the bridge (which is usually the centerline of the main span of the structure). As shown in Figure 1, PG becomes the area under the normal distribution defined by the location of the pier away from the normal vessel transit path, and bounded by the width of the bridge pier plus one-half of the width of the vessel on each side of the pier.

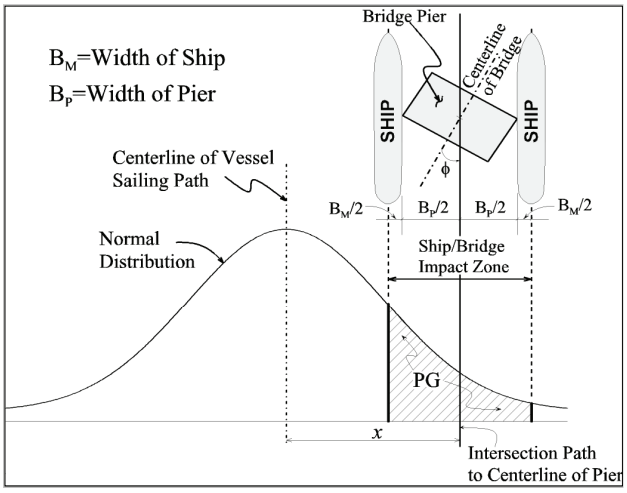


Figure 1: Geometric Probability Distribution

Probability of Collapse, PC

The probability of collapse, PC, is a function of many variables, including vessel size, type, forepeak ballast and shape, speed, direction of impact, and mass. It is also dependent on the ultimate lateral load strength of the bridge pier (particularly the local portion of the pier impacted by the bow of the vessel). Based on collision damages observed from numerous ship-ship collision accidents which have been correlated to the bridge-ship collision situation, an empirical relationship has been developed based on the ratio of the ultimate pier strength, H, to the vessel impact force, P. As shown in Figure 2, for H/P ratios less than 0.1, PC varies linearly from 0.1 at H/P=0.1, to 1.0 at H/P=0.0. For H/P ratios greater than 0.1, PC varies linearly from 0.1 at H/P=0.1, to 0.0 at H/P=1.0.

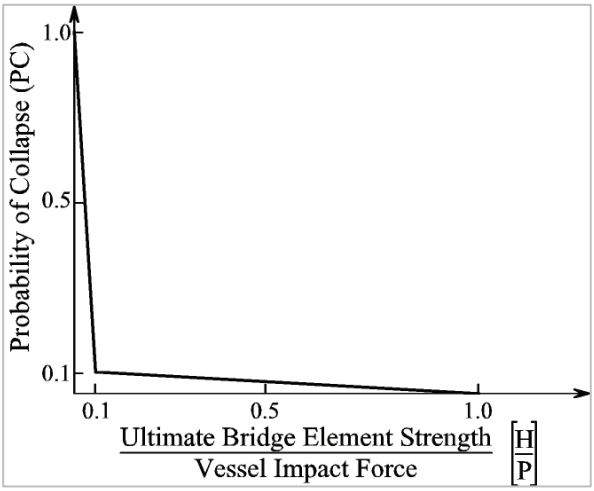


Figure 2: Probability of Collapse Distribution

Design Vessel Acceptance Criteria

A design vessel (including impact force and energy) is selected for each individual pier in the waterway such that the annual frequency of collapse of the entire bridge due to the vessels equal to, and larger than, the design vessels are less than a predetermined risk acceptance criteria based on the structure's importance classification. The AASHTO Guide Specification contains a two-category importance classification system in which bridges are classified as either “critical” or “regular.” The risk acceptance criteria associated with these two classifications are as follows:

A. Critical Bridges: AF should be equal to, or less than, 0.01 in 100 years (AF=0.0001). This represents a return period of bridge collapse equal to 1 in 10,000 years.

B. Regular Bridges: AF should be equal to, or less than, 0.1 in 100 years (AF=0.001). This represents a return period of bridge collapse equal to 1 in 1,000 years.

The structure classification of critical or regular is based on social/survival and security/defense considerations for the bridge and is dependent on the importance of the bridge link in the local/regional highway transportation system, as well as the availability of alternate travel routes in the event of a bridge collapse.

Vessel Impact Speed

For ship and barge tows transiting the waterway under their own power, the primary area of vessel collision concern is a central region or zone near the main navigation span of the bridge. The width or boundary of this navigation zone used in the vessel collision analysis is defined as a distance equal to 3xLOA on each side of the vessel transit path (which coincides with the channel centerline for most bridges).

The 3xLOA distance is also used to distribute the vessel impact speed over each of the piers located in the navigation zone as shown in Figure 3, where V = design impact speed; V_T = typical vessel transit speed in the channel; V_{MIN} = minimum impact speed (associated with the current in the waterway); x = the distance to the bridge pier; x_C = distance to the edge of channel; and x_L = 3xLOA from the centerline of the vessel transit path

VESSEL IMPACT FORCES

General

The AASHTO Code provides several empirical relationships for computing an equivalent static impact force associated with a head-on collision of a ship or barge with the bridge. The impact force equations were developed from published research by G. Woisin (for ships) and by K. Meir-Dornberg (for barges) based on large-scale physical model studies conducted in Germany to determine the crushing strength of typical vessel bows under dynamic testing conditions. Figures 4 and 5 depict typical vessel impact forces developed using the AASHTO equations.

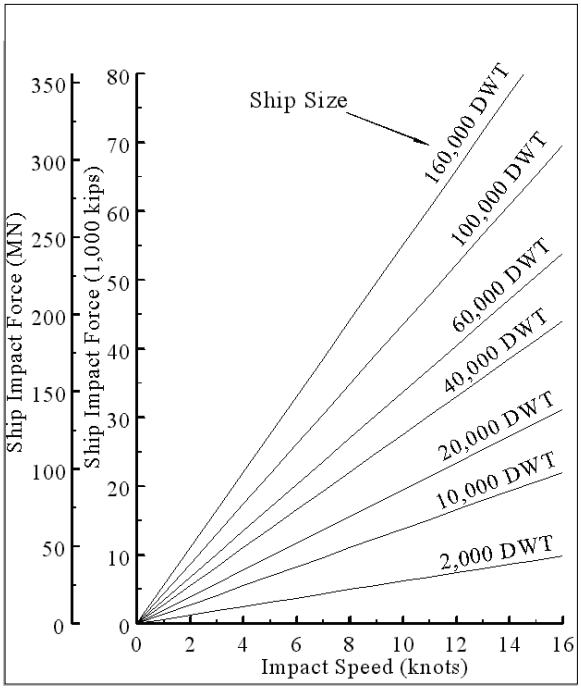


Figure 4: Ship Impact Forces

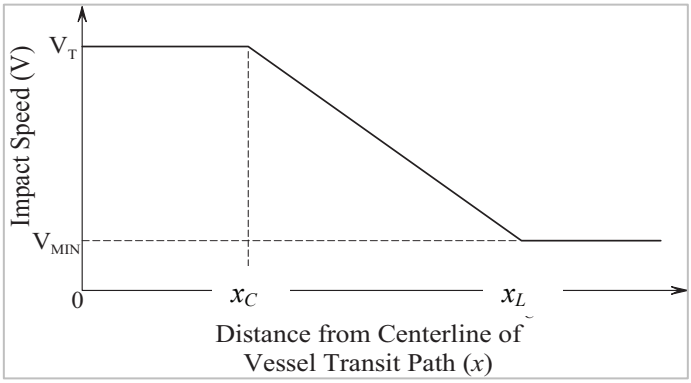


Figure 3. Vessel Impact Speed Distribution

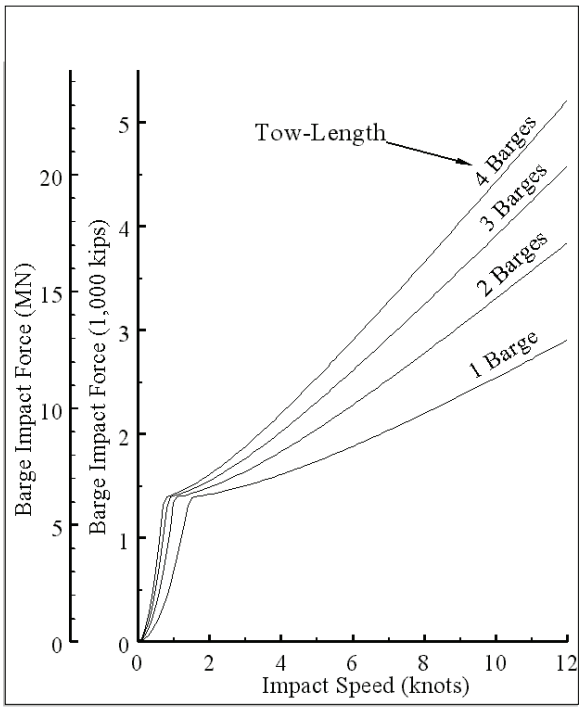


Figure 5: Barge Impact Forces

Ship Impact Forces

The ship impact force is computed by:

$$P_S = 220(DWT)^{1/2}(V/27) \qquad (1.3)$$

where,

P_S = equivalent static impact force (kips);

DWT = deadweight tonnage of the ship (metric tonnes); and

V = ship impact speed (feet per second).

A schematic representation of a typical impact force time-history is shown in Figure 6 based on Woisin's test data. As seen in Figure 6, Woisin measured a large variability of the load lasting approximately 0.1 to 0.2 seconds for the real ship (out of total impact durations exceeding 3 to 4 seconds). During this oscillation (which occurred at the very beginning of the time-history) the force amplitude sometimes increased to more than twice the mean value of the impact force.

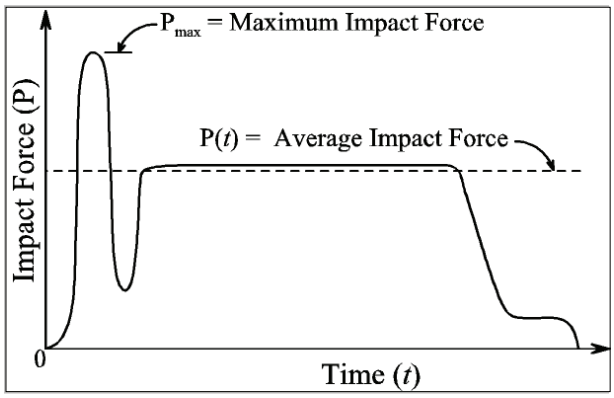


Figure 6: Typical Ship Impact Force Time History by Woisin

The impact force in Equation 1.3 represents the 70% fractile of the average ship impact force as measured over time by Woisin in his collision tests. This design impact force is shown graphically in Figure 7 (the units in the figure are metric), and its use implies that this force will be used to evaluate the bridge response to impact and to size members to resist the impact forces. The use of the maximum impact force (i.e., twice the mean) was not recommend for use by the AASHTO Specification since it was considered that the time duration of the maximum force (0.1 to 0.2 seconds) at the beginning of the collision was too brief to cause major problems to most structures. It was believed that the overall response of the structure would be more appropriately evaluated by using the average impact force over time (increased to a 70% fractile level to stay on the conservative side of the analysis).

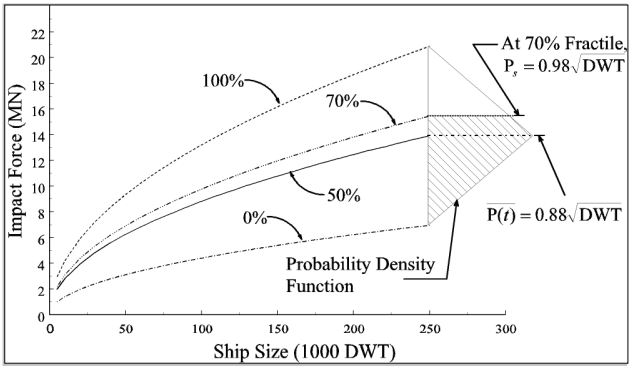


Figure 7: Probability Density Function of Ship Impact Force

Minimum Impact Force

Because a significant number of bridge collisions occur due to empty barges which break loose from moorings during storm events and drift down a waterway to strike a bridge, the AASHTO Specification requires that a minimum impact force be applied to all bridge piers located in water depths greater than 2 feet (especially piers located outside of the 3xLOA navigation zone). The minimum impact force is based on an empty 35x195 foot hopper barge (approx. 1,540 DWT) drifting into the bridge at a minimum speed equal to the yearly mean current for the waterway location.

The need for a minimum impact force, particularly for approach piers, was clearly demonstrated by the 1990 collapse of the Bonner Bridge in North Carolina. Five spans of the approach bridge collapsed when a 200-foot-long hopper dredge broke loose in a storm (while dragging its anchors and trying to stop) and drifted into the structure.

Application of Impact Forces

The AASHTO Specification requires that all portions of a bridge pier or substructure exposed to physical contact by any portion of the design vessel's hull, shall be either protected or proportioned to resist the applied loads. The bow overhang, rake, or flair distance of ship and barge vessels should be considered in determining the portions of the pier and substructure exposed to contact by the vessel.

The bow overhang of ships and barges is particularly dangerous and needs careful consideration by the bridge designer, especially for movable bridges with relatively small navigation clearances. As shown in Figure 8, the main cause of collapse of the Sunshine Skyway Bridge was a failure of the anchor pier column at a location 45 feet above the waterline where the overhang of the ship's bow contacted the structure at a weak point.

Pier Protection Systems

Bridge elements exposed to collision can be designed to withstand the impact loads or a protection system can be developed to prevent, redirect, or reduce the impact loads to non-destructive levels. The protective structures may

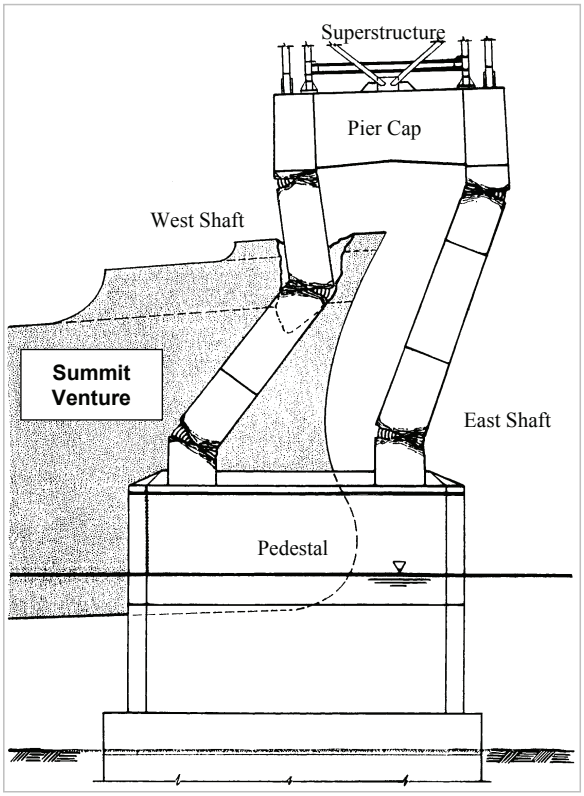


Figure 8: Collapse of the Sunshine Skyway Bridge due to Bow Overhang Collision

be located directly on the bridge (such as a fender), or placed independent of the bridge

(such as dolphins, islands, and pile supported structures). Protective structures are usually designed using energy methods in which the vessel impact energy is absorbed by the deformation of the protection structure; the deformation of the vessel's bow; or by a combination of both.

CODE EXPERIENCE

General

Since its adoption by AASHTO in 1991, the Guide Specification has been used to design numerous new bridges, and to evaluate existing structures for their susceptibility to vessel collision in the U.S. and worldwide. Because the code was published as a "guide specification", its use by the State Departments of Transportation (DOTs) was optional (i.e., its use was not mandatory).

In general, the use of the code was well received in the engineering community. The major drawbacks in the early implementation of the specification involved lack of experience in collecting the large amount of vessel fleet data needed to perform the risk analysis for each bridge, as well as a general unfamiliarity of most bridge designers (and bridge owners) in directly using risk concepts in structural design.

Historically in the U.S., the risk of structural collapse and potential loss of life have been (and to a great extent still are) buried in various "safety factors", "reliability indexes", etc., used in structural design equations within the design codes. Similar to most countries, the U.S. has a great amount of difficulty in dealing directly with engineering risks in a public environment (and this is reflected in our design codes). Defining an acceptable level of risk is a value oriented process, and is by nature subjective. This subjectiveness, and the wide range of public opinion concerning risk acceptance levels, results in an engineering issue that most bridge designers would rather leave alone.

The vessel collision code is somewhat unique in the U.S. in that the acceptable risk of collapse is clearly stated by the guide specification, and risk analysis procedures are directly used to design the structure. Experience to date has shown that the use of the vessel impact and bridge protection requirements of the AASHTO Guide Specification for planning and design of new bridges has resulted in a significant change in proposed structure types over navigable waterways. Incorporation of the risk of vessel collision and cost of protection in the total bridge cost has almost always resulted in longer span bridges being more economical than traditional shorter span structures. This is a consequence of the fact that bridge designs involving longer spans require fewer piers, and therefore fewer pier protection systems, thus producing lower total (bridge plus protection system) costs.

Experience has also shown that it is less expensive to include the cost of protection in the planning stages of a proposed bridge than to add it after the basic span configuration has been established without considering vessel collision concerns. Typical costs for adding protection, or for retrofitting an existing bridge for vessel collision, have ranged from 25% to over 100% of the existing bridge costs.

Extreme Event Combinations (Scour)

The AASHTO Guide Specification recommends a load combination of vessel impact plus dead load for bridge design under ultimate (survivability) conditions. It was not anticipated that scour (or other extreme events) would occur simultaneous with vessel collisions.

It should be noted that the magnitudes and consequences of individual extreme events such as ship and barge collisions; scour due to flooding; earthquakes; ice flows; hurricane driven storm surge and waves; terrorist attacks, etc., usually govern the design process for new highway bridges. If the simultaneous occurrence of two or more of these events is considered (for example, a ship collision or earthquake occurring on a bridge pier whose foundation had been subjected to scour during a flood event), the combination of these separate extreme events will generally result in a dominating load combination with significant cost consequences.

Design based on superposition of extreme loads (as currently advocated by some engineers and government agencies) can lead to a considerable over design costing millions of dollars on each project. Since a simultaneous occurrence of two or more extreme events with maximum magnitudes is unlikely, a rational design approach must be formulated for use by bridge engineers. Toward this end, the FHWA sponsored a conference in Atlanta, Georgia, on December 1996, entitled *The Design of Bridges for Extreme Events*. The conference proceedings contain a collection of papers dealing with vessel collision, scour, and earthquake design for highway bridges (FHWA 1996). Concerning the possible combination of vessel collision and scour, Nowak & Knott recommended an evaluation of the following two load cases (Nowak 1996):

A. A drifting empty barge breaking loose from its' moorings and hitting a bridge (potentially during storm and high water conditions). The drifting barge impact loads should be combined with one-half of the predicted long term plus one-half of the predicted short term scour. The short term scour should be the scour associated with a 100-year flood event.

B. A ship or barge tow striking the bridge while transiting the navigation channel under typical

waterway conditions (i.e., not during extreme storm events and high water conditions). The vessel impact loads should be combined with one-half of the long term scour (no short term scour is included).

In the U.S., historical data indicates that merchant ships and barge tows will not transit river and harbor areas during periods of high water and flood events which cause abnormal and dangerous water currents in the navigation channel. During such flood events, vessels will normally leave the harbor, tie-up at docks, or anchor in designated areas of the waterway. Following the passage of the flood stages of the waterway, and once currents return to normal levels, merchant shipping will recommence in the waterway. By that time it is anticipated that the short term scour areas near the bridge piers will have been significantly refilled by sediment transport mechanisms in the waterway. It is of interest to note that no records of any scour concerns are reported on any of the 31 major bridge collapses mentioned at the beginning of this report.

AASHTO LRFD Bridge Design Specification

The *AASHTO LRFD Bridge Design Specification (3rd Edition 2004 with approved 2005 Interim Revisions)* incorporates all of the analysis and design requirements of Method II of the AASHTO Guide Specification for Vessel Collision. Unlike the guide specification, for which usage is optional, the vessel collision requirements are now mandatory for users of the LRFD Bridge Design Code.

In the LRFD Code, design values of factored load combinations were determined using rigorous statistical analysis procedures and were based on a target beta reliability index of $\beta = 3.5$. However, the statistical analysis was performed only for the basic load combinations with dead load and live load. Extreme loads and their combinations were not considered in the LRFD calibration because of the lack of statistical data concerning the correlation of such extreme events (vessel collision, scour, earthquake, etc.). Therefore, the development of rational design criteria for extreme load events will require future research and the collection of extensive statistical data. Because of the rare nature and large variability of magnitudes associated with extreme events, some researchers believe that the current bridge design methods, statistical analysis models, and calibration procedures used in the development of LRFD load combinations are inappropriate for application to extreme event design.

The vessel collision force in the LRFD Code (designated as CV) is considered an "Extreme Event II" load combination, in which a load factor of 1.0 is used for the vessel collision force in combination with the dead load, 50% of the live load, water loads and stream pressure, and friction (no other extreme events are combined with the vessel collision force). No requirements are provided for combining the "Extreme Event II" loads with scour, however under "Extreme Event I" (Earthquake), the LRFD commentary states that " … unless specific site conditions dictate otherwise, local pier scour and contraction scour depths should not be included in the design."

COMPARISON WITH INTERNATIONAL CODES

Other than AASHTO, the only major international design code that contains provisions for vessel collision is the European Standard (Eurocode). The current provisions for vessel collision are contained in *Eurocode 1 – Actions on Structures – Part 1-7: General Actions – Accidental Actions, prEN 1991-1-7, Final Draft dated September 2005*. The Eurocode is similar in principle to the overall philosophy of the AASHTO LRFD bridge code. For vessel collisions the Eurocode provides for general (deterministic) forces for typical barge and ship collision situations, as well as procedures for performing detailed analysis using probabilistic analysis and dynamic modeling methods. The level of risk acceptance for accidental actions (including vessel collisions) is ultimately determined by the owner or national government, however a probability value of $p = 1 \times 10^{-4}$ is recommended in the code as a representative acceptance value in determining the risk that the accidental action might occur. This Eurocode risk acceptance value is the same as the 1 in 10,000 year Critical Bridge acceptance criteria found in the AASHTO vessel collision requirements.

Barge Impact Forces

A comparison of typical barge impact forces (taken from Table C.3 in the Eurocode) with similar impact forces from AASHTO are shown

in Table 1 below. The AASHTO forces in Table 1 are based on a 35x195 foot barge at a speed of 6 knots (Figure 5).

The Eurocode barge forces in Table 1 are based on different sized barges and displacement tonnages than the U.S., and the impact speed associated with the forces are not clearly stated (though a footnote in the Eurocode indicates that the impact speed should be approximately 5.8 knots plus the speed of any current).

In AASHTO, the displacement tonnage for a single 35x195 foot barge is approximately 1,900 tons, therefore 2 barges would be 3,800 tons, and 3 barges would be 5,700 tons. The AASHTO code only counts the number of barges in the length of the tow (the barges in the width of the tow are assumed to break-away quickly upon impact and are not included in the kinetic energy and force computations). A comparison of the Eurocode barge impact forces and the AASHTO barge impact forces are in general agreement based on forces computed using the displacement tonnage, however the Eurocode forces are higher for the larger tow sizes – probably because the barges in the width of the tow are included in the Eurocode force computation.

A significant difference between the Eurocode and the AASHTO code is that the Eurocode recommends that the quasi-static impact forces shown in Table 1 (which include the dynamic effects of the colliding barge, but not in the structure) be increased by multiplying by an appropriate dynamic amplification factor.

The Eurocode recommends a dynamic amplification factor of 1.3 for frontal (head-on) impacts and 1.7 for lateral impacts. The recommended Eurocode lateral impact forces for barge collision are based on a value equal to approximately 50% of the head-on impact force (similar to AASHTO).

Ship Impact Forces

Recent investigations associated with the Great Belt Bridge in Denmark (Larsen 1993, and Pedersen 1993), have indicated that the maximum ship impact force over time should be considered in the vessel collision analysis and protection system design, rather than the average impact force over time recommended by the AASHTO Specification, and in Eurocode 1, part 2.7 which had a similar equation which resulted in only slightly higher ship impact forces. Sophisticated time-domain computer finite element analysis studies and low strain rate (essentially "static") physical model tests of ship bows conducted by Pederson in Denmark, have indicated a time-history behavior different than that measured by Woisin (Figure 9). It is possible that the differences indicated in Figure 9 are attributable to the dynamic versus static methods used in the physical model tests.

Table 1: Comparison of AASHTO & Eurocode Barge Impact Forces

Eurocode			AASHTO
Barge Towl Description	Displacement Tonnage (tons)	Impact Force (kips)	Impact Force (kips)
Class Vb – Tow + 2 Barges (2x1)	3,000 – 6,000	2,250	1,850
Class VIa – Tow + 2 Barges (1x2)	3,000 – 6,000	2,250	2,270
Class VIb – Tow + 4 Barges (2x2)	6,000 – 12,000	3,150	2,270
Class VIc – Tow + 6 Barges (2x3)	10,000 - 18,000	3,825	2,685
Class VII – Tow + 9 Barges (3x3)	14,000 – 27,000	4,500	2,685

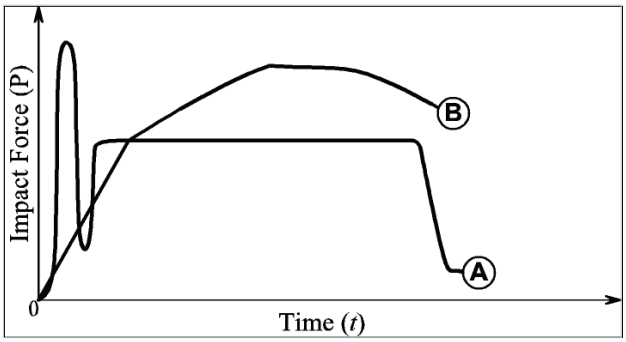


Figure 9: Comparison of Ship Impact Force Time Histories by Woisin (A), and recent research by Pedersen (B)

The consequences of using the maximum impact force for design are significant, since the impact force is approximately twice the average value. A comparison of typical ship impact forces (taken from Table C.4 in the current Eurocode based on Pedersen's equations) with similar forces from AASHTO are shown in Table 2 below. The forces in Table 2 are based on an impact speed of 10 knots, with the Eurocode ship impact forces based on Pederson's equations for computing the maximum impact force.

Similar to the barge forces previously discussed, a significant difference between the Eurocode and the AASHTO code is that the Eurocode recommends that the quasi-static impact forces in Table 2 (which include the dynamic effects of the colliding ship, but not in the structure) be increased by multiplying by an appropriate dynamic amplification factor. The Eurocode recommends a dynamic amplification factor of 1.3 for frontal (head-on) impacts and 1.7 for lateral impacts. The recommended Eurocode lateral impact forces for ship collision are based on a value equal to 50% of the head-on impact force (similar to AASHTO).

BARGE IMPACT RESEARCH IN THE U.S.

Since the AASHTO Guide Specification's adoption in 1991 and its use in analysis and design of bridges for vessel collision in the past 15 years, the specification has spurred a variety of research projects to better understand the mechanics associated with barge collisions on bridges located on the inland waterway system. Of particular note is recent research conducted

by FDOT (Henry Bollmann) and the University of Florida (Gary Consolazio, Ronald Cook, Marc Hoit, and Michael McVay); and recent research conducted by the KYDOT and the University of Kentucky (Hassam Harik).

The research by these institutions reflect the need for the development of dynamic analysis programs and procedures to estimate barge impact forces, rather than the use of quasi-static forces as currently included in the LRFD and Guide Specification for collision forces.

A key research program recently completed by FDOT and the University of Florida (UF) involved the use of full-scale barge impact testing on several bridge piers of the St. George Island Bridge across Florida's Apalachicola Bay. The existing bridge was being replaced by a new bridge, so two of the abandoned bridge piers (a channel pier with a relatively massive mudline foundation, and an approach pier with two waterline footings) were studied in three different structural configurations in a full-scale test program which included ramming a small 600 ton barge against the piers at various speeds (some with the superstructure in-place and others with the superstructure removed) and measuring a wide variety of responses in the structure and soil using extensive measurement and recording systems.

Table 2: Comparison of AASHTO & Eurocode Ship Impact Forces

Eurocode			AASHTO
Ship Description	Displacement Tonnage (tons)	Impact Force (kips)	Impact Force (kips)
Small Ship	3,000	6,750	6,900
Medium Ship	10,000	18,000	12,300
Large Ship	40,000	54,000	25,800
Very Large Ship	100,000	103,500	41,300

The research by these institutions reflect the need for the development of dynamic analysis programs and procedures to estimate barge impact forces, rather than the use of quasi-static forces as currently included in the LRFD and Guide Specification for collision forces.

A key research program recently completed by FDOT and the University of Florida (UF) involved the use of full-scale barge impact testing on several bridge piers of the St. George Island Bridge across Florida's Apalachicola Bay. The existing bridge was being replaced by a new bridge, so two of the abandoned bridge piers (a channel pier with a relatively massive mudline foundation, and an approach pier with two waterline footings) were studied in three different structural configurations in a full-scale test program which included ramming a small 600 ton barge against the piers at various speeds (some with the superstructure in-place and others with the superstructure removed) and measuring a wide variety of responses in the structure and soil using extensive measurement and recording systems.

The final UF report entitled Barge Impact Testing of the St. George Island Causeway Bridge (March 2006) is a valuable addition to the understanding of barge impact behavior. Following the test program, UF and FDOT have developed a bridge analysis software program (FB-MultiPier) available in the public domain that can perform a dynamic analysis of barge impacts in a matter of minutes. Other public domain structural analysis programs have also been used in the bridge design industry to model the dynamic behavior of bridges under vessel collision impacts.

Based on the UF test data from the St. George Bridge program several general observations can be made in comparing the measured barge impact forces with those predicted by the AASHTO equations. For relatively stiff piers with pedestal type substructures extending from underwater pile-supported footings buried under the mudline, the measured impact forces ranged from 50% to 100% of the AASHTO force (with most measurements near the 50% level). For relatively flexible piers with the footings at or above the waterline and supported by piling extending through the water column into the soil below, the measured impact forces ranged from 100% to 130% of the AASHTO forces (with most measurements near the 130% level). The test results indicate that the dynamic response of the structure and the stiffness of the underlying soil are key components in the development of the barge impact force transmitted to the pier.

The UF barge test data also indicated that the differences in load effects (e.g., displacements, shears, moments, etc.) that arise from application of AASHTO static loads versus the dynamic loads of the test data were, in some cases, even more pronounced than the differences in load magnitudes. The differences identified in the UF research were attributed to dynamic effects. Some of the effects relate to increased levels of response due to the inertia (or momentum) of the structure once it has been accelerated, while others involve short-term restraint of displacements that are associated with inertia resistance (e.g., of the bridge superstructure).

FHWA TECHNICAL ADVISORY

The author is currently assisting the Federal Highway Administration (FHWA) Bridges and Structures Division in the development of an FHWA Technical Advisory on Vessel Collision Design and Vulnerability Assessments of Highway Bridges. Included will be a series of FHWA reports on vessel collision risk assessment and design issues (publication is anticipated in the latter part of 2006). Recommendations being considered (though not yet officially adopted by FHWA) are summarized below

IMMEDIATE NEEDS

Until the results of the barge testing and research being conducted in the U.S. becomes available and has undergone technical review by bridge design practitioners, it is recommended that for the immediate future (the next 2-3 years) that the current vessel collision provisions of the AASHTO Guide Specification and LRFD Code be used by the industry with the incorporation of the minor adjustments noted below:

Recommended Immediate Revisions

The following revisions in the existing AASHTO procedures are recommended based on research, feedback from engineers using the existing codes, and to clarify certain portions of the original Guide Specification provisions.

Annual Frequency of Collapse, AF

It is recommended that a "Protection Factor (PF)" be added to the computation of AF (Equation 1.1 above). The revised equation for AF would become:

AF = (N)(PA)(PG)(PC)(PF) (1.4)

The concept of the protection factor is indirectly discussed in the existing AASHTO Guide Specification, but the above revision would make the concept explicit and therefore clearer to bridge engineers. The purpose of the protection factor is to adjust AF for full or partial protection of selected bridge piers against vessel collisions due to protection measures (dolphins, islands, etc.) or due to existing site conditions such as a parallel bridge protecting a bridge from impacts in one direction; or a feature of the waterway (such as a peninsula extending out on one side of the bridge) that may block vessels from hitting bridge piers; or a wharf structure near the bridge that may block vessels from a certain direction.

PF should be computed as:

PF = 1 – (% Protection Provided/100) (1-5)

If no protection of the pier exists, then PF=1.0. If the pier is 100% protected, then PF=0.0. If the pier protection (say a dolphin system) provides 70% protection, then PF would be 0.3. Values for PF may vary from pier to pier and may vary depending on the direction of the vessel traffic (i.e., vessel traffic moving inbound versus traffic moving outbound). A general procedure to estimate PF is shown in the AASHTO Guide Specification commentary (Figure C4.9.3-1) for estimating the reduction in annual frequency due to pier protection structures (such as large diameter dolphins).

Computation of PG and Impact Speed Distribution Based on LOA

When the original Guide Specification was developed in the late 1980s most analysis was done by hand calculators, therefore the specification provisions included some simplifying requirements to minimize the hand analysis effort. With modern personal computers and software programs such as Excel spreadsheets and MathCAD, the vessel collision risk analysis procedures can be easily programmed, therefore these simplifications can now be removed.

The existing Guide Specification (Section 3.7 on Design Impact Speed and Section 4.8.3.3 Geometric Probability) require the use of a vessel length overall (LOA) selected in accordance with the Method I criteria for use in estimating the impact speed and geometric probability for all vessel classifications. This provision should be revised to allow for the LOA of each specific vessel category to be used in determining the vessel speed distribution and geometric probability associated with that specific vessel category.

Water Depths

Section 4.2.2 of the Guide Specification states that, "The ability of a vessel to strike a pier or span shall be determined based on the design water depth at the location of the bridge element, and the draft of the vessel." This statement should be clarified by stating that the water depth at the pier should not include any short-term scour. In addition, the water depth should not just be evaluated at the specific pier location itself, but also at locations upstream and downstream of the pier – which may be shallower and would block certain deeper draft vessels from potentially hitting the pier.

Vessel Collision Load Combinations (Scour)

Unless DOTs have established different procedures based on scour observations within their respective States, it is recommended that the combination of vessel collision impact forces with scour be based on the recommendations of discussed above.

Electronic Navigation Aids and PA

Following the terrorist attacks upon the U.S. on 9/11, the USCG has required that all foreign ships entering the U.S. waterway system to be equipped with a variety of advanced electronic navigation aids and tracking systems. These requirements do not extend to domestic barge tows on the inland waterway system. An argument could be put forth that the use of such advanced navigation aids may reduce the risk of vessel collision with bridges and should be accounted for in the computation of the probability of aberrancy (PA).

At present however, no studies have been performed to analyze and document the potential reduction in PA due to such electronic aids-to-navigation. If a case can be made at a particular waterway and bridge site that improved electronic navigation aids would reduce PA, then such a factor could be used in the equation - provided it is approved by the owner (these type of changes based on the owners approval are allowed in the Guide Specification).

As an example, such a reduction was recently used in the design of a new cable-stayed bridge in Argentina. The thought process proceeded as follows: 1) approximately 60-90% of all accidents are caused by pilot error (a value of 70% was chosen for the analysis); 2) the bridge owner firmly believed that improvements to electronic navigation would result in a decrease in the rate of pilot error – however there were no studies or data to really support this belief or what the reduction should be; 3) though no actual data existed, the design team believed, and the owner agreed, that the pilot error rate could conservatively be reduced by 30% due to the electronic aids; therefore 0.3 x 0.7 = 0.21 was used to reduce the ship accident rate by about 20% for the risk analysis (i.e., a reduction factor of 0.8 was applied to the PA equation).

LONG TERM NEEDS

Compared to more mature and established fields such as wind and earthquake engineering, vessel collision design is in its infancy stages. Although there are a number of important research needs within the discipline, the following key areas are highlighted based on experience using the AASHTO code:

Ship Impact Forces

As noted in Section 5.2 above, there is a large discrepancy between the design values for ship impact in AASHTO based on a 70% fractile of the average ship impact force, and the maximum dynamic impact force contained in the Eurocode based on the Pederson equation. This matter will require further research and discussion in the U.S. on the appropriate course of action. Recent research conducted in China indicates that ship impact forces are only slightly higher then those computed using the AASHTO equations, versus those computed using Pederson's equations.

The consequences of using the maximum ship impact force for design are significant. Further research into accurate time-histories of ship impact forces, especially under dynamic loading conditions, is critical in resolving the current discussion on which impact force is the most appropriate to use for design.

In addition the use of a "dynamic amplification factor" to further increase the ship impact force to be applied as a quasi-static force to the structure (as contained in the Eurocode) will require future research.

Barge Impact Forces

Most of the bridges which cross navigable waterways in the U.S. are structures over rivers on our inland waterway system, and are therefore limited to collisions from shallow draft vessels such as barge tows. Because of the large number of these bridges, the development of accurate impact forces and time-histories associated with barge collisions is very important. As noted above, fundamental research is currently underway at the University of Florida and the University of Kentucky which will be a basis for potential future revisions of the AASHTO barge collision provisions.

One specific area requiring additional research is the behavior of long barge tows during a collision. In the U.S, such barge tows can contain as many as 15 to 20 barges and approach 1000 feet in total length. Currently, the AASHTO Code requires that the number of barges in the length of the tow be included in the determination of the barge impact force (based on observed historical behavior of barge tow accidents the side barges in the tow are assumed to quickly break away during the collision and not have a significant effect on the tow impact force). Some believe that this approach is too conservative, and that the barges in the length of the tow will buckle (like an accordion) and that the resultant impact forces would be reduced.

In addition the use of a "dynamic amplification factor" to further increase the barge impact force to be applied as a quasi-static force to the structure (as contained in the Eurocode) will require future research. With currently available computer software and hardware, development and use of simplified dynamic barge collision analysis models is also a viable means of

addressing dynamic amplification effects and may lead to greater uniformity in safety and economy of design than would quasi-static analysis with amplification factors. It is recommended the problem be approached from both directions: development, implementation, and practical use of simplified dynamic analysis procedures, as well as determination of simple, yet conservative, dynamic amplification factors for use in quasi-static analysis.

Risk Acceptance Criteria

Further research is needed to establish an appropriate risk acceptance level for vessel collision design, and for load combinations involving vessel collisions. It is also critical that the risk level be consistent with that established for other extreme events used for bridge design.

Current bridge structure codes in the U.S. are not well defined with regard to the combination and simultaneous occurrence of extreme events, nor are the selection of the individual extreme events consistent with each other. In the AASHTO LRFD Code for example, scour is considered for 100-year and 500-year flood events; earthquakes are considered for a 475-year return period event for regular bridges, and 2,500-years for critical bridges; and vessel collisions are considered for a 1,000-year return period for regular bridges, and 10,000 years for critical bridges. As can be seen, there is a real need for a common basis of design.

Some bridge designers in the U.S. believe that the vessel collision risk criteria may be set too high, and should possibly be reduced to the 475 and 2,500 year return period levels used for earthquake design. This is opposite to some current discussions in Europe, where it is believed that the vessel collision risk levels may be too low and should be increased to 10,000 years for regular bridges, and as high as 1,000,000 years for critical bridges.

Physical Protection Systems

The AASHTO Guide Specification provides examples and contains a relatively extensive discussion of various types of physical protection systems, such as fenders; pile supported structures; dolphins; protective islands; and floating structures. However, the code does not include specific procedures and recommendations on how to actually design such protection structures. Further research is critically needed to establish consistent analysis and design methodologies for protection structures, particularly since these structures undergo large plastic deformations during the collision.

Aids-to-Navigation Improvements

Research is needed to assess the reduction in the risk of vessel collision due to improvements to aids to navigation in the waterway, such as buoys; range markers; vessel traffic control systems; and electronic navigation systems onboard merchant vessels. Studies have indicated that improvements in the aids to navigation near a bridge can provide extremely cost-effective solutions to reducing the risk of collisions to acceptable levels.

The cost of such aid to navigation improvements and ship board electronic navigation systems is usually a fraction of the cost associated with expensive physical protection alternatives. However, few electronic navigation systems have ever been implemented (worldwide) due to legal complications arising from liability concerns; impacts on international laws governing trade on the high seas; and resistance by maritime users.

It should be noted that the traditional isolation of the maritime community must come to an end. In addition to the bridge costs, motorist inconvenience, and loss of life associated with a catastrophic vessel collision, significant environmental damage can also occur due to spilled hazardous or noxious cargoes in the waterway.

The days when the primary losses associated with an accident rested with the vessel and her crews are over. The $13 million value of the M/V Summit Venture was far below the $250 million replacement cost of the Sunshine Skyway Bridge which the vessel destroyed. The losses associated with the 11 million gallons of crude oil spilled from the M/V Exxon Valdez accident off the coast of Alaska in 1989 are over $3.5 billion. Both of these accidents could have been prevented using shipboard advanced electronic navigation systems.

CONCLUSIONS

Large lateral forces on bridge foundations due to extreme events such as vessel collisions, earthquakes, and wave forces on storm surges during hurricane events are often the controlling design condition for bridge foundations. The AASHTO Guide Specification requirements for vessel collision design have provided a rational methodology for determining the risk of vessel collision with bridges, and for the development of structures with improved resistance to catastrophic collapse due to ship and barge impacts. The experience to date by bridge engineers using the AASHTO vessel collision codes has been reasonably positive. This report contains immediate and long-term recommendations concerning improvements in the current AASHTO procedures.

It is recognized that vessel collision is but one of a multitude of factors involved in the planning process for a new bridge. The designer must balance a variety of needs including political, social, and economic in arriving at an optimal bridge solution for a proposed highway crossing. Because of the relatively high bridge costs associated with vessel collision design for most waterway crossings, it is important that additional research be conducted to improve our understanding of vessel impact mechanics, the response of the structure, and the development of cost-effective protection systems.

Reference List

AASHTO 1991. Guide Specification and Commentary for Vessel Collision Design of Highway Bridges, American Association of State Highway and Transportation Officials, Washington D.C.

AASHTO 1994. LRFD Bridge Design Specifications and Commentary, American Association of State Highway and Transportation Officials, Washington D.C.

FHWA 1996. The Design of Bridges for Extreme Events, Federal Highway Administration, Conference Proceedings, Atlanta, Georgia.

IABSE 1983. Ship Collision with Bridges and Offshore Structures, International Association for Bridge and Structural Engineering, Colloquium Proceedings, Copenhagen, Denmark, 3 Volumes (Introductory, Preliminary, and Final Re-ports).

Larsen, O.D. (ED) 1993. Ship Collision with Bridges - The Interaction Between Vessel Traffic and Bridge Structures, International Association for Bridge and Structural Engineering (IABSE), Structural Engineering Document No. 4.

Nowak, A. & Knott, M. 1996. Extreme Load Events and Their Combinations, FHWA Conference Proceedings, the Design of Bridges for Extreme Events, Atlanta, Georgia.

Pedersen, P.T. 1993. Ship Impacts: Bow Collisions, Conference Proceedings from the Third International Symposium on Structural Crashworthiness and Failure, University of Liverpool, U.K.

Report of The U.S. Coast Guard – American Waterways Operators Bridge Allision Work Group, USCG – AWO Safety Partnership, May 2003.

Barge Impact Testing of The St. George Island Bridge (March 2006), by G. Consolazio, R. Cook & M. McVay, et. al., University of Florida, Civil and Coastal Engineering Department, Report 2006/26868.

THE UNDERWATER CUT-OFF AT THE WALTER F. GEORGE DAM

Gianfranco Di Cicco, Area Manage Special Project and Riccardo Pertocelli CEO,
TREVIICOS Corporation, Boston, MA, USA

Seepage problems were recorded for more then 40 years at the Walter F. George lock and dam. In 2001 the Mobile district of The U.S. Army Corps of Engineers turned to the installation of a 200 feet deep cut-off in a final attempt to remedy the situation. The advertised design-built contract requested the installation of the cutoff wall in front of the concrete structure of the dam starting from 90 feet of water, cutting through a concrete lock structure, a submerged retaining wall and extending on both sides on the earthen embankments.

This paper summarize the history of the project and the installation of the first recorded cut-off wall constructed under deep water, upstream to an existing dam structures and under an existing concrete lock.

The technology used combined with the project's results may be considered a milestone in the marine foundation and the marine cut-off wall construction technology.



Project Location

HISTORY

The Walter F. George lock and dam was constructed on the Chattahoochee River between 1955 and 1963 with the double function of improving navigation and generating power. Its 82 ft. by 450 ft. lock can accommodate large barge traffic and its four generating units with a plant capacity of 150 MW have an average energy output of 453,000 MWH.

The dam consists of a 1,496 ft. long concrete structure housing the spillway, a non overflow portion, the power units and two earthen wing dams extending to the Georgia and Alabama sides, respectively 5,810 feet and 6,130 feet long.

As soon as the reservoir was impounded it became apparent that excessive seepage was occurring.

In October 1961, during stripping operations on the final stage of construction of the Alabama dike, two sinkholes occurred.

In 1962, still during construction, boils developed along the downstream toe of both Alabama and Georgia.

In order to control the seepage below the dam structure, relief wells were installed at the toe of the embankments and the foundation beneath the dikes was drilled and grouted.

Subsequently, after completion of the project, a large spring developed near the downstream lock guide wall and sinkhole activity increased on the Georgia side.

In 1968 sinkhole activity increased and a new phase of remedial work began.

Initially, the remedial work consisted of grouting a small area of the foundation under the Georgia

dike, filling the sinkholes with sand and grouting around each sinkhole periphery.

In February 1969 a sinkhole was discovered in the reservoir near the Georgia dike and it was filled and grouted in a similar manner.

A surface investigation downstream of the Georgia dike was carried out, a number of piezometers were installed and information concerning solution channels was obtained. After the evaluation of the new data, a sand filled filter trench was constructed downstream of the lock guide wall in order to intercept the water bearing solution channels which were discharging through a spring. The objective was to reduce the water velocity in order to prevent the movement of solid material.

In 1970 a line of grout holes was performed downstream of the Georgia dike.

During 1971, several small sinkholes were discovered at the Alabama dike toe and simultaneously pin boils were found in the relief well collector ditch in the same area.

In 1978 a new design recommended the installation of a positive cut-off wall under the earth embankment to upgrade the dam to current standards.

This recommendation was adopted, and a 24 inches thick concrete cut-off wall was installed to the bottom of the shell layer within the earthy limestone. In limited areas, in accordance with a previous soil investigation, the cut-off was installed deeper, generally to the bottom of the Shell Limestone.

Phase I of the cut-off was installed under a portion of the Georgia dike in 1981 and Phase II was installed beneath an additional portion of the Georgia dike and the Alabama dike between 1983 and 1985. In 1982, between the two phases of construction, a boil was observed on the water surface immediately downstream of the Power House. The entrance point, called the "Hungry Hole". was plugged with a tremie pipe. The eroded channel under the Power House was filled with 175 c.y. of tremied concrete. Additional grouting was performed along the upstream face of the power house and part of the spillway.



Figure 1: Aerial View of Cut-Off Wall

Those efforts were only partially successful and resulted in a concentration of the seepage below the concrete structure. The seepage problems at the W. F. George dam continued to worsen.

Discharges from piezometers SP-5 and from the power House drainage system increased. As the Shell Limestone material was piped from under the concrete structure, the passage ways through which the flow was occurring were being enlarged resulting in greater erosion.

This situation compromised the generating potential of the dam as well as potentially jeopardized its stability.

Finally, the decision was made to construct a deep cut-off primarily under the concrete portion of the dam to remedy the problem. (See Figures 1 and 2.)

PROCUREMENT

On July 5th, 2001, best and final offers were solicited by the Corps of Engineers (COE) for the construction of a deep cut-off to be built in front of the concrete portion of the dam from the bottom of the lake and tied into it. The cut-off had to cross an existing lock structure and an underwater retaining wall, as well as the remnants of a steel coffer cell left in place from the initial construction.

The specifications required that the wall be built with a minimum thickness of 24" and that it extended from the bottom of the lake to elevation -5 into the Providence formation, an impervious layer.

While the land portions of the wall were on average 208 feet deep, the marine portion started from up to 90 feet of water and continued through different rock formations for another 100 feet.

Contractors were invited to propose their own method of constructing the cut-off and offers were evaluated using several criteria, including technical, economic, and organizational and experience.

Three proposals were received and on August 14, 2001 an award was made to the Joint Venture (JV) of Treviicos and Rodio.

GEOLOGICAL CHALLENGES AND PROPOSED TECHNOLOGIES

The geological challenges to overcome during the cutoff wall construction consisted in the existence of a very hard stratum (up to 14000 PSI) overlaying a loose sand layer, the presence of voids, fractures and pathways in the rock mass and the existence of sediments and various debris at the lake bottom.

Nevertheless it was not requested; the proposal contemplated a preliminary drilling and grouting campaign in order to verify ground conditions and to fill any large voids which could disrupt the orderly progress of the work.

Treviicos-Rodio proposed to do the marine portion of the work with secant piles installed using reverse circulation top-pile rigs and using water as drilling fluid, while the land portion would be a slurry wall done by Hydromill, using bentonite as a stabilizing fluid.

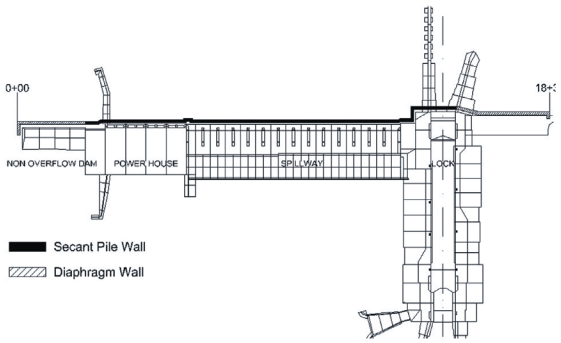


Figure 2: Plan View of the Cut-Off Wall

The chosen method for the marine work construction was the result of detailed analysis of safety, quality, environmental, technical and economical conditions and requirements.

Safety was considered in employing a technology able to reduce to the minimum the diving operation and the risks involved in performing underwater work at depths of almost 100 feet and in such operation.

Quality was considered in employing the secant piles technology as the most reliable to do the marine portion of the work.

Environmental concerns were considered in employing a reverse circulation methodology which allowed the use of water as circulation fluid and the elimination of any type of slurry from contaminating the lake environment.

Technical concerns were considered in researching and detailing each different phase and challenge of the various areas of the project.
Economical concerns were reduced in evaluating and implementing all the above considerations and insuring that the project team was formed by experienced personnel.

A very detailed technical proposal containing documents, drawings and method of statements were submitted with the bid. However, to insure the client that the proposal and the project challenges were studied, detailed and covered by the design and build proposal, it was decided to include in the presentation a video CD showing and describing the various phases of the marine work.

CONSTRUCTION METHODS

The construction methods used are summarized in the following sequence of mainly marine operations:

Drilling and Grouting Campaign

As explained, the specifications were not requiring the performing of any extra soil investigation. However, since the bid preparation it was decided to propose to drill a series of exploratory holes along the axis of the cut-off wall. (See Figure 3.) The results expected and obtained were to reduce the uncertainties over the extent of the Karstic phenomenon. The exploratory investigation,

which was the first of the marine operation performed, consisted in:

- Localized borings to ascertain:
  - Depth of sediments
  - Presence of fill materials placed upstream of the dam during construction
  - Thickness of hard sandy limestone layer
  - Characteristic of sand layer (apparently none cemented) within the sandy limestone
- Grout holes to fill major cavities, possibly with high water flows



Figure 3: Drilling and Grouting

Cleaning of the Lake Bottom and Constructing a Working Apron

The construction underwater of an apron was required to insure the correct installation and positioning of the cutoff wall at the lake bed elevation.

A cleaning operation in front of the dam structure was requested before the apron installation. Obstructions and debris were found in large quantities from the dam construction and from years of operation.

After all the obstructions were removed the apron was installed excavating a six foot minimum trench was and then backfilled with engineering material along the cut-off wall alignment.

Installing Casing Templates Tied to the Concrete Dam

Whenever possible, guide beams and templates were installed and secured to the concrete dam structures. The main beam was mounted on the props connected to the fenders of the dam. Its position and alignment was checked using reference points previously installed on the dam during the initial survey. (See Figure 4.)



Figure 4: Standard Templates

When it was possible to attach the template to the dam, temporary piles were driven to support the original or a modified template. The templates were used to insure the correct piles positioning and to guide the temporary casing while installing and driving them into the apron.

Drilling and Concreting Piles

The cutoff wall designed using 50 inch secant piles, spaced 33 inches center to center. The piles were installed in a sequence of primary and secondary, in which the secondary piles were drilled between the two adjacent primary piles. (See Figures 5 and 6.)

The piles were installed to form a continuous wall of the minimum thickness of 24 inches, from the lakebed to El - 5 MSL, into the Providence formation.

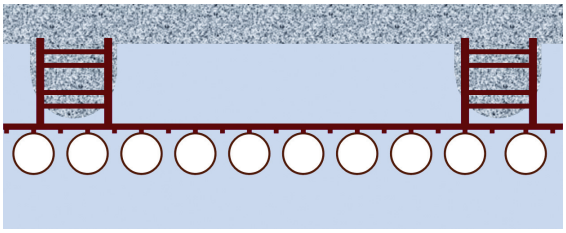


Figure 5: Phase I – Primary Piles Installation

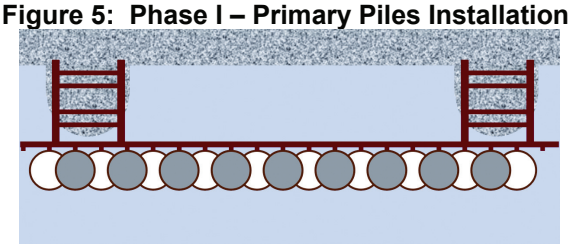


Figure 6: Phase II – Secondary Piles Installation

Typically, the execution of the piles entailed the following steps:

- Installation of the temporary casing supported and guided for the steel template
- Setting the reverse circulation rig on top of the temporary casing
- Drilling to design depth
- Removal of the drilling string
- Setting tremie pipes and pouring concrete
- Withdrawal of casing and setting in a new pile position

Water pumped from the lake was used as drilling fluid.

The main equipment for the installation of the secant piles was the following:

- Pontoons and spoil barges
- Manitowoc 4000 Crawler service cranes positioned on the pontoons
- Templates for the installations of casings
- Wirth PBA 612 reverse circulation rig
- ICE 66-80 hammers to install the casing
- ICE 160 Hydraulic pile hammers to install the casing through hard strata
- IR 960 high pressure compressors
- Vertically control device

The secant pile cut-off wall was drilled to full depth using the Wirth PBA 612 reverse circulation rig mounted on top of the 50 casing.

It has a rotary drill table mounted on the top of a frame, and a working platform. The rig is fixed on the top of the casing by means of clamps. A jib positioned on the top pile rig platform facilitates handling of rods. (See Figure 7.)



Figure 7: Reverse Circulation Rig

On the top of rotary table there is a two way swivel, discharging the cuttings into a 10 hose. The compressed air for drilling is supplied by means of 4pipes and hoses, connected to a swivel below the rotary table.

Specially designed stabilizers were used in order to maintain the verticality of the drilling string during drilling operations.

Flanged double wall drillings rods, 10 feet long with 6 " inner cuttings conduit and air conduit and the drilling bit completed the drilling equipment

All the cuttings excavated by the reverse circulation rigs passed through a 10 discharge pipe and were delivered to the hopper barge. From this barge the cuttings were deposited to the bottom of the lake. Silt curtains, installed around the hopper barge, prevented the

contamination of the lake water by the spoil material.

Constructing the Slurry Wall

Slurry wall installation was the technology chosen to install the land portion of the cut-off wall, to cut the lock concrete monolith and the underwater retaining wall. (See Figure 8.)

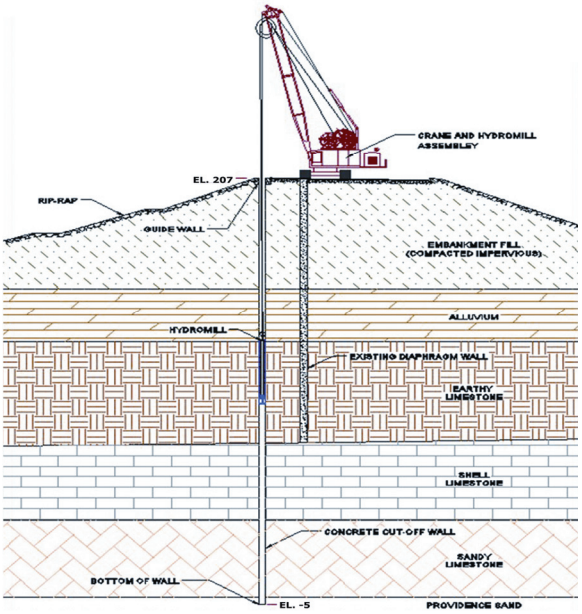


Figure 8: Construction of Slurry Wall on Land

The cut-off wall installed using the slurry wall was built by primary and secondary panels using a Soletanche HI 2000 series Hydromill.

The primary panel was formed by single or multiple bites with a total excavation length of 8 to 24 feet. The secondary panels overlapping the primaries were a single 8 foot bite.

The de-sanding plant was a Sotres-450 consisting of a series of vibrating screens and cyclones capable of screening all the cutting sizes with a capacity of 500 cu. yd. per hour.

Constructing the Cut-Off through the Lock Structure

The crossing of the lock structure was accomplished by using the Hydromill on the Georgia side to cross the eastern retaining wall, while secant piles did the rest of the crossing. (See Figure 9.)

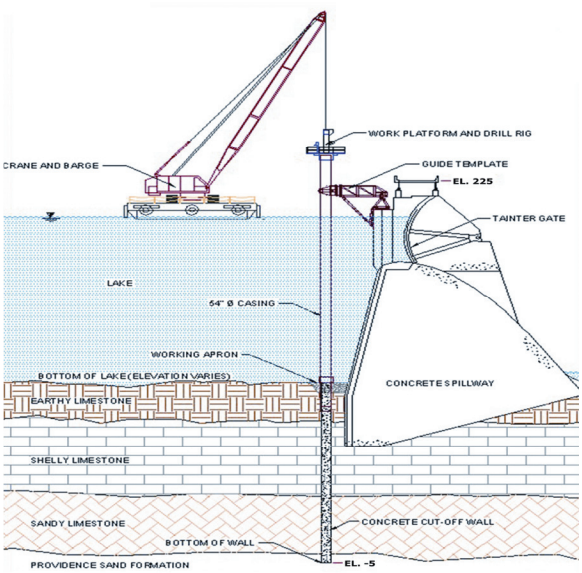


Figure 9: Construction of the Secant Pile Wall in the Water

With the Hydromill equipment, vertical excavation within required tolerance is assured when both cutter wheels mill similar material in terms of hardness and consistency. (See Figure 10.)

On the Georgia side, the sloping contact between the soil embankment and the monolithic wall did not allow for the wall to be built in the correct sequence of primary and secondary panels, due to the fact that no panel could be excavated through the inclined concrete surface without a vertical guide

The solution was to re-create in advance a uniform condition where:

- The inclined surface had been removed by a preliminary reaming of the wall
- The adjacent soil had been replaced by concrete

Under this modified conditions, the standard sequence of overlapped primary and secondary panels was correctly carried out.

In detail the following steps were adopted:

- Construction of the slurry wall up to the last panel touching the monolithic wall foundation
- Milling the first adjacent bite passing through the wall for a certain depth



Figure 10: Hydromill and Guide Pipes

- Note that when the Hydromill reached the inclined hard surface, it reacted against and was guided by the previously concreted panel acting as a shoulder. This did not allow any lateral deviation
- After entering in the entire concrete mass for several feet, the excavation was stopped and the panel was concreted
- The same procedure was repeated in single bites in an uphill progression until the entire inclined surface was entirely reamed and the soil replaced by concrete. The last panel in this sequence was excavated and left open.

After this operation, the slurry wall was built at full depth, re-excavating the newly placed concrete as well as the remaining portions of the lock wall with the proper sequence of primary and secondary panels. (See Figure 11.)

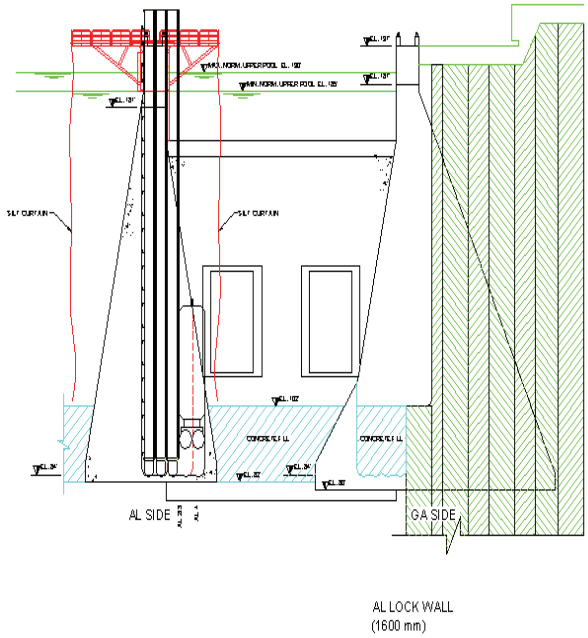


Figure 11: Lock Structure Crossing

Connection to Secant Pile Wall

The connection between slurry wall and secant piles was located in the footprint of the eastern monolith.



Figure 12: Hydromill on Pontoon

The following steps were carried out:

- The soil between the walls of the Lock was excavated under water from El 108 to the bottom of the walls at El 81, for a width of 15 feet. The lakebed westwards of the western monolith was dredged as well to the bottom of the wall
- The excavation as filled with 3000 psi concrete to elevation 108
- The Hydromill then continued to remove the concrete from the center of the Eastern wall, progressing westward until the concrete has been removed to El 108. Cutter wheels on the Hydromill for this operation were 63 inches in width in order to accommodate the casings for the secant piles.
- The progression was aided by installing a steel casing to act as a vertical guide
- Construction of the wall by the secant pile method was advanced eastward using the guiding template across the lock, until it encountered the lock wall.
- A secondary pile overlapping the last panel and the first primary pile was the joint element between secant pile wall and slurry wall.
- At the completion of the secant pile portion, the cut of the retaining wall was repaired.

Constructing the Permanent Concrete Cap Tying the Cut-Off to the Dam

The construction of the cap beam was done upon completion of the cut-off installation. Depending on the cut-off wall's position and the apron elevation, a portion, or all, of the engineered backfilling between the cut-off wall and the dam was removed in order to install the cap beam.

The surfaces of the monoliths and of the cut-off wall were cleaned to insure a proper joint before pouring the 3000 psi. concrete of the cap beam.



Figure 13: Cutting East Lock Monolith with Hydromill

CONCLUSIONS

The construction of a deep under water cut-off had never been attempted before and its successful completion will open new possibilities to Engineers and Owners on how to deal with difficult underwater seepage problems.

The result obtained were the consequence of awarding the project to qualified companies and the assembling of a team of highly qualified experts working together from the bid preparation and through the completion of all the difficult phases of the project.

CURRENT STATE OF PRACTICE OF CORRISION PROTECTIVE SYSTEMS FOR TIERODS AND TIEBACKS USED IN MARINE APPLICATIONS

Thomas A. Printz P.E. and Tom Bird, Williams Form Engineering Corp., Goldon, CO, USA
John A. White P.E., Williams Form Engineering Corp., Belmont, MI, USA

INTRODUCTION

The wide use of carbon steel in construction and engineering projects makes this engineering material accountable for approximately 85% of the total annual steel production worldwide. Despite the lack of corrosion resistance of carbon steel, it is incorporated into the permanent work for marine applications, power plants, transportation projects, chemical processing, mining, petroleum production and refining, pipelines, mining and construction equipment.

Corrosion is an electro-chemical process that occurs in the presence of water and air. When an electric current is introduced to water or soil, the rate of carbon steel corrosion increases rapidly. Gaseous atmospheric constituents that are capable of electrolytic activity can also increase the rate of corrosion. Corrosion tends to be more rapid in environments in which the steel is exposed to water, and then air, rather than being constantly submerged. The exposure to seawater increases steel pitting because the electrical conductivity is improved in salt water.

The corrosion of carbon steel costs the global economy hundreds of millions of dollars a year. Carbon steel usage is the largest among building materials in terms of tonnage as well as total material cost, therefore, the corrosion process and corrosion protection systems are of great interest to owners and designers to determine the design life of construction and engineering projects.

Corrosion protection systems may consist of protective coatings, such as, fusion bonded epoxy coating, coal tar epoxy coating, or steel elements that are pre-grouted inside a corrugated HDPE duct.

Hot dipped galvanizing is another corrosion protection system that protects the steel by sacrificing its own electrons and corroding prior to the carbon steel that it is protecting. There are many advantages of each form of corrosion protection provided by these methods.

FUSION BONDED EPOXY COATING

Fusion Bonded Epoxy Coating is a protective coating applied to deformed and plain steel reinforcing bars. The coating is applied by the electrostatic spray method, which consists of electrostatically charged dry powder sprayed onto a grounded bar. The bar is heated to a temperature that is specified by the powder manufacturer prior to the application of the powder. The specifications that govern the application and the material used for the coating process are ASTM A775 (rebar green), ASTM A934 (purple marine coating), and AASHTO M284 (rebar green).

The steel bar surface preparation includes abrasive blast cleaning to near white metal. After cleaning, the bars are handled by personnel with gloves to prevent the contamination of the clean steel. ASTM A775 and AASHTO M284 allow the coating to take place up to 8 hours after the cleaning operation, while ASTM A934 requires that the steel bars be coated within 3 hours after cleaning.



Figure 1: Plain bars are tagged with heat numbers and cut to length prior to being coated. There is visible surface oxidation on the bars that is mechanically cleaned prior to coating.

The coating is applied per the powder manufactures recommendations for steel temperature during application as well as epoxy coating cure time after application.

The coating thickness per ASTM and AASHTO specifications is 7-12 mils, however, some government agencies, project owners, owners representatives, as well as independent engineering firms may specify a thicker coating. The epoxy coating applicator accomplishes a thicker coating by slowing the speed of the coating line and adding powder spraying nozzles if necessary. It is possible for epoxy coating applicators to accomplish thicknesses of 12-16 mils on the steel product or greater. The bar supplier should have the ability to supply hardware, such as hex nuts and couplings, that are tapped slightly oversized to accommodate the thickness of the coating, without sacrificing the strength of the connection. The oversized hardware should exceed the strength of the bar and should be able to break a plain, uncoated bar in a tensile load test. If the coated product has more than 16 mils of epoxy coating, the threadability of even the oversized fasteners become an issue.

The quality of the coating is closely monitored by the coating applicator. The thickness of the coating is monitored and averaged over the entire length of the bar. The unaided eye examines the continuity of the coating. Any examined deficiencies in the coating are addressed by patching with approved materials and methods per the patch kit manufacturer. Typical patch kit material for epoxy-coated bar is in accordance with ASTM D3963.

The bar is also tested for holidays using a 67.5volt d-c holiday detector. A holiday is a pinhole in the coating that is not visible to the human eye. The ASTM A775 as well as the AASHTO M284 specifications allow for two holidays per lineal foot of coated bar, while the ASTM A934 coating specification only allows one holiday per lineal foot of bar.

One of the major differences between the ASTM A934 and the ASTM A775/ AASHTO M284 coatings is in the coating flexibility, which directly affects the coating adhesion to the steel in bent bars.

ASTM A775 and AASHTO M284 requires bend tests on production bars using a mandrel diameter 8 times the bar diameter. The exceptions are #14 and #18 bar where the mandrel diameters are 17 inches and 23 inches respectively. The bars are bent to 120 degrees, after rebound, at a constant rate.



Figure 2: ASTM A775 and AASHTO M284 coated bars. The coating is used for tension elements, but are more flexible than the "purple" ASTM A934 coating.

ASTM A934 specification uses the same mandrels for the bend test as ASTM A775 and AASHTO M284 for all bar diameters; however, the degree of bend is much less. The ASTM A934 specification requires #3 to #5 bar be bent at a constant rate to 9-degrees, after rebound. Bar diameters #6 and greater are bent at a constant rate to 6- degrees, after rebound. Additional adhesion testing is completed for the

ASTM A934 coating and evaluated by cathodic disbondment testing. Visual disbonding or cracking of the coating on the outside of the bend is cause for rejection of the coated bar.



Figure 3: ASTM A934 Coated Bars. The coating is preferred for tension elements in corrosive environments.

The ASTM A775 and AASHTO M284 specifications apply to a coating that is much more flexible than that of ASTM A934. The ASTM A934 coatings are typically applied to products that will be used in direct tension and will not be subjected to bending stresses. While, the ASTM A775 and AASHTO M284 are also used in tension members, it is more predominately used for reinforcing steel, which is manufactured in straight as well as bent shapes.

The ASTM A934 epoxy coating is much more brittle as well as more abrasion resistant than the ASTM A775. A bar coated to ASTM A775 standards may experience a tear in the epoxy coating when in contact with an abrasive surface. In comparison, a bar coated to ASTM A934 standards, under the same abrasive condition, may only experience a non-penetrating scratch in the coating, leaving the epoxy coating intact and the bar uncompromised.

All epoxy-coated bars should be packaged, handled and transported with extreme care. Bundles of coated steel bars should have padding between the steel bands and the coated bars or utilize banding material that will prevent damage to the coating. The material must be placed on dunnage, with padding between the dunnage and the coated bars for shipping.

Bundles of bars should be lifted with equipment utilizing spreader beams. The use of spreader beams will keep the material from sagging and the deformations of the steel bar from rubbing the epoxy coating off the bar.

The epoxy-coated bar should be stored on racks in the field to prevent the bar from contacting the ground. The final configuration of the epoxy-coated bar should also be assembled on racks to prevent scratching of the coating. The patch kit material can be used to patch any damaged areas on the bar that occur in the field. The area must be clean and the patching material applied to the affected area.

ASTM A934 and ASTM A775 specifies that the area of the bar needing repair should not exceed 1% of the total surface area in 1 foot of length of bar. AASHTO M284 specifies that the area of patch material not exceed 5% of the total bar surface. All bars should be examined prior to being incorporated into the permanent work for damaged coating needing repair. The patch material should be applied to the coated bar and allowed to cure prior to being installed.

The specifications for the powders used for the epoxy protective coating are outlined in Annex A1; requirements for organic coatings, in each of the Standard Specifications for Fusion Bonded Epoxy Coating (ASTM A775, ASTM A934 and AASHTO M284).

The epoxy coating applicator receives steel bar from the bar manufacturer with the bundles of steel bar tagged with the steel heat number and other information pertaining to the length and diameter of the steel bar. The epoxy coater applies the batch number of the epoxy powder to the appropriate heat numbers of the bar. A powder batch consists of 25,000 pounds of material. The steel heat numbers, as well as the powder batch number and the certification stating that the coating was in conformance to ASTM A775, ASTM A934 or AASHTO M284, are all tied together. This provides adequate traceability for all materials and workmanship that is involved with the final epoxy coated product.

The epoxy coating applicator certifications also included the powder batch numbers, the manufacturer of the powder, the average coating thickness along the length of the bar, how many thickness readings were taken along the length

of the bar, the bar preheat temperature, the surface profile and the average number of holidays per bar.

Epoxy coating as a corrosion protection system is fairly economical costing $0.30/ lb to $0.35/ lb (2007) depending on the bar diameter and weight. Epoxy coating has a very large cost savings advantage, however, epoxy coating does not have the self-healing properties that the galvanized bar offers, therefore, the cost benefit must be weighed with the cost of onsite inspection and material quality control. Compromised epoxy coating provides isolated areas along the bar that are going to be susceptible to corrosive attack. Since the areas are isolated, the corrosion process is accelerated, whereas an uncoated bar would have more surface area and the reduction of the cross-sectional area of the steel would actually take longer. The epoxy protective coating does take additional efforts in inspection and quality control to ensure that the material has not been compromised.

HOT DIP GALVANIZING

Hot-dip galvanizing has been used since the 1800s and is one of the oldest metallurgical coating processes there is in the world. (See Figure 4.)

To understand the process of galvanization, one must first be somewhat familiar with the element Zinc. This nonferrous metal is primarily used in the galvanizing process to protect iron and steel from corrosion. In addition to protecting steel from corrosion, zinc is essential for the development of almost all life. The World Health Organization has recommended a daily zinc intake for adults of 15 milligrams. Zinc is a silvery blue-gray substance and makes up an estimated 0.004 percent of the earth's crust.



Figure 4: Freshly galvanized components being pulled from the hot zinc bath.

The hot dip galvanizing process works by cleaning steel multiple times to remove any dirt, oil or rust. The cleaned steel is then lowered into an 850 degree F molten bath of zinc metal. When the steel reaches the temperature of the bath metal, the iron from the steel and zinc from the bath mix to form distinct inter-metallic layers. Once removed from the galvanizing bath, draining, vibrating or centrifuging for small items removes excess zinc. Coating thickness and surface condition inspections complete the process. The galvanized protective coating on a steel surface is usually 4 to 8 mils thick and uniform on all surfaces.

Infrequently, a reddish stain of newly galvanized steel will occur. This staining is not rusting; it is simply caused by the amount of iron in the zinc-iron alloy layers.

The dense, adherent zinc coating is effective for protecting steel in marine environments. The surface has a rate of corrosion some 10 to 100 times slower than that of the ferrous metal it's protecting. Even when the steel is embedded into grout or concrete, the zinc surface is more resistant to chloride ions than bare steel by a factor of five to ten. [A zinc coating will be self-sacrificing by *galvanic action* to protect the base material.] In general, a typical galvanized coating can now be expected to last 70 to 150 years without maintenance in most urban and rural atmospheres. The American Galvanizing Association estimates for marine environments containing more aggressive corrosive elements, such as chlorides and sulfides, galvanized steel may last for between 50-100 years as seen in Figure 5, showing the coating life of galvanization.

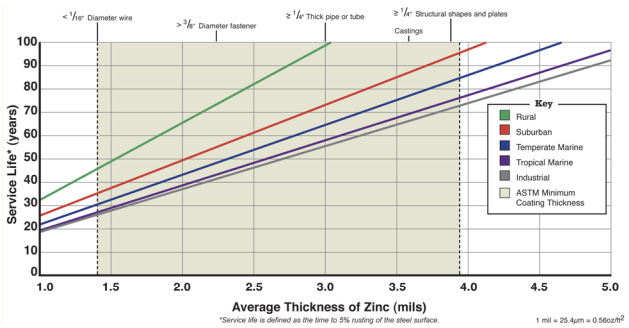


Figure 5: Above determinations of the coating life of galvanized steel are by means of collecting data and extrapolating corrosion rates via means of temperature, airborne salinity, sulfur dioxide concentration, relative humidity, rainfall, and sheltering condition.

Corrosion is an inherent tendency of metal, occurring when subjected to air or moisture and is caused by an electro-chemical process. More specifically, corrosion occurs when an electric current passes between the corroding metal and any other metal with which it has an electrical contact. The zinc (being anodic to iron) prevents this corrosive electrical current from generating by actually giving up its electrons or corroding first and protecting the steel. In this form of protection, known as cathodic protection, the base metal becomes the cathode in the corrosion cell, and the coating metal (zinc) becomes the anode. Even in areas where galvanized steel surfaces come into contact with adjacent surfaces resulting in wearing or exposed surfaces of unprotected steel, the surrounding zinc still protects these exposed areas without touch-up generally being necessary due to the zinc being anodic to iron. This particular effect is known as the self-healing property of galvanized coatings.

In today's construction practices, threaded bars, hex nuts and couplings are hot-dip galvanized to ASTM A-153 compliance and non-threaded accessories to ASTM A-123. Prior to galvanizing, high strength steel bars (150 KSI) are mechanically blasted clean rather than acid pickled to prevent hydrogen embrittlement from occurring.



Figure 6: Galvanized high strength steel bars (150 KSI)

Bars longer than 8 feet typically cannot be - centrifuged following galvanizing, so they are normally brushed clean to remove excess zinc and allow free rotation of fasteners. It is essential to remove the excess zinc prior to the galvanized item cooling. Fasteners are slightly oversized tapped to allow proper fit to a galvanized steel bar. ASTM A-153 allows for fasteners to be machined tapped following the galvanizing process. Oversized fasteners are designed to exceed the ultimate strength of the bar, even when oversized fasteners are used with an uncoated bar. Due to its very adherent coating and self-healing properties, galvanized steel components are less susceptible to corrosion resulting from handling or transporting abrasions versus epoxy or paint type coatings.

Galvanizing costs for high strength steel bars average around $1.00 per pound (2007) and fasteners/non-threaded components average around $0.60 per pound (2007).

One final point should be noted in this paper. It is often misunderstood the difference between hot-dip galvanizing and zinc plating. Hot-dip galvanized components generally contain about 10 times as much zinc on their surface than the same zinc-plated components. Only hot-dip galvanized components should be used in outdoor applications and especially in marine environments.

COAL TAR EPOXY COATING

Coal Tar Epoxy coating (CTE) is a protective coating applied to steel bars, sheet piles and concrete foundation elements for use in the construction industry, and is most prominent in marine construction. The Society for Protective Coatings (SSPC) Paint Specification No. 16 specifies the coating material and the material

application for coal tar epoxy coatings. Other specifications for the CTE material and application are the Corp of Engineers C-200 and C200a, the AWWA C-210 for exterior and Steel Tank Institute Corrosion Control System STI-P.

The steel bar surface preparation includes abrasive blast cleaning to near white metal with a combination of steel shot and grit per SSPC-SP 6. The surface may also be prepared by SSPC-PA 1, “pickling”. Pickling is a process in which the steel product is dipped in an acid bath to clean prior to coating.

The coating is applied per the CTE manufactures recommendations. The coating is self-priming and exhibits very good adhesion to clean concrete and structural steel surfaces. CTE coating is acceptable for use in environmental exposure zone 2A, which is frequently wet by fresh water; 2B, which is frequently wet by salt water; 2C, which is fresh water immersion; 2D, which is salt water immersion; 3A, which is chemical, acidic, 3B, which is chemical neutral and 3C, which is chemical alkaline.

The coating consists of two parts, Component A being a coal tar pitch, a liquid type polyamide resin, and a polyamine promoter. Component B is a liquid epoxy resin, which is added to Component A just prior to application. The mixture is four parts Component A, which is commonly referred to as paint; to one part Component B, which is referred to as the hardener. The color of the CTE is black or dark red.

The application should be accomplished using airless spraying equipment capable of developing 2000 psi of spray pressure. The coating thickness is normally specified as 16-mil dry film thickness, which is applied in two 8-mil coats. The wet application is more near 12-mil to achieve the 8-mil dry film thickness in a single coat. The second coat should be applied as soon as possible after the application of the first, so the inter-coat adhesion is not sacrificed. The maximum drying time between two coats should be no more than 72 hours, however, the quicker the second coat can be applied the better, especially in regions with high temperatures.

To ensure a quality adhesion to the steel, there should be a five-point spread between the steel temperature and the dew point. This will ensure that moisture does not form on the steel prior to the application of the coating. The coating should not be applied when the steel or ambient temperatures are at or below 50 degrees Fahrenheit. If ambient temperatures are between 50 and 60 degrees Fahrenheit, the mixed coal tar epoxy coating should be allowed to stand for 30 minutes prior to application.

The quality of the coating is closely monitored by the coating applicator. SSPC-PA 2 determines the thickness of the coating, which is the measurement of dry paint thickness with magnetic gauges.

The coating is also tested for sag, where a 14-mil minimum application of the coating is applied to a solvent clean 3”x6” cold-rolled steel panel. The cold rolled steel panel has a 1” strip of masking tape across the width of the panel and is parallel to and centered on the shorter axis of the panel. Immediately after the coating is applied to the steel panel, the masking tape should be removed and the panel should be stood in a vertical position. The temperature should be between 75 and 80 degrees Fahrenheit. The panel is observed for four hours and if sagging is observed to cross into the base area, it constitutes failure of the sag test. The balance of the mixed coating should be saved for the Penetration and Adhesion Tests.

The penetration test uses two 3”x6” samples of solvent cleaned steel panels. The coating mix that was used in the sag test is drawn down in accordance with FED-STD-141, method 2161 and is applied to the two 3”x6” panels. The film is allowed to dry 18 to 24 hours at a temperature between 75 and 80 degrees Fahrenheit and a relative humidity not over 60%. A second coat is applied to the panels at right angles to the first coat, this time using a freshly mixed sample. Both the drawn down sample and the freshly mixed sample are used in the adhesion test. After 120 hours of cure time the samples are clamped under a penetrometer so the needle is over an area of the prescribed thickness range. The penetration is determined by loading the penetrometer to 200 grams applied for five seconds at 77 degrees Fahrenheit. Five readings are taken within a 1 cm square, the average of the three lowest readings shall not exceed 0.03 cm after 120 hours of curing.

To test the adhesion of the coating a two- coat sample is applied to blast clean steel. The coats shall be applied at 10-14 mil. The first coat shall be allowed to cure 18 to 24 hours at 74 to 80 degrees Fahrenheit, before applying the second coat. The second coat should be allowed to cure 120 hours at 74 to 80 degrees Fahrenheit, before the adhesion is tested with a sharp knife. The coating shall strongly resist being removed from the steel. Using the knife to separate the two coats of epoxy should also test intercoat adhesion. If any delamination between layers occurs, it shall constitute intercoat adhesion failure.

The pot life of the CTE material is considered satisfactory when the mixed material remains in a fluid condition or when thinned with 100 ml of thinner remains lump free and brushable.

Each container of each component is marked with the product name, specification that the product is in accordance with (SSPC-Paint 16), component, color, lot number, stock number, date of manufacture, quantity of paint in each container, any information or warnings required by Federal Law and the name and address of the manufacturer. The lot numbers for the coal tar epoxy are attached to the heat numbers for the steel that has been coated to ensure there is traceability between the steel and the coating.

CTE coated material should be packaged handled and transported with extreme care. Bundles of coated steel members should have padding between the steel bands and the coated bars or utilize banding material that will prevent damage to the coating. The material must be placed on dunnage, with padding between the dunnage and the coated members for shipping.

Coated material should be lifted with equipment utilizing spreader beams. The use of spreader beams will keep the material from sagging that causes abrasion between the coated materials. Also, the coated material should be stored in the field on racks to prevent the coated members from contacting the ground. For any visual imperfections in the CTE coating, patch kits are available for field touch-up. Any damaged areas that are visible by the naked eye should be addressed prior to incorporating the coated member into the permanent work.

Threaded bars that are CTE coated with a thickness of 16 mil, have oversized hardware available to accommodate the thickness of the coating. The oversized hex nuts and couplings develop the full strength of the threaded bars. Even the oversized hardware exceeds the strength of the bar and is capable of breaking bare threaded bar.

Although CTE coating is more durable than fusion bonded epoxy coating, it is commonly used in conjunction with other corrosion protection systems. It is common to have a CTE coated bar wrapped with tapecoat with a PVC pipe placed over the tapecoat to provide several levels of corrosion protection prior to being incorporated into the permanent work.

CTE coating as a corrosion protection system is a fairly economical system. Pricing varies depending on the steel section that the coating is being applied to. Typically, deformed steel bars and other structural steel sections will cost between $2.05 and $2.35 per foot (2007) for 16-mil dry film thickness coating. Hardware for threaded bars tends to cost more.

GROUT ENCAPSULATION OF TIE-RODS AND TIEBACKS USED IN MARINE APPLICATIONS

Corrosion protection of steel tendons that are used to provide support for sheet pile retaining walls is a very important element of the design. Bare tendon steel in contact with other steel and/or the ground can accelerate the corrosion process and cause premature rupture of the tendon under load. Protecting the tendon against corrosion by encapsulating the steel with cement grout and a plastic containment sheath is one method to prohibit the forces of corrosion acting on the steel. (See Figure 7.)

Grout protected steel has (2) main protection mechanisms. One is to prohibit contact of the tendon with water and air and the other is a passive chemical resistance inherent with cement grout.

The first mechanism is that the plastic sheath that surrounds the steel is watertight to prohibit intrusion of the elements to get to the steel. The annular space between plastic sheath and the tie-rod tendon is then filled with neat cement (no aggregates or sand used) further providing a barrier from moisture to attack the steel.



Figure 7: The plastic sheath can be made from polyvinyl chloride, polypropylene or polyethylene and have a wall thickness not less than .040". The sheath can be either smooth or deformed (corrugated) depending on the application and preference of the designer.

Metal sheathing is discouraged since galvanic cells are created when dissimilar metals are in contact with one another and although the tierod tendon may not be in contact with the sheath, the sheath may contact other features of the sheet pile retaining wall.

The second mechanism that protects the steel is the inherently high PH of the surrounding cement. Cement grout is strong alkalinity by nature and therefore the steel it's protecting is rendered passive and not subject to corrosion. This protection occurs after the concrete has hydrated and the molecular water particles are not prevalent in the concrete matrix. Therefore, proper water to cement ratios must be used for the encapsulation grout. An encapsulation to protect any steel tendon shall be from a shrinkage compensated or expansive Portland cement grout.

Tie-rod manufacturers most often construct the encapsulation under factory-controlled conditions. Control over grouting equipment, potable water sources, tendon inclination to insure complete encapsulation, and cost inefficiency usually makes field encapsulation prohibitive.

Encapsulated tie-rods are constructed by placing the steel bars in the sheath. The bars are centered in the sheath using non-corrosive plastic centering devices (Centralizers). Different approaches to centralizing the bar exist but the main objective is to use a non-corrosive device that centers the bar and will not prohibit grout flow around the steel during the grouting operation. The size of the sheath and the selection of the centralizers should be such that it leaves a minimum of 0.5" of grout cover in all tendon locations, including any coupled splices. The assembled bars are then placed side by side to facilitate grouting of several tendons concurrently. The assemblies should be placed on an inclined bed or have some means to insure that all air is removed and displaced by the inner grout. It is common to have holes drilled at each end of the assembly to provide for grout entrance at one end, allow air to escape at the other end and to provide a visual indication that grout has completely filled the sheath. These holes then must be subsequently filled with silicon sealant or covered with heat shrink sleeving to regain its watertight construction.

Grouting occurs using proper mixing and pumping equipment. It is recommended that a high shear mixer, often referred to as colloidal mixer, be used to ensure proper cement particle wetting under low W/C ratio formulations. An example of a high shear mixing field grout plant (self contained power pack) is below: (See Figure 8.)



Figure 8: Typical High Shear Mixer

Proper handling of the grouted tendons is required to make sure the corrosion protection system remains functional. Metal banding of pre-grouted tie-rod bundles is discouraged unless a layer of cardboard or other barrier exists between the band and the plastic corrugation. Any tears or visible cracks in the

plastic sheathing should be repaired using heat shrink tubing or other means that keeps the sheath watertight.

Bundles of pre-grouted tie-rods should be kept to a size that is easily handled by both plant and field personnel. Long tie-rods (over 20') should be supported in multiple spots along the bundle length to make sure no more than 20' of unsupported length exists between supports. Spreader beams or other metal support devices may be used to facilitate this.

Tie-rods longer than 50' or placed in an area with excess constraint issues may require field splices to couple two or more grout protected tie-rods together. This requires additional field procedures to insure that the field splice has the same level of corrosion protection as the rest of the tie-rod.

The typical connection detail of a grout-protected tie-rod includes a full strength mechanical coupling of the same thread type as the connecting tie-rods. These couplings must be assembled with care to ensure that the mating bars are equally engaged within the coupling. Couplings without a positive stop in the coupling center should use jam nuts or a visible marking on the mating bars to insure positive engagement. (See Figure 9.)

If the tie-rod bars have a coating in addition to the layer of pre-grout, such as galvanizing, coal tar epoxy or epoxy coating according to ASTM A775, then the coupling should have the same coating applied to its exterior.

To equal the two layers of corrosion protection barriers that the rest of the tie-rod possesses, the splice must also have two layers of barrier protection to include the passive protection of the grout formulation as well as the watertight protection offered by the plastic sheath.

Field grouting operations can accomplish the passive protection as well. This may be difficult to accomplish since high shear mixing equipment and properly trained field personnel are not always available. If field grouting the splice is chosen, then the assembled splice must have a sheathing placed over it that is compatible to the sheathing over the tie-rod. Optimally they should screw together or use a coupling specially designed for use with that sheath. If the diameter of the coupling is too large to fit inside the same diameter sheath as used on the tie-rod, then a transition coupling should be threaded onto the tie-rod sheath. The transition coupler steps up to a minimum 0.5" grout cover over the coupling. Both connected end of this sheathing should have an additional layer of heat shrink tubing properly installed to water tighten the interface. See illustration below:

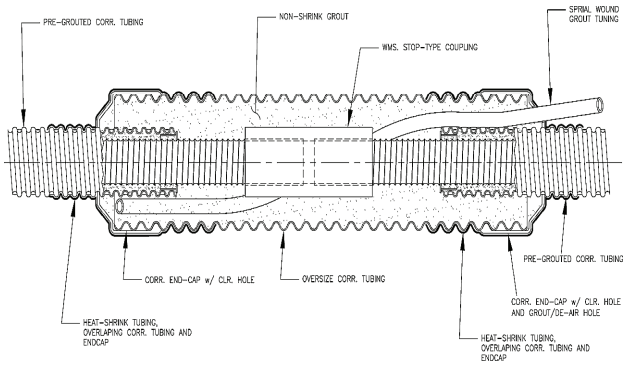
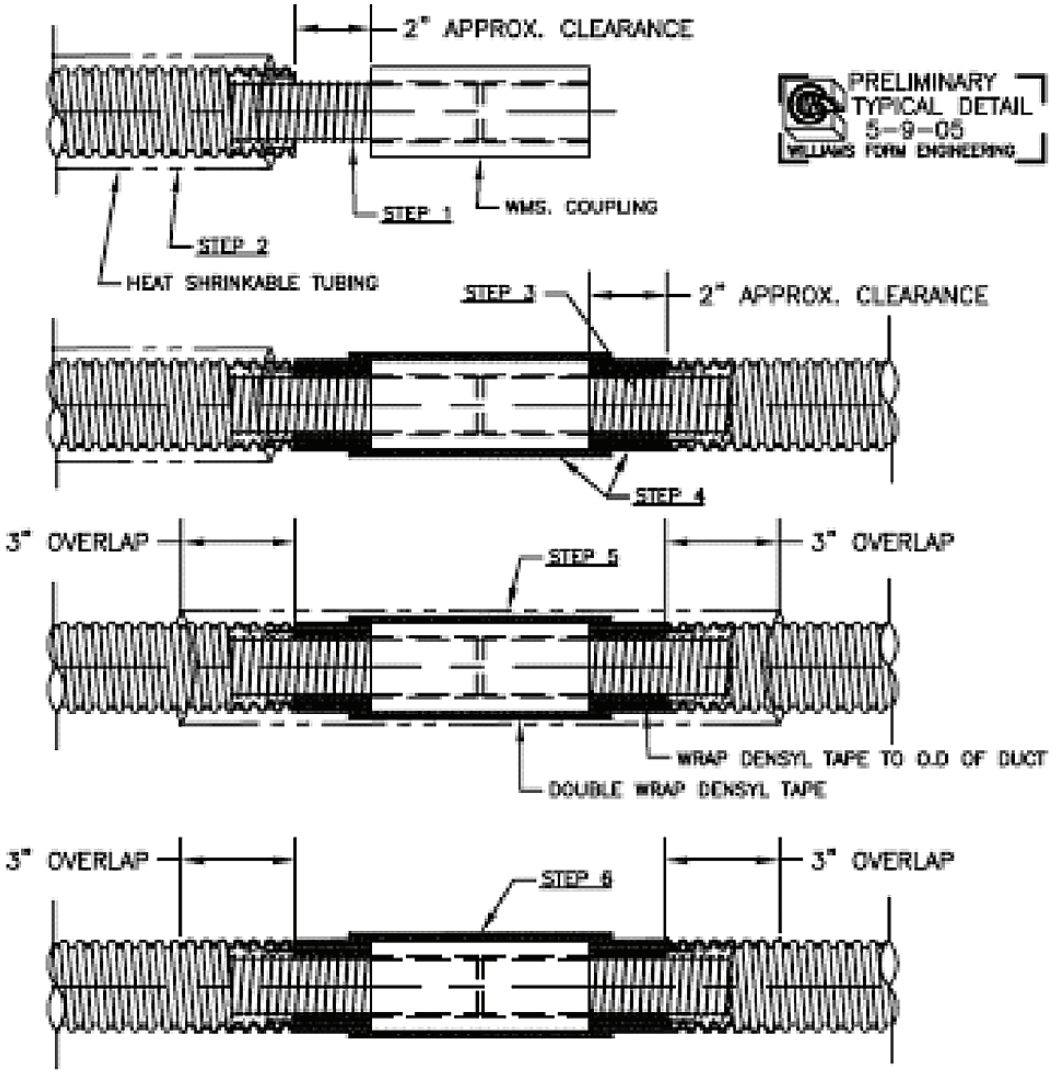


Figure 9: Typical Connection Detail

In the majority of instances, it is not practical to sheath and grout in spliced locations, so a special corrosion inhibiting grease or a grease-impregnated tape may be used as an accepted alternative to grout encapsulation. An example of this is the Denso Primer & impregnated Densyl Tape, which should be applied with a 50% overlap. The primer and the tape must cover all exposed metal surfaces including the protruding ends of the pre-grouted tie-rod and the coupling. Once the tape is fully applied, a layer of heat shrink sleeve is applied to overlap the greased-impregnated tape. The heat shrink sleeve then effectively serves as an impervious barrier, much the same as the plastic sheathing for the cement grout. See illustration in Figure 10.



STEP: 1.) FULLY ENGAGE THREADS AND TIGHTEN COUPLING ON ONE BAR. ASSURE APPROXIMATELY 2" CLEARANCE BETWEEN ENDS OF COUPLING AND (PREGROUTED) CORRUGATED DUCT.

STEP: 2.) PRECUT A MINIMUM LENGTH OF HEAT SHRINKABLE TUBING EQUAL TO THE COUPLING, CLEARANCES, AND A 3" OVERLAP OF EACH CORRUGATED DUCT. PLACE THE HEAT SHRINKABLE TUBING OVER THE CORRUGATED DUCT ON ONE OF THE BARS.

STEP: 3.) FULLY ENGAGE THREADS OF THE OTHER BAR AND TIGHTEN. AGAIN ASSURE APPROXIMATE 2" CLEARANCE BETWEEN THE COUPLING AND CORRUGATED DUCT.

STEP: 4.) FILL THE 2" CLEARANCE AREAS WITH DENSYL TAPE TO THE DIAMETER OF CORRUGATED DUCT AND DOUBLE (TWO) WRAP THE OUTER SURFACE OF THE COUPLING.

STEP: 5.) POSITION AND CENTER THE PRECUT HEAT SHRINKABLE TUBING OVER THE COUPLING TO ASSURE THE 3" OVERLAP ON BOTH CORRUGATED DUCTS.

STEP: 6.) SHRINK THE HEAT SHRINKABLE TUBING EVENLY OVER COUPLED JOINT STARTING FROM ONE END AND PROGRESSING TO THE OUTER END. TUBING MAY REQUIRE A SECOND HEATING TO ASSURE THAT IT HAS FULLY SHRUNK.

Figure 10: Coupler with Shrink Sleeve

It cannot be stressed enough how important the design and construction details are for the end attachment (or “end anchorage”) is. This is the portion of the tie-rod most susceptible to corrosion for a number of reasons:

1) There has to be threaded tie-rod bar (i.e. no grout or sheathing) to allow for load transfer to the structure.
2) It is most likely that this area will have the presence of water or saltwater.
3) Unless specific details prohibit it, the metal connection will be in contact with the air around it.
4) Various metals are in direct contact with each other.

As the bar transitions from its grout-encapsulated sheath, the tie-rod typically goes through a whaler design to transfer the tie-rod load to the retaining structure. The bar normally goes through a carbon steel plate and terminates with a hardened washer, beveled washer if necessary, and hex nut to properly transfer the load. All of these components and the conduit that the tie-rod goes through should be examined. (See Figure 11.)

It is common to galvanize or coal tar epoxy coat the hex nut, plate and washers to enhance their protection against corrosion.

Caps are often used to further protect the exposed tie-rod bar, nut washers and sometimes the entire bearing plate surface. Caps can be made from plastic or from steel. Plastic should be specified with care to ensure UV compatibility and also to make sure that no impact loads during normal wall use will damage the protective covers.

Steel caps are more durable during construction and therefore can withstand impact loads better than plastic. Steel caps should be secured to the bearing plate with fasteners to insure the cap remains on the plate.

Both steel and plastic caps should be either corrosion inhibiting grease or grout filled. Some caps have zerk fittings or other porting, which allows the cap to be filled. In all cases a rubber type gasket seal should be used between the tendon bearing plate and the protective end cap.

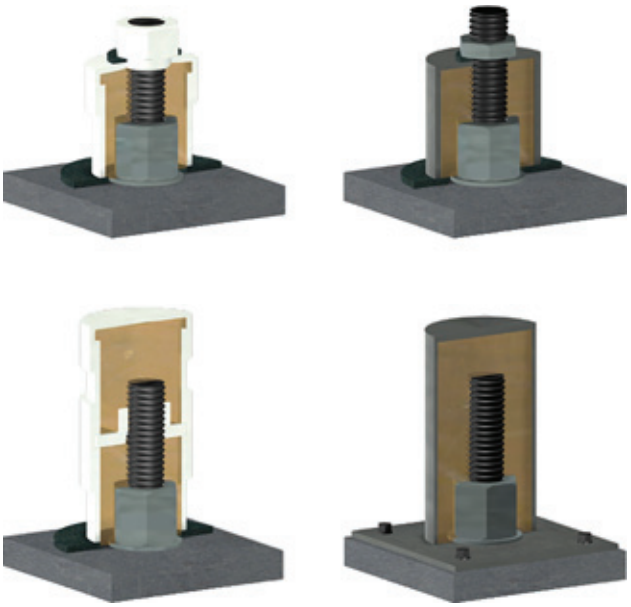


Figure 11: Typical Bar Terminations

HYBRID MULTIPLE CORROSION SYSTEMS

Many of the corrosion protection systems available to the engineering and construction community are also being used with additional materials to form several levels of protection as listed**:**

***** Tapecoat is commonly used in conjunction with coal tar epoxy (CTE) coated tie-rods, with a PVC pipe over both the CTE bar with the tapecoat being applied to the bar, overlapping half the width of the tape.

* Fusion Bonded Epoxy Coated and Galvanized Bars are being encapsulated in a grouted HDPE Corrugated tubing.

* Plain threaded bars are being wrapped with grease-impregnated tape, with densyl tape over the top of it as a form of multiple corrosion protection. Each layer of grease-impregnated tape and densyl tape are overlapped by half the width of the tape on each wrap.

* Encoat product, which is a 25 mil thick extruded HDPE over a bitumastic material is being applied over smooth galvanized bars.

* Epoxy, galvanized and CTE coated bars are used inside a PVC sleeve with corrosion inhibiting grease.

CONCLUSION

Fusion Bonded Epoxy Coating, Coal Tar Epoxy Coating, Hot Dip Galvanizing and Pre-Grouted Encapsulations are the most common base protections for the majority of engineered construction applications.

Fusion bonded epoxy coating is a very economical protective coating, however, it does require very good quality control and inspection to ensure that the coating is not compromised. Patching may be necessary in the field prior to incorporating the element into the permanent work.

Coal tar epoxy coating is another economical coating that tends to be more abrasion resistant than fusion bonded epoxy coatings. Coal tar epoxy can also be applied to several structural sections that are utilized in engineering projects, unlike the fusion bonded epoxy coatings. Coal tar epoxy coating is also a very economical coating, but also has to be inspected very well to address any damage that may have occurred during transportation and handling.

Hot dip galvanizing is a sacrificial zinc anode that corrodes prior to the carbon steel member that it is protecting. The zinc has very good self-healing properties and visual inspection or patching is not required with hot dipped galvanized products. The material handling of the hot dipped galvanized product becomes less of an issue than it is with the applied protective coatings of fusion bonded and coal tar epoxy coatings. Zinc has been escalating over the past several years and has increased the price of hot dip galvanizing to double the cost of fusion bonded and coal tar epoxy coatings.

Encapsulated tie-rods, tiebacks, soil nails and micropiles have gained much popularity in recent years in very aggressive environments. The protection offers a watertight plastic sheath and 0.2” of grout cover around the steel element inside the corrugated. Inspection of the pre-grouted elements is very simple. Damage to the corrugated tubing is patched with heat-shrink to maintain a water-tight corrosion protection system. There is additional material and labor involved with producing an encapsulated tendon, therefore, the cost of the product is greater.

There are several options to accomplish multiple corrosion protection to the most common protection systems of fusion bonded or coal tar epoxy coating, hot dip galvanizing and grout encapsulation. The project site, site conditions, aggressiveness of the soils, construction time and design life of the project should be considered prior to deciding which corrosion protection system will be used on the project. All of these factors determine how durable the coating needs to be, how the material will be handled and how the material will be installed. The decision should be made to choose a system that will protect the steel elements to provide the expected service life of the structure as well as keep the project economical.

REFERENCES

Personal conversation with Mr. Martin Gandarilla, quality control and quality assurance documents, Commercial Resins, Epoxy Coating applicator, Henderson, Colorado.

ASTM A934/A 934M-01, Standard Specification for Epoxy-Coated Prefabricated Steel Reinforcing Bars.

ASTM A775/ A775M-93a, Standard Specification for Epoxy-Coated Reinforcing Steel Bars.

AASHTO M284/M284M-87, Standard Specification for Epoxy Coated Reinforcing Bars.

ASTM D3963/ D3963M-87, Standard Specification for Epoxy Coated Reinforcing Bars.

American Galvanizers Association, n.d. 23 Feb. 2007 <www.galvanizeit.org>.

ASTM A-123, Standard Specification for Zinc (Hot-Dip Galvanized) Coatings on Iron and Steel Products

ASTM A-153, Standard Specification for Zinc Coating (Hot-Dip) on Iron and Steel Hardware

"Stacking the Decks." Bridge Builder Magazine January 2005

Personal conversation with Mr. George Foster, Womble Company, Coal Tar Epoxy Coating Applicator, Houston, Texas.

The Society for Protective Coating, SSPC Paint Specification No. 16

Carboline Bitumastic 300M, product data sheet.

Amercoat 78HB, product data sheet.

Army Corp of Engineers, C-200, C200a

National Resources Conservation Service, Material Specification 583 Coal Tar Epoxy Coated Paint, 10/1998.

PTI, Recommendations for Prestressed Rock and Soil Anchors.

DEEP COMPACTION USING VIBRATORY PILE HAMMERS

Dennis Nottingham, P.E., President, PND Incorporated, Anchorage, AK, USA

The need for deep compaction of submerged granular soils has led to improvements in this area. In 1971, L.B. Foster Company personnel patented a method of deep compaction using a vibratory pile hammer and pile probe. The technique had some success, but did not produce consistent results and thus found its way to obscurity. Other patents attempted to modify the technique by various probe modifications, but again without measurable improvement from a practical point of view. Solutions to economical deep compaction up to 100 foot depths particularly in saturated granular soils would have a great impact on the construction industry and new bulkhead structures being developed, thus PND was prompted into related research and development. The advent of higher horsepower vibratory hammers, coupled with PND engineers' experiments, observations and measurements, led to an "H" pile probe design which has produced measured soil density improvements up to 250% using SPT "N_{60}" values as a measure.

INTRODUCTION

The condition requiring deep compaction in fill placed below water level is a problem particularly for various bulkheads. During construction, sheet piles are placed before final filling operations, thus fill below water table will either be uncompacted or must be compacted after the structure is in place. Compaction causes fill settlement which can load tiebacks and cause distress in some cases.

The open cell type bulkhead was developed to avoid this problem, but nevertheless still needs compaction to ensure strength and help prevent long-term settlement. This is particularly true in high seismic areas where loose granular soils (i.e., less than "N_{60}" of 25 or so) might liquify and cause temporary loss of strength.

Other construction such as tubular tunnel backfill or large marine filled areas could also benefit from improved compaction techniques. Since vibratory type compaction effectively locally "liquifies" soil temporarily, affected soil must be of a granular nature with probably less than 15% by weight passing the No. 200 sieve.

Compaction of fine granular soils can be also use a variation of this method, but soils will not immediately densify. Instead, granular filled columns can be created for longer term stabilization.

VIBRACOMPACTION DEVELOPMENT

PND has researched deep compaction for several years, trying various methods including large surface vibratory compactors and various probes using vibratory pile hammers common to Alaskan marine construction. None of these methods were entirely successful until a new type probe surfaced through PND research and development.

It soon became apparent that previous deep compaction procedures using vibratory hammers and probes were simply not transmitting hammer energy into the surrounding soil. New probe designs began to evolve in concert with larger horsepower vibratory hammers with obvious increased ability to densify soil.

One project on the Mississippi River with fine uniform sand backfill produced average SPT N_{60} increases of over 250%. This was based on a limited number of pre- and post-compaction comparative soil tests.

Further probe improvements were finally tested on a large scale project in the summer of 2003 at the Alaska Port MacKenzie project involving stabilization of a large fill extending 800 feet seaward fronted by a 500 foot Open Cell bulkhead used as a barge dock.

COMPACTION EQUIPMENT

Equipment specified for vibracompaction was a minimum 500 hp vibratory pile hammer with a HP14 probe. The probe was specified to include a series of angles welded to the web (see Figure 2). Previous PND experience had shown that the angles help to increase densification. This is accomplished as angles help push material laterally as the probe is raised and lowered.



Figure 1: Port MacKenzie



Figure 2: Vibracompaction probe

For this project, the contractor provided an APE model 300 vibratory hammer. The contractor removed the counterweight from their crane and welded a framework to support the power pack of the hammer, while the probe and hammer were hung from a set of leads (Figure 3). This setup allowed the crane and compaction equipment to be portable and only required the contractor to have two workers on-site throughout the vibracompaction effort.



Figure 3: Vibracompaction equipment



Figure 4: Fill added to vibracompaction probe depression

PROCEDURE

The two types of fill materials present on-site were gravelly sands and fine-grained soils overlying hard silty clays. The properties for each soil type required different probing requirements. Loose, gravelly sand is more permeable and susceptible to consolidation under vibratory loads when saturated. Because of these material properties, most of the compaction of this type of material takes place during and shortly after the probing process is completed. Essentially, the probe vibrates the soil particles vertically and laterally as the probe is lowered and raised. The soil particles achieve a state of localized instability and the soil particles densify as the soils settle as the excess pore water pressure is relieved. Raising and lowering the probe in a series of cycles allows for additional material to enter the hole and fill the voids created.

Consolidation of fine-grained soils requires substantially more time than the gravelly sand material and can take years depending upon the length of the drainage path, permeability, gradation, and cohesive qualities of the material. Because of these factors, consolidation of the soil matrix is usually very slow. The probing procedure used for the sandy soils was also used for the fine-grained soils, except that a coarser fill material was used (Figure 4). This procedure creates a series of granular fill columns within the fine-grained soil matrix which increases the overall bearing capacity. The granular fill columns will also function as vertical drains. In general, water will be able to dissipate laterally towards the drains at an increased rate. Therefore, the bearing capacity of the fill material will continue to increase with time.

PRODUCTION PROGRAM

Pattern and Procedure

After SPT calibration and probe spacing testing programs were completed, the contractor continued probing holes and placed fill material at each probe location.

Production Rate

The vibracompaction effort consisted of 1792 probe locations which consisted of:

- 1043 probes in the gravelly sand area requiring 7,020 cy of gravelly sand fill material.
- 749 probes in the fine-grained soils requiring 5,022 cy of three inch minus granular fill material

On average, the vibracompaction required 6.7 cy of fill per probe location at an average depth of over 40 feet. Some probe locations were reported to take up to 12 cy of fill material. Overall volumes were computed by truck load count.

The contractor averaged 27 probes per day (typical range between 22 to 35 probes per day). During one ten hour shift, 41 probes were completed.

Post Trip Hammer "N"

Analysis of the Post SPT data shows the average N_{60} of the perimeter gravelly sand fill material within the Below Water Table (GWT) increased significantly. There was no significant change in strength of the hard fine-grained seabed soil. The auto trip hammer results were corrected to N_{60} and are shown following.

Perimeter Fill Area
Gravelly Sand underlain by the seabed
Gravelly Sand (above water table) $N_{60} = 36$
Gravelly Sand (below water table) $N_{60} = 66$

Interior fill
Fine-grained soil underlain by the seabed
Fine-Grained Soils (above water table) $N_{60} = 2$
Fine-Grained Soils (below water table) $N_{60} = 12$

SUMMARY

The vibracompaction program has shown immediate improvements in the density of the perimeter gravelly sand fill material. Additionally, the post vibracompaction average blow count, (N_{60} = 66), of the soil below the GWT is clearly higher than required for liquefaction stability.

Gravelly Sand Fill
Blow Count Summary

Location	Pre N_{60}	Post N_{60}	Ratio (Post/Pre)
Above GWT	14	36	2.5+
Below GWT	26	66	2.5+

OTHER PROJECTS

Many other projects have had vibracompaction activity during research and development and with the final production system. Granular soils of many types have been compacted including soils ranging from fine sands to shot rock fill.

Open Cell bridge abutments founded on loose granular soils can readily be area stabilized using the vibracompaction process. An example is the Alaska Iliamna River Bridge. This was permitted, designed and constructed in 14 weeks in late 2003, complete with vibracompacted stabilized Open Cell abutment.

A dock at King Cove, Alaska, is typical of many docks built on loose, but stabilized granular soils.

Figure 8 shows a typical situation requiring deep compaction for a bulkhead. Figure 9 shows another potential use involving backfill compaction of a buried subsea tunnel or conduit.



Figure 5: Vibracompaction of shot rock fill at Dutch Harbor, Alaska

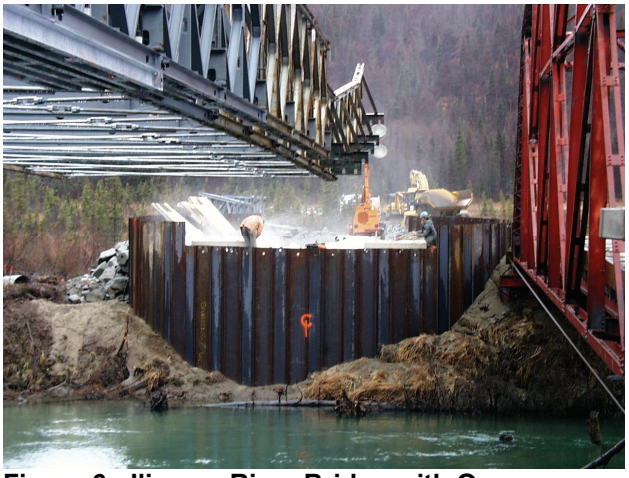


Figure 6: Iliamna River Bridge with Open Cell abutment and Bailey Bridge launch in progress



Figure 7: King Cove Dock

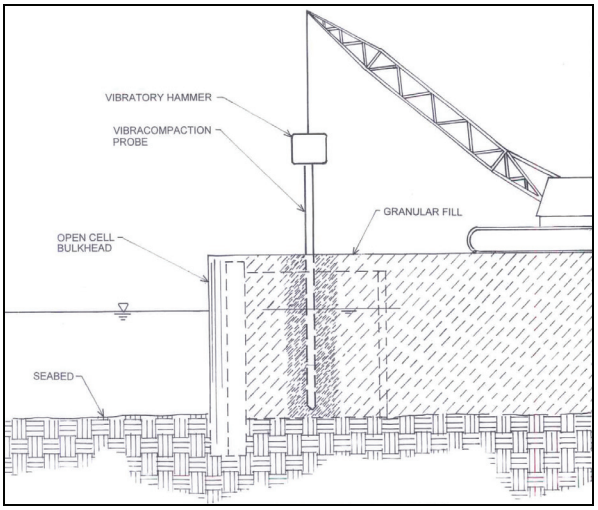


Figure 8: Compaction below water table in fill

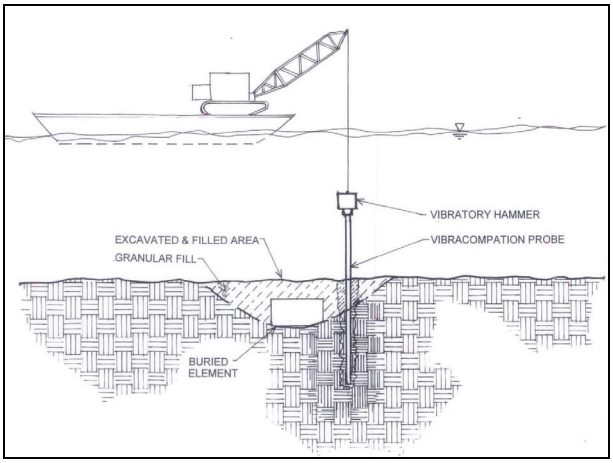


Figure 9: Use of vibracompaction for deep water compaction

CONCLUSION

Deep vibracompaction such as described in the preceding has important application in high seismic areas with loose soils. The ability to compact to great depths now gives the engineer more tools with which to provide greater safety with lower cost to the public.

Other deep compaction methods are really not comparable to this method, which uses large-horsepower vibratory hammers coupled with the new probes capable of reaching far below groundline.

REFERENCES

Anderson, Robert D., Alvin E. Herz, Clabeorn Jones, Harold Strickland and William K. Wilson, Nov. 23, 1971, U.S. Patent No. 3,621,659, Methods of Soil Compaction.

ASTM D-1586, 1999, Standard Test Method for Penetration Test and Split-Barrel Sampling of Soils, pg 145.

Laidlaw, Amy, Executive Director, Construction Innovation Forum, March 12, 1998, “Open-Cell Bulkheads Wins Prestigious NOVA Award” (press release).

STATNAMIC LOAD TESTING OF HIGH CAPACITY MARINE FOUNDATIONS

Mike Muchard, P.E., Applied Foundation Testing, Inc., Tampa, FL, USA

STATNAMIC load testing augmented with embedded instrumentation has been successfully used to obtain structural and geotechnical design information on large diameter spun cast concrete cylinder piles on many large marine construction projects. The paper focuses on one particularly interesting large marine project involving a new bridge to St. George Island, Florida where instrumentation and STATNAMIC load testing was used in conjunction with static load testing on high capacity piles. The information presented includes embedded instrumentation measurements taken during pile fabrication (post-tensioning), during pile driving, during static load testing, and STATNAMIC load testing. As much of this data is the first of its kind on concrete cylinder piles, it is exciting to present the foundation industry with this additional insight as to the behavior of this pile type and the accuracy of the methods used to test them.

INTRODUCTION

Construction projects in marine applications require demanding foundation designs. Large diameter spun cast concrete cylinder piles have many advantages in this application, most notable is their ability to resist large axial and lateral loads. As designers continue to push the capacity envelope, STATNAMIC load testing augmented with embedded instrumentation has become the preferred method of testing these “high capacity” foundations. Mainly because STATNAMIC load testing is a very efficient, cost effective, and reliable means of applying the large test loads needed to verify these demanding designs. Test loads up to 4,500 tons are available with current STATNAMIC equipment. The largest STATNAMIC load test to date on a concrete cylinder pile was 2,500 tons. The St. George Island Bridge project was the first in a long line of high capacity cylinder pile projects where STATNAMIC load testing was successfully used.

The St. George Island Bridge project included a pile load test program consisting of 4-static load tests and 6-STATNAMIC load tests, all of which included multiple levels of embedded strain gages. Dynamic pile testing was also performed on the test piles and upwards of 50 production piles. All dynamic pile testing and static load testing was performed independently by the project geotechnical consultant. The data obtained from embedded instrumentation, dynamic, STATNAMIC and static load testing provided engineers a better understanding of cylinder pile structural and geotechnical performance as well as a perspective on the methods used to test them.

Monitoring the embedded strain gages during post tensioning showed pre-stress magnitudes ranging from 760 psi to 1,010 psi and that some eccentricity was locked-in the pile during the process. Using these measurements, a composite modulus of elasticity of 5,725 ksi was calculated. The eccentricity is believed to be partly from non-uniform contact points between the segments and arching of the pile during tensioning.

Strain measurements made during the pile driving show the propagation of the stress wave and actual driving stresses within the pile. This information was useful in demonstrating the differences between dynamic testing and STATNAMIC testing.

Capacity predictions from dynamic testing showed as much as 41-percent under-prediction between the CAPWAP restrike and the static load tests. The CAPWAP derived skin friction and end bearing compared to the measured load distribution during the static tests showed a much greater disparity to the point of being totally unreliable.

During subsequent STATNAMIC and static load testing, the instrumentation was used to determine load distribution e.g. side shear and end bearing resistance. The data also shows the high reliability of STATNAMIC load testing of cylinder piles when compared to static testing. In three of four piles tested, the STATNAMIC

method was within 2-percent of the maximum static capacity. In the fourth case, STATNAMIC was 9-percent below the maximum static capacity because with only 2-days between tests the pile did not re-gain its full side shear capacity.

CYLINDER PILE DESCRIPTION

Cylinder piles are constructed by spin casting multiple cylindrical segments and post-tensioning them together to make up the desired length. The most popular pile diameters vary from 36 inches to 66 inches with wall thicknesses of 5 to 8 inches. Individual segment lengths which make up a pile typically range from 4 feet to 16 feet. The piles discussed in this paper were all 54 inches O.D. by 8 inch wall thickness and comprised of five 16-foot sections for a total length of 80 feet. The pile segments were constructed with longitudinal ducts in which post-tensioning strands were threaded after castings. High strength, low slump concrete was placed in the rotating forms. The centrifugal forces impel the concrete to the walls of the forms which results in a very strong and dense structural element.

The 54 inch piles on this project had ultimate capacities ranging from 750 tons to 900 tons. But ultimate capacities as much as 1,630 tons have been used on 54 inch cylinder piles in the Chesapeake Bay Area.

INSTRUMENTATION

Due to the manufacturing process of cylinder piles, successful instrumentation presents many challenges. Figures 1 and 2 show some of the instrumentation processes. To the author's knowledge, this was the first time cylinder piles were successfully instrumented with embedded strain gages. Embedded strain gages were installed in the test piles for the purpose of measuring load distribution during STATNAMIC and static load testing. However, to gain additional knowledge of this pile type, the gages were monitored during the post tensioning process and during pile driving as well. As shown in Figure 6 following the Reference section. The bottom 4-sections of the piles were instrumented with 3 gages on a plane for a total of 12 gages per pile.





Figures 1 and 2: Instrumentation of cylinder piles.
Courtesy of Applied Foundation Testing, Inc.

PILE INSTALLATION

Installation of cylinder piles are most commonly done by means of large air, steam or hydraulic powered hammers. Heavy ram - short stroke hammers seem to be the preferred combination in the industry. Typical air and steam hammers driving cylinder piles are shown in Figures 3, 4 and 5. The 54 inch diameter piles presented in this paper were driven with a 40,000 lb ram air-hammer capable of a maximum stroke of 3-feet. Therefore providing a maximum rated energy of 120,000 ft-lbs. As is typical of air-steam hammers, this hammer was equipped with half-stroke capabilities. Three of the test piles (LT-1, LT-2 and LT-3) were driven to practical refusal of 20 blows per inch. Test Pile LT-5 was driven to a final blow count of 10 blows per inch. This was the only pile of the four stopped prior to practical refusal.



Figures 3, 4 and 5: Driving of cylinder piles with 40,000 lb air hammer (left) and 60,000 lb ram steam hammer (center and right). ***Courtesy of Boh Brothers and Weeks Marine Construction, Inc.***

SOIL CONDITIONS

The subsurface conditions at the project generally consisted of four major strata. Water depths ranged from 10 to 20 feet. The upper layer was soft or loose silty bay bottom soils with N-values from 0 to 2. Underlying this was a more dense silty fine sand layer with N-values from 20 to 50. This strata was underlain by a weathered limestone formation ranging in thickness from 7 to over 15 feet. Below the limestone, dense silty fine sands and stiff sandy silts were present with N-values of 70 decreasing to 30 with depth. Soil conditions at each test pile location are shown in Figure 6 attached following the References.

DYNAMIC TESTING METHOD

Dynamic pile testing was performed on all of the test piles at the St. George Island Bridge project using a Pile Driving Analyzer® (PDA). Dynamic testing techniques are well documented in many references. It was accomplished by externally attaching accelerometers and strain transducers near the pile top and taking measurements during driving. Pile capacity during driving was estimated by the Maximum CASE Method. Other data obtained include maximum compression stress, maximum tension stress and hammer energy transferred to the pile at the gage locations. It should be common practice to use 4-sets of external gages due to the large diameter of typical cylinder piles.

A signal matching approach was used to back calculate various dynamic soil parameters and estimate pile load distribution. The computer program CAPWAP® uses the data measured during a single blow as a boundary condition and the user performs many iterations on soil parameters to make a calculated force wave match the measured one. This approach is highly user dependent and does not provide a unique answer.

STATNAMIC LOAD TEST METHOD

The STATNAMIC load test is based on Newton's second and third laws which state that force is equal to mass times acceleration and that for every action there is an equal and opposite reaction. Loads up to 4,500 tons can be generated (axially or laterally) by propelling a reaction mass off the foundation. Since the mass is in contact with the foundation prior to the test, the force associated with propelling of this mass acts equally and oppositely onto the foundation. STATNAMIC load testing requires no reaction piles, no reaction beam, and no

hydraulic jack. The STATNAMIC device (Figure 7) mounts on the pile top and includes a load cell and displacement measuring system. Although not necessary, embedded strain instrumentation is always recommended in the foundation.

A special solid fuel is burned to generate gas pressure inside a cylinder and ram (analogous to a gas actuated jack). As the pressure builds, it reacts against a heavy mass above the pile. The pressure eventually builds high enough to propel the reaction mass upward; in turn a downward load is simultaneously applied to the pile top which is many times greater than the weight of the reaction mass. The stages of a STATNAMIC test are shown in Figure 8. The STATNAMIC device typically produces a time dependent load on the order of 1/2 second or less. The fuel burn rate produces a smooth increasing force and controlled venting of the pressure produces a soft unloading. The load produced is not an impact which makes the analysis more simplified and reliable than dynamic testing. Load is measured with a calibrated load cell and displacement is measured with a photo-voltaic sensor triggered by a stationary laser reference. Three to four additional motion sensors also provide measurement of displacement at the pile top.

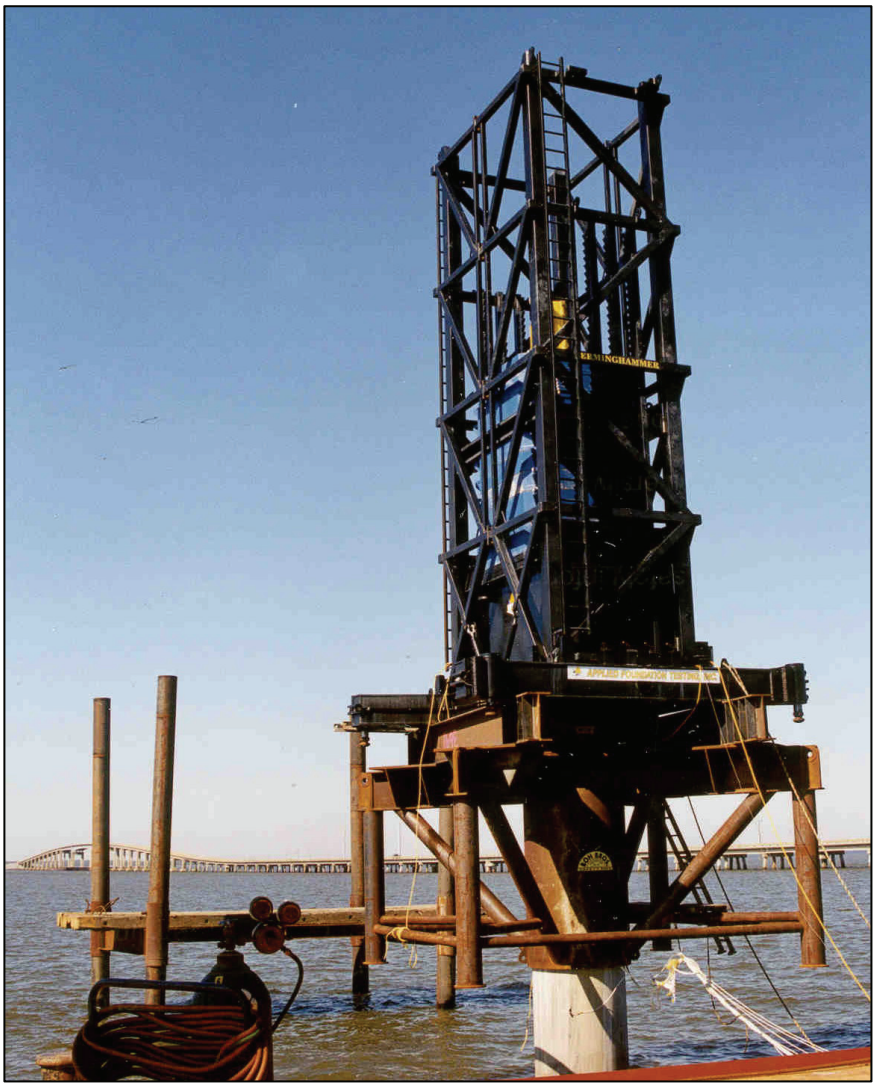
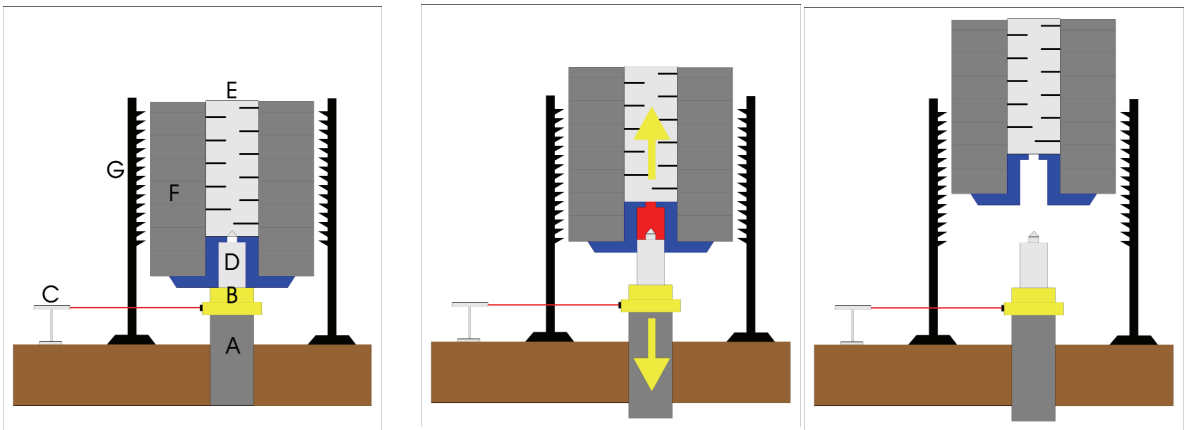


Figure 7: 2,200 Ton STATNAMIC Load Test device used on cylinder piles at St. George Island Bridge.
Courtesy of Applied Foundation Testing, Inc.



A - Foundation Member
B - Calibrated Load Cell
C - Laser Displacement System
D - Piston & Cylinder
E - Silencer
F - Reaction Mass
G - Catch Mechanism

Stage 1 - Before The Test - reaction mass is in contact with pile.
Stage 2 - The Test - Burning fuel creates high pressures, simultaneously propelling the reaction mass up and loading the pile in downward compression. The applied load and pile displacement are measured using high precision instrumentation and a data acquisition systems.
Stage 3 - After The Load Test - The reaction mass is safely caught using hydraulic systems or by mechanical means. It is easily lowered for cyclic loading on the same pile.

Figure 8: Stages of a STATNAMIC Load Test

STATIC LOAD TESTING METHOD

The load test set-up shown in Figures 9 and 10 was capable of applying almost 1,600 tons. As one can imagine from these photos, this test was very time consuming and costly. The axial load was applied to the pile using three 600 ton hydraulic jacks coupled in parallel. Multiple load cells (one above each jack) within this system provided a direct within this system provided a direct measure of the applied force. Multiple LVDT's were used to measure displacement. All instrumentation including the strain gages were used to measure displacement. All instrumentation including the strain gages were monitored with a data acquisition system. Reaction load was provided through frame supported water filled barges. Four pipe piles supported his weighted box apparatus. Loading rate was generally governed by filling the barges with water. The barge filling rate was about 7 tons of water per minute. The total duration of the test including loading and unloading was in most cases over 5 hours. In the interest of safely, the load on the test pile was always kept a minimum of 200 tons below the dead weight of the reaction mass. Thus, the four reaction piles were constantly under an approximate load around 50 tons each. The same is true for the unloading, where the pressure on the jack was slowly released as the water was drained from the tanks. Since the pipe pile supports were nearly 25-feet clear distance from the test pile and under minimal compression load, side effects on the test results from reaction piles were effectively negated.

POST TENSION MONITORING RESULTS

Sixteen tendons were stressed two at a time, 180 degrees from each other to a force of 63 kip each. Strand loading was monitored via gage pressure on the two calibrated jacks.

Figure 11 contains the strain measurements from 11 individual gages (one gage did not survive the casting process). The data shows significant eccentricity to the point of going into tension in one line of gages. However, when gages at each level are averaged the eccentric stress appear more uniform. The eccentricity is believed to be partly from non-uniform contact points between the segments and arching of the pile during tensioning. It is also interesting to note that the point of jacking was only 2.5 feet from the yellow gage level which shows the

highest average strain but also the most uniform strain. Since we know the jacking force, strain in the pile and the cross section area, the overall pile modulus was measured. The modulus based on the average of all strain gages was 5,725 ksi and corresponds to a concrete compressive strength of over 10,000 psi. The stress in the pile can then be determined based on the calculated modulus which is shown in Figure 12. This information can be used to validate structural design assumptions and also be used to more accurately determine allowable driving stresses for spun cast concrete cylinder piles.



Figure 9: Static load test set-up.
Courtesy of Boh Brothers Constructions Co.

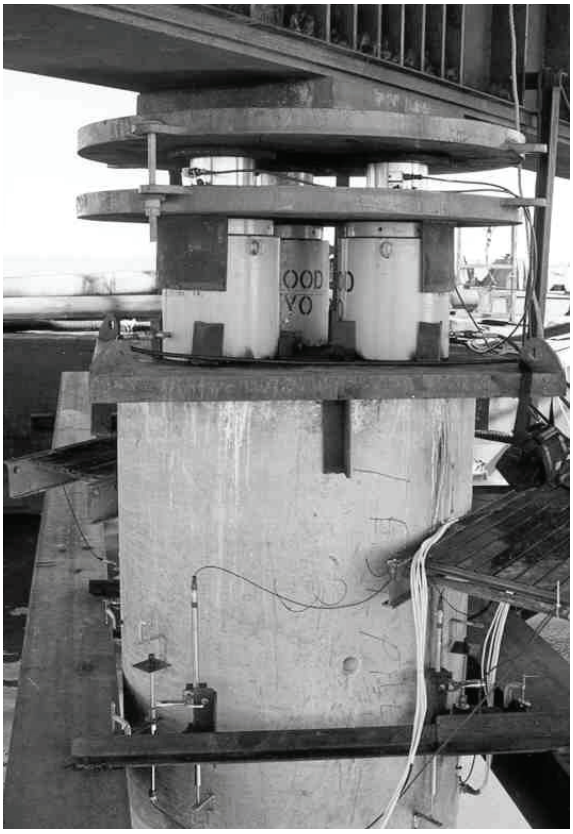


Figure 10: Detail pile top of static load test set-up.
Courtesy of Boh Brothers Construction Co, Inc.

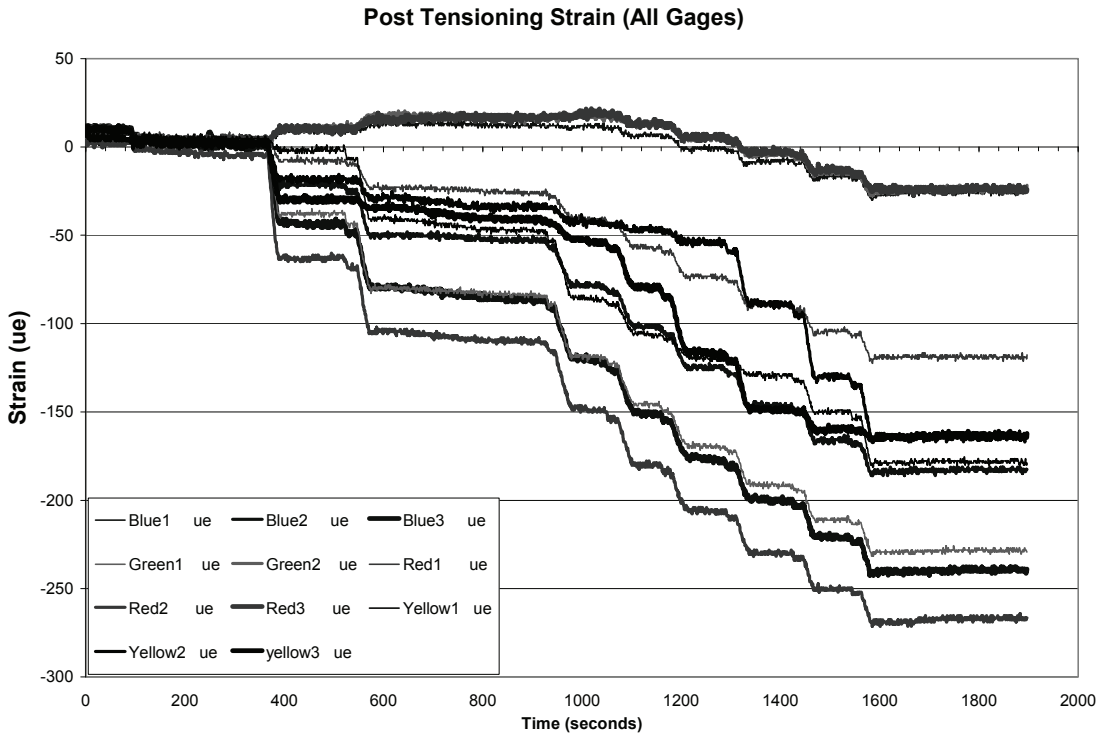


Figure 11: Strain measurements during post tensioning

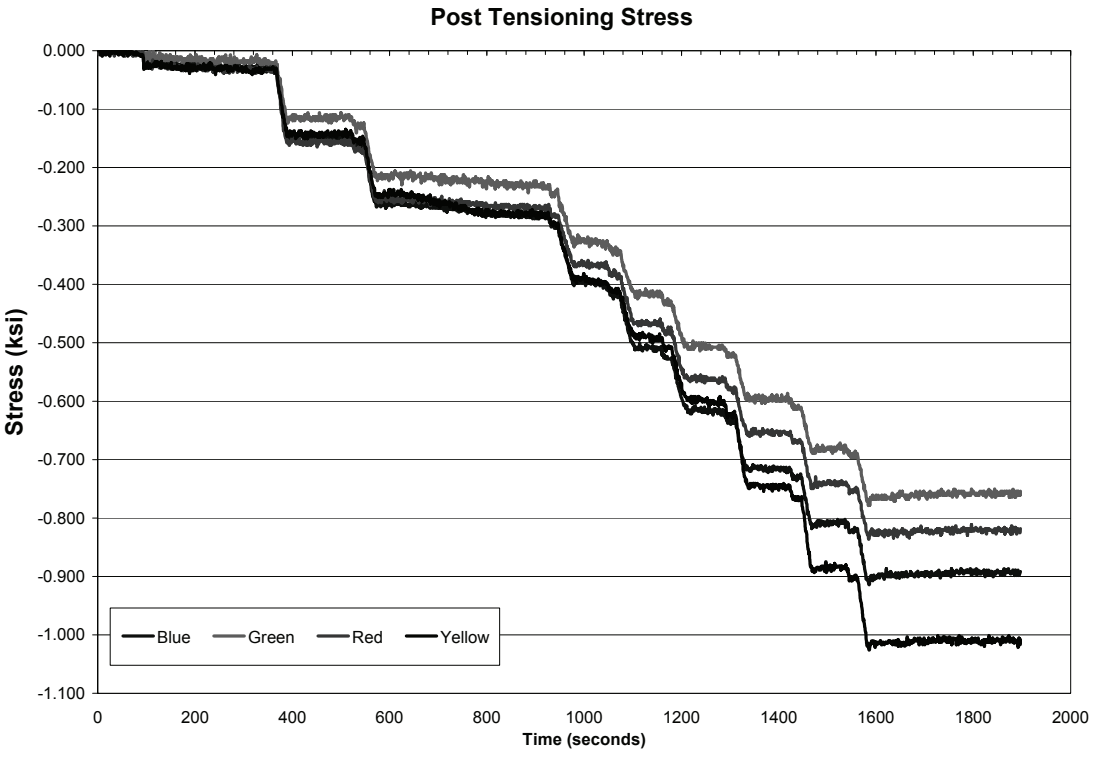


Figure 12: Average stress at each gage level during post tensioning

MEASUREMENTS DURING DRIVING

Measurements of the embedded strain gages were made during pile driving on selected test piles. Conventional dynamic monitoring was also performed on all test piles during initial drive and restrike. An example of the calculated force datfrom the strain measurements within the pile for a single hammer blow is shown in Figure 13. The force measured with the PDA is also superimposed on this figure. The internal measurements clearly indicate the effects of stress wave propagation. Due to this wave propagation, load distribution can not be simply interpreted from these data. The data shows the presence of compression and tension waves in the upper gages but the toe gages remain in compression. It is interesting to note that the highest tension was recorded near the head of the pile after several wave periods. It is also noted that the maximum compression and tension forces corresponded very well to the calculated values from the PDA.

An interesting comparison of the mechanics of a hammer impact and the STATNAMIC test may be made from this information.

The hammer blow impact duration is approximately 1 millisecond as shown in Figure 13. The STATNAMIC load test produced a compressive load lasting 100 milliseconds as shown in Figure 15. The STATNAMIC load is applied in a linearly increasing manner with a gradually decreasing unloading. The load is not an impact because the reaction mass is in contact with the pile prior to the test.

Because the STATNAMIC load duration is sufficiently longer than the natural period of the foundation, a much simpler and more accurate analysis can be made. The natural period of the pile is its length divided by its overall wave speed, L/c or 6 milliseconds for this pile. The STATNAMIC loading duration was approximately 16 times longer than the natural period of the pile. Where, a hammer impact is many times shorter than the natural period of the pile. This longer loading duration has several interesting characteristics. The most important is tensile stress waves are not present. This is shown in Figures 13 and 15 where the hammer blow produces over 800 kips of tension and the STATNAMIC test none. The figures also show that the pile is straining in-phase during the STATNAMIC test compared to those from an impact load. Therefore, the pile may be analyzed as a unit with all parts mobilizing capacity along its length simultaneously, like in a conventional static load test. But the static capacity is not simply the measured load and deflection. Because the pile, as a whole, undergoes rapid translation during the compressive loading, inertia and damping forces are easily subtracted.

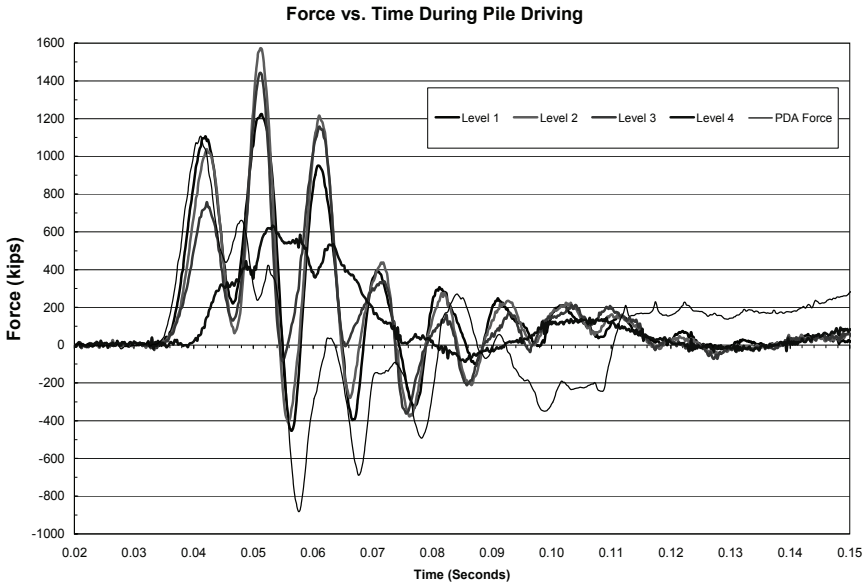


Figure 13: Measured Driving Forces in a Cylinder Piles

In contrast to the STATNAMIC loading, a hammer blow produces a wave down and wave back up the pile several times which mobilizes resistance at different locations at different points in time. This is especially noticeable in the upper strain gages. Thus, a more complex analysis technique involving a signal match approach is required to determine the resistance distribution. The signal match approach introduces approximately 18 unknowns and has no unique solution.

CAPWAP analyses were performed on the dynamic test data at end of initial drive and restikes with elapsed times ranging from 7 to 17 days. Only the CAPWAP restrike results are presented in Table 1.

Table 1: CAPWAP results from restrike tests

Pile No.	CAPWAP Total (kips)	CAPWAP Skin Friction (kips)	CAPWAP End Bearing (kips)
LT-1	1950	625	1325
LT-2	2016	735	1281
LT-3	1820	170	1650
LT-5	2028	474	1554

STATNAMIC AND STATIC LOAD TEST RESULTS

The load applied during a STATNAMIC test is of sufficient duration to maintain the pile in compression during the entire load event (like a static test). But because the pile is pushed rapidly, the loading force is also resisted by damping and inertia forces from the soil. Therefore, these forces must be subtracted to obtain the static resistance component. The derived static capacity from the STATNAMIC tests was determined using the Segmental Unloading Point Method (SUP) developed at the University of South Florida (Mullins et al., 2002). The Segmental Unloading Point Method (SUP) discretizes a foundation into segments defined by the locations of the embedded strain gages. This allows the standard Unloading Point Method (UPM) to be applied to each segment using measured data. Then the total derived static response is calculated as the sum of the derived static response from the individual segments. The applied STATNAMIC load and derived static load (via SUP method) for test pile 3 at the St. George Island project is shown in Figure 14. The difference between these two curves in Figure 14 is the inertia and damping components. The load calculated at each strain gage versus time from the same STATNAMIC test is shown in Figure 15. The loads in this figure are not corrected for inertia and damping. Note that the upper three levels of strain gages showed almost no load transfer with all the capacity being contributed by the bottom 16 feet of pile.

The physical set-up of the STATNAMIC equipment devised by the Contractor was quite ingenious in that it was self supported solely by the test pile. Therefore, falsework piles were not necessary to support the test equipment. This set up produced an atypical “bouncing effect” of the pile caused when the reaction mass was caught. This can be seen at the end of the data set in the load-displacement data as well as the strain data.

Data reduction of the static load test is very straight forward. A typical plot of the measured load versus measured displacement is shown in Figure 16 for test pile 3. The load distribution calculated from the strain gages as a function of time during the static test are shown in Figure 17. As was typical for most of the piles, the strain data for LT-3 show that all the load was transferred to the bottom 16 feet of pile.

Using these data reduction approaches, the static and STATNAMIC results were plotted together in Figures 18 through 21. As shown in these figures the ultimate capacity was achieved in two of the piles (LT-1 and LT-5). In pile LT-1, Figure 18, the STATNAMIC testing was done in three load cycles to a maximum of 2,166 kips following the static test which went to 2,136 kips. The STATNAMIC test showed both the stiffness and ultimate capacity that would be expected during a reload. It is also interesting to note that the pile developed more end bearing and less skin friction in the subsequent STATNAMIC test. The test order was reversed for LT-2, which is shown in Figure 19. STATNAMIC testing of LT-2 included three load cycles to a maximum of 3,372 kips. The following static test was taken to the limits of the equipment at 3,109 kips. Since this pile demonstrated an elastic response in each test, the comparison should be based on loads from similar deflections. Using this logic, the results were nearly identical from each test

method. The STATNAMIC and Static load test results for Pile LT-3 were plotted on top of each other in Figure 20 to show the nearly perfect agreement in every way. It is believed that this pile was on the “verge” of achieving plunging failure. The skin friction and end bearing distribution on pile LT-2 and LT-3 also had very good agreement. Test pile LT-5 shown in Figure 21 had a different response than the other test piles in that it had the most skin friction capacity of the four piles. The pile had a maximum static capacity of 2,889 kips of which 1,280 kips was end bearing. The STATNAMIC test was performed only two days later and showed a lower capacity of 2,631 kips. What is interesting is the STATNAMIC test showed a similar end bearing of 1,300 kips. So it is reasonable to assume the difference in capacity was due to a loss in skin friction between tests. A summary of results from the static and STATNAMIC tests is presented in Table 2.



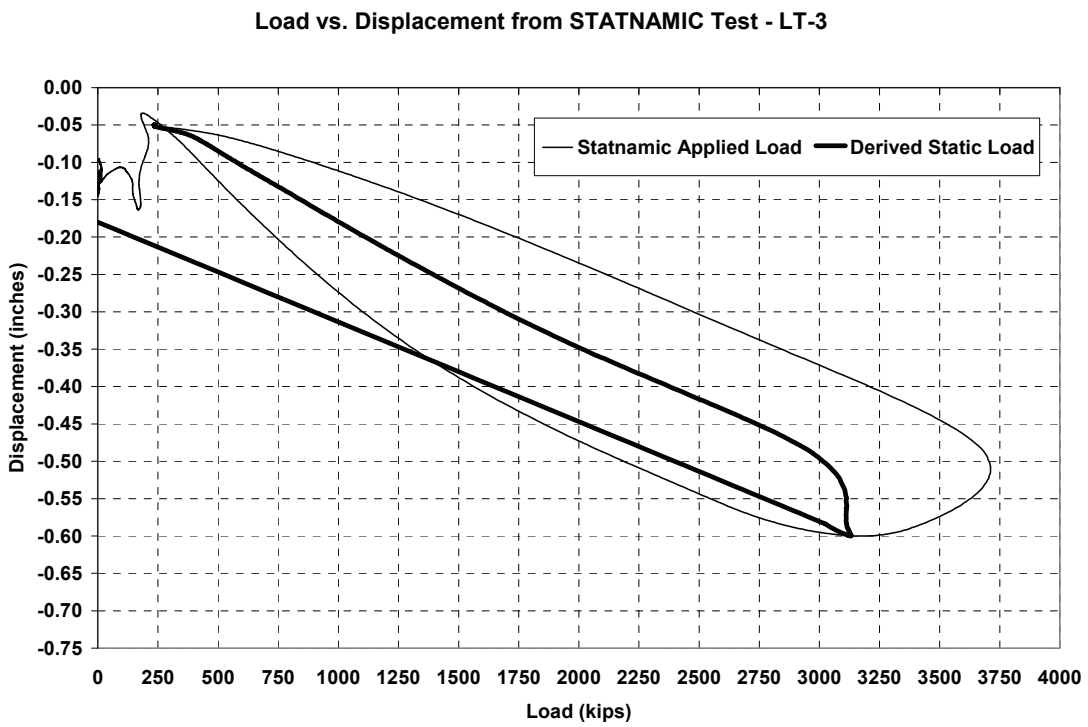


Figure 14: Applied STATNAMIC load and derived static load based on SUP method

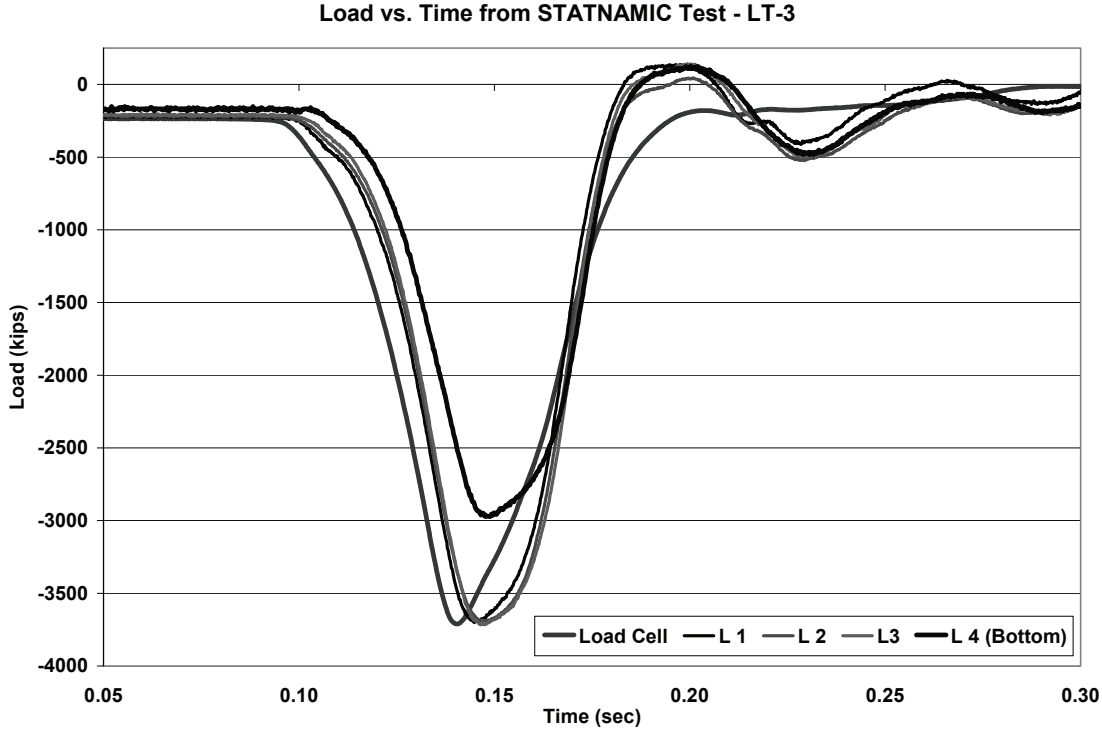


Figure 15: Load distribution within the pile during the STATNAMIC load test (uncorrected for inertia and damping)

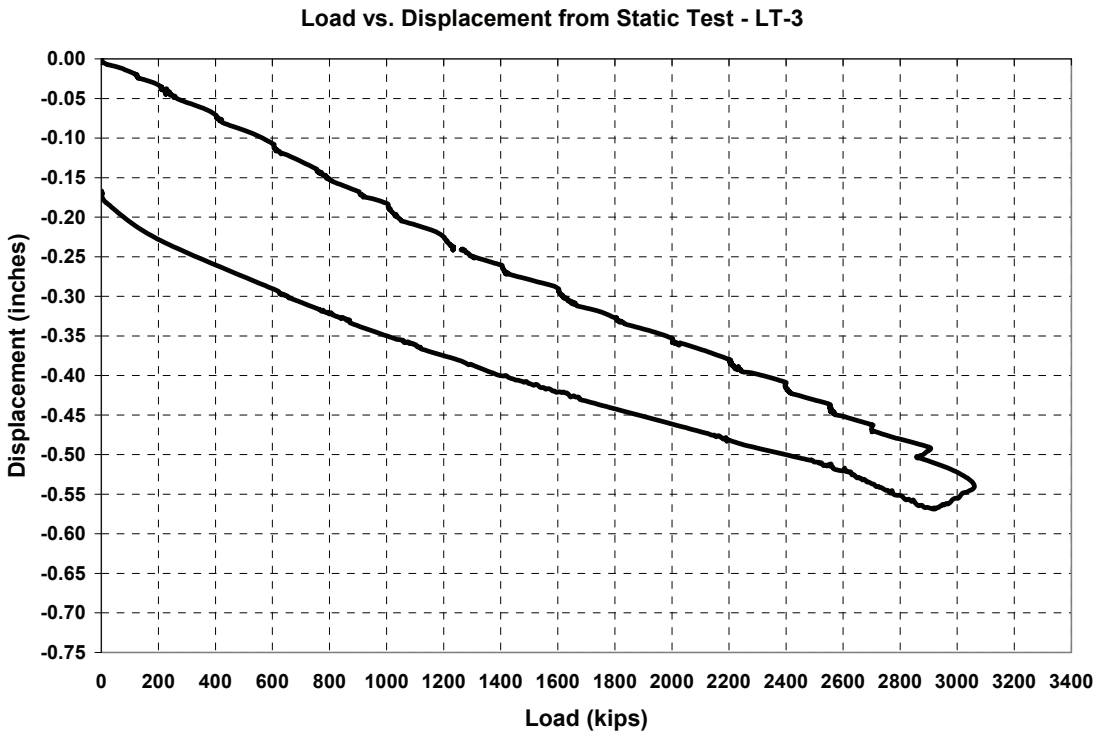


Figure 16: Applied load vs displacement during static load test of LT-3

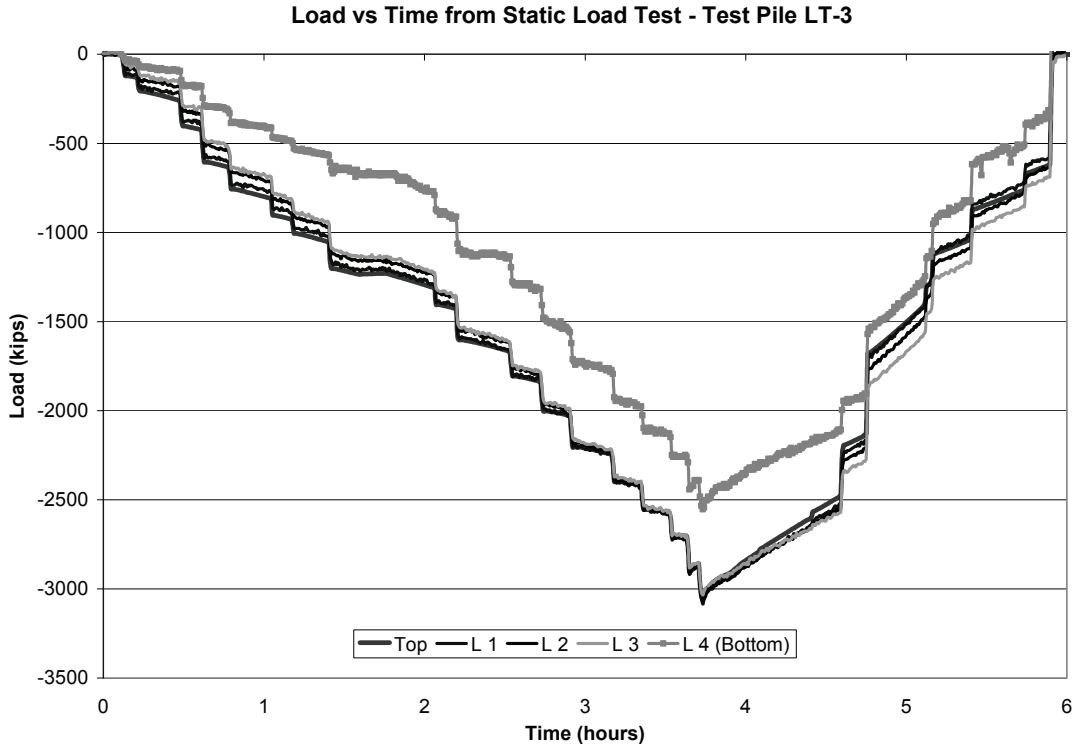


Figure 17: Load distribution based on strain measurements during the Static load test of LT-3

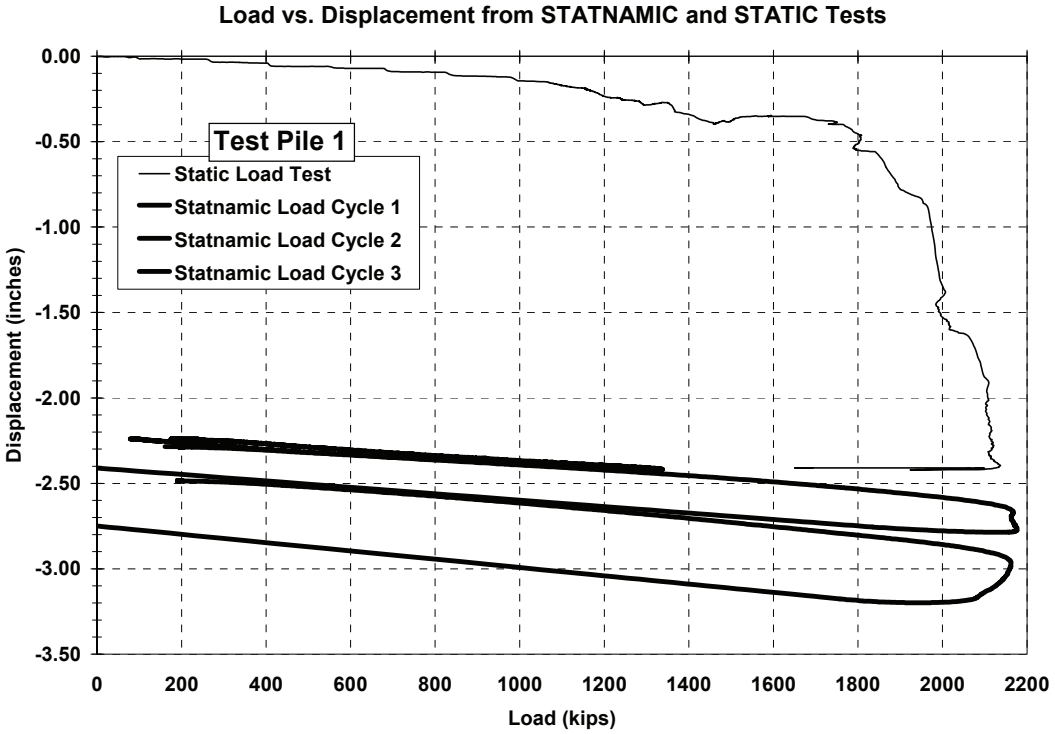


Figure 18: Static and STATNAMIC load test results from LT-1

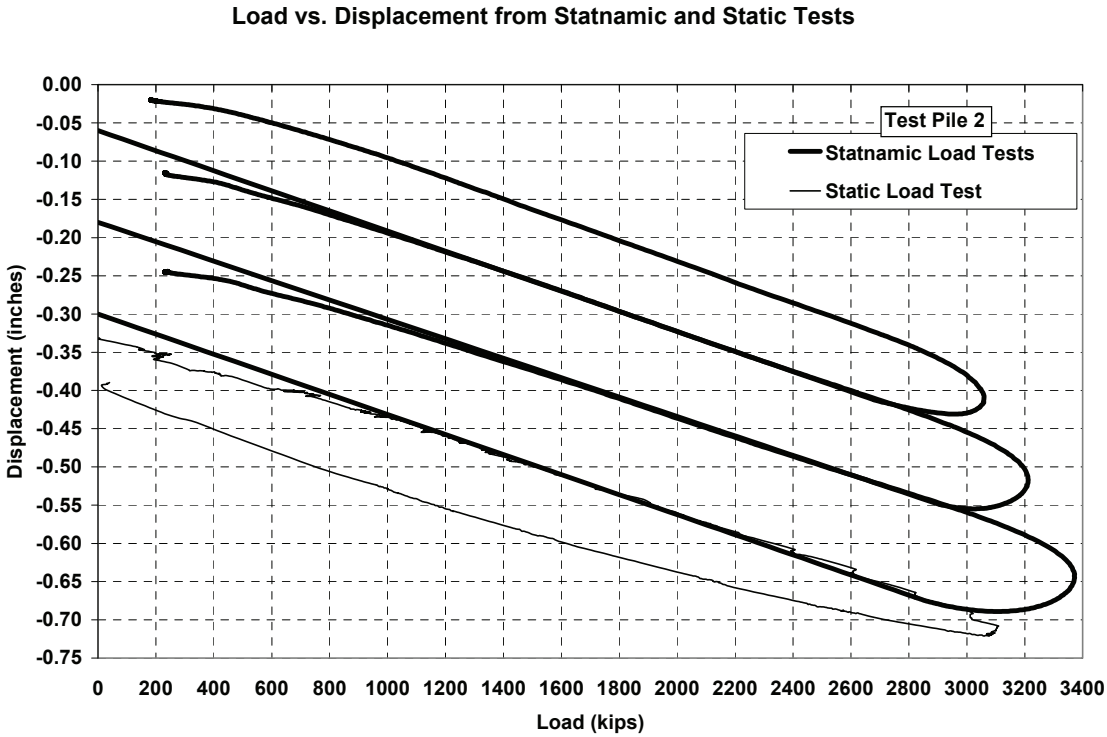


Figure 19: Static and STATNAMIC load test results from LT-2

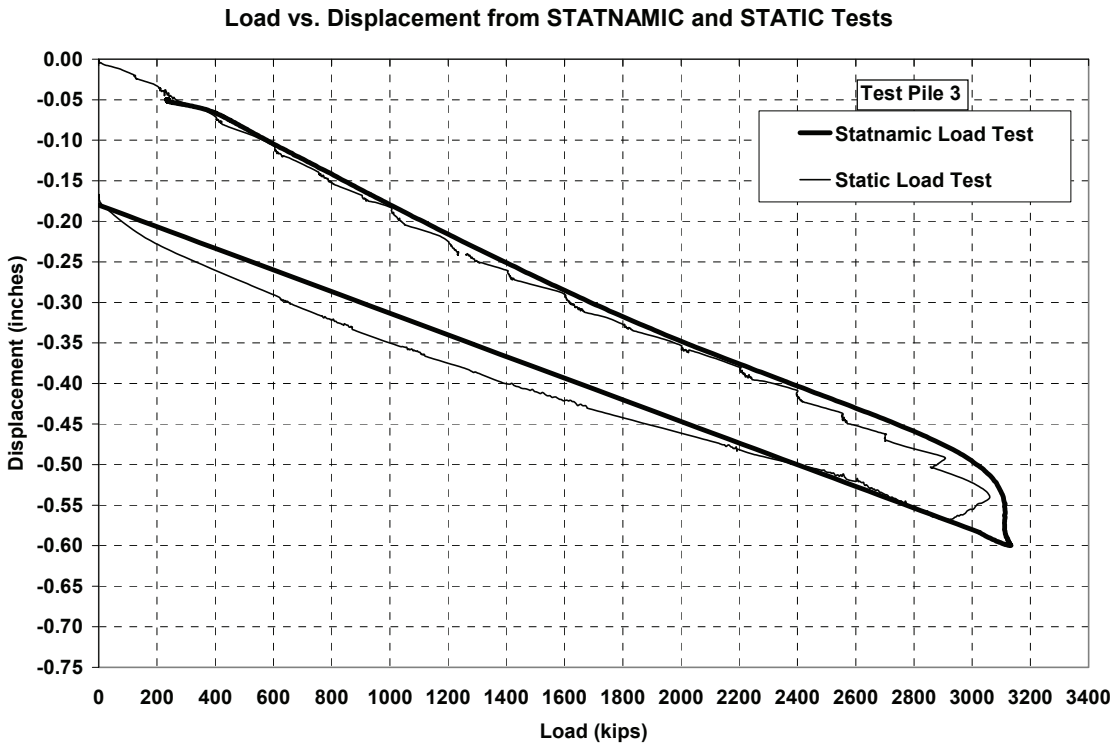


Figure 20: Static and STATNAMIC load test results from LT-3

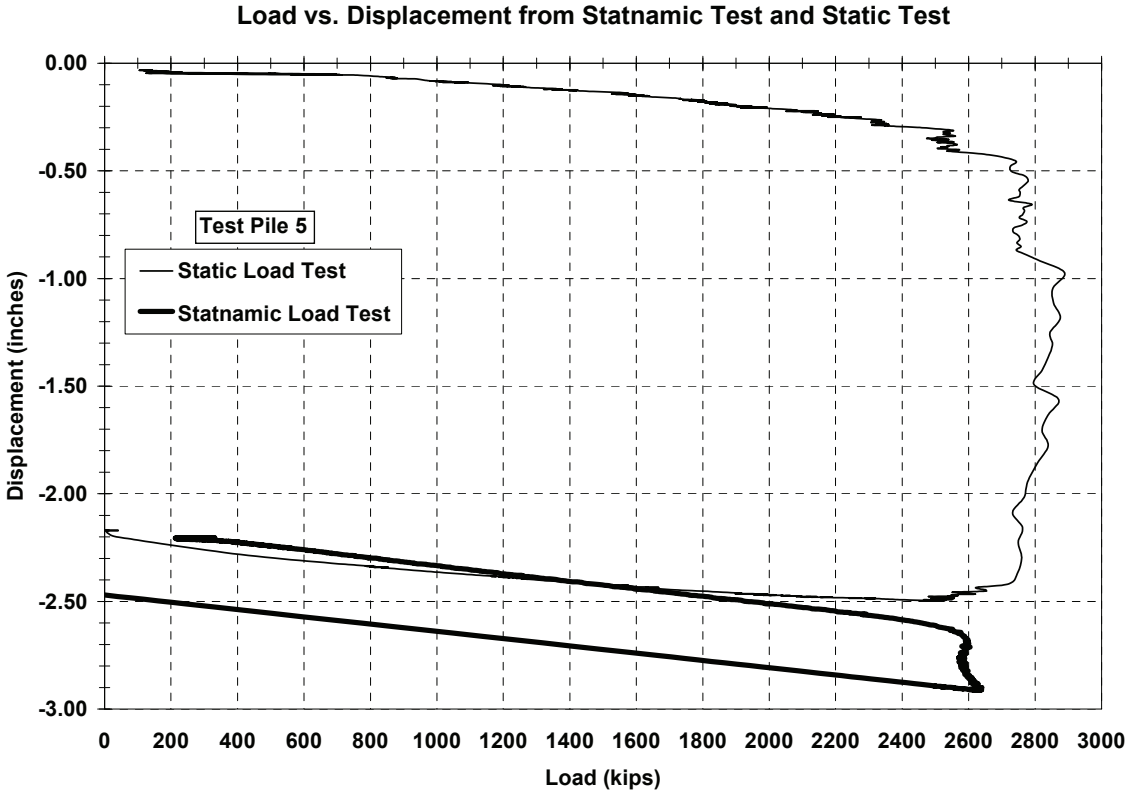


Figure 21: Static and STATNAMIC load test results from LT-5

Table 2: Summary of static and STATNAMIC load test results

Pile No.	Static Total (kips)	Static Skin Friction (kips)	Static End Bearing (kips)	STATNAMIC Total (kips)	STATNAMIC Skin Friction (kips)	STATNAMIC End Bearing (kips)
LT-1	2136	1392	740	2166	901	1265
LT-2	3109	324	2785	3052	217	2835
LT-3	3060	507	2553	3113	513	2600
LT-5	2889	1609	1280	2631	1300	1300

CONCLUSIONS AND COMPARISON OF THREE TEST METHODS

Three types of load tests were performed on the St. George Island Bridge project consisting of dynamic testing, STATNAMIC load testing, and static load testing. Four of the test piles utilized all three methods on the same pile which are the focus of this paper. In these comparisons, the static load test was selected as the bench mark reference test. Of the four piles tested, only two (LT-1 and LT-5) achieved the ultimate pile capacity.

In all cases, the CAPWAP restrike under-predicted the total pile static capacity. These under-predictions ranged from 9 percent to 41 percent as shown in Figure 22. The predicted load distribution from CAPWAP had much larger disparities though.

The best CAPWAP comparison was at LT-1, where the restrike was only 9 percent below the ultimate static capacity. However, it did not match so favorably to the skin friction and end bearing distribution where it under-predicted the skin friction by 222% and over-predicted the end bearing by 79%.

At LT-5, the CAPWAP restrike under-predicted the ultimate static capacity by 30 percent. It also under-predicted the skin friction by 245% and over-predicted the end bearing by 21%.

In LT-2 and LT-3, the CAPWAP restrike again showed significant under-prediction of 35% and 41%, respectively. At LT-2, the skin friction was over-predicted by 127% and the end bearing was under-predicted by over 117%. Similar magnitude discrepancies were shown in LT-3 with an under-prediction on skin friction of 194% and 54% under-prediction of end bearing.

In three of the four piles, STATNAMIC derived static capacities were within 2 percent of the static load tests. In the fourth pile, the STATNAMIC derived capacity was 9 percent below the static load test primarily due to the short time interval (only 2 days) between the static test and the STATNAMIC test. Figure 23 graphically depicts this comparison.

In LT-1 the end bearing during the reload was 71 % greater than the initial static test. Also accompanied by a reduction in side shear capacity of 35%. In LT-2 the STATNAMIC showed 107 kips lower side shear capacity and 50 kips higher end bearing capacity than in the static test. The side shear and end bearing capacity from STATNAMIC was within 1% to 2% of the static test for LT-3. In LT-5 the STATNAMIC end bearing was within 2 % of the static test, but was 17% lower on side shear as discussed above.

Although CAPWAP significantly underpredicted the pile capacity as illustrated in Figure 22, dynamic testing of cylinder piles still adds benefit in gaining driving stress and hammer energy data.

The high reliability of determining pile capacity with STATNAMIC load testing augmented with strain instrumentation was demonstrated on this project and illustrated in Figure 23. In this application, STATNAMIC has demonstrated it can provide engineers, owners and contractors a more cost effective means to test high capacity marine foundations.

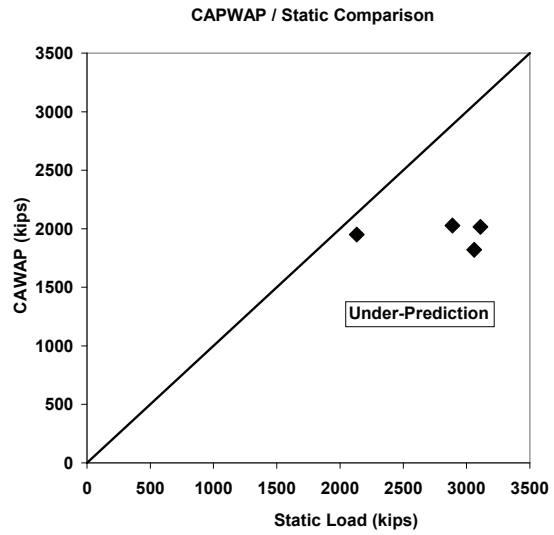


Figure 22: CAPWAP restrike to static test

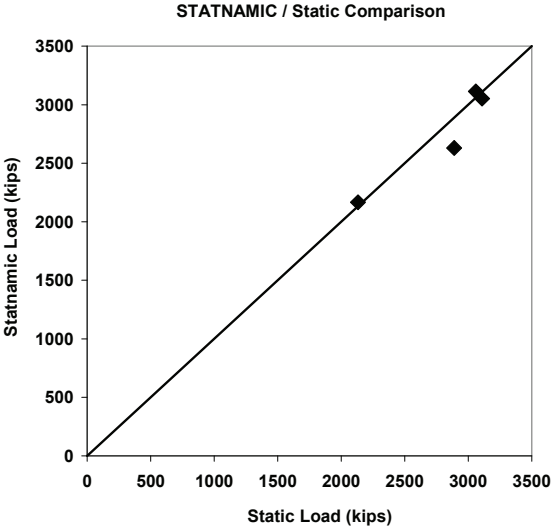


Figure 23: STATNAMIC to static test

REFERENCES

Mullins, G., Lewis, C., and Justason, M.D., 2002. Advancements in Statnamic data Reduction Techniques. ACSE Geotechnical Special Publication 116, pp. 915-928.

Williams Earth Sciences, Inc. Report of Load Test Results (Static, STATNAMIC, and PDA), St. George Island Bridge – SR 300 over Apalachicola Bay, January, 31, 2001

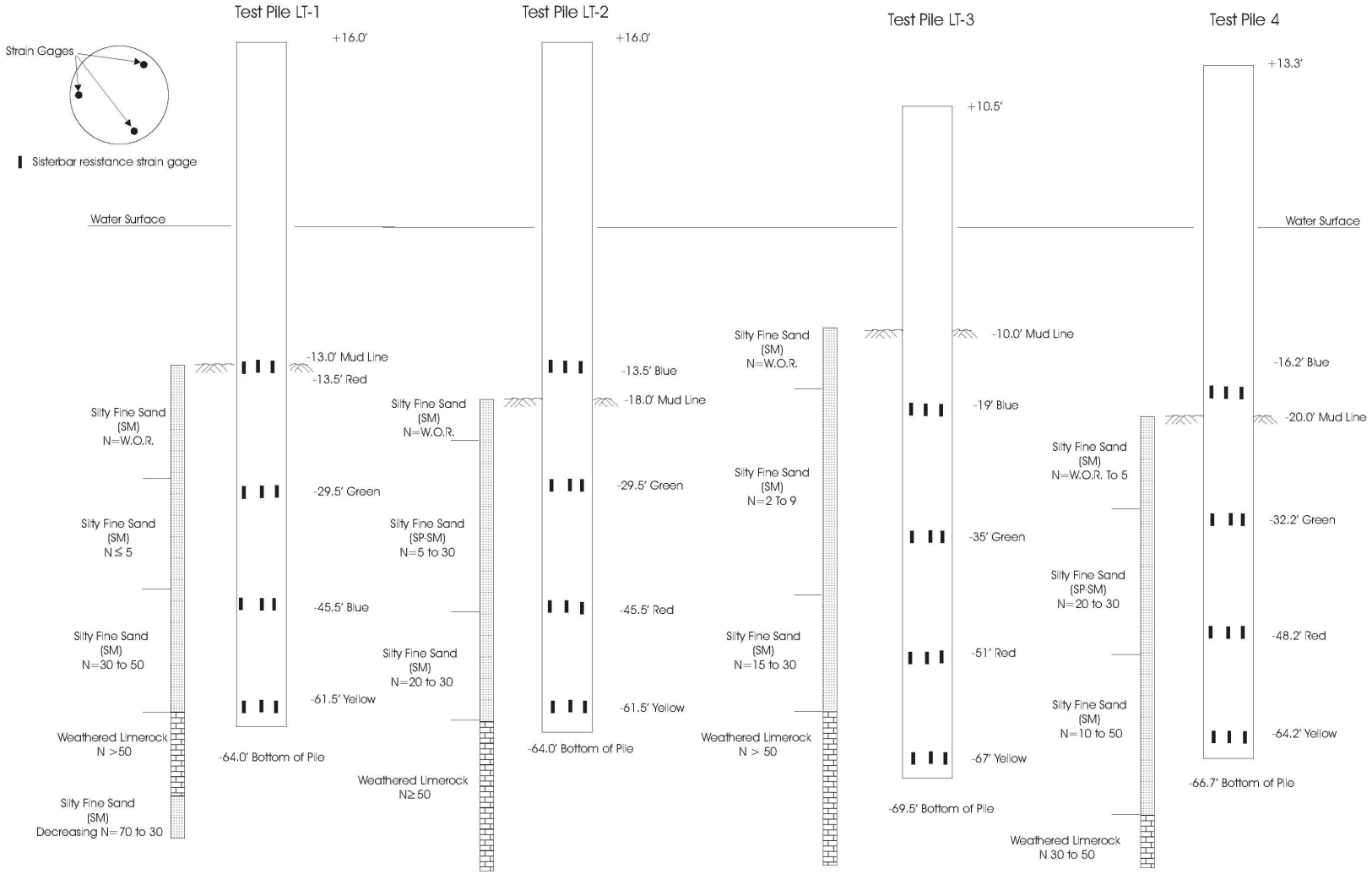


Figure 6: Soil and pile profiles St. George Island Bridge

FOUNDATIONS FOR OFFSHORE WIND ENERGY CONVERTERS – A REVIEW OF SOME CURRENT SCANDINAVIAN DEVELOPMENT PROJECTS

Viking, K., Ramboll Sverige AB, Stockholm, Sweden, <kenneth.viking@ramboll.se>
Johansson, Lars, Ramboll Sverige AB, Malmo, Sweden, <lars.johansson@ramboll.se>

This article deals with some of the civil engineering related problems to be encountered when offshore wind energy projects transform from prototype offshore wind energy converter farms, developed and installed during the 1990's, to commercial farms that's currently planned to be built. The offshore wind energy converter (OWEC) installations encounter a wide range of problems, only partial of these are geotechnical.

In Europe both onshore and offshore wind farms have, from a historical point of view, usually been founded by using the monopole technique, installed with traditional impact hammers, or by using gravitational foundations. However, the rapid development of bigger turbines and larger wind farms, together with increasing considerations of fatigue aspects, has lead to financial benefits of developing and exploring other foundation techniques. This paper reviews some Scandinavian experiences regarding critical components of the design phase in relation to connecting the superstructure to the ground, and some of the main considerations of how the loads applied to the structure are transferred to the surrounding soil.

Keywords: Offshore Wind Turbines, Wind Farms, Foundation, Pile, Gravity Structures

INTRODUCTION

For a long time sufficient supply of electric energy has not been a pronounced problem in Sweden. Traditionally, rivers in the Northern parts were used for water power plants, combined with power plants burning coal or oil. In the end of the 70's, increased concerns about environmental aspects however made it impossible to further develop water power, as the natural river environment was more or less destroyed. Several alternative energy sources were investigated to ensure a sufficient electric energy supply also in the future. Nuclear power was chosen as the alternative, however not entirely without protests – also within the political sphere.

An election was held in 1980 to support the government's decision to what extent nuclear power should be developed. There may be many opinions about the outcome of this election. Basically, there were three alternatives (called Line 1, Line 2, and Line 3). Line 3 represented the "No to nuclear power alternative" and even if this Line got the most number of votes, the results of Line 1 and Line 2 (both representing nuclear power alternatives) was in the end added, giving together more votes than Line 3. So, it was decided that there should be 12 nuclear power turbines in Sweden, which should all be closed by the year 2010.

The intention was that there should be a vast research program leading to effective alternative energy resources until 2010, which then could gradually substitute nuclear power. However, energy prices have since then been low in Sweden, in fact leading to no real incitement to develop other sources. None of them would simply be economically competitive. Probably also the thought of being able to run nuclear power stations longer than until 2010 was somewhat a 'zero alternative', even if it has never been officially presented.

Now, five years before 2010, the shut down of nuclear turbines has been initiated with two of the oldest. The price of electric energy has risen substantially, and as the government clearly indicates that their intention is to fulfil the outcome from the elections in 1980 to end nuclear energy production, the incitements for developing other sources is suddenly more real than ever.

WIND POWER IN SCANDINAVIA

As can be understood from the Introduction, wind energy converters have so far not been extensively used in Sweden. There have been some converters installed, mainly in the Southern parts of the country, but more or less only from private initiatives, e.g. farmers or local industries. The main electric energy production has still been based on nuclear and water power, and, in the south, also based on energy imported from neighboring countries, especially during peak situations.

In Denmark –a country about the size of Maine – generates some 20% of its power from wind. It is the nation in Scandinavia that gets the highest

percentage of its electricity from wind. Main reason for this is the lack of rivers to be used for water power plants. Originally, mainland based converters were used, and lately, also off-shore based. Off-shore based converters are mainly erected on shallow, near-cost areas. The competence of Danish consult firms and contractors within the field of wind energy converters is also well known.

The situation in Finland is obviously somewhere between the Swedish and Danish situation. Also in Finland, water power production has played an important role.

Historical Review

In Sweden, the use of wind energy converters has so far been limited, however is expected to change in the near future. The main reason is economical aspects. With low energy prices wind energy converters have not been able to compete with e.g. water power. For most of the converters installed, state subsidies were given. Without subsidies no converters at all would probably have been installed.

Traveling around in Sweden, converters can be seen mainly in the Southern parts. However, the number of offshore converters is far from what can be found in e.g. Denmark. The latest Swedish demonstration project named Bockstigen, is located south-west of the Swedish island Gotland in the Baltic Sea.

Finland have just confide its first offshore wind farm, consisting of five 2.3MW wind turbines at Brahestad, Baltic Sea.

In Norway; currently a power company together with the oil based Norsk Hydro, plans to erect an offshore farm mid-Norway, North Sea.

Environmental Aspects

There are widely spread protests against the erection of wind energy converters in Sweden. While people in general could accept a few of them installed locally, but discussing wind energy converter farms with forty and sometimes even a hundred converters, the reaction didn't wait.

Discussing mainland based converters; reactions are mostly of esthetic nature. People in general tend to think that converters have a negative impact on view and landscape. In addition, arguments against noise and ice (ice formed along the rotor blades can fall down and damage structure or hurt people and animals) are also raised.

When it comes to offshore converters, the conditions for fishes and birds are introduced to the arguments. Changes in water current conditions, impact on water vegetation are another set of arguments often used. Another aspect is the creation and spreading of fine grained sediments from drilling operations. Such sediments would settle on top of and cover the sea bottom.

In Sweden, many decisions are decentralized and taken by the local authorities, such as the permission to build or erect structures. Local politicians are, of course, opinion sensitive, and whereas there is a strong opinion against the localization of wind energy converters, companies involved in obtaining permissions would probably face time-consuming and difficult processes. One of the southernmost Swedish cities just recently tripled the application fee for wind energy converters under the argumentation that such processes are more complicated than for other structures.

RECENT PROJECTS AND FOUNDATION ASPECTS

In contrast to typical offshore structures, (like oil & gas structures), the support structure, tower + foundation, of a wind converter may account for up to 30-40% of the total installation cost. One of the reasons is simply the size of today's wind converters. Figure 1 illustrates some typical dimensions of a 2.5MW turbine. The turbine is elevated at approximately 90-100m (295-328ft) above mean sea level, having a rotor diameter in the order of 70-90m (230-295ft), and installed in relatively shallow waters 5-20m (16-65ft).

Standards and Certification of Offshore Wind Farms

Despite the huge installation costs and risks involved with erecting commercially based wind farms, with 3 to 5 MW turbines set as new targets. No national nor international Standard or Codes covering offshore wind turbines as an integrated system exist; however the following standards are used and cover the following areas:

ICE 61400-1 and ICE WT01 cover onshore wind turbines but not foundations.
ICE 61400-1 (not finalized) covers offshore wind turbines but not foundations.
Euro codes cover onshore buildings (with high safety class) but no wind turbines.
ISO 19902 and API cover fixed offshore oil- and gas structures (high safety class, but without covering wind turbines).
GR-Regulations cover the entire system.
DNV-OS-J101 cover the support structure and foundation, not the entirely system.

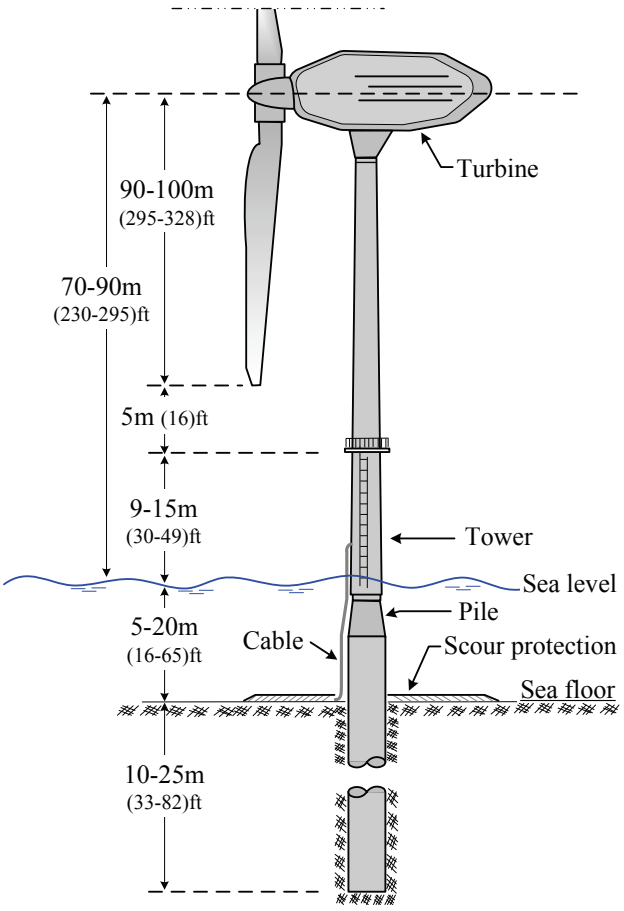


Figure 1: Typical dimensions of a 2.5MW turbine

Today's certifications are more frequently carried out on the basis of the Germanisher Lloyd's "Regulations for the Certification of Offshore Wind Energy Conversion Systems" (first published -95, supplemented -98, current -00 version on CD, with the latest to be released -05). GL Wind is accredited for type certification/approval according to Danish, Dutch, German, ICE and GR-Regulations.

However, Det Norske Veritas (DNV) still maintains its position as the leading international provider of certification services of offshore wind farm projects.

The Design Calculations and Foundation Problem

The design of offshore wind support structures (tower and foundation) is assessed on the basis of the site specific parameters in an integrated process, see Figure 2. This process contains considerations of the dynamic response of the; tower, foundation and soil behavior, due to the defined load assumptions. With the combined load assumptions due to; wind, wave and ice, as detailed assessments on both the static and fatigue related strength of all critical hot spots of the support structure.

Furthermore, it's also desirable to have one and the same design and installation procedure that can be mass-produced for the whole wind farm site, rather than having each foundation individually engineered. The combination of above-mentioned aspects leads to a very interesting engineering problem, where the foundation design becomes crucial to the economics of the whole project.

Classical design principles is normally subdivide into the following methods; the LRFD method, design by direct simulation of combined load effects of simultaneously acting load processes, testing assisted design, and the probability-based design. However, the main differences in the design approach of a standard offshore oil- and gas structure (jacket) with an OWT is the fact that the combined wind and wave loading on an OWT cannot simply be added up nor linearised. It's therefore inevitable to perform time domain simulations for extreme loading as well as for fatigue checks. For a normal jacket, fatigue calculations can be linearised and treated in the frequency domain, which significantly reduces the calculation time.

The Loads

The loading of an offshore wind turbine structure represents a major point in all related standards and guidelines. These loads will off course vary with; the size, design (structural stiffness) and the site specific parameters, e.g. the local environmental conditions such as:

- soil conditions,
- wind conditions,
- water depth,
- wave height,
- current,
- carrion, and
- combined wind-wave and wind-ice.

The loads comprised of wind and waves are cyclic in nature. It's normally not the combination of extreme sea and wind states that corresponds to the critical load case. Since the wave direction might not coincident with the prevailing wind direction and fluctuate rapidly with time, rather than remaining constant as would be typical assumptions in traditional offshore design.

However, the gravity load V of a wind turbine, that is, the weight of the construction, will be comparatively small compared with the horizontal load H and the overturning moment M caused by the action of waves and wind. The effect of the overturning loads will be further increased by the action of ice in winter time. Information of loads involved in the design of OWEC is found in [1]. The weight, e.g. vertical load V, will be comparatively small (~6MN (1,350 kips)), in comparison with the overturning moment M and horizontal load H.

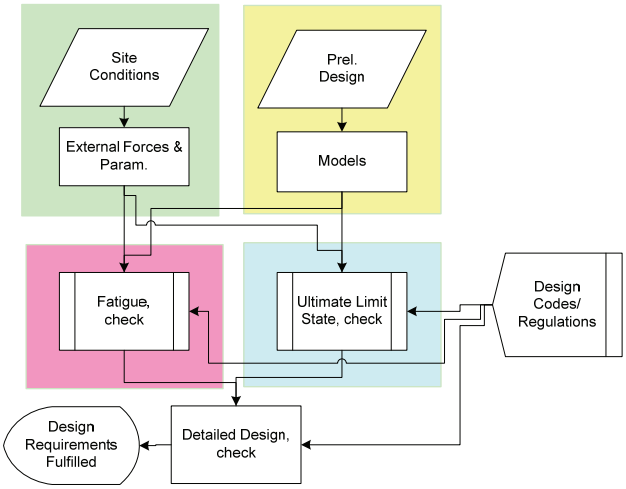


Figure 2: Design process of OWEC, after [9]

The overturning moment will be in the order of 120MN-m (22,500kip-ft) and the horizontal load in the range of 4-5MN (900-1,124kip).

Fatigue

Another very important load situation to consider is the Fatigue Loads (Forces) and the corresponding frequency of the external forces and its effects on each component of the system. Since wind turbines are subject to fluctuating winds, hence fluctuating forces. Components may eventually develop fatigue cracks, which ultimately may result in the failure of the component. For example, an 80-90m (260-290ft) tall wind turbine tower will have a tendency to swing back and forth, say, every third second. The frequency with which the tower oscillates back and forth depends on both the height of the tower, the thickness of its walls, the type of steel, and the weight of the nacelle and rotor. The swinging of the tower comes from the fact that each time a rotor blade passes the wind shade of the tower, the rotor will push slightly less against the tower. If the rotor turns with a rotational speed such that a rotor blade passes the tower each time the tower is in one of its extreme positions, then the rotor blade may either dampen or amplify (reinforce) the oscillations of the tower. As can be understood, it is very important to know both the frequency of the external loads and the natural frequency of the system, due to the risk of transferring the energy to the system with the risk of having the amplitude of the oscillations increased to an uncontrolled level; a condition called resonance.

Load-Foundation Structure–Soil Interaction

The support structures (tower + foundation) of wind farms can reach as high as 30-40% of the total investment. Knowledge of the soil conditions existing in the considered site is necessary to develop a safe and economical design. Thus geophysical surveys should be performed first followed by a geotechnical investigation as the main parts of the main analyses. The structure-foundation interaction analysis should be modeled non-linearly. For piled foundations the non-linear behavior of axial and lateral pile-soil interaction should be modeled explicitly in order to ensure the load-deflection compatibility between the structure and the pile-soil system. For pile analyzes, effects of geometrical and material non-linearities should be accounted for within the structure-pile-soil system. Effects of cyclic-loading on potential reduction of the shear strength and bearing capacity of the soil conditions should also be carefully considered and investigated.

However, it's normally both difficult and enormously time as well as computer capacity consuming to perform these time-domain simulations on all parts of the above mentioned foundation non-linearity issues. In practice, the p-y curves are approximated by linear springs (representing the modulus of subgrade reaction) which differ with respect to the considered load situation. With the implications that the different natural frequencies are derived for; extreme and fatigue load analysis, as well as for different load situations.

Type of OWEC Foundations

Today's option for offshore foundations of wind energy converters consists of the following three types:

- piled,
- gravity based, and
- skirted.

However, other concepts include types such as; jackets, hybrids, floating foundations and suction caissons. From the Danish '96 R&D project, which amongst many things, compared advantages and disadvantages of three typical foundations which are here described and further summarized in Tab 1.

Installing structures offshore is hardly novel, however these structures are different from typical offshore structures in two aspects; which relates to applied loads and hence on the type of foundation.

Gravity base structures/foundations most of the existing offshore wind parks use concrete gravitation foundations, due to the Scandinavian geology i.e. firm limestone. Lately a newer alternative have become more widely used, which consists of a flat steel box filled with gravity instead of the older solution consisting of reinforced concrete caissons. However, the shear size of gravity based foundations affects both waves and current. The base can be as big as 25-30m (82-98ft) in diameter and 3.5-4m (11-13ft) high. Advantages are the possibility to produce the foundation onshore, and the solution of gravity structures might be used on almost all types of seabeds.

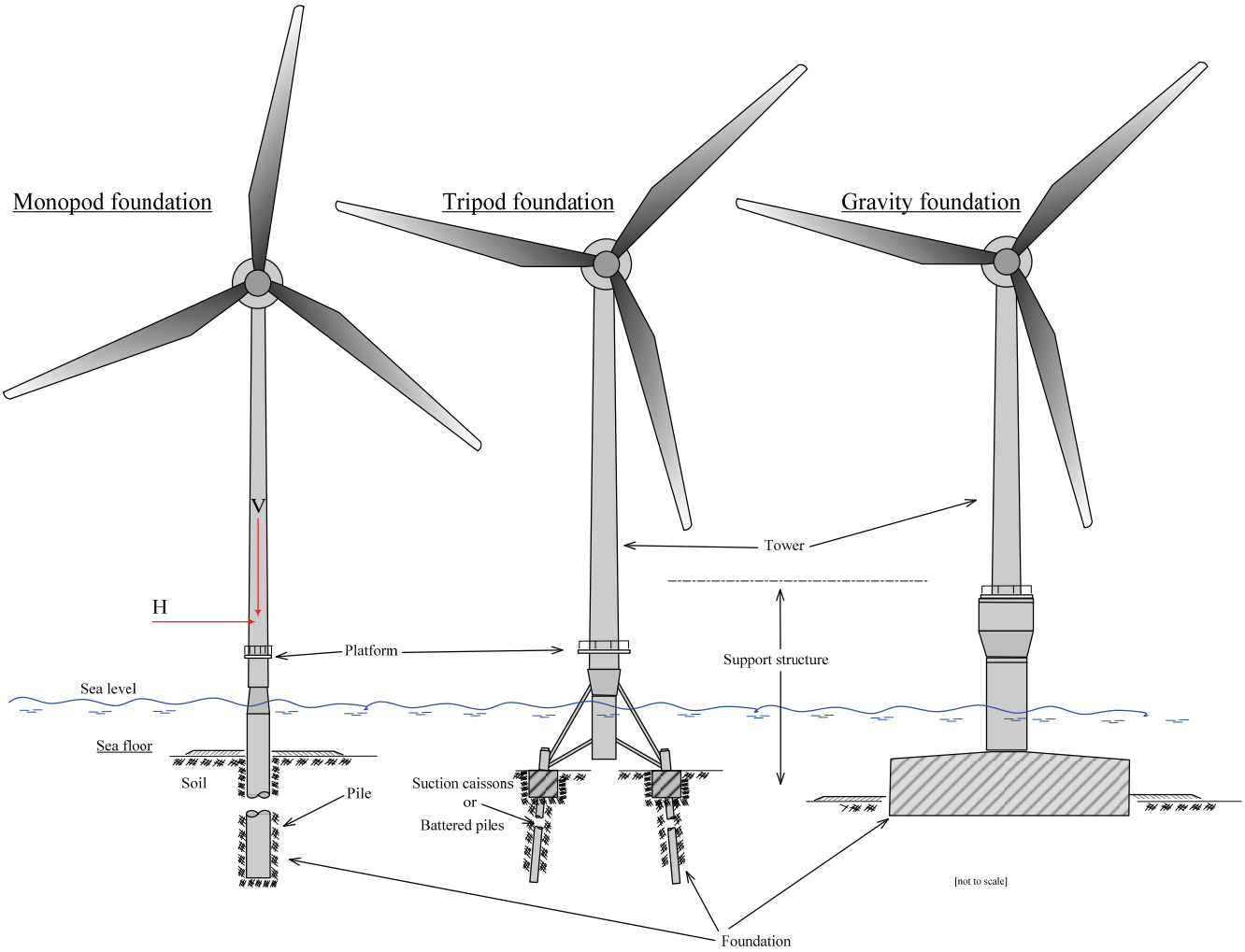


Figure 3: Type and definitions of offshore wind turbine sections, after [7]

However, preparations of the seabed are always required; softer sediments need to be removed and a smooth horizontal bed of shingles need to be prepared (usually by divers) before the foundation can be positioned. Gravitational solutions are frequently reinforced by drilling 'ground anchors' through the slab into the underlying limestone. The surrounding seabed needs also to be protected due to scour, accomplished by placing boulders or rocks around the edges of the base. Protection of pack ice might also be needed in the Baltic Sea.

Monotower structure/foundations are the simplest of them; it normally consists of a steel pipe with a diameter between 3-4m (10-13ft). The pile is either driven and/or drilled to ~10-20m (32-65ft) into the seafloor depending on type of underground. The advantage of this alternative is that no preparations of the seabed are necessary. On the other hand, it requires radar heavy piling and/or drilling equipments, and the foundation type is less suitable for locations with large boulders.

Tripod structures/foundations are an alternative to the monotower concept, originally developed for marginal offshore fields in the oil and gas sector. A steel pile beneath the tower transfers the load to a tripod, which is in each corner is anchored to the seafloor by smaller (~0.9m diameter) steel pipe piles. Pile anchored tripod structures share the same characteristics as monopod structures, apart from being:

- more suitable for deeper sites (>20m (65ft)),
- cheaper than monopods in deeper waters, and
- less suitable in shallow waters, as the tripods may obstruct approaching vessels.

Decommissioning of OWEC Foundations

There are to the author's knowledge so far no published materials regarding the decommissioning of OWEC structures as they are relatively new developments. However, the removal of a monopole and/or multiple piled structures would probably be less complex as well as cheaper compared to a gravity based structure. The removal of a piled structure would most likely involve methods such as cutting the pile at sea bed level.

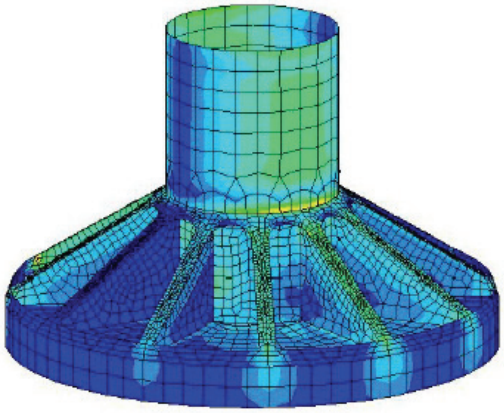


Figure 3a: FEM-analysis of a concrete gravity based foundations, Enercon 4.5MW, in Germany, [5]

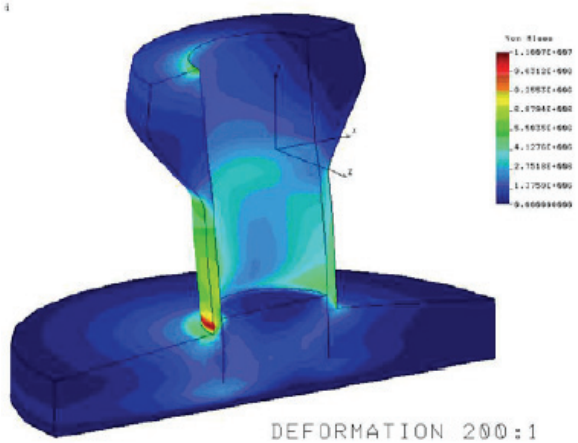


Figure 3b: FEM-analysis of a concrete gravity based foundations, Middelgrund 2MW, in Denmark, [5]

SOME RECENT SCANDINAVIAN PROJECTS

Lillgrund

Lillgrund is a shallow area located in Øresund between Sweden and Denmark, on the Swedish territorial water. The water depth on top of Lillgrund is just a couple of meters while it might be 5 to 10 m along the periphery of the shallow area. Lillgrund is located not far from Middelgrund on Danish territorial water, where wind energy converters had already been erected. The total number of converters intended to be erected has varied, but would probably be around 40 in the final design.

The process of building wind energy converters on Lillgrund has been long and far from straight forward. Already more than five years ago begun preliminary studies and design projects. Geotechnical and geological investigations were carried out to give basis for decisions regarding e.g. foundation methods. However, the process of building the converters has been postponed, much because changed conditions for state subsidies. The tender process has however begun in the middle of 2005.

Typical soil profiles in the area consist of uppermost sediments (clayey soils, sands, gravel mostly depending on the water current conditions and water depth) resting on clay till on bedrock, consisting of limestone. Locally, especially if the water depth is small, all sediments have been eroded, and the sea bottom exhibits clay till only. The limestone profile typically consists of an uppermost part with a thickness of about 1 to 2m (3-6ft) which is much fissured and of relatively bad quality. Flint nodules are commonly present. This part of the limestone profile is denominated Copenhagen limestone. Below is found a more competent cretaceous limestone of relatively good quality.

The traditional foundation for wind energy converters in this area is by making use of gravitational foundation, which was e.g. done for Middelgrund. Both the sediments, at least if they are not clayey, and the uppermost limestone, offer a good support for foundations from all relevant aspects.

It was however also considered to use monopile foundations. A monopile can be compared to a console installed vertically. The mechanical function is based on the assumption of the lowest part affixed in the bedrock and an upper part free to move in all directions.

The function of the monopile foundation is partly based on the strength and deformation of the bedrock in which it is installed, partly on the free length, that is, the length in water. It is generally assumed that monopile foundations are suitable to water depth of up to about 20m (65ft).

The installation of monopiles, which usually is carried out with the same technique more or less than for a battered pile, requires relatively homogeneous sediments to be penetrated. Sediments with a large content of stones, pebbles and blocks may prohibit installation. At Lillgrund, sediments are rather homogeneous with limited content of coarser material.

Kriegers Flak

Kriegers Flak is a shallow area located about 30km (19mi) south of the Swedish city Trelleborg on the southern coast, at the boarder point between the Swedish, German and Danish economical zones.

OWEC are being projected on the German side of the shallow area, and now also on the Swedish side. The number of converters being considered exceeds a hundred.

Table 1: Advantages and disadvantages for three foundation types, [10]

Foundation type	Advantages	Disadvantages
Gravity steel structures	No pile driving. Can be removed and possibly repositioned. All parts are visible for inspection.	Seabed preparations needed. Time consuming welding details. The space requirements at the site.
Mono pile steel structures	Simplicity No need of seabed preparations.	The requirements of heavy pile driving equipments. Less suitable for sites containing large boulders.
Tripod steel structures	Adaptable to increased water depth. Low blocking effects. Minimum seabed preparations.	Specialised fabrication methods. Not suitable for sites containing large boulders. Not suitable for shallow waters (<6m (20ft)).

As Kriegers Flak is located further away from the Swedish coast line, esthetic values are maybe less pronounced in the argumentation against the localization of the converters. However, all other issues are present. Also arguments from shipping companies can be seen. However, the application and approval process will in spite of this be quicker and less problem filled compared to that for Lillgrund.

The typical soil profile at Kriegers Flak consists of an uppermost layer of sediments, mainly sand on the shallow parts, sand being covered with clayey soils with a water depth exceeding about 12m (39ft). Sediments are underlain by clay till resting on limestone. The thickness of the sediments varies between a few meters to more than 20 meters. On the shallowest parts of the area, like at Lillgrund, the finest grained sediments have been eroded exhibiting only clay till. The water depth varies from about 5m (16ft) to about 20m (39ft).

The limestone profile resembles to a great extent to that for Lillgrund, besides that the Copenhagen part maybe being thinner. Otherwise, the quality in terms of strength and deformation properties can most probably be assumed as more or less identical.

As the water depth at Kriegers Flak is larger, gravitational foundations might not be suitable. This decision must be taken after a detailed study. Other foundation methods which can be applied are the monopile technique and the triode technique.

The applicability of the monopole technique is partly limited by the water depth, partly by the quality of the sediments and bedrock in which it is installed. Even if the clay till is a firm type of soil with relatively high quality, it might still not be competent enough to result in the lower part of the monopole foundation being affixed. Installation in the limestone might thus be necessary. Detailed studies will show this.

At larger water depths than about 20m (39ft), monopole foundations are considered less suitable. Other options would then be the tripod foundation. Also if the installation depth of the monopole would be too large, e.g. through sediments and in limestone, the tripode foundation may be considered.

The sediments at Kriegers Flak contain coarse material, such as stones and blocks. The distribution is partly in layers, if yet not present all over the area, partly randomly distributed in the sediments in the area. Such conditions can lead to difficulties trying to install piles by battering. Combinations of drilling and battering might therefore be necessary, alternatively making use of a foundation method, which does not require large installation depths.

CONCLUSIONS

It has been concluded that the major geotechnical task considering the foundation of off-shore wind converters is to find a cost effective common approach and design methodology for all foundations. The challenging task for the soil mechanical engineer is to really optimize the performance of all soil materials so that the foundations is neither over-dimensioned – which will not be economically sound - nor under-dimensioned which will vilolate safety conditions.

Geotechnical/geological investigations should be carried out in a systematic step-wise way so as to gather appropriate information to precede with evaluations of appropriate foundation techniques. Possible steps could be

- geophysical methods to get an overview of the area
- division of the actual area in sub-areas with similar conditions.
- detailed investigations in each sub-area, e.g. sounding, sampling etc.
- if appropriate evaluation of the drivability of sediment layers if battered pile foundations are considered.

For each sub-area the foundation technique is optimized which can lead to different techniques used in different areas. However, in order to get economically acceptable solutions, only one technique should be chosen for each sub-area.

ACKNOWLEDGEMENTS

The work was sponsored by Ramböll Sverige AB. The authors wish to thank Håkan Sandstedt, Eva Petersson and Annika Holmqvist for the moral and financial support.

REFERENCES

[1] Houlsby, G.T., Kelly, R.B., Byrne, B.W., (2005), Field trials of suction caissons in clay for offshore wind turbine foundations, Géotechnique 55, No. 4, 287-296.

[2] Camp, T.R. et al. (2003), Design methods for offshore wind turbines at exposed sites, Garrad Hassan and partners Ltd.

[3] Feld, T, Lorin, J, Hald Sorensen, P, Structural and Economic Optimization of Offshore Wind Turbine Support Structure.

[4a] Trumars, J, Bergdahl, L, (2002), Numeriska modeller av vågutbredning för beräkning av våglaster mot vindkraftverk till havs, Rapport nr 2002:2, Vatten Miljö Transport, Chalmers Tekniska Högskola, ss. 40, (in Swedish).

[4b] Schwarts, S., (2003), Certification of Offshore Wind Farms, Germanisher Lloyd WindEnergie GmbH, Steinhöff 9, Hamburg, Germany.

[5] Petersen, P, (2003), Project Certification of Offshore Wind Farms, Workshop.ppt presentation, 24/08/2003, DNV.

[6] Behrendt Ibs∅, J, (2003), Support Structures for Offshore Wind Turbines –Design standards Design Optimisation, Workshop.ppt presentation, 24/08/2003, DNV.

[7] Ferguson, M.C., M. Kühn, G.J.W. van Bussel, W.A.A.M. Bierbooms, T.T. Cockerill, B. Göransson, L.A. Harland, J.H. Vughts, (1998), Opti-Owecs report volume 4, "a typical design solution of an offshore wind energy conversion system". Institute for wind energy ISBN90-76468-05-2, Delft, The Netherlands, 100 p.

[8] Behrendt Ibs∅, J, (2003), Offshore Wind Turbines –Design standards, Workshop.ppt presentation, 24/08/2003, DNV.

[9] Camp, T.R., Morris, M.J., van Rooij, R., van der Tempel, J., Zaaijer, M., Henderson, A., Argyriadis, K., Schwartz, S., Just, H., Grainger, W., Pearce, D., (2003), Design methods for offshore wind turbine at exposed sites., EU Joule III Project JOR3-CT95-0284.

[10] Feld, T., Rasmussen, L., Hald S∅rensen, P., (1999), Structural and economic optimization of offshore wind turbine support structure and foundation, Proc. of 18th Int. Conf. on Offshore Mechanics and Artic Engineering, 9pp.

ABBREVIATIONS

DK	Denmark
DNV	Det Norske Veritas
GL-Wind	Germanischer Lloyd WindEnergie GmbH
ICE	International Electro technical Commission
LRFD	Linear Combination of Individual Load Processes
OWEC	Offshore Wind Energy Converters
OWT	Offshore Wind Turbine
R&D	Research and development

GEOPHYSICAL METHODS FOR SITE CHARACTERIZATION FOR MARINE FOUNDATIONS

Richard E. Sylwester, Golder Associates Inc., 18300 NE Union Hill Road, Redmond, WA, USA

Evaluating surface and subsurface conditions for marine foundations (bridges, causeways, terminals, etc.) is often done with a limited amount of data. Subsurface information for these projects is primarily acquired using traditional methods, such as boreholes, test pits or divers, which tend to be expensive and limited in the area of coverage. A number of geophysical methods, including precision bathymetry, sidescan sonar, and seismic reflection or subbottom profiling are extremely cost-effective and obtain significantly more data than can be acquired using traditional intrusive methods. These geophysical methods provide detailed surface images and continuous profiles of the subsurface stratigraphy. This information can be invaluable for selecting the best location for geotechnical boreholes and to map potential geohazards such as submarine slides and filled or open scour holes. Offshore investigations conducted for a proposed highway bridge (Knik Arm Bridge, Cook Inlet, AK), the retrofit of two existing bridge (Antioch and Dumbarton Bridges, CA) and a proposed cruise ship terminal (Ketchikan, AK) used a combination of geophysical methods to map water depth, detect and map debris on the seabed, map the thickness of unconsolidated sediment, determine the depth to bedrock and identify potential geohazards such as scour holes. The results of the geophysical investigations will be used to select locations for obtaining geotechnical borings, to extrapolate geologic information between existing or proposed boreholes, evaluate the potential depth of scour and design a pile support pier. Geotechnical engineers, offshore contractors and bridge designers are realizing the importance of the early use of offshore geophysics for (i) site characterization, (ii) to reduce the uncertainty of geotechnical conditions thus avoiding designs that may be overly conservative and thus more expensive and (iii) to assist in selecting locations for geotechnical borings.

INTRODUCTION

Subsurface information for marine projects is primarily acquired using traditional intrusive methods such as boreholes, test pits or with divers offshore. Geophysics, the study of the earth and its physical and material properties, can provide a cost-effective, non-intrusive approach for initial site reconnaissance and/or detailed investigation. The use of surface and borehole geophysical methods for onshore projects is well documented and a number of publications are available describing these methods (see Bibliography). However, technical information and case histories on the application of offshore geophysical methods for bridges, terminals, or causeways that span or are located adjacent to waterway are not as readily available in the literature.

Geophysical methods based on the physics of acoustics include precision echosounding, sidescanning sonar and subbottom or seismic reflection profiling. These techniques provide a cost-effective means to investigate and map surface and subsurface sediment and other geologic features offshore. This paper introduces the fundamentals of these methods and presents three case histories demonstrating how offshore geophysics provided invaluable information that would have been prohibitively expensive had it been acquired by traditional intrusive methods.

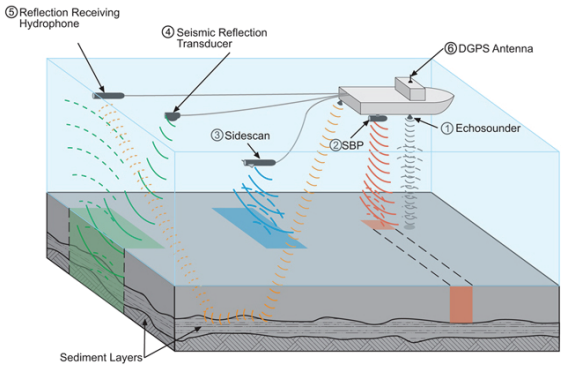
CONSIDERATIONS FOR CONDUCTING OFFSHORE GEOPHYSICAL SURVEYS

The primary considerations when planning an offshore geophysical investigation are the selection of the survey vessel, geophysical instrumentation and navigation or positioning. The selection of these parameters depends on a number of factors including the location of the study area (ocean, river, lakes, etc.) project

objectives, how the data are to be used, size of the survey area, expected subsurface geology and possible operational limitations (tides, currents, obstacles, shallow water vessel traffic, etc).

The use of acoustics or sound is the primary technique for performing offshore geophysical investigations. The acoustic methods are echosounding, sidescanning sonar, subbottom profiling and seismic reflection profiling. Each method provides different information that together produces a comprehensive understanding of surface and subsurface conditions. As shown in the following illustration, data from the four methods can be acquired simultaneously.

The following is a brief discussion of the techniques or methods that make use of the principals and physics of sound. Three case histories that illustrate the use of these methods are presented in the last section.



FUNDAMENTALS OF INSTRUMENTATION AND METHODS

The instrumentation required for the subsurface investigations discussed in this paper are relatively portable and can easily be transported to remote sites and installed on small vessels. For in-land waterway projects vessels of opportunity can almost always be found locally or easily transported to the site. Vessels ranging in size from 15 to 20 feet are generally adequate in protected water areas. On larger bodies of water (lakes, estuaries, and large rivers) it is generally necessary to use vessels that are 20 to 25 feet in length with a covered area for the instruments.



Geophysical survey from small inflatable (above) and barge (below)





Dedicated survey vessel

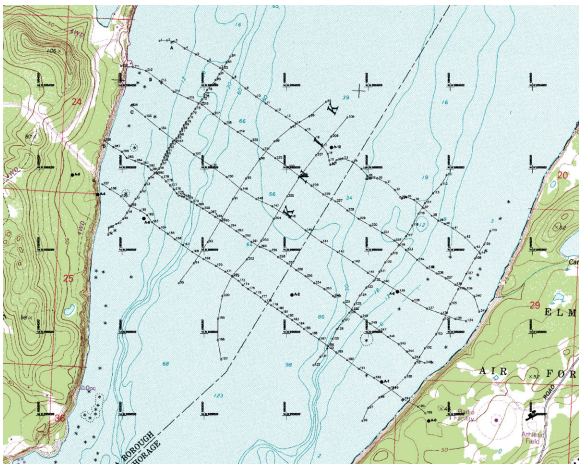
A complete offshore geophysical system (navigation, seismic source, sidescan sonar and digital acquisition) typically weighing less than 500 lbs can be transported in 4 to 5 shipping boxes (24in.X 24in. X 20 in.). Generators (1 to 2kw) are usually rented on site although they can be shipped if necessary. These instruments can be installed on a vessel in two to three

hours and the survey can proceed following a brief operational check.

Navigation and Survey Transects

Offshore geophysical investigations use the global positioning system (GPS) for determining the position of the survey vessel. The GPS navigation system obtains information from satellites while underway with an accuracy of approximately +/- 10 feet. However, the position accuracy can be significantly improved (+/- 1 foot) using differential GPS. This method, which is routinely used, consists of correcting the position data by comparing the onboard GPS receiver data to data acquired by a receiver located on accurately known positions (U.S. Coast Guard beacons, GPS receivers placed on monuments located in the survey area, or from a commercial satellite system that broadcasts corrections for specific areas). The "difference" between the two is the correction that is applied to the onboard GPS data. This can be done in real-time or information from land based receivers for a given area and time period can be downloaded on the internet and the corrections can be made post-survey.

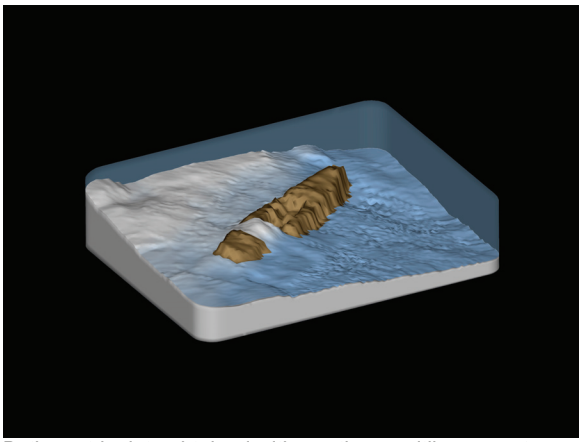
The survey consists of running a series of transects across the area of interest, such as a parallel to a proposed bridge crossing, in addition to several cross lines. The desired transects are displayed on an LCD monitor which also shows in real-time the actual transects being run by the vessel. The position information, acquired 1 to 10 times each second, is stored digitally and is used for producing a trackline map needed for the data analysis phase.



Example of survey tracklines with navigation event numbers.

Bathymetry-Precision Echosounder

A survey grade precision echosounder is used to obtain accurate measurement of the water depth. The data are obtained with a high frequency transducer (100 to 200 kHz typical), which can resolve very small changes in bottom relief (+/- 0.1 foot). For surveys of large areas or areas with complex bottom conditions bathymetric data is often acquired with a multibeam or swath system. These systems acquire 50 to 150 depth measurements over a swath that is typical equal to 3 to 10 times the depth of water. Although the use of this system is considerably more expensive than a single beam echosounder it may be more cost-effective under some situations. For example dense coverage (soundings on 3 to 5 foot grid spacing) in an extended area would be nearly impossible to achieve using the single beam echosounding method (almost impossible to run transects on 5 foot line intervals) as well as time-consuming and expensive.

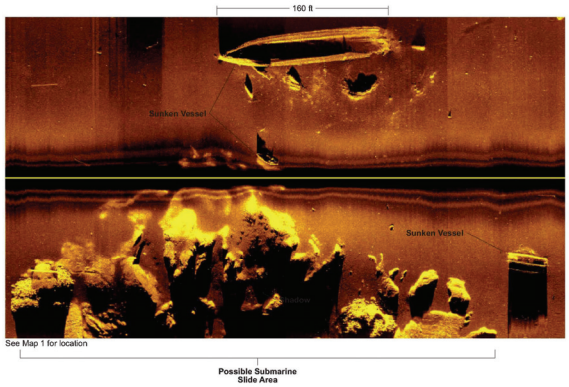


Bathymetric data obtained with swath or multibeam system showing sunken vessel

Sidescan Sonar

Sidescan sonar produces a plan view image of the bottom to either side of the survey vessel trackline. As the survey vessel moves along the track line the sonar transmits a fan-shaped acoustical signal. The full width of this image, which is controlled by the operator, typically ranges from 150 to 500 feet. This image is used to map lateral variations in soil type (sand, gravel, mud etc.), identify exposed bedrock and geologic hazards such as landslides, depressions and surface faults, as well as to detect and map the location of cultural artifacts

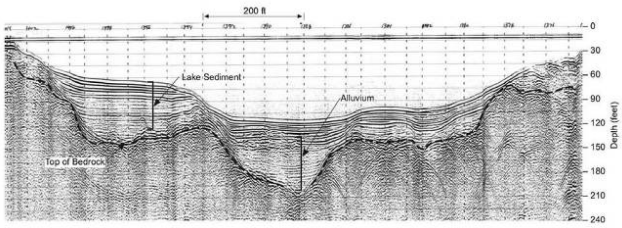
such as pipelines, sunken vessels and discarded debris.



Sidescan sonar image showing sunken vessels and submarine slide located on the route proposed for a new bridge.

Seismic and Subbottom Reflection

Subsurface reflection methods are used to image sediment layers, depth to top of bedrock, detect discrete objects such as pipeline, boulders etc, that are located below the bottom of water covered areas The data are obtained using various types and sizes of acoustic sources and receivers. The choice of instruments depends on the geologic characteristics of the bottom, the desired resolution or details to be mapped and the required depth of subsurface penetration. High-frequency acoustic systems (3 to 10 KHz) can be expected to penetrate 5 to 30 feet of fine-grained sediment with excellent vertical resolution (0.3 to 1 foot). On the other hand lower frequency seismic reflection systems (400 Hz to 1 KHz) can achieve 50 to hundreds of feet of penetration in medium- to coarse-grained sediment with a reduced resolution of 1 to 3 feet.



Examples of seismic reflection field record that is displayed in real-time during the survey. This profile was obtained in 5 minutes.

The reflected energy is received at the water surface by a hydrophone or in the case of subbottom profilers by the same transducer that transmitted the signal. The received signal is converted to an electrical signal and printed in real-time on a graphic recorder that displays a continuous cross-section image of the subsurface along the survey trackline. The data can also be collected digitally. The data are acquired at vessel speed of 3 to 4 mph and a subsurface reflection is obtained two to four times each second. This represents a data point every 5 to 10 feet. Each data point has a corresponding position coordinate so that during data analysis it is possible to accurately map subsurface geology, stratigraphy or other features of interest.

PRESENTATION OF DATA

There are several options for presentation of the interpreted data, as well as the field or actual geophysical data, for each geophysical methods employed for the investigations. Several presentation examples are included in the section on case histories. The following summarizes some of the options for presentation of the interpreted data.

Trackline Data

The trackline data, illustrating the survey coverage or survey tracklines, are presented on a CAD or GIS compatible maps. These maps can be used to review a specific piece of geophysical data. Event numbers are shown on the tracklines, typically at a fixed interval of time or distance (30 seconds, 100 feet etc) that correspond with event numbers on the geophysical data. The event numbers and the corresponding geographic coordinates can also be provided in digital or tabular format.

Bathymetric Data

These data are presented as contour maps, in tabular format (x, y, and z) and as isometric, 3-D or shaded view images. All maps can be GIS or CAD-compatible at a scale specified by the client. The data can also be superimposed on orthophotographs of the site.

Sidescan Sonar Data

The sidescan sonar data is usually presented on a surficial features map which represents an interpretation of the data. This map shows the location of debris, the interpreted lithology of the bottom (silt, sand, gravel), biohabitats and

distribution of marine or aquatic plants, potential archeological or other cultural features, and geohazards such as fault lines, zone of subsidence or submarine slides. The data can also be presented as a mosaic which is an acoustic photograph of the bottom constructed from the individual sidescan records made on adjacent transects. The mosaic image can be placed on an orthophotograph of the site.

Subbottom and Seismic Reflection Data

The subsurface reflection data is presented on a series of interpreted profiles that represent the subsurface stratigraphy and geology in the area of interest. The interpreted data are also presented on a series of maps that might include a map of the thickness of unconsolidated sediment (isopach map), a map of the depth or elevation of top of bedrock, and a structural map. The availability of borehole data provides a means to apply geologic names to the interpreted seismic units or reflectors.

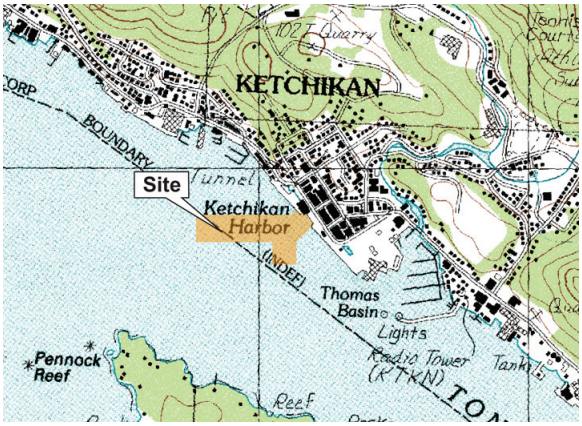


Contour map of top of bedrock based on seismic reflection data.

CASE HISTORIES

Three representative examples of offshore geophysical investigations conducted in support of projects are now discussed. The three studies were performed in entirely different environments and required different considerations with regards to survey vessel, instrumentation, and operations to achieve the project objectives.

Ketchikan Harbor Cruise Ship Terminal



Location of geophysical survey conducted for proposed cruise berthing terminal, Ketchikan, AK

Ketchikan Alaska has seen a significant increase in the number of cruise ships arriving during the summer tourist season. Often two to three of these deep-draft vessels, 600 to 900 in length, arrive simultaneously. The existing pile supported facility, located at the city dock, may be unable to handle an anticipated increase in vessel arrivals in future years. Therefore alternative locations are being considered for developing new berthing facilities.

Project Objectives

The objective of the geophysical survey was to obtain information that would be used to select a new location offshore of the existing docks and to obtain subsurface data to assist in the design of a proposed pile-supported berthing facility. The specific information requested included accurate depth of water, qualitative classification of the seafloor sediment (silt, sand, till, etc), identification of debris, bedrock knobs, biohabitats, etc. on the seafloor that might adversely impact construction and the depth to top of bedrock. This information was critical for determining the amount of dredging that might be required, addressing potential environmental issues, estimating length of piles and selecting locations for borings for determining geotechnical properties of soil and bedrock.

Survey Operations

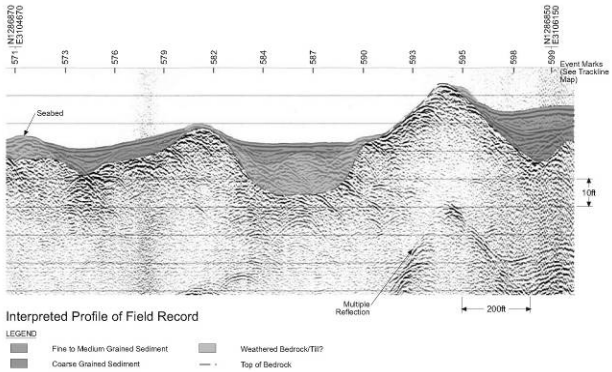
The investigation was performed using DGPS, a single beam precision echosounder and high-resolution seismic reflection system. The instruments were flown to Alaska and installed on a small fishing vessel (24 feet) in one day. The geophysical data were then collected in one day, on a series of transects that were laid out on a grid (50 foot spacing) over the proposed berthing site and approaches to the site.

Summary of Survey Results

The results of the investigation were presented on a series of AutoCAD maps and interpreted profiles showing bathymetric contours, surficial features including lateral distribution of sediment the location of shallow bedrock exposures, thickness of fine-grained sediment and a plan and profile of the interpreted surface and subsurface geology along the area of the proposed berthing facility.

The water depth ranged from 80 to 120 feet which was more than sufficient for safe operation of the cruise ships and it was clearly apparent that the proposed berthing area would not require dredging. However, the presence of a bedrock shoal immediately to the south of the proposed berth was of concern because it was a potential hazard to navigation when entering or exiting the berth. In addition, the bedrock knob was a significant biological habitat.

The seismic reflection data identified an additional problem. It was quite evident that the geology of the proposed site was considerably different than the geology at the existing terminal. At the existing terminal the marine and glacial marine sediment were 40 to 60 feet thick and provided sufficient support for the piles. However, the seismic reflection profiles clearly showed that at the proposed berthing site the thickness of sediment was extremely variable (0 to 20 feet), and mantled a highly irregular bedrock surface. This finding resulted in reconsidering as to whether the project could proceed considering the potential costs associated with having to socket the piles into holes drilled into bedrock.



Seismic reflection profile showing unconsolidated sediment (fine-grained, coarse-grained) overlain on weathered bedrock and bedrock. This is the field record that was obtained in 3 minutes.

Knik Arm Bridge Crossing-Cook Inlet Alaska

Cook Inlet extends north and then east from the Gulf of Alaska. It divides into two arms: Knik Arm on the north and Turnagain Arm on the south, with Anchorage on the peninsula between the two. The Knik Arm Bridge and Toll authority is studying the feasibility and cost for constructing a bridge across Knik Arm providing easy access from the City of Anchorage to the east shore of Knik Arm. During early stages of this study a number of offshore borings were obtained to obtain geotechnical data for conceptual studies of the crossing. The borings were done from a jackup barge which was unable to work in the deeper water along the center of Knik Arm and was also unable to drill to bedrock. A geophysical survey was requested by Alaska Department of Transportation (ADOT) to fill in these data gaps.

Unusual Operation Conditions

Cook Inlet and its two arms (inlets) have extreme tidal range (30 to 35 feet) producing large tidal currents, and at low tide large areas of the two arms are exposed mud flats. Because of the currents and shallow water it was necessary to use a survey vessel with considerable power, enough space to carry the primary geophysical equipment and backup equipment, and have a shallow draft to work in the nearshore area. The large tidal currents restricted the survey time to approximately 2 to 3 hours during relatively slack water conditions.

Survey Operations

The geophysical data were acquired with a precision echosounder, high-resolution reflection system (sparker) and deep penetration reflection system (airgun). The two acoustic systems, with different output characteristics, provided higher resolution information on the upper 200 feet (sparker) and deeper information with less resolution to a depth of 800 feet. Navigation was provided with a differential GPS.

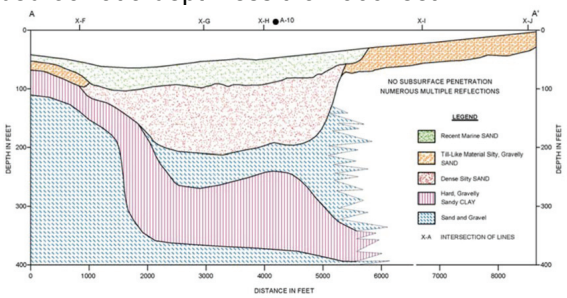
The survey consisted of running a series of parallel transects across the inlet spaced at an interval of approximately 500 feet. A second set of transect was run perpendicular to these spaced at an interval of 2,000 feet.

Summary of Results

The bathymetric data, acquired on wide line spacing, were used to produce a reconnaissance level contour map. The water depth within the survey area ranged from –5 feet to -90 feet referenced to mean lower low water. The data were interpreted using the method of seismic facies analysis. This method identifies various reflection patterns (uniform horizontal reflectors, discontinuous reflectors, chaotic reflectors, etc.) on the graphic records and then assumes they are characteristic of a particular lithology or depositional environment. For example, a geophysical facies on the record consisting of continuous, thin layers suggests fine-grained sediment deposited in a low energy environment. Sediments deposited in a high-energy environment usually produce very strong reflections (dark layers on the records) and the reflectors are often discontinuous. The availability of borehole data (11 boreholes) made the interpretation process considerably easier and more reliable.

Interpreted subsurface features or boundaries, sediment thickness and depth to subsurface reflectors from both data sets (sparker and airgun) were integrated and used to produce interpreted profiles or cross sections for each of the survey transects. In the shallow water areas the near-surface deposits are interpreted to be predominantly sand and sandy gravel and where there was limited subsurface penetration, are very dense, and contain cobbles. In the deep-water central area the seafloor is mantled with recent marine deposits of loose sediment that typically ranged in thickness from 5 to 40 feet.

Underlying the surficial deposit is approximately 100 feet of dense to very dense silty sand that is underlain by hard, gravelly clay. This sediment is deposited on what are interpreted to be sand and gravel and marine or glacial marine deposits. There was no evidence on the reflection data to suggest the presence of bedrock at a depth less than 900 feet.



Interpreted geophysical record, Knik Arm Alaska. Contacts based on interpreted geophysical data and geology based on borehole data.

Retrofit of Antioch and Dumbarton Bridges

The California Department of Transportation (Caltrans) and the Bay Area Toll Authority (BATA), plan to undertake seismic evaluations of the Dumbarton and Antioch Bridges to withstand potential future earthquakes. Under this contract Earth Mechanic Inc. is providing geotechnical engineering services necessary to support the retrofit designs and collaborate with Caltrans design engineers on the retrofit project. To assist in the retrofit design program an offshore geophysical program was conducted at the two bridges.

Project Objectives

The specific objectives of geophysical program and the methods used to achieve these objectives included:

- Provide detailed bathymetric map and evidence of scour around the bridge piers.
- Locate and map debris on the seafloor that might impact emplacement of new piers.
- Continuous profiles of the subsurface stratigraphy and geology.

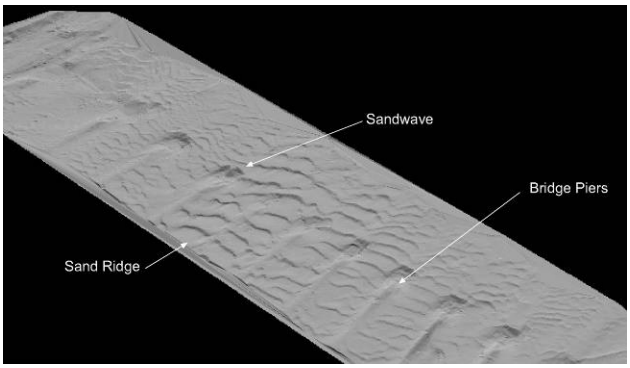
Survey Operations

The survey vessel was mobilized in Seattle and driven to California for this project. Although the equipment and geophysical crew could have flown to California and rented a vessel it was determined that it was more cost- effective to mobilize a vessel in Seattle (where the geophysical equipment is located) and drive the 12 hours to California.

The survey at each bridge consisted of running a series of parallel transects on either side of the bridge and cross lines between the bridge piers. The geophysical investigation, which included multibeam bathymetry, sidescan sonar and seismic reflection and subbottom profiling, was completed in one day at each bridge.

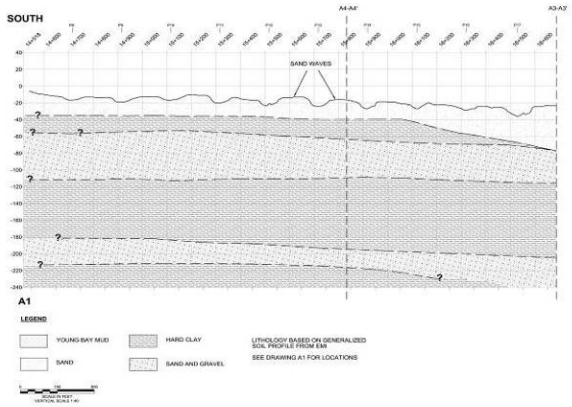
Summary of Results

The multibeam bathymetric data, displayed as shaded relief images and contours, produced detailed image of the seabed at each of the bridges. Subtle geomorphologic features, produced by the hydrodynamic regime of tidal currents, such as small sand waves, depressions and ridges of sand, could be clearly identified. The sidescan sonar data also detected these features in addition to the bridge piers, a number of localized pieces of debris including cables, pipes and unidentified small discrete targets. The exact location of these objects was determined from the sidescan sonar data that were digitally acquired.



Multibeam bathymetric data from Antioch Bridge

The subbottom and seismic reflection data were able to map the shallow stratigraphy as well as deeper reflectors to a subsurface depth of 250 feet below the seabed. The seismic reflection data were correlated with borehole data that had been acquired during construction of the bridges. Additional interpretation of the data will be conducted following completion of a new ongoing drilling program.



Interpreted geophysical profile, Antioch Bridge. Geological classification based on borehole data.

CONCLUSIONS AND SUMMARY

Offshore geophysical investigations provide a rapid and cost-effective means for obtaining surface and subsurface data. In addition to providing detailed images of the subsurface, the data are extremely useful for planning cost-effective sampling programs that use traditional, but often more expensive, geologic, geotechnical and engineering methods.

When planning an offshore geophysical investigation it is extremely important to clearly define the objectives of the investigation, the desired deliverables and how the data are to be used in conjunction with existing data or data that may be acquired with other methods. A clear presentation of this information may significantly affect on whether or not the results of the geophysical investigation are successful and provide added value to the project.

REFERENCES

Federal Highway Administration, 1989. Proceedings of the Bridge Scour Symposium, Report No. FHWA-RD-90-035.

Golder Associates Inc., 2002. Geophysical technology for identification of geology/geotechnical characteristics, Report to Transportation and Public Facilities, State of Alaska.

Golder Associates Inc., 2003. Report on the Knik Arm geophysical investigation, Cook Inlet Alaska; prepared for Alaska Department of Transportation and PBD&Q.

Golder Associates Inc., 2004. Report on the Ketchikan proposed cruise terminal; Prepared for Hart-Crowser Associates, Seattle, Washington.

Golder Associates Inc., 2006. Report on the offshore geophysical investigation for the Hwy 520 floating bridge: Prepared for Washington State Department of Transportation.

Golder Associates Inc., 2007. Report on the geophysical investigation of the Antioch and Dumbarton Bridges, California; Prepared for Earth Mechanics Inc. and CALTRANS.

Golder Associates Inc., 2007. Report on the geophysical investigation for replacement of the Hwy 59 Bridge, Kansas; Prepared for the Kansas Department of Transportation.

NCHRP Project 20-5, 2004. Synthesis of highway practice 36-08, Use of geophysics for transportation projects.

Sylwester, R. E., 2005. Geophysical methods for site characterization of offshore highway structures; 56th Highway Geology Symposium.

Sylwester, R. E., 1983. Single-channel, high-resolution, seismic-reflection profiling: An introduction to the fundamentals and instrumentation: Geophysical Exploration at Sea, Geyer, R., Editor, CRC Press, Boca Raton, Florida.

Sylwester, R. E. and Anderson, R., 1997. A view below the surface: Civil Engineering News, January, 1997, pp. 8-11.

Sylwester, R. E., LOWELL, S., Cromwell, R., AND D. Hrutfiord, 1997. A geologic and geophysical investigation to determine the impact of marine erosion on SR-105, Willipa Bay, Washington: AEG 40th Annual Meeting, Portland, Oregon, September 1997.

WWW.cflhd.gov: Geophysical Imaging Resource Site; Federal Lands Highway Program

OFFSHORE WIND TURBINE FOUNDATIONS – IN DENMARK AND BELGIUM

Jørn H. Thomsen, COWI A/S, Denmark
Torben Forsberg, COWI A/S, Denmark
Robert Bittner, P.E., Ben C. Gerwick, Inc. San Francisco, CA, USA

INTRODUCTION

This paper presents the experience gained and the lessons learned over the last decade within the numerous offshore foundation projects undertaken in the offshore waters of Denmark and Belgium by COWI A/S of Denmark. This experience derives from the close collaboration with, and interaction between the owners, contractors, and engineers in the various stages of project development. In turn, the experience draws on COWI's experience within foundation of large bridges world wide over half a century.

Focus is on two pioneering gravity base foundation projects:

- Nysted in Denmark, currently the largest offshore windfarm worldwide with 72 Nos Bonus 2.3 MW turbines in water depths up to 10 m in the relatively benign inner Danish waters
- Thornton Bank in Belgium, where the first phase - comprising 6 Nos REpower 5MW-turbines of a total of 60 - are planned to be built in the rough North Sea in water depths exceeding 25 m.

The two projects illustrate the speed at which the structural concept must keep pace with increases in turbine size. The projects exemplify how a tailor made design is made fit for purpose. The latter case uses state-of-the-art designs for thin-walled reinforced concrete shell structures.

Offshore wind turbine foundation design requires development of highly cost effective concepts, because the share of the cost of the foundation relative to that of the complete wind turbine installation is considerably higher than that of an onshore foundation. Further, environmental and energy gain considerations require that windfarms be located farther from shore at consequently deeper waters. With this trend of ever larger turbines in deeper and rougher waters, the design and construction challenges and complexity increase proportionally, and both become closer to or beyond normal experience.

Thus, value engineering becomes crucial for development of foundation concepts that are sufficiently robust to be carried through to site installation without impacting the economic viability of the projects.

This engineering approach is described in the following sections.

ENGINEERING CONSIDERATIONS

In all project phases from concept phase to detailed design, consideration of operational and environmental loads and hydrographic and geotechnical conditions needs to be given interactively with fabrication, installation and logistic demands.

While design develops, focus shifts towards the implementation aspects of the project.

Design, construction and installation of gravity base foundations for offshore wind turbines are similar to those of large bridge foundations, and experience from the latter is valuable for the former.

However, wind turbine foundation design imposes special challenges, in that

- the combined soil-foundation-wind turbine structure is a dynamic system
- hence, loads depend on the response of the system, i.e. are dictated by the overall stiffness of the system
- soil stiffness is load dependent in a nonlinear manner
- therefore, several load iterations are required between wind turbine and foundation designers to arrive at the design loads
- industry practise has it that turbine supply and design of turbines and foundations,

respectively, are carried out under separate contracts with associated demands for strong interface management on the part of the owner

- the dominant loads are horizontal forces from wind, currents and waves
- hence, for gravity base foundations the challenge is to provide sufficient dead weight in the permanent stage through ballasting, while minimising structural dead weight within available equipment range in the installation phase during lifting and transportation
- therefore a close collaboration between the designer and the contractor is crucial in the design stage
- the cost share of the foundation relative to the complete turbine installation may be decisive for the viability of the offshore windfarm development

NYSTED WINDFARM

Background

The design and construction of the gravity foundations for the Nysted Offshore Windfarm, located some 10 km off the southern coast of Lolland, Denmark, (Figure 1) is an example of concept development and design as a result of close collaboration between the contractor and the designer. The foundation concept was developed jointly between the contractor P. Aarsleff A/S and the contractor's consultant COWI A/S in the tender stage and detailed after award of the contract to P. Aarsleff A/S.

The owner was a joint venture between energy companies which have today merged into DONG Energy of Denmark. In this case, the owner had selected to define a comprehensive design basis with all interfaces defined, including stiffness requirements of the foundation.

Project

The project comprises 72 windmill foundations for 2.3 MW Bonus wind turbines, arranged in 8 lines each with 9 turbines. Height of hub above the sea is 68.8 meters and rotor diameter is 82.4 meters, giving a total height of 110 m. The windmills with foundation level from -7.5 to -12.75 m MSL at natural water depths 6 - 9.5 m (MSL), and soil conditions are generally stiff moraine clay.

Concept Development

It was immediately evident that a monopile solution was not feasible due to a high content of boulders. At the same time, these soil conditions were favourable for a gravity foundation, as generally high bearing capacity was met near the natural sea bed.

In the course of tender design, the contractor found that the most cost-effective solution overall would be concrete foundations fabricated in Swinoujscie, Poland, where cheap and skilled labour was available. In turn, this required transport by barges to the site. On site, a floating crane would pick the units up and place them on pre-prepared stone beddings, thus maximising the effective time of the crane.

The transport and installation procedures required that the weight of the concrete foundation units be minimised. This was achieved by the concept of a hexagonal base structure with six open cells, and a shaft and an ice cone at top.

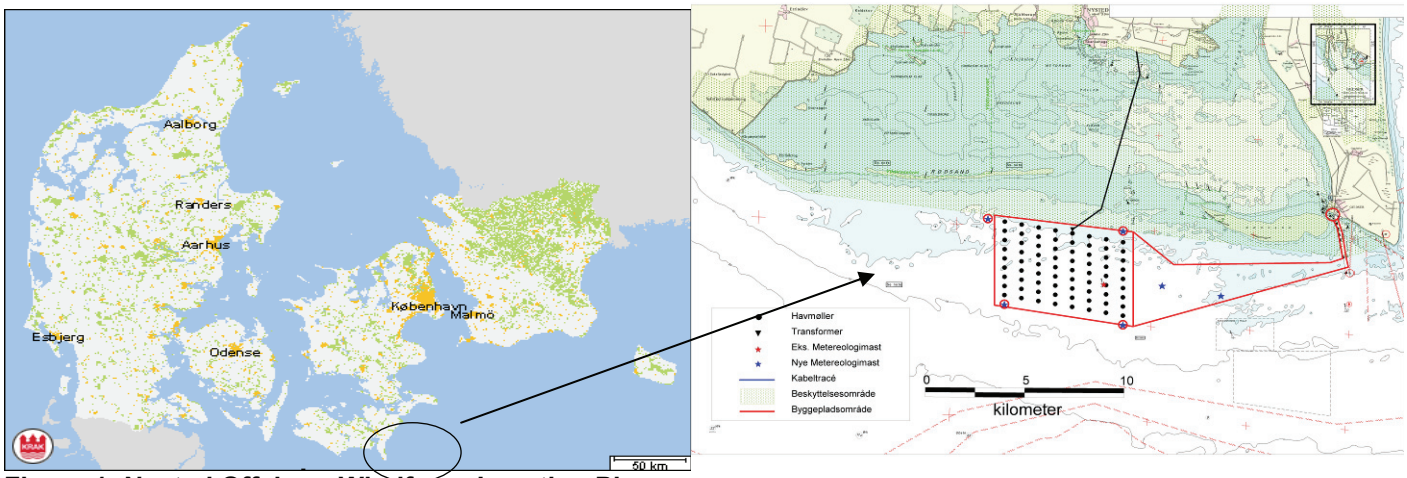


Figure 1: Nysted Offshore Windfarm, Location Plan

The necessary weight was achieved by filling on site with heavy duty ballast in the shaft and the chambers.

Foundation Design

The design appears from Figure 2. The base dimension is 15 m and the maximum height 16.25 m. A concrete weight (in air) under 1300 t was achieved, corresponding to the operational limits set by the floating equipment. The additional weight necessary to provide stability against sliding and overturning was provided by heavy duty olivine material filled in the cells and the shaft, adding another 500 t to the weight.

Note the conical shape at top, which in accordance with Danish practise was required by the owner's specifications to minimise ice loads.

The Contractor and the crane subcontractor Eide Marine designed a purpose built lifting device, shaped as a cone to fit the ice cone. The lifting forces were thus distributed over a large area of the solid concrete ice cone, reducing the local installation stresses to a minimum.

Foundation Installation

The actual performance proved the adequacy of the concept, as a production cycle for 4 foundations on one 10,000 t barge was carried through in 30 days or less, once teething troubles were overcome. With 3 barges in the line, 4 foundations were placed every 10 days, weather permitting. (See Figures 3a and 3b.) The project was carried out according to schedule, from contract award in March 2002 to all foundations in place in the summer of 2003, ready for reception of the wind turbines, Figure 8.

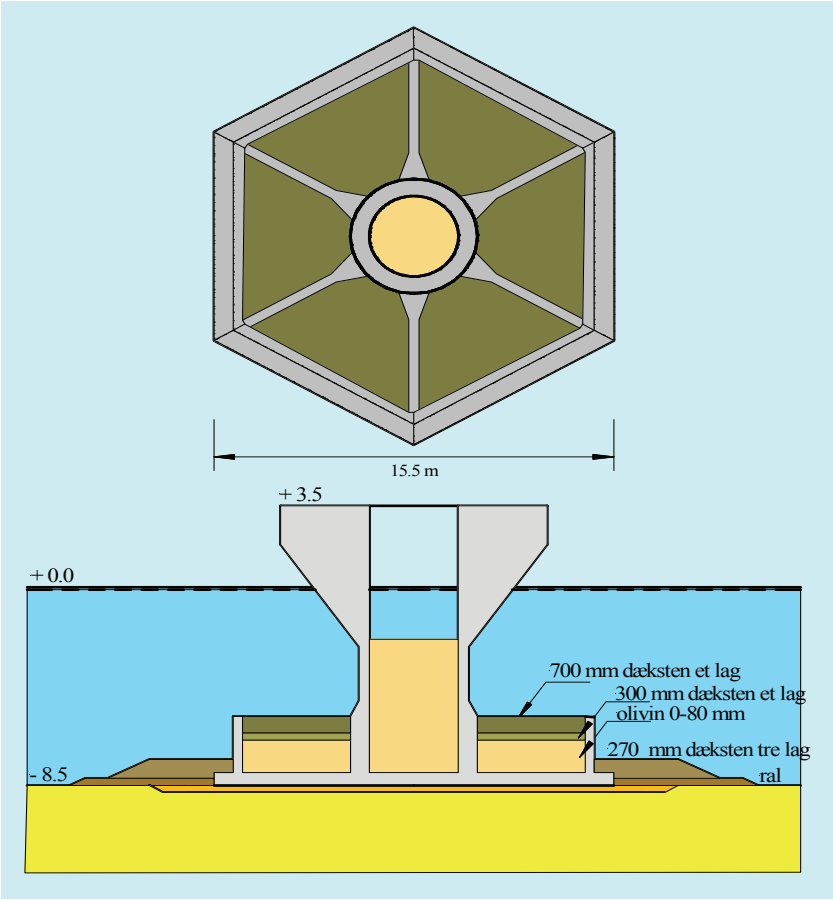


Figure 2: Nysted Offshore Windfarm, Gravity Foundation Concept

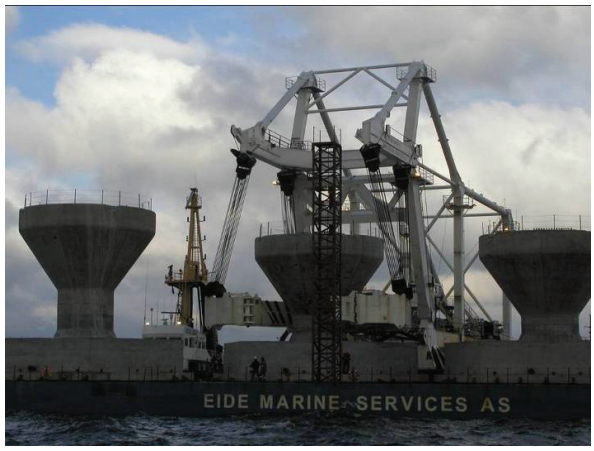


Figure 3a: Nysted Offshore Windfarm, Installation of Foundations

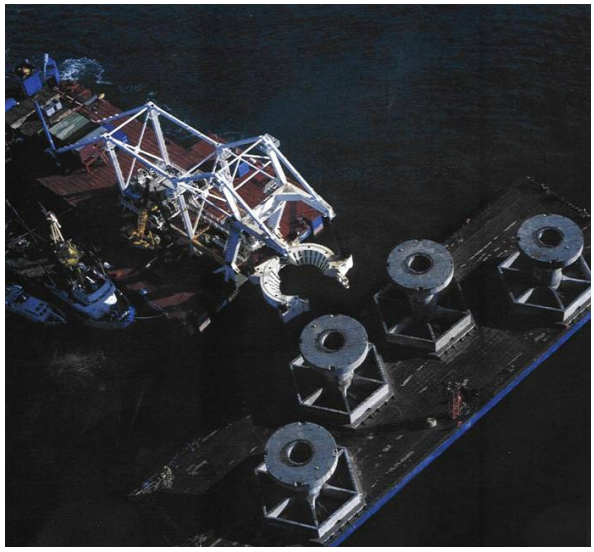


Figure 3b: View of Installation Equipment from above

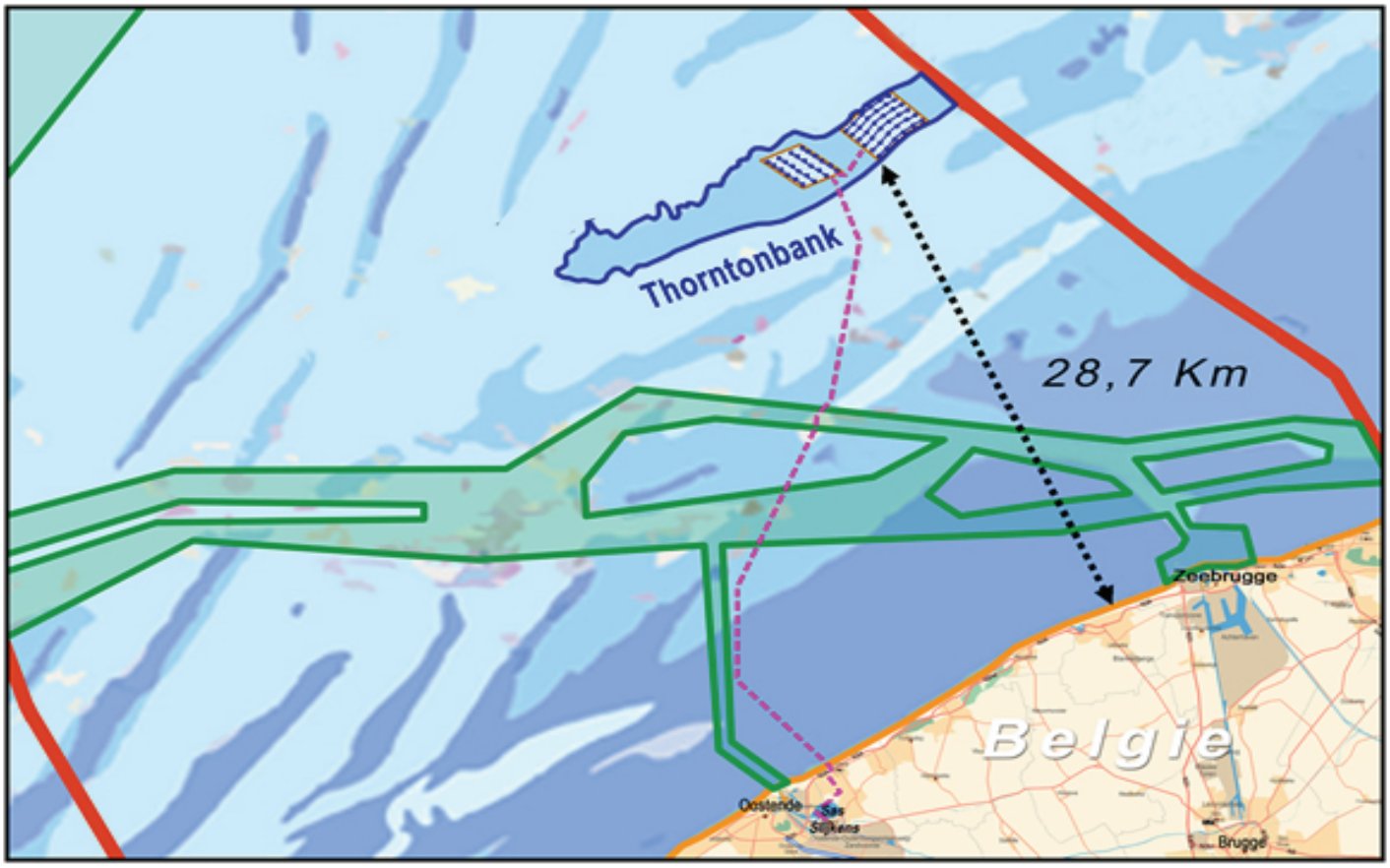


Figure 4: Thornton Bank Windfarm, Location Plan

THORNTON BANK OFFSHORE WINDFARM

Background

One of the most challenging offshore wind turbine projects is currently being developed for the Thornton Bank in Belgium, planned for installation in 2008.

The owner is C-Power n.v. of Belgium, who is undertaking this development of the first offshore windfarm in Belgium. Due to the level of development at the time of writing, only general information is provided.

In this case the owner has decided that the foundation design be carried out as a process between the Owner's Engineer - Technum n.v. of Belgium in cooperation with DONG Energy of Denmark; the turbine supplier - REpower Systems AG of Germany, and the Marine Contractor - Dredging International with its consultant COWI A/S of Denmark as designer.

Project

The final project will comprise 60 wind turbines, arranged in 2 arrays each with 4x6 and 6x6 turbines, respectively, (See Figure 4.) The development is planned in three design/construction phases, of which the current first phase comprises 6 turbines.

The turbines, located some 30 km off the Belgian coast, are planned to be REpower 5 MW turbines, with hub above the sea is 95 m TAW (chart datum corresponding to LAT). The windmills are founded at -21.5 to -27 m TAW and soil conditions are generally sand of medium grain size.

Concept Development

This concept was initially developed as a result of collaboration between the marine contractor and his designer.
Given the rough environment of the North Sea, it was evident that construction procedures at sea should be kept at a minimum. Therefore, the Nysted solution with external chambers was not relevant as infill works would be vulnerable to adverse sea conditions.

For the large water depths and the increasing size of wind turbines, structural stiffness and fatigue issues become decisive. A post-tensioned concrete structure offered solutions to these issues.

Further, structural weight minimisation consideration led to the conclusion that a conical shell structure would be most efficient in terms of:

- providing sufficient volume for ballast material
- direct load transfer from turbine base to foundation level
- slender structure, yet with high stiffness
- one set-up for in-fill operations
- no need for diver assistance

An important feature at the location is that sediment transport takes place, causing sand dunes to move along the area. Foundation level should therefore be selected to ensure that troughs of the sand dunes would not jeopardise the integrity of the foundation layers. This aspect has been dealt with by the owner's engineer in subsequent design phases.

For the sake of comparison to the Nysted project, it should be mentioned that no ice cone is needed at this location.

Foundation Design

At the time of writing, the design process is ongoing, with design loops between the foundation and turbine designers. The design is presented at this preliminary stage of the project.

The structure is composed of a cylindrical shaft on top of a conical base transferring the loads from the turbine directly to the base slab. The base slab is designed with a central void fille with soft material in order to ensure that the dynamic loads do not create a hump with risk of rocking.

The structure is post tensioned in order to provide sufficient strength and linear stiffness properties as well as fatigue and crack resistance.

The design features appear in Figure 5. At the deepest location the foundation extends from foundation level -27m TAW to top level +17 m TAW. The foundation base diameter is 21.5 m and the shaft diameter is 6.5 m, matching the diameter of the turbine tower.
The structural concrete weight is about 2700 tonnes. The ballast will be a combination of sand and heavy fill, sufficient to ensure the stability against the overturning moments. The total dry weight may be up to 7000 tonnes, depending on quantity and type of heavy fill.

The scour protection, designed by the owner's engineer, is arranged at a level below the trough of moving sand dunes.

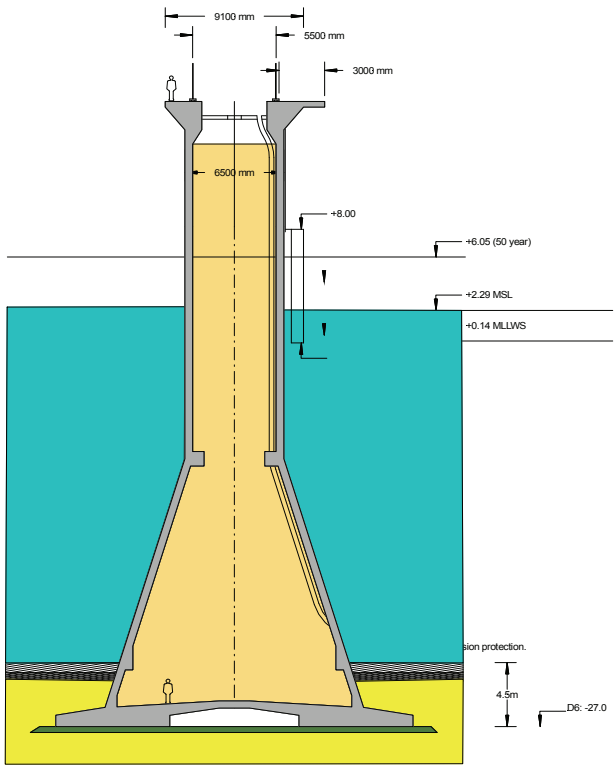


Figure 5: Thornton Bank Windfarm, Gravity Foundation Concept

Installation Considerations

The design assumes that the foundations will be constructed onshore at a yard with necessary quay facilities. The lifting and transport consideration are based on use of a floating crane.

Installation procedures are being developed at the time of writing and further detailing is referred to the future. However, given the size and the environment it is a prerequisite that marine equipment and operators be of capacity and experience capable of meeting the challenges met.

Figure 6 shows the installation of a REpower 5MW turbine for the Beatrice Windfarm Demonstrator project August 2006.



Figure 6: Installation of Repower 5MW Turbine for the Beatrice Windfarm Demonstrator Project, Scotland

LESSONS LEARNED

Development Trends

The presented projects demonstrate the speed at which wind turbine industry is developing in general, and offshore windfarms in particular.

Obviously, the economic viability of offshore windfarms is depending on the competitiveness relative to other energy sources. The introduction of the Clean Development Mechanism (CDM), see e.g. [1], of the Kyoto Protocol in 2008 is believed to further favour the competitiveness of renewable energy projects. This is argued for in a recent publication issued by Vestas [2].

It has been said that the current development stage of the wind industry is comparable to that of the aeroplane industry in the fifties and sixties: any prediction of the limits to turbine and windfarm sizes are quickly surpassed by the actual developments.

Figure 7 visualizes the case, showing the two foundation concepts of Nysted and Thornton, respectively, to same scale. Over a short span of years, the limits for offshore gravity foundations have been pushed to meet the increased demands from the increased turbine size and the rough environmental conditions associated with the interesting wind fields for this category of wind turbines.

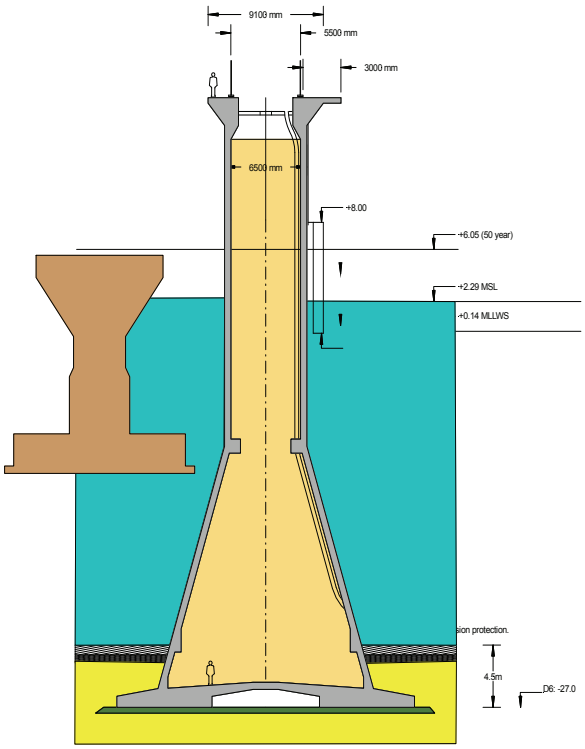


Figure 7: Comparison of Nysted and Thornton Windfarm Foundations

Project organisation

Also offshore windfarm project organisation practises are in a development stage, and it can hardly be claimed that a general industry practise has been established.

Split design and build contracts

The first Danish offshore windfarms were contracted on separate design-and-build contracts for turbine, cables, and foundations, respectively. The client tendered out the project based on front end engineering designs (FEED) and actively took on the responsibility for design and construction management.

This contracting model implies that the foundation designer works directly for the contractor. Therefore, the design is tailor made to suit the contractor's construction, installation and construction procedures and equipment.

Consequently, the foundation design can be optimised with regard to the actual construction methods.

Tenders are based on tender designs from the three main contractors.

The tender designs will then have to be merged in the detailed design phase following award of contracts.

As mentioned above, interface management on the part on the Client is crucial under this model. The interface to the cable contractor is fairly straightforward. In contrast, the design loops between the turbine and the foundation designers are time consuming and may reveal requirements that could not be taken into account in the tender design.

Turn key contracts (EPC)

In recent years, windfarm developers have tendered offshore windfarms on a turn key basis. Under this model, the turbine contractor is typically the main contractor with the cable and the foundation contractors being subcontractors. Interface management is thus largely taken on by the main contractor, shortening the communication and responsibility lines.

The benefits of this model are similar to the split contract model. In addition, the tender design benefits from the joint design between the turbine and the foundation at tender design stage.

Also this contracting model require a substantial design work to be carried out after award of contract, although the key issues are solved in the early design loops between the turbine and foundation contractor.

It appears that in spite of the apparent advantages of this contracting model, the industry does not seem to be ready to adopt it in practise. Recent tenders have returned to the split contract model.

Split contracts based on detailed design

Most recently some developers are turning towards a contracting model based on detailed design carried out by the client. In turn, it requires that the client has in-house design and construction management resources.

The advantage of this model for the client is control of the project both in terms of designs and cost at an early date. Risks are often identified in the detailed design phase and can be mitigated before tender.

The number of potential tenderers is increased, as they do not have to possess or acquire specialist engineering resources. Hence, competition is expected to be increased.

Tender costs, and therefore also overall construction costs, will decrease, as the tenderers will not have to make parallel, expensive tender designs.

Overall time is expected to decrease, as all major constraints should be identified and dealt with at an early date.

However, for the foundation designer new challenges emerge. Designs will have to be generic, and rather than designing for specific construction/installation methods and equipment the objective will be shifted to designing for a wider range of methods and equipment.

CONCLUSION

It follows from the above considerations that offshore wind turbine foundation design is subject to a developing project environment.

Every project has unique features, which have to be taken into consideration. The combination of

- integral wind turbine - foundation structure
- soil conditions
- hydraulic conditions
- construction methods
- transport/installation equipment and methods

- project organisation

sets the frame for the individual project, and the solution has to be optimised with respect to all elements.

For large water depths and turbines no standard solution exists. This is true for both concrete gravity base foundations and steel foundations, as the simple monopile concept would exceed the limits for fatigue and stiffness.

The elements of particular concern are:

- the turbine loads and the design loop process between the foundation and the turbine designer
- variations in water depths over project area
- the soil conditions, which are the most varying element and therefore need to be designed for each individual turbine location;
- weight limits for lift/installation and consideration of the working procedures related hereto
- the interface issues set by the project organisation

ACKNOWLEDGMENTS

The authors wish to thank the companies mentioned below for permission to reference the projects described in this paper and to use maps and pictures in their custody.

C-Power n.v. of Belgium for permission to reference the Thornton project and to use site map.

To the construction companies P. Aarsleff A/S of Denmark, and Dredging International b.v. for the joint project development discussion and for sharing their knowledge on construction procedures with the designers in the concept development phases and for valuable comments during the detailed design phase.

REpower Systems AG of Germany is thanked for their permission to include the photo from the Beatrice Windfarm Demonstrator project.

REFERENCES

UN, 2006, United Nations Climate Change Conference - Nairobi, 6 - 17 November 2006 http://unfccc.int/2860.php

Vestas, 2007, "Wind power is competitive", http://www.vestas.com/vestas/global/en/



Figure 8: Nysted Windfarm, Turbine Installation

BERTH DEEPENING A THREE DECADE OLD WHARF STRUCTURE FOR THE NEXT GENERATION OF CONTAINER SHIPS

Bill Paparis, P.E. and Michael Quadagno, P.E. Han-Padron Associates, LLP, New York, NY, USA
Guy Buzzoni, P.E. and James McQueen, P.E., APM Terminals N. America, Inc., Charlotte, NC, USA
John Lizzo, P.E., Port Authority of NY & NJ, Newark, NJ, USA

The thirty year old wharf structures at the Port Authority of New York & New Jersey's Port Elizabeth Marine Terminal are being modernized for the next generation of Post-Panamax container ships, which require deeper water and larger container cranes. The terminal operator is upgrading the wharf in order to remain competitive, now and into the future. The upgrade coincides with the Army Corps of Engineers' $733 million project to deepen the main shipping channel in New York Harbor.

This paper focuses on the structural modifications to accommodate berth deepening and to support the heavier loads of the new cranes. An overview is provided of the design and actual construction, including typical problems encountered when combining new and existing structures. The wharf improvements included:

- Installation of a steel king pile/sheet pile cutoff wall along the face of the wharf to permit increasing the depth from –12.2 m + 0.61 m to –15.2 m + 0.61 m (–40 ft + 2 ft to –50 ft + 2 ft)
- Removal of the existing crane rail support beams and installation of new piles and beams to support the increased crane loads
- Replacement of the existing timber fender system with a new system capable of resisting the berthing energy of a 152,000 MT displacement vessel, and having dedicated sections for berthing barges
- Replacing the existing overhead, landside crane electric feeder system with a waterside, cable reel trench system. The work included upgrading the transformer capacity at the terminal for increased crane power demands

This paper provides a case history for port administrators, terminal operators, engineers, and shipping lines challenged with upgrading aging terminals.

INTRODUCTION

The thirty year old wharf structures at Berths 82 through 98 at the Port Authority of New York and New Jersey's Port Elizabeth Marine Terminal are currently being modernized for the next generation of Post-Panamax vessels, which require deeper water and higher capacity container cranes. The terminal operator is upgrading its wharves in combination with the Army Corps of Engineers' $733 million dollar dredging project to deepen the main shipping channels in New York Harbor, thereby permitting larger vessels to enter the port. The channels are scheduled to be dredged to a depth of 13.7 m (45 ft) by 2005, and to a depth of 15.2 m (50 ft) by 2009. These wharf improvements are part of the $650 million terminal redevelopment program that the Port Authority is currently making at Port Elizabeth/Port Newark.

The existing wharf structures are only capable of berthing vessels with drafts up to 11.6 m (38 ft). Six of the eight low profile container cranes were built in the early 1970's, and are only capable of offloading vessels thirteen containers wide. The improved wharf structures will be able to berth vessels with drafts as deep as 14.6 m (48 ft) and support sixteen new Post-Panamax cranes, servicing vessels up to eighteen containers wide. Wharf improvements were sequenced in five phases in order to maintain on-going vessel berthing and container operations at the existing terminal during construction. Phase 1 construction was completed in 2002 and Phase 2 was substantially completed in January 2004. The

remaining phases are scheduled to be completed by 2009.

This paper focuses on the structural modifications made to accommodate the berth deepening and the heavier new container crane loads. The design process is discussed, outlining how it was determined that combining new construction with the existing wharf structures was the optimal improvement alternative. The paper addresses the electrical upgrades that were implemented so that the terminal would be capable of supplying the increased future crane power demands. An overview of the actual construction is also provided, including a discussion of some typical problems encountered when retrofitting existing structures.

EXISTING WHARF AND CRANES

Berths 82 through 98, which consist of 1,830 m (6,000 lin ft) of wharf, are located on the southeast corner of Port Elizabeth, as shown in Figure 1. The wharf structures were originally constructed in the early 1970's to serve general cargo operations, not container operations. Subsequent to the original wharf construction, Port Elizabeth was modified to accommodate container terminal operations by adding crane rails supported on concrete crane rail beams. The wharf and cranes were designed for Panamax container vessels, which have beams less than the Panama Canal limit of 32.2 m (105.75 ft), (thirteen 2.44 m (8 ft) wide containers) and drafts less than 12.2 m (40 ft).

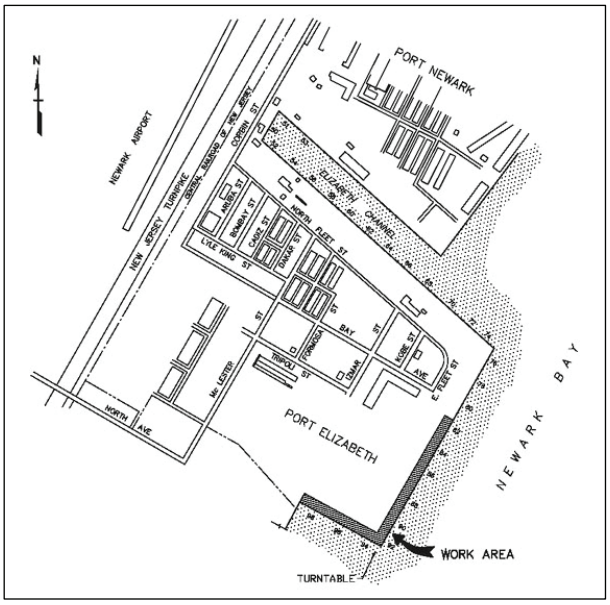


Figure 1: Wharf improvements, Berths 82 Through 98

Berths 82 through 88 were originally designed for a dredge depth of 11.6 m + 0.61 m (38 ft + 2 ft), while Berths 90 through 98 were originally designed for a dredge depth of 12.2 m + 0.61 m (40 ft + 2 ft). In 1996, a king pile/sheet pile cutoff wall was installed along Berth 98 and part of Berth 96, and these berths were deepened to 13.7 m + 0.61 m (45 ft + 2 ft).

Berths 82 through 98, similar to most of the wharf structures throughout Port Elizabeth/Port Newark, consist of a 15.24 m (50 ft) wide low level platform comprised of a 12 in. thick concrete deck slab supported by 27.2 MT (30 ton) timber piles. The piles are arranged in bents spaced at 2.44 m (8 ft) on center, with nine piles per bent.

The concrete deck supports 1.5 m (5 ft) of earth fill and bituminous concrete pavement. A concrete fascia wall at the outboard edge of the platform retains the fill. Lateral stability for the wharf structure is provided by a lower level tie rod and deadman system, spaced on 2.44 m (8 ft) centers. The structure was designed for a uniform live load of 24 kPa (500 psf).

The waterside crane rail is located 3.28 m (10 ft-9 in.) inshore of the wharf face, while the landside crane rail is located 30.48 m (100 ft) inshore of the waterside rail. The waterside crane rail beam is supported by a combination of relieving platform timber piles and additional timber piles. The landside crane rail beam is supported on pairs of steel piles that are spaced 3.66 m (12 ft) on center. The landside crane beam is connected to the wharf structure by upper level tie rods spaced on 7.32 m (24 ft) centers. Both the waterside and landside crane rail beams were designed for a live load of 290 kN per meter (20 klf).

STRUCTURAL ASSESSMENT OF EXISTING WHARF

The existing berths were initially assessed to determine what structural upgrades were required to accommodate the berth deepening and support for the heavier loads from the new cranes. The following factors were evaluated:

- Global and local stability of the wharf under-deck slope after deepening the berth from –12.2 m + 0.61 m (40 ft + 2 ft) to –15.2 m + 0.61 m (50 ft + 2 ft);
- Structural capacity of the existing crane beams and piles to resist the increase in crane loads from 290 kN per meter (20 klf) to 730 kN per meter (50 klf);

- Seismic loading; and
- Condition and remaining service life of existing wharf structure

The assessment of the existing wharf and design of the structural upgrades were dependent on the geotechnical conditions. The general geological profile throughout Berths 82 to 98 consists of hydraulic fill above soft and loose varved silt and clays, over a strata of dense sand and gravel (glacial till), underlain by sandstone and shale bedrock.

Wharf Reinforcement For Increased Water Depth

In order to deepen the berth from –12.2 m (40 ft) to –15.2 m (50 ft) mean low water (MLW), a steel king pile cutoff wall was installed at the wharf face. This wall permitted dredging seaward of the wharf, while still maintaining the stability of the riprap slope beneath the relieving platform.

The king pile cutoff wall system was determined to be the most economical structure. H-piles with interlocks on their flanges were driven along the face of the wharf. Pairs of intermediate sheet piles were then installed underwater between the H-pile interlocks, so that the tops of the sheets were just above the toe of the existing underwater slope.
The local stability of the under-deck riprap slope after dredging is maintained by the new cutoff wall. However, the overall global stability of the wharf due to the deepening needed to be evaluated. The principal concern was a slip-circle type of failure, under both static and seismic conditions. Slope-stability analyses of the riprap slope and underlying soil determined that the tips of the intermediate sheet piles needed to be driven into the glacial till, i.e., below the clay layer, in order to achieve this stability. Driving the king piles through the glacial till layer also resulted in the optimum wall design. This maximized the passive pressure on the wall and eliminated the need to socket the king piles into the underlying bedrock.

The king piles are anchored into the concrete fascia wall for lateral support. Analysis of the original tie rod deadman system revealed that in some locations it is marginally capable of resisting additional lateral loading of the cutoff wall when combined with the higher mooring loads from the new bollards. However, due to concern over potential corrosion, some of the tie rods were upgraded. Figure 2 shows a typical section through the upgraded wharf and cutoff wall, and Figure 3 shows the typical wall installation.

Crane Rail Capacity Increase

The upgrading of the existing crane rail support system to accommodate substantially larger cranes was a major element of this project. The new cranes have substantially higher container lifting capacity and reach than the existing cranes. They also weigh considerably more, and impose considerably higher loading on the crane rails. The new cranes impose a vertical load of 2.5 times and a lateral load of several times those imposed by the existing cranes.

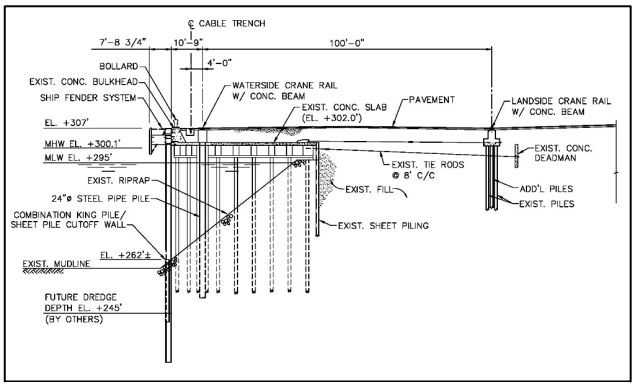


Figure 2: Typical upgraded wharf section.



Figure 3: Installation of cutoff wall along face of wharf

Preliminary analyses of the existing crane foundations indicated that the waterside and landside reinforced concrete crane beams had sufficient capacity to support the new cranes, but the piles did not. Several alternatives were explored in order to develop the optimum crane rail foundation upgrade. One preliminary design option was locating the new rails either landward or seaward of the existing rails. Another alternative was to drive new piles adjacent to the existing beam, and then tie them together. Ultimately, it was determined that demolishing both the waterside and landside crane beams and installing new reinforced concrete beams in the same location as the existing beams was the most economically feasible option.

New 610 mm (24 in.) diameter steel pipe piles were installed at 2.44 m (8 ft) on center, adjacent to the existing timber piles. Since the steel piles needed to be installed through the existing wharf deck and within a very confined area between the existing timber piles, it was determined that fewer high capacity 227 MT (250 ton) piles were the most economical solution. The existing timber crane support piles were found to be in good condition. However, since the axial stiffness of the new steel pipe piles is considerably greater than that of the existing timber piles, the steel piles were designed to carry the entire load of the new cranes.

New steel piles were also installed as part of the landside crane beam upgrades. However, they required less capacity than the new waterside piles because they were designed to work in combination with the existing steel piles that supported the existing landside crane beam. The existing landside crane beam foundation consisted of pairs of 254 mm (10 in.) diam steel pipe piles spaced at 3.66 m (12 ft) centers along the beam. The upgrade consisted of driving two new HP14 piles (99.8 MT/110 ton capacity) between the pairs of existing pipe piles. New pile caps were also constructed as part of the modifications, in order to tie the existing piles into the new crane beam.

Tiedown pins were incorporated into both the waterside and landside crane beams to provide anchorage for the cranes during severe storms and hurricanes. The wind loads generated by the cranes due to severe storms produce substantial uplift forces. In order to resist the uplift, tension anchors were installed below the tiedown pins, and in order to resist the jacking loads, the size of the concrete beam was increased along portions of its length. The tension anchors along both the waterside and landside crane rail beams consist of pairs of concrete-filled 610 mm (24 in.) diam. steel pipe piles socketed into the underlying bedrock. Figure 4 shows the crane beams under construction.



Figure 4. Installation of new crane rail beams

Wharf Seismic Analysis

When the existing Port Elizabeth wharf structures were built, requirements for seismic design were not included in the local building codes. Consequently, the wharves were not designed to withstand a seismic event. As part of the wharf improvements, a seismic analysis was performed to insure that new structural elements comply with current codes applicable to waterfront structures in the New York City region.

Several of the wharf improvement elements were governed by the seismic loading, including the size of the cutoff wall king piles and anchor bolts, and the pile/crane beam connections.

Evaluation of Existing Wharf

An above water and underwater inspection of the existing wharf structure was performed at the start of the wharf improvement design. The purpose of the inspection was to determine the general condition of the wharf and to assess whether its structural capacity and remaining service life were compatible with the proposed wharf improvements. The assessment also addressed any future maintenance repairs that may be required in order to assure the existing structure will have the same design life as the new construction. This evaluation particularly focused on the potential of future marine borer deterioration of the existing timber wharf piles, and the preventative maintenance required to protect against borer infestation.

The inspection found the wharves to be in good condition and in need of only minor future preventative maintenance in order to assure that

their service lives will be compatible with the new construction.

MOORING FITTINGS, FENDER SYSTEM, PAVING, AND DRAINAGE UPGRADES

As part of the wharf improvements, the mooring fittings, fender system, pavement, and drainage were also upgraded. Figure 5 shows these newly installed elements immediately after the completion of the Phase 1 construction.

Mooring Fittings

At the time the existing wharf and its mooring fittings were designed, vessels as large as 152,000 MT were not contemplated. The mooring fittings consisted of 77 MT (85 ton) bollards spaced at 36.6 m (120 ft) on center, with smaller cleats midway between each bollard. This "mixing" of mooring fittings is considered poor practice by modern standards because the relatively low capacity cleats are inadequate to secure the heavily loaded mooring lines. The existing mooring fittings were replaced with new 150 MT bollards spaced at 12.2 m (40 ft) on center. The lateral loads from the higher capacity moorings resulted in the need to replace some of the tie rods with tie rods of increased capacity.

Fender System

The existing fender system consisted of timber piles spaced at 2.44 m (8 ft) on center, with timber wales and chocks, and 254 mm (10 in.) diameter by 305 mm (12 in.) long end-loaded cylindrical rubber elements between the timber and the concrete wharf face. The fender system was designed in the early 1970's and had only a small fraction of the energy absorbing capacity required by modern practice, especially considering the larger vessels that will call at the terminal. Therefore, the existing timber fender system was replaced with buckling type rubber units, as shown in Figure 5.

The new buckling type fenders, spaced at 12.2 m (40 ft) on center along the face of the wharf, are capable of accommodating the berthing energy of a 152,000 MT vessel. This modern resilient fender system not only has high energy absorption capacity, which provides maximum protection to the berthing vessels as well as the wharf structure, but it is more cost effective than the existing timber system due to its low maintenance cost.

An approximately 109.7 m (360 ft) long, continuous solid faced fender system was also installed along portions of the wharves to accommodate barges.

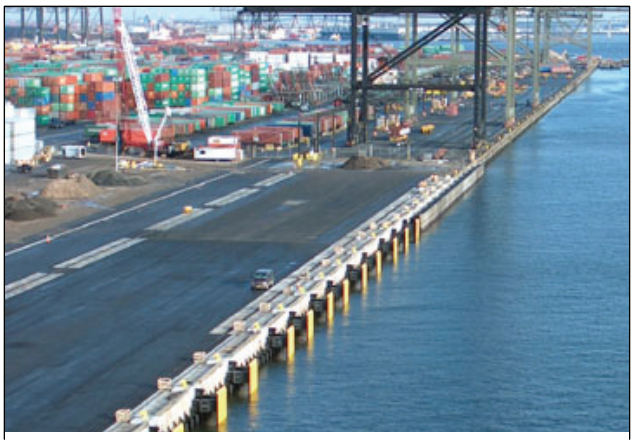


Figure 5: Overall view of newly installed mooring fittings, fender system, and pavement

Since the ship fenders are discrete units, they are not well suited for the barges used for container feeder service. Barges generally have a squared-off bow and stern, and may be berthed without the assistance of a tug. Thus, the barge usually berths at a relatively steep angle in relation to the face of the wharf, resulting in the corner of the bow or stern contacting the fender system. The corner of the barge can pass in between adjacent ship fender units and contact the wharf structure, potentially damaging the wharf and/or the barge. Therefore, a continuous face with no gaps must be provided for the barge.

The barge fender system consists of a solid timber face attached to 12.2 m (40 ft) long steel panels supported on H-piles by pin connections, which are necessary to prevent overstress in the steel frames. Rubber energy absorbing units are fitted between the panels and the wharf structure to absorb the energy of the berthing vessels. The barge fender system also works in conjunction with the ship fender system when berthing large vessels. Similar to the ship fenders, the barge fender system provides maximum protection to the vessels and the wharf, while requiring far less maintenance than the timber system it replaces.

Pavement and Drainage

The existing wharf pavement was typically in good condition. As part of the wharf improvements, most pavement was only milled and resurfaced. Full depth pavement replacement was only performed along the new crane rail beams and where trenches were dug to replace tie rods and install electrical duct banks. As part of the resurfacing work, the pavement was re-graded to improve the drainage.

A continuous trench drain was also installed parallel to the wharf, 15.2 m (50 ft) inshore of the landside crane rail.

ELECTRICAL SERVICE UPGRADES

Another major element of the wharf improvements was upgrading the existing 4.16 kV electrical power supply and distribution system to the existing shore cranes at the terminal, to allow it to handle the future increased power demands of the new 13.8 kV Post-Panamax cranes. These improvements included providing redundant transformer capacity and feeder cables for up to sixteen new cranes.

The main electrical substation was expanded by constructing a replica of the existing one in layout and type of equipment. This included installing two new separate incoming 26 kV feeders from the utility company (PSE&G), and two 7,500 kVA main step-down transformers to 13.8 kV. After the new substation expansion was in place, the old substation was refurbished, which included the replacement of the two original 7,500 kVA transformers.

Other electrical upgrades included the installation of new electrical and communication ductlines and manholes, and new crane loop switches along the wharves. The existing overhead, landside crane electrical collector bar system was also replaced. Power is supplied to the new cranes by a waterside cable and reel system, with the cable laid in a trench below the pavement surface, powered via a cable reel mounted on the crane legs. The existing 4.16 kV cranes will also be converted to this new 13.8 kV power supply system.

OVERVIEW OF THE CONSTRUCTION

The wharf improvements are being performed in five phases so that the terminal can remain operational during construction. The construction duration of each phase, which is approximately 305 m (1,000 ft) long, is 9 to 12 months. Phase 1 was performed from January through December 2002, and Phase 2 was carried out from May 2003 through January 2004. The remainder of the phases are scheduled to be completed by 2009. The phases were sequenced so that Phases 1 and 2 were designed and constructed before the design of the subsequent phases. This allowed any “lessons learned” from initial construction to be incorporated into the design of the future phases. Figure 6 shows an overall view of the completed Phase 1 wharf improvements, including three new Post-Panamax container cranes.



Figure 6: Overall view of the completed wharf improvements, including the first three Post-Panamax container cranes

Although the combination of the new construction with the existing wharf structures was the optimal wharf improvement alternative, this combined approach was subject to frequent field changes during the construction, resulting from the as-found conditions differing from as-built plans. This was particularly the case for the new waterside and landside piles, which were installed between the existing crane beam and wharf piles. The locations of the new piles were determined from the as-built drawings. However, upon demolishing the old crane rail beams, it was discovered that the spacing and/or location of many of the existing piles deviated from what was shown. Also, the locations of several new waterside crane beam piles had to be changed slightly because there were abandoned timber piles under the wharf deck in the proposed design locations. Ultimately, some of the new crane beam piles were spaced further apart than initially intended, and some of the landside pile cap sizes were increased. However, the new crane beam piles, pile caps, and beams were over-designed with enough flexibility such that no major re-designs were required when these problems were encountered.

CONCLUSION

Many marine container terminals in operation today were built over thirty years ago, in the era of the Panamax vessel. Similar to Port Elizabeth, these terminals will likely also require upgrades to accommodate Post-Panamax ships in order to remain competitive. This paper serves as a valuable case history to port administrators, terminal operators, engineers, and shipping lines that will be faced with the challenges of upgrading these terminals.